VIBRATION OF BEARINGS

K.M. RAGULSKIS A.Yu. JURKAUSKAS
V.V. ATSTUPĖNAS A.Yu. VITKUTĖ A.P KULVEC

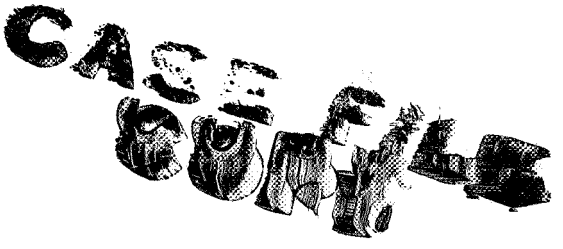

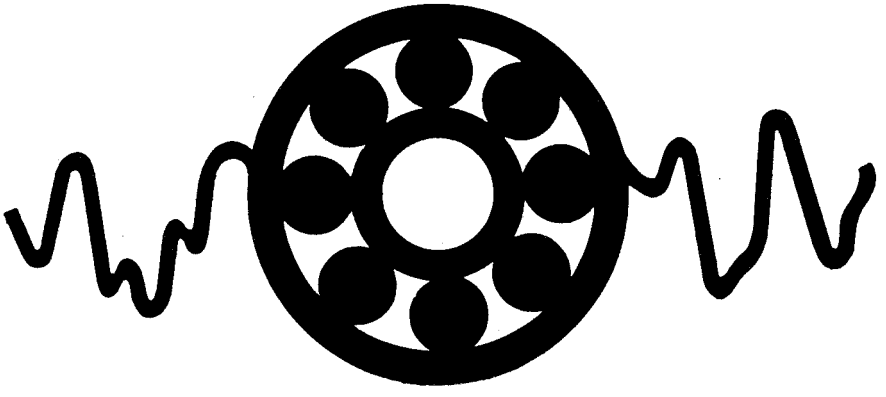

Published for the National Aeronautics and Space Administration,
and the National Science Foundation, Washington, D.C.
by Amerind Publishing Co. Pvt. Ltd., New Delhi

VIBRATION OF BEARINGS
K.M. RAGULSKIS A.Yu. JURKAUSKAS
V.V. ATSTUPĖNAS A.Yu. VITKUTĖ A.P. KULVEC

Amerind

Analytical determination of vibrations and friction torque due to rotation, taking into account the hydrodynamic action of a lubricating oil film, and determination of the elastic and damping characteristics of bearings and bearing assemblies are some of the problems considered in this book. The methodology and techniques of measuring the dynamic characteristics of bearings are presented. Experimental data and the methodology of statistical analysis are also given.

The book is intended for scientists and engineers engaged in the instrument manufacturing and machine building industries.

TT 75-52090
NASA TT F-679

KAUNSKII POLITEKHNICHESKII INSTITUT
Tsentral'naya Nauchno-Issledovatel'skaya Laboratoriya Vibrotekhniki

KAUNSK POLYTECHNICAL INSTITUTE
Central Scientific-Research Laboratory of Vibrotechniques

VIBRATION OF BEARINGS

[Vibratsiya Podshipnikov]

K.M. RAGULSKIS, A.YU. JURKAUSKAS,
V.V. ATSTUPĖNAS, A.YU. VITKUTĖ, A.P. KULVEC

Mintis Publishers, Vilnyus, 1974

Translated from Russian

Published for the National Aeronautics and Space Administration,
and the National Science Foundation, Washington, D.C.
by Amerind Publishing Co. Pvt. Ltd., New Delhi
1979

© 1979 Oxonian Press Pvt. Ltd., New Delhi

Translated for the National Aeronautics and Space Administration, pursuant to an agreement with the National Science Foundation, Washington, D.C., by Amerind Publishing Co. Pvt. Ltd., 66 Janpath, New Delhi

Translator: Dr. N.M. Shivaramkrishnan
General Editor: Dr. V.S. Kothekar

Available from the U.S. Department of Commerce, National Technical Information Service, Springfield, Virginia 22161

Published and printed at Oxonian Press Pvt. Ltd., Faridabad, India

UDC 621

Analytical determination of vibrations and friction torque due to rotation, taking into account the hydrodynamic action of a lubricating oil film, and determination of the elastic and damping characteristics of bearings and bearing assemblies are some of the problems considered in this book. The methodology and techniques of measuring the dynamic characteristics of bearings are presented. Experimental data and the methodology of statistical analysis are also given.

The book is intended for scientists and engineers engaged in the instrument manufacturing and machine building industries.

CONTENTS

INTRODUCTION 1

CHAPTER 1. ANALYTICAL DETERMINATION OF FRICTION TORQUE . . . 2

1.1 Friction Torque in Rolling-Contact Bearings 3

1.1.1 Rolling friction in bearings 3

1.1.2 Total friction torque in rolling-contact bearings . . . 6

1.1.3 Analytical determination of total friction torque in rolling-contact bearings 15

1.2 Analytical Determination of Variable Component of Friction Torque 19

1.2.1 Determination of the load acting on the *i*-th ball bearing 29

1.2.2 Computation and analysis of variable component of friction torque 30

1.3 Determination of the Friction Torque in Ball Bearing due to Rolling Friction, Taking into Account Exponential Dependence of Viscosity on Pressure 34

References 40

CHAPTER 2. DETERMINATION OF ELASTIC AND DAMPING CHARACTERISTICS OF ROLLING-CONTACT BEARINGS 44

2.1 Determination of Static Stiffness of Rolling-Contact Bearings 46

2.2 Errors in Manufacture and Their Effect on the Stiffness of Rolling-Contact Bearings 65

2.3 Identification of Elastic and Damping Characteristics of Bearings Based on the Results of Vibration Tests 74

References 84

CHAPTER 3. ANALYSIS OF RADIAL VIBRATIONS OF BEARINGS AND BEARING ASSEMBLIES 89

3.1 Dynamics of Ball Bearing Assembly 94

3.2 Vibration of the Outer Ring of Ball Bearing and Conservative Friction Torque 101

3.3 Vibrations of Shaft Rotating in Two Ball Bearings with Preload 112

3.3.1 Statistical characteristics of vibrations of shaft in standard ball bearings 114

3.4 Equation of Radial Vibrations of a Shaft in a Bearing During Random Excitation 118

3.5 General Formulation of the Problem of Probability Modelling 123

References 134

CHAPTER 4. MEASUREMENT TECHNIQUES AND INSTRUMENTS FOR MEASUREMENT OF DYNAMIC CHARACTERISTICS OF BEARINGS . . . 145

4.1 Measurement of Friction Torque and Vibrations of Bearings 146

4.2 Setup for the Measurement of Friction Torque in Rolling-Contact Bearings 151

4.2.1 Electrical instruments for the measurement of friction torque coefficients in bearings 167

4.3 Apparatus for the Analysis of Friction Torque in Sliding Bearings 175

4.4 Apparatus for the Measurement of Dynamic Parameters of High-Speed Ball Bearings in Specific Conditions 179

References 189

CHAPTER 5. ERRORS IN THE MEASUREMENT OF FRICTION TORQUE AND THEIR REDUCTION 199

5.1 Additive Error in the Measurement of Friction Torque and Its Reduction 199

5.2 Dynamic Condition of Correction of Additive Error. . . . 201

5.2.1 Energy spectrum of residual error 206

5.3 Some Problems of Correction Procedure 211

5.3.1 Analysis of the effect of interrupting measurement . . . 212

5.3.2 Determination of the parameters of error 215

5.3.3 Evaluation of the effectiveness of correction 217

5.4 Friction Torque Measuring Instrument (FTMI) with Correction for Additive Error 218

5.5 Other Sources of Error in the Measurement of Friction Torque 223
References 228

CHAPTER 6. STATISTICAL ANALYSIS OF EXPERIMENTAL RESULTS OF PRECISION BEARING DYNAMICS 233

6.1 Requirements for the Evaluation of Statistical Characteristics and Preparation of Experimental Material 235

6.2 Estimation of Statistical Characteristics 252

6.2.1 Special correlation characteristics of rolling-contact bearing parameters and the dependence of friction torque on different operating conditions 265

6.3 Determination of Relations between Bearing Parameters . . 274

References 292

CHAPTER 7. EXPERIMENTAL STUDY OF THE DYNAMIC CHARACTERISTICS OF PRECISION BEARINGS AND ASSEMBLIES 296

7.1 Study of Friction Torque in Bearings and Bearing Assemblies . 296

7.1.1 Dependence of friction torque on loading 297

7.1.2 Study of friction torque in bearing assemblies . . . 301

7.1.3 Dependence of friction torque (M_B) in bearings on other factors 304

7.2 Effect of Lubricant on Friction Torque in Bearings 307

7.3 Study of the Dynamic Parameters of High-Speed Rotors in Ball Bearing Supports 318

7.4 Experimental Study of Heating, Friction Torque and Lubricating Conditions of High-Speed Ball Bearings 327

7.5 Investigation of Friction Torque in Precision Slide Bearings . 343

7.6 Diagnosis of Errors and Mounting-cum-Operational Defects in Bearings according to Characteristics of Friction Torques . 356

7.6.1 Effect of the shape of bearings 358

7.6.2 Effect of the cage 358

7.6.3 Effect of the surface smoothness 360

7.6.4 Effect of dirt 361

7.6.5 Effect of lubrication 362

7.6.6 Effect of ring deformation 362

References 366

CHAPTER 8. WAYS OF REDUCING FRICTION TORQUE AND VIBRATIONS IN BEARINGS 372

8.1 Effect of Vibrations on Friction Torque in Ball Bearings . . 372

8.2 New Designs of Rolling-Contact Bearings and Assemblies with Reduced Friction Torque 377

8.3 New Designs of Slide Bearings with Reduced Friction Torque 383

References 387

INTRODUCTION

It is impossible to imagine the progress of modern science and technology without the wide application of bearings, which form an integral part of the majority of machines, instruments and assemblies. The accuracy and sensitivity of the majority of precision instruments and assemblies have improved considerably in the recent past. Tremendous progress has also been made in achieving reduction in the sizes of machines, their weight and power requirements. All this led to the development of new types and designs of mounting and more stringent requirements of the quality of bearings and assemblies. These developments stimulated theoretical and experimental research on the dynamic characteristics of bearings.

The large amount of work (theoretical and experimental) devoted to the study of bearings and their mountings has yet to cover every aspect of the phenomena occurring in this dynamic domain.

In recent times such characteristics of precision mechanisms as spatial vibrations of rings, friction torque and elastic and damping properties have assumed the highest importance. It is necessary to study these characteristics theoretically and experimentally using statistical analysis.

Problems related to the computation of vibrations, friction torque and stiffness of bearings taking into account the enhanced qualitative requirements of bearing assemblies are considered in this book. Methods and experimental setups for the determination of the dynamic characteristics of the mounting are described and the methodology of the statistical analysis of experimental results is given.

The following scientists of the central interdepartmental research laboratory, Kaunasskii Polytechnic Institute, have contributed to this book: A.B. Palionis (1.2, 1.3, 7.2, 8.2); R.P. Atstupenene (2.3); R.V. Kanapenas (4.3, 7.5, 8.3); V.I. Zdanavichyus (4.4, 7.3, 7.4); V.N. Augutis (5.1, 5.2, 5.3, 5.4); I.P. Zhitkevichyus (8.1).

1

ANALYTICAL DETERMINATION OF FRICTION TORQUE

The total resistance in roller-contact bearings is dependent on a number of factors, the most important of which are given in the work [36]. It is necessary to mention that in all the works devoted to the investigation of friction only the constant resistance component is considered. In a deeper analysis of the phenomenon it is possible to separate out the variable resistance component from the constant one during the relative displacement of parts in contact. The presence of the variable component in roller-contact bearings is primarily due to geometrical errors in raceways, rollers and balls, nonuniform properties of the material, nonuniform loads, solid intrusions, etc.

There are various ways of reducing the variable component of the friction torque in bearings (VFT): reduction of loads acting on the bearing, reduction of clearances, increase in accuracy, etc. In this difficult and complex field the study of the effect of the kind of lubricant has been inadequate.

Since all types of resistances act simultaneously in the bearing, it is possible to use analytical method of research in order to find the resistance in the lubricating material. Preliminary studies show that the lubricant itself does not create VFT. Consequently the effect of lubricant on VFT has to be considered in conjunction with the working conditions, faults in the bearing, etc.

The different types of resistances in bearings, their contribution to the total resistance and the prevailing methods of computation are described in this chapter.

On the basis of known solutions of the contact-hydrodynamic problem formulas are obtained for computing VFT due to differential sliding, taking into account the deformation of bearing surface elements, the hydrodynamic action of the lubricating film, etc. The results of the computations are presented.

A formula is developed for the computation of the friction torque due to rolling, assuming an exponential relationship between the viscosity of the lubricant and pressure.

1.1 FRICTION TORQUE IN ROLLING-CONTACT BEARINGS

1.1.1 Rolling Friction in Bearings

The resistance to relative motion in rolling-contact bearings is due to many factors, the basic one being rolling friction. This was long assumed to be the only resistance to motion in rolling-contact bearings. After further studies of rolling-contact bearings it was established that the contribution of rolling friction in bearings is small though its effect on wear and tear and operating temperature conditions is important. These factors are especially important for miniature instrument rolling-contact bearings operating in the very accurate mechanisms of servo-systems, magnetic recorder mechanisms and other precision parts of instruments.

The first experimental research on rolling friction was carried out by Leonardo da Vinci in 1508. The concept of the coefficient of external friction arose as a result of these experiments. Leonardo da Vinci concluded that for identical surface smoothness this coefficient is a constant for different bodies and equals 0.25.

In early research the rolling friction was treated as a mechanical process, i.e. the interaction of rough surfaces of absolutely rigid solid bodies was considered.

The concept of rolling friction as a mechanical process was introduced by I. Delagir and was further developed and studied by A. Parin, L. Euler, D. Lesley and others [20, 21].

M. Coulomb was the first to introduce the hypothesis of the dynamic nature of external friction. The experimentally obtained relationship of the frictional force F due to rolling along a plane is given by the classical equation

$$F=f\frac{P}{r}=\mu\cdot P, \tag{1.1}$$

where f is the coefficient of rolling friction, having the dimension of length;

P is the normal load;

r is the radius of roll;

μ is a coefficient similar to the coefficient of sliding friction.

This relationship known as the Amon-Coulomb law, relating frictional force and normal load, appeared to mark the end of a long period in the development of the science of friction [21].

In 1876 O. Reynolds [36, 38] was the first to propose the hypothesis of relative slipping according to which the frictional force due to rolling of a perfectly elastic body along a perfectly elastic base appears as a result of relative slipping of contact surfaces due to their deformation. It can be seen from Fig. 1.1 that in the region AC surface layers of the roller are compressed (in a direction along the area of contact) and in the plane, elongated. In the

region *CB* of the contact area these deformations take place in the opposite direction, as a result of which microslipping occurs.

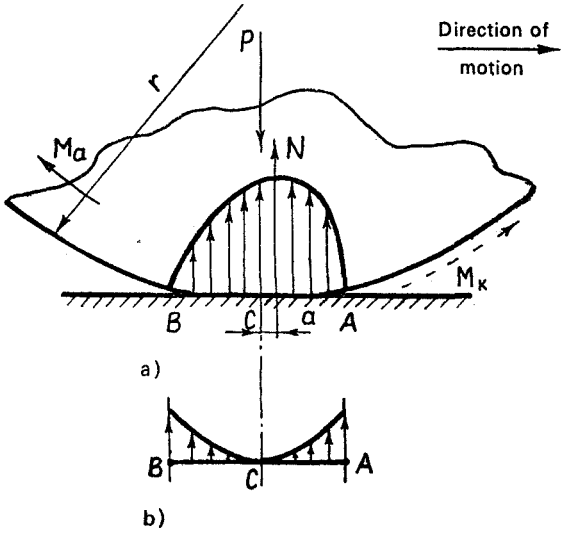

Fig. 1.1. Explanation of O. Reynolds' hypothesis.

A.S. Ahmatov, D. Taybor and A. Tomlinson [2, 49, 50] have shown that slipping in the contact zone is not the only source of frictional loss in rolling. In this connection the hypothesis of molecular interaction was put forward. G. Tomlinson and D. Taybor showed experimentally that even during the rolling of two cylinders or two balls of identical size made of identical material loss of energy occurs. According to G. Tomlinson, when two bodies approach each other atomic and molecular interactions appear and energy is lost in overcoming them, which accounts for the additional energy loss.

Taking into account the forces of molecular interaction during the rolling of a cylinder along a plane G. Tomlinson determined the frictional coefficient as follows:

$$K=\frac{3}{4}\sqrt{\frac{\pi}{2}\frac{ef}{\sqrt{P\cdot r\cdot\Theta}}}, \tag{1.2}$$

where K is the coefficient of rolling friction;

P load on the cylinder;

r radius of the cylinder;

e crystal lattice constant;

f coefficient of sliding friction;

Θ is a function of the elastic constants of the materials of the bodies in contact.

G. Tomlinson carried out experimental verification of the coefficient of

rolling friction by introducing an additional coefficient λ related to the coefficient of rolling friction K (mm) by the expression $K=\lambda \cdot l$, where l is the moment arm applied to the rolling body. The coefficient λ was determined by the damping of the oscillations of a pendulum. The value of λ thus obtained was twice the theoretical value for amplitudes of pendulum oscillation ranging from 4 to 0.61° and this is explained by the fact that the relative displacement and molecular sizes are commensurable.

A.S. Ahmatov developed formulas for determination of the coefficient of rolling friction based on perfect contact between the friction surfaces. Pitting of metal was established by V. Gardi, F. Banden and R. Ridler [41, 43].

The works of A.Yu. Ishlinskii [6, 7], R.S. Drutovski [42], A. Palmgren [46], D. Taybor [49] and others have great practical importance. They have studied the appearance of internal friction as a result of the imperfect elastic properties of true solids. In order to prove this hypothesis A.Yu. Ishlinskii considers the rolling resistance in the case of the rolling of a perfectly hard roller along a viscoelastic surface and along a yielding surface. The load distribution on the roller is shown in Fig. 1.2. The presence of frictional force in this case is explained by the unsymmetric load distribution [33].

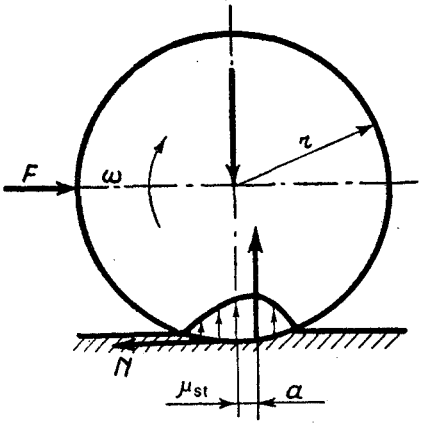

Fig. 1.2. Appearance of frictional force with asymmetric distribution of rolling pressure on ground along contact surface.

A.Yu. Ishlinskii developed the relationship for the determination of resistance F (at small rolling speeds) in the case of the rolling of a perfectly hard body along a yielding surface:

$$F=\frac{\mu \cdot v}{C \cdot r} P, \tag{1.3}$$

where P is the load on the cylinder;
v rolling speed;
μ coefficient of internal friction of the base material;
r radius of cylinder;
C hardness coefficient of the base.

The coefficient of rolling friction is thus obtained as:

$$K=\frac{\mu \cdot v}{C} \cdot \tag{1.4}$$

The corresponding corrections, especially in the mechanical and molecular

concepts of external friction, led to further development of this science. The large amount of work, basically of the applied kind, devoted to the mechanical concept has enriched our understanding of the laws of elastoplastic deformation and destruction. The latter concept is closely bound up with the molecular concept, based on the analysis of the physics of the boundary layer and the thin metal structure of rubbing surfaces.

1.1.2 Total Friction Torque in Rolling-Contact Bearings

In 1919 A. Palmgren developed a theory of resistance of roller bearings assuming differential slipping as the cause of rolling friction.

The roller bearings widely used now have undergone hardly any change in form since they first appeared in 1900–1920. The major thrust of research concerned the life, load-bearing capacity and wear resistance of roller bearings. Research on friction in roller bearings started in 1940 when friction torque became a basic problem and—for certain instrument bearings—the basic criterion determining usefulness.

A. Palmgren's works [27, 46] are among the most important in this field. It is necessary to consider load, number of revolutions, shape and quantity of lubricant as basic factors affecting the energy loss in rolling contact bearings.

According to Palmgren, the contact region is a point or a line in the case of an unloaded bearing but in the case of a loaded bearing contact surfaces appear due to elastic deformations. The surfaces cannot be generated either theoretically or experimentally and hence there appear, even though small, local displacement and slipping even when the rolling body is completely displaced as in pure rolling. The energy spent on this displacement is considered lost.

The hysteresis loss is added to the losses due to friction arising from elastic slipping. These losses depend on load but not on the convergence of rolling bodies with the ball race.

In 1949 G.V. Poritskii and others [47] extended the theory of friction in roller bearings by analyzing the loss resulting from sliding friction caused by gyroscopic effect. However, Poritskii's studies are too specialized to be considered a general theory of roller bearing friction.

Ito [44] in 1957 analyzed roller bearing friction under axial load as the friction due to differential slipping but did not consider the loss to friction due to slip arising from the motion of the rollers.

In 1959 A.B. Johns [45] took the movement of the rollers of roller bearings as his basis to develop a theory of friction but he did not take into account all the factors acting on the roller either, in particular the losses due to elastic hysteresis. At present there is a tendency to generalize the early theories into a common theory on the total friction torque of roller bearings.

The works of N.A. Spintsyn, B.Ya. Kraskovskii, A.I. Sprishevskii, K. Kakuty, R. Barnard and others [8, 36] encompass all the above-mentioned factors affecting friction torque. Approximate formulas have been developed for analytical determination of friction torque.

When considering friction torque as the result of a number of factors affecting the bearing it is necessary to break down the torque into its components with the following interpretation:

Friction torque in bearings represents a complex physical process [37] which can be expressed as follows:

$$M=(M_{ds}+M_{gyr}+M_{hys}+M_{de}+M_c+M_e+M_m+M_T)\cdot K, \qquad (1.5)$$

where M_{ds} is the friction torque due to differential slipping of roller on contact surface;

M_{gyr} friction torque arising from gyroscopic spin or deviation of the axis of rotation of rollers;

M_{hys} friction torque due to losses on elastic hysteresis in the material of bodies in contact;

M_{de} friction torque as a result of the deviation of bearing elements from the correct geometric shape and microroughness of contact surfaces;

M_c sliding friction torque along the guide edges of the ball race and torque arising from the contact of rollers with the ball race housing;

M_e friction torque due to shear and bleeding of the lubricant;

M_m friction torque due to the working medium of the bearing (gas, liquid, air, vacuum);

M_T complex increase in friction torque due to increase in temperature;

K correction coefficient taking into account complex change in the friction torque due to the action of forces not taken into account in computing the individual components. The

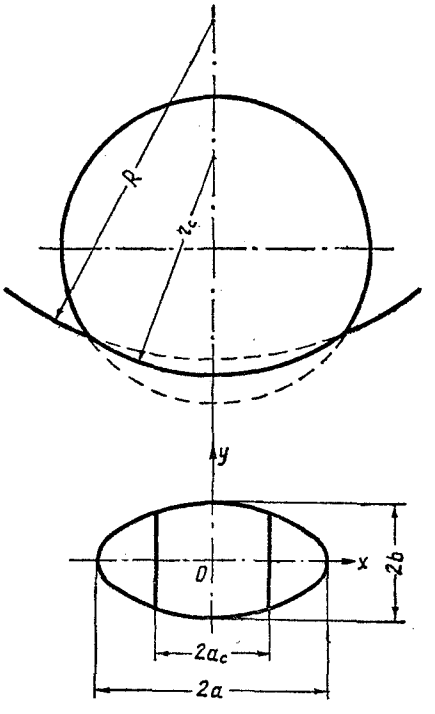

Fig. 1.3. Differential sliding.

action of axial, radial, and rolling forces, vibrational effects and other unconsidered factors are involved.

Friction torque to differential sliding (M_{ds})**:** Let us consider the friction torque due to differential sliding (M_{ds}) for the case where the ball rolls along a groove with radius of curvature R in a plane perpendicular to the direction of rolling. Pure rolling will occur along two lines (Fig. 1.3) located on an ellipse of contact at a distance 2 a_c. In other parts of the ellipse between balls and grooves of rings there will be sliding because of the unequal distance of contact points from the axis of rotation.

Friction torque due to differential sliding of rollers on the contact area is expressed in terms of work done (A) by the roller bearing in unit time as a result of differential sliding friction

$$A=(F_i\, l_i+F_o\, l_o)\cdot z, \tag{1.6}$$

where F_i, F_o is the sliding friction caused by differential sliding during the rolling of the ball along the surface of inner and outer rings respectively;

l_i, l_o are the distances moved in unit time by the point of contact of the ball with inner and outer rings respectively;

z is the number of balls.

$$l_i=2\pi R_{li}\, n_b=\frac{\pi}{2}\, d_b\left(1-\frac{d_b^2}{D_0^2}\cos^2\alpha\right)\cdot n; \tag{1.7}$$

$$l_o=2\pi R_{lo}\,(n-n_b)=\frac{\pi}{2}\, d_b\left(1-\frac{d_b^2}{d_0^2}\cos^2\alpha\right)\cdot n. \tag{1.8}$$

The relation (1.6) is valid for the case where the inner ring rotates and the outer one is fixed. In the expressions (1.7)–(1.8):

n is the rotational speed of the inner ring of the bearing;

n_b is the rotational speed of the ball;

d_b is the diameter of the ball;

D_0 is the pitch circle diameter of the ball;

R_{li}, R_{lo} are the radii of curvature of the roller groove of the inner and outer rings respectively;

α is the contact angle.

Then the friction torque resulting from differential sliding of a ball bearing will be

$$M_{ds}=\frac{A}{2\pi\cdot n} \tag{1.9}$$

or after expansion

$$M_{ds}=\frac{P\cdot D_0\cdot z}{4d_b}\left(1-\frac{d_b^2}{D_0^2}\cos^2\alpha\right)\cdot(r_oB_o-r_iB_i)\cdot f, \tag{1.10}$$

where f is the coefficient of sliding friction;

B_i, B_o are coefficients determined by the geometric conditions of deformations;

r_i, r_o are the respective radii of deformed surfaces of the ball race of the inner and outer rings.

Friction torque due to gyroscopic spin (M_{gyr}): Friction torque arising from gyroscopic spin appears in the presence of contact angle α on the balls.

To find M_{gyr} it is necessary to determine the moment of inertia of the ball, I, obtained from the expression

$$I=\frac{\pi}{60}\, d_b^2 \frac{\gamma}{g}\,, \tag{1.11}$$

where γ is the density of steel ball $=7.8$ gm/cm^3.

Friction torque due to gyroscopic spin equals

$$M_{gyr}=I\cdot\omega_b\cdot z\cdot\sin\alpha, \tag{1.12}$$

where $\omega_b=\frac{\pi n_b}{30}$, i.e. the angular velocity of the ball and

$$n_b=n_{shaft}\,\frac{D_0^2-d_b^2\cos^2\alpha}{2\,D_0 d_b}\,, \tag{1.13}$$

where n_{shaft} is the rotational speed of the shaft.

Friction torque M_{gyr} increases with an increase in contact angle α and attains a maximum when $\alpha=\pi/2$. Thrust bearings have such an angle. In individual cases, for radial bearings $\alpha=0$, so that $M_{gyr}=0$.

In order to avoid gyroscopic spin of balls it is necessary to satisfy the inequality

$$M_{gyr}<A\cdot d_b\cdot f\cdot z, \tag{1.14}$$

where A is the axial load.

The effect of gyroscopic spin is especially noticeable in radial thrust bearings.

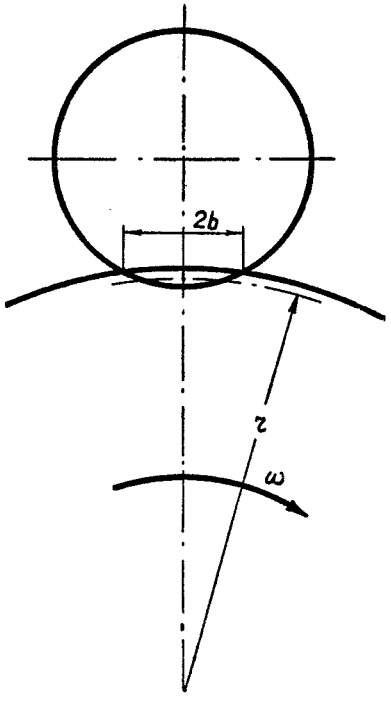

Fig. 1.4. Hertz's contact ellipse.

Friction torque due to elastic hysteresis in the material of the bodies in contact (M_{hys}): Energy losses due to elastic hysteresis in the material of the bearing can be determined assuming that during the loading cycle a specific quantity

of kinetic energy is expended. Friction torque caused by elastic hysteresis has been adequately studied for the case of slow-running roller bearings. However, in the case of high speed, large centrifugal forces arise and they create additional load. Hence in all the expressions developed below friction torque M_{hys} must be treated as a function of rotational speed.

When the ball rolls along the ball race Hertz's contact ellipse is formed between them (Fig. 1.4).

Energy developed during the rolling of the body about one point of the ball race is proportional to the load p and to the magnitude of deformation δ [32].

Contact time t of the rolling body with the ball race is directly proportional to the extent of the contact surface in the direction of motion $2b$ and inversely proportional to the circumferential velocity $r \cdot \omega$ (Fig. 1.5):

$$t \approx \frac{2b}{r \cdot \omega}. \tag{1.15}$$

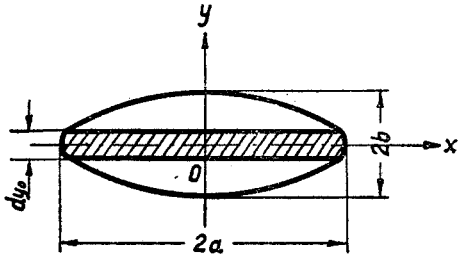

Fig. 1.5. Ball contact with groove to determine elastic hysteresis losses.

Energy losses during the contact of the rolling body with one point of the ball race are

$$M_{hys} \cdot \omega \cdot t \approx p \cdot \delta. \tag{1.16}$$

According to Hertz's theory, where there is point contact between two steel bodies the magnitude of deformation is expressed as

$$\delta = K \sqrt[3]{p^3 \Sigma\rho}, \tag{1.17}$$

where $\Sigma\rho$ is the sum of the reciprocal of the principal radii of curvature, i.e.

$$(\rho_1 + \rho_2)_I / (\rho_1 + \rho_2)_{II}, \text{ mm}^{-1},$$

here ρ_1 and ρ_2 are the reciprocals of the principal radii of curvature of the bodies at the point of contact;

K is a coefficient depending on the auxiliary function $F(\rho)$:

$$F(\rho) = \left| \frac{(\rho_1 - \rho_2)_I + (\rho_1 - \rho_2)_{II}}{\Sigma\rho} \right|. \tag{1.18}$$

Coefficient $F(\rho)$ is usually determined from tables. It is possible to consider approximately:

$$M_{hys} = \Sigma p^{4/3}. \tag{1.19}$$

The expression (1.19) is valid for point contact when $\delta \approx p^{2/3}$ and $b \approx p^{1/3}$. A more exact expression for loss caused by elastic hysteresis is given in the work [37]:

$$M_{\text{hys}} = 1.25 \times 10^{-4} D_0 \cdot d_b^{-2/3} \cdot \Sigma_i \cdot p_i^{4/3}, \tag{1.20}$$

where p_i is the load on the i-th ball.

Hysteresis losses are practically independent of the shape of the ball race.

Friction torque due to geometric errors and the effect of microroughness of contact surfaces (M_{de}): The main cause of changes in friction torque are errors in the geometric shape of the bearing elements (ovality, edges of rings and balls, form of roughness and others).

According to [29] let us write the additional active friction torque:

$$M_{\text{de}} = \frac{dx}{dk} N, \tag{1.21}$$

where k is the turn angle of the moving ring of the bearing relative to the stationary one;

x is the linear displacement of the moving ring of the bearing in the direction of the load N acting on it and arising due to the deviation in the geometric shape and microsurface roughness of the contact surfaces from the ideal.

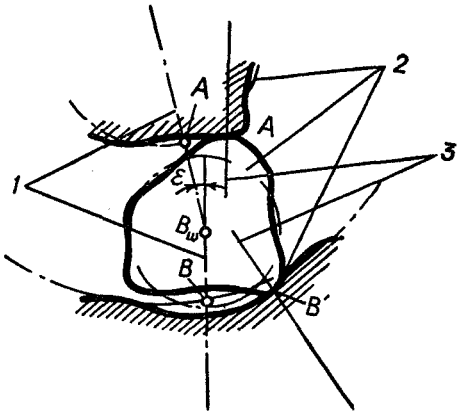

Fig. 1.6. Creation of friction torque due to defects in shape of bearing components.

The process of the formation of M_{de} is shown in Fig. 1.6.

The line of action is formed at every given instant. In an ideal bearing (in which balls and rings have ideal form) this line passes through the center of the loaded ball. In a real bearing the line of action does not coincide with the direction of the theoretical line of action.

In a real radial bearing center O (Fig. 1.7) of the race circle of the moving inner ring does not coincide with the theoretical center O_1. Total errors Δz_1 and Δz_2 [29] arise due to geometric nonuniformities. While determining the center O_1 it is assumed that the radial bearing is loaded purely by radial load R applied at the point O_1. Here the radial load is taken by two balls which roll without slipping. Then

$$M_{de}=R\frac{dx}{dk}=\frac{R}{\sin\frac{\alpha\pi}{z}}\left[\frac{dz_1}{dk}\sin\left(\frac{2\pi}{z}-\alpha_1\right)\right.$$

$$\left.-\Delta z_1\frac{d_i}{2D_0}\cos\left(\frac{2\pi}{z}-\alpha_1\right)+\frac{dz_2}{dk}+\Delta z_2\frac{d_i}{2D_0}\cos\alpha_1\right], \qquad (1.22)$$

where d_i is the diameter of the race circle of the inner ring;

Δz_1, Δz_2 are the total errors;

Δz_n is the metrological and actual error of the inner ring in the zone of contact with the ball;

ΔR_n is the metrological and actual error of the outer ring in the zone of contact with the ball;

$\Delta\rho_1, \Delta\rho_2$ are the errors in the ball in the zone of contact with the inner and outer rings respectively.

Thus it is possible to consider the effect of certain specific errors as an exception for individual errors.

Friction torque due to the effect of the ball race (M_c): If we assume that the inner ring of the bearing rotates about a vertical axis and the ball race

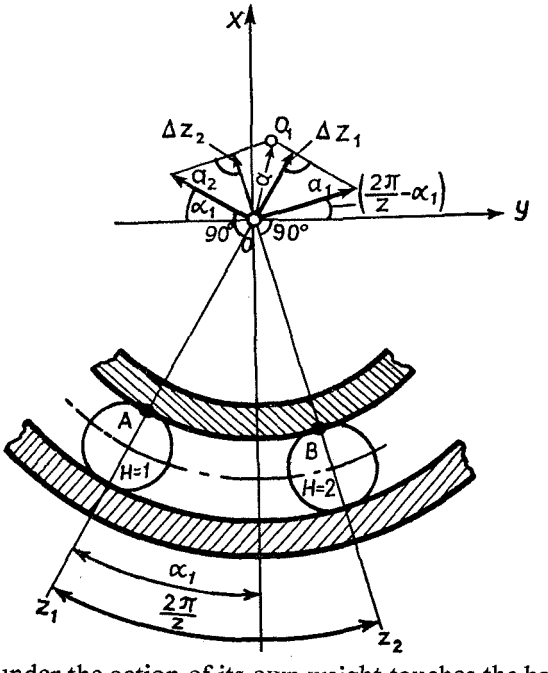

Fig. 1.7. Determination of total errors due to geometric defects.

under the action of its own weight touches the ball only at one point, then the friction torque due to the contact of the rolling bodies with the ball race housing (M_{c_1}) is expressed in the form

$$M_{c_I}=\frac{D^0}{4}\left(1-\frac{d_b^2}{D_0^2}\cos^2\alpha\right)\sin\left[\alpha+\tan^{-1}\left(\frac{d_b\sin\alpha}{2R_r}\right)\right]G_c f_c \qquad (1.23)$$

where G_c is the ball race housing mass;

R_r is the radius of the ball race of the inner ring;

f_c is the friction coefficient of balls about the ball race housing.

The bearing housing is on the rim of the inner or outer ring and hence at the time of operation there appears frictional force as a result of contact of the housing with the guiding edges. Correspondingly the frictional force is reduced or increased depending on the load pressing the housing onto the guide rings. Depending on which ring (outer or inner) the housing rests on, the working formula takes the following form [37]:

$$M^{o}_{c_{II}} = 1.38 \times 10^{-4} G_c f_c n^2 D_{o_e} \varepsilon \left(\frac{D_0 - d_b \cos \alpha}{D_0} \right)^2 ; \tag{1.24}$$

$$M^{i}_{c_{II}} = 1.38 \times 10^{-4} G_c f_c n^2 D_{i_e} \varepsilon \left(\frac{D_0 - d_b \cos \alpha}{D_0} \right)^2 , \tag{1.25}$$

where D_{o_e} is the diameter of the outer edge;

D_{i_e} is the diameter of the inner edge;

ε is the eccentricity of the housing with respect to the bearing axis.

The total M_c is given by

$$M_c = M_{c_I} + M_{c_{II}} . \tag{1.26}$$

The housing is in its most suitable position when it rests on the outer rings: there is an improvement in lubrication in the clearance and the deformation of the housing due to centrifugal forces is reduced [37].

Friction torque due to shear and bleeding of lubricant (M_e): The presence of lubricant between rolling bodies in a bearing leads to additional energy losses due to the viscosity of the lubricant, its physical characteristics, pressure, relative velocity of oil flow, temperature range and design features of the bearing assembly. P.L. Kapitsa developed the hydrodynamic theory of lubricant in rolling [10].

The intermediate layer of oil formed in the bearing prevents direct contact of the rolling bodies, thereby reducing wear and tear and stress in the metal at points of contact and increasing the area of resistance.

Power spent on overcoming friction in the intermediate layer of oil per unit length of a cylindrical roller bearing is given by

$$W^{c}_{o} = \frac{6.5 \cdot v^2 \cdot \mu}{\sqrt{h_0 \cdot \alpha}}, \text{ when } \alpha \, l_2^2 \gg h_0 , \tag{1.27}$$

where $v = \dfrac{\partial x}{\partial t}$ is the longitudinal velocity of the point of contact during the rolling of the cylinder;

μ is the viscosity of the lubricant;

h_0 is the clearance filled with lubricant;

$$\alpha=\frac{1}{2}\left(\frac{1}{R_x}\mp\frac{1}{R_1}\right),$$

here R_x is the radius of curvature of the cylinder surface at point O;

R_1 is the radius of curvature of the rolling surface.

The cylinder cross section with a viscous intermediate layer is shown in Fig. 1.8.

The frictional loss for a ball has the following form:

$$W_o^b\approx\frac{6\pi v^2\cdot\mu\sqrt{\alpha}}{(2\beta/3\alpha)\sqrt{\beta}}\ln\left(\frac{4m^2\beta}{h_0}\right)\text{ for }4m^2\beta\gg h_0, \tag{1.28}$$

where $2m$ is the thickness of the intermediate layer of oil;

$$\alpha=\frac{1}{2}\left(\frac{1}{R_x}\mp\frac{1}{R_1}\right);\qquad \beta=\frac{1}{2}\left(\frac{1}{R_y}\mp\frac{1}{R_2}\right),$$

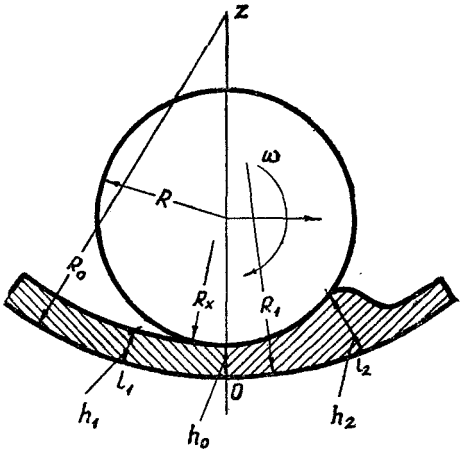

Fig. 1.8. Cross section of cylinder with viscous intermediate layer.

here R_y and R_2 are the radii of curvature perpendicular to the direction of rolling.

Power expended on overcoming friction in this case is sensitive to changes in the values of m and h_0 and has a logarithmic dependence on the thickness of the intermediate layer.

The resistance moment due to lubricant can be approximately expressed in the following way:

$$M_e=z\cdot 2\cdot W_o^b. \tag{1.29}$$

However, we must remember that the losses due to friction along the outer and inner rings during the rolling of a ball will be different.

Friction torque caused by the working medium of the bearing (M_m): The progress of space research made a series of specific demands on the working of roller bearings. In outer space conditions there are many factors that appreciably modify the nature of friction torque: low pressure of the surrounding medium, ionizing radiation, meteorites, absence of gravitation, presence of substances in the state of plasma, etc. [39].

It is well known that under low-pressure conditions surface films evaporate from rolling bodies, as a result of which the friction between filmless surfaces reaches a large value due to strong adhesion and the welding of surfaces. According to the experiments of F. Boyden and D. Taybor [40], when there

is a complete dehydration of samples in a vacuum and at high temperatures (800–900°C) the frictional coefficient increases more than tenfold. To create a protective film under low-pressure conditions it is proposed to utilize helium having low vapor pressure (which can remain in the liquid state for a wide range of temperatures) and good wetting characteristics.

Friction torque caused by temperature increase (M_T)**:** Temperature does not uniformly affect friction torque. With an increase in temperature to 100–120°C friction torque decreases, which is explained by the decrease in the viscosity of the lubricant. An increase in temperature beyond 100–140°C causes an appreciable increase in the constant component of the friction torque as a result of changes in the geometric dimensions of individual components of rolling contact bearings [5].

The housing material affects the change in the resistance moment depending on temperature. This is explained by the unequal effect of temperature on the material. For example, starting from temperatures of 60–70°C a housing made of Maslyanite B-2 gives out liquid phase which leads to a reduction in frictional torque. An analogous picture is observed in the case of bearings with a housing made of Aman-24 and FN-202.

A more accurate dependence for the effect of temperature on friction torque has not been developed.

1.1.3 Analytical Determination of Total Friction Torque in Rolling Contact Bearings

So far we have considered the existing state of the theory of friction torque in roller bearings and its components. However, because of the difficulties these methods are not useful for practical application, nor do they take into account real factors that result in friction torque.

It is occasionally sufficient to determine friction torque approximately when computing less important bearing units.

Let us consider, so far as possible, most of the existing expressions, which in practical work give more accurate values for friction torque in specific concrete conditions. The suggested expressions should not be used for important units and mechanisms where, taking into account the complex process of the appearance of the friction torque, it is necessary to make experimental verification.

The majority of the expressions mentioned contain a well-founded constant friction coefficient varying over large intervals depending on the working conditions, though for approximate computations it is sufficient to use an average value chosen for a particular load and rotational speed n.

Then the friction coefficient f_F for self-aligning ball bearings will equal 0.0010, for cylindrical roller bearings 0.0011, for thrust ball bearings 0.0013, for deep groove ball bearings 0.0015, for tapered and beveled roller bearing

0.0018 and needle roller bearings 0.0045. These coefficients are used by the Swedish firm SKF for computing the friction torque of bearings having an operational life of 10^9 revolutions. Then

$$M = f_F \cdot F \cdot \frac{d}{2}, \tag{1.30}$$

where F is the load on the bearing, kg;

d is the diameter of the bearing clearance, mm.

The coefficient of friction in bearings has been extensively studied by Eshman and also by A. Palmgren.

According to the laws established by G. Amonton and confirmed by S. Coulomb, the friction coefficient is determined by the ratio of effort T to the normal load N

$$f = \frac{T}{N}. \tag{1.31}$$

The friction coefficient is found empirically, taking friction torque in a bearing instead of effort. Friction torque of rolling contact bearings, forming part of the assembly, and also torque due to individual bearings, are determined in different ways by different researchers. According to Palmgren, the torque of running resistance is expressed in the form:

$$M = M_1(F) + M_0(n), \tag{1.32}$$

where

$$M_1(F) = f_1 \cdot F \cdot d_b \left(\frac{F}{C_s}\right)^c,$$

$$M_0(n) = f_0 \, d_b^z \, (\gamma \, . \, n)^{2/3},$$

where f_0, f_1 are the factors depending on bearing design, load and lubrication method;

C is the power index depending on the type of bearing;

γ is the kinematic viscosity;

C_s is the static carrying capacity of the bearing;

d_b is the average diameter;

z is the number of rolling bodies;

F is the load on the bearing;

n is the speed of rotation.

Other researchers determine the torque of running resistance by other methods but Palmgren's formula is considered to be the most dependable and the best. I. Figatner analyzed experimental results using Palmgren's formula and obtained

$$M = m \cdot F + M_s, \tag{1.33}$$

where m is a coefficient;

M_s is the torque component independent of load. The value of the coefficient m according to Palmgren and experimental data are shown in Table 1.1 for $n = 1{,}000$ rpm.

TABLE 1.1

Radial two-row radial spherical ball bearings	2211	2311	1311
Coefficient according to A. Palmgren	0.031	0.025	0.028
Coefficient obtained from experimental data	0.023	0.024	0.021

Considering the large scatter (see Table 1.1) in the value of coefficients of friction m in rolling contact bearings, some researchers either avoid using it altogether in the formula for determination of friction torque or take a value based on their own empirical data.

The torque of running resistance in a bearing for radial loading can be approximately calculated using the empirical formula

$$M = \frac{Q \cdot f \cdot d}{2}, \tag{1.34}$$

where Q is the radial load on one bearing;

f is a transformed friction coefficient, equal to 0.004–0.010 (the coefficient changes depending on size, type and operating conditions of the bearing),

d is the diameter of the bearing clearance.

The expression for the determination of friction torque with the rolling frictional coefficient has the following form [31]:

$$M = 1.4 \cdot Q \cdot \left(\frac{D_0}{d_b} + 1\right) \cdot \delta, \tag{1.35}$$

where D_0 is the diameter of the ball race of the inner ring;

δ is the friction coefficient, equal to $(5\text{–}10) \cdot 10^{-6}$ m.

A more general expression for the approximate determination of friction torque is given in [30]. It is worth pointing out that the coefficient of rolling friction δ in the expression (1.35) lowers the actual friction torque.

When radial loads act

$$M = M_0 + 1.25\, \delta \frac{D_0}{d_b} \cdot R, \tag{1.36}$$

where $M_0 = 0.04\, D_0$.

For a bearing under axial loads only

$$M = M_0 + 1.5 \cdot \delta \frac{D_0}{d_b} \cdot A. \tag{1.37}$$

When both radial and axial loads act simultaneously on a rolling contact bearing,

$$M = M_0 + (1.5\,A + 1.25\,R)\,\delta \cdot \frac{D_0}{d_b}. \tag{1.38}$$

All these expressions give an approximate value of friction torque since they do not take into account the influence of many factors present during the operation of a rolling contact bearing. The following formula for the determination of friction torque, taking into account lubricant, the number of revolutions and other effective factors is given in [26, 38], based on experimental data:

$$M = -\mu \cdot \pi \cdot z \cdot \frac{D_0}{2} \cdot L_F \frac{D_1 \cdot n}{30 \cdot d_b} \left[\frac{4.5\, d_b\, a_0 \left(\frac{d_b\, h_0 + a_0^2}{2\, h_0} \right)}{a_0^2 + h_0 \cdot d_b} + \frac{9 d_b \cdot a_0 \left(\frac{d_b \cdot h_0 + a_0^2}{2\, h_0} \right)}{4\, a^2 + h_0\, d_b} + \left(\frac{15 \left(\frac{d_b}{2} \right)^{3/2}}{2 \sqrt{2\, h_0}} - \frac{9\, a_0^2 \sqrt{\frac{d_b}{2}}}{2\, h_0 \sqrt{2\, h_0}} \right) \times \left(\tan^{-1} \frac{a_0}{\sqrt{h_0\, d_b}} + \tan^{-1} \frac{2\, a_0}{\sqrt{h_0\, d_b}} \right) + 16.5\, a_0 \right], \tag{1.39}$$

where μ is the viscosity of the lubricant;

n is the number of revolutions of the inner ring;

D_1 is the diameter of the ball race of the outer ring;

L_F is a coefficient, depending on the ball race radius of curvature;

a_0 is the length of the hydrodynamic lubricating film;

h_0 is the minimum lubricant thickness.

However, formula (1.39) is not useful for practical applications because it is complicated and because it contains parameters whose determination in actual conditions is not possible (it is possible to compute these parameters only theoretically). Parameters a_0 and h_0 can be found using the hydrodynamic theory of lubricant developed by P.L. Kapitsy.

It is possible to use the following relation [3] as a working formula:

$$M = 0.452 \frac{(1-\xi)(1+\xi)^2}{\xi} D_0^2 \left(0.625 \cdot 10^{-3} \frac{\sigma}{\lambda_K \sqrt{r}} \right)^{6.5} d_b^{-0.65} \cdot z, \tag{1.40}$$

$$\xi = \frac{d_b}{D_0};\ \lambda_K = \frac{1}{1 + \xi \sin \beta};$$

where

β is the contact angle;

D_0 is the pitch circle diameter of balls, mm;

σ is the contact load, usually taken in the range 85–280 kg/mm^2;

r is the radius of ball race.

Formula (1.40) may be used to compute radial-thrust ball bearings working at operating speeds of 50–3,000 rpm.

In modern machinery and assemblies subjected to the influence of vibrations it is important to know and compute the torque of running resistance when the bearing functions under vibration conditions [33]. In this case if the bearing axis is horizontal the friction torque can be computed using the formula

$$M=\mu_b \cdot Q \cdot \frac{d_s}{2}, \tag{1.41}$$

where Q is the radial load on the bearing;

d_s is the diameter of the shaft neck;

$$\mu_b=k\frac{2.8\,(1+\alpha)}{d_s \cdot g}\cdot\frac{D_0}{d}V_m \cdot V_{m\cdot v},$$

where $V_{m\cdot v}$ is the mean relative collision velocity of the inner ring and balls with the outer ring of the bearing;

V_m is the mean frequency of impacts of the inner ring of bearing and balls about the outer bearing ring;

k is the rolling friction coefficient;

d is the ball diameter;

g is the acceleration due to gravity;

α is the coefficient of speed restoration during impact.

In the case of vertical vibration of a bearing with a vertical axis of rotation friction torque has the form

$$M=f_A \cdot Q\frac{d_s}{2}, \tag{1.42}$$

where

$$f_A=\left(\frac{D_r}{d}+\cos\beta\right)\frac{2k\,(1+\alpha)}{f_n\, d_s\, g \sin\beta}\,V_{m\cdot v}\cdot V_m,$$

where D_r is the diameter of the ball race on the inner ring of the bearing;

f_n is the coefficient of nonuniformity of load distribution between balls, $f_n=0.9$ (usually);

β is an angle at which the load acts on the ball.

All these formulas give only an approximate value of friction torque or contain parameters which can be determined only experimentally.

1.2 ANALYTICAL DETERMINATION OF VARIABLE COMPONENT OF FRICTION TORQUE

The friction torque when a ball rolls along the ball race is expressed in the general form by the formula

$$M=\frac{W}{\omega}, \tag{1.43}$$

where ω is the angular velocity of rolling of the ball;

W is the power expended during the rolling of the ball.

The following formula based on the work [10] is obtained for power expended during the rolling of the ball along the ball race, taking into account the contribution of the oil film:

$$W=\frac{17.3\,\pi v^2\,\mu_0\,\sqrt{\alpha}}{(2\beta+3\alpha)\,\sqrt{\beta}}. \tag{1.44}$$

Here the speed v is practically constant, the viscosity μ_0 can be considered independent of pressure and α and β are parameters depending on the radii of curvature of the balls and the ball race:

$$\alpha=\frac{1}{r}\mp\frac{1}{R_{\text{in, ot}}};\quad \beta=\frac{1}{r}+\frac{1}{r_z}. \tag{1.45}$$

For bodies and ball races of ideal geometric form the radii r, $R_{\text{in, ot}}$ and r_z are constants. In actual bearings they are variables.

The geometric errors in ball races can be expressed in terms of a Fourier series [1, 4, 11, 23]. In the case of the ball race of the outer ring the function for errors has the expression

$$\Phi_1(\varphi)=\sum_{k=1}^{m} A_k\cos(k\varphi+\varphi_k), \tag{1.46}$$

and for the ball race of the inner ring

$$\Phi_2(\psi)=\sum_{k=1}^{m} B_k\cos(k\psi+\psi_k), \tag{1.47}$$

where m is the number of harmonics;

A_k, B_k are the amplitudes of the harmonic components;

φ_k, ψ_k is the corresponding phase angle.

The amplitude of the harmonic components is expressed in the form

$$A_k=\sqrt{a_k^2+b_k^2}, \tag{1.48}$$

where

$$a_k=\frac{1}{\pi}\int_0^{2\pi}\Phi_1\cos k\varphi\,dx=\frac{1}{\pi}\sum_{i=1}^{N}\rho_{o_i}\cos ki\,\Delta\varphi\,\Delta x,$$

$$b_k=\frac{1}{\pi}\int_0^{2\pi}\Phi_1\sin k\varphi\,dx=\frac{1}{\pi}\sum_{i=1}^{N}\rho_{o_i}\sin ki\,\Delta\varphi\,\Delta x. \tag{1.49}$$

Here $\Delta\varphi$ is the interval for computing the circle diagram of errors in the ball race. Usually $\Delta\varphi \leqslant 1°$. Phase angles are expressed in the following way:

$$\varphi_k = \tan^{-1}\frac{b_k}{a_k}.$$

It follows that the radius of curvature varies along the length of the ball race. The radius of curvature at a given point is obtained by mathematical analysis:

$$R_{ot}(\varphi) = \frac{\left\{R_{ot} + \sum_{k=1}^{m} A_k \cos(k\varphi + \varphi_k) + \left[\sum_{k=1}^{m} kA_k \sin(k\varphi + \varphi_k)\right]^2\right\}^{3/2}}{R_{ot} + \sum_{k=1}^{m} A_k \cos(k\varphi + \varphi_k) + 2\sum_{k=1}^{m} kA_k \sin(k\varphi + \varphi_k)\Big]^2 + \left[R_{ot} + \sum_{k=1}^{m} A_k \cos(k\varphi + \varphi_k)\right]\left[\sum_{k=1}^{m} k^2 \cos(k\varphi + \varphi_k)\right]}. \quad (1.50)$$

An analogous expression is obtained for the ball race of the inner ring. Consequently with a change in the radius of curvature the geometric coefficients α and β also vary and with them the power loss.

However, analyses carried out for the variable component of friction torque (VFT) according to formulas (1.43) and (1.50) show that the magnitude of this component is negligibly small compared to (VFT), obtained experimentally. Consequently it is not possible to describe (VFT) from this point of view.

The second approach to the description of (VFT) is as follows: Let us assume that the ball rolls between two surfaces (Fig. 1.9). The lower surface differs slightly from a plane surface and is stationary, the upper surface is an ideal, plane surface and moves with velocity v in such a way that at any moment of time any point on it does not change its position along the height (Fig. 1.9 a). For the displacement of the upper plane it is necessary to overcome a certain rolling friction force Q_c. Here the ball will be either in the trough or on the projection. During the rolling of the ball across the projection (Fig. 1.9 b) it is necessary to do work proportional to the magnitude of deformation and the height of the projections. The force Q_c will also change. Here it is assumed that sliding is absent. If the magnitude of the projection depends on its position along the length, then the force Q_c will be a function of time. Further, this model helps explain the effect of lubricating oils of different viscosities on $Q_c(t)$. It is well known that the lubricant forms an oily film, thereby increasing the contact area. In the work [10] it is mentioned that with the increase in viscosity the dimensions of the film of oil increase. Consequently, with an increase in viscosity the amount of work done in-

creases, since the deformation takes place in a larger volume. The force Q_c changes proportionally to the work done. So with an increase in the viscosity of the oil the amplitudes of the variable component of friction torque increase. Besides this, when the viscosity of the oil increases the microsurface roughness affects the variable component of force—the high-frequency components are "cut off". These assumptions tally very well with the results of experiments, showing that with the increase in viscosity high-frequency components of VFT are damped but the amplitudes of lower components are increased.

However, we have no expressions describing the dimensions of the intermediate layer of oil because of the difficulty of obtaining them. Consequently it does not seem possible to use this model (Fig. 1.9).

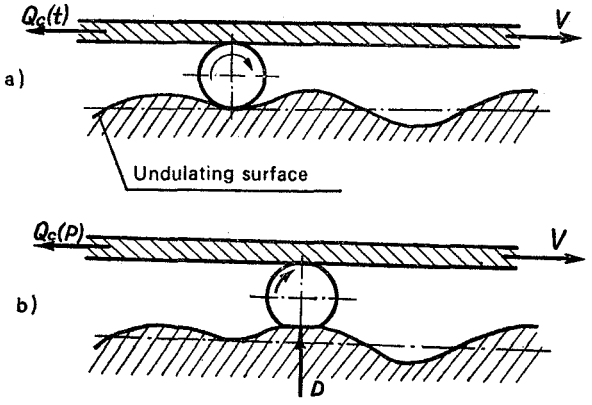

Fig. 1.9. Motion of ball along a wavy surface.

In the model shown in Fig. 1.9 b it may be seen that Q_c (t) can be related to the force developed by the deformation of the projection and acting in the normal direction. The magnitude of the force when the ball approaches the uneven surface depends on the height of the bump and is described by Hertz's theory of "Contact of Elastic Solids" [28]. It is possible to write $Q_c = F(P)$.

Let the friction torque when the ball rolls along the ball race [25] be expressed by

$$M = \left\{ 11.24 \frac{\mu_0}{h_0} a_0^5 b_0 \left[\frac{r_r + 0.5\, d_b}{r_r\, d_b} \right]^2 \frac{e^{n\sigma_0}}{(n\sigma_0)^{3/2}} \times \left[\left(\frac{y}{a_0} \right)^4 - \frac{1}{n\sigma_0} \left(\frac{y}{a_0} \right)^2 + \frac{3}{4\,(n\sigma_0)^{3/2}} \right] \right\} \omega, \tag{1.51}$$

where μ_0 is the dynamic viscosity of the lubricant;

h_0 is the thickness of the lubricating layer;

a_0, b_0 are the major and minor axes of the ellipse of contact (Hertz), respectively;

r_r, d_b are the radius of the ball race and diameter of the ball, respectively;
n is the piezocoefficient of the lubricant;
σ_0 is the maximum stress at the center of the contact area (according to Hertz);
ω is the angular velocity of rolling of the ball.

Expression (1.51) has been obtained on the basis of the solution of the contact hydrodynamic problem. Since the major axis of the contact ellipse is larger than the minor axis by one order of magnitude it is assumed that the lubricant flows only in the direction of rolling (plane contact hydrodynamic problem). The expression given for friction torque has been obtained on the basis of resistance to differential slipping when the ball rolls along the ball race. In this expression the hydrodynamic flow of lubricant, deformation of surfaces and exponential dependence of viscosity on pressure have been assumed. Formula (1.51) is preferred for the case of heavily loaded surfaces.

In the work [16] a nomogram is suggested to solve the contact hydrodynamic problem of determining the thickness of the lubricating layer between rubbing surfaces rolling about each other with slipping. The thickness of the lubricant layer h_0 as a function of total velocity of rolling U_a+U_b of the contact of surfaces, given by the profiles Σ_ρ, viscosity of lubricant μ_0, its piezocoefficient n and linear load K_0, can be directly determined by computing a set of interrelated auxiliary parameters with the help of such nomograms.

The accuracy of determining the thickness of lubricating layer h_0 is insufficient when obtained with the nomogram of a smaller scale but it is very difficult to get the nomogram of a bigger scale. Besides, it is necessary to compute the nondimensional parameters using the respective physical quantities.

Therefore, in order to simplify the computations and to obtain more accurate dependence of the quantity h_0 on a number of basic factors, the following formula is used to determine h_0 [24]:

$$h_{0_{\text{in(ot)}}}=\frac{3\cdot 17\,[\mu_0\,(U_a+U_b)]^{0.75}\,n^{0.6}}{K_0^{0.15}(\Sigma\rho)^{0.45}}. \tag{1.52}$$

Here
$$K_0=\frac{3\sqrt[3]{3}}{8\mu}\sqrt[3]{P^2E(\Sigma\rho)^2};\ \Sigma\rho=\frac{4}{d_b}-\frac{1}{R_{\text{in}}}\pm\frac{1}{R_{\text{in(ot)}}}; \tag{1.53}$$

$$R_{\text{in}}=\frac{0.5\,D_{\text{in}}+r_{\text{in}}}{\cos\beta_{\text{in}}};\ R_{\text{ot}}=\frac{0.5\,D_{\text{in}}-r_{\text{in}}}{\cos\beta_{\text{ot}}}-(r_{\text{in}}-0.5\,d_b)\frac{\cos\beta_{\text{in}}}{\cos\beta_{\text{ot}}}+0.5\,d_b;$$

$$U_a\approx U_b\approx(\omega_{\text{in}}-\omega_0)\,D_{\text{ink}}/2,$$

where U_a, U_b are the relative speeds of surfaces with respect to the contact point;
μ, ν are the coefficients which are functions of elliptic integrals;
P is the normal effort at the contact point;
E is the elastic modulus;

Indices 'in, ot' represent inner and outer rings.

ω_{in} is the angular velocity of the inner ring;

ω_0 is the angular velocity of the center of the ball.

To make it easier to determine friction torque at different loads, after a series of transformations expression (1.51) can be written in the form:

$$M=\left\{\frac{6.11\,\mu_0\,\mathbf{s}^6\,\mu^5\nu}{\mathbf{k}\mathbf{t}^{3/2}}\left(\frac{r_{in}+0.5\,d_b}{r_{in}\,d_b}\right)^2\mathbf{P}^{1.6}\,\mathbf{e}^{3/2\mathbf{t}\,\mathbf{P}\,1/3}\right.$$
$$\left.\times\left[\left(\frac{y_m}{a_0}\right)^4-\frac{2}{3}\,\frac{1}{\mathbf{t}\mathbf{P}^{1/3}}\left(\frac{y_m}{a_0}\right)^2+0.407\,\frac{1}{\mathbf{t}^{3/2}\,\mathbf{P}^{1/2}}\right]\right\}\omega, \tag{1.54}$$

where

$$\mathbf{t}=\frac{n}{\pi\mathbf{s}^2\,\mu\nu};\quad \mathbf{s}=1.08\cdot10^{-3}\,(1/\Sigma\rho)^{1/3};$$
$$\mathbf{k}=\frac{3.48\,\mu^{0.15}\,\mu_0^{0.75}\,(U_a+U_b)^{0.75}\,n^{0.6}}{E^{0.05}\,(\Sigma_\rho)^{0.45}}; \tag{1.55}$$

y_m/a_0 is the relative position of trace of pure rolling;

a_0 is determined using the graph or formula given in [25].

Computations show that the sum of two terms

$$\left(\frac{y_m}{a_0}\right)^4-\frac{2}{3}\,\frac{1}{\mathbf{t}\mathbf{P}^{1/3}}\left(\frac{y_m}{a_0}\right)^2$$

does not exceed 5 percent of the term $0.407\,\frac{1}{\mathbf{t}^{3/2}\,\mathbf{P}^{1/2}}$. Hence we will neglect it in further discussions.

In Fig. 1.10 the dependence of friction torque is shown per unit effort for different viscosities of the oil. From this it can be seen that friction torque even at small sliding velocities sharply increases and can reach astronomical values, which contradicts experiments. This is due to the close dependence of viscosity on pressure: ($\mu=\mu_0\,e^{n\sigma 0}$).

The dependence of $e^{3/2t}$ on the viscosity of the lubricating oil is shown in Fig. 1.11. It can be seen from this that the variation in $e^{3/2t}$ is similar to the variation in friction torque. Consequently the term $e^{3/2t}$, which depends on the piezocoefficient and pressure, according to Hertz, has an important role in the expression for friction torque. Analysis shows that a 20 percent error in the piezocoefficient of the lubricant alters the above-mentioned term several hundred-fold.

From what has been said it follows that the expression developed in [25] is not applicable in this particular case.

In [19] a formula has been obtained for shear stress which takes into account the dependence of the viscosity of the lubricant on pressure by the exponential law and on temperature by the polytropic law:

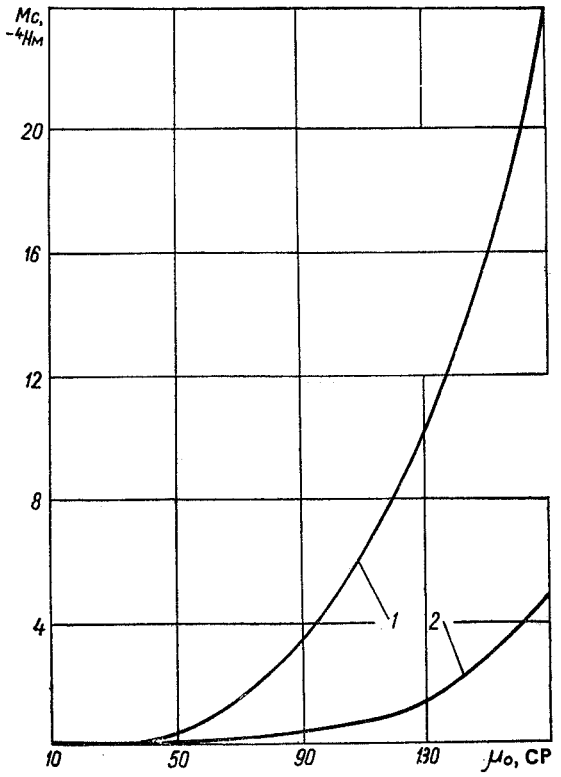

Fig. 1.10. Relation between friction torque and viscosity of lubricant with unit load.

$$\tau=\frac{2\sqrt{427\,\lambda T_s\,\mu_s}}{h_0\sqrt{\gamma}\,\sqrt{k^2\gamma+2-1/(a_1+1)}}\ln$$
$$\times\frac{\sqrt{a_1+1}\,[k^2\gamma+1+\sqrt{k^2\gamma[k^2\gamma+2-1/(a_1+1)]}]}{\sqrt{k^2\gamma+(1+a_1)}}, \qquad (1.56)$$

where

$$k=\frac{(U_a-U_b)\sqrt{\mu_s}}{2\sqrt{427\lambda T_s}};$$

T_s is the temperature of the lubricant at the surface, °C;

μ_s is the viscosity of the lubricant at the given pressure and temperature T_s;

λ is the coefficient of heat conductivity of the lubricant;

γ and a_1 are the coefficients obtained empirically.

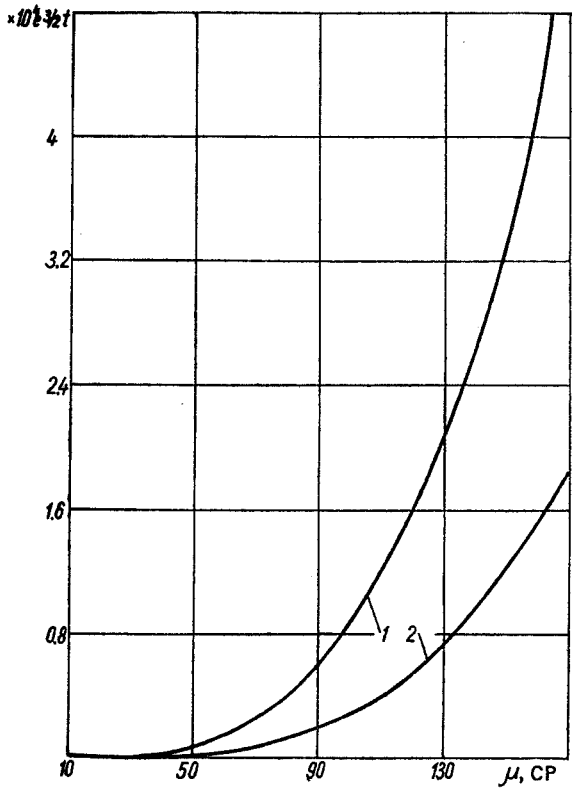

Fig. 1.11. Relation between $e^{3/2t}$ and lubricant viscosity with unit load.

The friction torque due to rolling equals

$$M_K = \int\int_F \tau dF. \tag{1.57}$$

Formula (1.57) is difficult to use due to its complexity.

In [10,19] it has been shown that at low sliding speeds and small loads the shear stress can be computed using the classical formula for the isothermal domain,

$$\tau = \mu_0 \frac{v}{h_0}. \tag{1.58}$$

Let us introduce the following simplifying assumptions:

1) The contact radius of curvature ρ_m (Fig. 1.12) is determined approximately by the formula

$$\rho_m = \frac{r_i d_b}{2r_i + d_b}; \tag{1.59}$$

2) The instantaneous rolling axis ω of the ball relative to the ball race

passes through the trace of "pure" rolling (rolling without slipping) in the plane passing through the axis of the ring and the center of the ball;

3) Since the stress in the contact zone is relatively small it is possible to consider that viscosity does not depend on pressure [10];

4) The area of contact in the outer direction along the axis is assumed to be plane.

According to Fig. 1.12 the distance from any point on the profile of the contact area to the axis of pure rolling ω is

$$z \approx \frac{1}{2\rho_m} y^2. \tag{1.60}$$

The sliding speed at the contact during rolling is

$$v = \frac{1}{2\rho_m} (y_m^2 - y^2)\, \omega. \tag{1.61}$$

Elemental resistance to sliding

$$dT = \mu_0 \frac{v}{h_0} dx\, dy = \frac{\mu_0 (y_m^2 - y^2)}{2\rho_m h_0} dx\, dy. \tag{1.62}$$

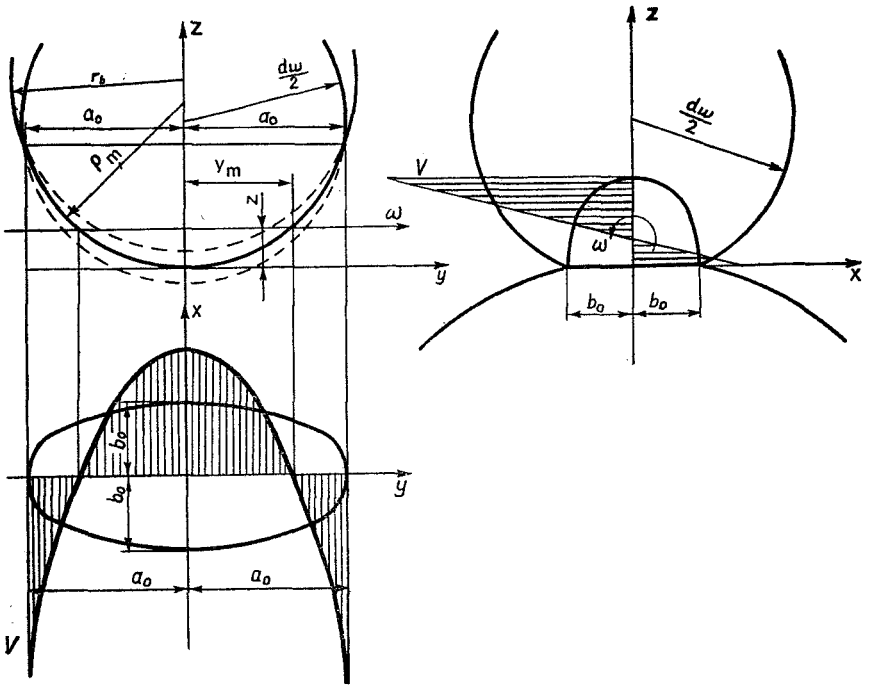

Fig. 1.12. Rolling of ball along raceway for determination of friction torque due to differential sliding.

Elemental friction torque in rolling with slipping:

$$dM=dT(z_m-z)=\frac{\mu_0}{h_0}\frac{\omega}{4\rho_m^2}(y_m^2-y^2)\,dxdy.$$

The friction torque

$$M=4\int_0^{a_0}\int_0^{b_0}dM=\frac{\mu_0\,a_0^5\,b_0}{h_0\rho_m^2}\left(\mathbf{y}_m^4-\frac{2}{3}\,\mathbf{y}_m^2+1/5\right)\omega, \tag{1.63}$$

where $\mathbf{y}_m=\mathbf{y}_m/a_0$, i.e. position of the trace of "pure" rolling.

Calculations show that $\left(\mathbf{y}_m^4-\frac{2}{3}\,\mathbf{y}_m^2\right)$ does not exceed 5 percent of the expression within brackets. Taking this into account, after transformation we get

$$M=\frac{0.8\,\mu_0\,\omega\,\mathbf{s}^6\,\mu^5\,\nu}{\mathbf{k}}\left(\frac{r_{in}+0.5\,d_b}{r_{in}\,d_b}\right)^2 P^{2.1}. \tag{1.64}$$

We will express (1.64) in the form

$$M=CP^{2.1}, \tag{1.65}$$

where C is a constant for the given type and identical geometric sizes of bearings.

Power spent in rotation of the inner ring of the bearing equals

$$N=N_{in}+N_{ot}, \tag{1.66}$$

where N_{in} and N_{ot} is power spent during the rotation of the ball along the raceway of inner and outer rings, respectively.

In order to overcome the resistance to inner ring of the bearing it is necessary to apply a torque

$$M=M_{in}+(M_{in}+M_{ot})\frac{\omega_b}{\omega}, \tag{1.67}$$

where ω_b and ω are angular velocities of the ball and the inner ring of the bearing respectively.

On the basis of the equation (1.64) for one ball it is possible to write

$$M=\left[C_{in}+(C_{in}+C_{ot})\frac{\omega_b}{\omega}\right]P_i^{2.1}, \tag{1.68}$$

for bearing with s balls

$$M=\left[C_{in}+(C_{in}+C_{ot})\frac{\omega_b}{\omega}\right]\sum_{i=1}^{s}P_i^{2.1}. \tag{1.69}$$

Here C_{in} and C_{ot} are constants for the inner and outer rings, respectively.

In order to bring out the variable component in the last expression it is necessary to relate resistance to geometrical errors in raceways of rings.

1.2.1 Determination of the Load Acting on the *i*-th Ball Bearing

In the case of point contact [38]

$$P_i = K\delta_i^{3/2}, \tag{1.70}$$

where P_i is the load acting on the i-th ball;

K is the coefficient depending on the curvature of the contact elements of the bearing at the contact points and on the elastic characteristics of materials from which these elements are made;

δ_i is the elastic convergence of contact bodies.

The deformation in the direction of the i-th ball depends not only on the force due to preliminary tension and due to the displacement of the rotor but also on the geometric errors in the rings [23].

Taking the above into account, the deformation in the direction of the i-th ball in the case of a radial bearing can be expressed in the form

$$\begin{aligned}\delta_i = \delta_0 + x\cos\varphi_i\cos\alpha_0 + y\sin\varphi_i\cos\alpha_0 + z\sin\alpha_0 \\ + \rho_{\text{in}}(\psi_i)\cos\alpha_0 - \rho_{\text{ot}}(\varphi_i)\cos\alpha_0,\end{aligned} \tag{1.71}$$

where x, y, z are displacements of the rotor center in the directions X, Y and Z, obtainable by the equation given in Chapter 3. However, determination of the complete solution of this equation is difficult. For moderate revolutions of the bearing the determination of static displacement of the bearing center is adequate.

The static displacement of the rotor center can be expressed by the equations

$$\begin{aligned} x &= F_1^{\text{ot}}(t) - F_1^{\text{in}}(t), \\ y &= F_2^{\text{ot}}(t) - F_2^{\text{in}}(t), \\ z &= F_3^{\text{ot}}(t) - F_3^{\text{in}}(t). \end{aligned} \tag{1.72}$$

For a radial bearing the radial load in the direction of the ball due to axial preload has the following expression:

$$\begin{aligned}P_{i_0} = K\{\delta_0 + [F_1^{\text{ot}}(t) - F_1^{\text{in}}(t)]\cos\varphi_i\cos\alpha_0 + [F_2^{\text{ot}}(t) - F_2^{\text{in}}(t)]\sin\varphi_i\cos\alpha_0 \\ + [F_3^{\text{ot}}(t) - F_3^{\text{in}}(t)]\sin\alpha_0 + \rho_{\text{in}}(\psi_i)\cos\alpha_0 - \rho_{\text{ot}}(\varphi_i)\cos\alpha_0\}^{3/2}.\end{aligned} \tag{1.73}$$

This formula is valid if the inequality $\delta_0 > \delta_x$ is satisfied, where δ_x is the variable component of deformation. The load acting in the direction of the i-th ball from the radial force is found [36] using the formula

$$P_{ip} = 4.37\frac{P}{s}(\cos\alpha_i)^{2/3}, \tag{1.74}$$

where P is the radial load;

α_i is the angle between the direction of radial load and the position of the i-th ball. In this case α_i coincides with φ_i.

Finally, the total load on the i-th ball, taking into account the prestress and radial load, takes the form

$$P_i = P_{i_0} + P_{i_p}. \tag{1.75}$$

The load computed using formulas (1.73) and (1.75) is made up of both constant and variable components.

1.2.2 Computation and Analysis of Variable Component of Friction Torque

For the bearing C201 the term $\sum_{i=1}^{s} P_i^{2.1}$ from the formula (1.69) can be given in the form

$$\sum_{i=1}^{s} P_i^{2.1} = \sum_{i=1}^{s=7} \left\{ 8.77 \cdot 10^5 \left[\delta_0 + x \cos \alpha_0 \cos \varphi_i + y \cos \alpha_0 \sin \varphi_i + z \sin \alpha_0 \right.\right.$$

$$\left.\left. + \rho_{in}(\psi_i) \cos \alpha_0 - \rho_{ot}(\varphi_i) \cos \alpha_0 \right]^{3/2} + 4.37 \frac{P}{s} (\cos \varphi_i)^{2/3} \right\}^{2.1},$$

where

$$\psi_i = \left\{ \frac{\omega_{in} t + 2\pi\, i/s}{2\pi} \right\};$$

$$\varphi_i = \left\{ \frac{\omega_c t + 2\pi\, i/s}{2\pi} \right\}.$$

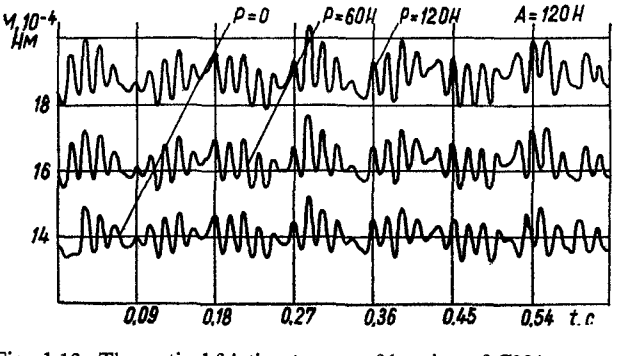

Fig. 1.13. Theoretical friction torque of bearing of C201 type as function of time. Working conditions: speed of rotation—50 rad/sec; viscosity—50 CP; P—90 N.

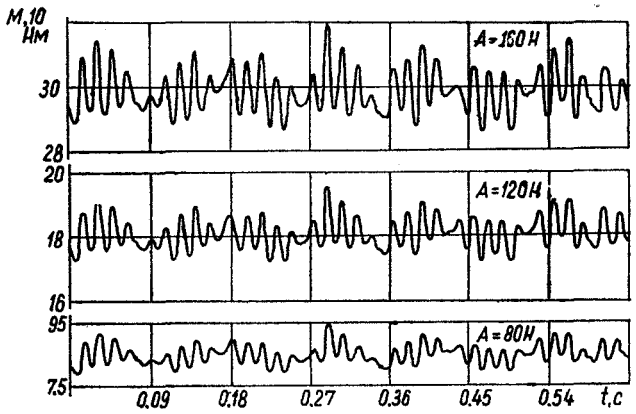

Fig. 1.14. Theoretical friction torque of bearing of C201 type as function of time. Working conditions: speed of rotation—50 rad/sec; Viscosity—50 CP; P—90 N.

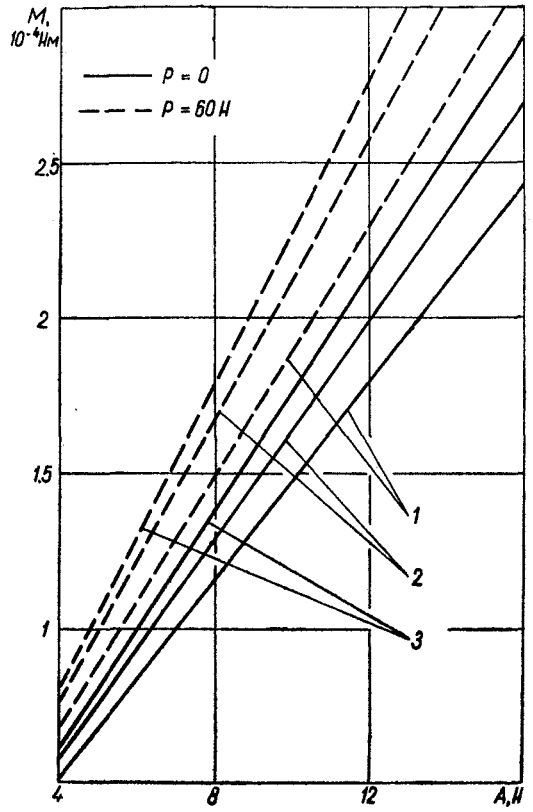

Fig. 1.15. Peak values of VFT in bearing of C201 type as function of axial load. Working conditions: ω=50 rad/sec; *1*—μ=50 CP; *2*—μ=90 CP; *3*—μ=130 CP.

The following are taken as initial data

$$\rho_{in}(\psi), \text{ for } \psi = l\Delta\psi,\ \Delta\psi = 1°,\ l = 1, 2, 3, \ldots 360°;$$
$$\rho_{ot}(\varphi), \text{ for } \varphi = l\Delta\varphi,\ \Delta\varphi = 1°,\ l = 1, 2, 3, \ldots 360°; \tag{1.76}$$

$$x = 0.29\left[\sum_{i=1}^{s} \rho_{ot}(\varphi_i)\cos\varphi_i - \sum_{i=1}^{s} \rho_{in}(\psi_i)\cos\varphi_i\right];$$

$$y = 0.29\left[\sum_{i=1}^{s} \rho_{ot}(\varphi_i)\sin\varphi_i - \sum_{i=1}^{s} \rho_{in}(\psi_i)\sin\varphi_i\right];$$

$$z = 0.14\left[\sum_{i=1}^{s} \rho_{ot}(\varphi_i) - \sum_{i=1}^{s} \rho_{in}(\psi_i)\right].$$

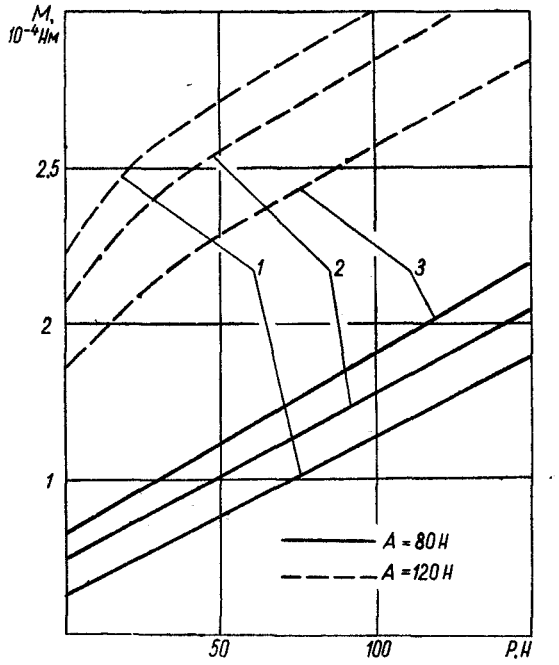

Fig. 1.16. Peak values of VFT in bearing of C201 type as function of radial load. Working conditions: $\omega = 50$ rad/sec; *1*—$\mu = 50$ CP; *2*—$\mu = 90$ CP; *3*—$\mu = 130$ CP.

The deviation from the correct geometric shape of the ball races of rings $\rho_{in}(\psi)$ and $\rho_{ot}(\varphi)$ is obtained with the help of a circular protractor and has the form of a circular diagram. The step size for calculating the deviation on the circular diagram equals 1°. The expression $\sum_{i=1}^{s} P_i^{2.1}$ is a function of time. It is solved on Minsk-22 computer at $\Delta t = 1/128$ sec. Multiplying $\sum_{i=1}^{s} P_i^{2.1}$ by

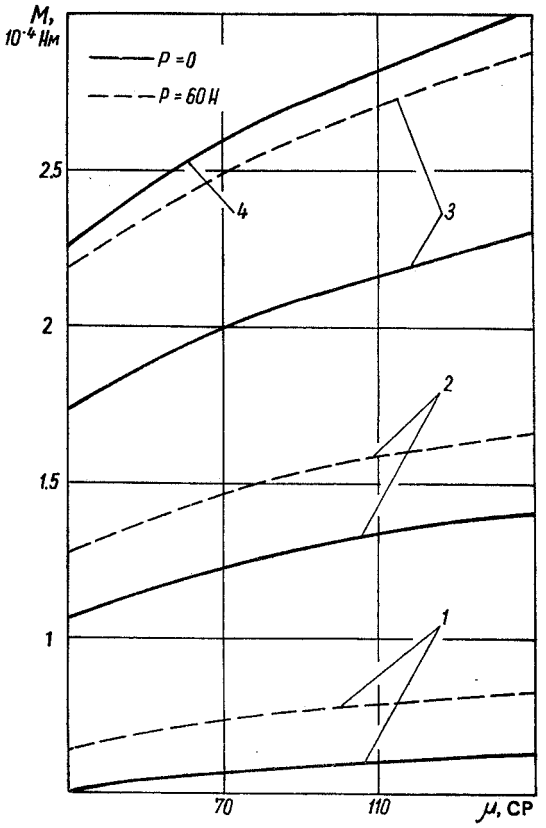

Fig. 1.17. Peak values of VFT as function of viscosity of lubricant:
1—A=40 N; *2*—A=80 N; *3*—A=120 N; *4*—A=160 N.

$\left[C_{in}+(C_{in}+C_{ot})\frac{\omega_b}{\omega}\right]$, we get the variation in the friction torque for the given bearing, lubricant, loads and speed of rotation.

In Figs. 1.13 and 1.14 the variation with time in friction torque is shown for various loads. As can be seen from the graphs, with the increase in radial loads (for constant preloading stresses) the variable and constant components increase appreciably (Fig. 1.13). When there is an increase in the value of preloading stresses the increase of composite forces is more marked (Fig. 1.14).

In Figs. 1.15 and 1.16 the dependence of peak values of VFT on axial and radial loads is shown for different viscosities of lubricant. It should be mentioned that to reduce VFT it is necessary to avoid large loads, especially axial.

The effect of increasing the viscosity of the lubricant is similar to that of

an increase in radial load. With an increase in viscosity the variable component of the torque increases (Figs. 1.17, 1.18). Comparing the dependences (Figs. 1.17, 1.18), we see that the increase in VFT is more sharply expressed where the load is greater (Fig. 1.18). Hence in order to reduce VFT it makes sense to use a lubricant with low viscosity.

In conclusion we may observe that the basic cause of the appearance of VFT is deviation from true of the geometric shapes of ball races. These deviations lead to a variable load (with time), which acts at contact points between the balls and the ball race and on which VFT depends. Changes in the viscosity of the lubricant, loads acting and speed of rotation only increase or weaken the action of geometric errors in the ball race. It follows that it is necessary to find means of eliminating variable components of loads at contacts.

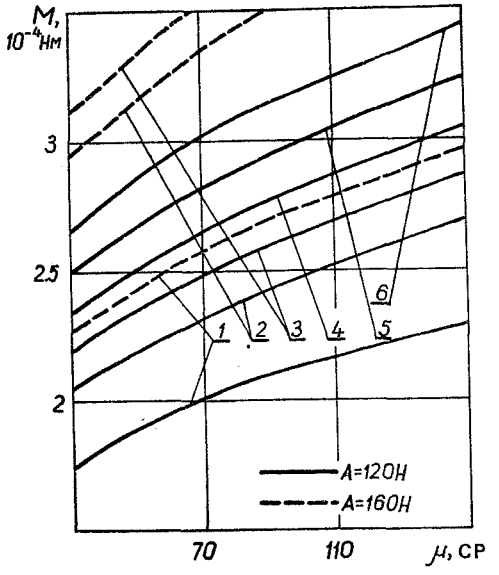

Fig. 1.18. Peak values of VFT as function of viscosity of lubricant: *1*—P=0; *2*—P=30 N; *3*—P=60 N; *4*—P=90 N; *5*—P=120 N; *6*—P=160 N.

1.3 DETERMINATION OF THE FRICTION TORQUE IN BALL-BEARING DUE TO ROLLING FRICTION, TAKING INTO ACCOUNT EXPONENTIAL DEPENDENCE OF VISCOSITY ON PRESSURE

The friction torque when a ball rolls along the ball race with an angular velocity ω is determined by formula (1.43).

Power W used by friction while rolling in the hydrodynamic lubricating film is determined in following way: Let an element of the surface of a ball move with velocity v to the left (Fig. 1.19). Obviously, h at a point $x=x_1$ is a function of time t. On the basis of elementary considerations we find

$$\frac{\partial h}{\partial t}=-v\tan\gamma;\ \tan\gamma=\frac{\partial h}{\partial x}. \tag{1.77}$$

Hence

$$\frac{\partial h}{\partial t}=-v\frac{\partial h}{\partial x}. \tag{1.78}$$

An element of the ball's surface touching the lubricant does an element of work on unit path—$p\,dx\,dy\,\Delta h$. The total work done is

$$F=\iint_S -p\,dx\,dy\frac{\partial h}{\partial t}\,dt.$$

Assuming the expression for the thickness distribution of film $h=h_0+\alpha x^2+\beta y^2$ [10], we determine the power required

$$W=2\alpha v\iint_S px\,dx\,dy, \tag{1.79}$$

where

$$p=-\frac{1}{n}\ln\left[1-\frac{12vn\,\mu_0\sqrt{\alpha}}{(2\beta+3\alpha)\sqrt{h_0^3}}p'\right]. \tag{1.80}$$

Here p' in nondimensional coordinates is expressed in the following way:

$$p'=\frac{\chi}{(1+\eta^2+\chi^2)^2}.$$

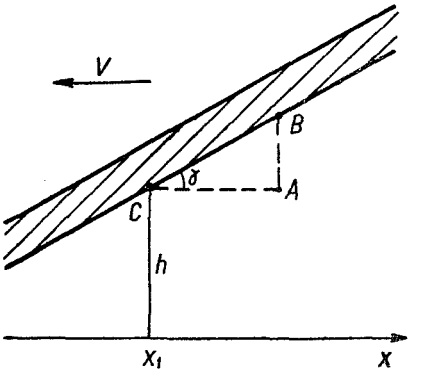

Fig. 1.19. Determination of power losses in lubricant.

In the expression for pressure distribution (1.80) the following exponential dependence of viscosity on pressure is assumed: $\mu=\mu_0 e^{np}$.

For further analysis we introduce the following notations:

$$R=\frac{2v\,h_0^{3/2}}{n\sqrt{\beta}};\ L=\frac{12v\,\mu_0\sqrt{\alpha}\,n}{(2\beta+3\alpha)\sqrt{h_0^3}}. \tag{1.81}$$

After transformation we get

$$W=-R\iint_\Omega x\ln(1-Lp')\,dx\,dy,\ p'=\frac{x}{(1+x^2+y^2)^2}. \tag{1.82}$$

The integration limits are determined by the following values

$$\Omega=\begin{cases}0<x<\infty\\ |y|\leqslant a.\end{cases} \tag{1.83}$$

From equations (1.80) and (1.82) it follows that the solution is meaningful in the interval

$$0<Lp'<1.$$

The function $\ln(1-Lp')$ is expanded in a Taylor series

$$\ln(1-Lp') = -\left(Lp' + \frac{(Lp')^2}{2} + \frac{(Lp')^3}{3} + \ldots + \frac{(Lp')^{\mathbf{n}}}{\mathbf{n}}\right)$$

$$= -\sum_{k=1}^{\infty} \frac{(Lp')^k}{k}. \tag{1.84}$$

Taking into account equations (1.82) and (1.84), where $k=1, 2, 3, \ldots$, the power loss is expressed in the form

$$W(L) = \iint_{\Omega} \sum_{k=1}^{\infty} \frac{R}{k} L^k \frac{x^{k+1}}{(1+x^2+y^2)^{2k}}\, dx\, dy. \tag{1.85}$$

Consider the integral

$$T_{\mathbf{n},\mathbf{m}} = \int_0^{\infty} \frac{x^{\mathbf{n}}}{(x^2+b^2)^{\mathbf{m}}}\, dx, \quad \mathbf{n} \leqslant \mathbf{m}, \quad \begin{matrix}\mathbf{n}=0, 1, 2, \ldots \\ \mathbf{m}=0, 1, 2, \ldots\end{matrix}$$

$$T_{0,0} = \infty;\ T_{0,1} = \pi/2b;\ T_{0,\mathbf{m}} = \frac{(2\mathbf{m}-3)!!\pi}{(2\mathbf{m}-2)!!\, 2b^{2\mathbf{m}-1}};$$

$$\mathbf{m} = 1, 2, 3, \ldots \tag{1.86}$$

$$T_{1,0} = \infty;\ T_{1,1} = \infty;\ T_{1,\mathbf{m}} = \frac{1}{2(\mathbf{m}-1)b^{2(\mathbf{m}-1)}};\ \mathbf{m} = 2, 3, 4, \ldots$$

$$T_{\mathbf{n},\mathbf{m}} = \int_0^{\infty} \frac{x^{\mathbf{n}}}{(x^2+b^2)^{\mathbf{m}}}\, dx = \frac{1}{2(-\mathbf{m}+1)} \left[\frac{x^{\mathbf{n}-1}}{(x^2+b^2)^{\mathbf{m}-1}}\right|_0^{\infty}$$

$$- \int_0^{\infty} \frac{(\mathbf{n}-1)\, x^{\mathbf{n}-2}}{(x^2+b^2)^{\mathbf{m}-1}}\, dx\Bigg].$$

$$\frac{x^{n-1}}{(x^2+b^2)^{\mathbf{m}-1}} \to 0 \text{ for } \mathbf{n} \geqslant 2,\ \mathbf{m} > \mathbf{n},\ 2\mathbf{m} \geqslant \mathbf{n}-1 \text{ and } x \to \infty. \tag{1.87}$$

From (1.87) we get

$$T_{\mathbf{n},\mathbf{m}} = \frac{\mathbf{n}-1}{2(\mathbf{m}-1)}\, T_{(\mathbf{n}-2),\,(\mathbf{m}-1)}. \tag{1.88}$$

Let $n=2k$, then

$$T_{2k,\,\mathbf{m}} = \frac{(2k-1)!!\,(\mathbf{m}-k-1)!}{2^k(\mathbf{m}-1)!}\, T_{0,\,\mathbf{m}-k}; \tag{1.89}$$

$$k = 1, 2, 3, \ldots;\quad \mathbf{m} = 2, 3, 4, \ldots.$$

Let $n=2k-1$, then

$$T_{2k-1,\,\mathbf{m}}=\frac{(2k-2)!!\;(\mathbf{m}-k)!}{2^{k-1}\,(\mathbf{m}-1)!}\,T_{1,\,\mathbf{m}-k+1} \tag{1.90}$$

$$\text{for } k=1,\,2,\,3,\ldots;\quad \mathbf{m}=2,\,3,\,4,\ldots.$$

Hence integrals $T_{\mathbf{n},\mathbf{m}}$ for even and odd $\mathbf{n}$ are expressed by different formulas.

In order to determine the factorials we use Stirling's formula:

$$\mathbf{n}!=\sqrt{2\pi\mathbf{n}}\left(\frac{\mathbf{n}}{e}\right)^{\mathbf{n}}e^{\Theta/12\mathbf{n}}\ \text{for}\ 0<\Theta<1. \tag{1.91}$$

For computations the following expression was used

$$\mathbf{n}!=\sqrt{2\pi\mathbf{n}}\left(\frac{n}{e}\right)^{\mathbf{n}}, \tag{1.92}$$

and the relative error δ was

$$\frac{\delta}{\mathbf{n}}\leqslant\left|\frac{1-e^{\frac{1}{12\mathbf{n}}}}{1}\right|\approx\left|1-\left(1+\frac{1}{12\mathbf{n}}+\frac{1}{(12\,\mathbf{n})^2\cdot 2}+\cdots\right)\right|\approx\frac{1}{12\mathbf{n}}.$$

Hence when $\mathbf{n}=10$ the error does not exceed 1 percent.

Taking this into account, we get

$$T_{\mathbf{n},\mathbf{m}}=\frac{\mathbf{n}!\,(\mathbf{m}-\mathbf{n}/2-1)!}{2^{\mathbf{n}}\,(\mathbf{n}/2)!\,(\mathbf{m}-1)!}\cdot T_{0,m-n/2} \tag{1.93}$$

for $\mathbf{n}=2,\,4,\,6,\ldots,\quad \mathbf{m}=2,\,3,\,4,\ldots;$

$$T_{\mathbf{n},\,\mathbf{m}}=\frac{\left(\frac{\mathbf{n}-1}{2}\right)!\left(\mathbf{m}-\frac{\mathbf{n}+1}{2}\right)!}{(\mathbf{m}-1)}\,T_{1,\,\mathbf{m}-\frac{\mathbf{n}-1}{2}} \tag{1.94}$$

for $\mathbf{n}=1,\,3,\,5,\ldots,\quad \mathbf{m}=2,\,3,\,4,\ldots.$

It is not difficult to show that expression (1.85) converges uniformly relative to k.

Putting $1+y^2=b^2$, we get

$$W(L)=R\sum_{k=1}^{\infty}\frac{2L^k}{k}\int_0^a dy\int_0^{\infty}\frac{x^{k+1}}{(b^2+x^2)^{2k}}\,dx. \tag{1.95}$$

Using (1.86) we get

$$W(L)=2R\sum_{k=1}^{\infty}\frac{L^k}{k}\int_0^a T_{k+1,\,2k}\,dy, \tag{1.96}$$

where

$$T_{k+1,\,2k}=\int_0^{\infty}\frac{x^{k+1}}{[b^2(y)+x^2]^{2k}}\,dx. \tag{1.97}$$

Putting

$$T_{k+1,\,2k}=A_k(y),\ C_k=\int_0^a A_k(y)\,dy,$$

we find

$$W(L)=2R\sum_{k=1}^{\infty}\frac{C_k}{k}L^k. \tag{1.98}$$

From (1.87) we get

$$T_{0,2k-\frac{k+1}{2}}=\frac{(3k-4)!!}{(3k-3)!!}\frac{\pi}{2b^{3k-2}},\quad k=3,5,7,\ldots, \tag{1.99}$$

$$T_{1,2k-\frac{k}{2}}=\frac{1}{(3k-2)}\frac{1}{b^{3k-2}},\quad k=2,4,6,\ldots. \tag{1.100}$$

Finally we have

$$T_{k+1,\,2k}=\begin{cases}\dfrac{\pi}{4}\dfrac{1}{b(y)}, & k=1\\[2ex] \dfrac{k!!\left(2k-\frac{k+1}{2}-1\right)!\,(3k-4)!!\,\pi}{2^{\frac{k+1}{2}}(2k-1)!\,(3k-3)!!\,2}\cdot\dfrac{1}{b^{3k-2}(y)}, & k=3,5,7,\ldots\\[2ex] \dfrac{k!!\left(2k-\frac{k+2}{2}\right)!}{2^{\frac{1}{2}k}(2k-1)!\,(3k-2)}\dfrac{1}{b^{3k-2}(y)}, & k=2,4,6\ldots.\end{cases} \tag{1.101}$$

$$\mathbf{T}_{k+1,\,2k}=\begin{cases}\pi/4, & k=1\\[2ex] \dfrac{k!!\left(\frac{3k-3}{2}\right)!\,(3k-4)!!\,\pi}{2^{\frac{k+1}{2}}(2k-1)!\,(3k-3)!!2}, & k=3,5,7,\ldots\\[2ex] \dfrac{k!!\left(\frac{3k-2}{2}\right)}{2^{\frac{1}{2}k}(2k-1)!\,(3k-2)}, & k=2,4,6,\ldots\end{cases} \tag{1.102}$$

$$A_k(y)=\mathbf{T}_{k+1,\,2k}/\sqrt{(1+y^2)^{3k-2}}. \tag{1.103}$$

Substituting (1.103) in expression (1.97):

$$C_k=\mathbf{T}_{k+1,\,2k}\int_0^a\frac{1}{\sqrt{(1+y^2)^{3k-2}}}\,dy. \tag{1.104}$$

The limits of integration are determined by the boundaries of GMP where

the pressure is zero. Since we do not have the dependence describing the dimension of GMP the limits of integration are taken as the mean value of isobars of pressure in the direction of the y-axis [10]. A few isobars are taken for this purpose with different values of pressure.

Apparently, $a=a\,(p')$ (Fig. 1.20). We will take the following expression as basic [10]:

$$\frac{x}{(1+x^2+y^2)^2}-p'=0\cdot \tag{1.105}$$

The value of a is found in the following way:

$$a\,(p')=\frac{1}{x_2-x_1}\int\limits_{x_1}^{x_2}\sqrt{\sqrt{\frac{x}{p'}}-(1+x^2)}\,dx, \tag{1.106}$$

where x_1 and x_2 are points of intersection of isobars with the x-axis. Values of $a\,(p')$ and C_k were computed for the following values of transformed pressure p': 0.01, 0.001 and 0.0001. For final computations of power losses the value of a is taken as the value corresponding to $p'=0.0001$. It is interesting that in spite of the fact that the values of a are different for different p', the integrals

$$\int\limits_0^a \frac{1}{\sqrt{(1+y^2)^{3k-2}}}\,dy$$

differ very little.

Thus the final expression for determination of power losses due to the rolling of a ball along the ball race, assuming exponential dependence of viscosity on pressure, takes the form

$$W=2R\,(2.4998\,L+0.03276\,L^2+0.002619\,L^3+0.0005112\,L^4+0.00009736\,L^5+0.00002076\,L^6)\cdot \tag{1.107}$$

Here R and L are determined from (1.81).

It is possible to use two terms of the series to compute the power loss in GMP. The error here will constitute not more than 0.5 percent.

The friction torque due to rolling of one ball is expressed in the following form:

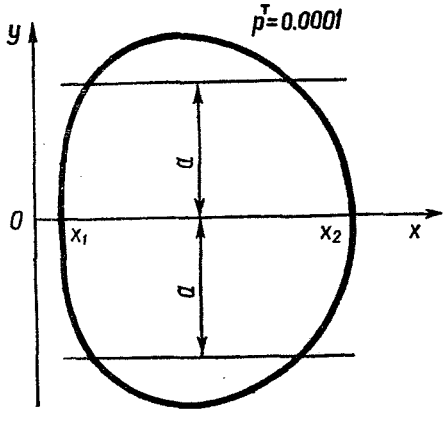

Fig. 1.20. Determination of integration limits perpendicular to rolling of ball.

$$M=\frac{2R}{\omega}(2.4998\,L+0.03276\,L^2), \tag{1.108}$$

where ω is the angular velocity of the ball.

The friction torque of the whole bearing when the inner ring rotates is expressed in the form

$$M=\frac{1}{\omega}\sum_{i=1}^{s}(W_{\mathrm{ot}_i}+W_{\mathrm{in}_i}), \tag{1.109}$$

where s is the number of balls;

W_{in_i}, W_{ot_i} are the power losses due to rolling of the ball along the inner and outer rings, respectively.

Analysis shows that in computing friction torque using formula (1.107) VFT contains all the terms except the first.

Expression (1.109) is recommended for use for computing the components of friction torque of bearings with a higher radius of curvature of the ball race, i.e. when $r>0.515\,d_b$. In such bearings differential slipping is negligible and hence rolling friction has the major role.

References

1. Atctupenas, V.R.V. 1969. Voprosy dynamiki pretsizionnogo zhestkogo rotora v uprugikh podshipnikakh kacheniya (Dynamics of a rigid precision rotor in flexible roller bearings). Avtoreferat Kand. dis., Kaunas.
2. Akhmatov, S.A. 1940. Vliyanie profilya i fiziko-khimcheskikh svoistv truschikhsya poverkhnostei na vid zavisimostei sil treniya ot smazki (Influence of profile and physico-chemical properties of rubbing surfaces on the type of dependence of frictional resistance on lubricant). *Trudy I Vsesoyuznoi konferentsii po treniyu i iznosu.* Moscow, Izd. AN SSSR.
3. Bochkov, V.S. and V.F. Starostin. 1968. Trenie v radialnoupornykh sharikopodshipnikakh (Friction in radial-thrust ball bearings). *Trudy VNIPP*, No. 2 (54).
4. Vitkute, A.E.Yu. 1970. Sluchainye vozmuscheniya i kolebaniya pretsizionnykh sharikonodshipnikov. (Random disturbances and vibration in precision ball bearings). Avtoreferat Kand. dis., Kaunas.
5. Zdanavichyus, V.V.I. and K.M. Ragul'skis. 1971. Issledovanie momenta treniya skorostnyh podshipnikov, rabotayuschikh v vakuume (Study of friction torque in high-speed bearings working in a vacuum). *Nauchnye trudy vuzov Lit. SSR, Vibrotekhnika*, No. 3 (16).
6. Ishlinskii, A.Yu. 1938. Prikladnaya Matematika i Mekhanika (Applied Mathematics and Mechanics). Vol. 2 vyp. 2.

7. Ishlinskii, A.Yu. 1940. Trenie i uznos v mashinakh (Friction and abrasion in machines). *Trudy Vsesoyuzngi konferentsii*, Vol. 2, Moscow, Izd. AN SSSR.
8. Kakuta, K.Zh. 1961. *Nihon kikai gakkoi rombonsyu*, Vol. 27, No. 178.
9. Cameron, A. 1962. Teoriya smazki b inzhenernom dele. (Theory of lubricant in engineering practice). Translation from English by V.K. Zhitomirskii. Moscow, Mashgiz.
10. Kapitsa, P.K. 1955. Gidrodinamicheskaya teoriya smazki pri kachenii (Hydrodynamic theory of lubricant in rolling). *Zhurnal Tekhnicheskoi fiziki*, Vol. 25, vyp. 4.
11. Kasnaukas, Yu.Yu. 1969. K. Voprosu issledovaniya dvizheniya zhestkogo rotora, vraschayuschegosya v Vysokotochnykh predvaritelno natyanutykh podshipnikakh kacheniya (Study of the motion of a rigid rotor turning in high-precision preloaded rolling contact bearings). *Nauchnye trudy vuzov Lit. SSR, Vibrotekhnika*, No. 3 (5).
12. Kovalev, M.P., I.M. Sivokonenko and K.I. Yavlenskii. 1967. Opory priborov (Instrument bearings). Moscow, Mashinostroenie.
13. Kodnir, D.S. and others. 1940. Raschet tolschiny smazochnogo sloya v zubehtykh peredachakh i podshipnikakh kacheniya (Computation of the thickness of the lubricating layer in gear transmission and rolling contact bearings). *Trudy Kuibyshevskogo aviatsionnogo instituta*. vyp. 40.
14. Kodnir, D.S. 1963. K. Voprosu o Metodike Kontaktno-gidrodinami cheskogo rascheta podshipnikov kacheniya i zubchatykh peredach. (Methodology for contact-hydrodynamic computation of rolling contact bearings and gear transmissions). *Trudy Kuibyshevskogo aviatsionnogo instituta*. vyp. 12.
15. Kodnir, D.S. 1963. Kontaktno-gidrodinamicheskaya teoniya smazki (Contact-hydrodynamic theory of lubricant). Kuibyshev.
16. Kodnir, D.S. 1965. Kontaktno-gidrodinamicheskaya teoriya smazki i raschet podshipnikov kacheniya i zubch. peredach. (Contact-hydrodynamic theory of lubricant and computation of rolling contact bearings and gear transmissions). In book *Teoriya treniya i iznosa*. Moscow, Nauka.
17. Kodnir, D.S. 1969. Kontaktno-gidrodinamicheskaya teoryia smazki primenitol'no k detalyam mashin (Contact-hydrodynamic theory of lubricant applied to machine parts). *Trudy Kuibyshevskogo aviatsionnogo in-ta*. vyp. 40.
18. Kodnir, D.S. 1950. Razrabotka metoda eksperimentalnogo i teoreticheskogo issledovaniya podshipnikov zhidkostnogo treniya s tselyu povyshcheniya ikh gruzopodemnosti (Development of empirical and theoretical methods of studying bearings with liquid friction to improve their load-bearing capacity). TsNIITMASh.
19. Kodnir D.S. and L.L. Savvin. 1969. Opredelenie kasatelnykh nagruzok i koeffitsientov troniya dlya poverkhnostei, rabotayuschykh v kontaktno-

gidrodinamicheskom rezhime (Determination of tangential loads and friction coefficients for surfaces operating in a contact-hydrodynamic domain). *Trudy Kuibysherskogo aviatsionnogo in-ta.* vyp. 40.

20. Kostetskii, B.I. 1970. Trenie, smazka i iznos v mashinakh (Friction, lubricant and wear and tear in machines). Kiev, Tekhnika.
21. Kostetskii, B.I. and F.C. Edigoryan. 1964. Klassifikatsiya osnovnykh vidov iznosa i elementy teorii iznosa pri trenii kacheniya (Classification of the basic types of wear and tear and elements of the theory of abrasion due to rolling friction). *Trudy Kievskogo in-ta grazhdanskogo vozdushnogo flota.* vyp. IV.
22. Kragelskii, I.V. 1968. Trenie i iznos (Friction and abrasion). Moscow, Mashinostroenie.
23. Kulvets, A.P. 1970. Voprosy dinamiki zhestkogo rotora, vrashchayuschegosya v pretisizionnykh podshipnikakh kacheniya (Dynamics of a rigid rotor turning in precision rolling contact bearings). Avtoreferat kand. dis., Kaunas.
24. Kurushin, M.I. 1967. K voprosu primeneniya kontaktno-gidrodinamicheskoi teorii smazki dlya analiza kinematiki i teplovydeleniya v radialno-upornom podshipnike (Application of the contact-hydrodynamic theory of lubricant in analysis of the kinematics and heat generation in radial-thrust bearings). In book. *Tezisy doklady yubilennoi nauchno-tekhnicheskoi konferentsii Kuibyshevskogo aviatsionnogo-in-ta.*
25. Kurushin, M.I. and D.S. Kodnir. 1969. Kinematika, napryazheniya i teplovydeleni v radialno-upornykh sharikopodshipnikakh s uchetom vliyaniya smazki (Kinematics, stress and heat generation in radial-thrust ball bearings and the effect of lubricant). *Trudy Kuibyshevskogo aviatsionnogo in-ta.* vyp. 40.
26. Nikitina, I.A. 1957. Eksperimentalnye issledovanie momentov treniya pribornykh sharikopodshipnikov (Empirical study of friction torque in instrument ball bearings). *Optikomekhanicheskaya promyshlennost*, No. 6.
27. Palmgren, A. 1961. O nekotorykh svoistvakh podshipnikov kacheniya (Some characteristics of rolling contact bearings). Geteborg, perevod GPNTB No. 28655.
28. Pinschin, S.V. 1969. Kontaknaya prochnost' i soprotivlenie kacheniyu (Contact strength and resistance to rolling). Moscow, Mashinostroenie.
29. Radionov, E.M. 1964. Momenty, voznikayushchie ot pogreshnosti formy poverkhnostei kacheniya sharikopodshipnikov (Torque due to defects in rolling surfaces of ball bearings). Moscow, Mashinostroenie.
30. Sannikov, K.A. 1948. Raschet usilii i momentov v schetno-reshayushchikh mekhanizmakh. (Computation of loads and torques in calculating machines). Moscow, Oborongiz.
31. Sivokonenko, I.M. 1952. Opory podvizhnykh sistem priborov (Bearings of moving system of instruments). Leningrad, Sudpromgiz.

32. Siwek i Sner. Teoriya podshipnikov kacheniya (Theory of rolling contact bearings). From the course of lectures on rolling contact bearings by the firm SKF.
33. Skorynin, Yu. 1965. V. Nadezhnost'i dolgovechsnost' opor podvizhnykh sistem priborov (Reliability and life of bearings of moving systems of instruments). Minsk, Nauka i tekhnika.
34. Solovev, A.I. 1963. Laboratornyi praktikum po teorii mekhanizmov i detalyam priborov (Laboratory course on the theory of machines and components of instruments). Moscow, Mashgiz.
35. Spitsyn, N.A. and others. 1968. Poteri na trenie v podshipnikakh kacheniya (Losses due to friction in rolling contact bearings). Spetsial'nyi informatsionnyi tsentr podshipnikovoi promyshlennosti. Msocow.
36. Spitsyn, N.A. and others. 1970. Opory osei valov mashin i priborov (Bearings of axles and shafts of machines and instruments). Leningrad, Mashinostroenie.
37. Sprishevskii, A.I. 1969. Podshipniki kacheniya (Rolling contact bearings). Moscow, Mashinostroenie.
38. Tyunina, N.A. 1955. Issledovanie momentov treniya pribornykh sharikovykh podshipnikov (Study of friction torque in instrument ball bearings). Avtoreferat kand. dis. LIGMO.
39. Bawden, F.P. and D. Tabor. 1950. The Friction and Lubrication of Solids. Clarendon Press, Oxford.

2

DETERMINATION OF ELASTIC AND DAMPING CHARACTERISTICS OF ROLLING CONTACT BEARINGS

The elastic characteristics of bearings and their variation in rotation, resulting in parametric excitation, are among the basic causes of the vibrational phenomena that occur during the rotation of a precision rotor in a rolling contact bearing, along with kinematic excitation. It is very difficult to study these characteristics because the rolling contact bearing is a complex mechanical system.

A number of works of Soviet and foreign authors wholly or partly devoted to the study of stiffness and elasto-static equilibrium in rolling contact bearings are well known. In the works of L.Z. Novikov [24–26] expressions have been obtained in a linearized form for axial and radial stiffness of a radial thrust bearing taking into account the nonlinearity of elastic characteristics. A methodology is given for computing the coefficient of proportionality in Hertz's formula [25]. Static equilibrium is considered for the radial thrust bearing without taking lubricant into account [26]. The results obtained are extended to the case of displacement of the inner ring relative to the outer ring in the axial direction toward increasing axial clearance [24].

S.A. Kharlamov [38] analyzes the case of static equilibrium of a radial thrust bearing when the axial load appreciably exceeds the radial load. Simple formulas for the radial, axial and transverse stiffness of the bearing have been obtained for this case by linearizing the equations. The formulas obtained for radial and axial stiffness have been compared with analogous linearized formulas obtained by L.Z. Novikov.

The works of V.S. Bochkov [9–14] comprise the most complete cycle of works devoted to the study of the elasto-static equilibrium of radial thrust ball bearings. The results of the study are valid on the assumption that the system is dynamically stable and all the rollers in the unit take part in transmitting the load. Equality of contact angles and an axial load considerably greater than the radial load are not assumed. Similar problems are highlighted in the works of V.I. Fedorov [37] and E. Meldan [23, 44–46].

In the theoretical work of T. Szucki [52] a procedure has been given for

computation of the elasticity of a ball bearing. 'The load is represented in the form of radial force, axial force and the torque in the plane of these forces. It is assumed that in a mounted bearing, clearance and preload are absent.

M.M. Dombrovska [15] and I.I. Chulkov [39] have contributed to the experimental research on deformations and stiffness of rolling contact bearings. In the work [43] the rigidity of rotating rolling contact bearings has been studied experimentally and the conclusion is drawn that it is independent of rotational speed.

The stiffness of rolling contact bearings for different values of clearance or loads has been studied by E. Wiche [55] and the stiffness of an assembly made up of two radial thrust rolling contact bearings with preloads by K. Karlheinz [42].

The following authors have also contributed to the study of the stiffness of rolling contact bearings: A.S. Saverskii [32], H. Perret [48], J. Scieszko [53], D. Gunther [41], H.H. Schreiber [49, 50].

In all the above-mentioned works the dependence of stiffness on angular rotation of the cage due to changes in the position of the rolling bodies and errors in components have not been taken into account. This theme is mentioned in the theoretical work [54] devoted to the analysis of the static rigidity and kinematic characteristics of bearings with three and four balls and in the work of G. Neubert [47]. Neubert mentions that the change in the stiffness of bearings during rotation depends on the number of rolling bodies in the bearing, load and clearance. It has been shown that for certain values of average stiffness its variation is equal to zero when the radial load is directed onto the rolling body and between rolling bodies. But the amplitude of variation in stiffness even in this case is more than zero.

In the works of V.O. Kononenko and N.P. Plakhtienko [19, 20, 29] a method based on the analysis of motion has been suggested for determination of the characteristics of nonlinear vibrational systems using the method of Krylov-Bogoljubov-Mitropolskii. This method can also be used for the determination of the elastic and damping characteristics of bearings based on the results of the analysis of forced vibrations.

In the present chapter the stiffness of bearings will be considered as a function of the displacement of the moving ring and the turn angle of the cage and formulas will be developed to determine it. The method of determining the elastic and damping characteristics of bearings will be described using the results of vibration tests.

In the first section of this chapter formulas are given for radial, axial and torsional stiffness of ball and roller bearings with the assumption that the components of the bearing are of ideal geometric shape and the rolling bodies are equal in diameter and made of materials with identical mechanical properties. The change in amplitude of the periodic component of stiffness is analyzed. Graphs are plotted for the analytical relations of stiffness, making it possible

to approximate these dependencies for concrete cases by comparatively simple expressions. All this allows a correct estimation of the effect of the nonlinearity of contact elasticity on the stiffness of bearings and the periodic component of stiffness on the change in the position of rolling bodies during rotation which is predominant in precision bearings with a small number of rolling bodies.

In the second section of this chapter the influence of nonuniform sizes, unequal elasticity of the rolling bodies and errors in the geometric shape of raceways on the periodic component of radial stiffness of bearings with preload is considered. It will be shown that the variable stiffness of the rolling bodies in the assembly of a precision bearing can affect the periodic component of stiffness more than their unequal dimensions. In the light of this it is proposed that the rolling bodies of precision bearings be sorted on the basis of stiffness. An automatic apparatus for such sorting is described.

In the third section a methodology is described and formulas are obtained for determination of the elastic and damping characteristics of bearings using the results of vibration tests. This method of determining the elastic and damping characteristics of bearings makes it possible to obtain the most reliable results.

2.1 DETERMINATION OF STATIC STIFFNESS OF ROLLING CONTACT BEARINGS

Radial stiffness of radial bearings. Let us assume that the bearing remains in static equilibrium throughout rotation. According to Hertz's theory of elasticity [7, 28, 31, 35] the total elastic force at the points of contact of the i-th ball with the inner and outer rings is expressed in the following way:

$$P_i = K\,\delta_i^{3/2}, \tag{2.1}$$

where δ_i is the deformation (mutual convergence of rings) in the direction of the i-th ball;

K is the coefficient of proportionality.

Formula (2.1) is also applicable for the case of roller bearings, only the exponential index is 10/9 [40]. Thus the total elastic force at the contact points of rolling bodies with the inner and outer rings can be expressed in the form

$$P_i = K\,\delta_i^n, \tag{2.2}$$

and the projection of this force on the line of action of the applied radial load on the bearing in the form

$$P_i = K\,\delta_i^n \cos\eta_i, \tag{2.3}$$

where n is the index of power for ball bearings ($n=3/2$ and for roller bearings $n=10/9$);

$\eta_i=\varphi+i\gamma$ is the angle between lines of action of radial load (direction of displacement of the moving ring) and the radius passing through the center of the i-th rolling body;

φ is the turning angle of the cage;

γ is the angular distance between rolling bodies; $\gamma=\frac{2\pi}{m}$;

m is the number of rolling bodies in the bearing;

$$i=0, 1, 2, \cdots, m-1.$$

Let us first assume that the bearing elements are ideal in shape, dimensions and material properties. Then the deformation in the direction of i-th rolling body is expressed by the relation

$$\delta_i=g\cos(0.5\,\Theta_{max}\sin\eta_i)+\delta_1+\delta_2\cos(\Theta_{max}\sin\eta_i), \tag{2.4}$$

where g is the radial preload or clearance*;

δ_1 and δ_2 are deformations caused by mutual displacement of rings at the contact points of the rolling body with the inner and outer rings, respectively.

The magnitude of the angle Θ_{max} (Fig. 2.1) is expressed by the formula

$$\Theta_{max}=2\sin^{-1}\frac{z}{d}, \tag{2.5}$$

where d is the diameter of the raceway of the bearing inner ring;

z is the mutual displacement of rings.

For example, a bearing of type 201 with a radial load of 150 N deforms by about 20 μ [15]. Diameter of the inner ring $d=19.22$ mm. Thus

$$\sin\Theta_{max}=2\sin^{-1}\frac{z}{d}=2\,\frac{0.02}{19.22}=0.00208,\ \Theta_{max}\approx 7'.$$

Since Θ_{max} is small it is possible to take it equal to zero. Then the formula (2.3) is transformed into:

$$P_i=K\,[g+x\cos\eta_i+y\sin\eta_i]^n\cos\eta_i, \tag{2.6}$$

where x is the displacement of the moving ring in the direction of the radial load;

y is the displacement of the moving ring in a direction perpendicular to the direction of the radial load.

The restoring force of the complete bearing is equal to the sum of elastic forces of all rolling bodies taking part in the transfer of load:

*Hereinafter the preload in the radial (or axial) direction means the radial (axial) component of the actual total elastic deformation due to preload at points of contact of the rolling body with the rings. When g is negative a preclearance exists.

$$P=\sum_i P_i=K\sum_{i=0}^{m-1}[g+x\cos(\varphi+i\gamma)+y\sin(\varphi+i\gamma)]^n\cos(\varphi+i\gamma). \qquad (2.7)$$

In expression (2.7) only the terms with positive values in the square brackets are summed, since the rolling body does not participate in load transfer when it enters the unloaded zone.

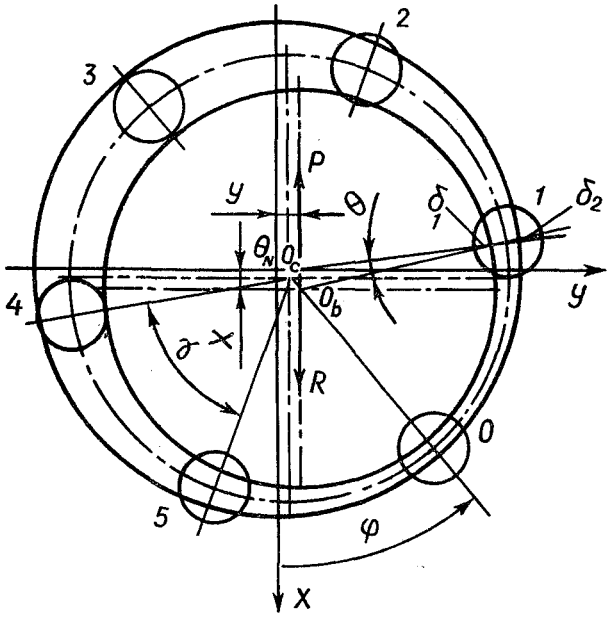

Fig. 2.1. Line diagram of loaded bearing.

For the determination of y we use the condition of zero elastic force of the bearing along axis y for slow rotation:

$$P_y=0. \qquad (2.8)$$

Since

$$P_y=\sum_i P_{yi}=K\sum_{i=0}^{m-1}\delta_i^n\sin\eta_i, \qquad (2.9)$$

where P_{yi} is the projection on the y-axis of the elastic force of the i-th rolling body, the condition (2.8) can be expressed in the following form:

$$K\sum_{i=0}^{m-1}[g+x\cos(\varphi+i\gamma)+y\sin(\varphi+i\gamma)]^n\sin(\varphi+i\gamma)=0. \qquad (2.10)$$

Expanding the expression (2.10) in a McLaurin series in powers of y and limiting it to the first two terms, we get

$$K\sum_{i=0}^{m-1}[g+x\cos(\varphi+i\gamma)]^n\sin(\varphi+i\gamma)$$

$$+y\,Kn\sum_{i=0}^{m-1}[g+x\cos(\varphi+i\gamma)]^{n-1}\sin^2(\varphi+i\gamma)=0. \tag{2.11}$$

Hence to the first order of approximation an expression for y is obtained:

$$y=\frac{\sum_{i=0}^{m-1}[g+x\cos(\varphi+i\gamma)]^n\sin(\varphi+i\gamma)}{n\sum_{i=0}^{m-1}[g+x\cos(\varphi+i\gamma)]^{n-1}\sin^2(\varphi+i\gamma)}\cdot \tag{2.12}$$

The elastic properties of bearings can be conveniently studied by operating on their stiffness determined as the first derivative of restoring force with respect to the displacement:

$$k=\frac{\partial P}{\partial x}\cdot \tag{2.13}$$

Substituting expression (2.7) in equation (2.13), taking into account expression (2.12), we get

$$k=K\sum_{i=0}^{m-1}\left[g+x\cos\eta_i-\frac{A}{Bn}\sin\eta_i\right]^{n-1}$$

$$\times\left\{\cos\eta_i-\frac{CBn-AF(n-1)}{(Bn)^2}\sin\eta_i\right\}\cos\eta_i\,, \tag{2.14}$$

where

$$A=\sum_{i=0}^{m-1}[\mathrm{g}+x\cos\eta_i]^n\,\mathrm{isn}\,\eta_i\,,$$

$$B=\sum_{i=0}^{m-1}[g+x\cos\eta_i]^{n-1}\sin^2\eta_i\,,$$

$$C=\sum_{i=0}^{m-1}[g+x\cos\eta_i]^{n-1}\sin\eta_i\cos\eta_i\,,$$

$$F=\sum_{i=0}^{m-1}[g+x\cos\eta_i]^{n-2}\sin^2\eta_i\cos\eta_i\,. \tag{2.15}$$

Thus the stiffness of each typical size of bearings depends on preload or

clearance g, mutual displacement of rings under the action of load x and angle of turn of cage φ. However, formula (2.14) does not give a clear picture of how k depends on these values and is not useful for direct application. This formula can be used to obtain graphs of functions $k(x)$ and $k(\varphi)$ using the computer for further approximation by simple analytical expressions.

In considering the stiffness of the bearing as a function of $k(x)$, depending on g as a parameter, it is useful to take $\varphi=\gamma/2$. For this position of the cage (radial load is directed exactly between two neighboring rolling bodies) $y=0$, and formula (2.14) is appreciably simplified. The value $y=0$ also corresponds to the value $\varphi=0$ but this position is unstable in a bearing with initial clearance and can be unrealizable in practice.

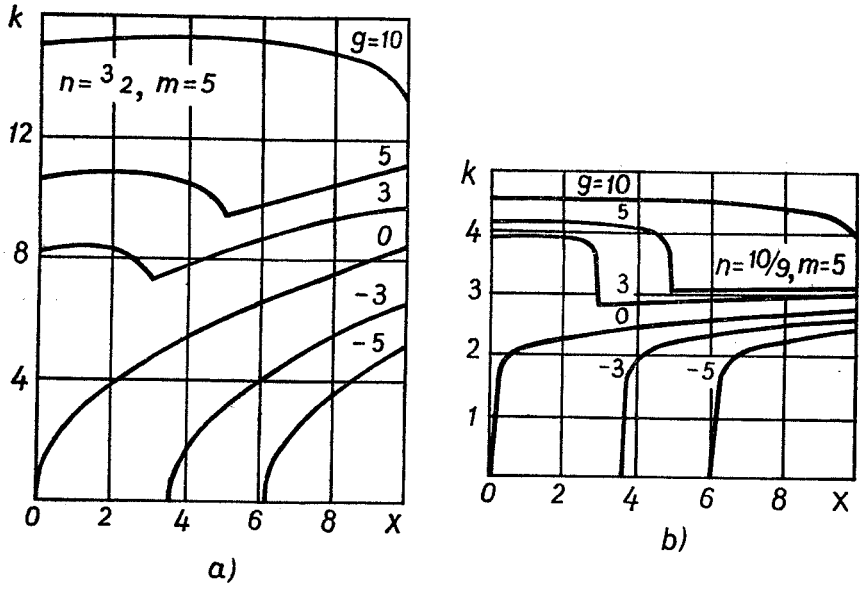

Fig. 2.2. Dependence of radial stiffness of (*a*) ball bearing and (*b*) roller bearing on displacement of moving ring for different values of preloading.

In Fig. 2.2 graphs of function $k(x)$ are shown for $K=1$ and for particular values of g for ball bearing (*a*) and roller bearing (*b*) with six rolling bodies. These graphs can be approximated by simple analytical expressions. For example, for a ball bearing in the case $g>0$

$$k(x)=a-bx^2 \text{ when } |x| \leqslant g, \tag{2.16}$$

$$k(x)=b_1 x^{2/3} \text{ when } |x| > g;$$

when $g=0$

$$k(x)=b_2 x^{2/3}; \tag{2.17}$$

and when $g<0$

$$k(x)=0 \text{ when } |x| < g, \qquad (2.18)$$
$$k(x)=b_3 x^{2/3} \text{ when } |x| > g.$$

The values of coefficients a, b, b_1, b_2 and b_3 can be obtained by substituting in formula (2.14) the values of $y=0$, $\varphi=\gamma/2$ and the corresponding values of x. When $x=0$ we get $k_0=a$, when $x=+g$ the equations $k_g=a-b^2$ and $k_g=b_1 g^{2/3}$, from which we find $b=\frac{k_0-k_g}{g}$, $b_1=k_g g^{2/3}$, etc.

The expression so obtained for stiffness has to be multiplied further by the coefficient K, which takes into account the design and material of the bearing elements. The formulas and methodology for computing the coefficient K are given, for example, in works [25, 30, 36].

Before going onto consider stiffness of a bearing as a function of $k(\varphi)$ let us look at the function $y(\varphi)$. Let us call it the transverse displacements of the moving ring in the radial plane and introduce some clarity regarding the effect of these displacements on the stiffness of radial rolling contact bearings.

The function $y(\varphi)$ when $K=1$, $x=1$ and some values of parameters $\zeta=g/x$, m and n are graphically shown in Fig. 2.3. As can be seen from the graphs, when $\zeta>1$ y varies according to a law which is nearly sinusoidal with period equal to γ. But when $1>\zeta>0$ and especially when $\zeta<0$ the periodic curve of variation in y depending on φ is far from sinusoidal by nature. Here the maximum values of y are obtained for different values of φ, not always in steps of $\gamma/4$.

The maximum value y_{max} of displacement of the center of the moving ring

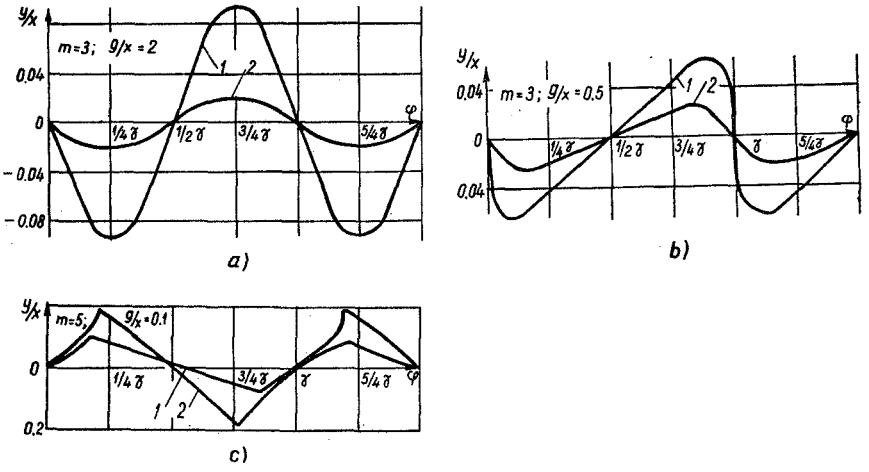

Fig. 2.3. Function $y(\varphi)$ for (*1*) ball bearing and (*2*) roller bearing for certain values of parameters m and $\zeta=g/x$, $x=1$.

along the y-axis is of greatest interest in relation to the effect on the stiffness of bearings. Calculations show that y_{max} depends not only on the number of rolling elements (m) and their geometric shape (n) but also on the ratio of preload or initial clearance and the displacement of the moving ring in the direction of action of the radial load.

In Fig. 2.4 the dependence $Y=y_{max}/x$ on $\xi=g/x$ is shown for some values of m and n. From the graphs it can be seen that Y increases fast with an increase in initial clearance and decreases with an increase in preload and the number of rolling elements. For $\xi>1$, practically $Y=0$. Both the magnitude and sign of Y depend on the value ξ. There are values of ξ for which $Y=0$ even given initial clearance. The values of Y with roller bearings are in general greater than with ball bearings with the same number of rolling elements but for particular values of ξ they could also be smaller, since the extrema of functions $Y(\xi)$ for one and the same m but for different n do not coincide.

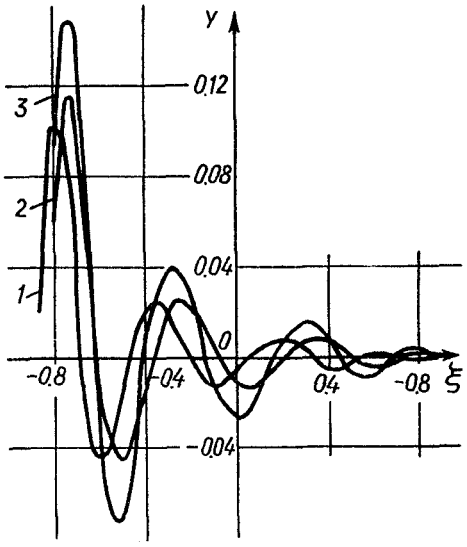

Fig. 2.4. Function $Y(\xi)$ for bearing with (*1*) 12 balls, (*2*) with 11 balls and (*3*) with 11 rollers.

It follows from what has been said that transverse displacements of the moving ring in a radial plane $y(\varphi)$ in bearings with preload should not appreciably affect stiffness. In bearings with initial clearance the effect should be considerable.

Considering the stiffness of the bearing as a function of $k(\varphi)$ depending on g as on a parameter, we take $x=\text{const}$. In Fig. 2.5 a comparison of graphs of function $k(\varphi)$ is given for $K=1$ obtained from formula (2.14) and by the formula

$$k=Kn\sum_{i=0}^{m-1}[g+x\cos(\varphi+i\gamma)]^{n-1}\cos^2(\varphi+i\gamma), \tag{2.19}$$

i.e. assuming $y=0$. From the Figure it can be seen that the consideration of free transverse displacements of the moving ring of the bearing in the radial plane changes the values of k, basically toward reduction. This difference is not great for $x<g$ even for a bearing with three rolling elements, more considerable for $x>g$ and still more when $g<0$. However the values of k when

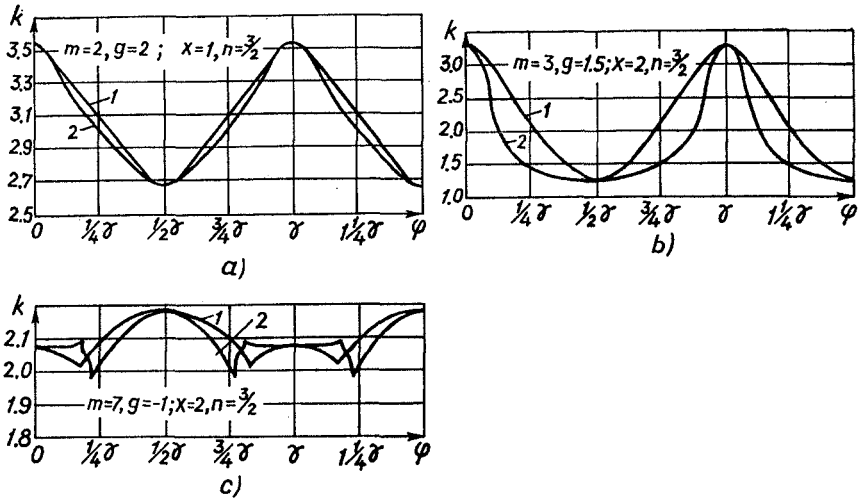

Fig. 2.5. Comparison of curves of k (φ) for $k=1$ (*1*) without taking Y into account and (*2*) taking Y into account: *a*—in bearings with large preload; *b*—with small preload; *c*—with clearance.

$\varphi=0$ and $\varphi=\gamma/2$ always coincide.

In Figs. 2.6 and 2.7 the variation in the difference in stiffness of bearings is shown for $\varphi=0$ and $\varphi=\gamma/2$ as a percentage of its mean value:

$$\varkappa=\frac{k_{\varphi=0}-k_{\varphi=\gamma/2}}{k_{\varphi=0}+k_{\varphi=\gamma/2}}\cdot 2\cdot 100, \tag{2.20}$$

depending on the ratio of radial displacement of the moving ring to the value of preload or initial clearance $\xi=x/g$. Graphs of function $\varkappa$ (ξ) are different for even and odd numbers of rolling elements: for even m graph $\varkappa-\xi$ is symmetric with respect to the $\varkappa$-axis, and for odd m with respect to the origin.

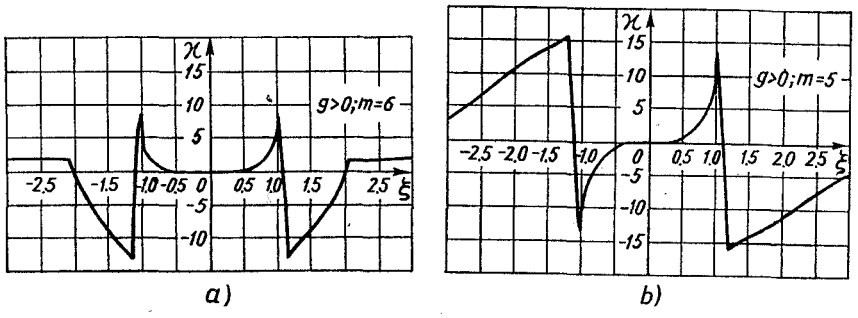

Fig. 2.6. Function $\varkappa$ (ξ) for ball bearings with preload with (*a*) even number of balls and (*b*) odd number of balls.

Figs. 2.8–2.11 show the dependence of the amplitude of variation in stiffness during rotation

$$\varkappa_1 = \frac{k_{max} - k_{min}}{k_{max} + k_{min}} \cdot 2 \cdot 100 \tag{2.21}$$

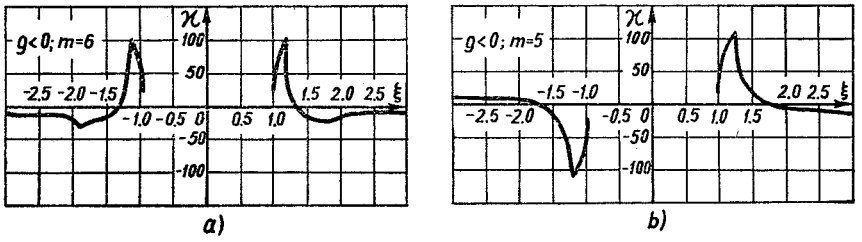

Fig. 2.7. Function $\varkappa(\xi)$ for ball bearings with clearance with (*a*) even and (*b*) odd number of balls.

and $\varkappa$ (2.20) (broken curve) as a percentage of the mean value of k on the ratio of preload or initial clearance to radial displacement of the moving ring $\zeta = g/x$ for ball bearings and roller bearings with the number of rolling elements equal to 3, 4, 5, 6 and 10. For preloaded bearings graphs of functions $\varkappa(\zeta)$ and $\varkappa_1(\zeta)$ coincide but for bearings with initial clearance these graphs coincide only for certain values of ζ and when $m < 5$.

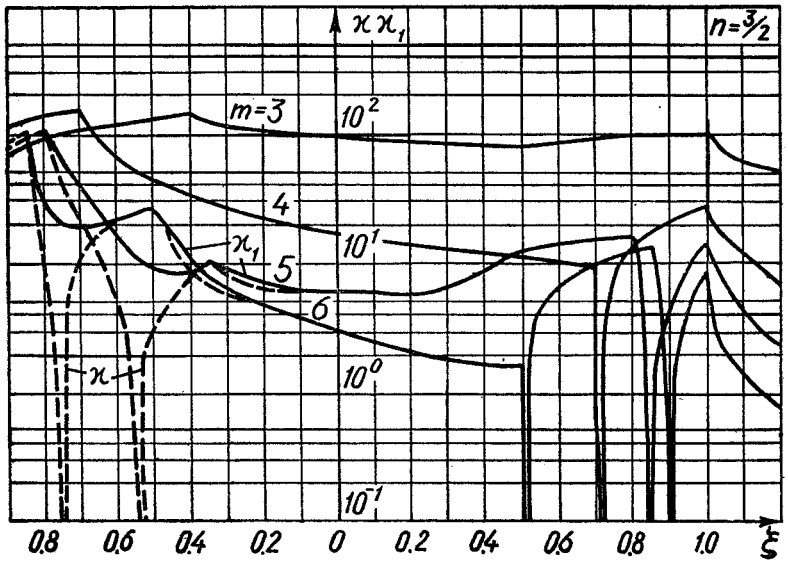

Fig. 2.8. Variation in stiffness during rotation of ball bearings with three, four, five and six rolling elements.

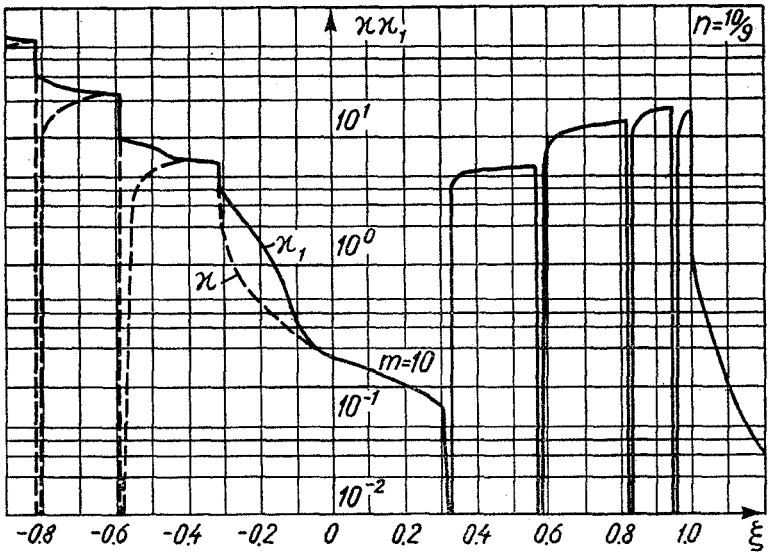

Fig. 2.9. Variation in stiffness during rotation of ball bearings with 10 rolling elements.

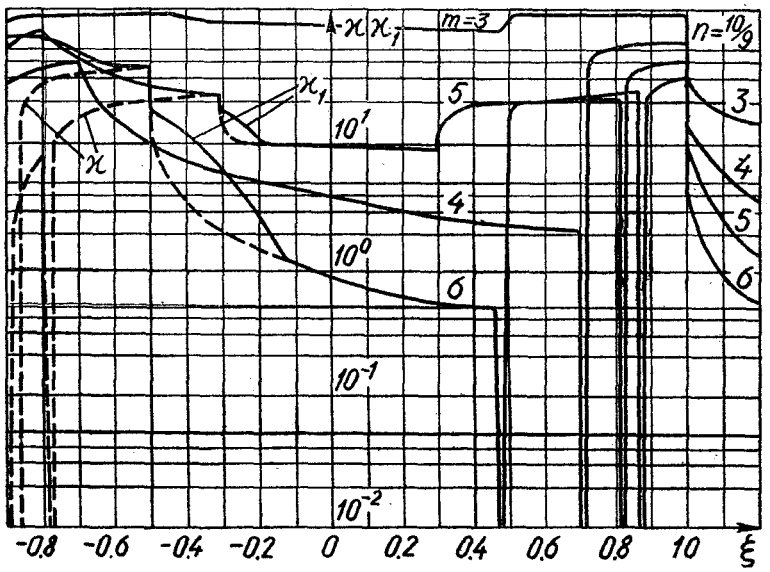

Fig. 2.10. Variation in stiffness during rotation of roller bearings with three, four, five and six rolling elements.

As per the behavior of curves of functions $\varkappa(\zeta)$ and $\varkappa_1(\zeta)$ (Figs. 2.6–2.11), so also according to the graphs of function $k(\varphi)$ (Fig. 2.12), analogous for ball bearings and roller bearings, it is possible to differentiate three basic cases:

1) bearing with large preload ($\zeta > 1$),
2) bearing with small preload ($1 > \zeta > 0$),
3) bearing with initial clearance ($\zeta < 0$ when $x > 0$).

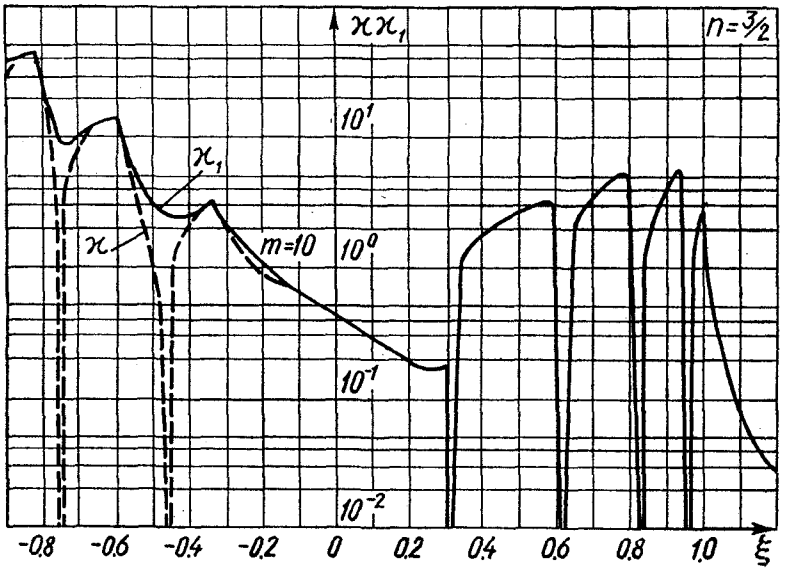

Fig. 2.11. Variation in stiffness during rotation of roller bearings with 10 rolling elements.

Knowing the behavior of the graphs of function $k(\varphi)$ and the order of their variation it is possible to switch over to approximation of the periodic component of stiffness of the bearing as functions of the turn angle of cage φ.

The periodic component of radial stiffness of the bearing with preload in the case $\zeta > 1$, and with a somewhat large error in the case $\zeta > 1$ (Figs. 2.5 and 2.12), can be expressed in the form

$$h \sin(m\varphi + \alpha), \tag{2.22}$$

where $h(\xi)$ is the amplitude of periodic component.

In the case of a bearing with initial clearance the function $k(\varphi)$ can be approximated by the expression

$$k(\varphi) = c + |h_1 \sin(m\varphi + \alpha) + b_4|, \tag{2.23}$$

where c, h_1 and b_4 are functions of the variable depending on g as on a parameter.

Expression (2.23) (Fig. 2.13) approximates with sufficient accuracy the curves of the function $k\ (\varphi)$ according to formula (2.19) and also, in a first approximation, according to formula (2.15) (Fig. 2.5 c). In order to find the

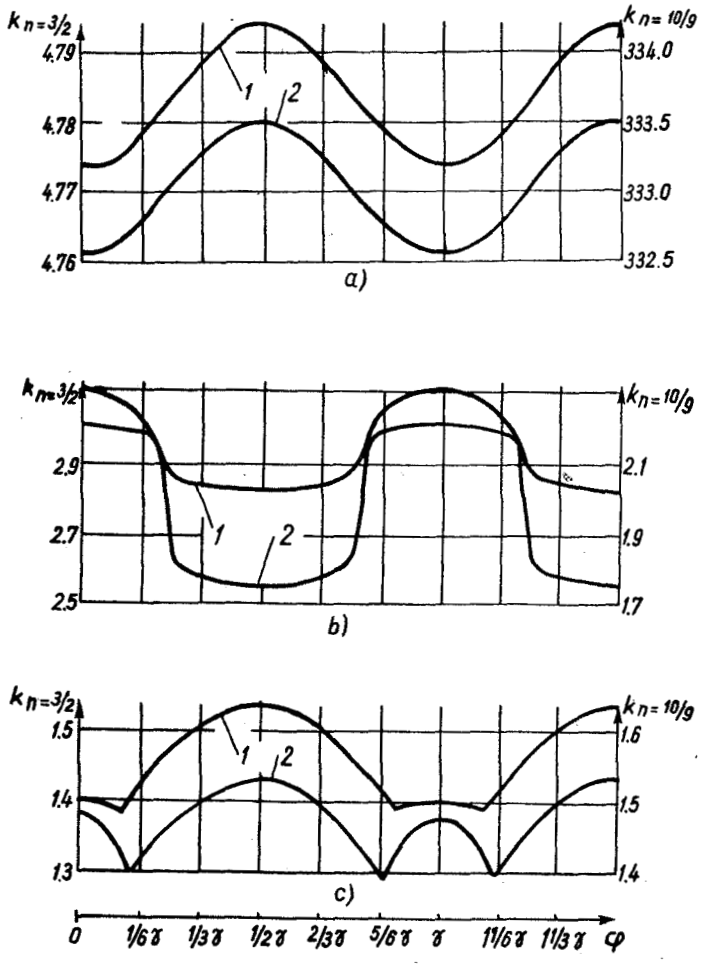

Fig. 2.12. Variation in radial stiffness during rotation of bearing with (*1*) six balls (*2*) rollers; *a*—when $\xi=1.3$; *b*—$\xi=0.7$; *c*—$\xi=0.4$.

approximating expressions of functions h, h_1 and b_4 we use the graphs of functions $\varkappa\ (\xi)$, $\varkappa\ (\zeta)$ and $\varkappa_1\ (\zeta)$. For example, for bearings with preload $h=\varkappa/2$ and for bearings with initial clearance $h_1=\varkappa_1-(\varkappa/2)$, $b_4=(3/2)\,\varkappa-\varkappa_1$, $c=k_m-(\varkappa_1/2)$, where k_m is the mean value of stiffness.

It is worth mentioning that if the angle φ is read from the direction of

action of the load on the rolling element, then the phase angle α in formulas (2.22) and (2.23) can have only two values: $\pi/2$ and $3\pi/2$. When the number of rolling elements in the bearing is even this angle is always constant and for an odd number m there is a jump in the value by π, when the quantity x changes sign.

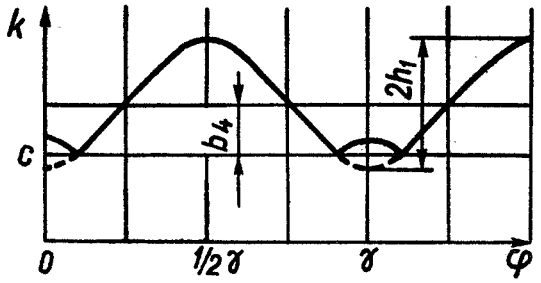

Fig. 2.13. Function $k\ (\varphi)=c+|h_1 \sin\ (m\varphi+\alpha)+b_4|$ when $\gamma=\frac{2\pi}{m}$ and $\alpha=\frac{3}{2}\pi$.

Radial and torsional stiffness of radial thrust bearings: We have been considering the stiffness of radial rolling contact bearings with preload or initial clearance. In practice, however, radial thrust bearings are usually assembled with preload or initial clearance. The formula for radial stiffness of a radial thrust bearing will be developed for the case of a ball bearing. Here let us assume that the contact angle of all balls is identical, i.e. does not depend on radial displacement of the moving ring, and the rotation of the cage remains constant. As is well known [34], the centrifugal forces that appear in the rotation of a cage with balls affect the value of the contact angle. As a result the angle between the balls and the outer ring somewhat decreases and that between the balls and the inner ring increases. However, this phenomenon can be realized in practice only when the inner ring rotates at high speed, at rates of tens and hundreds of thousands of RPM, and is observed only in ball bearings.

Let the outer ring of the bearing remain stationary while fixing the load, and let the inner ring and rolling elements be displaced to the right (Fig. 2.14). The radial clearance of the free bearing g_0 has an effect only on the value of contact angle β. When the ball is displaced from the initial position (the location of the center of the ball is at point O_1) to a position with its center at point O_3 deformation takes place only in the region of displacement of the center O_2, O_3 equal to the axial load g_a. This load corresponds to radial load g and gives the total given contact deformation of the ball resulting from preload:

$$\delta_g=g/\cos\beta. \tag{2.24}$$

The total contact deformation is equal to

$$\delta_1=\delta_g+\delta_{xi}+\delta_{yi}, \tag{2.25}$$

where $\delta_{xi}+\delta_{yi}$ is the deformation of the i-th ball caused by the radial displacement of the inner ring. Thus

$$\delta_i=\frac{g}{\cos\beta}+x\frac{\cos\eta}{\cos\beta}+y\frac{\sin\eta}{\cos\beta}\,. \tag{2.26}$$

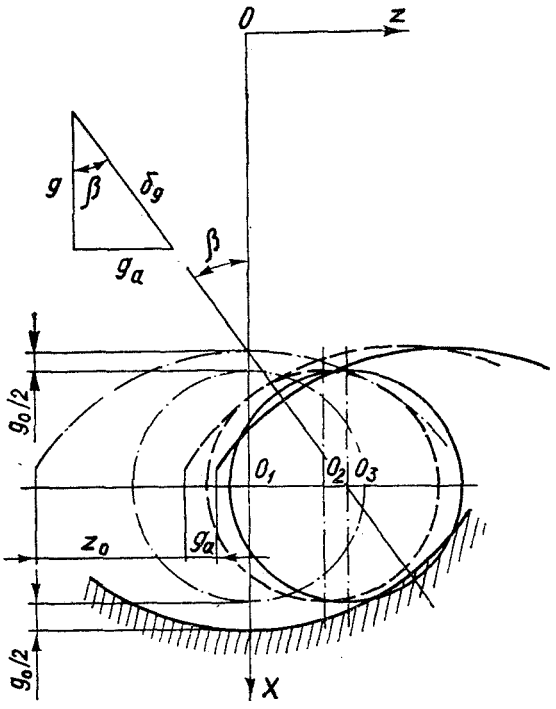

Fig. 2.14. Contact deformation of balls due to axial tension in radial-thrust bearing.

Substituting expression (2.26) in equation (2.2) and adding the projections P_i on the radial plane and on the x-axis, we obtain

$$P=K\sum_{i=0}^{m-1}\left[\frac{g}{\cos\beta}+x\frac{\cos\eta_i}{\cos\beta}+y\frac{\sin\eta_i}{\cos\beta}\right]^n\cos\beta\cos\eta_i. \tag{2.27}$$

Using this, we may determine the radial stiffness of a radial thrust bearing ignoring transverse displacements of the moving ring:

$$k=Kn\cos^{1-n}\beta\sum_{i=0}^{m-1}[g+x\cos(\varphi+i\gamma)]^{n-1}\cos^2(\varphi+i\gamma). \tag{2.28}$$

Comparing expressions (2.28) and (2.19), we see that formula (2.28) is similar to the formula for stiffness for a radial bearing and differs only by the coefficient $\cos^{1-n}\beta$.

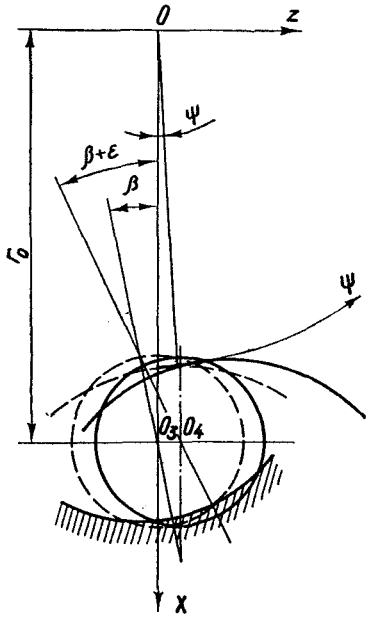

Fig. 2.15. Contact deformation of balls due to mutual twisting of rings in radial-thrust bearings.

Now let torque act in the plane xOz (Fig. 2.15) on a radial thrust ball bearing with preload. As a result there appears a mutual torque of rings through an angle φ. Let us assume that the twist appears only in the plane xOz, and angular free transverse displacement is absent. Then the contact angle of each ball is changed by a value ε_i, depending on ψ and η_i ($\varepsilon_i=\varepsilon\cos\eta_i$):

$$\beta_i=\beta+\varepsilon\cos(\varphi+i\gamma). \qquad (2.29)$$

The angle ε is very small when compared to the angle β and hence it can be neglected. In such a case it is assumed that the contact angle of all balls remains unchanged and equal to β. Then the deformation of the i-th ball caused by the twisting of rings will be expressed by the formula

$$\delta_{\varphi i}=\frac{r_0\sin\varphi\cos(\varphi+i\gamma)}{\sin\beta}. \qquad (2.30)$$

where $r=\frac{d_k+d_b}{2}$, i.e. radius of the circle passing through the centers of balls;

d_k is the diameter of the raceway of the inner ring;

d_b is the ball diameter.

The total contact deformation of the i-th ball is determined by the expression:

$$\delta_i=\frac{g}{\cos\beta}+\frac{r_0\sin\psi\cos(\varphi+i\gamma)}{\sin\beta}. \qquad (2.31)$$

After summing i elastic moments from each rolling element we obtain an expression for elastic torque about the axis y:

$$M=Kr_0\cos^{-n}\beta\sum_{i=0}^{m-1}[g+\sin\psi\, r_0\cot\beta\cos(\varphi+i\gamma)]^n\cos(\varphi+i\gamma). \qquad (2.32)$$

Considering the smallness of angle ψ, it may be presumed that $\sin\psi\approx\psi$. Then the contact hardness of a radially supported bearing is determined from

angle ψ as the first derivative of the elastic moment:

$$k_\psi = Knr_0 \sin^{-1}\beta \cos^{1-n}\beta \sum_{i=0}^{m-1} [g + \psi r_0 \cot\beta \cos(\varphi + i\gamma)]^{n-1} \times \cos^2(\varphi + i\gamma). \quad (2.33)$$

This formula is also analogous to the formula for radial stiffness of a radial bearing (2.19).

Consequently the regularity of the variation in stiffness of a radial bearing is true for radial and torsional stiffness of a radial-thrust bearing. Although formulas (2.28) and (2.33) have been developed for ball bearings they are valid for roller bearings too if we take $n = 10/9$.

Radial stiffness of thrust and radial-thrust bearings. For a thrust bearing, for example, a ball bearing (Fig. 2.16), deformation of the i-th rolling element caused by the displacement of the inner ring in the axial direction with axial preload and mutual twist of rings is determined by the expression

$$\delta_i = g_a + z + r_0 \sin\psi \cos\eta_i \cos\psi, \quad (2.34)$$

where g_a is the axial preload;

z is the displacement of the moving ring in the axial direction.

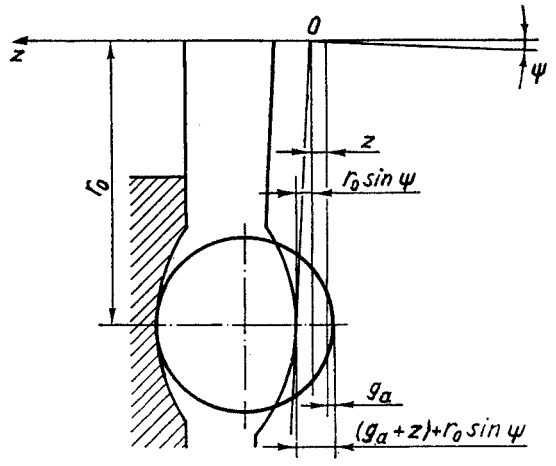

Fig. 2.16. Contact deformation of rolling elements due to displacement of rings in thrust bearing.

Considering the low value of the angle ψ and formula (2.2), the axial load transferred by the whole bearing is expressed by the relation

$$P_a = K \sum_{i=0}^{m-1} [g_a + z + r_0 \psi \cos\eta_i]^n, \quad (2.35)$$

and axial stiffness by the formula

$$k_a=\frac{\partial P}{\partial z}=Kn\sum_{i=0}^{m-1}[g_a+z+r_0\,\psi\cos(\varphi+i\gamma)]^{n-1}. \tag{2.36}$$

In this formula, as in the expressions for rigidity developed so far, $\delta_i<0$ means that the i-th rolling element does not take part in the load transfer and hence the terms in the square brackets whose sign is negative are not summed. If the value of g_a is negative (bearing with initial axial clearance), then for $z+\psi r_0\leqslant|g_a|$ the axial rigidity of the bearing is equal to zero.

For a radial-thrust bearing the deformation of the i-th rolling element comprises

$$\delta_i=g_a+z+r_0\sin\psi\cos\eta_i+\frac{x\cos\eta_i}{\cos\beta_i}, \tag{2.37}$$

and axial load transferred by the bearing is expressed in the form:

$$P_a=K\sum_{i=0}^{m-1}\left[g_a+z+r_0\,\psi\cos\eta_i+\frac{x\cos\eta_i}{\cos\beta}\right]^n\sin\beta. \tag{2.38}$$

In this case it is assumed that for small values of ψ $\sin\psi\approx\psi$ and $\beta_i\approx\beta$.

Differentiating expression (2.38) with respect to z, we get

$$k_a=K\sin\beta\sum_{i=0}^{m-1}\left[g_a+z+\left(r_0\,\psi+\frac{x}{\cos\beta}\right)\cos(\varphi+i\gamma)\right]^{n-1}. \tag{2.39}$$

In the case where $g_a<0$ the axial rigidity of a radial thrust bearing is equal to zero when

$$z+\left(r_0\,\psi+\frac{x}{\cos\beta}\right)\leqslant|g_a|.$$

From formulas (2.36) and (2.39) we find that when there is no radial load or angle of mutual twist of the rings of the bearing, axial stiffness does not depend on the turn angle of the cage if the bearings are mounted ideally and accurately on a perfectly rigid rotor without radial load. If the shaft allows a constant deflection both in magnitude and direction or if the moving ring is skewed or $x\neq0$ the axial rigidity of the bearing varies periodically as it rotates.

Hence in actual conditions axial stiffness of the bearing k_a, like radial or torsional stiffness, depends on the turn angle of the cage φ.

Let us consider another characteristic case. Let the moving ring of the bearing have a twist with respect to the axis of the shaft. Then the deformation of the i-th rolling element is expressed by the formula

$$\delta_i = g_a + z + \left(r_0 \psi + \frac{x \cos \eta_i}{\cos \beta} \right) \cos \eta_i + r_0 \psi_0 \cos q \eta_i, \tag{2.40}$$

and the axial stiffness of the bearing by the formula

$$k_a = K_n \sin \beta \sum_{i=0}^{m-1} \left[g_a + z + \left(r_0 \psi + \frac{x}{\cos \beta} \right) \cos (\varphi + i\gamma) + r_0 \psi_0 \cos q (\varphi + i\gamma) \right]^{n-1}, \tag{2.41}$$

where ψ_0 is the angle of twist of the moving ring with respect to the axis of rotation;

q is a coefficient depending on the relation of rolling element diameters to the circle of their centers.

Since in the general case φq and φ are not repeated values, then here k_a is not a periodic function if simultaneously $\varphi \neq 0$ and $\psi_0 \neq 0$.

In Fig. 2.17 the stiffness of bearings is shown graphically as a function of axial displacement z using formula (2.41) for certain values of the parameters. In Fig. 2.18 the corresponding curves are shown for roller bearings. The axial stiffness more roughly depends on displacement than radial or torsional stiffness and only for roller bearings with a few rolling elements and quite large displacement can this dependence be neglected.

In Fig. 2.19 graphs of axial stiffness are plotted as functions of angular turn of the cage corresponding to formula (2.41) for certain values of parameters. In both cases the function $k_a(\varphi)$ is approximated with a small error by the expression

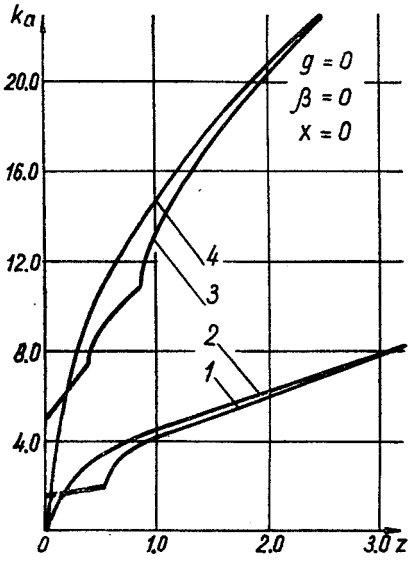

Fig. 2.17. Relation between axial stiffness of ball bearings and axial displacement ($K=1$): *1*—for $m=3$, $r_0 \psi=1$; *2*—for $m=3$, $r_0 \psi=0$; *3*—for $m=10$, $r_0 \psi=1$; *4*—for $m=10$, $r_0 \psi=0$.

$$k_a = k_0 + k_1 \left| \sin (m\varphi + \alpha) \right|, \tag{2.42}$$

where for curve *1* the phase angle $\alpha=0$, and for curve *2*—$\alpha=\pi/2$. The value of the phase angle in general depends on the ratio (g_a+z) to $(r_0 \psi)$ or to $(r_0 \psi_0)$.

Fig. 2.20 illustrates the varying difference between the axial stiffness of ball and roller bearings with three rolling elements for $\varphi=0$ and $\varphi_2=\gamma/2$ as a percentage of the mean value:

$$\varkappa=\frac{k_{a\,(\varphi=0)}-k_{a\,(\varphi=\gamma/2)}}{k_{a\,(\varphi=0)}+k_{a\,(\varphi=\gamma/2)}}\cdot 2\cdot 100 \tag{2.43}$$

depending on the ratio $\xi_a=\frac{r_0\,\psi}{g_a}$ for certain values of parameters. Similar graphs can be approximated, for example, by functions which are linear in part.

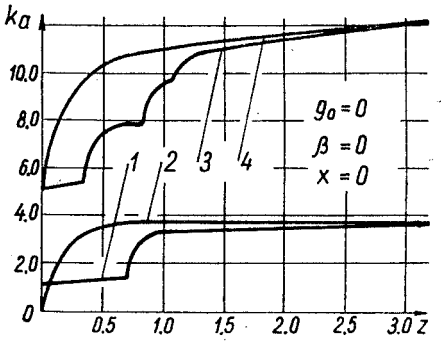

Fig. 2.18. Relation between axial stiffness of roller bearings and axial displacement ($K=1$): *1*—for $m=3$, $r_0\psi=1$; *2*—for $m=3$, $r_0\,\psi=0$; *3*—for $m=10$, $r_0\,\psi=1$; *4*—for $m=10$, $r_0\psi=0$.

The above methodology makes it possible to develop formulas for the stiffness of bearings, corresponding to any one coordinate and taking into account the dependence of stiffness on other coordinates. As an example we will give a formula for the radial stiffness of a radial thrust bearing, corresponding to the x coordinate and taking into account the dependence of k_x on all other independent coordinates (except the rotation of the moving ring

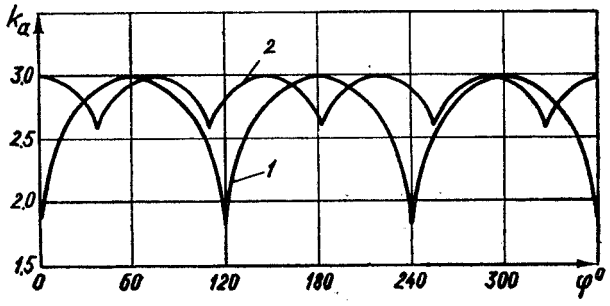

Fig. 2.19. Function $k_a\,(\varphi)$ for $K=1$, $g_a+z=3$, $m=3$; $q=1.64$: *1*—for ball bearings with $r_0\,\psi=1$; $r_0\,\psi_0=0$; $x=0$; *2*—for ball bearings with $r_0\psi=0$; $r_0\psi_0=0.5$; $x=0$.

around its own axis, since in this direction stiffness is equal to zero):

$$k=K_n\sum_{i=0}^{m-1}[\cos^{-1}\beta\,(g+x\cos\eta_i+y\sin\eta_i)+\sin^{-1}\beta\,(\psi\,r_0\cos\eta_i+\chi\,r_0\sin\eta_i+z)]^{n-1}\cos^2\eta_i, \tag{2.44}$$

where χ is the angle of rotation of the moving ring around the x-axis.

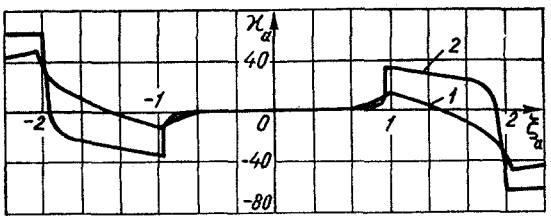

Fig. 2.20. Function $\varkappa_a$ (ξ_a) for (*1*) ball bearing (*2*) roller bearing with three rolling elements.

2.2 ERRORS IN MANUFACTURE AND THEIR EFFECT ON THE STIFFNESS OF ROLLING CONTACT BEARINGS

Although the components of precision rolling contact bearings can be manufactured with high accuracy, certain errors in the geometric shape and dimensions and deviation in the properties of the material are unavoidable. These errors basically have an effect only on the periodic component of stiffness. As shown in the previous section, even in ideal bearings the amplitude of the periodic component of stiffness is considerable in the case of initial clearance. Hence the effect of errors is considered only for the case of preloaded bearings when the change in stiffness caused by imperfections of geometric shape and the characteristics and sizes of components outdo the change in stiffness in ideal bearings.

Let us confine ourselves to consideration of the unevenness of raceways and the variable dimensions and variable elasticity of rolling elements. Unevenness of the rollers of roller bearings can also be taken into account without special difficulties. As far as errors in the geometric shape of the balls are concerned it is difficult to take them into account because the axis of rotation of a ball changes during operation of the bearing.

Formula for the radial stiffness of a rolling contact bearing including errors in components. During the rotation of a bearing the rolling elements roll along the raceways of the outer and inner rings and hence their contact points continuously change. In the case of an ideal bearing this condition has no significance. In actual bearings, the rolling elements are either climbing over bumps or entering troughs while rolling along the raceway and the mutual position of the unevenness of the outer and inner rings changes continuously.

At the initial moment of time let the ball (or roller) be in contact with point *1* (Fig. 2.21) of the stationary outer ring and with point *2* of the inner ring rotating in an anticlockwise direction. After a time t point *2* moves away from the stationary point *1* by an angle $\omega_{in}\, t$, where ω_{in} is the angular velocity of the inner ring. The ball is displaced during this time in the same direction

by an angle ωt, where $\omega t < \omega_{in} t$ since the angular velocity of the cage ω is less than ω_{in}. Then the rings make contact with the ball at points $1'$ and $2'$. This means that the point of contact of the ball with the outer ring moved along the profile of the ring in an anticlockwise direction through an angular distance ωt, and the point of contact of the ball with the inner ring moved in a clockwise direction through a distance $\omega_{in} t - \omega t = (\omega_{in} - \omega)t$, or $q\omega t$, if $q = \frac{\omega_{in}}{\omega} - 1$.

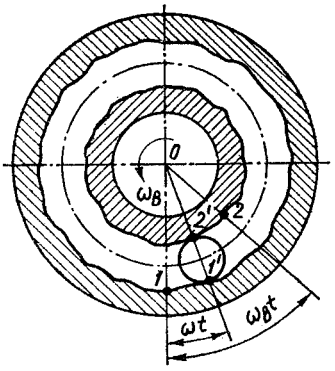

Fig. 2.21. Displacement of contact points of outer and inner rings of bearing with same rolling element during rotation of inner ring.

So during the rotation of the cage through an angle $\omega t = \varphi$ the contact point between the stationary ring and the ball moves through an angular distance φ and the contact point of the inner ring with the ball through a distance $q\varphi$. For the i-th rolling element these angular distances can be written respectively in the form $\varphi + i\gamma$ and $q\varphi + i\gamma$, where γ and i are the same as in the previous section.

It is possible to consider the raceway as a circle with a variable radius. Since its graph is a closed curve this function is periodic and can be expanded in a Fourier series [18]. Taking the above into account the profile of the raceway of the outer ring can be written in the form

$$R_0 + \sum_l \Delta R_l \sin\{l(\varphi + i\gamma) + \alpha_l\}, \tag{2.45}$$

and the profile of the raceway of the inner ring, along which the ball rolls simultaneously, in the form

$$r + \sum_p \Delta r_p \sin\{p(q\varphi + i\gamma) + x_p\}. \tag{2.46}$$

Here R_0 and r_0 are the constant components of the radii of the raceways of the outer and inner rings respectively;

l and p are the order of the harmonic of unevenness in the raceways of the outer and inner rings respectively;

ΔR_l and Δr_p are the amplitudes of these harmonics;

α_l and α_p are the phase angles.

Let us determine the limits of the summation of the series (2.45) and (2.46). Obviously it is meaningful to take the upper limit as infinity, since for suffi-

ciently large values of l and p unevenness of raceways is covered by the contact area and stops affecting periodic component of stiffness. Besides, the upper limit of the quantities l and p (we will call it s) cannot be found rigorously and uniquely since it depends on the value of preload, mutual displacement of rings, mechanical properties of the materials of the components and other factors. The lower limit in the expression (2.46) is equal to unity since without exception all lower harmonics of errors in raceways of a rotating ring affect the change in contact deformation during rotation under the condition of $x=$constant. It is impossible to say this about the stationary outer ring. The first harmonic of unevenness is caused by eccentricity which does not affect the change in contact deformation since the bearing is automatically centered in the inner ring. If due to design or some other factor the center of the outer ring still does not coincide with the center of rotation of the inner ring this misalignment is taken as the value of x in the formula (2.47). Thus the lower limit of summation in the series (2.45) or minimum value of l should be taken equal to two but the minimum value of p in the series (2.46) as equal to unity.

Let the value of radial displacement x of the inner ring with respect to the outer remain constant during the rotation of the bearing. Then the total contact deformation at places where the rings rub against the rolling elements is determined by the expression

$$\delta_i=\Big[g_i+(x_1+x_0)\cos(\varphi+i\gamma)+(y_1+y_0)\sin(\varphi+i\gamma)+\sum_{l=2}^{s}\Delta R_l \times \sin\{l(\varphi+i\gamma)+\alpha_l\}+\sum_{p=1}\Delta r_p \sin\{p(q\varphi+i\gamma)+\alpha_p\}\Big], \qquad (2.47)$$

where $g_i=g+\Delta D_i$,

ΔD_i is the deviation of the actual diameter of the i-th rolling element from the normal;

x_1 is the mutual displacement of rings in the direction x under the action of radial load;

x_0 is the mutual displacement of rings in the direction x for zero radial load;

y_1 is the mutual displacement of rings in the direction y under the action of radial load in an ideal bearing;

y_0 is the mutual displacement of rings in the direction y for zero radial load $x_0=x-x_1$.

Substituting the expression for total contact deformation (2.47) in equation (2.3) and summing with respect to i, we get the formula for radial elastic force for the entire bearing:

$$P=\sum_{i=0}^{m-1} K_i\Big[\, g_i+(x_1+x_0)\cos(\varphi+i\gamma)+y_0\sin(\varphi+i\gamma)$$
$$+\sum_{l=2}^{s}\Delta R_l\sin\{l(\varphi+i\gamma+\alpha_1\}$$
$$+\sum_{p=1}^{s}\Delta r_p\sin\{p(q\varphi+i\gamma)+\alpha_p\}\Big]^n\cos(\varphi+i\gamma), \tag{2.48}$$

where K_i is the coefficient of proportionality in formulas (2.1) and (2.2), in this case different for contacts of rolling elements with rings. Its value, except for a number of geometric parameters, depends on the mechanical properties of the material of the rolling elements and the rings of the bearing, namely, on the modulus of elasticity E and Poisson's ratio Σ.

So other things being equal, coefficient K for the contact of each rolling element with the rings depends on the quantities E and Σ of the material of this rolling element. It can be used to describe the difference in the mechanical properties of the material of the rolling element. In expression (2.48) usually $y_1=0$, because only a bearing with preload is being considered, when the values of y_1 are small and only slightly affect stiffness (see Figs. 2.3, 2.4 and 2.5).

Values x_0 and y_0 are determined from the condition that the projections of the elastic force of the complete bearing on the axes x and y are equal to zero (in the absence of radial load):

$$P=0,\ P_y=0. \tag{2.49}$$

In this case $x_1=0$, $y_1=0$ and the condition (2.49) takes the form:

$$P_y=\sum_{i=0}^{m-1} K_i\Big[\, g_i+x_0\cos(\varphi+i\gamma)+y_0\sin(\varphi+i\gamma)$$
$$+\sum_{l=2}^{s}\Delta R_l\sin\{l(\varphi+i\gamma)+\alpha_l\}$$
$$+\sum_{p=1}^{s}\Delta r_p\sin\{p(q\varphi+i\gamma)+\alpha_p\}\Big]^n\sin(\varphi+i\gamma),$$

$$P=\sum_{i=0}^{m-1} K_i\Big[\, g_i+x_0\cos(\varphi+i\gamma)+y_0\sin(\varphi+i\gamma)$$

$$+\sum_{l=2}^{s}\Delta R_l \sin\{l(\varphi+i\gamma)+\alpha_l\}$$

$$+\sum_{p=1}^{s}\Delta r_p \sin\{p(q\varphi+i\gamma)+\alpha_p\}\Big]^n \cos(\varphi+i\gamma). \tag{2.50}$$

By expanding expression (2.50) in a McLaurin series in powers of x_0 and y_0 and limiting the terms containing x_0 and y_0 to the zeroth and first order we get

$$\left.\begin{aligned} A+Bn\,y_0+Cn\,x_0=0\\ B+Cn\,y_0+En\,x_0=0\end{aligned}\right\}, \tag{2.51}$$

where

$$A=\sum_{i=0}^{m-1}K_i\Big[g_i+\sum_l+\sum_p\Big]^n \sin\eta_i,$$

$$B=\sum_{i=0}^{m-1}K_i\Big[g_i+\sum_l+\sum_p\Big]^n \sin^2\eta_i,$$

$$C=\sum_{i=0}^{m-1}K_i\Big[g_i+\sum_l+\sum_p\Big]^{n-1} \sin\eta_i\cos\eta_i,$$

$$D=\sum_{i=0}^{m-1}K_i\Big[g_i+\sum_l+\sum_p\Big]^n \cos\eta_i,$$

$$E=\sum_{i=0}^{m-1}K_i\Big[g_i+\sum_l+\sum_p\Big]^{n-1} \cos^2\eta_i,$$

$$\sum_l=\sum_{l=2}^{s}\Delta R_l \sin\{l(\varphi+i\gamma)+\alpha_l\},$$

$$\sum_p=\sum_{p=1}^{s}\Delta r_p \sin\{p(q+\varphi i\gamma)+\alpha_p\}.$$

Solving the system of equations (2.51) with respect to x_0 and y_0, we find

$$x=\frac{AE-CD}{n(C^2-BE)};\quad y=\frac{BD-AC}{n(C^2-BE)}. \tag{2.52}$$

After substituting these expressions in (2.48) and differentiating with respect to x_1 we get the formula for radial stiffness of a radial bearing, taking into account the errors in the components:

$$k=n\sum_{i=0}^{m-1}K_i\Big[g_i+x_1\cos(\varphi+i\gamma)+\frac{AE-CD}{n(C^2-BE)}\cos(\varphi+i\gamma)$$
$$+\frac{BD-AC}{n(C^2-BE)}\sin(\varphi+i\gamma)+\sum_{l}+\sum_{p}\Big]^{n-1}\cos^2(\varphi+i\gamma). \qquad (2.53)$$

The effect of variable dimensions and variable stiffness of rolling elements on bearing stiffness. In order to bring out the effect of variable dimensions and variable elasticity of rolling elements on the radial stiffness of the bearing we assume that there are no other errors, that the bearing has an even number of rolling elements and that there are two identical "defective" rolling elements placed opposite each other. Under such conditions $y_1=y_0=x_0=0$ and formula (2.53) is considerably simplified.

$$k=n\sum_{i=0}^{m-1}K_i\,[g_i+x\cos(\varphi+i\gamma)]^{n-1}\cos^2(\varphi+i\gamma). \qquad (2.54)$$

The maximum allowable value of variable dimensions of the rolling elements depends on the class of accuracy and the dimensions of the bearing. For example, if the dimensions of the balls of a bearing of type 200 of super-high accuracy satisfy conditions by 01 degree of accuracy, then the allowable deviation in variable dimensions is 0.3 μ [7]. The coefficient K_i takes into account the difference in the mechanical properties of the rolling elements, as already mentioned. Any difference in this coefficient as between the rolling elements included in one assembly is due to the prevailing manufacturing technology. The assembly of bearings does not guarantee that rolling elements made from steel of absolutely identical mechanical properties will be fitted in a particular bearing. Nor does it exclude the possibility of a difference in mechanical properties arising during heat treatment [35]. The deviation in the value K_i in formula (2.54) is equal to the deviation in the contact rigidity of the ball, since

$$k_i=n\,K_i\,\delta_i^{n-1}. \qquad (2.55)$$

Preliminary experiments to determine the elastic properties $\delta_i(p)$ of balls of unused C36204E and H303 bearings showed that in certain assemblies variable rigidity of the order of a few percent was characteristic of balls.

In Fig. 2.22 the function $k(\varphi)$ is graphically shown using expression (2.54) for $m=6$, $n=3/2$. The graphs correspond to the following values of K_i and g_i:

1) $K_i=1$ and $g_i=20\ \mu$ for all values of i (ideal bearing);

2) $K_i=1$ for all values of i, $g_0=g_3=19.7\mu$, $g_1=g_2=g_4=g_3=20\mu$ (stiffness of all balls is identical but deformation, due to preload, of two balls is less than the deformation of the remainder by 1.5% because of negative deviation in their diameters);

3) $K_0=K_3=0.985$, $K_1=K_2=K_4=K_5=1$, $g_i=20\mu$ for all values of i (stiffness of two balls less than the rigidity of the remainder by 1.5%, diameters of all balls identical).

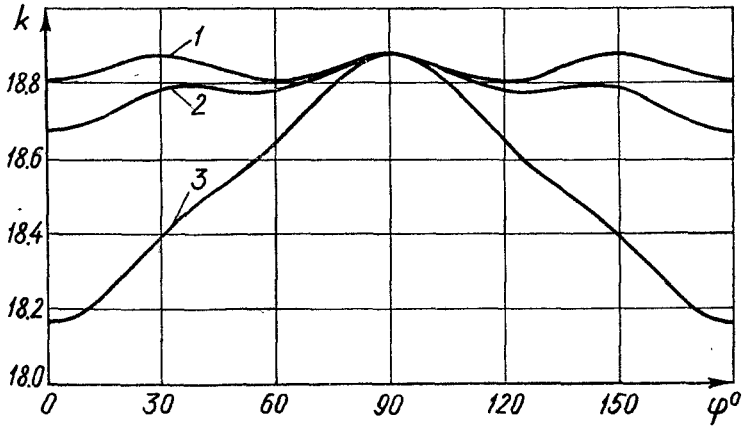

Fig. 2.22. Variation in radial stiffness during rotation of bearing with six balls: *1*—ideal bearing; *2*—zeroth and fourth balls smaller than rest; *3*—stiffness of zeroth and fourth balls less than stiffness of other balls.

A comparison of the graphs shows that classification of the rolling elements of bearings, especially precision bearings with preload, based only on dimensional-geometric parameters is not enough. It is necessary to verify the rigidity of the rolling elements too. Besides, it is not rational to manufacture precision bearings with a small number of rolling elements since the change in their rigidity during rotation is considerable even in the case of absolute identity of the rolling elements.

A method for automatic selection of the elements of rolling contact bearings, taking into account the variable stiffness of rolling elements. In Fig. 2.23 a scheme is shown for one possible variation in a setup to collect the elements of bearings. After classification by their dimensional-geometric parameters, before storage, individual groups of rolling elements are gathered in a setup for measuring their stiffness, thereby forming different dimensional-stiffness groups of rolling elements. This information is fed to the computer.

The outer ring moving in jerks along the transmission line *1* enters the measuring position *2* where the measurement of rolling elements is carried out and information on the results of measurement (number of selective group of the outer ring) is fed to a computer *9*. Similarly, the inner ring enters the measuring position *5* along the transmission line *4* and information as to the number of its selective group is fed into the computer *9*. In exactly the same way the rolling elements enter the measuring section *8* along the transmission

line *7*. The rolling elements being measured are initially sorted according to geometric parameters and then the rolling elements found in one group are sorted according to stiffness. Thus dimensional-stiffness groups are formed. For sorting out by stiffness, for example, workability is tested by determining the deformation of each rolling element under the action of one and the same load. The rolling elements fall into one or other dimensional-stiffness group, depending on the value and tolerance of the deformation. Various dimensional-stiffness groups of rolling elements are placed in bunkers *10*. Any dimensional-stiffness group of rolling elements is placed in a particular bunker except the groups already lying in other bunkers. Information as to the number of the group of rolling elements placed in the given bunker is fed into the computer *9*, which checks the number of the ring lying in the first position for outer rings, with the number of the inner ring at the last position (position '*y*' *6*) and successively with all the numbers of rolling elements in '*z*' bunkers,

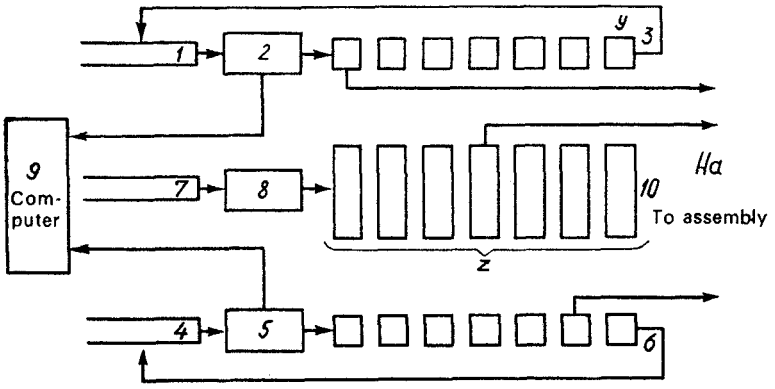

Fig. 2.23. Block diagram of unit for automatic selective assembly of bearings.

then with the same outer ring and inner ring in the last but one position ('*y*' *1*) and again with all rolling elements, etc. (including the number of inner ring in first position). Then a cross check is carried out for the inner ring in the first position with the outer ring in the last position (position '*y*' *3*) and successively with all rolling elements and then with the same inner ring and with the outer ring on the second-to-last position ('*y*' *1*), and so on to the outer ring on the first position. If the necessary combination of components is found for the given radial clearance then the computer gives the output of these components in the assembly, after which checking is temporarily suspended.

The rings are moved in to the positions of rings with a single step filling the vacated positions and the next rings follow to the first position from the measuring positions.

If the complete cycle of checking does not give even a single required as-

sembly combination then the rings from the last position ('y' *3* and 'y' *6*) are thrown out and returned to the corresponding transmission lines. Then the rings move in, filling the last places and correspondingly vacating the first. A new cycle of checks is started.

The effect of waviness of raceways of rings on the stiffness of bearings. Assuming that the unevenness of the raceway of the outer and inner rings of the bearing comprises only harmonics whose order is equal to m, or less or more than that by a multiple of two, and that phase angles of all harmonics are equal (then $x_0=y_0=0$), it is possible to simplify formula (2.53) appreciably:

$$k=n\sum_{i=0}^{m-1}K_i\Big[g_i+x\cos(\varphi+i\gamma)+\sum_{l=2}^{s}\Delta R_l\sin\{l(\varphi+i\gamma)+\alpha_l\}+\sum_{p=1}^{s}\Delta r_p\sin\{p(q\varphi+i\gamma)+\alpha_p\}\Big]^{n-1}\cos^2(\varphi+i\gamma). \tag{2.56}$$

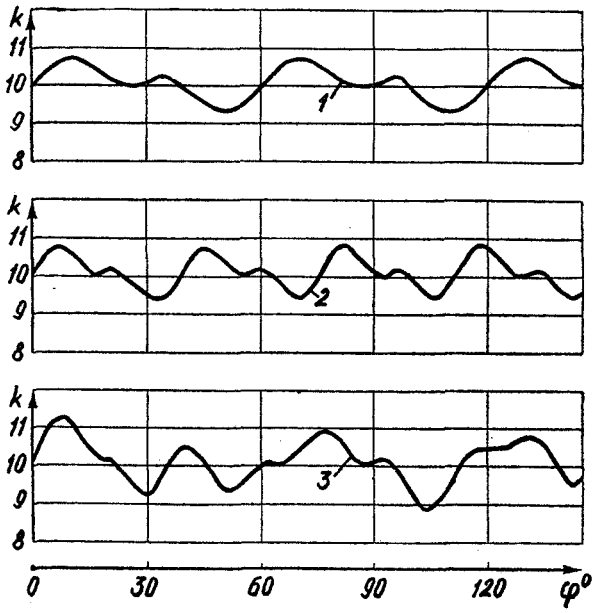

Fig. 2.24. Variation in radial stiffness of bearing with 6 balls due to waviness of stationary (*1*) outer ring; (*2*) inner ring and (*3*) both rings.

In Fig. 2.24 graphs of function $k(\varphi)$ are shown using formula (2.56) for $m=6$, $x=0$, $K_i=K=1$, $g_i=g=5$, $q=1.64$, $\alpha_l=\alpha_p=0$, corresponding to three cases: 1) the inner ring is ideal, raceway of outer ring has three harmonics of unevenness whose amplitudes are $\Delta R_3=1$, $\Delta R_6=0.5$ and $\Delta R_{12}=0.3$; 2) the outer ring is ideal but the inner ring has the same type of unevenness; 3) both

rings have the above-mentioned unevenness simultaneously. As a result of superposing the periodic component due to the unevenness of the raceways of the inner ring on the component due to the unevenness of the outer ring, and in the general case also due to variable dimensions, variable elasticity and change in the position of rolling elements during rotation (when $x \neq 0$) the function $k(\varphi)$ becomes almost periodic because the rotational speed of the moving ring and the cage are in general not repeated.

The repetition of the rotational speeds is characterized by the quantity q, which is determined by the relation

$$q = \frac{\omega_{in}}{\omega} - 1. \tag{2.57}$$

According to [8]

$$\frac{n_{in}}{n_c} = \frac{2D_0}{D_0 - d_r \cos \beta}, \tag{2.58}$$

where n_{in} and n_c are the rotational speeds of the inner ring and cage, rpm;

$$\frac{n_{in}}{n_c} = \frac{\omega_{in}}{\omega};$$

D_0 is the diameter of the circle passing through the centers of the rolling elements, mm;

d_r is the diameter of the rolling elements, mm.

By substituting the expression (2.58) in (2.57) we get

$$q = \frac{2D_0}{D_0 - d_r \cos \beta}. \tag{2.59}$$

Thus the quantity q depends not only on the dimensional geometric parameters of the bearing (D_0, d_r, β) but also on the value of preload. With changes in this the effective values of diameters D_0 and d_r and constant angle β change. Consequently the quantity q not only cannot be computed with great accuracy but also does not remain a constant during the working of the bearing.

2.3 IDENTIFICATION OF ELASTIC AND DAMPING CHARACTERISTICS OF BEARINGS BASED ON THE RESULTS OF VIBRATION TESTS

The complexity of the analytical determination of the elastic properties of rolling contact bearings is responsible for some unreliability in the results obtained for each concrete case. This relates to qualitative and especially to quantitative aspects of the problem. Sometimes it is difficult to judge the degree of legitimacy of an assumption and the influence of factors not taken into account. Therefore in important cases theoretical computations, as a rule, are accompanied by experimental verification including the determination of the elastic properties of the bearing using the static loading technique. However,

the results obtained by this and other methods do not take into account the actual conditions of the dynamic domain. The method of determining the characteristics of bearings based on the results of vibration tests is free of such disadvantages and allows determination not only of elastic but also of damping characteristics.

It is possible to consider the bearing as a nonlinear vibrational system comprising mass m (moving ring with attached mass, if the bearing is mounted), connected to the casing (stationary ring) with the help of spring and dash pot. The vibration of such a system under strong harmonic excitation along one of the independent coordinates will predominate over vibration along other independent coordinates. Hence such a system can be considered as a single degree of freedom system (Fig. 2.25).

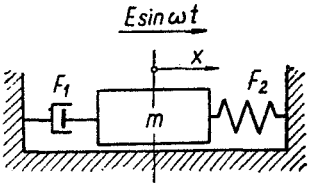

Fig. 2.25. A simplified dynamic model of bearing.

Such a vibrational system is described by differential equations of the type

$$m\ddot{x}+F_1(\dot{x})+F_2(x)=E\sin\omega t. \tag{2.60}$$

Let us assume that with harmonic excitation it is possible to have very nearly sinusoidal vibrations (but not necessarily symmetric) in the system, i.e. the solution of equation (2.60) can be approximately expressed in the form

$$x=x_0+a\sin(\omega t+\varphi)=x_0+x_1, \tag{2.61}$$

where x_0 is the constant component of vibration (mean deviation);

a is the amplitude of vibrations;

φ is the phase angle.

Equation (2.60) can be charged by an equivalent linear equation:

$$m\ddot{x}+F_{10}(v)+\lambda(v)\dot{x}+F_{20}(a)+k(a)\,x_1=E\sin\omega t. \tag{2.62}$$

Here x and $\dot{x}=v\cos(\omega t+\varphi)$ are the displacement and speed of the equivalent system;

$$v=a\omega,$$

$\lambda(v)$ and $k(a)$ are equivalent coefficients of damping and stiffness;

$F_{10}(v)$ and $F_{20}(a)$ are constant components of the equivalent damping and elastic forces.

The constant components of forces and equivalent coefficients of damping and stiffness can be determined from the condition of probable equivalence [16] of nonlinear and linearized forces of damping and stiffness although in the given case the functions being compared are damped.

As an approximate theory operating on the moments of first and second-

order random functions it is natural to consider as statistically equivalent functions which have correspondingly identical mathematical expectation and correlated functions for the given law of distribution. On the basis of this two criteria are considered in practice for approximation of random functions [16, 17]. The first criterion involves the satisfaction of the condition of equality of mathematical expectations and dispersion of true and approximating functions, the second criterion involves the satisfaction of the condition of minima of mathematical expectation of the square of the difference of true and approximating random functions.

We will use the second criterion because it gives the best results for quasi-harmonic vibrations. After carrying out the corresponding operations we get:

$$F_{10}(v) = -\int_{-v}^{v} F_1(\dot{x})\, w(\dot{x})\, d\dot{x}, \tag{2.63a}$$

$$\lambda(v) = \frac{1}{D_{\dot{x}}} \int_{-v}^{v} F_1(\dot{x})\, \dot{x} w(\dot{x})\, d\dot{x}, \tag{2.63b}$$

$$F_{20}^{*}(a, x_0) = -\int_{x_0-a}^{x_0+a} F_2(x)\, w(x)\, dx, \tag{2.63c}$$

$$k^{*}(a, x_0) = \frac{1}{D_x} \int_{x_0-a}^{x_0+a} F_2(x)\,(x - x_0)\, w(x)\, dx, \tag{2.63d}$$

where $F_{20}^{*}(a, x_0)$ and $k^{*}(a, x_0)$ are the constant components of elastic force and stiffness coefficient corresponding to the periodic component of unsymmetric vibrations;

$D_{\dot{x}}$ and D_x are the dispersion of velocity and displacement;

$w(\dot{x})$ and $w(x)$ are differential functions of the velocity and displacement distribution.

Constant components of damping and elastic forces appear as a result of the unsymmetry of $F_1(\dot{x})$ and $F_2(x)$ and are determined by their even components. However, coefficients λ and k are determined by odd components of functions $F_1(\dot{x})$ and $F_2(x)$. In connection with this, functions F_1 and F_2 will be expressed in the form of even (P) and odd (Q) components:

$$\begin{aligned} F_1(\dot{x}) &= P_1(\dot{x}) + Q_2(\dot{x}). \\ F_2(x) &= P_2(x) + Q_2(x). \end{aligned} \tag{2.64}$$

By substituting the even components in equations (2.63 a) and (2.63 c) and

odd components in equations (2.63b) and (2.63d) of these functions and differential functions of distribution corresponding to the harmonic case we get

$$F_{10}(v) = -\frac{2}{\pi}\int_0^v \frac{P_1(\dot{x})}{\sqrt{v^2-x^2}}d\dot{x}, \tag{2.65a}$$

$$\lambda(v) = \frac{4}{\pi v^2}\int_0^v \frac{Q_1(\dot{x})\,x}{\sqrt{v^2-x^2}}d\dot{x}, \tag{2.65b}$$

$$F_{20}^*(a, x_0) = -\frac{2}{\pi}\int_{x_0-a}^{x_0+a} \frac{P_2(x)}{\sqrt{a^2-(x-x_0^2)}}dx, \tag{2.65c}$$

$$k^*(a, x_0) = \frac{4}{\pi a^2}\int_{x_0-a}^{x_0+a} \frac{Q_2(x)(x-x_0)}{\sqrt{a^2-(x-x_0)^2}}dx. \tag{2.65d}$$

In equations (2.65c) and (2.65d) we introduce the variable $x_1 = x - x_0$ and express even and odd components of elastic characteristic by x_1 in parallel systems of coordinates with the origin at points $[x_0; P_2(x_0)]$ and $[x_0; Q_2(x_0)]$ respectively. Then

$$F_{20}^*(a, x_0) = \frac{2}{\pi}\int_0^a \frac{P_2^*(x_1)}{\sqrt{a^2-x_1^2}}dx_1, \tag{2.66a}$$

$$k^*(a, x_0) = \frac{4}{\pi a^2}\int_0^a \frac{Q_2^*(x_1)\,x_1}{\sqrt{a^2-x_1^2}}dx_1. \tag{2.66b}$$

Equations (2.65a), (2.65b), (2.66a) and (2.66b) lead to integral equations of the Abel type, which can be solved.

Taking equation (2.64) into account, we get

$$F_1(\dot{x}) = \int_0^x \frac{d}{d(v^2)}[v^2\lambda(v)]\frac{v\,dv}{\sqrt{x^2-v^2}} - \frac{d}{d\dot{x}}\int_0^{\dot{x}_1} \frac{F_{10}(v)\,v}{\sqrt{\dot{x}^2-v^2}}\cdot dv, \tag{2.67a}$$

$$F_2(x) = \int_0^{x_1} \frac{d}{d(a^2)}[a^2 k^*(a, x_0)]\frac{ada}{\sqrt{x_1^2-a^2}} - \frac{d}{dx_1}\int_0^{x_1} \frac{F_{20}^*(a, x_0)\,a}{\sqrt{x_1^2-a^2}}\cdot da. \tag{2.67b}$$

The function $F_2^*(x_1) = P_2^*(x_1) + Q_2^*(x_1)$ represents the dynamic elastic characteristic of the bearing, depending not only on the displacement but also on the amplitude, frequency, damping characteristics and constant compo-

nent of the excitation force if this is not equal to zero. For the determination of static elastic characteristics the functions $P_2^*(x_1)$ and $Q_2^*(x_1)$ have to be expressed in the initial system of coordinates:

$$P_2(x)=P_2(x_0+x_1)=P_2^*(x_1),$$
$$Q_2(x)=Q_2(x_0+x_1)=Q_2^*(x_1). \tag{2.68}$$

However, it is possible to determine the elastic characteristic by other, simpler methods based on the coincidence of functions $F_2^*(x_1)$ and $F_2(x)$ in interconnected systems of coordinates. In this particular case, when $x_0=0$, $F_2^*(x_1)=F_2(x)$. To obtain the expression for $F_2(x)$ it is necessary to substitute the quantities x, $k(a)$ and $F_{20}(a)$ in formula (2.67b) instead of the quantities x_1, $k^*(a, x_0)$ and $F_{20}^*(a, x_0)$. The last functions are determined by eliminating terms containing x_0 from the empirically obtained expressions for $k^*(a, x_0)$ and $F_{20}^*(a, x_0)$. Hence

$$F_2(x)=\int_0^x \frac{d}{d(a^2)}[a^2 k(a)]\frac{a\,da}{\sqrt{x^2-a^2}}-\frac{d}{dx}\int_0^x \frac{F_{20}(a)\,a}{\sqrt{x^2-a^2}}\,da. \tag{2.69}$$

It is worthwhile noticing the condition that in a particular case k^* and F_{20}^* can be completely determined by the amplitude of vibrations, if x_0 depends only on a (the case where the only cause for the appearance of x_0 is the unsymmetry of elastic characteristic). In this case the functions $k^{**}(a)$ and $F_{20}^{**}(a)$ can be obtained experimentally. They are not useful for substitution either in formula (2.67b) or in formula (2.69), since

$$k^{**}(a)\neq k(a),\ F_{20}^{**}(a)\neq F_{20}(a).$$

Approximate formulas (2.67a) and (2.69) are comparatively cumbersome. It is desirable to have simpler, though less accurate, formulas, all the more because the functions $F_{10}(v)$, $F_{20}(a)$, $\lambda(v)$ and $k(a)$ obtained as a result of the analysis of experimental data cannot be absolutely accurate.

With the aim of obtaining more convenient approximate formulas for the determination of elastic and damping characteristics of bearings we make use of one of the formulas of numerical integration due to Steklov [51]:

$$\frac{1}{\pi}\int_{-1}^{1}\frac{f(z)}{\sqrt{1-z^2}}\,dz=\frac{1}{6}\left[f(1)+f(-1)+2f\left(\frac{1}{2}\right)+2f\left(-\frac{1}{2}\right)\right]+R, \tag{2.70}$$

where R is the remainder given by

$$R=-\frac{f^{(6)}(\zeta)}{2^5\cdot 6!},\quad -1<\zeta<+1. \tag{2.71}$$

After the corresponding transformation of the right-hand sides of equa-

tions (2.65a), (2.65b), (2.66) and applying the formula (2.70) to them without the remainder term we get

$$F_{10}(v)=-\frac{1}{3}\left[P_1(v)+2P_1\left(\frac{v}{2}\right)\right],$$

$$\lambda(v)=\frac{2}{3}\left[Q_1(v)+Q_1\left(\frac{v}{2}\right)\right],$$

$$F_{20}(a)=-\frac{1}{3}\left[P_2(a)+2P_2\left(\frac{a}{2}\right)\right],$$

$$k(a)=\frac{2}{3a}\left[Q_2(a)+Q_2\left(\frac{a}{2}\right)\right]. \tag{2.72}$$

The presence of the values of functions P and Q in equation (2.72) for two values of the arguments makes their solution difficult with respect to these functions. From formulas (2.72) it can be seen that F_0 depends on the argument the same way as P, ak or $v\lambda$, the same as Q. Let us assume that the functions P and Q are developed from basic elementary functions without the operations of addition and subtraction. Then

$$\frac{P_1\left(\frac{v}{2}\right)}{P_1(v)}=\frac{F_{10}\left(\frac{v}{2}\right)}{F_{10}(v)};\quad \frac{Q_1\left(\frac{v}{2}\right)}{Q_1(v)}=\frac{\frac{v}{2}\lambda\left(\frac{v}{2}\right)}{v\lambda(v)};\quad \frac{P_2\left(\frac{a}{2}\right)}{P_2(a)}=\frac{F_{20}\left(\frac{a}{2}\right)}{F_{20}(a)};\quad \frac{Q_2\left(\frac{a}{2}\right)}{Q_2(a)}=\frac{\frac{a}{2}k\left(\frac{a}{2}\right)}{ak(a)}. \tag{2.73}$$

Equation (2.72) then takes the form:

$$F_{10}(v)=-\frac{1}{3}P_1(v)\left[1+2\frac{F_{10}\left(\frac{v}{2}\right)}{F_{10}(v)}\right],$$

$$\lambda(v)=\frac{2}{3v}Q_1(v)\left[1+\frac{\lambda\left(\frac{v}{2}\right)}{2\lambda(v)}\right], \tag{2.74}$$

$$F_{20}(a)=-\frac{1}{3}P_2(a)\left[1+2\frac{F_{20}\left(\frac{a}{2}\right)}{F_{20}(a)}\right],$$

$$k(a)=\frac{2}{3a}Q_2(a)\left[1+\frac{k\left(\frac{a}{2}\right)}{2k(a)}\right].$$

Introducing new variables $x=a$, $\dot{x}=v$ and taking into account equation (2.64), we then get

$$F_1(\dot{x})=\frac{3\dot{x}\lambda(\dot{x})\operatorname{sign}\dot{x}}{2+\dfrac{\lambda\left(\dfrac{\dot{x}}{2}\right)}{\lambda(\dot{x})}}-\frac{3F_{10}(|\dot{x}|)}{1+2\dfrac{F_{20}\left(\dfrac{|\dot{x}|}{2}\right)}{F_{20}(|\dot{x}|)}},$$

$$F_2(x)=\frac{3xk(x)\operatorname{sign}x}{2+\dfrac{k\dfrac{x}{2}}{k(x)}}-\frac{3F_{20}(|x|)}{1+2\dfrac{F_{20}\left(\dfrac{|x|}{2}\right)}{F_{20}(|x|)}}. \tag{2.75}$$

The term in these formulas is taken with the sign of the argument and $\dot{x}$ and x in the second term with their absolute value, since Q_1 and Q_2 by definition are odd and P_1 and P_2 even functions.

If the analytical expressions F_{10}, F_{20}, λ and k are formed from the sum of functions of the class mentioned above, then formulas (2.73) are applied to each additive separately and the characteristics are obtained term by term.

Simpler approximate formulas for the determination of elastic and damping characteristics of bearings based on the results of vibration tests can be obtained by using the well-known tool [21] for expressing the differential function of distribution through the δ-function:

$$w(u)=\lim_{T\to\infty}\frac{1}{T}\int_0^T\delta[u-x(t)]\,dt \tag{2.76}$$

and approximating it in the form of a linear combination of δ-functions:

$$w(u)=\sum_{l=0}^{s}\alpha_l\,\delta(u-x_l). \tag{2.77}$$

Here x_l is a certain value of x lying between x_{min} and x_{max};

α_l are positive numbers whose sum is equal to unity.

The method for the determination of x_l and α_l is given in the works of M.Z. Kolovskii [21, 22]. In the case of harmonic vibrations, when $x_0=0$

$$w(\dot{x})=\frac{1}{3}\,\delta(\dot{x})+\frac{1}{3}\left[\delta\left(\dot{x}-\frac{\sqrt{3}}{2}\,v\right)+\delta\left(\dot{x}+\frac{\sqrt{3}}{2}\,v\right)\right],$$

$$w(x)=\frac{1}{3}\,\delta(x)+\frac{1}{3}\left[\delta\left(x-\frac{\sqrt{3}}{2}\,a\right)+\delta\left(x+\frac{\sqrt{3}}{2}\,a\right)\right]. \tag{2.78}$$

By substituting expressions (2.78) in the equations (2.65) and (2.66), where $x_0=0$, taking the equation (2.64) into account, we get

$$F_{10}(v)=-\frac{2}{3}\,P_1\left(\frac{\sqrt{3}}{2}v\right),$$

$$\lambda(v)=\frac{2\sqrt{3}}{3v}Q_1\left(\frac{\sqrt{3}}{2}v\right), \tag{2.79}$$

$$F_{20}(a)=-\frac{2}{3}P_2\left(\frac{\sqrt{3}}{2}a\right),$$

$$k(a)=\frac{2\sqrt{3}}{3a}Q_2\left(\frac{\sqrt{3}}{2}a\right).$$

In the equations (2.79) let us replace the variables: $\frac{\sqrt{3}}{2}v=\dot{x}$, $\frac{\sqrt{3}}{2}a=x$ and solve them with respect to P and Q. As a result, by taking equation (2.64) into account we get approximate formulas for the determination of damping and elastic characteristics:

$$F_1(\dot{x})=\dot{x}\lambda\left(\frac{2\sqrt{3}}{3}\dot{x}\right)\operatorname{sign}\dot{x}-\frac{3}{2}F_{10}\left(\frac{2\sqrt{3}}{2}|\dot{x}|\right), \tag{2.80}$$

$$F_2(x)=xk\left(\frac{2\sqrt{3}}{3}x\right)\operatorname{sign}x-\frac{3}{2}F_{20}\left(\frac{2\sqrt{3}}{3}|x|\right).$$

Formulas (2.80) are considerably simpler than formulas (2.67a) and (2.69) and even somewhat simpler than formulas (2.75), though to some extent they are inferior to the last in accuracy. They are convenient for use in computation. It is possible to judge the value of error resulting from the use of formulas (2.75) and (2.80) when compared to the more accurate formulas (2.67a) and (2.69) with the help of the given data in Tables for even and odd components of elastic characteristics.

TABLE 2.1

$k(a)$	$Q(x)$		
	Formula (2.69)	Formula (2.75)	Formula (2.80)
c	cx	cx	cx
ca	$\frac{3\pi}{8}cx^2\operatorname{sign}x$	$\frac{6}{5}cx^2\operatorname{sign}x$	$\frac{2\sqrt{3}}{3}cx^2\operatorname{sign}x$
ca^2	$\frac{4}{3}cx^3$	$\frac{4}{3}cx^3$	$\frac{4}{3}cx^3$
ca^3	$\frac{15}{32}\pi cx^4\operatorname{sign}x$	$\frac{24}{17}cx^4\operatorname{sign}x$	$\frac{8\sqrt{3}}{9}cx^4\operatorname{sign}x$
ca^4	$\frac{8}{5}cx^5$	$\frac{16}{11}cx^5$	$\frac{16}{9}cx^5$
ca^5	$\frac{35}{64}\pi cx^6\operatorname{sign}x$	$\frac{96}{65}cx^6\operatorname{sign}x$	$\frac{32\sqrt{3}}{27}cx^6\operatorname{sign}x$
ca^6	$\frac{64}{35}cx^7$	$\frac{64}{43}cx^7$	$\frac{64}{27}cx$
ca^7	$\frac{315}{512}\pi cx^8\operatorname{sign}x$	$\frac{384}{257}cx^8\operatorname{sign}x$	$\frac{128\sqrt{3}}{31}cx^8$

TABLE 2.2

$F_{10}(a)$	$-P(x)$		
	Formula (2.69)	Formula (2.75)	Formula (2.80)
c	c	c	$3/2\,c$
ca	$\frac{\pi}{2} c \lvert x \rvert$	$\frac{3}{2} c \lvert x \rvert$	$\sqrt{3}\, c \lvert x \rvert$
ca^2	$2cx^2$	$2cx^2$	$2cx^2$
ca^3	$\frac{3\pi}{4} c \lvert x \rvert^3$	$\frac{12}{5} c \lvert x \rvert^5$	$\frac{4\sqrt{3}}{3} c \lvert x \rvert^3$
ca^4	$\frac{8}{3} cx^4$	$\frac{8}{3} cx^4$	$\frac{8}{3} cx^4$
ca^5	$\frac{15}{16} \pi c \lvert x \rvert^5$	$\frac{48}{17} c \lvert x \rvert^5$	$\frac{16\sqrt{3}}{9} c \lvert x \rvert^5$
ca^6	$\frac{16}{5} cx^6$	$\frac{32}{11} cx^6$	$\frac{32}{9} cx^6$
ca^7	$\frac{35}{32} \pi c \lvert x \rvert^7$	$\frac{192}{65} c \lvert x \rvert^7$	$\frac{64\sqrt{3}}{27} c \lvert x \rvert^7$

The formulas for the determination of the elastic and damping characteristics of a bearing allow us to determine these characteristics if the constant part and equivalent coefficients are known. These values are determined empirically by vibration tests on the bearing for different amplitudes of vibration.

Equivalent coefficients of damping $\lambda\,(a\omega)$ and stiffness $k\,(a)$ are determined separately for certain values of amplitudes. The graphs obtained in this way are approximated by analytical expressions and can be used for substitution in the respective formulas. As far as the constant part of damping $F_{10}\,(a\omega)$ and elastic $F_{20}\,(a)$ forces is concerned we get their sum directly from the empirical results:

$$F_0\,(a, \omega) = F_{10}\,(a\omega) + F_{20}\,(a) = k\,(a)\, x_0\,(a\omega). \tag{2.81}$$

The causes of the appearance of the constant part of deviation x_0 representing the mean displacement of the vibrating mass for the period in question are the unsymmetry of damping and the elastic characteristics for a symmetric excitation force. Hence the value x_0 is made up of two components:

$$x_0\,(a, \omega) = x_{10}\,(a\omega) + x_{20}\,(a), \tag{2.82}$$

where $x_{10}\,(a\omega)$ is the constant part of deviation caused by unsymmetry of the damping characteristic;

$a\omega = v$ is the amplitude of variation in vibrational speed;

$x_{20}\,(a)$ is the constant part of the deviation caused by the unsymmetry of the elastic characteristic.

Both components of the quantity x_0 can be expanded in series in powers of $a\omega$ and a without the free term, since when $a=0$ and $\omega=0$ the system is in a state of static equilibrium and unsymmetry of characteristics is not to be found. Consequently

$$x_{10}(a\omega)=\beta_1 a\omega+\beta_2(a\omega)^2+\beta_3(a\omega)^3+\ldots,$$
$$x_{20}(a)=\gamma_1 a+\gamma_2 a^2+\gamma_3 a^3+\ldots. \tag{2.83}$$

Putting $a=$constant in equation (2.83) and adding them, we get

$$x_0(a\omega)=x_{10}(a\omega)+x_{20}(a)=\Gamma+\beta_1 a\omega+\beta_2 a^2\omega^2+\beta_3 a^3\omega^3+\ldots, \tag{2.84}$$

where $\Gamma=\gamma_1 a+\gamma_2 a^2+\gamma_3 a^3+\ldots=$const, i.e. for a constant amplitude of vibrations the relationship for $x_0^*(\omega)$ can be empirically obtained as a result of approximation by a polynomial with the free term

$$x_0^*(\omega)=\Gamma+\beta_1^*\omega+\beta_2^*\omega^2+\beta_3^*\omega^3+\ldots \tag{2.85}$$

It is possible to determine the value of coefficient β_1:

$$\beta_1=\frac{\beta_1^*}{a},\quad \beta_2=\frac{\beta_2^*}{a^2},\quad \beta_3=\frac{\beta_3^*}{a^3},\ \ldots \tag{2.86}$$

We observe that the quantity Γ cannot be obtained directly. It has to be considered as a value to which the function $x_0^*(\omega)$ tends when the frequency ω tends to zero.

Let us then put $\omega=$const in equation (2.83). After adding them we get

$$x_0(a,\omega)=(\beta_1\omega+\gamma_1)a+(\beta_2\omega^2+\gamma_2)a^2+(\beta_3\omega^3+\gamma_3)a^3+\ldots, \tag{2.87}$$

i.e. it is necessary to approximate the relationship for $x_0^{**}(a)$ for $\omega=$const obtained empirically by a polynomial not containing the free term:

$$x_0^{**}(a)=d_1 a+d_2 a^2+d_3 a^3+\ldots \tag{2.88}$$

The value of coefficients γ_i is obtained from the formulas

$$\gamma_1=d_1-\beta_1\omega,\quad \gamma_2=d_2-\beta_2\omega^2,\quad \gamma_3=d_3-\beta_3\omega^3,\ \ldots, \tag{2.89}$$

since the quantities β_1 and d_1 are already known.

After determination of the values of coefficients β_1 and thence the function $x_{20}(a\omega)$, the value of function $x_{20}(a)$ can be obtained as a difference in the values of functions $x_{20}(a)$ and $x_{10}(a\omega)$ for various values of a and ω, though it is more useful to use this criterion for verification of the correctness of the results obtained.

To get the constant components of forces $F_{10}(v)$ and $F_{20}(a)$ separately it is necessary to take the experimental characteristics $x_0^*(a)$ for $a=$const and $x_0^{**}(\omega)$ when $\omega=$const. After analysis it is possible to obtain functions $x_{10*}(a)$ and $x_{20}(a)$, whose product with the stiffness coefficient corresponding to symmetric vibrations gives

$$F_{10*}(a)=k(a)\,x_{10*}(a),$$
$$F_{20}(a)=k(a)\,x_{20}(a). \tag{2.90}$$

By replacing the variable using the formula $v=a\omega$ the function $F_{10*}(a)$ is brought to the form of $F_{10}(v)$.

The above method in principle can also be used for determination of the periodic component of the stiffness of bearings. For this it is necessary to determine the elastic property of the bearing for different positions of the cage and the moving ring.

References

1. Atstupenas, V.R.V. 1969. Vliyanie peremeshcheniya tel kacheniya na zhestkost' podshipnikov s uchetom poperechnykh kolebanii vnutrennego koltsa (Effect of displacement of rolling elements on the stiffness of bearings with transverse vibrations of inner ring). *Nauchnye trudy vuzov Lit. SSR, Vibrotekhnika*, No. 1 (6).
2. Atstupenas, V.R.V. 1968. O zhestkosti opor kacheniya ustanovlennykh s predavaritelnym natyagom (On the stiffness of rolling contact bearings with preload). *Nauchnye trudy vuzov Lit. SSR, Vibrotekhnika*, No. 3 (5).
3. Atstupenas, V.R.V. 1969. Ob osevoi zhestkosti podshipnikov kacheniya (On the axial stiffness of rolling contact bearings). *Nauchnye trudy vuzov Lit. SSR, Vibrotekhnika*, No. 2 (7).
4. Atstupenas, V.R.V., Yu.Yu. Getsevichyus and K.M. Ragulskis. 1970. Vliyanie raznouprugosti tel kacheniya na postoyanstvo zhestkosti podshipnikov (Effect of variable elasticity of rolling elements on the constancy of stiffness of bearings). *Nauchnye trudy vuzov Lit. SSR, Vibrotekhnika*, No. 1 (10).
5. Atstupenas, V.R.V. and R.P. Atstupeniene. 1971. Opredelenie kharakteristik nelineinykh kolabatelnykh sistem s odnoi stepenyu svobody po resultatam vibroispitanii (Determination of the characteristics of nonlinear vibrational systems with one degree of freedom based on the results of vibration tests). *Nauchnye trudy vuzov Lit. SSR, Vibrotekhnika*, No. 3 (16).
6. Atstupeniene, R., V. Atstupenas and K. Ragulskis. 1972. Netiesiniu virpanciu sistemu identifikacija. *Mokslas ir technika*, No. 3.
7. Beiselman, R.D., B.V. Tsipkin and L.Ya. Perel. 1967. Podshipniki Kacheniya (Rolling contact bearings). Moscow, Mashinostroenie.
8. Bonch-Osmolovskii, A.M. and V.F. Nabatov. 1964. Avtomatizatsiya komplektovaniya radialnykh sharikopodshipnikov s primeneniem vychislitelnykh ustroistv (Automation of sorting of radial ball bearings using the computer). Moscow, TsNIITMASh.
9. Bochkov, V.S. 1965. Zhestkost pretsizionnykh opor kacheniya tochnykh sistem (Stiffness of precision rolling contact bearings of accurate sys-

tems). Avtoreferat kand. diss. VNIPP.
10. Bochkov, V.S. 1966. Issledovanie tochnosti vrascheniye radialno-upornykh sharikopodshipnikov (Study of the accuracy of rotation of radial-thrust ball bearings). *Trudy VNIPPa*, Vol. 48, No. 4.
11. Bochkov, V.S. 1966. Statika radialno-upornogo sharikopodshipnika (Statics of radial-thrust ball bearings). *Trudy VNIPPa*, Vol. 47, No. 3.
12. Bochkov, V.S. 1962. Staticheskoe ravnovenie podshipnika na zhestkom valu pod deistviem priozvolnoi nagruzki (Static equilibrium of a bearing on a rigid shaft under the action of arbitrary load). *Trudy VNIPPa*, Vol. 31, No. 3.
13. Bochkov, V.S. 1962. Teoreticheskoe issledovanie smeshcheniya tsentra tyazhesti radialno-upornogo podshipnika pri kombiniro-vannoi nagruzke (Theoretical study of the displacement of the center of gravity of a radial-thrust bearing under combined loading). *Trudy VNIPPa*, Vol. 32, No. 4.
14. Bochkov, V.S. 1964. Teoreticheskoe i eksperimentalnoe issledovanie osevoi zhestkosti radialno-upornogo podshipnika pri kombinirovannoi nagruzke (Theoretical and empirical study of axial stiffness of a radial-thrust bearing under combined loading). *Trudy-VNIPPa*, Vol. 38, No. 2.
15. Dombrovskaya, M.M. 1961. Eksperimentalnoe issledovanie deformatsii shariko-podshipnikov (Empirical study of the deformations of ball bearings). *Izv. vuzov, Priborostroenie*, No. 4.
16. Kazakov, I.E. and B.T. Dostupov. 1962. Statisticheskaya dinamika nelineinykh avtomaticheskikh sistem (Statistical dynamics of nonlinear automatic systems). Moscow, Fizmatizdat.
17. Kazakov, I.E. 1969. Statisticheskie metody proektirovaniya sistem upravleniya (Statistical methods of control systems design). Moscow, Mashinostroenie.
18. Kasnauskas, Yu.Yu. 1967. Analiz geometricheskikh pogreshnostei dorozhek kacheniya podshipnikovykh kolets i tel kacheniya (Analysis of geometric errors in the raceways of bearing rings and rolling elements). In book: *Materialy Nauchnoi konferentsii molodykh uchenykh Lit. SSR, posvyashchennoi 50-letiyu Velikogo Oktyabrya*, Tekhnika, Vilnyus.
19. Kononenko, V.O. and N.P. Plakhtienko. 1969. Opredelenie kharakteristik nelineinykh elementov kolebatelnykh sistem iz analiza dvizheniya (Determination of the characteristics of nonlinear elements of vibration systems in the analysis of motion). *Prikladnaya Mekhanika*, Vol. 5, vyp. 10.
20. Kononenko, V.O. and N.P. Plakhtienko. 1970. Opredelenie kharakteristik nelineinykh kolabatelnykh sistem iz analiza kolebanii (Determination of nonlinear vibration system characteristics from the analysis of vibrations). *Prikladnaya Mekhanika*, Vol. 6, vyp. 9.
21. Kolovskii, M.Z. 1966. Nelineinaya teoriya vibrozashchitnykh sistem (Nonlinear theory of vibration-isolating systems). Moscow.

22. Kolovskii, M.Z. 1964. O vybore zakona raspredeleniya pri linearizatsii-nelineinykh differentsialnykh uravnenii (On the choice of the distribution law in the linearization of nonlinear differential equations). *Trudy Leningr. politekhn. in-ta*, No. 235.
23. Meldau, E. 1952. Dvizhenie osi podshipnika kacheniya pri malykh chislakh oborotov (Movement of the axis of a rolling contact bearing at low turning speeds). *Prikladnaya Mekhanika i Mashinostroenie*, No. 4.
24. Novikov, L.Z. 1964. Ob uprugikh kharakteristikakh radialno-upornogo sharikovogo podshipnika (On the elastic characteristics of radial-thrust ball bearings). *Izv. AN SSSR, OTN, Mekhanika i mashinosroenie*, No. 3.
25. Novikov, L.Z. 1961. Opredelenie sobstvennykh chastot kolebanii elektrodvigatelya, svyazannykh s nelineinoi uprugostyu podshipnikov (Determination of eigen frequencies of vibrations of an electric motor due to nonlinear elasticity of bearings). *Izv. AN SSSR, OTN, Mekhanika i Mashinostroenie*, No. 6.
26. Novikov, L.Z. 1963. Statika radialno-upornogo sharikovogo podshipnika (Statics of radial-thrust ball bearings). *Izv. AN SSSR. OTN, Mekhanika i Mashinostroenie*, No. 5.
27. Panovko, Ya.G. 1967. Osnovy prikladnoi teorii uprugikh kolebanii (Fundamentals of the applied theory of elastic vibrations). Moscow, Mashinostroenie.
28. Pinegin, S.V. 1965. Opory kacheniya v mashinakh (Rolling contact bearings in machines). Moscow, Nauka.
29. Plakhtienko, N.P. 1971. Vosstanovlenie kharakteristik avtokolebatelnykh sistem iz analiza vynuzhegennykh kolebanii (Restoration of the characteristics of self-vibrating systems from the analysis of forced vibrations). *Prikladnaya Mekhanika*, Vol. 8, vyp. 7.
30. Reshetov, D.N. 1955. Raschety podshipnikov kacheniya, ustanovlennykh po dva opore (Design of rolling contact bearings installed two to a mounting). In book: *Raschety i issledovaniya nekotorykh detalei mashin.* Moscow, Mashgiz.
31. Ryzhov, E.V. 1966. Kontaktnaya zhestkost detalei mashin (Contact stiffness of machine parts). Moscow, Mashinostroenie.
32. Saverskii, A.S. 1963. Issledovanie zhestkosti radialnoupornykh odinarnykh i sdvoennykh sharikopodshipnikov pri chisto osevoi nagruzke (Study of radial-thrust single-row and double-row ball bearings under purely axial loading). *Trudy VNIPPa*, Vol. 34, No. 2.
33. Spitsyn, N.A., M.Z. Narodetskii and I.Ya. Lysenko. 1963. Novae v teorii rascheta podshipnikov kacheniya (A new technique in the theory of rolling contact bearing design). *Trudy VNIPPa*, Vol. 35, No. 3.
34. Spitsyn, N.A. and others. 1968. Raschet i primenenie radialnoupornykh sharikopodshipnikov v uzlakh mashin i priborov (Design and application of radial-thrust ball bearings in assemblies of machines and instru-

ments). Moscow.
35. Sprishevskii, A.I. 1969. Podshipniki kacheniya (Rolling contact bearings). Moscow, Mashinostroenie.
36. Starostin, V.F. and A.A. Sorochinskaya. 1967. Vspomo-gatelnyi material dlya rascheta napryazhenii i deformatsii v mestakh kontakta detalei radialno-upornykh sharikopodshipnikov (Computation of stresses and deformations at contact points of radial-thrust ball bearing components). *Trudy VNIPPa*, Vol. 50, No. 2.
37. Fedorov, V.I. 1963. O zonakh ustoichivosti radialnykh podshipnikov kacheniya (Stability regions of radial rolling contact bearings). *Vestnick mashinostroeniya*, No. 4.
38. Kharlamov, S.A. 1962. O zhestkosti radialno-upornykh sharikovykh podshipnikov s osevym natyagom (Stiffness of radial-thrust ball bearings with axial loading). *Izv. AN SSSR, OTN, Mekhanika i mashinostroenie*, No. 5.
39. Chulkov, I.I. 1965. Eksperimentalnoe opredelenie deformatsii v mestakh kontakta tel kacheniya s koltsami podshipnikov (Experimental determination of the deformations at contact points between rolling elements and bearing rings). *Vestnik mashinostroenie*, No. 5.
40. Bielicki, H. 1962. Wplyw luzu poprzecznego w lozyskach tocznych na dragania walow wirujacych. *Przeglad mechaniczny*, No. 7.
41. Gunther, D. 1964. Untersuchung der Federung von Hauptschpingel-Lagerungen in Werkzeugmaschinen. Aachen.
42. Karlheinz, K. 1960. Die Starrheit des vorgespannten Schragku-gellagerpaares bei radialer Belastung. *Industrie-Anzeiger*, Vol. 82, No. 103.
43. Korren, H.W., W. Kircher and E. Back. 1964. Die Bestimmung der Federkennlinien an umlaufenden Walzlagern. *Industrie-Anzeiger*, Vol. 86, No. 92.
44. Meldau, E. 1954. Druckverteilung im Radialrillenkugellager. *Werkstatt und Betrieb*, Vol 87, Heft 2.
45. Meldau, E. 1956. Druckverteilung im Radialrillenkugellager bei Belastung durch Einzelkraft und Moment. *Werkstaff und Betrieb*, Vol. 89, Heft 4.
46. Meldau, E. 1955. Druckverteilung im Radialrillenkugellager bei reiner Moment Belastung. *Werkstatt und Betrieb*, Vol. 88, Heft 4.
47. Neubert, G. 1968. Der Einfluss der Lager auf den Lauffehler einer Walzgelagerten Werkzeugmaschinen-Hauptspindel. *Maschinen-bautechnik*, Vol. 17, Heft 6.
48. Perret, H. 1950. Die Berechnung der elastischen Vervormung von Rillenkugellagem. *Konstruktion*, Vol. 2, Heft 5.
49. Schreiber, H.H. 1961. Die axiale Federung von Kugellagern. *Industrie-Anzeiger*, Vol. 83, No. 79.
50. Schreiber, H.H. 1936. Die Steifigkeit des vorgespannten Zylinderrollenlagers. *Walzlagertechnik*, Heft 1.

51. Stekloff, W. (Steklov, V). 1918. Sur les quadratures. Note I, *Izvestiya Rossiiskoi Akademii Nauk*, ser. VI, No. 17.
52. Szucki, T. 1955. Obliczenie sztywnosci lozyska kulkowego zwyklego, Zeszyty Naukowe politechniki Warszawskiej. *Budownictwo*, No. 27.
53. Sciezzko, J. 1966. Odksztalcenia sprezyste walcowych lozysk tocznych. *Przegland mechaniczny*, Vol. 25, No. 24.
54. Tamura, H. and H. Shimizu. 1967. Vibration of Rotor Based on Ball Bearing. 2 rept., Static stiffness of ball bearing containing a small number of balls. *Bull. JSME*, Vol. 10, No. 41.
55. Wiche, E. 1967. Radiale Federung von Walzlagern bei beliebiger Lagerluft. *Konstruktion*, Vol. 19, No. 5.

3

ANALYSIS OF RADIAL VIBRATIONS OF BEARINGS AND BEARING ASSEMBLIES

With the increase in shaft speeds and demands on precision bearing assemblies (rotors of gyroscopes, precision lathe spindles, low-noise electric motors, shafts of information carriers and others) there is need of a more accurate description of the dynamics of their operation. Much effort is devoted both in our country and abroad to study of the causes of vibrations and noise in ball bearing assemblies and remedial measures. Only particular cases have been studied so far and there is no general theory for these problems. The complexity of the phenomena of the vibrational process of a bearing and the dependence of these phenomena on a large number of factors render the subject difficult. However, the amount of work devoted to analytical and experimental study of rolling contact bearings and the vibrations and noise they caused has been continuously increasing. In recent times, both in the Soviet Union and abroad, there has appeared a series of surveys [73, 74, 104] of the most important contributions. These help to spread the flow of information, highlight the most significant achievements and pose problems for further research.

In one such survey S.V. Pinegin and K.V. Frolov analyze a number of publications by Soviet and foreign authors, commenting on the successes achieved in research on the steady-state working of bearings and the reduction of vibrations and noise transmitted by the bearings to the machine casing.

O.I. Shevchenko's survey is wide-ranging and interesting. In his work he considers various causes of the production of noise and vibrations in rolling-contact bearings. Some of the basic causes, according to the majority of researchers, are the cyclic change in the flexibility of the bearing with loading (these vibrations appear even in the case of a geometrically ideal bearing) and geometric errors in the bearing components arising when the rolling elements turn. The opinions of various researchers and the results they have obtained are given for study of the following causes of noise and vibration in rolling contact bearings: uneven raceways of the rings, sizes of ball bearings, shaft speed, load, design and material of cage, lubricant, etc. As can be seen from

this list, almost all the causes of noise and vibrations in bearings have been dealt with in this survey. Such surveys which not only equip the researcher to follow the flow of information on this subject but also point the way for further research are undoubtedly very useful.

Many authors have studied both experimentally and analytically the effect of unevenness of rings and rolling elements on the level of vibrations of the bearing [29–32, 56, 105–107 and others], indicating that unevenness is determined by wavelength and amplitude. Based on the wavelength, the unevenness is conditionally divided into various groups: oval, straight edged, wavy and rough. When the unevenness has a wavelength between 1/3 and 1/18 of the circumference of the circle, it is called straight-edged. Unevenness with a wavelength between 1/18 and 1/360 of the circumference of the circle is called wavy and unevenness with a wavelength less than 1/360 of the circumference of circle is called rough. It has been shown that of all varieties of unevenness of raceways waviness has the maximum influence on the level of vibrations of a bearing.

The works of P.D. Volkov, N.N. Gerasimova and V.V. Sukhanova [29–31] are devoted to the experimental determination of the individual and combined effect of geometric errors in the raceways of rings and rolling elements on the level of vibrations in ball bearings. As a result of the analysis of experimental data it has been concluded that the waviness of balls has maximum influence on the level of vibrations, the waviness of the rotating inner ring has less effect and waviness of the outer ring has the least effect. These results were obtained while characterizing the vibrations of the free outer ring. It is shown that while mounting the bearing in the casing the waviness of the outer ring may have a greater effect on the vibrations of the assembly. The spectral composition of the vibration in a bearing and the magnitude of the amplitude for various harmonics of errors in rings are not dealt with in this work. As mentioned in the work [92], certain values of waviness in the raceways of rings are more prone to excite vibrations than others. Hence the general level of vibrations is the result not only of the amplitude of waviness but also of the spectral composition of geometric errors in the manufacture of the raceways of rings and rolling elements.

In the works of B.T. Sheftel', K.M. Sivyakov, V.A. Guschin and G.K. Lipskii [105–107] and others analytical and experimental research is described on the effect of waviness in the raceways of the inner ring on the vibration of ball bearing. The waviness of the raceway is expressed by a polar equation, and not by a sinusoidal curve, combined with the conditionally straightened arc of a circle. This equation is obtained analytically when determining the trajectory of the grinder disc.

In the work [82] it is assumed that two balls interact with the raceway of an inner ring with a wavy surface. The frequency and amplitude of vibrational acceleration corresponding to the fundamental harmonic of the waviness in

the raceway have been obtained. It has been established that the amplitude of vibrational acceleration depends on the relation between the number of balls and the number of waves on the circumference of the raceway of the ring. In the above-mentioned works only purely kinematic factors that excited vibrations are considered.

In the works of L.Z. Novikov [65–66] the motion of the rotor relative to the casing has been considered for elastic radial thrust ball bearings with preload. Analysis of eigen frequencies of vibrations connected with the nonlinear elasticity of bearings has also been carried out. It has been assumed that all the bearing components are of ideal geometric shape.

The works of V.S. Boyarinov and Yu.I. Neimark [19–23] are devoted to research on the radial vibrations of a horizontal shaft rotating in ball bearings. It has been shown that depending on the ball bearing and shaft parameters two types of motion are possible: unseparated motion, when the shaft vibrates without losing contact with the balls, and impact, when the shaft separates from the balls and creates an impact load on them. Continuous (unseparated) motion is described by Mate's equation, including the right hand side.

Axial vibrations of a horizontal rotor are described in the works of A. Tamura and O. Taniguti [94–95] in which analytical and experimental research is described on subharmonic vibrations of the order of 1/2 [94] and the axial harmonic vibrations of a horizontal rigid rotor due to the motion of the balls [95]. On the basis of analytical study of Hill's equations stable and unstable domains of motion are obtained.

In A. Tamura's work [145] the effect of variable dimensions of the balls on the axial vibrations of the rotor is shown. The experiments were run on a special stand. The bearing being studied had two large-diameter balls placed side by side. Measurements were carried out for different initial misalignment of rings. The relationship between the stiffness of the bearing in the axial direction and the angular position of the cage has been shown as a function of the change in the number of balls in the loaded zone. Resonance was observed at shaft speeds where the frequency of the eigen vibrations of the system was a multiple of the angular speed of the cage. The analytical study included the formulation and study of the Mate equation with the right-hand side.

A number of works by Yu.Yu. Kasnauskasa [37–42] are devoted to experimental and analytical research on the vibrations of a vertical rigid rotor rotating in a radial thrust ball bearing with preload. The momentum equations of the rotor axis obtained by Lagrange's method are considered in the analytical treatment. It is established that the dynamic characteristics of the outer ring fixture appreciably affect the intensity of excitation of the spectral component amplitudes of the rotor vibrations. The resonance frequency shift is mentioned. The experiments were run on a special stand in which the ball bearings being studied served as the direct support of the rotor. The spectral compo-

nent and the general level and amplitudes of the fundamental components of the spectrum of vibrations were measured.

A study of the statics and dynamics of the rotor in actual bearings is to be found in the works of V.F. Zhuravlev [34, 35], in which the equilibrium of the bearing [34] and dynamics of the rotor in ball bearings with axial preload [35] are examined. The geometric defects in the shape of raceways and balls are given. Stress and deformation in contact groups of the bearing are related to Hertz's law. The mass of the balls is taken as zero and the relation between the balls and the rings is ideal and not uniform. The energy of the bearing in the deformed state is determined. The momentum equations are derived using Lagrange's method and these equations are linearized. The structure of the disturbing forces is also studied. As a result of the analysis of expressions (regarding disturbing forces) it has been established that the forced motion of the rotor is the sum of harmonic vibrations with frequencies which depend on the angular speed of the rotor, the cage and the number of balls. In the linear approximation not all the harmonics of the Fourier series expansion of the ring surface cause rotor vibration. The rotor vibration and the imbalance are due to the vibrations that are even multiples of the speed of rotation.

From this short survey of basic work to date on the causes of noise and vibrations in rolling contact bearings and of rotor vibrations in rolling contact bearings we may conclude that along with the appreciable successes in this field there are still many unsolved problems. As is mentioned in the surveys [73–74], to date there has not been enough work on the analysis of vibrations and noise in rolling contact bearings and there are no general conclusions and recommendations. Vibrations of precision rotors caused by errors in the manufacture of components and the mounting of rolling contact bearings have not been adequately studied. The problem of determining the statistical characteristics of vibrations of similar rotors working in standard bearings has not been solved.

This lag is partly explained by the fact that the problem of determining the statistical characteristics of nonlinear dynamic systems has been solved with a certain accuracy by analytical methods for relatively simple cases. For the study of nonlinear systems for random effects the Markovian theory for random processes (Fokker-Planck-Kolmogorov equation [75]) is widely used. From the point of view of mathematics the study of the behavior of heterogeneous nonlinear vibrational systems in the case of disturbance caused by "white noise" boils down to study of one class of quasi-linear stochastic differential equations and the determination of certain results by simultaneous application of the methods of nonlinear mechanics and the theory of probability [51]. Here the expression obtained for steady-state density of the probability distribution of the amplitude of a vibrational system is used for the determination of the most probable steady-state amplitudes of vibrations of the basic system.

In more complex cases when the disturbance is not a "white noise" or when the system of equations is "highly" nonlinear (the method of averages is not valid) the above methods are not applicable. Current practice is to tackle such problems using approximation and numerical methods which give the desired accuracy.

Even N.E. Zhukovsky [33] seriously considered the possibility and effectiveness of simulation methods for the study of complex dynamic systems.

Numerical methods are best suited for analysis of nonlinear systems. The basic disadvantage of these methods (large computations) was dispelled with the development of computers.

In carrying out purely mathematical operations (integration of a system of equations) "classical" numerical methods often do not bring out the physical meaning of the processes being studied, i.e. the intermediate stages of computation, lacking explicit system interpretation, do not allow determination of the causes of the resulting behavior of the system.

In this sense a more convenient method is direct probability simulation [13, 103], leading to the generation of the sequence of realizations of initial random processes, their functional (algorithmic) transformation consistent with the structure of the system being simulated and, finally, statistical analysis of the sequence of realizations at the output of the system. Analytical study of the mathematical model is replaced here by an experiment with a physical model reproduced on a computer.

The realizations of initial (real) random signals are usually reproduced with the accuracy of indentity of the first two moments (average and correlation function). Hence research that uses the method of statistical experimentation must be preceded by an experiment whose aim is to explain the nature and probability characteristics of the signals occurring in the given system.

The principles of the mathematical formalization of the relations and processes appearing during the operation of any system are described in the works [14, 15, 82, 96].

The present chapter deals with vibrational processes appearing during the rotation of a rigid shaft in radial thrust ball bearings of high accuracy with preload. The effect of errors in the manufacture of components and the torque of bearings on the excitation of shaft vibrations and vibrations of the outer ring of the ball bearing will be examined. The statistical characteristics of the vibration of a similar shaft rotating in rolling contact bearings will also be determined.

The case where the system can be considered to be quasi-linear will be singled out. The method of solution for such a system will be described and that for the system of stochastic differential equations of Ito. The computational method will be described using the method of statistical tests. The determination of relations will be given to obtain random sequences which in their probability characteristics are similar to the observed characteristics of

the real system when in operation. The methodology and results of the solution of the differential equations of the dependence of vibrations of a ball bearing on geometric errors in the manufacture of components will also be described. An estimation is provided of the function of probabilistic densities of solutions of the same equation at different moments of time for initial conditions having normal distribution with zero mathematical expectation and unit dispersion.

3.1 DYNAMICS OF BALL BEARING ASSEMBLY

First let us consider the vibrations of the shaft in a radial thrust ball bearing with preload (a radial thrust ball bearing has been chosen for the sake of concreteness; all the following results are valid both for radial and thrust ball bearings).

The dynamic model of the system is shown in Fig. 3.1. The shaft and bearing components (rings and balls) of this model are assumed to be perfectly rigid. The displacements of rings are possible thanks to the flexibility of the contacts between the balls and the raceways of the rings and also because of the elasticity of the mounting of the outer ring and related components to the casing. This is the most general case, where the shaft connected to the outer ring has six degrees of freedom. The ball and the cage are considered to be massless in further computations and hence they do not increase the number of degrees of freedom. It is assumed that the force of preload is sufficient to ensure continuous motion of the balls, i.e. for continuous contact with the raceways of both rings. This condition is usually satisfied in precision rotor assemblies. Besides this, the angles between balls are changed within the limits allowed by the cage. The above assumption makes it possible to neglect the effect of the cage and considerably simplify the procedure.

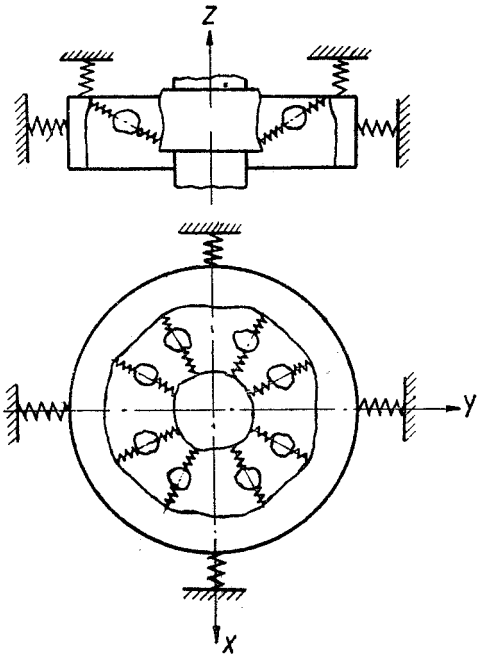

Fig. 3.1. Dynamic model of ball bearing assembly.

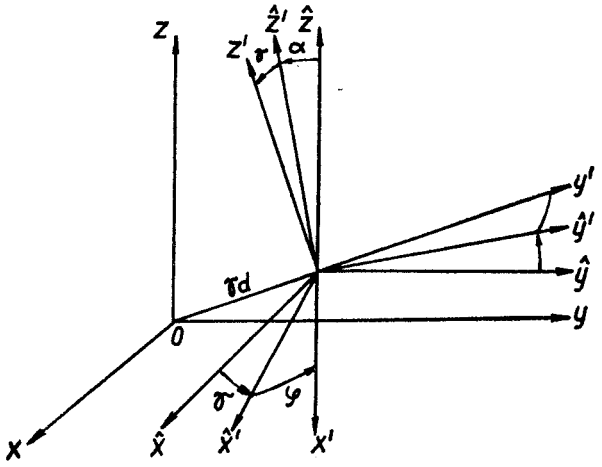

Fig. 3.2. Coordinate system for determination of position of shaft and rings.

Let us now consider the coordinate description of the position of the center of mass and angular position of the shaft and outer ring. Hereinafter by the mass of the outer ring we mean the mass of all components (for example pulley) connected with the outer ring. The shaft has a frame of reference with the moving system of coordinates $x'\ y'\ z'$ with origin at the center of mass C. The coordinate axes x', y', z' represent the major central inertial axes. In the fixed coordinate system $x\ y\ z$ the position of the shaft is determined by the vector $\mathbf{r}_0$ or by the three coordinates x, y, z of the position of its center of mass and by the angles α, γ, φ (Fig. 3.2). The angular transformation of coordinates is formulated by three successive rotations: rotation through an angle α around the axis $\hat{x}$, rotation through an angle β around the axis $\hat{y}$ and rotation through an angle γ around the axis z'. The transformation of the vector components in the coordinate system $x'\ y'\ z'$ into the components of the same vector in the coordinate system $\hat{x}$, $\hat{y}$, $\hat{z}$ is given by the orthogonal matrix

$$A=\begin{Vmatrix} \cos\gamma\cos\varphi & -\cos\gamma\sin\varphi & \sin\gamma \\ \cos\alpha\sin\varphi & \cos\alpha\cos\varphi & \\ +\sin\alpha\sin\gamma\cos\varphi & -\sin\alpha\sin\gamma\sin\varphi & \sin\alpha\cos\gamma \\ \sin\alpha\sin\varphi & \cos\alpha\sin\gamma\sin\varphi & \\ +\cos\alpha\sin\gamma\cos\varphi & -\sin\alpha\cos\varphi & \cos\alpha\cos\varphi \end{Vmatrix}. \quad (3.1)$$

Thus the position of a point in the coordinate system $x'\ y'\ z'$ is related to the position of the same point in the coordinate system $x\ y\ z$ by the matrix equation

$$X = AX' + \mathbf{r}_0. \tag{3.2}$$

where X, X' are column vectors;

$\mathbf{r}_0$ is the vector that determines the position of the center of mass of the shaft.

Similarly the position of a point in the coordinate system $x''\ y''\ z''$ (moving system of coordinates connected with the outer ring, axes $x''\ y''\ z''$—major central inertial axis) and its position in the coordinate system $x\ y\ z$ are mutually connected by the relation

$$X = A'\ X'' + \mathbf{r}_{0''}, \tag{3.3}$$

where A' is a matrix similar to matrix A (only instead of angles α, γ, φ there must be the corresponding angles α', γ', φ', which determine the angular position of the outer ring);

$\mathbf{r}_{0''}$ is a vector which determines the position of the center of the mass of the outer ring.

The projections of the angular velocity of the shaft on the coordinate axis $x'\ y'\ z'$ are expressed by the angular coordinates α, γ, φ of the following equation:

$$\Omega = \begin{Vmatrix} \omega_{x'} \\ \omega_{y'} \\ \omega_{z'} \end{Vmatrix} = B \begin{Vmatrix} \alpha' \\ \gamma' \\ \varphi' \end{Vmatrix}, \tag{3.4}$$

where

$$B = \begin{Vmatrix} \cos\gamma\cos\varphi & \sin\varphi & 0 \\ \cos\gamma\sin\varphi & \cos\varphi & 0 \\ \sin\gamma & 0 & 1 \end{Vmatrix}.$$

In a similar way the projections of the angular speed of the outer ring on the coordinate axes $x''\ y''\ z''$ are related to the angular coordinates $\alpha'\ \gamma'\ \varphi'$. Knowledge of the projections of angular velocity of the shaft and outer ring on the corresponding moving coordinate axes is necessary for computation of the kinetic energy of the system.

In the case in question the basic factors causing the rotor vibrations are manufacturing errors in the rings and rolling elements. These errors appear during manufacture as a result of the occurrence of vibrations in the product when it is turned. The profiles of the raceways of rings in the radial section can be considered as periodic functions of polar angles with a period 2π. Since the displacements in the axial direction are negligible the profile of the raceways in this direction can be considered ideal, such that in rolling the balls have contact all the time with one and the same raceway on the outer and on the inner ring. Then the geometric profile of the outer and inner rings will depend on one angle in the radial plane. The above profiles can be conveniently expressed in cylindrical coordinates

$$\rho = \rho^{(\eta)}, \qquad (3.5)$$
$$z = a_0.$$

Cylindrical coordinates are related to the corresponding moving coordinates of shaft $x'\ y'\ z'$ and outer ring $x''\ y''\ z''$ by the well-known relations

$$z = z',$$
$$\rho = (x'^2 + y'^2)^{1/2}, \qquad (3.6)$$
$$\eta = \tan^{-1}\left(\frac{y'}{x'}\right).$$

The function ρ can be expressed as a periodic function in a Fourier series. Then profiles of the raceways of the outer and inner rings, respectively, are expressed by the following equations:

$$\rho_{\text{ot}}(\eta) = R_{\text{ot}} + \sum_{k=1}^{n} A_k \cos(k\eta + \eta_k), \qquad (3.7)$$

$$\rho_{\text{in}}(\psi) = R_{\text{in}} + \sum_{k=1}^{n} B \cos(k\psi + \psi_k), \qquad (3.8)$$

where R_{ot}, R_{in} are mean radii of the outer and inner rings, respectively;

A_k, B_k are amplitudes of the k-th harmonic component of the profile of corresponding rings;

η_k, ψ_k are phase angles of the k-th harmonic component; n is the number of harmonic components.

It is assumed that the axis of a ball's rotation in an ideal bearing is parallel to the tangent to the profiles along which it rolls. In a real bearing, however, the position of this axis depends on frictional torques appearing at contact points between the ball and the outer and inner rings. As a result both rolling and sliding take place at these points of contact. But due to the different forms of the contact surfaces at points where the ball touches the raceways of the rings the resistance to sliding will also vary. During the rotation of the rotor in radial thrust ball bearing with preload pure rotation usually takes place at the contact point with one ring (where the resistance to sliding is greater). In this case the contact of the ball with the outer and inner rings takes place along two circles: this has been confirmed experimentally by K. Kakyta [43]. After long use, the circle along which contact takes place changes as a result of the influence of the cage and other causes. But it can be taken approximately that the contact of the ball with the rings takes place along a circle and the profile of the ball in contact with the rings is also a periodic function of the polar angle with a period 2π. As in the case of the profiles of the raceway, let us express this function in a Fourier series. The profile of the i-th ball is determined by the following equation:

$$\rho_m^i(\Theta_i)=R_m^i+\sum_{k=1}^{n} C_k^i \cos(k\Theta_i+\Theta_k^i), \tag{3.9}$$

where R_m^i is the mean radius of the i-th ball;

C_k^i, Θ_k^i are the amplitude and phase of the k-th component of harmonic expansion of the profile of the i-th ball.

As mentioned above, the angles between balls are assumed constant. In such a case, for small displacements of the shaft and outer ring the position of the i-th ball is expressed through the angular position of the first ball

$$\varphi_i=\varphi_1+\frac{2\pi_i}{s}, \tag{3.10}$$

where s is the number of balls in the ball bearing.

We will now move on to determination of the potential energy of the system. It is made up of: potential energy caused by the force of gravity; potential energy of the elastic fixture of the outer ring and the potential energy of other deformations of the contacts between the balls and the rings. The relation between the acting force and deformation of the contacts of balls with rings (convergence of rings) in accordance with the Hertz theory of elasticity is expressed in the following way:

$$N=k\,\delta^{3/2}, \tag{3.11}$$

where k is a coefficient that depends on the parameters of the ball bearing [8, 90 and others];

δ is the convergence of rings.

Let us consider how the loading of an ideal ball bearing takes place with the force of preload. By "ideal" we mean a ball bearing whose ball surfaces are spherical and identical, the raceways are ideal toroidal surfaces, there are no mounting defects and the axis of the outer ring coincides with the shaft axis and axis of the inner ring. At the initial moment all the balls make contact with the rings and there are no contact deformations. Let us assume that under the action of the force due to preload (axial force) only the outer ring was displaced by an amount z_δ. In the general case the displacement of the outer ring relative to the shaft $z_\delta - z_0$ affects the convergence of the rings. In the ideal bearing the convergence of rings in the direction of any ball exactly corresponds to each other (Fig. 3.3). As we mentioned, the profiles of the rings in the axial direction in the dynamic model are assumed to be ideal. Hence the ball contact with rings takes place along a straight line passing

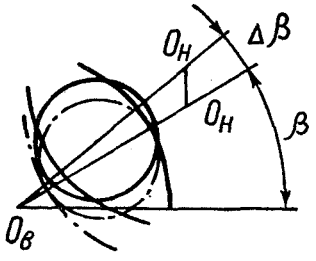

Fig. 3.3. Deformation of contact group (ball-ring).

through O_{ot} and O_{in} (center of curvature of the outer and inner rings in the axial plane). The variation in the distance O_{in} and O_{ot} corresponds to the convergence of rings.

In the case considered above the change in distance $O_{ot}\,O_{in}$ took place on account of the displacement of the outer ring by an amount z_0. In the general case the convergence of rings takes place on account of a change in the relative positions of the shaft and the outer ring along all coordinates. Hereinafter we will be concerned with the convergence of rings in the direction of each of the balls, i.e. for a fixed value of the angle φ_i which determines the position of the i-th ball. Here the fixed position in the moving system of coordinates is occupied by the respective centers of curvature of the outer and inner rings in the axial plane O_{ot} and O_{in}. In the cylindrical moving system of coordinates the position of these centers is given by the following equations:

$$\begin{aligned} z &= z_{ot}, \\ \rho &= R_{ot}, \\ \eta &= \eta_i. \end{aligned} \tag{3.12}$$

In the fixed system of coordinates $x\ y\ z$ the position of centers of curvature $(O_{ot})_i$ and $(O_{in})_i$ is determined by vectors $(r_{ot})_i$ and $(r_{in})_i$ which are expressed through fixed coordinates in moving systems of coordinates (3.2), (3.3)

$$\begin{aligned} r_{ot_i} &= AX'_{in_i} + r_{0'}, \\ r_{in_i} &= A'X''_{ot_i} + r_{0''}. \end{aligned} \tag{3.13}$$

Using equations (3.12) the convergence of rings in the direction of the i-th ball can be expressed in the following way:

$$\delta_i = |\, r_{ot_i} + r_{in_i} \,| - l_0, \tag{3.14}$$

where l_0 is the distance between centers of curvature $O_{ot}\,O_{in}$ in the ideal free bearing without loads.

It follows from equations (3.1), (3.12) and (3.14) that the expression for the convergence of rings δ_i through the coordinate system is difficult and so a linear approximation will be used henceforth:

$$\begin{aligned} \delta_i = \delta_0 + \delta_{0i} + (x - x_1)\cos\beta\cos\varphi_i + (y - y_1)\cos\beta\sin\varphi_1 + (z - z_1)\sin\beta \\ + (\gamma b_1 - \gamma b'_1)\cos\varphi_i + (\alpha\, b_2 - \alpha\, b'_2 \sin\varphi_i) + \rho_{in}(\psi_i)\cos\beta - \rho_{ot}(\eta_i)\cos\beta + d_i(\Theta_i), \end{aligned} \tag{3.15}$$

where $\delta_0 = z_0 \sin\beta$ is the convergence of rings in the ideal ball bearing under the action of the force due to preload;

β is the contact angle;

δ_{0_i} is the convergence of rings in the direction of the i-th ball due to noncoincidence of axes of moving and fixed systems of coordinates at the start;

$b_i,\ b'_i$ are the coefficients;

$\rho_{in}(\psi_i)$ is the magnitude of error in the profile of the inner ring at the contact point with the i-th ball;

$\rho_{ot}(\eta_i)$ is the same for the outer ring;

$d_i(Q_i)$ is the magnitude of error in the diameter of the i-th ball, coinciding with the straight line $(O_{ot})_i\,(O_{in})_i$.

But even in the linear approximation the expression for the convergence of rings δ_i (3.15) is very complex and requires further simplification. In the linear approximation convergence of rings is equal to the sum of projections on the straight line $O_{ot}\,O_{in}$ of the displacements of shaft and outer ring.

The convergence of rings (compression of contacts of balls with rings) is possible not only on account of change of distance $(O_{ot})_i\,(O_{in})_i$, but also as a result of the effect of geometric defects in the raceways of the rings and the balls. By increasing the profile radius of the raceway of the ring additional compression of contacts takes place, which depends, on the basis of linear approximation, on the projection of the geometric error in the ring on the straight line $(O_{ot})_i\,(O_{in})_i$. Thus the effect of geometric defects in the raceways and balls on the compression of rings is taken into account in formula (3.15).

Coefficients b_i, b_i' depend on the fixed coordinates $(z_{in}, z_{ot}, r_{in}, r_{ot})$ of the centers of curvature of the raceways of the rings in the axial plane

$$\begin{aligned} b_1 &= -z_{in}\cos\beta + r_{in}\sin\beta,\ b_1' = z_{ot}\cos\beta - r_{ot}\sin\beta, \\ b_2 &= +z_{in}\cos\beta - r_{in}\sin\beta,\ b_2' = -z_{ot}\cos\beta + r_{ot}\sin\beta. \end{aligned} \tag{3.16}$$

The compression of rings in the direction of the i-th ball and δ_{0_i} is possible as a result of the action of various constants of forces or moments and defects in mounting. One may instance as a constant of forces the force of gravity in the case of a horizontal shaft. During the test on a bearing using flexible joints of small stiffness radial force is developed. This practically does not change for a small displacement of outer ring and can be considered a constant. Among the defects in mounting the most frequent is the twist that can be given in terms of angles α_0 and γ_0. In order to ensure correspondence in the system of the assumed dynamic model the action of the above-mentioned factors should not cause separation of the balls from the raceway, i.e. should not exceed a certain value depending on the force due to preload.

For analytical study of the dynamics of a ball bearing assembly let us formulate the differential equations. The kinetic energy of the system can be expressed in the form

$$\begin{aligned} T = {} & \frac{1}{2} m_s (\dot{x}^2 + \dot{y}^2 + \dot{z}^2) + \frac{1}{2} I (\omega_{x'}^2 + \omega_{y'}^2) + \frac{1}{2} I_p \omega_{2'}^2 \\ & + \frac{1}{2} m_{ot} (\dot{x}_1^2 + \dot{y}_1^2 + \dot{z}_1^2) + \frac{1}{2} I_{ot} (\omega_{x''}^2 + \omega_{y''}^2) + \frac{1}{2} I_{pot} \omega_{2''}^2, \end{aligned} \tag{3.17}$$

where m_s, m_{ot} are the mass of the shaft and the outer ring respectively;

I, I_p, I_{ot}, I_{pot} are the moment of inertia and polar moment of inertia of the shaft and the outer ring respectively;

$\omega_{x'}$, $\omega_{x''}$, $\omega_{y'}$, $\omega_{y''}$ are the projection on the corresponding coordinate axes of the instantaneous angular velocity of the shaft and outer ring, respectively.

The expression of projections of instantaneous angular velocity ω_q' and $\omega_{q'}^*$ through angular coordinates γ, α, φ was shown above (3.4).

The potential energy of the system is expressed in the following way:

$$\Pi = \Pi_p + \Pi_{ot} + \frac{2}{5} K \sum_{i=1}^{s} \delta_i^{3/2}, \tag{3.18}$$

where Π_p is the potential energy due to gravitational force;

Π_{ot} is the potential energy accumulated in the elastic fixture of the outer ring.

The last term in expression (3.18) is the potential energy of compressed contacts of balls with the outer and inner rings of the ball bearing.

To formulate the momentum equations we use Lagrange's method

$$\frac{d}{dt}\left(\frac{\partial T}{\partial \dot{q}}\right) + \frac{\partial T}{\partial q} = Q_k - \frac{\partial \Pi}{\partial q}. \tag{3.19}$$

It follows from expressions (3.17) through (3.19) that the dynamics of a bearing assembly is described by a system of 12 nonlinear differential equations of the second order.

In order to formulate these equations in the general form, besides kinetic and potential energies of the system it is necessary to know the external torque and loads acting on the system. In what follows, a few particular cases are considered with external loads absent except for the torque.

3.2 VIBRATION OF THE OUTER RING OF BALL BEARING AND CONSERVATIVE FRICTION TORQUE

Let us consider the most general case where the outer ring has five degrees of freedom: the position of the outer ring is determined by the three coordinates of the center of mass x_1, y_1, z_1 and angles α_1, γ_1.

The variable friction torque of the bearing is small and does not affect the shaft rotation. The outer ring cannot rotate ($\varphi_1 = 0$).

This is the particular case of the general system considered in the previous paragraph (Fig. 3.1) when the motion of the shaft is described by one equation

$$\varphi = \omega t,$$

where ω is the constant angular speed of the shaft.

*Should be ω_y' and ω_y''—Gen. Editor.

The derivative of potential energy (3.18) with respect to coordinates q_1 ($q_1 = x_1, y_1, z_1, \alpha_1, \gamma_1$) is given by the equation

$$\frac{\partial \Pi}{\partial q_1} = -P_{q_1} + Cq_1 + a \sum_{i=1}^{s} \partial_1^{3/2} \frac{\partial \delta_i}{\partial q_1}, \tag{3.20}$$

where P_{q_1} is the projection of the mass of the outer ring on the corresponding coordinate axis;

C is the column-vector of the stiffness coefficients of the outer ring fixture;

q_1 is the column-vector of coordinates.

The stiffness characteristics of the outer ring fixture are assumed to be linear, as is usually observed for small vibrations of a system. The values of the stiffness coefficients depend on the design of the fixture.

The last term in formula (3.20) is the sum of the loads and torque appearing during displacement of the outer ring in nonlinear springs corresponding to contacts of the balls with the rings. In order to simplify this complex expression we will take the following into account: The deformation caused by the preload δ_0 exceeds the deformation of contacts caused by small displacements of the outer ring, geometrical defects in the raceways of rings and balls and defects in the mounting. In other words, the value of δ_0 forms the major part of the expression for δ_i (compression of rings in the direction of the i-th ball). Hence the expression under the summation sign can be expanded in a power series in terms of the difference $(\delta_1 - \delta_0)$. This difference represents the additional deformation in the direction of the i-th ball and is denoted by δ_i'. Then the last term in expression (3.20) can be represented in the form

$$\frac{\partial \Pi_k}{\partial q_1} = a\delta_0^{3/2} \sum_{i=1}^{s} \left[1 + \frac{3}{2\delta_0} \delta_i' + \cdots + \frac{\prod_{k=1}^{n} (5-2k)}{(2\delta_0)^n n!} (\delta_i')^n \right] \cdot \frac{\partial \delta_i}{\partial q_1}, \tag{3.21}$$

where n is the number of terms in the series to be considered.

This number depends on the ratio δ_i/δ_0. For a relatively large preload and consequently for a large initial deformation δ_0 it is possible to limit ourselves to a linear approximation or to two terms of the series. For smaller preloads (depending on the accuracy desired) it is necessary to consider more terms of the series. In further analysis three terms are taken into account and this allows us to consider the qualitative effect of nonlinearity on the dynamics of the system.

It follows from expression (3.15) that the compression of rings in the direction of the i-th ball depends on the profile radius of the raceways of the rings at the contact points with the balls. When the shaft rotates the ball makes contact with different points of the profile of the raceways. This is explained in the layout in Fig. 3.4. The angular position of the i-th ball and the value of

profile radii of the raceways at the contact points during rotation of the shaft depend on time. When the shaft rotates at a constant speed ω, the expressions for the respective angles will be the following:

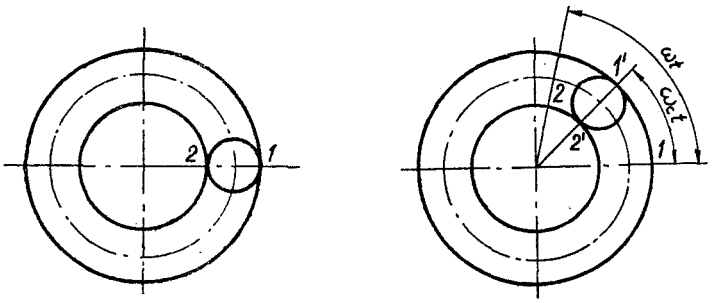

Fig. 3.4. Change in angular position of ball and rings with rotation.

$$\varphi_1 = \omega_c t + \frac{2\pi i}{s}, \tag{3.22}$$

$$\eta_i = \omega_c t + \frac{2\pi}{s}, \tag{3.23}$$

$$\psi_i = (\omega_c - \omega) t + \frac{2\pi i}{s}, \tag{3.24}$$

$$\Theta_i = \omega_b t, \tag{3.25}$$

where ω_c is the angular speed of the cage;

ω_b is the angular speed of the ball with respect to the cage.

The dependence of the values ω_c and ω_b on the angular speed of the shaft and the ball bearing parameters is given in the handbook [90]. In formulas (3.22) through (3.25) it has been assumed for concreteness that at the initial moment ($t=0$) the last ball crosses the x-axis.

Using formulas (3.23) through (3.25) the change with time in the values of geometric errors in the raceways of the rings and the balls can be expressed in the form

$$\rho^i_{ot}(t) = \sum_k A_k \cos\left[k\left(\omega_c t + \frac{2\pi i}{s}\right) + \eta_k\right], \tag{3.26}$$

$$\rho^i_{in}(t) = \sum_k B_k \cos\left[k\left(\omega_{in} t + \frac{2\pi i}{s}\right) + \psi_k\right], \tag{3.27}$$

$$d^i_b(t) = \sum_k 2C^i_{2k} \cos(2k\omega_b t + \Theta^i_{2k}). \tag{3.28}$$

The odd harmonics of the expansion of the ball profile do not affect the compression of the rings (3.15), which depends only on even harmonics and the deviation of the mean diameter from the normal. This last is considered as the component of the expansion $k=0$ in expression (3.28).

The inner ring of the ball bearing can be placed eccentrically on the shaft. The magnitude of the eccentricity in expression (3.27) corresponds to the amplitude of the first harmonic B_1. The geometric axis of the raceway of the outer ring also need not coincide with the axis passing through the center of mass. The value of this eccentricity corresponds to the amplitude of the first harmonic A_1.

The outer ring can be initially displaced by a constant radial load (mass of outer ring, if its axis is not vertical) or by radial load arising from flexible connections of small stiffness (in this case the values of initial displacement are calculated using the formulas of Chapter II). Besides this, the outer ring can have an initial twist due to various mounting defects. The value of the initial twist is given by angles d_{10} and γ_{10}. Thus the additional initial displacement in the direction of the i-th ball δ_{0i} can be expressed in the form:

$$\delta_{0i}=x_{10}\cos\beta\cos\varphi_i+y_{10}\cos\beta\sin\varphi_i+\alpha_{10}\,b\sin\varphi_i+\gamma_{10}\,b\cos\varphi_i. \quad (3.29)$$

All the components of the compression of rings in the direction of the i-th ball are thus determined. Let us return to expression (3.21). The expressions under the summation sign indicate loads caused in the direction of the corresponding coordinate axis by the i-th ball during deformation in this direction. But the rotor is subject to the cumulative load of all the balls and it is desirable to determine the cumulative load. For this we have to sum the loads imposed by individual balls. Under the summation sign the trigonometric functions of sines and cosines in the expression for the deformation δ_i' and its derivatives depend on the order number of the balls. These functions and their derivatives will be under the summation sign when the terms of expansion (3.21) are taken into account. In other words, expressions under the summation sign can be represented in the form of the product of coefficients not depending on the order number of the ball but on the trigonometric functions of cosines and sines of angles that determine the position of each individual ball.

Besides this, under the summation sign there will be terms, not dependent on the order number of the ball, whose summation does not pose any difficulty.

It is possible to show that when the remaining terms are summed with respect to i-the result will be different from zero only in the case where $k=js$, where $j=1, 2, 3, \ldots$:

$$\sum_{i=1}^{s}\cos k\left(\omega_c\,t+\frac{2\pi i}{s}\right)=\begin{cases}0, & k\neq js\\ s\cos k\,\omega_c\,t, & k=js,\end{cases} \quad (3.30)$$

$$\sum_{i=1}^{s}\sin k\left(\omega_c\,t+\frac{2\pi i}{s}\right)=\begin{cases}0, & k\neq js\\ s\sin k\,\omega_c\,t, & k=js.\end{cases} \quad (3.31)$$

The differential equations of motion of the outer ring, taking into account three terms of series (3.21) and correspondingly terms up to the second order of the derivatives of kinetic energy, can be represented in the form:

$$m\ddot{x}+\sum k_{1q}\dot{q}_1+\sum_q c'_{11}q_1+c_{11}x+c_{15}\gamma+r_{11}z+r_{12}xz+r_{13}\gamma z+\sum_q \mu_q q_1=E_x(t),$$

$$m\ddot{y}+\sum k_{2q}\dot{q}_1+\sum c'_{2q}q_1+c_{22}y+c_{24}\alpha+r_{21}z+r_{22}yz+r_{23}\alpha z+\sum \mu_{2q}q_2=E_y(t),$$

$$m\ddot{z}+\sum k_{3q}\dot{q}_1+\sum c'_{3q}q_1+\sum c_{3q}z+r_{31}x+r_{32}y+r_{33}\alpha+r_{34}\gamma+r_{35}x\gamma+r_{36}y\alpha+r_{37}x^2+r_{38}y^2+r_{39}z^2+r_{310}\alpha^2+r_{311}\gamma^2+\sum \mu_{3q}q_1=E_1(t), \tag{3.32}$$

$$I\ddot{\alpha}-I_P\omega\dot{\gamma}+Ek_{4q}\dot{q}_1+\sum c'_{4q}+c_{42}y+c_{44}\alpha+r_{41}z+r_{42}\alpha z+r_{43}yz+\sum \mu_{4q}q_2=E_\alpha(t),$$

$$I\ddot{\gamma}+I_P\omega\alpha+\sum k_{5q}\dot{q}_1+\sum c'_{5q}q_1+c_{51}x+c_{55}\gamma+r_{51}z+r_{52}xz+r_{53}\gamma z+\sum \mu_{5q}q_1=E_\gamma(t)\cdot$$

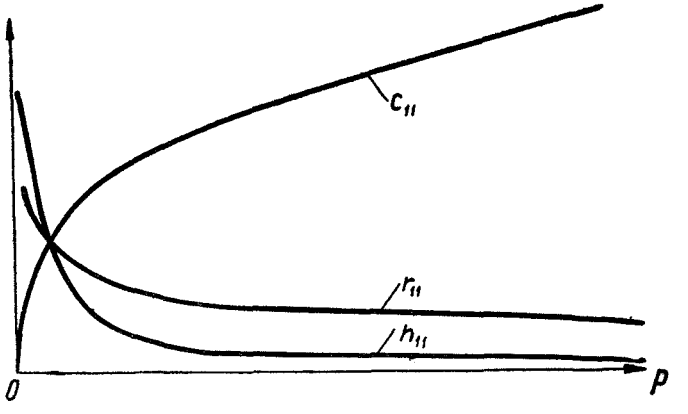

Fig. 3.5. Relation between coefficients c_{11}, r_{11} and h_{11} with rotation.

It follows from these equations that the motion of the outer ring of a ball bearing is described by a system of five nonhomogeneous nonlinear differential equations of the second order with coefficients depending on time.

The values of the stiffness coefficients c'_{iq} are determined by the design of the outer ring mounting. The value of coefficients c_{ij} and r_{ij} depend on the parameters of the ball bearing and on the initial compression of rings δ_0 or on the preload. The dependence of coefficients c_{11}, r_{11} and h_{11} on the force due to preload (Fig. 3.5) is given by the following:

$$\begin{aligned} c_{11} &= a_1 P^{1/3}, \\ r_{11} &= a_2 P^{-1/3}, \\ h_{11} &= a_3 P^{-1}, \end{aligned} \tag{3.33}$$

where a_i are coefficients depending on the ball bearing parameters;

h_{11} is a coefficient of the product of three independent variables in the series for the derivative of potential energy.

It follows from formulas (3.33) and Fig. 3.5 that with an increase in force due to preload the coefficient C_{11} increases but coefficients r_{11} and h_{11} are reduced. Consequently the accuracy of the linear approximation increases.

The quantities r_{ij} in the system of differential equations (3.32) are the coefficients not only of the product of two variables but also of one variable, for example, of the variable r_{11}. In this case coefficients r_{ij} depend not only on the ball bearing parameters and the preload but also on the initial deformations in the direction of the i-th ball δ_{0i} and the eccentricity of the assembly of the rings.

In equations (3.32) coefficients of the variables of the r_{11}-th order depend on time, and μ_{ij} depends on the geometric defects in the raceways of the rings and the balls. As an example, the following are the values of the two coefficients $\mu_{11}(t)$ and $\mu_{33}(t)$ calculated on the assumption that the balls have ideal geometric shape (balls are usually made considerably more accurately than rings):

$$\begin{aligned} \mu_{11}(t) = r_{12} \cot \alpha \sum_j [B_{js} \cos (js\omega_{\text{in}} + \psi_{js}) + 0.5\, B_{js\pm 2} \\ \times \cos (js\omega_{\text{in}} t \pm 2\omega t + \psi_{js\pm 2}) - A_{js} \cos (js\omega_{\text{c}} t + \varphi_{js}) \\ - 0.5\, A_{js\pm 2} \cos (js\omega_{\text{c}} t + \varphi_{js\pm 2})]; \end{aligned} \tag{3.34}$$

$$\mu_{33}(t) = 2r_{12} \tan \alpha \sum [B_{js} \cos (js\, \omega_{\text{in}} t + \psi_{js}) - A_{js} \cos (js\, \omega_{\text{c}} t + \varphi_{js})].$$

From expressions (3.34) it may be seen that the periodic coefficients depend only on certain harmonic components of the series for the ring profiles, and in particular on js, $js \pm 1$; $js \pm 2$ ($j = 0, 1, 2, 3, \ldots$). The first and second harmonics of the series for the profile of the inner ring enter the expressions

for periodic coefficients when $j=0$. The frequencies of periodic coefficients are the following:

$$js\,\omega_c,\ js\,\omega_{in},\ js\,\omega_{in}\pm\omega,\ js\,\omega_{in}\pm 2\omega.$$

In periodic functions corresponding to the action of the outer ring there is one frequency $js\omega_c$ for all equations of the system (3.32). Three different frequencies of periodic functions correspond to the inner ring. If the effect of geometric defects in the rolling elements were considered the frequencies of the periodic functions they caused would be

$$2k\omega_b,\ 2k\omega_b\pm\omega_c,\ 2k\omega_b\pm 2\omega_c.$$

For a more accurate computation and, specifically, with more than three terms in the series (3.21) periodic coefficients would have depended on all the harmonics of the series for ring profiles and the frequencies would have been linear functions of ω and $s\omega_c$.

It is well known [12] that the presence of coefficients that depend on time can lead to sharp increases in the amplitude of vibrations for certain relations of the parameters of the system. These relations of parameters determine the region of dynamic instability of the system. The presence of damping narrows down the region of dynamic instability and the presence of nonlinear terms limits the enlargement of amplitudes.

The zones of instability are distributed near the frequencies that are determined by the simple relation

$$\Theta^*=\frac{2\Omega_i}{k}, \tag{3.35}$$

where Θ^* is the critical value of the frequency of the periodic function $\mu_{ij}(t)$;

Ω_i is one of the eigen frequencies of the system;

$k=1, 2, 3\ldots.$

Usually the geometric defects in the raceways of rings and balls of ball bearings are negligible and hence the excitation coefficients are also small. A dangerous increase in excitation coefficients can be observed only for appreciable eccentricity of the inner ring. Hence it is desirable that all the circular eigen frequencies of the system differ from $0.5\,\omega$. Damping in the bearing as a result of the contact of many elements is relatively large and the system usually works beyond the limits of the region of dynamic instability.

Damping coefficients k_{ij} depend on the damping in the bearing itself and also on the damping of the outer ring mounting. Damping in the dynamic model in question has a linear dependence on speed.

For small vibrations of the system and loads due to preload which ensures unseparated motion of the balls it is possible to consider linearized differential equations. The inclusion of nonlinear terms and terms with coefficients depending on time is necessary only for vibrations in the resonance zone and

zones of dynamic instability. The linearized differential equations of motion of the outer ring have the following form:

$$M\ddot{q}_1 + K\dot{q}_1 + Cq_1 = E_q(t), \tag{3.36}$$

where M is the diagonal inertia-matrix;

K is the matrix of damping coefficients;

C is the matrix of stiffness coefficients.

Coefficients r_{ij}, like c'_{ij} and C_{ij}, form part of the stiffness coefficients matrix. It is necessary to take into account the coefficients r_{ij} for an appreciable twist in the outer ring α_{10}, γ_{10} or with constant radial load.

$$C = \left\| \begin{array}{ccccc} c'_{11}+c_{11} & c'_{12} & c'_{13}+r_{11} & c'_{14} & c'_{15}+c_{15} \\ c'_{21} & c'_{22}+c_{22} & c'_{23}+r_{21} & c'_{24}+c_{24} & c'_{25} \\ c'_{31}+r_{31} & c'_{32}+r_{32} & c'_{33}+c_{33} & c'_{34}+r_{34} & c'_{35}+r_{35} \\ c'_{41} & c'_{42}+c_{42} & c'_{43}+r_{41} & c'_{44}+c_{44} & c'_{45} \\ c'_{51}+c_{51} & c'_{52} & c'_{53}+r_{51} & c'_{54} & c'_{55}+c_{55} \end{array} \right\| \tag{3.37}$$

The matrix of damping coefficients is similar to the above matrix.

The generalized disturbances $Eq(t)$, when we consider n terms of the series of derivatives of potential energy in a power series (3.21), are expressed in the form

$$E_q(t) = K\delta_0^{3/2} \sum_{i=1}^{s} \left(1 + \frac{3}{2\delta_0} f_i + \frac{3}{8\delta_0^2} f_i^2 + \ldots + \frac{\Pi(5-2k)}{(2\delta_0)^n n!} f_i^n\right) \frac{\partial \delta'_i}{\partial q_1}, \tag{3.38}$$

where

$$f_i = \delta_{0i} + [\rho_i^{\text{in}}(t) - \rho_i^{\text{ot}}(t)] \cos\beta + d_i(t).$$

In the linear approximation or taking two terms of the series (3.38) without the effect of the ball, we get the generalized disturbance $Eq(t)$:

$$E'_1(t) = c_{11} \sum_j [A_{js\pm1} \cos(js\omega_i t + \eta_{js\pm1}) - B_{js\pm1} \cos(js\,\omega_{\text{in}} \pm \omega t + \psi_{js\pm1})], \tag{3.39}$$

$$E'_2(t) = c_{11} \sum_j [A_{js\pm1} \sin(js\,\omega_c t + \eta_{js\pm1}) - B_{js\pm1} \sin(js\,\omega_{\text{in}} t \pm \omega t + \psi_{js\pm1})], \tag{3.40}$$

$$E'_3(t) = c_{33} \sum_j [A_{js} \cos(js\,\omega_c t + \eta_{js}) - B_{js} \cos(js\,\omega_{\text{in}} t + \psi_{sj})], \tag{3.41}$$

$$E'_4(t) = c_{11} \sum_j [A_{js\pm1} \sin(js\,\omega_c t + \eta_{js\pm1}) - B_{js\pm1} \sin(j\omega_\Theta st \pm \omega t + \psi_{js\pm1})], \tag{3.42}$$

$$E_5'(t)=c_{51}\sum_j [A_{js\pm1}\cos(js\,\omega_c\,t+\eta_{js\pm1})-B_{js\pm1}\cos(js\,\omega_c t\pm\omega t+\psi_{js\pm1})]. \tag{3.43}$$

On the basis of expressions (3.39) through (3.43) it is possible to conclude that only certain harmonics of the series for ring profiles affect the vibrations of the outer ring in the linear approximation. Harmonics of the series of profiles of the order js cause axial vibrations but harmonics of the $(js\pm1)$ order cause radial and torsional vibrations. Frequencies of vibrations caused by harmonics of the outer ring profile series are given by $js\omega_c$; frequencies of vibrations caused by harmonics of the inner ring profile series are equal to $js\omega_{in}\pm\omega$ (radial and torsional vibrations) and $js\omega_{in}$ (axial vibrations); and frequencies of vibrations caused by geometric defects in balls from $2k\omega_b$ (axial vibrations) and $2k\omega_b+\omega_c$ (radial and torsional vibrations). Each one of the balls influences the vibrations of the outer ring individually. The total effect depends on the sequence of distribution and phases during assembly. Hence the composition of vibrations caused by balls is very difficult. It will be carried out in what follows with the help of the theory of random functions. The initial compression of rings in the directions of the i-th ball δ_{0i} does not cause vibrations in the linear approximation.

In the second approximation in the excitation of vibrations of the outer ring all the harmonics of the series expression for profiles of raceways of rings participate. As an example we will give the generalized disturbances $E_x''(t)$ and $E_z''(t)$ (as before, without the effect of balls);

$$E_x''(t)=0.5\,r_{12}\cot\beta\sum_j\left\{\left[\sum_{l\,b}A_e\,A_m\cos(js\omega_c\,t+\eta_c+\eta_m)\right.\right.$$
$$\left.+B_c\,B_m\cos(js\omega_{in}\,t\pm\omega t+\psi_e\pm\psi_b)-2A_e\,B_m\cos(js\omega_c\,t\pm m\omega t\pm\eta_e\pm\psi_b)\right]$$
$$+\frac{b\gamma_{10}}{\cos\beta}\cdot[A_{js}\cos(js\omega_c\,t+\eta_{js})+A_{js\pm2}\cos(js\omega_c\,t+\eta_{js\pm2})-B_{js}\cos(js\omega_{in}\,t$$
$$+\psi_{js})-B_{js\pm2}\cos(js\omega_{in}\,t\pm2\omega t+\psi_{js\pm2})]+\frac{b\beta_0}{\cos\beta}[A_{js\pm2}\sin(js\omega_c\,t+\eta_{js\pm2})$$
$$\left.-B_{js\pm2}\sin(js\omega_{in}\,t\pm2\omega t+\psi_{js\pm2})]\right\}, \tag{3.44}$$

$$E_2''(t)=0.5\,r_{12}\tan\beta\sum_j\left\{\sum_{l\,b}[A_eA_b\cos(js\omega_c\,t+\eta_e\pm\eta_b)\right.$$
$$+B_c\,B_b\cos(js\omega_{in}\,t+\psi_e\pm\psi_b)-2A_eB_b\cos(js\omega_c\,t\pm m\omega t$$
$$+\eta_e\pm\psi_b)]+\frac{2b\gamma_{10}}{\sin\beta}[A_{js\pm1}\cdot\cos(js\omega_c\,t+\eta_{js\pm1})-B_{js\pm1}$$
$$\left.\times\cos(js\omega_c\,t\pm\omega t\pm\psi_{js\pm1})]\right\}. \tag{3.45}$$

It follows from expressions (3.44) and (3.45) that by including the third term of the series (3.38) further generalization of disturbance depends on the product of amplitudes of the harmonic components of the series for the profiles of raceways of rings and balls and the initial compression of rings δ_{0i}. The orders of the harmonic components contributing to the creation of disturbance should satisfy the following relations:

For generalized disturbances in radial and angular directions

$$m+l\pm 1=js,$$
$$m-l\pm 1=js, \tag{3.46}$$

and for the generalized disturbance in the axial direction

$$m\pm l=js. \tag{3.47}$$

This means that the m-th harmonic of the series for the profile of rings takes part in the excitation of vibrations not with all the components of the harmonic series but only with those satisfying the relations (3.46), (3.47). The second approximation obtained allows us to evaluate the effect of defects in the manufacture of rings on the excitation of rotor vibration. The generalized disturbance $E_q(t)$, which in the linear approximation depends only on certain harmonics of the series for the profile of rings, in the second approximation depends on all the harmonics. Consequently the inclusion of the second approximation is necessary, especially in the cases where the amplitudes of harmonic components js and $js+1$ are small or where certain harmonic components have large amplitudes compared to others. In actual bearings, oval and polygon usually have maximum values, i.e. a few first harmonics of the series for the profiles of rings. Defects in mounting and constant radial forces do not affect the vibration of the outer ring of the ball bearing in the linear approximation. But with geometric defects in the profiles of rings they can cause intense vibrations. Frequencies of vibrations caused by errors in profiles of rings and initial displacement of rings δ_{0i} can be expressed in the following form according to formulas (3.44) and (3.45):

$$is\,\omega_c-n\,\omega, \tag{3.48}$$

where

$$j=0, 1, 2, 3, \ldots; \; n=0, 1, 2, 3, \ldots,$$

and frequencies of vibrations caused by geometric defects in balls in combination with the errors in rings and mounting in the following form:

$$2k\,\omega_b\pm n\,\omega_c\pm p\omega, \tag{3.49}$$

where $p=0, 1, 2, 3\ldots$

In the above analysis the vibrations of the outer ring were considered along five coordinates, i.e. a system with five degrees of freedom. Besides vibrations of rings, as already mentioned, friction torque of the ball bearing

is also measured. Friction torque depends on many factors and has a constant and a variable component. A more detailed description of friction torque in ball bearings will be given in the following chapters. Here we will consider only one of its components, i.e. restoring torque.

Restoring torque is a derivative of φ of the expression for potential energy. In the first approximation, when considering only one term of the power series of the derivatives of potential energy (3.21), restoring torque is expressed in the form

$$M_k' = ks\,\delta_0^{3/2}\left\{\sum_j\left[\frac{js\,\omega_c}{\omega}A_{js}\cos(js\,\omega_c t+\eta_{js})\right.\right.$$
$$\left.+\frac{js\,\omega_{in}}{\omega}B_{js}\cos(js\,\omega_{in}t+\psi_{js})\right]\cos\beta$$
$$\left.+\frac{2k\,\omega_b}{\omega}\sum_{i=1}^{s}\sum_k 2\,C_{2k}^i\cos(2k\,\omega_b t+\Theta_{2k}^i)\right\}. \tag{3.50}$$

It follows from expression (3.50) that restoring torque in the first approximation is directly proportional to the force caused by preload and depends only on certain harmonic components of the series for profiles of rings, in particular on the order js, but does not depend on small displacements of the outer ring along the coordinates q_1 and defects in the mounting (initial compression in the direction of the i-th ball).

In the second approximation, including two terms of the power series (3.21), restoring torque depends on all the harmonic components of the series for the profiles of rings and also on the initial compression in the direction of the i-th ball and displacements of the ring along coordinates q_1. In order to determine restoring torque in the second approximation it is better to solve the system of differential equations (3.36) simultaneously with the equation

$$\frac{\partial\Pi}{\partial\varphi}=k\delta_0^{3/2}\sum_i\left[1+\frac{3}{2\delta_0}\delta_i'+\ldots+\frac{\Pi(5-2k)\,\delta_i^n}{(2\delta_0)^n\,n!}\right]\frac{\partial\delta_i}{\partial\varphi}. \tag{3.51}$$

In certain cases, for a mounting of the outer ring ensuring very small vibrations, it is possible to assume that restoring torque does not depend on displacements of the outer ring. When considering two terms of the power series (3.21) the expression for additional restoring torque becomes

$$M_k''=c_{33}\sum\left\{\sum_{lm}\left[\frac{l\omega_c}{\omega}A_e A_m\cos(js\,\psi_c t+\eta_l\pm\eta_m)+\frac{l\omega_c}{\omega}B_l B_m\right.\right.$$
$$\times\cos(js\,\omega_{in}t+\psi_l\pm\psi_m)-A_l B_m\frac{m\omega+js\,\omega_c}{\omega}\cos(js\,\omega_c t\pm m\omega$$
$$\left.+\psi_m\pm\eta_{js-m})\right]+\frac{2b\,\gamma_{10}}{\sin\beta}\frac{js\,\omega_c}{\omega}[A_{js+1}\cos(js\,\omega_c t$$
$$\left.+\eta_{js\pm1})-B_{js\pm1}\cos(js\,\omega_c t\pm\omega t\pm\psi_{js\pm1})]\right\}. \tag{3.52}$$

It follows from equation (3.51) that when considering the second term of the power series (3.21) restoring torque depends on the product of amplitudes of harmonic components of the series of profiles of rings. The sequence numbers of harmonics must satisfy the relation (3.47). The components M_k'' caused by inaccuracies in balls are not included in formula (3.51).

As already mentioned, restoring torque forms part of the total friction torque of the ball bearing. The above analysis explains the presence of the components of variable friction torque caused by geometrical defects in the manufacture of the raceways of rings and balls.

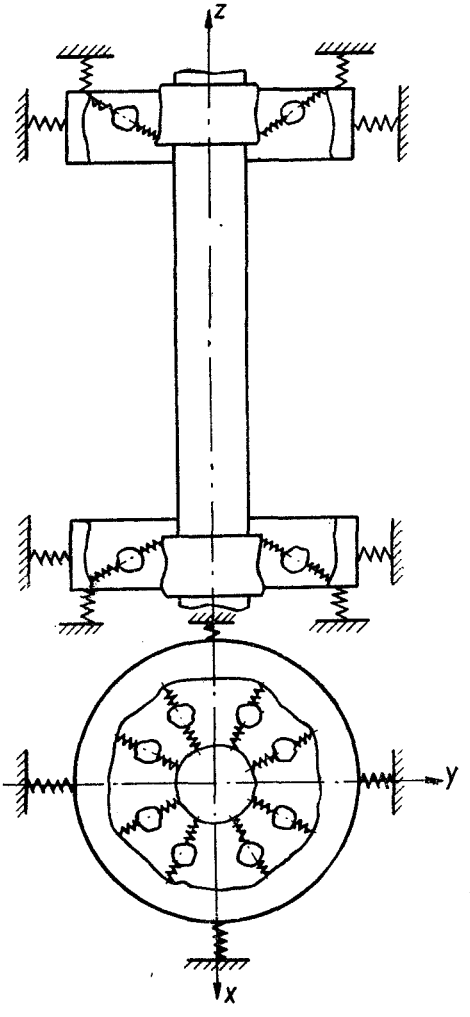

Fig. 3.6. Dynamic model of shaft rotating in two radial-thrust ball bearings with preload.

3.3 VIBRATIONS OF SHAFT ROTATING IN TWO BALL BEARINGS WITH PRELOAD

In the last section we considered the vibrations of the outer ring of a ball bearing without shaft vibrations. In the present section we will consider the vibrations of a shaft rotating at a constant angular velocity in two radial thrust ball bearings with preload. In actual assemblies the shaft mass considerably exceeds the mass of the outer rings and hence the mass of the latter will be neglected. This is also a particular case of the more general system described in section 2.

Fig. 3.6 shows a dynamic model corresponding to a shaft rotating in two ball bearings. In the general case this would have been a system with 18 degrees of freedom. The ball and both the outer rings of the ball bearing would have had six degrees of freedom each. If the shaft rotates at constant speed and if it is possible to neglect the mass of the rings the dynamics of this system can be described by a

system of five second-order differential equations. As we mentioned in the last section, for small amplitudes of shaft vibrations (usually found in precision assemblies) it is possible to consider linearized differential equations. In these nonresonant cases the size of amplitudes of vibrations with and without damping differ negligibly. Hence the motion of the system is described by a system of differential and algebraic equations

$$\begin{aligned} M\ddot{q}+K\dot{q}+C_1(q-q_1)+C_2(q-q_2)&=E_1(t)+E_2(t), \\ C_1'q_1+C_1(q_1-q)&=-E_1(t), \\ C_2'q_2+C_2(q_2-q)&=-E_2(t), \end{aligned} \tag{3.53}$$

where C_1, C_2 are matrices of stiffness coefficients of the 1st and 2nd ball bearings respectively, caused by the elasticity of contacts of balls with rings;

$E_1(t)$, $E_2(t)$ are disturbances caused by geometric defects in the raceways of the 1st and 2nd ball bearings respectively;

C_1', C_2' are matrices of stiffness coefficients of the mountings of the outer ring of the first and second ball bearings respectively.

After some simple transformations the system of equations (3.53) can be brought to the form

$$M\ddot{q}+K\dot{q}+Cq=E(t). \tag{3.54}$$

Here the matrices of stiffness coefficients C and matrix of generalized disturbances $E(t)$ are expressed in the following way:

$$C=C_1-C_1(C_1'+C_1)^{-1}C_1+C_2-C_2(C_2'+C_2)^{-1}C_2, \tag{3.55}$$

$$E(t)=[I-C_1(C_1'+C_1)^{-1}]E_1(t)+[1-C_2(C_2'+C_2)^{-1}]E_2(t), \tag{3.56}$$

where I is a unit matrix,

$(C_1'+C_1)^{-1}$, $(C_2'+C_2)^{-1}$ are inverse matrices.

The matrix of damping coefficient K has the form

$$K=\begin{Vmatrix} k_{11} & k_{12} & k_{13} & k_{14} & k_{15} \\ k_{21} & k_{22} & k_{23} & k_{24} & k_{25} \\ k_{31} & k_{32} & k_{33} & k_{34} & k_{35} \\ k_{41} & k_{42} & k_{43} & k_{44} & k_{45}-I_p\omega \\ k_{51} & k_{52} & k_{53} & k_{54}+I_p\omega & k_{55} \end{Vmatrix}. \tag{3.57}$$

In the matrix (3.57), besides damping coefficients k_{ij}, for the sake of convenience the kinetic moment of the rotor $I_p\,\omega$ has also been conditionally included.

The matrix of stiffness coefficients of ball bearings has the following form:

$$C_1=\begin{Vmatrix} c_{11} & 0 & r_{11} & 0 & c_{15} \\ 0 & c_{22} & r_{21} & c_{24} & 0 \\ r_{31} & r_{32} & c_{33} & r_{34} & r_{35} \\ 0 & c_{42} & r_{41} & c_{44} & 0 \\ c_{51} & 0 & r_{51} & 0 & c_{55} \end{Vmatrix}. \tag{3.58}$$

Here the coefficients C_{ij} and r_{ij} are determined as in the previous section.

The generalized disturbance $E(t)$ (3.56) depends on geometric errors in the raceways of rings and balls of ball bearings and also on the initial compression of rings in the direction of the i-th ball δ_{0i} (3.29). It is the sum of disturbances caused by each ball bearing individually. The latter was considered in detail in the last section. Terms that account for the residual imbalance of the shaft also have a place in the composition of generalized disturbance. The type of these terms is given in the works [69, 102]. In addition the shaft may be affected by external forces and torques that depend on the actual conditions of the working of the assembly. These must also be taken into account when forming the differential equations (3.19).

3.3.1 Statistical Characteristics of Vibrations of Shaft in Standard Ball Bearings

In the previous sections we have considered the vibrations of the outer ring of a ball bearing and a shaft rotating in two ball bearings. These vibrations are caused by defects in manufacture, assembly and mounting of ball bearings and depend on a very large number of factors. For an accurate determination, for example, of the motion of a shaft rotating in two ball bearings, it is necessary to know the exact profiles of the raceways of all the rings and all the balls, the sequence and phase of all balls during assembly, location of rings with respect to one another and all mounting errors. Determination of all these factors encounters serious technical difficulties and besides, some of them change during the operation of the assembly.

In actual conditions the shaft rotates in standard ball bearings with previously unknown errors in both of them. Often it is necessary to know the limits of possible amplitudes of the components of the spectrum of shaft vibrations. This problem can be solved by using the methods of the theory of random functions.

The profile of the raceways of rings and balls of a ball bearing can be considered as a random function having its statistical characteristics for each specific size of ball bearings. The profile of the raceways of each particular ring represents the realization of this random function. In the mathematical operations with random functions the canonical series developed by V.S. Pugachev [76] is widely used, thanks to its simplicity. It is convenient to express random profiles of raceways of rings and balls (3.26) and (3.28) in the form of canonical series:

$$\rho^i_{\text{ot}}(t)=\sum_k\left[H_k\cos k\left(\omega_C t+\frac{2\pi i}{s}\right)+G_k\sin k\left(\omega_C t+\frac{2\pi i}{s}\right)\right], \quad (3.59)$$

$$\rho^i_{\text{in}}(t)=\sum_k\left[U_k\cos k\left(\omega_{\text{in}} t+\frac{2\pi i}{s}\right)+F_k\sin k\left(\omega_{\text{in}} t+\frac{2\pi i}{s}\right)\right], \quad (3.60)$$

$$d_b^i(t)=\sum_k (S_{2k}^i \cos 2k\,\omega_b\, t+T_{2k}^i \sin 2k\,\omega_b\, t). \tag{3.61}$$

Canonical expansion with coordinate functions $\cos k\varphi$, $\sin k\varphi$ is called spectral expansion of the random function. Random coefficients H_k and G_k of spectral expansion (3.59) can be expressed according to expression (3.26) in the form

$$H_k=A_k \cos \eta_k;\ G_k=A_k \sin \eta_k. \tag{3.62}$$

In a similar way the coefficients of spectral expansions (3.60) and (3.61) can be expressed in terms of random amplitudes and phases of series (3.22) and (3.32).

The numerical characteristics of random numbers H_k and G_k can be expressed in terms of the numerical characteristics of random amplitude A_k and random phase η_k. Random amplitude A_k is distributed very nearly according to normal distribution [38, 42] with a mathematical expectation m_{Ak} and dispersion D_{Ak}. It is possible to consider the random phase η_k as distributed according to the law of uniform density in the interval $|-\pi, \pi|$, since any value from this interval is equally probable. Consequently the density of probabilities and numerical characteristics of this random number are equal to

$$f(\eta)=\begin{cases} \dfrac{1}{2\pi}, & -\pi \leqslant \eta \leqslant \pi \\ 0, & -\pi > \eta > \pi, \end{cases} \tag{3.63}$$

$$m_\eta=0,\ D_\eta=\frac{1}{2}\pi^2.$$

The graph of the probabilistic density corresponding to expression (3.63) is shown in Fig. 3.7 a. In Fig. 3.7 b the graph of the function $W=\cos\eta$ in the interval $|-\pi, \pi|$ is shown. The function of the distribution of random function W is expressed in terms of the probabilistic density of random phase η:

$$F(W)=\int_{-\pi}^{-\cos^{-1} W} f(\eta)\, d\eta+\int_{\cos^{-1} W}^{\pi} f(\eta)\, d\eta. \tag{3.64}$$

The probabilistic density and the numerical characteristics of random value W can be expressed on the basis of expression (3.64) in the form

$$f(W)=\begin{cases} \dfrac{1}{\pi\sqrt{1-W^2}}, & -1 \leqslant W \leqslant 1 \\ 0, & -1 > W > 1 \end{cases}$$

$$m_W=0,\ D_W=\frac{1}{2}. \tag{3.65}$$

The graph of probabilistic density $f(W)$ of the random number W is shown in Fig. 3.7 c. The random values A_k and W are independent. Hence the mathematical expectation and dispersion of the random coefficient H_k from expression (3.62) have the following form:

$$m_{H_k}=m_{A_k}\cdot m_W=0, \tag{3.66}$$

$$D_{H_k}=\frac{1}{2}(D_{A_k}+m_{A_k}^2). \tag{3.67}$$

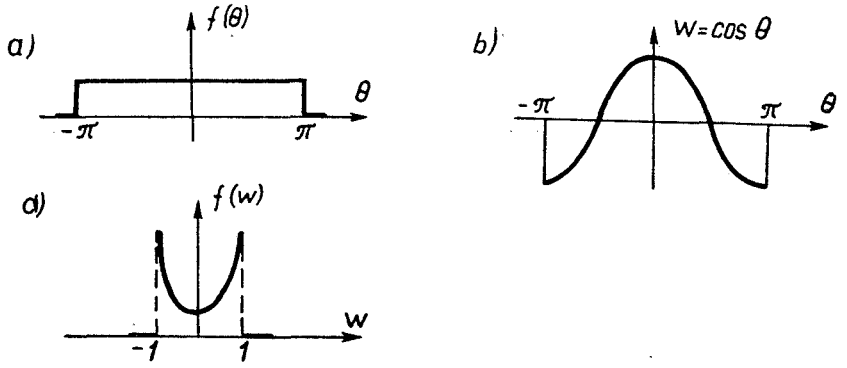

Fig. 3.7. Graphs: *a*—Probabilistic densities of random phase; *b*—function W of random argument; *c*—probabilistic densities of function W.

After similar transformations we obtain the same values of mathematical expectation and dispersions for the random coefficient G_k and also for coefficients U_k, F_k, S_k and T_k.

In the foregoing analysis expressions for the generalized disturbance in linear and second approximations (3.39) and (3.45) were given. When considering the vibrations of a set of shafts in standard ball bearings the respective amplitudes and phases of harmonic components of the series expansion for the profiles it is necessary to take into account random values. Expressions for generalized disturbances can be rearranged using coefficients H_k, G_k, U_k, F_k. For example, the expression for generalized disturbance along the coordinate x in linear approximation, neglecting the effect of balls [equation (3.39)], can be written in the form

$$E_x'(t)=C_{\|}\sum_j [H_{js\pm1}\cos js\omega_c t+G_{js\pm1}\sin js\omega_c t$$
$$+U_{js\pm1}\cos(js\omega_c t\pm\omega t)+F_{js\pm1}\sin(js\omega_c t\pm\omega t). \tag{3.68}$$

The cumulative effect of the balls on the vibrations of the shaft can be more or less than the effect of one ball taken separately (Figs. 3.8 a, 3.8 c, where the effect of the second harmonic is shown conditionally, corresponding to ovality of balls, on the excitation of vibrations). All the balls (Fig. 3.8 a) have identical

ovality and identical phases relative to the rotor. In this case the ovality of the balls does not cause radial vibrations of the shaft. In Fig. 3.8 c the case of relatively large radial vibrations of the shaft caused by the ovality of balls is shown (two groups of balls with opposite phases). This represents the limiting cases. In an actual bearing the phases of the various harmonics of the series expansion for the profile of the balls with respect to the shaft will be different. Hence it is possible to evaluate quantitatively the effect of balls on the excitation of shaft vibrations only by using the principle of random functions.

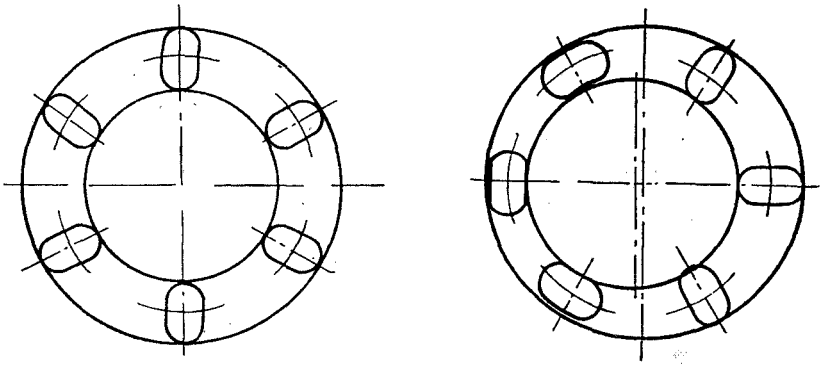

Fig. 3.8. Effect of ovality of balls on vibration of shaft: *a*—all balls having identical phase relative to shaft; *b*—two groups of balls with opposite phases.

Part of the generalized disturbance along the coordinate x caused by balls has the following form in the linear approximation:

$$E'_{xb}(t)=\frac{c_{||}}{s\cos\alpha}\sum_{k}[S_{2k}\cos(2k\,\omega_b\pm\omega_c)\,t+T_{2k}\sin(2k\,\omega_b\pm\omega)\,t], \quad (3.69)$$

where S_{2k} and T_{2k} are random coefficients.

Since each ball affects the excitation of vibrations individually, independent of the others, it is possible to consider the random coefficients S_{2k_i} and T_{2k_i} of different balls to be independent, random values. In this case coefficients S_{2k} and T_{2k}, which are the sum of the corresponding random values S_{2k_i} and T_{2k_i}, have zero mathematical expectation and dispersion

$$D_{S_{2k}}=D_{T_{2k}}=SD_{S_{2ki}}. \quad (3.70)$$

On the basis of the above analysis it is possible to determine the probability characteristics of generalized disturbances $E(t)$ if the probability characteristics of geometric errors in raceways of rings and balls and also the probability characteristics of mounting defects are known. The mounting defects are determined by the method of statistical tests.

3.4 EQUATION OF RADIAL VIBRATIONS OF A SHAFT IN A BEARING DURING RANDOM EXCITATION

Let us assume that an ideally balanced vertical rigid rotor of mass m rotates at a constant speed ω in ball bearings and that it can vibrate only in the radial direction. The scatter of energy in the bearing is assumed to be proportional to the velocity of vibrational motion of the mass.

The stiffness of the bearing is considered as a function of displacement x of the moving ring from the equilibrium position, angle of turn φ of the cage with rolling elements and the preload or initial clearance g. The stiffness is analytically expressed by the relations (2.16) through (2.18).

Let us examine the vibration equation for a setup consisting of bearing with preload whose vibrations considerably exceed the maximum radial displacement of ring-rotor, with a large number of rolling elements. In this case the range of variation in the stiffness of the bearing during rotation is not large and it can be approximated by the expression

$$k=k(x, \varphi, g)=a-bx^2,$$

where coefficients a and b are determined from (2.14).

The equation of the dependence of vibration x of a rigidly balanced shaft in a ball bearing with preload on geometric defects in the manufacture of bearing components that rub together during rotation can be written in the form

$$m\ddot{x}+\beta\dot{x}+ax-bx^3=y(t), \tag{3.71}$$

where $y(t)$ is the random effect caused by the surface roughness of components.

For medium- and large-size ball bearings the coefficient can be considered as relatively small, and equation (3.71) takes the form

$$\ddot{x}+\omega^2 x=\varepsilon(p\dot{x}+qx^3)+\sqrt{\varepsilon}\,h(x, \dot{x})\,y_1(t), \tag{3.72}$$

where $\omega^2=\frac{a}{m}$, $p=-\frac{\beta}{m\varepsilon}$, $q=\frac{b}{\varepsilon m}$; ε is a small positive parameter;

$h(x, \dot{x})$ characterizes the intensity of "white noise" $y(t)$ at the point $(x, \dot{x})$.

Equation (3.72) will henceforth be considered as a system of Ito's stochastic differential equations. By introducing symbols it can be written in the form

$$\begin{cases}\dot{x}=z,\\ \dot{z}=-\omega^2 x+\varepsilon(pz+qx^3)+\sqrt{\varepsilon}\,hy_1(t).\end{cases} \tag{3.73}$$

As is well known, there is a unique Markovian recursive process $\{x(t), z(t)\}$, satisfying the system (3.73) for the initial conditions.

As in the case considered, for the undisturbed system

$$\ddot{x}+\omega^2 x=\varepsilon\,(p\dot{x}+qx^3)$$

the resonance and non-resonance cases are distinct.

In the non-resonance case the variables in equations (3.72) or in the system (3.73) are changed:

$$x=a\cos\psi,$$

$$\dot{x}=z=-a\omega\sin\psi,\quad \psi=\omega t+\varphi \tag{3.74}$$

and we get

$$\begin{aligned}\frac{da}{dt}&=-\frac{\varepsilon}{\omega}\,[qa^3\cos^3\varphi-pa\omega\sin\psi]\sin\psi\\&\quad-\frac{\sqrt{\varepsilon}}{\omega}\,h\,(a\cos\psi_1-a\sin\psi)\,\varphi_1\,(t)\sin\psi_1,\\\frac{d\varphi}{dt}&=-\frac{\varepsilon}{a\omega}\,[qa^3\cos^3\psi-pa\omega\sin\psi]\cos\psi\\&\quad-\frac{\sqrt{\varepsilon}}{a\omega}\,h\cdot(a\cos\psi_1-a\omega\sin\psi)\,\varphi_1\,(t)\cos\psi.\end{aligned}\tag{3.75}$$

It can be seen that a and φ are slowly varying random functions in the interval of time equal to the period of free vibrations $T=2\pi/\omega$.

A two-dimensional Markovian process will be the solution of system (3.75). In order to study it we use the Fokker-Planck-Kolmogorov equation [15] for density $P=P\,(a,\,\varphi,\,t/a_0,\,\varphi_0,\,t_0)$, of simultaneous distribution of amplitude and phase. For the case in question this will be the equation

$$\begin{aligned}\frac{\partial P}{\partial t}&=-\frac{\partial}{\partial a}\,[K_a\,D]-\frac{\partial}{\partial\varphi}\,[K_\varphi\,P]+\frac{1}{2}\,\left\{\frac{\partial^2}{\partial a^2}\,[D_a\,P]\right.\\&\quad\left.+2\,\frac{\partial^2}{\partial a\,\partial\varphi}\,[Da\varphi\,P]+\frac{\partial^2}{\partial\varphi^2}\,[D_\varphi\,P]\right\},\end{aligned}\tag{3.76}$$

where

$$K_a=\lim_{\Delta t\to 0}\frac{M_\Delta\,a}{\Delta t}=-\frac{\varepsilon}{\omega}\,[qa^3\cos^3\psi-\omega ap\sin\psi]\sin\psi,$$

$$K_\varphi=\lim_{\Delta t\to 0}\frac{M_\Delta\,\varphi}{\Delta t}=-\frac{\varepsilon}{a\omega}\,[qa^3\cos^3\psi-\omega ap\sin\psi]\cos\psi,$$

$$D_a=\lim_{\Delta t\to 0}\frac{M_\Delta\,a^2}{\Delta t}=\frac{\varepsilon}{\omega^2}\,h^2\,(a\cos\psi_1-a\omega\sin\psi)\sin^2\psi,$$

$$D_{a\varphi}=\lim_{\Delta t\to 0}\frac{M_\Delta\,a_\Delta\,\varphi}{\Delta t^2}=\frac{\varepsilon}{a\omega^2}\,h^2\,(a\cos\psi_1-a\omega\sin\psi)\sin\psi\cos\psi,$$

$$D_\varphi=\lim_{\Delta t\to 0}\frac{M_\Delta\,\varphi^2}{\Delta t^2}=\frac{\varepsilon}{a^2\omega^2}\,h^2\,(a\cos\psi_1-a\omega\sin\psi)\cos^2\psi,$$

where K_a and K_φ are transfer coefficients;

D_a and D_φ are the coefficients of recursion of amplitude and phase respectively;

$D_{a\varphi}$ is a mixed coefficient of recursion of amplitude and phase.

In solving equation (3.76) as an initial distribution, as is usually done, we take Dirac's distribution

$$P(a_1, \mu_1, t/a_0, y_0, t_0) = \delta(a-a_0)\cdot\delta(\varphi-\varphi_0).$$

This means that $a=a_0$, $\varphi=\varphi_0$ when $t=0$.

One of the relations is the boundary condition which must be satisfied by the solution as distribution function, i.e. $P(a, \varphi, t)\to 0$ when $a\to\infty$, $0\leqslant\varphi\leqslant 2\pi$ and for all t.

It is difficult to obtain the analytical solution of equation (3.76) in the general form. By applying Bogoljubov's mean value theorem it is possible to obtain a solution [10, 11, 64] of equation (3.76) when $\varepsilon\to 0$ to converge uniformly in a rather large but finite interval of time to the solution of the following equation:

$$\frac{\partial P}{\partial t} = \varepsilon\left\{-\frac{\partial}{\partial a}[\overline{K}_a P]-\frac{\partial}{\partial\varphi}[K_\varphi P]\right\}+\frac{\varepsilon}{2}\left\{\frac{\partial^2}{\partial a^2}\left(\overline{D_a(a)}P\right)+2\frac{\partial^2}{\partial a\,\partial\varphi}[\overline{D}_{a\varphi}(a)P]+\frac{\partial^2}{\partial\varphi^2}[\overline{D_\varphi(a)}\cdot P]\right\}, \tag{3.77}$$

where

$$\overline{K}_a(a) = -\frac{1}{2\pi\omega}\int_0^{2\pi}\left(-\frac{\varepsilon}{\omega}\right)[qa^3\cos^3\psi-\omega ap\sin\psi]\sin\psi\,d\psi,$$

$$\overline{K}_\varphi(a) = -\frac{1}{2\pi\omega}\int_0^{2\pi}\left(-\frac{\varepsilon}{a\omega}\right)[qa^3\cos^3\psi-\omega ap\sin\psi]\cos\psi\,d\psi,$$

$$\overline{D}_a(a) = -\frac{1}{2\pi\omega^2}\int_0^{2\pi}h^2(a\cos\psi_1-a\omega\sin\psi)\sin^2\psi\,d\psi,$$

$$\overline{D}_{a\varphi}(a) = \frac{1}{2\pi a\omega^2}\int_0^{2\pi}h^2(a\cos\psi_1-a\omega\sin\psi)\sin\psi\cos\psi\,d\psi,$$

$$\overline{D}_\varphi(a) = \frac{1}{2\pi a^2\omega^2}\int_0^{2\pi}h^2(a\cos\psi_1-a\omega\sin\psi)\cos^2\psi\,d\psi.$$

If the process of vibrations as a random process becomes steady $\left(\frac{\partial p}{\partial t}=0\right)$ with the passage of time it does not depend on initial conditions: the probabilistic density distribution will depend only on the amplitude and phase and will satisfy the steady-state equation in partial derivatives:

$$-\frac{\partial}{\partial a}[\bar{K}_a(a)P_s(a,\varphi)]-\frac{\partial}{\partial\varphi}[\bar{K}_\varphi(a)P_s(a,\varphi)]$$
$$+\frac{1}{2}\left\{\frac{\partial^2}{\partial a^2}[\bar{D}_a(a)P_s(a,\varphi)]+2\frac{\partial^2}{2a\partial\varphi}[\bar{D}_\varphi(a)P_s(a,\varphi)]\right\}=0. \quad (3.78)$$

The stationary density of the amplitude distribution is of greatest interest because its steady-state points (if they exist) correspond to the most probable stable and unstable values of amplitudes of vibrations of the initial system, depending on whether maximum or minimum is obtained at the steady-state points.

When the intensity of "white noise" is expressed by the complete polynomial in cos vt, sin vt, x and $\dot{x}$, then we get the resonance case, i.e. the case where the value of ω is in the neighborhood of one of the numbers $r/s\ v$ or $\omega^2=(r/s)^2+\varepsilon\Delta$, where the expression Δ characterizes the disorder of the system. The system (3.72) takes the form

$$\ddot{x}+\left(\frac{l}{s}v\right)^2 x=\varepsilon[p\dot{x}+qx^3]+\sqrt{\varepsilon}\,h(vt,x,\dot{x})\,y_1(t)-\varepsilon\Delta x. \quad (3.79)$$

After replacing the variables

$$x=a\cos\psi,$$
$$\dot{x}=-\frac{ar}{s}v\sin\psi_1,\ \frac{s}{r}vt+\varphi=\psi_1$$

we obtain a system of equations for the determination of amplitude a and phase φ:

$$\frac{da}{dt}=\frac{\varepsilon\Delta s}{nv}a\sin\psi_1\cos\psi-\frac{\varepsilon s}{rv}\left[a^3 q\cos^3\psi-\frac{ar}{s}vp\sin\psi_1\right]$$
$$\times\sin\psi_1\frac{\sqrt{\varepsilon}s}{rv}h(\acute{vt},a\cos\psi_1-a\omega\sin\psi_1)\sin\psi_1\,y_1(t),$$
$$\frac{d\varphi}{dt}=\frac{\varepsilon\Delta s}{rv}\cos^2\psi-\frac{\varepsilon s}{rva}\left[a^3 q\cos^3\psi_1-\frac{arv}{s}p\sin\psi_1\right]$$
$$\times\cos\psi_1-\frac{\sqrt{\varepsilon}s}{rva}h(vt,a\cos\psi_1-a\omega\sin\psi_1)\cos\psi_1\,y_1(t). \quad (3.80)$$

The system (3.80) also describes a two-dimensional Markovian recursive process with an accuracy to the order of 0 (ε^2):

$$K_a(a,\varphi,t)=\frac{\varepsilon\Delta s}{rv}\sin\psi_1\cos\varphi_1-\frac{\varepsilon s}{rv}\left[qa^3\cos^3\psi_1-p\frac{arv}{s}\sin\psi\right]\sin\psi_1,$$
$$K\varphi(a,\varphi,t)=\frac{\varepsilon\Delta s}{rv}\cos^2\psi_1-\frac{\varepsilon s}{rv}\left(qa^3\cos\psi_1-p\frac{arv}{s}\omega\sin\psi_1\right)\cos\psi_1,$$
$$D_a(a,\varphi,t)=\frac{\varepsilon s^2}{r^2v^2}h^2\left(vt,a\cos\psi_1,-\frac{arv}{s}\sin\psi_1\right)\sin^2\psi_1,$$

$$D_a\varphi(a,\varphi,t)=\frac{\varepsilon s^2}{r^2v^2a}h^2\left(vt,a\cos\psi_1,-\frac{arv}{s}\sin\psi_1\right)\sin\psi_1\cos\psi_1,$$

$$D\varphi(a,\varphi,t)=\frac{\varepsilon s^2}{r^2v^2a}h^2\left(vt,a\cos\psi_1,-\frac{arv}{s}\sin\psi_1\right)\cos^2\psi_1. \quad (3.81)$$

The averaged Fokker-Planck-Kolmogorov equation takes the following form:

$$\frac{\partial P}{\partial t}=\varepsilon\left\{-\frac{\partial}{\partial a}[\overline{K}_a(a,\varphi)P]-\frac{\partial}{\partial t}[\overline{K}_\varphi(\overline{a,\varphi})P]\right\}+\frac{\varepsilon}{2}$$
$$\times\left\{\frac{\partial^2}{\partial a^2}[\overline{D}_a(a,\varphi)P]+2\frac{\partial^2}{\partial a\,\partial\varphi}[\overline{D}_{a\varphi}(a,\varphi)P]+\frac{\partial^2}{\partial\varphi^2}[\overline{D}_\varphi(a,\varphi)\cdot P]\right\},$$

where

$$\overline{K}_a(a,\varphi)=\lim_{T\to\infty}\frac{1}{T}\int_0^T\frac{s}{rv}\left[qa^3\cos^3\psi_1-\frac{parv}{s}\omega\sin\psi_1\right]\sin\psi_1\,dt,$$

$$\overline{K}_\varphi(a,\varphi)=\lim_{T\to\infty}\frac{1}{T}\int_0^T\frac{s}{rva}\left[qa^3\cos^3\psi_1-\frac{1}{s}par\omega\sin\psi_1\right]\cos\psi_1\,dt+\frac{\Delta s}{2rv},$$

$$\overline{D}_a(a,\varphi)=\lim_{T\to\infty}\frac{1}{T}\int_0^T\frac{s^2}{r^2v^2}h^2\left(vt,a\cos\psi_1,-\frac{ar}{s}v\sin\psi_1\right)\sin^2\psi_1\,dt,$$

$$\overline{D}_{a\varphi}(a,\varphi)=\lim_{T\to\infty}\frac{1}{T}\int_0^T\frac{s}{ar^2v^2}h^2\left(vt,a\cos\psi_1,-\frac{ar}{s}v\sin\psi_1\right)\sin\psi_1\cos\psi_1\,dt,$$

$$\overline{D}_\varphi(a,\varphi)=\lim_{T\to\infty}\frac{1}{T}\int_0^T\frac{s^2}{r^2v^2a^2}h^2\left(vt,a\cos\psi_1,-\frac{ar}{s}v\sin\psi_1\right)\cos^2\psi_1\,dt. \quad (3.82)$$

Correspondingly, the stationary Fokker-Planck-Kolmogorov equation for the density of amplitude and phase distribution $P_s(a,\varphi)$ in the general case has the expression:

$$-\frac{\partial}{\partial a}[\overline{K}_a(a,\varphi)P_s]-\frac{\partial}{\partial\varphi}[\overline{K}_\varphi(a,\varphi)P_s]+\frac{1}{2}\int\frac{\partial^2}{\partial a^2}[\overline{D}_a(a,\varphi)P_s]$$
$$+2\frac{\partial^2}{\partial a\,\partial\varphi}[\overline{D}a\varphi(a,\varphi)P_s]+\frac{\partial^2}{\partial\varphi^2}[D\varphi(a,\varphi)P_s]=0. \quad (3.83)$$

The condition that in the resonance case coefficients of transfer and diffusion depend not only on amplitude a, but also on phase φ, somewhat complicates the solution of equation (3.83). The stationary density of amplitude distribution can be found only in a few particular cases obtained with assumptions that impose rigid working conditions on the actual system.

Finally we may mention that an analogous statement of the problem is possible in the case where random perturbations is the normal process with a

correlation function which can be expressed analytically as the sum of damping cosines. In this case it is assumed that the perturbations process can be obtained from "white noise" by allowing the latter to pass through the linear system that is mathematically equivalent to the solution of linear differential equations with random disturbance in the form of "white noise" ξ:

$$\frac{\partial^{\alpha} y_1}{\partial t^{\alpha}}+\beta_{\alpha-1}(t)\frac{\partial^{\alpha-1} y_1}{\partial t^{\alpha-1}}+\ldots+\beta_1(t)\frac{\partial y_1}{\partial t}=\xi. \tag{3.84}$$

Equation (3.84) can be reduced to a system of first-order equations

$$\begin{cases} \dfrac{\partial y_1}{\partial t}=v_1 \\ \dfrac{\partial y_1^2}{\partial t}=\dfrac{\partial v_1}{\partial t}=v_2 \\ \cdot \\ \cdot \\ \cdot \\ \dfrac{\partial v_{\alpha-2}}{\partial t}=v_{\alpha-1} \\ \dfrac{\partial v_{\alpha-1}}{\partial t}=\dfrac{\partial^2 y_1}{\partial t^2}=\beta_{\alpha-1}(t)\, v_{\alpha-1}+\ldots+\beta_1 v_1=\xi. \end{cases} \tag{3.85}$$

By combining the systems of equations (3.85) and (3.73) it is possible to write the Fokker-Planck-Kolmogorov equation corresponding to the new system from $\alpha+2$ equations.

3.5 GENERAL FORMULATION OF THE PROBLEM OF PROBABILITY MODELLING

In the most general case, useful for all classes of probability problems involving dynamic systems, it is possible to suggest the following mathematical formulation:

Let us assume that the system of differential equations is given with respect to the output coordinates $x_1, x_2, \ldots, x_n$ of the dynamic system

$$\frac{dx_i}{dt}=f_i(t_1, x_1, x_2, \ldots, x_n, z_1, z_2, \ldots, z_k, \Theta_1, \Theta_2, \ldots, \Theta_n) \tag{3.86}$$

with initial conditions $x_i(t_0)=x_{i0}$, $i=1, 2, \ldots, n$,

where f_i in the general case is some nonlinear function of the above arguments;

$z_1, z_2, \ldots, z_k$ are random functions of time that model the random effects on the system;

$Q_1, Q_2, \ldots, Q_n$ are random values that model random deviations of the parameters of the dynamic system.

Probability characteristics of random functions $z_1, z_2, \ldots, z_n$ and random

numbers $Q_1, Q_2, \ldots, Q_n$ are also given in the form of moments or distributive laws.

It is necessary to determine the mathematical expectation $M(Z_k)$ based on the system of equations (3.86) and the probability characteristics of random functions and random numbers $\Theta_1, \Theta_2, \ldots, Q_s, z_1, z_2, \ldots, z_m$. In particular cases the latter can be expressed by mathematical expectation and dispersion of output coordinates, integral relations of distribution for certain functions on the output coordinates.

In solving problems in the analysis of dynamic systems using the computer, random functions and random numbers present on the right-hand side of the given system of equations are modeled along their given characteristics. For each selection of values of these random numbers and realization of random functions by numerical methods the system of differential equations is integrated and the numerical integration is carried out a number of times. As a result a number of solutions of the system (3.86) are obtained for different variations in the values of the random numbers and realizations of random functions. Then, depending on the chosen method of analysis, the necessary probability characteristics are computed.

The various methods differ in regard to computation only by the way we choose the variations for the computation using formulas for probability characteristics and by the total number of variations for which it is necessary to carry out numerical integration.

The simplest is the computational scheme (we will be using it) of algorithms developed on the basis of the method of statistical tests (Monte-Carlo).

The sequence of operations by the Monte-Carlo method for the solution of our problem consists of the following stages (we should mention that in the case being analyzed the right-hand sides of equations (3.86) do not depend on the values $\lambda_1, \ldots, \lambda_s$):

1. The selection of random numbers that represent sequences of the corresponding random functions $z_1, \ldots, z_m$, i.e. the selection of the values of random numbers, is made according to the laws of distribution and correlational-spectral characteristics of random functions observed during normal working of the system or at the time of the experiment.

2. Using numerical methods, integration is carried out for the system of differential equations that describe the system being studied for zero initial conditions and concrete numerical values of random functions obtained in step 1.

3. Steps 1 and 2 are repeated a number of times ($10^3 - 10^4$ times). As a result we get a few variations of the solutions of the system for different choices of random functions, i.e. we obtain statistical results

$$y_{1k}(t), y_{2k}(t), \ldots, y_{nk}(t),$$

where k is the number of the variation.

4. The values of the required statistical characteristics of output processes are computed using the formula

$$M(\Phi_k)=\frac{1}{N}\sum_{l=1}^{N}\Phi_{kl}, \tag{3.87}$$

where Φ_{kl} is the required characteristic for the variations.

With the increase in the number of variations N the error decreases at the rate of $1/\sqrt{N}$ [63]. So to obtain the desired accuracy of results by the method of statistical tests it is necessary to carry out numerical integration of the system being analyzed for a large number of variations (10^3-10^4).

Fig. 3.9. Block diagram of statistical tests.

A probability model of the system is built with the help of the computer in the form of individual functional blocks (programs) (Fig. 3.9). The block-diagram GRS works as the generator of independent uncorrelated random signals $q_1, q_2, \ldots, q_n$, and is one of the basic blocks of the probability model. The total number of independent sources of random signals n is determined by the structure of the model of the dynamic system being studied.

In order to transform random signals generated by the block-program GRS into random signals with the given distribution law the block program NT (nonlinear "transformer") is retained in the structural scheme of the probability model. Of course, not all n signals are subjected to transformation because a certain number of them correspond to the requirements of the model.

When designing the probability model it is sometimes necessary to generate correlated random signals for which the dependence of two quantities $x_i(t)$ and $x_i(t+\tau)$ is characterized by a certain correlation function. The block-program described in Fig. 3.9 is also meant for the formulation of dependent random processes with given correlation functions from steady-state random processes with uncorrelated values.

Block-program DS is the model of the dynamic system. In this block input effects x_i are transformed into outputs y_i characterizing the output coordinates of the system.

In order to automatize the process of analyzing the results of the investigation, block-program MSC (measurement of statistical characteristics) is introduced (see Fig. 3.9).

In order to solve equation (3.71) numerically it is converted into a system of two equations

$$\dot{x}_1=\frac{1}{m}\,[y\,(t)-ax_2+bx_2^3-\beta x_1],$$

$$\dot{x}_2=x_1, \tag{3.88}$$

where $$x=x_2,\ \dot{x}=x_1.$$

We will now describe how to solve the system of equations (3.88).

There are different well-known methods of programmed generation of random numbers on the computer [15, 32, 63, 96]. The method we have chosen is based on the fact that while carrying out logical operations of shifts of machine codes, units and zeros fall out randomly because the probability of their appearance depends very little on their presence in the initial numbers. By realizing this method we get a universal data unit of uniformly distributed pseudo-random numbers since in the presence of the data unit uniform numbers in the interval [0, 1] can in principle be realized by any distribution [63].

It has been established by the study of real signals that the magnitudes of the function of geometric errors have normal distribution. The effect of geometric errors is expressed by a linear relation of these same errors. Hence the total effect will also have normal distribution with zero mathematical expectation and dispersion equal to the dispersion of geometric errors multiplied by the number of balls.

Errors in manufacture also have normal distribution and this is taken into account in calculations using a computer by an appropriate change in the dispersion of random numbers.

Uniformly distributed pseudo-random numbers are transformed asymptotically by normal transformation:

$$\eta=\sqrt{3/5}\left(2\sum_{i=1}^{5}g_i-5\right),$$

$$\xi=\eta-0.01\,(\eta^3-3\eta). \tag{3.89}$$

The cumulative value of the effect of errors in the manufacture of components on variable friction torque or on vibrations is given by the signal with the correlation function

$$K_y\,(\tau)=\sum_{k=1}^{n}D_k\,e^{-\alpha_n|\tau|}\cos\beta_k\,\tau. \tag{3.90}$$

This is formed from the signal with the correlation function

$$K_\xi\,(\tau)=G^2\,\delta\,(\tau) \tag{3.91}$$

on the basis of the use of relations

$$S_{yk\,yk}\,(\omega)=|\,W_k\,(j\omega)^2\,|\,S_{\xi\xi}\,(\omega),\qquad k=1,2,\ldots,n, \tag{3.92}$$

connecting the spectral density of the signal and the signal having the correlation function

$$K_{yk}(\tau) = D_k\, e^{-\alpha_k |\tau|} \cos \beta_k \tau$$

which is one of the additives of the formed signal y determined by using the general scheme shown in Fig. 3.10.

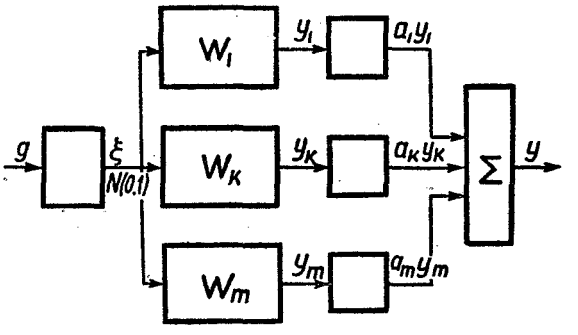

Fig. 3.10. Block diagram for generation of signal having given correlation function.

On the basis of expression (3.92) it is possible to obtain an infinite number of functions $W_k(j\omega)$. The sequential link to the system from transformation function $W_k(j\omega)$ of the element with transformation function

$$W_k(j\omega) = \frac{a - j\omega}{j\omega + a}, \tag{3.93}$$

whose zero and pole are situated symmetrically with respect to the ordinate axis of the plane of the argument ω, does not change the steady-state correlation function of the output signal. The property of invariance of the steady-state correlation function is maintained if a few statistically neutral links with different or identical parameters a in expression (3.93) are linked successively with the system. Of the possible solutions we have to choose the one that describes the stable minimal phase system and is most easily realized, for example, using the method described in the work [87].

In the case in question the system has a transformation function

$$W = \frac{\sqrt{2\alpha_k D_k}\,(\sqrt{\alpha_k^2 + \beta_k^2} + j\omega)}{G\,(\alpha_k^2 + \beta_k^2 + (j\omega)^2 + 2\alpha_k j\omega)}. \tag{3.94}$$

Using this function we determine the equivalent function of digital filter which transforms the uncorrelated numerical sequence $\{\xi(i)\}$ into the sequence $\{y_k(i)\}$, i.e. when random processes ξ and y_k are measured at discrete moments of time $t = i\Delta t$, $y_k = 0, 1, 2, \ldots$. To do this we find the weighted function corresponding to the transformation function (3.94), apply z-trans-

formation (see, for example [97]) and after simple transformations obtain

$$y_k(i)=2e^{-\alpha_k \Delta t}\cos\beta_k \Delta t y_k(t-1)-e^{-2\alpha\Delta t}y_k(i-2)+\frac{\sqrt{2\alpha_k D_k}}{G}$$
$$\times\left\{\xi(i)+\left[\frac{\sqrt{\alpha_k^2+\beta_k^2}}{\beta_k}\sin\beta_k\Delta t-\cos\beta_k\Delta t\right]e^{-\alpha_k\Delta t}(i-1)\right\}. \quad (3.95)$$

The required signal y is determined from the equation

$$y=\sum_{k=1}^{n}a_k y_k, \quad (3.96)$$

where a_k ($k=1, \ldots, n$) is the weighted coefficient equal to unity if the sequence is modeled with the constant interval of "discretization" Δt. When it is necessary to change the interval of "discretization" during the computations we change a_k ($k=1, \ldots, n$) according to the relation [12]

$$D_y=\frac{1}{a}, \quad (3.97)$$

connecting dispersion of the output process y with the number a, which indicates how much the "discretization" interval Δt has been increased. Usually $a=2^m$, $m=\pm1, \pm2$.

In the case of different damping coefficients of correlation functions having analytical expressions (3.90) it is assumed that

$$\frac{S_y{}^i(\omega)}{S_{y_j}(\omega)}=\frac{D_i\alpha_j}{D_j\alpha_i}. \quad (3.98)$$

The accuracy of the working of the algorithm described is illustrated in Fig. 3.11, where the theoretical (continuous line) function is shown along with the function of spectral density obtained by using the algorithm corresponding to the correlation function

$$K(\tau)=e^{-0.01|\tau|}\cos 62.8\tau+0.9e^{-0.021|\tau|}\cos 171.5\tau$$
$$+0.5e^{-0.015|\tau|}\cos 290.4\tau+e^{-0.01|\tau|}\cos 363\tau+e^{-0.5|\tau|}\cos 1{,}042\tau.$$

The solution was obtained for $\Delta t=0.001$ and $\Delta\omega=0.1$.

Let us return to the solution of the system of differential equations.

Equations (3.98) are solved by the Runge-Kutta method [9]. Here we use the particular variation of the Runge-Kutta formulas with an order of accuracy of h^5 at each step (the interval in our case is equal to the step size of the qualification of input signal $h=\Delta t$):

$$\Delta x_i(j)=\frac{1}{6}[k_{1i}+2k_{2i}+2k_{3i}+k_{4i}], \quad (3.99)$$

where Δx_i is the increment in the output signal corresponding to the interval Δt,

$$k_{1i}=\Delta t f_i\left[j\Delta t, x_1(j-1), x_2(j-1)\right],$$

$$k_{2i}=\Delta t f_i\left[\left(j+\frac{1}{2}\right)\Delta t, x_1(j-1)+\frac{k_{11}}{2}, x_2(j-1)+\frac{k_{12}}{2}\right],$$

$$k_{3i}=\Delta t f_i\left[\left(j+\frac{1}{2}\right)\Delta t, x_1(j-1)+\frac{k_{21}}{2}, x_2(j-1)+\frac{k_{22}}{2}\right],$$

$$k_{4i}=\Delta t f_i\left[(j+1)\Delta t, x_1(j-1)+k_3, x_2(j-1)+k_{32}\right]. \qquad (3.100)$$

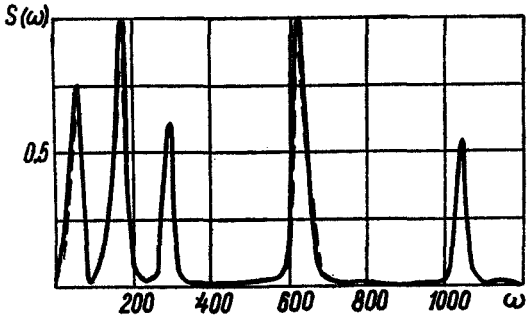

Fig. 3.11. Spectral densities computed from given correlation function (solid line) and from signal developed in computer (broken line).

To save time, the step size can be increased in the neighborhood of values for which the output signal is comparatively large and the error h_5 for $\Delta t_1 = k\Delta t$, $k>1$ is relatively small. In this case the condition of doubling of the step size of "discretization" is determined by the relations

$$\delta_{1i}=8\{\bar{\bar{x}}_i(j)-\bar{x}(j-1)-\tilde{x}(j+1)\},\ \delta_{1i}<\varepsilon_1,\ \delta_{2i}<\varepsilon_1,\ i=1,2, \qquad (3.101)$$

where ε_1 is the required accuracy of the computations;

$\bar{\bar{x}}_i$ is the solution of the system at the point $(j+1)\Delta t$, computed with a step size Δt;

$\bar{x}$ is the solution of the system at the same point but computed with step size $\Delta t/2$;

$\tilde{x}(j)$ is the solution of the system at a point $(j+1)\Delta t$; the values of ε_{1i} can be constant, variable and dependent on the allowable relative error δ, %,

$$\varepsilon_{1i}=\frac{x_j(j)\,\delta}{100}, \qquad (3.102)$$

Here ε_2 is the accuracy to be obtained for doubling the step size of integration.

If even one of the values δ_{1i} is greater than ε_2 the step size remains as before. The solution of the system at the point $(i+1)\,\Delta t$ is corrected using the formula

$$x_i(j+1)=\bar{x}_1(j+1)-\frac{1}{15}\bar{\bar{x}}_i(j+1)-\tilde{x}_1(j+1). \tag{3.103}$$

If even one of the values δ_{1i} is greater than ε_1 the desired accuracy is not achieved, the step size is halved and the integration is continued with a new step size $h_n=\Delta t/2$.

The random sequences obtained for the magnitudes of output signal with the help of the method of linear interpolation are converted into a sequence determined at equidistant points.

Finally let us move on to the determination of the probability characteristics of the output process. The method of determining them for the given solution is described in Chapter IV.

Repetition of the above operation a number of times gives a number of probability characteristics corresponding to each solution of the system. By averaging these characteristics based on their number we obtain the required spectral density and distribution function.

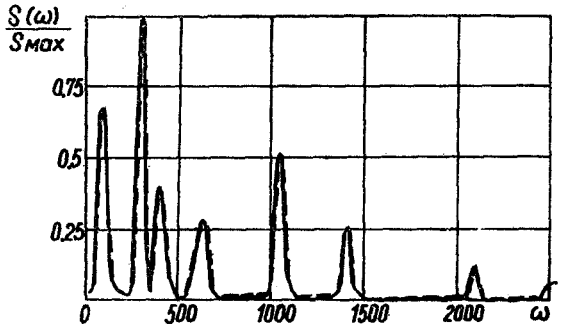

Fig. 3.12. Spectral density of radial vibrations of shaft when $a=4.17$; $b=0.01$; $m=7.14$.

Fig. 3.12 shows the spectral density. In Fig. 3.13 the histogram of the solution of equation (3.71) is shown for the ball bearing C36204E for $a=4.17$ kg/μ, $b=0.01$ kg/μ, $m=7.14$ kg/μ and a rotor angular speed of 900 rpm. The maximum allowable deviation from the circular of the profile of the raceway is taken equal to 5 μ. It has been assumed that there is unevenness with wavelengths equal to 1/3rd, 1/10th and 1/15th of the circumference of the circle. The effect of this surface roughness is explicitly expressed in the spectrum of solution of equation (3.71). According to the formula of combinational frequencies:

$$\Omega=mp+n\omega,$$

where Ω is the combinational frequency of the vibration of the system;

p is the eigen frequency of the system;

ω is the frequency of excitation force;

m and n are integers.

We easily determine that when $m=0$ and $n=1$ and 2 we get frequencies that are multiples of 104 Hz, i.e. equal to 310 and 635 Hz. The latter corresponds to the passage of balls which in this case are six in number. The vibrations with frequencies of 1,040 and 2,080 Hz are explained by the effect of error with the wavelength 1/10th the circumference of the circle. The frequency of 2,550 Hz corresponds to the harmonic with wavelength equal to 1/15th of the circumference.

Verification of the hypothesis on normality according to the criterion χ^2 with 5% level of significance shows disagreement between empirical results and hypothetical assumptions. The Edgeworth series gives a good approximation. Here the mathematical expectation m is equal to 7, dispersion σ^2 is equal to 23, coefficient of asymmetry is equal to 0.021 and coefficient of excess E_k is equal to 0.8720.

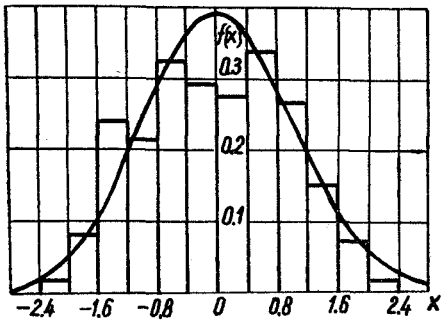

Fig. 3.13. Histogram of radial vibrations of shaft for $a=4.17$; $b=0.01$; $m=7.14$. Continuous line is function of density with normal distribution.

The most complete characteristic of the condition of the dynamic system is the probability description by its laws of distribution of coordinates or functions of the distribution of probabilistic densities. Such a problem has been framed many times, starting with the works of M. Cmonukhovkii and A. Einstein based on the theory of Brownian motion. This direction is connected with the application of the theory of Marcovian processes. The solution of this problem in this case leads to the integration of partial differential equations or to an integral differential equation for the determination of characteristic functions of the coordinate system. These methods are accurate in principle though they lead to difficult algorithms. The complexity of computations is especially marked if the initial random disturbances do not have δ-correlations.

The general equations for determination of the distribution function of the probabilistic density of the integral of the system of differential equations containing random parameters are given in works [53, 77]. Solution of these equations involves massive computations.

Functions of the distribution of vibrations of a rigid shaft in a bearing, caused by geometric errors in the manufacture of the components, are deter-

mined by the method of statistical tests. For this we integrate differential equations (3.88). It is assumed that initial values of the effects have normal distribution corresponding to the actual, since functions of geometric defects in the manufacture of components are subject to this distribution.

Starting from the given initial conditions we integrate equation (3.88) by the Runge-Kutta method and register the values of solution at instants of time where the distribution function is determined.

Since the law of distribution is not unknown in advance the number of variations (repetition of solution) necessary to plot the histogram with the desired accuracy is evaluated by successive analysis of the results obtained in the process of plotting the histogram: after a series of numerical integrations of the system the question of stopping or going on is settled depending on whether the results so far can be trusted for accuracy.

For the purpose of plotting the histogram let the domain of the change in the values of the solution at a given instant of time be divided into certain intervals $\Delta_0, \Delta_1, \ldots, \Delta_m$. Suppose that after carrying out a series of tests consisting of N solutions of the system n_j values fall in the interval Δ_j. A question arises: With what probability can we maintain that the inequality is fulfilled

$$\left| P_{\Delta_j} - \frac{n_j}{N} \right| \leqslant \varepsilon, \tag{3.104}$$

where P_{Δ_j} is the true probability of the random number falling in the interval Δ_j;

ε is the accuracy.

From Chebyshev's theorem it follows that the larger the value, the greater the probability P_0 of the relation (3.104) being fulfilled.

Let us assign the probability P_0. If it is possible to compute the probability

$$P_{j,\,N}\left\{ \left| P_{\Delta_j} - \frac{n_j}{N} \right| \leqslant \varepsilon \right\}, \tag{3.105}$$

then to find the probability P_{Δ_j} it is necessary to continue the numerical integration of the system of equations (3.88) until the following inequality is fulfilled:

$$P_{j,\,N}\left\{ \left| P_{\Delta_j} - \frac{n_j}{N} \right| < \varepsilon \right\} \geqslant P_0. \tag{3.106}$$

From what has been said it is meaningful to develop an algorithm for the computation of a histogram in the following way: Let us carry out a series of integrations consisting of N_1 variations and for each interval Δ_j compute the probability $P_{j,\,N_1}$ using formula (3.105). If for all values j (for all intervals Δ_j) the relation (3.106) holds good, then the computation of the histogram is complete. If not, we carry out a new series of integrations of N_2 variations, for each interval the probability $P_{j,\,N_1+N_2}$ is again calculated, and so on until the inequality (3.106) is fulfilled for all intervals Δ_j.

The probability P_{jN} can be computed using the Moire-Laplace integral theorem [10],

$$P_{j,N}\left\{\left|P_{\Delta_j}-\frac{n_j}{N}\right|\leqslant\varepsilon\right\}\geqslant\frac{2}{\sqrt{2\pi}}\int_0^{\varepsilon\sqrt{N/(1-p)\,p}}\exp\left\{-\frac{x^2}{2}\right\}dx, \qquad (3.107)$$

where

$$p=\frac{n_j}{N}\cdot$$

Using the table of probability integrals we find that a reliability, for example, equal to 90% (2×0.45), corresponds to the argument $x=1.65$. Consequently, to satisfy the last inequality the following condition should be fulfilled:

$$\varepsilon\sqrt{N/(1-p)\,p}\geqslant1.65$$

or

$$\gamma=\varepsilon^2\frac{N^3}{n_j(N-n_j)}\geqslant2.722.$$

The asymptote of the Moire-Laplace formula has sufficient accuracy for values of P that are not too small and not very close to unity. Hence for the evaluation of small probabilities (at the extreme intervals Δ_j) it is better to use Poisson's distribution, whose asymptote is good for small probabilities and probabilities close to unity.

In this case the formula for the computation of probability (3.107) has the form

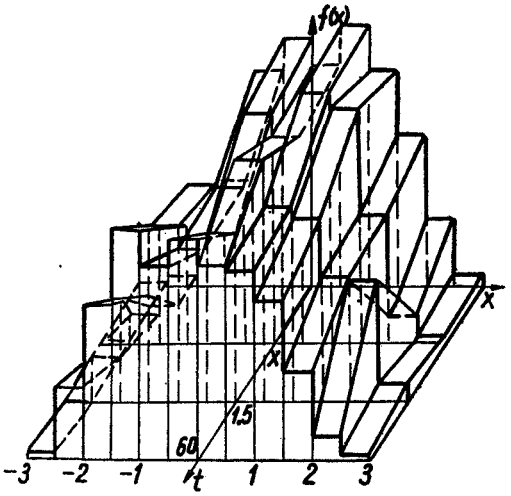

Fig. 3.14. Variation histograms with time for $a=4.17$; $b=0.01$; $m=7.14$ as function of normally distributed N (0; 1) initial conditions.

$$P\left\{\left|P_{\Delta_j}-\frac{n_j}{N}\right|\leqslant\varepsilon\right\}=\sum_{k=1}^{m}\frac{n_j\,k}{k!}\,\mathrm{e}^{-n_j}\,, \tag{3.108}$$

where $$k=n_j-\varepsilon N,\ m=n_j+\varepsilon N.$$

If the histograms are computed for certain values of time the above relations determining when computations may be suspended and the chosen values of time must be satisfied for all the histograms.

In Fig. 3.14 distribution functions are shown for instants of time t equal to 15, 30, 45, 60 sec, obtained as a result of solving equation (3.88) for $a=4.17$, $b=0.01$, $m=7.14$ and for initial values with normal distribution with zero mean values and unit dispersion N (0, 1).

The verification of normality does not show agreement of the experimental results with the hypothesis using the criterion χ with 5% level of significance in any of the above instants of time. The change in the parameter of the functions of the distribution density (we have in mind the mathematical expectation, dispersions, coefficients of asymmetry and excess) indicates in the general case an unsteady process of vibration of the shaft in the bearing.

References

1. Same as [1], Chapter I.
2. Same as [3], Chapter II.
3. Same as [4], Chapter II.
4. Atstupenas, V.R.V. and K.M. Ragulskis. 1969. Vibratsii pretsizionnogo barabana ustroistva magnitnoi zapisi (Vibrations of precision drum of a tape recorder). *Nauchnye Trudy vuzov Lit. SSR, Vibrotekhnika,* No. 3 (8).
5. Banakh, L.Ya., F.M. Dimentberg and N.V. Zvinogrodskii. 1961. O vozniknovenii parametricheskogo resonansa gorizontalno raspolozhennogo vala s gruzom, imeyushchego podshipnik s radial'nym zazorom (Development of the parametric resonance of a horizontal shaft with weight having a bearing with clearance). *Izv. AN SSSR, OTN, Mekhanika i Mashinostroenie,* No. 6.
6. Banakh, L.Ya. 1965. Nekotorye yavleniya, voznikayuskhie pri dvizhenii vala v podshipnike s zazorom (Some aspects of the motion of a shaft in a bearing with clearance). Mashinostroenie.
7. Baranov, I.A. and E.M. Radionov. 1968. Vliyanie tsentrobezhnykh sil, deistvuyushchikh na shariki, na osevuyu zhestkost, bystrovraschayuschegosya radialnoupornogo podshipnika (Effect of centrifugal forces of balls on axial stiffness of a high-speed radial-thrust bearing). *Izv. vuzov, Priborostroenie,* No. 10.

8. Same as [7], Chapter II.
9. Berezin, I.S. and I.P. Zhidkov. 1962. Metody vychislenii. ch. P. [Numerical analysis, Volume I] , Moscow, Fizmatgiz.
10. Bogolyubov, N.N. 1945. O nekotorykh statisticheskikh metodakh v matematicheskoi fizike (Statistical methods in mathematical Physics). Izd. AN SSSR.
11. Bogolyubov, N.N. and Yu.A. Mitropolskii. 1963. Asimptoticheskie metody v teorii nelineinykh kolebanii (Asymptotic methods in the theory of nonlinear vibrations). Moscow, Nauka.
12. Bolotin, V.V. 1956. Dinamicheskaya ustoichivost uprugikh sistem (Dynamic stability of elastic systems). Moscow.
13. Buslenko, N.P. and D.I. Golenko. 1962. Metod statisticheskikh ispitanii (Statistical test techniques). Moscow, Fizmatgiz.
14. Buslenko, N.P. 1964. Matematicheskoe modelirovanie proizvodstvennykh protsessov na tsifrovykh vychislitelnykh mashinakh (Mathematical modeling of production processes on digital computers). Moscow, Nauka.
15. Buslenko, N.P. and Yu.A. Shreider. 1961. Method statisticheskikh ispitanii (Techniques of statistical tests). Moscow, Fizmatgiz.
16. Bochkov, V.S. 1962. Teoreticheskoe issledovanie smescheniyatsentra tyazhesti radialno-upornogo podshipnika pri kombinirovannoi nagruzke (Theoretical study of displacement of the center of gravity of a radial-thrust bearing with combined loading). *Trudy VNIPPa*, 1962, Vol. 32, No. 4.
17. Bochkov, V.S. 1964. Teoreticheskoe i eksperimentalnoe issledovanie osevoi zhestkosti radialno-upornykh sharikopodshipnikov (Theoretical and empirical study of the axial stiffness of radial-thrust ball bearings). *Trudy VNIPPa*, Vol. 38, No. 2.
18. Bolotov, V.E. and I.I. Panov. 1957. Ustanovka dlya izmereniya vibratsii podshipnikov kacheniya (Setup for measurement of the vibrations in rolling contact bearings). *Izmeritelnaya Tekhnika*, No. 4.
19. Boyarinov, V.S. 1966. Issledovanie vibratsii vala, vrashchayuschegosya v sharikopodshipnikakh (Study of the vibrations of a shaft turning in ball bearings). Avtoreferat kand. diss. Gorkii.
20. Boyarinov, V.S. 1966. K voprosu ob usloviyakh vozniknoveniya radialnykh kolebanii vala s udarami v sharikopodshipnikakh (Conditions for radial vibrations in a shaft with shocks in ball bearings). *Izv. vuzov, Radiofizika*, Vol. 9, No. 2.
21. Boyarinov, V.S. 1965. Ob usloviyakh vozniknoveniya radialnykh kolebanii vala s udarami v sharikopodshipnikakh (Radial vibrations in shaft with shocks in ball bearings). *Izv. vuzov, Radiofizika*, Vol. 8, No. 5.
22. Boyarinov, V.S. and Yu.I. Neimark, 1965. O vibratsiyakh vala v sharikopodshipnike (Vibrations of shaft in ball bearing). *Izv. AN SSSR, Me-*

khanika, No. 3.
23. Boyarinov, V.S. and Yu.I. Neimark. 1966. O kolebaniyakh vala v sharikopodshipnike (Vibrations of shaft in ball bearing). In book: *Dinamika Mashin*, Moscow, Mashinostroenie.
24. Brozgol, I.M., E.S. Kuznetsov and K.S. Kogan. 1965. Vliyanie gabritnykh razmerov sharikopodshipnikov na uroven' vibratsii (Effect of the size of ball bearings on the vibration level). *Trudy VNIPPa*, Vol. 43, No. 3.
25. Bykhovskii, I.I. 1969. Osnovy teorii vibratsionnoi tekhniki (Fundamentals of the theory of vibrations). Moscow, Mashinostroenie.
26. Baldman, A.P. and I.A. Tomashuns. 1966. O parametricheskom rezonanse rotora na rolikovykh podshipnikakh (Parametric resonance of the rotor in roller bearings). *Izv. AN Latv. SSR, Seriya fizicheskikh i tekhnicheskikh nauk*, No. 3.
27. Vergiles, A.M., N.A. Spitsyn and L.N. Blokhin. 1968. Stokhasticheskaya model' fluktuatsii momenta sil soprotivleniya vrashcheniyu podshipnikov kacheniya (Stochastic model of fluctuation in friction torque of rolling contact bearings). *Trudy VNIPPa*, No. 3.
28. Vergiles, A.M. 1969. Issledovanie fluktuatsii momentov sil treniya sharikopodshipnikov v atmosfere i vakuume pri povyshennykh temperaturakh (Study of the fluctuations in friction torque of ball bearings in the atmosphere and in a vacuum at high temperatures). Avtoreferat kand. diss. Moscow.
29. Volkov, P.D. and C.G. Atras. 1961. Grannost' rolikov i ee vliyanie na vibratsiyu rolikovykh podshipnikov (Polygonal deformation of rollers and its effect on the vibration of roller bearings). *Trudy, VNIPPa*, Vol. 27, No. 3.
30. Volkov, P.D. and N.N. Gerasimova. 1961. Volnistost' zhelobov naruzhnykh kolets i ee vliyanie na vibratsiyu sharikovykh radialnykh podshipnikov (Waviness of the grooves of outer rings and its effect on the vibration of radial ball bearings). *Trudy VNIPPa*, Vol. 26, No. 3.
31. Gerasimova, N.N. and V.V. Sukhanova. 1965. Issledovanie vliyaniya volnistosti rabochikh poverkhnostei detalei radialnykh sharikopodshipnikov na uroven' vibratsii (Effect of waviness of working surfaces of radial ball bearing components on the vibration level). *Trudy VNIPPa*, 2 (42).
32. Golenko, D.I. 1965. Modelirovanie i statisticheskii analiz psevdoslu-chainykh chisel na elekronnykh vychislitelnykh mashinakh (Modeling and statistical analysis of pseudo-random numbers on computers). Moscow, Nauka.
33. Zhukovskii, I.E. 1937. Analogiya dvukh zadach mekhaniki (Analogy of two problems of mechanics). *Poln. Sobr. Soch.*, Vol. 5.
34. Zhuravlev, V.F. 1970. Zadacha o ravnovesii neidealnogo sharikovogo

podshipnika (Equilibrium of a real ball bearing). *Izv. AN SSSR, Mekhanika tverdogo tela*, No. 4.

35. Zhuravlev, V.F. 1971. Dinamika rotora v neidealnykh sharikovykh podshipnikakh (Dynamics of a rotor in real ball bearings). *Izv. AN SSSR, Mekhanika tverdogo tela*, No. 5.
36. Zmanovskii, V.A. and A.I. Gibert. 1966. Issledovanie dinamikivala v podshipnike s zazorom primenitelno k zadacham akusticheskoi diagnostiki (Dynamics of a shaft in a bearing with clearance, applicable to problems of acoustic diagnostics). *Nauchnye Trudy Sibirskogo filiala VNII mekhanizatsii sel'skogo khozyaistva*, vyp. 3.
37. Same as [18], Chapter II.
38. Kasnauskas, Yu.Yu. 1969. Veroyatnostye otsenki dinamicheskoi tochnosti rotorov, vrashchayuschikhsya v predvaritelno natyanutykh vysokotochnykh sharikopodshipnikakh (Probability estimates of dynamic accuracy of rotors turning in preloaded high-precision ball bearings). *Nauchye trudy vuzov Lit. SSR, Vibrotekhnika*, No. (6).
39. Kasnauskas, Yu.Yu. 1969. Issledovanie dvizheniya vertikalnykh zhestkikh rotorov, Vrashchayuschikhsya v vysokotochnykh, predvaritelno natyamutykh sharikopodshipnikakh (Study of the motion of vertical rigid rotors turning in preloaded high-precision ball bearings). Avtoreferat kand diss., Kaunas.
40. Kasnauskas, Yu.Yu. 1968. Issledovanie dvizheniya vertikalnogo zhestkogo rotora uchetom dinamicheskikh kharakteristik konstruktsii perepleniya naruzhnogo koltsa predvaritelno natyamutogo sharikopodshipnika (Study of the motion of a vertical rigid rotor and dynamic characteristics of fixture design of the outer ring of a preloaded ball bearing). *Nauchnye trudy vuzov Lit. SSR, Vibrotekhnika*, No. 3 (5).
41. Same as [11], Chapter I.
42. Kasnauskas, Yu.Yu. 1968. Eksperimentalnoe issledovanie spektra kolebanii sverkhtochnykh sharikopodshipnikov (Empirical study of the vibration spectrum of super-precision ball bearings). *Nauchnye trudy vuzov Lit. SSR, Vibrotekhnika*, No. (3).
43. Kakuta, K. Issledovanie momenta treniya sharikopodshipnika, nakhodyashchegoya pod oseroi nagruskoi (Study of the friction torque of a ball bearing under an axial load). GPNTB No. 83390, (Translation).
44. Knenidzu, Kh. and Kh. Tamura. Vibratsiya tel kacheniya v sharikopodshipnikakh (ob osevoi vibratsii, vyzvannoi naklonom ploskosti povorota). [Vibration of rolling elements in ball bearings (axial vibration due to inclination of the plane of rotation)]. GPNTB, No. 46743, (Translation).
45. Knenidzu, Kh. and Kh. Tamura. Vibratsiya tel kacheniya v sharikopodshipnikakh (o vliyanii smazki) [Vibration of rolling elements in ball bearings (influence of lubrication)]. GPNTB No. 46742, (Translation).

46. Knenidzu, Kh. and Kh. Tamura. Vibratsiya tel kacheniya v sharikopodshipnikakh (O vzaimosvyazi radialnoi i osevoi vibratsii. (Vibration of rolling elements in ball bearings. Mutual relation between radial and axial vibration). GPNTB No. 46741, (Translation).
47. Knenidzu, Kh. and Kh. Tamura. Vibratsiya tel kacheniya v sharikopodshipnikakh (O zavisimosti mezhdra kriviznoi ploskosti povorota i osevym treniem) [Vibration of rolling elements in ball bearings (relation between curvature of the plane of rotation and axial friction)]. GPNTB No. 46745/1, (Translation).
48. Knenidzu, Kh., Kh. Tamura and Yu. Yaneguti. Vibratsiya tel Kacheniya v sharikopodshipnikakh (o ressopnykh kharak teristikakh) [Vibration of rolling elements in ball bearings (Spring characteristics)]. GPNTB No. 46745/3, (Translation).
49. Same as [12], Chapter I.
50. Same as [15], Chapter I.
51. Kolomiets, V.G. 1968. Sluchainye kolebaniya neavtonomnykh kvazilineinykh stokhasticheskikh sistem (Random vibrations of dependent quasilinear stochastic systems). *Ukrainskii Matematicheskii zhurnal*, Vol. 20, No. 3.
52. Kramer, G. 1948. Matematicheskie metody statistiki (Mathematical methods of statistics). Moscow, IL.
53. Krendel, G.G. 1963. Sluchainye kolebaniya sistem s nelineinymi vostanavlivayuschimi silami (Random vibrations of systems with nonlinear restoring forces). *Trudy Mezhdunarodnogo simposiuma po nelineiinym kolebaniyam Kiev*, Izd. An SSSR.
54. Kryuchkov, Yu.S. 1959. Vliyanie zazora na vibratsii i shum podshipnikov kacheniya (Effect of clearance on the vibrations and noise of rolling contact bearings). *Vestnik Mashinostroeniya*, No. 8.
55. Kryuchkov, Yu.S. 1959. Strukturnyi shum sudorykhmekhanizmov s podshipnikami kacheniya (Structural noise of ship machinery with rolling contact bearings). *Sudostroenie*, No. 2.
56. Kubinek, M. 1964. K voprosu shumnosti podshipnikov kacheniya (The problem of noisy rolling contact bearings). *Trudy VNIPPa*, Vol. 38, No. 2.
57. Kulvets, A.P. 1970. O kolebaniyakh vertikalnogo zhestkogo rotora, vrashchayuschegosya v predvonitelnonatyanutom radialnoupornom sharikopodshipnike (Vibrations of a vertical rigid rotor turning in a preloaded radial-thrust ball bearing). *Nauchnye trudy vuzov Lit. SSR, Vibrotekhnika*, No. 3 (12).
58. Kulvets, A.P. 1970. O kolebaniyakh rotora, vyzyvaemykh netochnostyu izgotovleniya sharikopodshipnikov (Vibrations of a rotor due to manufacturing defects in ball bearings). In book: *Materialy Vsesoyuznogo simpoziuma' novye metody issledovanii shumov i vibratsii kibernetiches-*

kaya diagnostika mashin i mekhanizmov, Kaunas.
59. Kulvets, A.P. 1971. Sluchainye kolebaniya rotora v pretsizionnykh sharikopodshipnikakh (Random vibrations of a rotor in precision ball bearings). In book: *Materialy 3-go Mezhdunarodnogo kongressa po teorii mashin i mekhanizmov.* Dubrovnik (Yugoslavia).
60. Lifschits, Z.B. 1962. Nekotorye voprosy vibratsii i shuma podshipnikov kacheniya (Vibration and noise in rolling contact bearings). *Podshipnikovaya Promyshelennost*, vyp. 3, Moscow. TsNIITMASh.
61. Lyubimov, Yu.K. 1965. Poluchenie na EVM diskretnykh znachenii statsionarnogo sluchainnogo protsessa v nepavnootstoyaschikh tochkakh (Use of the computer to obtain discrete values of a stationary random process at unequally spaced points). *Avtomekhanika i telemekhanika*, Vol. 26, No. 12.
62. Marinin, V.B. 1969. Issledovanie effektnykh metody snizheniya shumnosti i vibratsii radialnykh sharikopodshipnikov (Study of effective methods of noise and vibration abatement in radial ball bearings). *Vibratsionnaya Tekhnika*, Collection 2, Moscow.
63. Metod statisticheskikh ispitanii (Metod Monte-Karlo) (Statistical test techniques. Monte-Carlo method). Ed. Yu.A. Shreider, Moscow, Fizmatgiz.
64. Mitropolskii, Yu.A. 1966. Lektsii po metody usredneniya v nelineinoi mekhanike (Lectures on study techniques in nonlinear mechanics). Kiev, Naukovaya dumka.
65. Same as [24], Chapter II.
66. Same as [25], Chapter II.
67. Same as [26], Chapter II.
68. Pavlov, B.B. 1967. Akusticheskaya diagnostika mekhanizmov (Acoustic diagnosis of mechanisms). Moscow, Mashinostroenie.
69. Same as [27], Chapter II.
70. Panovko, Ya.G. and I.I. Gubanova. 1967. Ustoichivost' kolebaniya uprugikh sistem (Stability and vibrations of elastic systems). Moscow, Nauka.
71. Pervozvanskii, A.A. 1962. Sluchainye protsessy v nelineinykh avtomaticheskikh sistemakh (Random processes in nonlinear automatic systems). Moscow, Fizmatgiz.
72. Same as [28], Chapter II.
73. Pinegin, S.V. and K.V. Frolov. 1966. Vibratsii i shum podshipnikov kacheniya (Vibrations and noise in rolling contact bearings). *Izv. AN SSSR, OTN, Mashinostroenie*, No. 2.
74. Pinegin, S.V. and K.V. Frolov. 1966. Sovremennye problemy vibratsii i shuma podshipnikov kacheniya (Current problems of vibration and noise in rolling contact bearings). In book: *Vibratsii v. mashinostroenie i sel'skokhozyaistvennoi tekhnike*, Erevan.

75. Pontryagin, L.S., A.A. Andronov and A.A. Vitt. 1956. O staticheskom rasmotrenii dinamicheskikh sistem (Static analysis of dynamic systems). *Sobr. Trudov A.A. Andronova.* Moscow, Izd. AN SSSR.
76. Pugachev, V.S. 1962. Teoriya sluchainykh funktsii i ee primenenie k zadacham avtomaticheskogo upravleniya (Theory of random functions and its application to problems of automatic control). Moscow, Fizmatgiz.
77. Pugachev, V.S. 1961. Primenenie teorii markovskikh protsessov k analizu tochnosti avtomaticheskikh sistem (Application of the theory of Marcovian processes to analysis of the accuracy of automatic systems). *Izv. AN SSSR, OTN, Energetika i avtomatika,* No. 3.
78. Reshetov, D.N. 1949. Sovmestnoe deistvie na sharikopodshipniki radialnoi i osevoi nagruzki (Simultaneous action of radial and axial loads on ball bearings). *Podshipniki,* Nos. 10–11.
79. Rodionov, E.M. 1957. O momente soprotivleniya Vroshcheniyu priornogo radialnogo podshipnika (Friction torque in an instrument radial bearing). *Trudy Moskovskogo aviatsonnogo tekhnologicheskogo in-ta,* vyp. 33.
80. Rodionov, E.M. 1964. Momenty, voznikayushchie ot pogreshnosti formy poverkhnosti kacheniya sharikopodshipnikov (Torque due to geometric errors in the rolling surface of ball bearings). *Trudy Moskovskogo aviatsonnogo tekhnologicheskogo in-ta,* vyp. 59.
81. Romanenko, A.F. and G.A. Sergeev. 1968. Voprosy prikladnogo analiza sluchainykh protsessov (Applied analysis of random processes). Moscow, Sov. radio.
82. Rotkop, L.L. 1967. Statisticheskie metody issledovaniya na elektronnykh modelyakh (Statistical study techniques with electronic models). Moscow, Energiya.
83. Rybin, I.I. 1966. Issledovanie vliyaniya pogreshnostei geometricheskoi formy podshipnikov kacheniya na tochnost' balancirovki zhestkikh rotorov na balansirovochnykh stankakh s podvizhnymi oporami i ramnogo tipa (Study of the effect of errors in the geometric form of rolling contact bearings on the accuracy of balancing rigid rotors on balancing machines with moving supports and of mounted type). Avtoreferat kand. diss. Kiev.
84. Same as [32], Chapter II.
85. Svednikov, A.A. 1971. Prikladnye metody teorii sluchainykh funktsii (Applied methods of the theory of random functions). Leningrad, Sudpromgiz.
86. Sivokonenko, I.M. and K.N. Yavlenskii. 1964. Metody izmereniya momenta sil treniya v oporakh tochnykh priborov (Measurement techniques for friction torque in bearings of precision instruments). *Ensiklopediya izmerenii kontrolya i avtomatizatsii,* vyp. 2, Moscow, Leningrad, E'nergiya.

87. Sklyarevich, A.N. 1965. Operatornye metody v statisticheskoi dinamike avtomaticheskikh sistem (Operation techniques in statistical dynamics of automatic systems). Moscow, Nauka.
88. Same as [33], Chapter II.
89. Same as [34], Chapter II.
90. Same as [35], Chapter II.
91. Same as [36], Chapter II.
92. Tallian, G. and O. Gustafsson. 1965. Uspekhi v issledovanii vibratsii podshipnikov kacheniya i snizheniya ikh urovnya (Progress in the study of vibrations in rolling contact bearings and ways to reduce them). *Mekhanika*, No. 6.
93. Tamura, A. 1962. Kolebaniya sharikopodshipnikov. (6-e soobschenie. Kolebaniya podshipnikov pod legkoi nagruzkoi). (Vibration of ball bearings. 6. Vibration of ball bearings under light load). *Nikon, Nikai, gakkai rombuesyu*, Vol. 23, No. 188, GPNTB N 63794, (Translation).
94. Tamura, A. and O. Taniguti. 1963. O subgarmonicheskikh kolebaniyakh poryadka 1/2, vozbuzhdennykh pri dvizhenii sharikov sharikopodshipnikov (Subharmonic vibrations of the order of 1/2 excited by the motion of balls in bearings). *Mekhanika*, No. 3.
95. Tamura, A. and O. Taniguti. 1963. Ob osevykh garmonicheskikh kolebaniyakh, obuslovlennykh dvizheniem sharikov v sharikopodshipnike (Axial harmonic vibrations due to the motion of balls in bearings). *Mekhanika*, No. 3.
96. Taran, V.A., S.S. Brudnik and Yu.N. Kofanov. 1968. Matematicheskie voprosy avtomatizatsii proizvodstvennykh protsessov (Mathematical problems of production processes). Moscow, Vysshaya shkola.
97. Tu Julius T. 1964. Tsifrovye i impulsynye sistemy avtomaticheskogo upravleniya (Digital and impulse systems of automatic control)—Translated from the English, Moscow, Mashinostroenie.
98. Walters. 1971. Dinamika sharikovykh podshipnikov (Dynamics of ball bearings). *Trudy amerikanskogo obshchestva inzhenerov mekhanikov* (ASME Transactions), ser. II, Vol. 93, No. 1.
99. Same as [38], Chapter II.
100. Khayasi, T. 1968. Nelineinye kolebaniya v fizicheskikh sistemakh (Nonlinear vibrations in physical systems). Moscow, Mir.
101. Khennan, E. 1964. Analiz Vremennykh ryadov (Analysis of time series). Moscow, Nauka.
102. Tsze, F.S., I.E. Morze and R.T. Khinkl. 1966. Mekhani-cheskie kolebaniya (Mechanical vibrations). Moscow, Mashinostroenie.
103. Chernetskii, V.I. 1962. Metody vychisleniya veroyatnostnykh Kharakteristik nelineinykh sistem avtomaticheskogo upravleniya (Numerical methods for the probability characteristics of nonlinear systems of automatic control). In book: *Avtomaticheskoe upravlenie i vychislitelnaya*

tekhnika. vyp. 5, Moscow, Mashgiz.
104. Shevchenko, O.I. 1968. Prichiny voznikroveniya Shuma i vibratsii sharikopodshipnikov (Sources of noise and vibrations in ball bearings). Moscow.
105. Sheftel, B.T. 1966. Raschet ozhidaemoi vibratsii sharikopodshipnika ot volnistosti zheloba vnutrennego koltsa (Computation of prospective vibration of a ball bearing due to waviness of inner ring groove). *Mashinostroenie*, No. 6.
106. Sheftel, B.T. and V.A. Gushin. 1964. Vibratsionny uskoreniya obuslovlennye volnistostyu zheloba vnutrennego koltra sharikopodshipnika (Vibrational acceleration due to waviness of the inner ring groove in a ball bearing). *Podshipnikovaya promyshlennost*, vyp. 5.
107. Shtaerman, I.Ya. 1941. K voprosu o mestnykh deformatsiyakh pri szhatii uprugikh tel (Local deformations due to compression of elastic bodies). *DAN SSSR*, Vol. 31, No. 8.
108. Shtaerman, I.Ya. 1949. Kontaktnaya zadach teorii uprugosti (Contact problem of the theory of elasticity). Moscow, Leningrad.
109. Allan, R. 1957. Internal load reactions in rolling bearings. *Mechanical World*, No. 9.
110. Allan, R. 1946. Rolling bearing technique. *Machinery*. London, Vol. 69.
111. Bassler, O. 1963. Der Einfluss von Walzlagern auf die Biegesch-wingungen von Wellen. *Konstruktion*, Heft 5.
112. Bielicki, H. 1962. Wplyw luzu poprzecnego w lozyskach tocznych na dragania walow wirujacych. *Przeglad mechaniczny*, No. 7.
113. Black, H.F. and A.J. Mcternan. 1968. Vibration of a rotating asymmetric shaft supported in asymptotic bearings. *J. Mech. Eng. Sc.*, Vol. 10, No. 3.
114. Ehrich, F.F. 1965. Bistable vibrations of rotors in bearing clearance. *Pap. Amer. Soc. Mech. Eng.*, No. WA/DM.
115. Gunther, D. 1964. Untersuchung der Federung von Hauptschpindel-Lagerungen in Werzeugmaschinen. *Aachen.*
116. Halm, G. 1967. Das Laugerausch von Walzlagen als Guterparameter. *Maschinenbautechnik*, 16, No. 4.
117. Igarashi, T. 1960. Noise of ball bearings. *Bull. JSME*, Vol. 3, No. 9.
118. Igarachi, T. and K. Lida. 1960. Axial vibration humming of small induction motors equipped with ball bearings. *Bull. JSME*, Vol. 3, No. 9.
119. A General Theory for Elastically Constrained Ball and Radial Roller Bearings under Arbitrary Load and Speed Conditions. *J. of Basic Eng., Trans. ASME, Ser. D.*, Vol. 82, No. 2, 1960.
120. Jones, A.B. Some Contributions to Ball Bearing Theory. "*SAE Spec. Public. s. a.*, No. 163.
121. Karlheinz, K. 1960. Die Starrheit des vorgespannten Schragkugellagerpaares bei radialer Belastung. *Industrie-Anzeiger*, Vol. 82, No. 103.

122. Korren, H.W., W. Kirchner and E. Back. 1964. Die bestimmung der Federkennlinien an umlaufenden Walzlagern. *Industrie-Anzeiger*, Vol. 86, No. 29.
123. Kunlenz, K. 1956. Laufgerauschprufung an Walzlagern. *Die Technik*, Heft 10.
124. Lohmann, G. 1953. Untersuchungen des Laufgerausches von Walzlagern. *Konstruktion*, Heft 3.
125. Meldau, E. 1954. Druckverteilung im Radialrillenkugellager. *Werkstatt und Betrieb*, Vol. 87, Heft 2.
126. Meldau, E. 1956. Druckverteilung im Radialrillenkugellager bei Belastung durch Einzelkraft und Moment. *Werkstaff und Betrieb*, Vol. 89, Heft 4.
127. Meldau, E. 1955. Druckverteilung in Radialrillenkugeller bei reiner Moment Belastung. *Werkstatt und Betrieb*, Vol. 88, Heft 4.
128. Mitra, G. and S.K. Basu. 1965. Preloading of Bearing in a Machine Tool. *J. Instr. Eng., Mech. Eng. Div.*, Vol. 45, No. 11.
129. Neubert, G. 1968. Der Einflus der Lager auf den Lauffehler einer Walzgelagerten Werkzeugmaschinen—Haupttspindel. *Maschinenbautechnik*, Vol. 17, Heft 6.
130. Neubert, G. 1968. Die Fehler der Walzlager im Zusammenhang mit dem Lauffehler einer Wekrzeugmachinen—Hauptspindel. *Machinenbautechnik*, Vol. 17, Heft 8.
131. Perret, H. 1950. Die Berechnung der elastichen Vervormung von Rillenkugellagern. *Konstruktion*, Vol. 2, Heft 5.
132. Perret, H. 1950. Elastisch Spielschwingungen konstant belasteter Walzlager. *Verkstatt und Betrieb*, Vol. 83, Heft 8.
133. Perret, H. 1952. Schwingengen in Walzlagern bei statisch bestimmter Abstutzung.—*VDJ—Forschungsheft*, Heft 434.
134. Pesante, M. 1962. Study on the Noise Induced by Rolling Bearings. *Rivista RJV*, No. 14.
135. Ropinceanu, N.G., D. Nastase, M.D. Gafiteanu, T. Giosan and M. Paun. 1962. Beitrag zue Untersuchung der Laufgerauschbestimmung an Walzlagern. *Bul. Inst. politechn. Jasi*, Vol. 8, No. 3–4.
136. Schreiber, H.H. 1961. Die axiale Federung von Kugellagern. *Industrie-Anzeiger*, Vol. 83, No. 79.
137. Schreiber, H.H. 1963. Die Steifigkeit des vorgespannten zylinder rollenlagers. *Walzlagertechnik*, Heft 1.
138. Stanl, U.K. 1967. Einflussee der Walzlagerung auf die Rotierende Welle. Stuttgart.
139. Streger, A. 1958. Theoretische Uberlegungen zue Entstehung des Laufgerausches von Walzlagern. *Die Technik*, No. 5.
140. Szoke, B. 1961. Die grunderscheinung der Kugellageraschwingung. *Maschinenbautechnik*, Vol. 10, No. 12.

141. Szoke, B. 1950. The possibility of Kinetik Vibrations in Autofriction Bearings. *Acta Technica Academiar Scientiarum Hungaricae*, Vol. 25, Fasc. 1–2.
142. Scucki, T. 1965. Obliczenie sztywnosci lozyska kulkowego zwyk lego. *Zeszyty Naukowe politechniki Warszawskiej, Budownictwo*, No. 27.
143. Szucki, T. 1966. Swobodne drgania walow zamocowanych w lozyskach tecznych kulkowych. *Archyvum budowy maszun*, Vol. 18, zeszyt 4.
144. Scieszko, J. 1960. Odksztelcenia sprezyste walcowych lozysk tocznych. *Przeglad mechaniczny*, Vol. 25, No. 24.
145. Tamura, A. 1968. On the Vibrations caused by Ball Diameter Differences in a Ball Bearing. *Bull. ISME*, Vol. 11, No. 44.
146. Tamura, H. and H. Shimizu. 1967. Vibration of rotor based on ball bearing, 2 rept. Static stiffness of ball bearing containing a small number of balls. *Bull. ISME*, Vol. 10, No. 41.
147. Tamura, A. and O. Taniguchi. 1960. Ball bearing vibrations, first report. On the radial vibration caused by bearing balls.—*Trans. ISME*, Vol. 26, No. 161.
148. Tamura, A. and O. Taniguchi. 1961. Ball bearing vibrations, Fourth Report. On the nonlinear vibrations in axial direction.—*Trans. ISME*, Vol. 27, No. 179.
149. Unterberger, M. 1956. Garauschuntersuchungen an Walzlagern in Elektromotoren. *VDJ—Zeitschrift*, Vol. 98, No. 6.
150. Wigotsky, V.W. 1964. Designing with noise-free ball bearings. *Design News*, Vol. 19, No. 6.
151. Wiche, E. 1967. Radiale Federung von Walzlagern bei beliebiger Lagerluft. *Konstruktion*, Vol. 19, No. 5.

4

MEASUREMENT TECHNIQUES AND INSTRUMENTS FOR MEASUREMENT OF DYNAMIC CHARACTERISTICS OF BEARINGS

The different parameters of bearings are checked by special setups and instruments. Depending on the nature of the requirements of instrument bearings verification of all the parameters of the bearings can often be replaced by determination of the friction torque and, when necessary, vibrations of the bearing rings.

In this case the friction torque and vibrations of the bearings to be measured can be divided into the following groups:

a) friction torque of bearing contact (contact torque);

b) friction torque in the dynamic condition consisting of constant and variable components of friction torque;

c) spatial vibrations of bearings consisting of vibrations of bearing rolling elements in the axial and radial directions.

These methods and instruments for the measurement of friction torque and vibrations can be classified into groups with the following general requirements:

1. High accuracy of measurements exceeding the accuracy of the instruments in which the bearings are mounted.

2. High sensitivity that allows measurement of the parameters of miniprecision bearings.

3. Conditions of measurement that must fully initiate the operational range of the bearings.

4. Minimum inertia of the sensing element of the measuring setup.

5. Minimum nonlinearity. The working conditions of many bearings differ so much that friction torque and vibrations during operation sometimes change by more than two orders of magnitude. Hence the range of measuring instruments should be large and linear.

6. Universality and simplicity of maintenance for different types of bearings (this is especially important for shop control).

7. The possibility of measurements with simultaneous recording of readings.

8. High productivity of measurements.

Such high demands sometimes involve finding different variations of the solution of the problem for each individual case so that the principle and methods vary for apparently similar measurements.

4.1 MEASUREMENT OF FRICTION TORQUE AND VIBRATIONS OF BEARINGS

The friction torque of a bearing is a function of many variables. Analytical determination is almost impossible where it appreciably affects the working of the complete assembly or machine. The study and determination of the components of friction torque in bearings started simultaneously with the appearance of precision instruments, in the first place, navigation instruments. In the last couple of decades this parameter has become the decisive factor in evaluating the quality and suitability of a bearing for application in instrument rolling contact bearings.

The working principle of the majority of instruments and stands for the measurement of friction torque is based on the fact that the forces acting on the moving part of the torque meter—transducers assembly deflect it from the initial equilibrium position. The moving part of the torque meter is maintained in equilibrium in this new position under the action of two opposing forces: the force due to the object being measured (in this case, the friction torque in the bearing) and the reacting force due to the elastic number of the torque meter that records the quantity to be measured.

In the majority of cases the measurement of vibrations is based on the contactless method of measuring displacements.

First of all, the methods for measuring friction torque can be divided into two groups: direct and indirect. The following methods belong to the first type:

1. Mechanical, in which the following methods are included:

Direct reading, where the torque to be measured is read and recorded directly from the instrument scale without additional effort or transformation. Instruments of the pendulum type, setups for rundown of the rotor, mechanical friction balances and others belong to this group. As a rule, direct reading instruments are meant for measurement of the mean value of the constant friction torque component and contact torque-static torque.

Pneumatic, based on the use of pneumatic systems for the creation of a force balancing the friction torque, for example, membranes and others.

Optical, in which optical systems are used to increase the accuracy of reading and recording the torque.

Strain gauge, which has high sensitivity and is very useful especially when using semiconductor resistance strain gauge transducers as a torque meter.

Piezoelectric, in which piezotransducers are used as the sensitive element

and the working principle is based on the formation of electromagnetic energy under the action of the load on the piezo-element. The temperature error in the transducer does not exceed $\pm 5\%$ in the interval $-10°$ to $+70°$C. However, the use of piezotransducers is restricted to measurement of the variable component of friction torque.

Capacitor type, in which the effect of a mechanical system is realized as torque in the capacitor transducer.

Mechanotron, in which a mechanotron is used as a transducer.

All the mechanical methods of measurement are based on the use of a mechanical system that introduces torque which balances the friction torque of the bearing. Depending on the method of reading, usually by the use of transducers, the mechanical measuring technique embraces the above methods. It would be possible to supplement this list by a full series of methods not mentioned here. The choice depends on the transducers used.

2. The next group of methods is electro-mechanical techniques. A series of instruments has been devised using this principle. In instruments embodying this method the balancing torque is created by electro-mechanical systems usually in association with signal indicators that show the change in friction torque and its constant component, which is proportional to the balancing torque. According to the torque transducers used to create the balancing force and signal transducers, the electro-mechanical method may be subdivided:

Photoelectric technique. This method is based on use of the large number of instruments and setups incorporating photoelectric elements, which far outnumber all others.

Inductive method. In instruments incorporating this method inductive transducers are used both to create balancing torque and to measure it.

Electro-magnetic technique. In some setups electro-magnetic systems are used.

Induction method. In instruments employing this method inductional functional converters with magnetic systems of the type of an electrical machine are used. The advantages of this method are the small ratio of residual signal to torque, the symmetry of the characteristic of output stress when the rotor is displaced to either side and the small balancing torque. As a rule a linear characteristic of the output stress in induction transducers makes up a few degrees, which is quite enough for the measurement of friction torques in bearings.

Transformer method. Rotating transformers with distributed windings and uniform air gap with rotor and stator having built-in poles are used.

3. Magnetic method. It is possible to classify this as a separate group since there are instruments in which permanent magnets are used and angular displacement is measured.

It would be possible to add a complete series of methods to the direct measuring techniques but all of them belong to the above three basic groups.

Besides direct methods there are indirect methods of determining the components of friction torque in rolling contact bearings. The method of measuring active electrical resistance and the method of measuring capacitance have found widest application. These methods boil down to measurement of the thickness of the lubricating film, which is directly connected with changes in friction torque. This problem has been and is being studied by many scientists [26, 90]. As mentioned earlier, the hydrodynamic theory of lubricants developed by Academician P.L. Kapitsa is the basis of this method.

The theoretical conclusions of the work of Academician Kapitsa on the study of hydrodynamic phenomena in rolling contact bearings objectively reflect the actual processes taking place therein.

Based on this theory it is possible to obtain analytical expressions for power spent on overcoming friction torque in rolling contact bearings.

The maximum power lost on friction U_m during the rolling of a ball is

$$U_m=\frac{12\ \pi\ v^2\mu\ \sqrt{\alpha}}{(2\beta+3\alpha)\sqrt{\beta}}\sin^{-1}h\sqrt{\frac{\beta}{h_0}} \tag{4.1}$$

for $\alpha l_2^2 \gg h_0$,

where $v^2=\omega_1\frac{R\cdot R_0}{R\mp R_0}$ is the velocity of longitudinal motion of the contact point during the rolling of the cylinder;

ω_1 is the angular speed of the ball with respect to the surface of the ring;

R is the ball radius;

R_0 is the raceway radius; the plus sign is used when the rolling takes place along the cylinder (the case of a ball rolling along the inner ring), the negative sign for rolling along the ring (along the outer ring) ($\mu=\mu_0\ e^{\gamma p}$ is the viscosity of the lubricant, where μ_0 is the viscosity at atmospheric pressure);

γ is the piezocoefficient of the lubricant;

p is the pressure;

$$\alpha=\frac{1}{2}\left(\frac{1}{R}\mp\frac{1}{R_0}\right);\quad \beta=\frac{1}{2}\left(\frac{1}{R}\mp\frac{1}{R_2}\right);$$

R_2 is the radius of the raceway (in the plane normal to the rolling plane). The plus sign is taken where the centers of corresponding circles of rolling R and R_0 or R and R_2 are on one side of the contact point;

$2m$ is the width of the lubricating layer;

h_0 is the thickness of the hydrodynamic film of lubricant.

If the value of β is small (radius of raceway close to the ball radius), then approximately

$$U_m = \frac{4\pi v^2 \mu m}{\sqrt{h_0 \alpha}} \text{ for } m^2 \beta \ll h_0 \text{ and } \beta \ll \alpha. \tag{4.2}$$

From this formula it is possible to obtain the value of the total maximum power in the bearing:

$$U_c = \sum_{i=1}^{z} U_{m_{1i}} + \sum_{i=1}^{z} U_{m_{2i}}, \tag{4.3}$$

where z is the number of balls;

$U_{m_{1i}}$, $U_{m_{2i}}$ are the power losses in the clearance between the ball and the inner and outer rings, respectively.

Then the friction torque in the bearing is written in the following way:

$$M_2 = \frac{U_c}{\omega}, \tag{4.4}$$

where ω is the angular speed of the ring.

When the value of β is small,

$$M_2 = \frac{4\pi\mu}{\omega}\left(\frac{v_1^2}{\alpha_1}\sum_{i=1}^{z}\frac{m_{1i}}{h_{01i}} + \frac{v_2^2}{\alpha_2}\sum_{i=1}^{z}\frac{m_{2i}}{h_{02i}}\right), \tag{4.5}$$

where indices 1 and 2 represent the inner and outer rings, respectively.

Here we assume that $\mu = \text{const}$ since the load in the bearing is assumed to be small. If we also neglect the sliding of balls we can assume $v_1 = \text{const}$, $v_2 = \text{const}$ and also $\alpha_1 = \text{const}$, $\alpha_2 = \text{const}$, since the defects in the bearing do not appreciably change these geometric relations and the deformations are small.

Thus we may conclude that one source of friction torque is change in the thickness of the lubricating layer caused by the geometric defects in the bearing components. By measuring the change in the thickness of this layer it is possible to determine the change in friction torque.

If β is large, then

$$U_m = \frac{6\pi v^2 \mu \sqrt{\alpha}}{(2\beta + 3\alpha)\sqrt{\beta}} \ln \frac{4m^2 \beta}{h_0} \text{ for } 4m^2 \beta \gg h_0. \tag{4.6}$$

For measurement of the thickness of the lubricating film light, X-rays or gamma rays are used. In rolling contact bearings the use of these rays encounters the obvious handicap of difficulty of access. Electrical methods of measurement are more suitable. The method for measuring the injection pressure of a lubricating film, being discrete, is not very suitable for measurement of vibrations. The method for measuring active resistance between bearing rings can be considered to be the more suitable. Rolling contact bearings are subjected to forced vibrations under the action of external forces.

The measurement of vibrations in bearings is a complex problem and includes the measurement of many parameters: frequencies of natural vibrations, frequencies of fundamental vibrations, amplitudes of vibrations, velocity and acceleration, displacements, peak values, etc.

Friction torque is also part of the vibrational characteristics of bearings but is dealt with in separate chapters of this book.

Measurement of the spatial vibrations of bearing elements is of interest in the context of vibrations of bearings [2, 21].

The measurement of vibrations can be classified into two groups: contact and contactless. Both groups of measurements are subdivided depending on the types of transducers used.

Vibration measurements using resistance transducers. Displacements and frequencies are basically recorded by contact methods. These include measurements using rheostatic transducers, transducers of contact resistance based on the dependence of contact resistance transfer from their compressive load. Electrolytic, electronic and ionic measuring techniques can also be included in this group.

Inductive measuring techniques are based on the change in inductance under the action of input value, in this case, of displacement.

Capacitance methods are based on the change in capacitance due to input value. As is well known, the capacitance of a condenser is

$$c=\frac{\varepsilon s}{\delta}, \tag{4.7}$$

where δ is the clearance between electrodes;

s is the area of the plates;

ε is the dielectric constant.

Radiation techniques are based on changes in the radiational energy as a result of displacement. Visible light is most often used. In cases where the displaced element is in a closed container penetrating rays are used—X-rays, γ and β rays. In certain cases it is convenient to use α radiation instead of light rays. Using various forms of radiational energy and different techniques for measuring the intensity of flow it is possible to obtain the required characteristics and properties of transducers.

Thermal methods are based on changes in electrical properties due to the effect of the temperature of the element. The dependence of heat transfer on different factors is determined by similarity criteria:

$$\mathrm{Nu}=\frac{\alpha \cdot l}{\lambda} \qquad \text{—Nusselt number;} \tag{4.8}$$

$$\mathrm{Pr}=\frac{c_p \mu}{\lambda} \qquad \text{—Prandtl number;} \tag{4.9}$$

$$\mathrm{Gr}=\frac{\beta \cdot g \cdot l^3 \Delta t \rho^2}{\mu^2} \quad \text{—Grashoff number;} \tag{4.10}$$

$$\mathrm{Re}=\frac{v \cdot l \cdot \rho}{\mu} \quad \text{—Reynolds number;} \tag{4.11}$$

where α is the heat transfer coefficient;
l is the reference length;
λ is the coefficient of heat conductivity;
c_p is the specific heat;
μ is the coefficient of dynamic viscosity;
β is the coefficient of volume expansion;
v is the velocity;
g is the acceleration due to gravity.

Pneumatic and hydraulic methods are based on changes in pressure in the system due to vibrations. These methods are simple, have considerable power output and are explosion proof.

In the computation of pneumatic systems for the subcritical region of flow we use the formula

$$G=\mu \cdot F \sqrt{\frac{2g}{RT}} \sqrt{P_1 (P_1-P_2)}, \tag{4.12}$$

where G is the weight of air discharged;
μ is the discharge coefficient;
F is the area of clearance;
R is the gas constant;
T is the absolute temperature;
g is the acceleration due to gravity;
P_1 and P_2 are the pressure before and after compression:

For hydraulic systems we use the formula

$$G=\mu \cdot F \sqrt{\frac{2g}{\rho}} \sqrt{P_1-P_2}, \tag{4.13}$$

Compensation methods are based on the comparison of input value with the analogous compensating quantity. Compensation systems are closed systems and are divided into static and nonstatic.

Besides the methods listed there are others which are not considered in this book.

4.2 SETUP FOR THE MEASUREMENT OF FRICTION TORQUE IN ROLLING-CONTACT BEARINGS

Depending on the measurement technique setups can be divided into different groups. The simplest are mechanical setups with direct reading. The

most widely used among them will be discussed [19, 97, 100]. Fig. 4.1 a shows a pendulum which is basically meant for determination of contact torque. But with its help it is also possible to determine the variable component of friction torque. During the rotation of axis *1* due to friction torque the pendulum *3* is displaced through an angle α proportional to the value M in the bearing being tested. The friction torque is computed using the expression

$$M = P \cdot l \cdot \sin \alpha, \tag{4.14}$$

where P is the mass of the pendulum;

l is the distance from the center of gravity of the pendulum to the center of the axis of rotation;

α is the angle through which the pendulum swings.

The setup is suitable for shop control because it does not require highly qualified personnel and has a sensitivity of up to 10^{-6} nm with an error of 10%. Using the variable guides *2* and weights *3* it is possible to carry out direct reading by graduating the scale in nm.

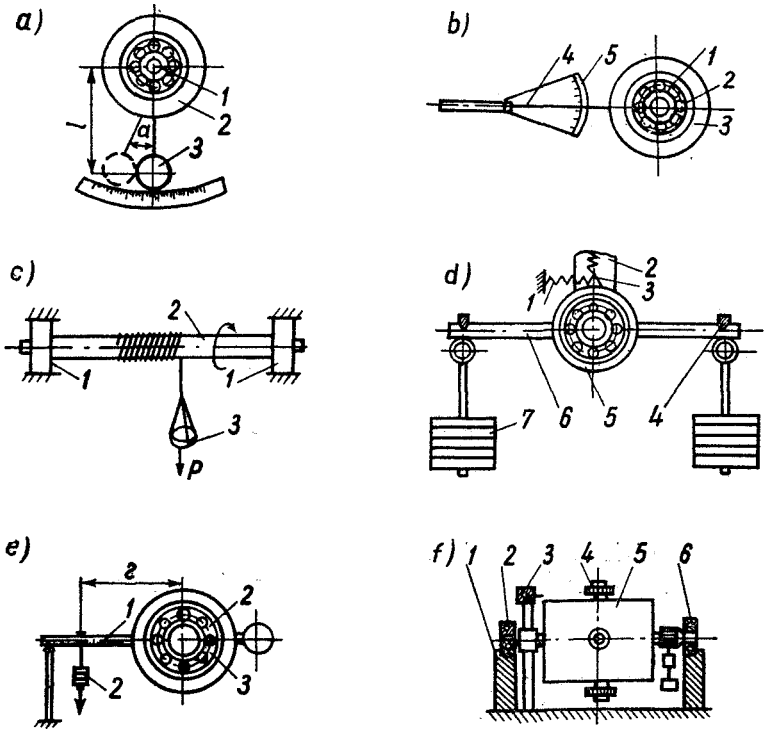

Fig. 4.1. Direct-reading mechanical devices for determination of contact torque: *a*—pendulum device; *b*—grammometer; *c*—balance device; *d*—mechanical balance of friction; *e*—lever device; *f*—instrument of C-21 type with drum.

It is possible to check friction torque directly in the assembly by means of a grammometer (Fig. 4.1 b). During rotation of the bearing about the axis *1* friction torque rotates the ring *3* and this presses the end of spring *4* and bends it. From the scale *5* the friction torque is read. When measuring contact torque the guide is pressed by the end of the spring until it begins to move.

The balance setup (Fig. 4.1 c) is widely used for measuring the torque of assembly units in bearings. The setup is suitable only for the measurement of contact torque. Weights are added to the pan *3* until the initial turn of axis *2* in bearings *1*. Friction torque for initial rotation (contact torque) is expressed by the formula

$$M_T = P \cdot r, \tag{4.15}$$

where P is the mass of the pan with weights;

r is the radius of the axis *2*.

Although mechanical balances (Fig. 4.1 c) of friction have poor sensitivity they can be used for preliminary control. Weights *7* are used to create radial load. For a more accurate balancing, weights are placed on prisms *4* and beam *6*. Friction torque during the rotation of the inner ring pulls the spring *1*, deflects scriber *3* and records on the paper tape *2*. By changing the stiffness of the spring it is possible to change the sensitivity of the setup.

A simpler setup is shown in Fig. 4.1 d. By rotating the axis *2* the friction torque in the bearing *3* turns the lever *1* with the moving weight *4*, whose displacement determines the friction torque in the bearing.

In order to measure the contact torque determined by the formula

$$M_T = (P_1 - P_2)\frac{d}{2}, \tag{4.16}$$

where P_1 and P_2 are the masses of weights;

d is the shaft diameter,

an instrument of type C-21 (Fig. 4.1 e) is used. Using this instrument it is possible to measure the contact torque of a pair of bearings *2* and *6*, fixed on prisms *1*, and to determine the contact torque of the drum from the place. Here the weights P_2 are shifted to the pan P_1.

There is a nut *4* on the drum *5* which makes it possible to ensure different angular positions of the outer ring of the bearings being tested.

It is worth mentioning that the setups shown in Fig. 4.1 (a, b, c, d) can be used for the measurement of constant and variable components of friction torque but with greater limitations of the dynamic range.

The setup shown in Fig. 4.2 a is meant for measurement of the constant component of friction torque and also for comparative measurements of bearings for which friction torque in the support (in the bearing under test) is proportional to the number of oscillations of the pendulum *1* from the start of the movement until it comes to rest or until the pendulum reaches a given angle φ_0:

$$M_T = \frac{P \cdot l\,(\cos\varphi_0 - \cos\varphi)\cdot 57.3}{(\varphi-\varphi_0)\,(3\cos\varphi_0 - 2\cos\varphi)2n}, \tag{4.17}$$

where P is the mass of the pendulum;

l is the distance from the center of gravity of the pendulum to the axis of rotation;

n is the number of periods of pendulum oscillations from the beginning of motion until it comes to rest or reaches the angle φ_0.

For comparative studies there is another setup (as shown in Fig. 4.2 b) suitable for measurement of the constant component of friction torque only. The friction torque in the support of the bearings being tested *1* is proportional to the number of periods of oscillation n of the balance *2* from the beginning of motion until its conclusion:

$$M = \frac{Ehb^3}{12\,l\,(1+2n)}\cdot\varphi, \tag{4.18}$$

where E is the modulus of elasticity of the spring material;

h and b are the height and thickness of the spring;

l is the length of the spring in the elongated form.

The setup shown in Fig. 4.2 c is for standard calibration of the friction torque of a bearing. The standard *2* and experimental *2'* bearings are placed on the counter-rotating axes *1* and *1'*. Depending on the value of the friction torque of the bearing under test the weight *4* connected with the flat spring *5* is displaced one way or the other and the friction torque is read from the scale *3*.

Determination of the friction torque of bearings by the rundown method is most commonly met with in practice. The simplest accessories are used (Fig. 4.2 d). The outer ring of the bearing is carefully moved by the fingers. Abrupt slowing or stopping indicates the presence of large friction torque or some defect in the elements of the rolling contact bearing.

In this case the friction torque in the bearing can be approximately computed from the formula

$$M = \frac{4\pi In}{T^2}, \tag{4.19}$$

where I is the moment of inertia of the bearing outer ring;

n is the number of revolutions;

T is the time, sec.

A more perfect setup for determination of friction torque in bearings using the run-down method is shown in Fig. 4.2 e. The bearing being tested *1* is mounted by the outer ring in the adjustable guide *2* fixed by the screw *3* in the support *4*. Replaceable journal *5* with flywheel *6* is placed in the inner ring of the bearing. On the outer surface of the flywheel a wire *7* is wound and fixed to the pin *8*. On the other end of the wire weight *10* is hung

through the block *9*. Before each measurement is taken this is placed on the table *11*. When the table is swung down the weight falls due to gravity and sets the flywheel *6* in motion. The flywheel along with the inner ring of the bearing continues to rotate due to inertia with gradual retardation which depends on the value of friction torque computed by formula (4.19). The run-down time of bearings varies from 2 to 4 min approximately depending on their quality and mass.

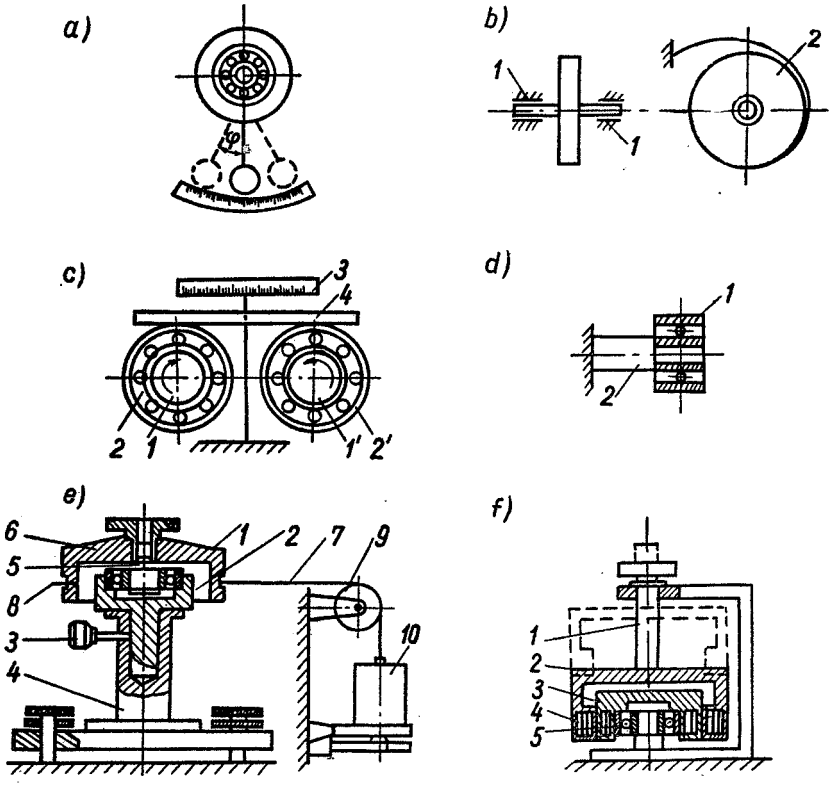

Fig. 4.2. Direct-reading mechanical devices for determination of constant component of friction torque: *a*—pendulum device; *b*—balancing unit; *c*—inertial setup; *d*—"run-down" type setup; *e*—instrument for determination of friction torque on basis of run-down; *f*—improved device for determination of friction torque on basis of run-down.

Another, more effective run-down method is used in the setup shown in Fig. 4.2 f. The guide *3* is placed on the outer ring of the bearing *5* and causes the required load. The outer ring is driven by the rotating magnetic field created by the winding *4*. On reaching a certain speed the stator *2* is screwed up with the help of the spindle *1*. The constant component of the friction torque, as in the previous setups, is determined by formula (4.19). This setup

widens the scope of the study of bearings since it allows a change of loads and an arbitrary choice of the speed range.

The pneumatic instruments and setups for the measurement of friction torque in bearings (Fig. 4.3) are not widely used because of the need for a source of compressed air, filtering and supply to the measuring setups.

The pneumatic instrument MDSL-1 (Fig. 4.3 a) which is the most well developed among them is meant for measurement of contact torque in radial bearings of an outer diameter up to 20 mm.

The bearing under test *1* is placed in the replaceable arbor *2* in the moving cup *3*. The cup can rotate on the rolling contact bearings *4* mounted on the stationary axis *5*. To ensure concentricity a rocker arm *7* is placed in the inner ring of the bearing with the help of conical pad *6* with replaceable weights *8* to create axial loading of the bearing. A hemisphere *9* and balancing weights *10* are fixed onto the rocker arm to receive the pressure of the air jet.

The torque needed to overcome the contact torque in the bearing is determined by the angle of turn of the rocker arm and is read from the graduated scale *11* on the flange of the cup *3*. The torque necessary to turn the rocker arm is created by the jet of air impinging from the calibrated nozzle *12*. The air pressure is regulated by a pneumatic valve and is measured using a manometer graduated in units of friction torque.

Before starting measurements the mark *1* is lined up with the indicator notch on the base of the instrument *13* and the end face of the hemisphere *9* with the stationary indicator *14*.

During measurement the air jet pressure on the hemisphere increases until the rocker arm is displaced.

By adjusting all the points simultaneously with the indicator notch the contact torque at various points in the raceway is measured for various locations of the rings of the bearing [16].

The pneumatic system ensures high sensitivity of the setup.

A more universal pneumatic instrument is shown in Fig. 4.3 b. The instrument allows measurement of the constant and variable components of friction torque. Corrugated diaphragms connected by an air tract with a projection micromanometer have the role of the sensitive measuring element in this setup. When the inner ring of the bearing under test *1* is rotated with the help of an electric motor the outer ring with the arbor *2* fixed on it and connected with the diaphragm *3* turns through a certain angle proportional to the constant component of the friction torque. The closed volume of air tract limited by the corrugated diaphragm of the manometer and measuring diaphragm *3* changes in proportion to the load applied to the diaphragm. As a result the air pressure changes, causing deflections of the diaphragm of the sensitive manometer. The mirror *5* which is fixed to the manometer turns under the action of the load in the direction of the diaphragm.

The variable component is recorded as the mirror turns one way or the other from the equilibrium position, corresponding to the constant component of friction torque [79].

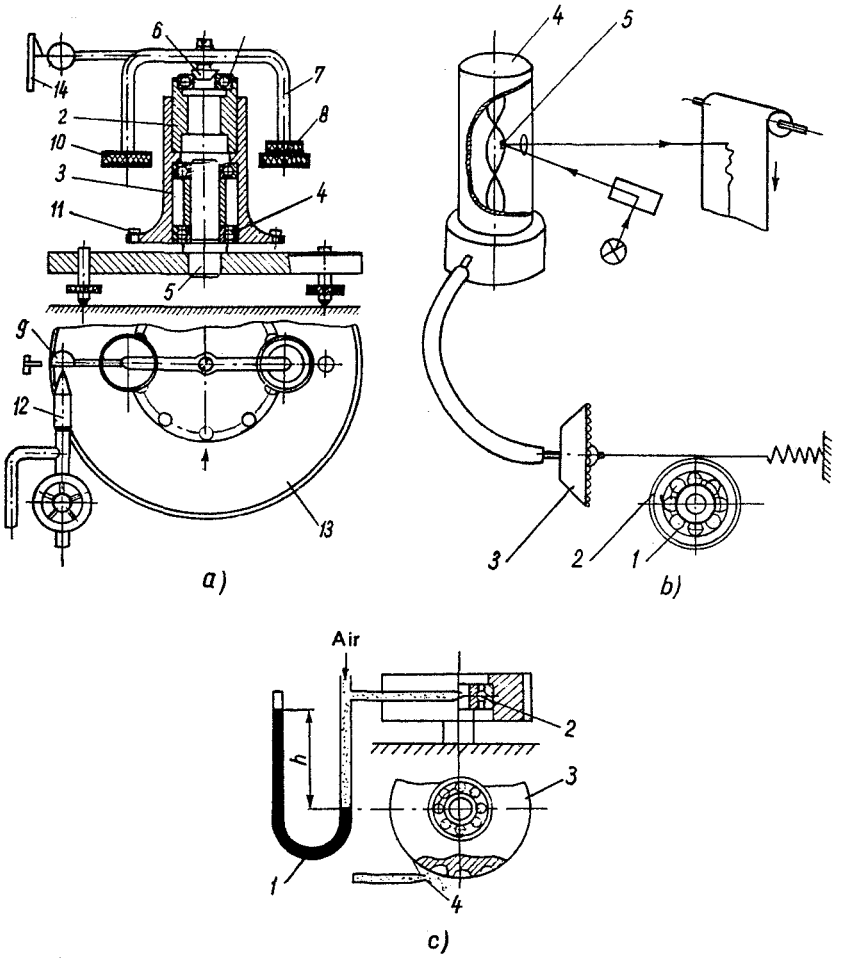

Fig. 4.3. Pneumatic instruments and devices for measurement of friction torque: *a*—MDSh-1 instrument; *b*—pneumatic diaphragm unit; *c*—instrument with liquid manometer.

Another variation of the pneumatic setup for the measurement of contact torque is shown in Fig. 4.3 c. The bearing *2* under test is placed in the arbor *3*. The arbor moves under the action of the jet of air issuing from the nozzle *4* with gradually increasing pressure. The value of the pressure at the instant of contact is recorded by the liquid manometer *1* which is graduated in terms of friction torque [88].

Optical instruments and setups form a small group because optical systems have only the role of recording element and the friction torque is balanced by pneumatic, elastic rods and other systems. Hence optical setups can be included in other groups.

The principal scheme for the setup with an optical system for reading and recording friction torque components is shown in Fig. 4.4 a [24].

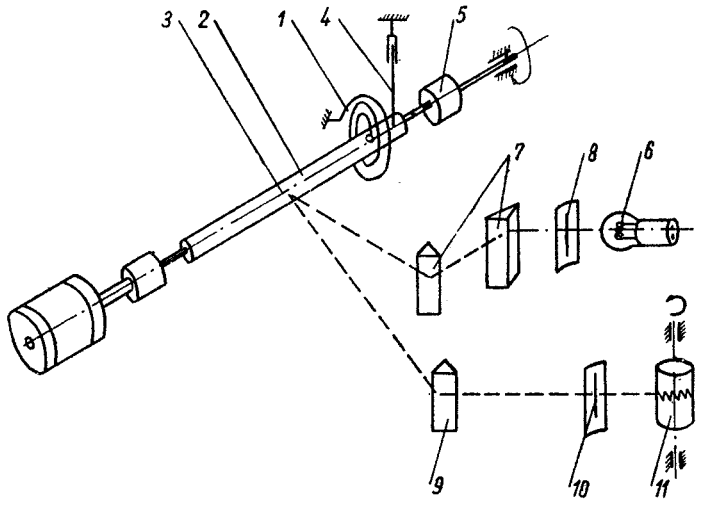

Fig. 4.4. Setup for measurement and recording of friction torque in bearings at low speeds.

Let us describe this scheme.

The bearing under test is placed in the chuck *5* and set in motion by an electric motor with reduction gear. The friction torque is balanced by the spiral spring *1* connected at one end with the stationary part of the casing and at the other with the axis *2*, on which mirror *3* and damper (dash-pot) *4* are fixed. Friction torques in the bearing move the measuring system by twisting the spring through an angle proportional to the friction torque being measured. Due to this, the ray of light falling on the mirror from the source of light *6* through the optical system *7* and *8* is deflected through the same angle and is recorded by the optical system *9* and *10* on the moving paper tape of the camera *11* in the form of a curve. A scale serves the purpose of visual reading.

Nowadays the strain gauge technique finds wide application in the measurement of friction torque in bearings. The basic principle of strain gauge transducers is the change in the resistance of the metal or semiconductor under the action of an applied load. The resistance strain gauge finds very wide application because of its small size and the possibility of measuring

both static and dynamic torques. Most popular are wire, foil and semiconductor resistance strain gauges.

The relative change in the resistance of a resistance strain gauge is determined by the relation

$$\frac{\Delta R}{R}=\frac{\Delta l}{l}(1+2\mu), \tag{4.20}$$

where Δl is the change in length;

μ is Poisson's ratio.

The basic parameter of the resistance strain gauge (gauge factor) is expressed in the following form

$$S=\frac{\Delta R/R}{\Delta l/l}=\frac{\Delta R}{R\varepsilon}, \tag{4.21}$$

where $\Delta R/R$ is the relative change in the resistance of the strain gauge;

$\varepsilon=\frac{\Delta l}{l}$ is the relative change in the length of the resistance strain gauge.

The value of the gauge factor depends on the properties of the material the resistance strain gauge is made of and on the technology of manufacture, since

$$R=\rho\frac{l}{F_0}, \tag{4.22}$$

where R is the electrical resistance of the strain gauge;

l is the length of the strain gauge;

F_0 is the area of its cross section;

ρ is the specific resistance.

Wire resistance strain gauges are most widely used in practice. Materials having a large gauge factor and small changes in resistance with temperature are used for the manufacture of these strain gauges. For this purpose the most suitable material is constantan wire bonded onto paper or on a film base. The film base is prepared from Bakelite lacquer, BF-2 gum and special compositions. Films can be prepared from BF gum in the temperature range of $-40°$ to $+70°$C. They are made on the Bakelite lacquer base and work up to 200°C.

The gauge factor of strain gauges manufactured by industry of the 2PKB and 2PKP types is 2 ± 0.2. The nominal operating current during bonding on the metal part is 30 μa. The maximum allowable strain does not exceed 0.3%. For constantan wire the temperature coefficient of resistance is $\pm50\times10^{-6}$ deg^{-1}, the coefficient of linear expansion $\alpha=15\times10^{-6}$ deg^{-1} and maximum working temperature 500°C.

The next type of resistance strain gauge is the foil type transducer made of thin strips of constantan foil of rectangular cross section ($b=4$–12 μ). Foil-

type strain gauges have a large area of contact with the object under test and hence the heat transfer is more than with wire gauges. This makes it possible to increase the supply current for the gauge and thereby increase the sensitivity of the gauge [72].

The first types of semiconductor strain gauges appeared in the Soviet Union and abroad during 1955–1958. They have found very wide application.

The gauge factor of semiconductor strain gauges, unlike wire- and foil-type gauges, closely depends on the level of deformation, temperature, specific resistance and crystal lattice direction.

The dependence of the gauge factor on the temperature of the surrounding medium is determined using the formula

$$\frac{\Delta S}{S_0} = -\gamma (T - T_0), \tag{4.23}$$

where ΔS is the absolute increment in the value of the gauge factor at a temperature T;

S_0 is the value of the gauge factor at a temperature T_0;

γ is the temperature gauge factor.

At present semiconductor strain gauges are made from silicon, germanium and the compounds galium arsenide (GaAs), galium-antimony (GaSb) and others. In strain gauges of germanium a dendritic germanium strip is used with a specific resistance $\rho = 1 \pm 0.2$ Ohm-cm.

The gauge factor of semiconductor strain gauges is 50–60 times more than wire resistance gauges.

The gauge factor of semiconductor strain gauges of the KTD type with a conductivity of p-type, KTE of p-type is 110 ± 10 and the working tempera-

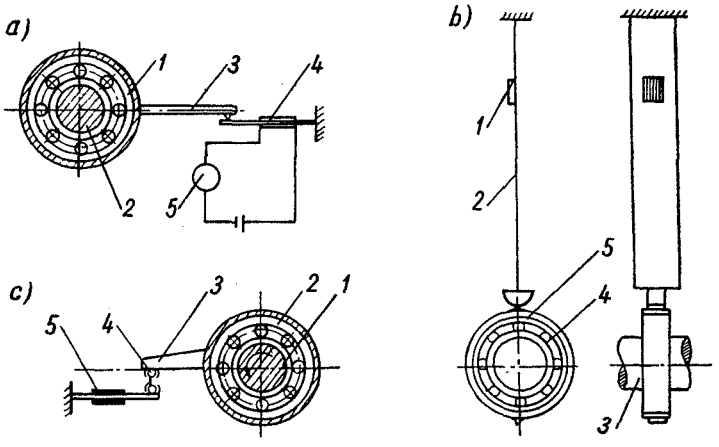

Fig. 4.5. Strain gauge setups for measurement of friction torque: *a*—friction torque measurement; *b*—setup with vertical flat spring; *c*—improved strain gauge device.

ture range lies between $-160°$ and $+300°C$. The temperature coefficient of resistance is determined as

$$(5\text{–}10)\cdot 10^{-4}\frac{\Delta R}{R}\ 1/°C. \tag{4.24}$$

Some of the disadvantages of semiconductor strain gauges are low mechanical strength, low flexibility and sensitivity to light and temperature [12, 38, 39, 40, 73, 108].

The components of friction torque in bearings are measured using strain gauges in the following way (Fig. 4.5 a). During the rotation of the axis *2* caused by the friction torque in the bearing its outer ring *1* acts through the lever *3* on the flat spring *4* with its bonded strain gauges. The deflection of the flat spring proportional to the friction torque in the bearing is recorded by the measuring instrument which receives the signal from the strain gauges. The setup has high sensitivity but is limited in dynamic range.

Another strain gauge variant for measurement of the friction torque components in bearings is shown in Fig. 4.5 b [31, 79]. A plane flat spring *2* made of beryllium copper is used as the balancing element and strain gauges are bonded onto it in a half-bridge, i.e. a bridge circuit is used. In this circuit, of which the strain gauge forms a part (Fig. 4.6), the bridge must be balanced to eliminate the initial constant component at the bridge output. The condition for balance is the relation

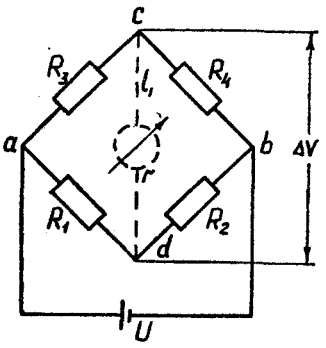

Fig. 4.6. Strain gauge bridge circuit.

$$R_1R_4=R_2R_3. \tag{4.25}$$

During the working of the electric motor the inner ring of the bearing *3* sets the outer ring with arbor *4* in motion as a result of friction torque. The outer ring rotates and deforms the flat spring *2* with strain gauges *1*. The deformation of the spring causes a change in the resistance of the strain gauge and the signal voltage at the output of the initially balanced bridge is determined in the case of complete symmetry as

$$\Delta V=\frac{U}{4}\frac{\Delta R}{R+2\Delta R} \tag{4.26}$$

or, considering that $2\Delta R \ll R$ with an error less than 1%,

$$\Delta V=\frac{U}{4}\frac{\Delta R}{R}. \tag{4.27}$$

In this case, when active strain gauges are placed on the two mixed arms, where R_1 increased during deformation and R_2 decreases (half-bridge circuit) or on all four arms (full bridge circuit), the voltages of signals at the bridge output will respectively have the form:

$$\Delta V_2 = \frac{U}{2}\frac{\Delta R}{R}, \tag{4.28}$$

$$\Delta V_{(4)} = U\frac{\Delta R}{R}. \tag{4.29}$$

In Fig. 4.5 c an improved design of strain gauge instrument is shown for the measurement of friction torque components in bearings and assemblies. The bearing *2* is fixed on the rotating shaft *1* and the resistance force is transferred from the outer ring through the pin *3* and the needle *4* with spherical ends to the strain gauges *5* bonded onto the plate *6* in the bridge circuit. The signals from the strain gauges are transmitted to an electronic strain amplifier.

The setup works in the following way: When the shaft *1* rotates the outer ring of the bearing *2* is displaced relative to the gauges *5* due to wobbling and vibrations. The pin *3* presses the plate *6* through the needle *4* and the plate deflects, thereby causing deformation of the strain gauges *5* and a change in the voltage to the strain gauges which is recorded by the strain amplifier. Since the friction of the end of the needle about the fulcrum is negligible the displacement caused by the bearing in a plane perpendicular to the needle practically does not cause additional tangential loads on the strain gauges.

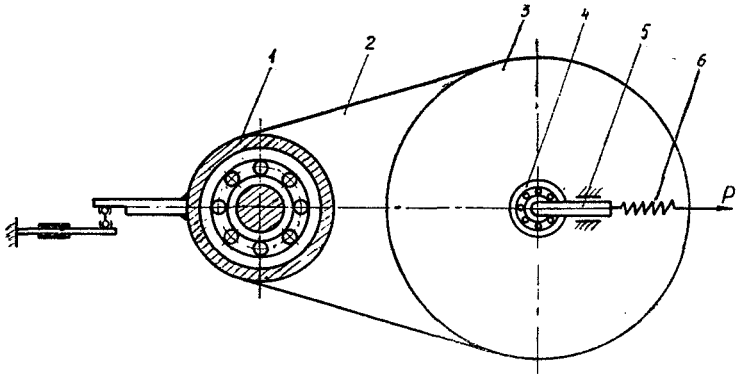

Fig. 4.7. Radial loading.

The instrument for measuring friction torque components includes the setup for radial loading (4.7) which consists of the bearing being tested *1*, unstretchable rope *2* enveloping the assembly and disc *3* at whose center there is an auxiliary bearing *4*. The axis of the latter is rigidly connected to the guides *5* and flexible element *6*.

The instrument works in the following way: The tension in the spring *6* is transmitted as radial load to the assembly *1* through the guide *5* with fixed axis, auxiliary bearing *4*, disc *3* and branches of the rope *2*.

The auxiliary bearing *4* was tested under the action of oscillatory motion with respect to the stationary axis through small angles. It has been experimentally established that in such operational conditions the values of friction torque in rolling contact bearings are a few orders of magnitudes lower than the value of contact torque for negligible angles of turn (not exceeding 1°). The maximum value of the contact torque is reached not immediately but gradually, after turning for 20 or 30 minutes (Fig. 4.8).

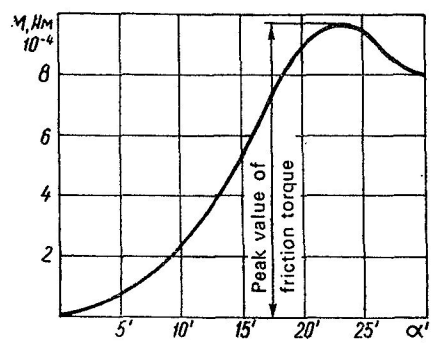

Fig. 4.8. Friction torque of bearing of C1000096 type.

This phenomenon takes place due to the elasticity of the contacts between the rolling elements and rings and also due to the cage. It is interesting to note that during the clogging of the bearing the zone of elastic increase in friction torque is prolonged occasionally up to one degree because the contact torque increases sharply.

During measurement of friction torque in the instrument the auxiliary bearing will rotate through an angle whose value depends on the value of the

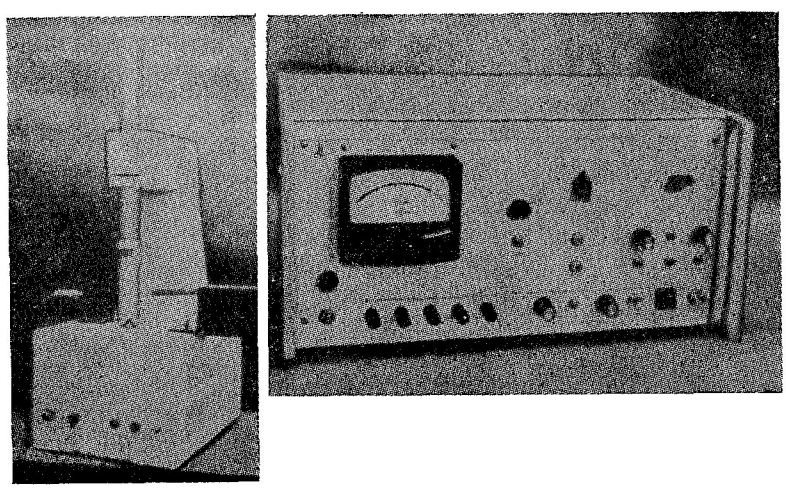

Fig. 4.9. Apparatus for measurement of friction torque components.

torque being measured and the size of the flat plate with strain gauge fixed to it (depending on its stiffness). During measurement of torque components, for example, 1.0×10^{-4} nm, by selecting the flat plate in such a way that the angle of turn of the auxiliary bearing is about 1′ we get a very small value of error.

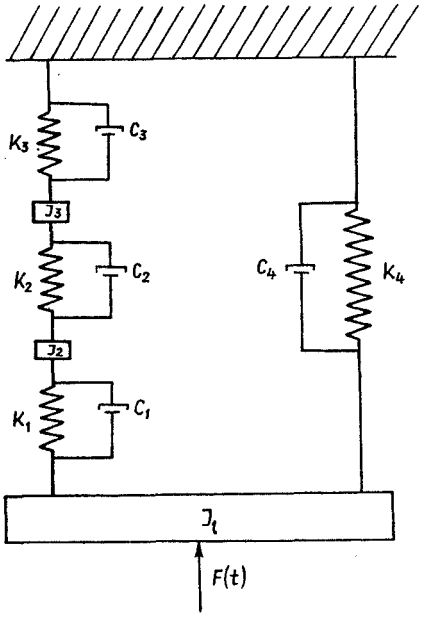

Fig. 4.10. Dynamic model of measuring system.

We can consider the dynamics of the measuring system of one of the strain gauge instruments (Fig. 4.5 c) as an example for all the above setups and instruments (Figs. 4.9 and 4.10).

The system we are studying in the general case is a system with three degrees of freedom.

Let us introduce the following notations:

k_1, k_2, k_3, k_4—elasticity of the pin *3*, needle *4*, spring *6* (Fig. 4.5 c), rope *2* and contacts in the bearing *4* between balls and raceways respectively (Fig. 4.7);

c_1, c_2, c_3, c_4—damping coefficients of the bearing *2*, contacts of needle *4*, spring fixture *6* (Fig. 4.5 c) and bearing *4* (Fig. 4.7) respectively;

I_1, I_2, I_3—moments of inertia of the moving parts of the assembly and disc *3* (Fig. 4.7), needle *4* and spring *6* (Fig. 4.5 c) respectively;

$\xi(t)$—disturbing torque appearing during the rotation of the bearing.

Moments of inertia I_2 and I_3 are negligible when compared to the value of I_1 and hence they are neglected in computations. Thus the dynamic model is simplified (Fig. 4.11).

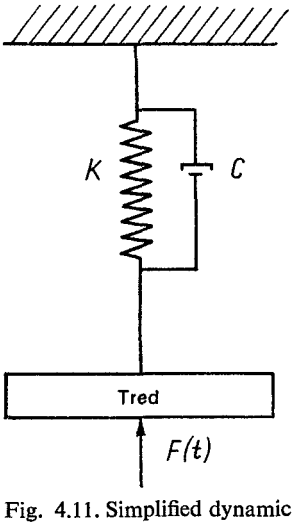

Fig. 4.11. Simplified dynamic model of measuring system.

Then
$$k=\frac{k_1 k_2 k_3}{k_2 k_3+k_1 k_3+k_1 k_2}+k_4, \tag{4.30}$$

$$c=\frac{c_4(c_1+c_2+c_3)}{c_1+c_2+c_3+c_4}. \tag{4.31}$$

Correspondingly, the differential equation for the free motion of the system takes the form

$$I\ddot{\varphi}+c\dot{\varphi}+k\varphi=0, \tag{4.32}$$

where $\ddot{\varphi}$ is the angular acceleration of the moving part of the system. The eigen frequency of torsional vibrations with damping is expressed in the following form:

$$\omega_d=\sqrt{1-\xi^2}\,\omega_n, \tag{4.33}$$

where ξ is the nondimensional damping coefficient having the form

$$\xi=\frac{c}{2I\omega_n}. \tag{4.34}$$

Here ω_n is the eigen frequency of torsional vibrations without damping determined from the expression

$$\omega_n=\sqrt{\frac{k}{I}} \tag{4.35}$$

or in another form

$$\omega_n=\sqrt{\frac{k_1 k_2 k_3+(k_1 k_2+k_1 k_3+k_2 k_3)}{I(k_1 k_3+k_1 k_3+k_2 k_3)}}. \tag{4.36}$$

Finally we obtain

$$\omega_d=\frac{1}{2I}\sqrt{4I\left[\frac{k_1 k_2 k_3+k_4(k_1 k_2+k_1 k_3+k_2 k_3)}{k_1 k_2+k_1 k_3+k_2 k_3}\right]-\left[\frac{c_4(c_1+c_2+c_3)}{c_1+c_2+c_3+c_4}\right]^2}. \tag{4.37}$$

The moment of inertia obtained is given by

$$I=I_1+i^2 I_2, \tag{4.38}$$

where I_1 is the moment of inertia of the moving part of the assembly;

I_2 is the moment of inertia of the disc with moving part of the bearing;

i is the transfer coefficient.

Let us now consider piezoelectric instruments for the measurement of friction torque using the piezoelectric effect. The piezo effect is linear, i.e. mechanical deformations of the crystal give rise to directly proportional electrical polarization P [32, 35]:

$$P=e\cdot r, \tag{4.39}$$

where e is the coefficient of proportionality (Piezoelectric modulus).

The sensitivity of piezotransducers is about 100–250 V/kW for an impulse duration of 0.1–0.2 μ sec. The temperature error of the transducer does not exceed $\pm 5\%$ in the range of temperatures from -10 to $+70$°C.

The measuring instruments using piezotransducers allow measurement only of the variable component of the friction torque in bearings.

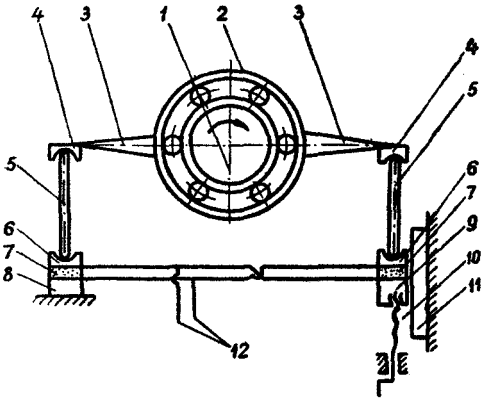

Fig. 4.12. Transmission of friction torque using two piezoelectric transducers.

The piezotransducers have insufficient directional properties. Hence for the direct transfer of torque to the piezotransducer from the moving part of the instrument, with the inescapable wobbling and vibrations of the latter, considerable tangential forces act on the transducers and result in errors which occasionally exceed the torque being measured. In order to avoid this the system (Fig. 4.12) is used. This system is analogous to the system used in the strain gauge setup (Fig. 4.5 c) meant for rigid transfer of force, which in essence consists of the use of a light steel needle and spherical pads made of solid stones fixed to the transducer and the moving part of the instrument.

Let us describe such a setup (Fig. 4.12).

The bearing is fixed on the rotating shaft *1* and the friction torque is transmitted from the ring *2* through pin *3*, spherical pads *4*, needles *5* and pads *6* to the transducers *7*. These are fixed to the bases *8* and *9* where the base *9* can be displaced by a microscrew *10* along the guide *11* until the compression of the needle to a small load which does not disappear during the wobbling of the bearing caused by the flexibility of the pins. Transducers *7* are electrically connected in parallel to opposite ends and a signal is received from ends *12*.

The setup works in the following way:

When the shaft *1* rotates the outer ring *2* is displaced with respect to transducers *7* due to the wobbling and vibrations. The displacement of the spherical supports *4* connected to the bearing in the plane perpendicular to needles practically does not result in additional tangential loads directed onto the transducer since the rolling friction of the end of the needle in the lower pad is negligible. The displacement in the direction of the needles simultaneously acts on both transducers and thanks to the transducers being connected to opposite ends it is mutually compensated. At the same time the change

in the friction torque causes cumulative signals of opposite signs in the transducers and these are transmitted through the conductors *12* and amplifier to the measuring instrument or analyzer. In the present setup, complete data on the characteristics of piezotransducers must be procured.

In the above group of instruments and setups the balancing torque was created by mechanical means. In order to suppress undesirable high frequencies damping units were included in many designs.

Capacitor type and electro-mechanical types of instruments for the measurement of friction torques in bearings are very rare among the known setups and instruments.

4.2.1 Electrical Instruments for the Measurement of Friction Torque Coefficients in Bearings

Among the electro-mechanical means of measuring friction torque components in bearings the most widespread is the photoelectric method. Examples of different schemes for the measurement of torques using photoelectric methods are shown in Fig. 4.13. Here the photoelectric method of registering torque is combined with other principles of balancing and operation of the setups. In the setup shown in Fig. 4.13 a [22] the stroboscopic disc *2* with alternating transparent and opaque sectors is fixed to the flywheel *1*. For a given interval of time the photoelement *3* receives a particular quantum of impulses of light rays. The change in the angular speed $\omega - \omega_0$ of the flywheel with the disc characterizes the constant component of the friction torque. The instrument scale receiving the signals from the photoelement can be graduated in terms of torque units.

In the electromechanical methods of measurement, as in others, the compensation of friction torque is widely used [46, 56, 57, 61, 112, 121, 125]. For example, in the setup shown in Fig. 4.13 b the bearing *1* is placed on the rotating shaft *2* and the outer ring of the bearing is mounted in the coupling *3* on which the frame *4* of the electromagnetic mechanism is fixed. The mirror *5* reflects a light ray from lamp *6* to the photomagnifier *7* fixed on the coupling *3*. The friction torque component of the bearing M_c that appears when the shaft *2* rotates is balanced by the torque M_b of the frame *4* as a result of the current I_b passing through the frame. The value of current necessary to balance the torque is automatically maintained by the setup consisting of lamp *6*, mirror 5, photoamplifier *7* and amplifier *8*.

When

$$\Delta M = M_c - M_b \tag{4.40}$$

the mirror turns and balances the friction torque of the bearing by the electromagnetic mechanism.

A photoelectric setup with inductance transformer [56] is shown in

Fig. 4.13 c. When the shaft *1* rotates at constant speed the outer ring of the bearing *2* along with the flywheel *3* and disc *4* is attracted as a result of the friction torque in the bearing. The friction torque is compensated by the torque M_b caused by inductance mechanism *5*:

$$M_b \approx c \frac{f}{\rho} I_1^2 \sin \psi, \tag{4.41}$$

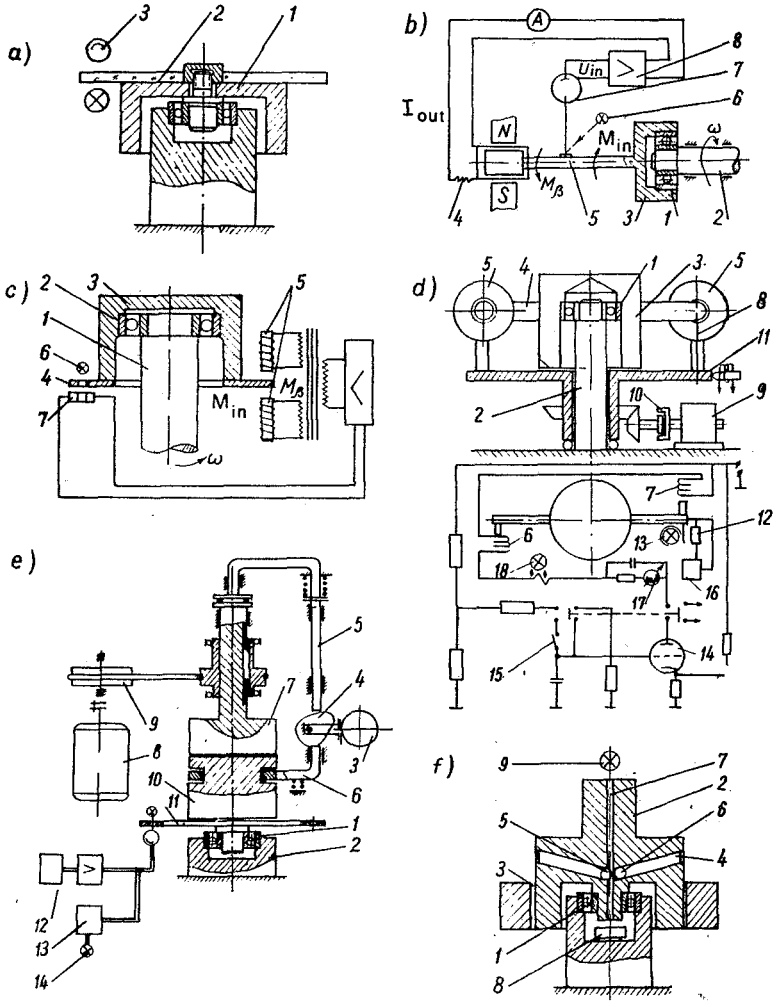

Fig. 4.13. Measurement of friction torque by photoelectric techniques: *a*—photoelectric unit for measurement of friction torque using method of "run-down"; *b*—compensating unit; *c*—photoelectric unit with inductance converter; *d*—photoelectric unit for controlling contact torque; *e*—setup for control of bearing by run-down; *f*—semi-automatic device for control of bearings.

where c is the coefficient of proportionality;

f is the frequency of alternating current;

ρ is the specific electrical resistance of the material of the disc;

I_1 is the current in the primary winding of the transformer;

ψ is the shift in the phase angle between magnetic fields.

If the condition

$$I_1 = K \cdot I_2, \tag{4.42}$$

where I_2 is the current in the secondary winding, is fulfilled, then the torque produced by the inductance mechanism can be determined from the reading of the ammeter that measures the current in one of the windings. The value of the current needed to produce compensating torque is automatically maintained by the uncompensated transformer consisting of lighting arrangement *6*, photoresistance *7* and an amplifier that changes the current in the windings of the transformer with any change in the intensity of the light.

In order to register the beginning of contact of the bearings a setup (Fig. 4.13 d) is used in which balancing torque is produced by an electromagnetic transformer [66]. The bearing *1* to be controlled is fixed on the stationary axis *2*. The requisite axial load is created by a detachable metal cup *3* whose center of gravity is lower than the plane of the bearing (in order to ensure uniform distribution of the load). The rocker arm is attached to this cup. The rocker arms *4* with cores *5* of ferromagnetic material are attracted by coils *6* and *7* when the current passes through them and thereby create the balancing torque. A shutter *8* with a narrow slit fixed to one of the beams forms part of the photoelectric transformer.

In order to control the contact torque of the bearing at different positions along the circumference there is an electric motor *9* with electromagnetic coupling *10* which automatically turns the moving part *11* to the appropriate position. In the initial position photoresistance *12* included in the circuit of the photo relay is illuminated through the shutter slit *8* of the lamp *13*. During this time there is no current in the anode circuit of the electronic lamp *14*.

After switching on the setup by the switch *15* the current in the anode circuit increases and simultaneously the friction torque increases in the coils *6* and *7*. As soon as the torque created by coils exceeds the contact torque in bearing then the moving part *11* of the setup is displaced and covers the photo resistance by the shutter. The photo relay *16* responds and the drive turns the moving part with the outer ring of the bearing to a new initial position.

Contact torque is determined using the instrument *17* which is graduated in units of torque. When the allowable level of contact torque is exceeded the signal lamp *18* is included in the circuit.

Photoelectric instruments for the control of bearings by run-down are shown in Fig. 4.13 e and f. B.S. Apirin [3, 4] developed a semiautomatic setup

for the control of the constant component of the friction torque in bearings (Fig. 4.13 e). The working principle is as follows: The bearing *1* placed in a replaceable seat *2* is raised to a given angular speed. On achieving the desired initial speed the coupling *7* is slightly lifted by turning the handle *3* and the drive is switched off. During the exposure time measurement of the angle of turn is carried out by a photoelectric transducer counting the number of light impulses. The run-down time is determined by electronic relay.

K.S. Liberson and G.I. Nedonoskov [68] developed a setup (Fig. 4.13 f) which works on the same principle. The inner ring of the bearing *1* is connected to the brass flywheel *2* whose lower part is placed in the magnetic field of the 3-phase stator *3*. In the body of the flywheel balls *5* and *6* freely move along the channels *4*. The flywheel is turned by the moving magnetic field. Under the action of centrifugal forces the balls are thrown out from the axis of flywheel *4* and photoresistance *8* is illuminated by the lamp *9*. After achieving the desired number of turns the time relay switches off the magnetic field and switches on the run-down time count. When the motion is reduced the balls slide down to the axial channel *7*, covering the light to the photoresistance. Covering it stops the counting of run-down time.

Inductance methods are based on the use of inductance transducers whose action consists in changing the inductive impedance of coils during the displacement of the moving part of the transducer-anchor.

Setups which use inductance methods of measurement include the magneto-inductive semiautomat (Fig. 4.14) containing two magneto-inductive transducers, two measuring instruments and stabilized transformer I [13, 22]. The magneto-inductive transducer used for determination of the reading time consists of coils *1*, two open steel cores *2* and brass flywheel *3*. The upper half of the flywheel is divided along the contour into two equal parts to one of

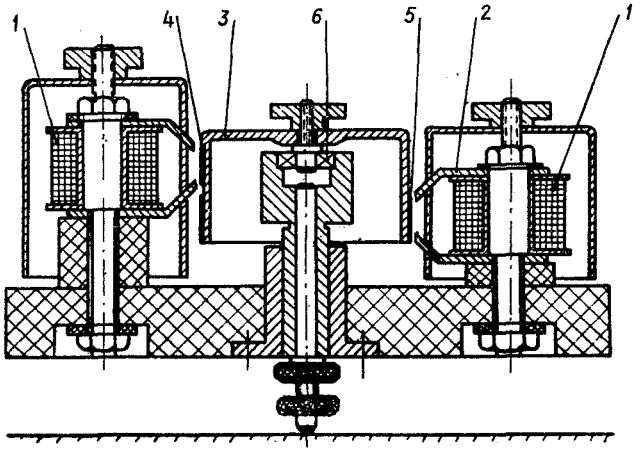

Fig. 4.14. Magnetic-inductive setup for measuring friction torque in bearings.

which a steel plate *4* is brazed. The lower half of the flywheel is divided into six equal parts to three of which the remaining plates *5* are brazed. The bearing being tested *6*, initially kept in an arbor, is installed in the slot of flywheel *3*. The measuring instrument or electrical stopwatch consists of the counting mechanism and relay which ensures prompt switching on and switching off of the electrical stopwatch.

When the flywheel rotates an electric current is induced in the coils and the signal from the coils goes to the polarized relay of the counter. The initial and final angular speeds are determined by the coils.

Examples of setups using the electro-magnetic methods are shown in Fig. 4.15. The torque balancing the friction torque in the bearing (Fig. 4.15 a) is created by the rotating electromagnetic field. An asynchronous electric motor *1* rotates ring *2* with the ball bearing under test installed in it. The axis *3* is installed in the slot of the inner ring and the copper disc *4* rotating between four poles is fixed on it. The excitation current passing into coils *6* ensures the appearance of a rotating magnetic field balancing the friction torque. The excitation current measured at the time of equilibrium determines the friction torque.

The following is the working principle of the instrument (Fig. 4.15 b) meant for the rejection of bearings based on the limiting value of friction torque [67]. The bearing *1* is installed on the shaft rotated by the motor *2*. The hub *3* covers the outer ring and creates the desired axial load. The outer ring of the bearing remains immobile since the lever *4* of the hub is pressed to

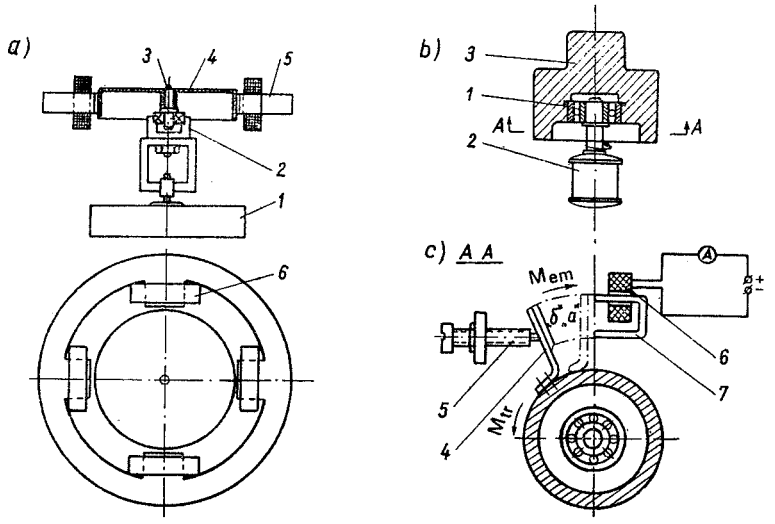

Fig. 4.15. Examples of designs:
a—device for controlling bearings by constant friction torque;
b—instrument for sorting ball bearings; *c*—electromagnetic device for controlling rolling contact bearing.

the support *5*. The compression force is determined by the value of friction torque. When current is passed through the coil *6* of the electromagnet *7* the balancing electromagnetic torque will act on the lever carrying the yoke of the electromagnet. This tends to move the yoke of the magnet from position 'b' to position 'a'. The strength, number of turns in the coil and distance from the magnet to the yoke in the position 'b'.

If the friction torque in the bearing is more than the balancing torque then the lever *4* remains pressed onto the support; if it is less than the allowable figure then the lever is moved to position 'a' and the fit bearing is moved to the anchor of the electromagnet.

The setup shown in Fig. 4.15 c basically provides for measurement of the contact torque of the bearings under test. The current in the coil *3* is gradually increased until the balancing torque exceeds the contact torque and the axis *1* in bearings *2* is deflected. The current in the coil *3* is proportional to the contact torque in the bearings. When the outer rings rotate it is also possible to measure the variable component of the friction torque but with large errors.

Induction and transformer methods can be considered together since basically transformer-type transducers are a variation of induction transformers. All these setups work according to the principle of "angle-amplitude" and "angle-phase." These transformers are electro-mechanical amplitude and phase modulators with carrier frequency corresponding to the supply voltage. They usually follow a linear law.

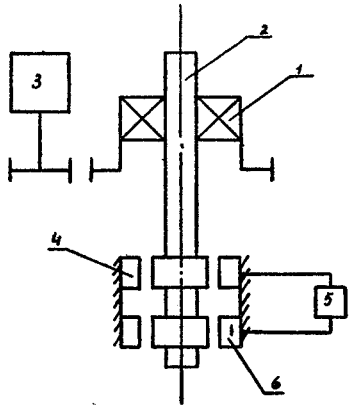

Fig. 4.16. Basic diagram of instrument measuring dynamic characteristics of bearings.

The principle scheme of the setup is shown in Fig. 4.16. This setup works on the principle of an electrical spring using transformer transducers.

The setup works like this: The bearing under test *1* is installed on the axis *2* of the transducer's rotor. The outer ring of the bearing is rotated by the electric motor *3*. The friction torque drives the rotor. The signal transducer *4* measures the deflection angle and converts it into an electrical signal. This signal is amplified by the amplifier *5* and reaches the transducer of torque *6*, creating a torque that balances the driving torque of the shaft.

Signal and torque transducers are similar in working principle and also in design. The working principle of transducers consists in destruction of the symmetry of the magnetic field in the magnetic conductor when there is a deviation of the differential transformer from its symmetric position. In the

initial condition the rotor remains in the mean position (Fig. 4.17) during which the flows φ_1, φ_2 and φ_3, φ_4 developed by the excitation coils 'b' in the cores of the signal coils 'c' are equal in magnitude. The signal coils are connected so that the induced emfs, E_1E_2 and E_3E_4, are opposite in phase. As a result of the equality of magnetic flows and opposite phases the total emf of the four series connected is around zero.

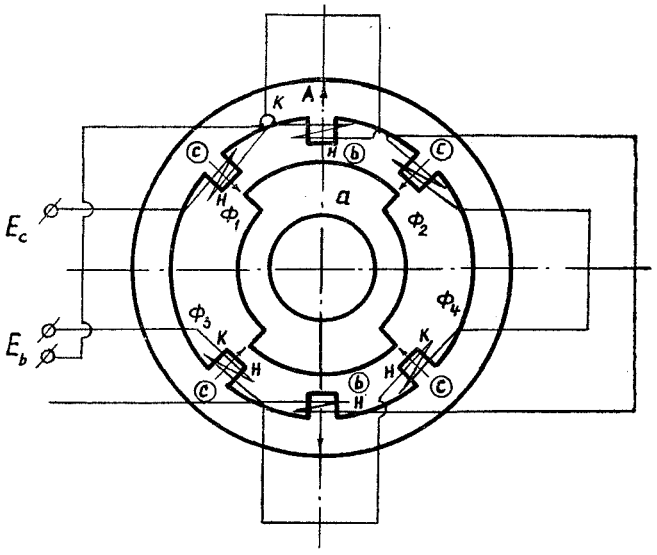

Fig. 4.17. Inductance transducer.

The appearance of "zero" signal is explained by the accuracy of manufacture of the transducers. The resistance of the magnetic circuit is changed during the displacement of the rotor, causing redistribution of magnetic flux φ_1, φ_2 and φ_3, φ_4. The latter gives out a signal in the form of the e.m.f. of the signal coils. The amplitude and phase correspond to the direction and magnitude of the angular displacement of the rotor.

The working of this instrument (Fig. 4.18) is as follows:

The experimental bearing *10* is installed on the axis *12*. The other end is guided by the agate bearing *17* whose friction torque is one order of magnitude less than that of the experimental bearings being tested. The outer ring of the bearing is pressed to the pulley-sleeve *4* which is rotated by the electric motor by a belt drive *3*. Rotors *13* and *15* of the signal *14* and torque *16* transducers are installed on the axis. These transducers are connected together by an inverse coupling through the amplifier-matching setup *20*.

The loads on the bearing under test are created by the electro-magnetic setup *19*. Damping elements *7*, *8* are installed in the instrument. The assembly of the apparatus (Fig. 4.19) consists of electronic and mechanical parts.

The magnetic method has not been considered among the electro-mecha-

nical methods. This method can be included in other groups but since mechanical and electrical setups do not form part of instruments incorporating this method it is better to consider it in a separate group.

An example of this group is the setup (Fig. 4.20). When the magnets *3* (leading) rotate the outer ring of the bearing *2* with the magnets *1* (follower) fixed on them also rotates. The lag angle between the two sets of magnets characterizes the friction torque of the bearing being tested. The setup lacks accuracy but cosidering its simplicity it occasionally finds application.

Analyzing the above instruments and setups, it is worth mentioning that a production model of an instrument to measure friction torque components in

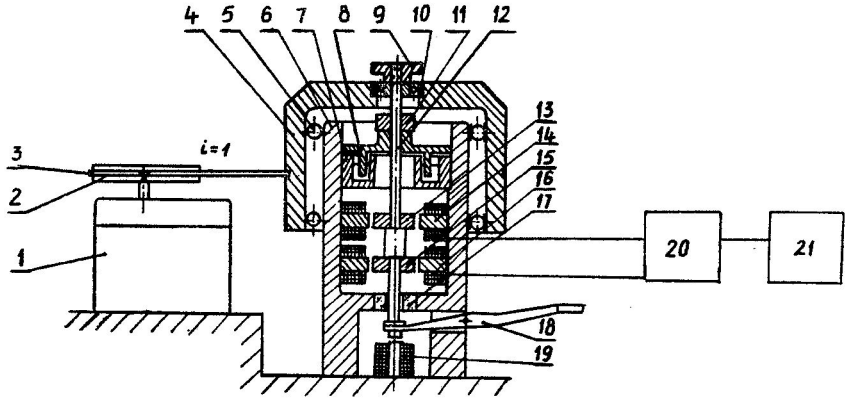

Fig. 4.18. Kinematic diagram of instrument measuring dynamic characteristics of bearings.

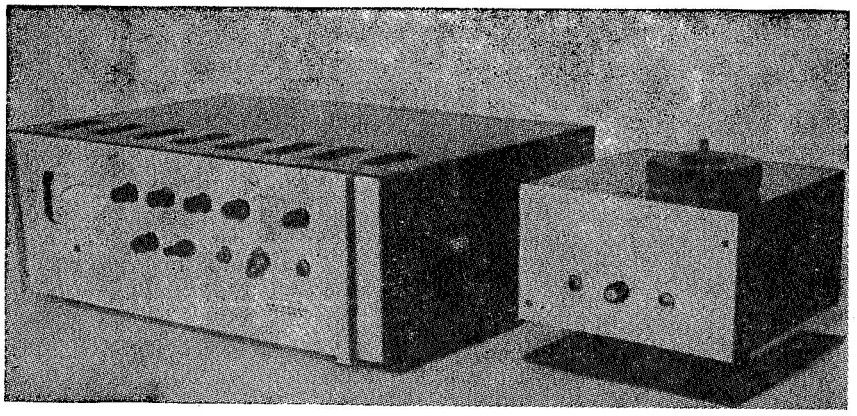

Fig. 4.19. General view of apparatus for dynamic characteristics of bearings.

bearings that fully simulates operating conditions is yet to be developed. Certain setups and instruments could be made to the requisite specifications and recommended for production.

Study of the instruments and setups for the measurement of the vibrations of bearings is beyond the scope of this book. This problem is considered in some detail in specialized works [7, 21, 23, 42, 43, 102, 112] and repetition is unnecessary.

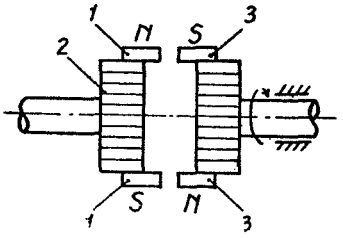

Fig. 4.20. Magnetic unit for measuring friction torque in bearings.

In the field of vibrations measurement we must mention a series of interesting new problems that have appeared with the development of laser technology, holography and introscopy which open up new vistas for the improvement of methods and setups for the measurement of vibrations.

4.3 APPARATUS FOR THE ANALYSIS OF FRICTION TORQUE IN SLIDING BEARINGS

In principle the setups for the measurement of friction torque in sliding bearings differ very little from setups measuring friction torque in rolling contact bearings.

The basic kinematic scheme for the measurement of friction torque components in precision sliding bearings [28, 41] is shown in Fig. 4.21. It works as follows: When the rotor *1* rotates in the support of instrument *2* the friction torque is disturbed. Under the action of the resistance the support *2* turns along with the rigidly connected casing *3* which is held on elastic crossed, for example, flat metal plates *4*. When the suspended casing *3* rotates with the support the load due to friction torque is transmitted through the lever *5*, rigid needle *6* and semiconductor strain gauge bonded to the elastic plate *7*, to the amplifying-recording apparatus (not shown in the Figure). The value of the constant component M_{cons} observed on the oscilloscope screen can be determined on the basis of the reading shown on the scale of the microammeter mounted in the strain gauge amplifier and recorded with the help of an automatic relay, etc. The variable component M_v can, however, be observed and recorded by an indicator in the shape of an oscillogram or photograph.

The needle *6* is suspended in a magnetic field in which the lines of force between poles coincide with its longitudinal geometric axis. Due to the permanent magnet *8* the fixture of the needle does not require additional mechanical tightening of the plate with the strain gauge *7* relative to the elastic suspension and this appreciably enhances the sensitivity of the turn of suspension around its geometric axis, i.e. the suspension in the static position has

practically zero restoring torque. This design of suspension works practically without friction torque for small angles (0–1°) of turn because the value of the friction of elasticity of plane elements is very small. The value of the torque M_i to be measured can be represented as a sum

$$M_i = M_s + M_r + M_r' + M_p, \tag{4.43}$$

where M_s is the friction torque of the rotating rotor in the support;
M_r is the restoring torque of the crossed elastic elements of suspension;
M_r' is the restoring torque of the suspension caused by the change in temperature of the surrounding medium;
M_p is the restoring torque of the elastic plate with the bonded strain gauge.

Under the action of friction torque the support turns through a certain angle φ_2 and the crossed plates adjust their length due to extension caused by the curvature of the plane element and compression caused by the displacement of the end of the elastic element along the inner radius of the cylindrical casing of the suspension.

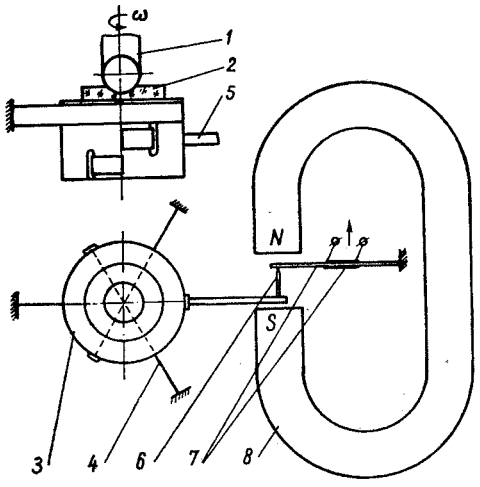

Fig. 4.21. Instrument for measuring friction torque in precision supports.

To change the sensitivity of turn of the suspension, the magnitude and direction of the restoring torque of the suspension can be regulated by using the regulating compression (not shown in the Figure), effectively changing the deforming length of one of the crossed elastic elements. By regulating the tensile or compressive loads acting on the elastic element the value of M_r can be reduced to zero. Under the action of the tensile P_T and compressive P_c loads on the elastic elements for small angles of turn of the suspension ($\varphi_2 = 0 - 1°$) the restoring torque can be computed using the formulas:

$$M_{rT} = n_e P_T \varphi_2 \frac{\cos i\beta}{\cos i\alpha - \cos i\beta} (l_{el} - \eta\, i \tan i\beta) \tag{4.44}$$

and

$$M_{rc} = n_e P_c \varphi_2 \frac{\cos \beta}{\cos \alpha - \cos \beta} (l_{el} - \eta \tan \beta), \tag{4.45}$$

where n_e is the number of crossed elastic elements;

$$\alpha=\frac{\tanh^{-1} l_{e_1}+l_{e_2}\cosh\chi-\eta\sinh\chi}{\eta(\cosh\chi-1)-l_{e_2}\sinh\chi}.$$

Hence

$$\gamma=\alpha+\frac{L_e}{\eta};\qquad \eta=\sqrt{\frac{EI_e}{P_{T,c}}};$$

$$I_e=\frac{b_e h_e^3}{12};\qquad \chi=\frac{L_e}{\eta};\quad i=\sqrt{-1};$$

where $l_e=l_{e_1}+l_{e_2}$ is the total length of the elastic flat element between the fixed points;

l_{e_2} is the length of the flat elastic plate equal to the inner radius of the cylindrical suspension;

E is Young's modulus of elasticity of the flat plate;

b_e and h_e are the thickness and width of the elastic element ($h_e \gg b_e$).

The restoring torque is equal to zero when $l_{e_1}=\eta i\tan i\beta$ for formula (4.44) and when $l_{e_1}=\eta\tan\beta$ for formula (4.45).

A change in temperature of the surrounding medium by $\Delta t°$ causes a compressive load and presses the elastic elements. Then the additional restoring torque of the suspension will be

$$M_r'=1.68\cdot 10^{-1}\cdot n_e\cdot\varphi_2\sqrt{\frac{E}{P_c}\,b_e^3\cdot b_e^5\cdot\alpha_t\cdot\Delta t°},\qquad (4.46)$$

where α_t is the coefficient of linear expansion of elastic elements.

A simplified kinematic scheme of the mechanical part of the instrument for the measurement of friction torque components of precision bearings with and without axial vibrations when the rotor is in the vertical, horizontal and inclined positions is shown in Fig. 4.22.

The instrument has high sensitivity of measurement, is universal and is meant basically for the measurement of friction torque in precision bearings of different sizes in air and in some special medium at high temperatures, different loads and velocity ranges of the rotor operation.

Let us analyze its working principle. The rotor *4* with the lower and upper test bearings is fixed to the lower *3* and upper *6* vibration elements which could be, for example, piezoelements of linear vibrations. Piezo crystals of inverse effect are electrically connected to the block for excitation and control of frequencies. The lower vibration element *3* is rigidly connected to a chuck in the same axis as the axis of rotation. The upper vibration element *6* is axially connected to the chuck holder *5*. The reciprocating-rotating motion of the chuck along with the lower *3* and upper *6* vibration elements and bearings is derived from the drive *14*, which through pulley *15*, belt transmission *13*, pulley *11*, worm gears *9* and hob *10*, transmits the rotation to the worm gear *2* on the shaft of which the chuck is rigidly fixed. In order to achieve accurate

coaxiality and normality and to eliminate radial wobbling of the axis of rotation of the rotor *4* in the direction of the working plane of the chuck the upper vibration element *6* can be shifted with the help of microscrews *17* and *18* in two perpendicular planes and roughly move along the guides in the vertical plane. This makes it possible to carry out the test with rotor systems of different sizes. The lower and upper vibration elements work independently of each other and allow axial vibrations which differ in amplitude and frequency.

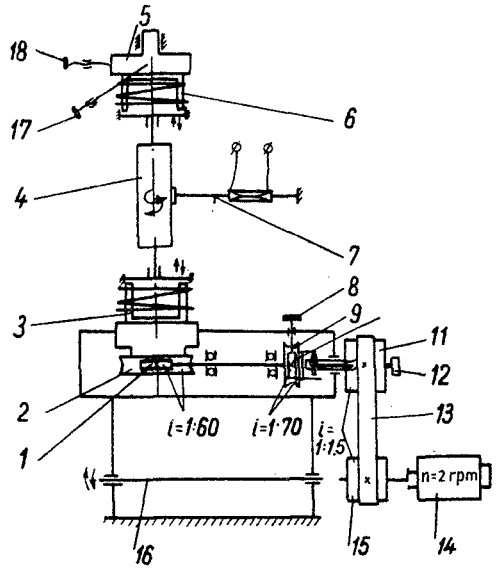

Fig. 4.22. Instrument for measuring friction torque in slide bearings.

For the measurement of M_{const} and M_{var} in a special medium, for example, in a special liquid and at high temperatures a photographic hermetically sealed chamber is used in which are installed the rotor *4*, vibroelement *3* and semiconductor strain gauge *7* movable in the radial direction. The temperature of the surrounding medium is controlled by a thermistor connected to a control block for temperature (not shown in Figure).

The angle of inclination of the rotor *4* with bearings to the vertical position is regulated by the turn of the whole upper part around the axis *16* along the dial. When the upper part turns, the electric drive *14* rotates accordingly when the tension in the belt *13* is maintained. The chuck can also be rotated by hand. In that case instead of the pully *11* a handle is installed which can be fixed with the help of a bolt *12*.

To change the drive ratio to the chuck there is another worm gear *9*, *10* on which instead of handle *8* a follower pulley *11* is fitted.

In all cases the friction torque being measured is transferred through the elastic deformable plate with the semiconductor strain gauge 7 bonded to it and the signal from it is amplified by a strain amplifier and transmitted to the indicator (not shown in the Figure). The sensitivity to changes in friction torque in the bearing is regulated by damping and displacement of the elastic plate with strain gauge. As a result it is possible to obtain dynamic characteristics of the instrument very nearly equal to the dynamic characteristics of the pairs being tested.

The general view of the working instrument is shown in Fig. 4.23.

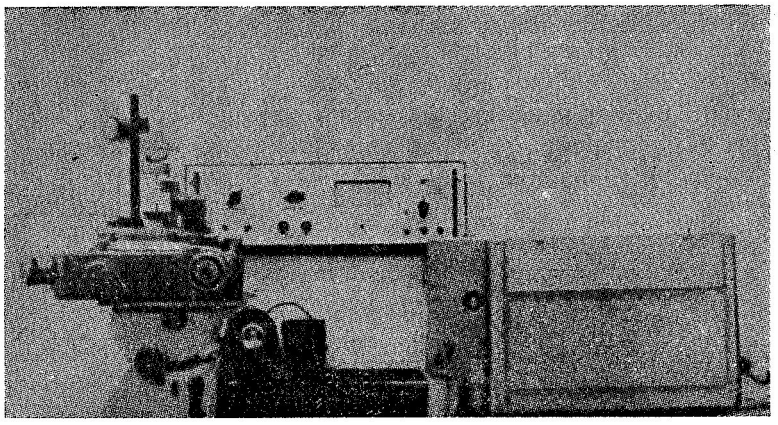

Fig. 4.23. General view of apparatus for measurement of friction torque in slide bearings.

For determination of the true value of the friction torque, semiconductor strain gauges connected to the measuring setup are calibrated under the same working conditions as in the case of measurement of the required values. Depending on the desired accuracy and the measurement scheme used it is possible to carry out the calibration of strain gauges by creating loads of known values acting at the point of application of the force due to the friction torque in the bearing being tested.

4.4 APPARATUS FOR THE MEASUREMENT OF DYNAMIC PARAMETERS OF HIGH-SPEED BALL BEARINGS IN SPECIFIC CONDITIONS

Determination of the nature of constant and variable components of friction torque of a pair of high-speed ball bearings under different working conditions is especially important in conjunction with analysis of the parameters that characterize the dynamics of the high-speed rotor.

The operation of rolling contact bearings in a vacuum is characterized by certain significant features of friction:

a) absence of effective heat transfer from the bearing components;

b) unsuitability of conventional liquid lubricants and use of solid lubricants to eliminate setting at points of friction.

Study of the friction torque in the working range of high-speed precision ball bearings of the 406075 type was carried out using a setup consisting of mechanical and electronic parts (Fig. 4.24). A high-frequency hysteresis synchronous motor of inverter design is placed at the base. The moment of inertia of the rotor was equal to 1.1 g cm sec^2 and it rotated on the test bearings.

The oscillations of the variable friction torque in high-speed ball bearings have quite a high frequency, reaching a few tens of kilohertz. However, only the components having much lower frequencies are of practical significance because in actual systems higher harmonics of vibrations are absorbed by mechanical components of the apparatus. In the vacuum chamber, in the synchronous range of rotation of the rotor, strain gauges register the changes in the torque of the motor. After switching off the motor these readings correspond to the value of friction torque in the bearings at that instant.

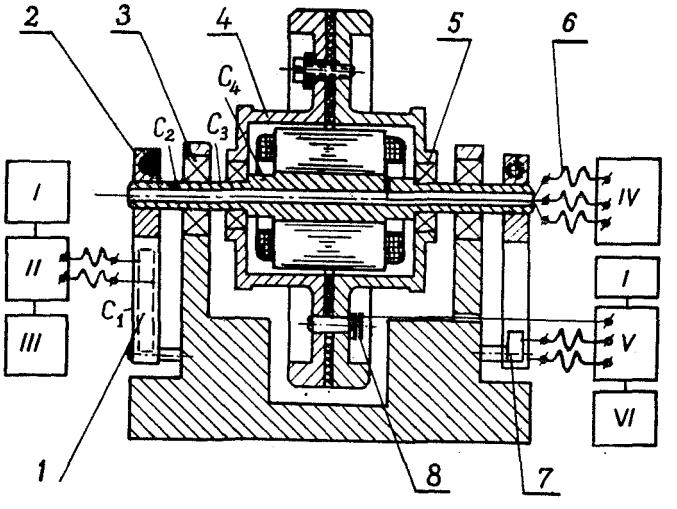

Fig. 4.24. Test stand: *1*—steel plate with bonded strain gauges; *2*—fastener for plate; *3*—sensitive bearing of 1000095 type; *4*—rotor; *5*—bearings under test; *6*—conductors; *7*—capacitor transducer for measuring friction torque; *8*—capacitor transducer for measuring rotor speed; C_1, C_2, C_3, C_4—stiffness of respective parts of vibrating system; *I*—*C*1-18 oscillograph; *II*—device for measuring dynamic friction torque in high-speed ball bearings; *III*—autorecording instrument of high sensitivity; *IV*—electronic statistical frequency converter; *V*—capacitor converter; *VI*—impulse counter.

However, during operation of a test stand (Fig. 4.25) of this design the amplitudes of torsion vibrations appearing in the stator and determined by function ξ (t) exceed by many times the amplitudes that appear during the

vibration of the moving ring of a sensitive ball bearing. On the basis of existing data [27] and additional measurements it has been established that for small angles of turn of the inner ring of a bearing of the 1000095 type the friction torque does not exceed 2×10^{-6} nm. Hence it is practically possible to neglect the effect of friction torque in sensitive bearings, determined by the function $\xi'(t)$ on the results of measurements. Besides, it has been established that

$$c_2+c_3+c_4\gg c_1\gg c_p,$$
$$\varphi_1\cong\varphi_2\cong\varphi_4=\varphi_3. \tag{4.47}$$

Simultaneously neglecting the effect of variable torque determined by the function $\varphi_r(t)$, vibrations of the system are described by the differential equation

$$\ddot{\varphi}_3+2h\dot{\varphi}_3+\omega_0^2\varphi_3=A\xi(t), \tag{4.48}$$

where the eigen frequency of the system ω_0 (when $c_4\to\infty$) is determined in the following way:

$$\omega_0=\sqrt{\frac{c_1c_2c_3+c_p(c_1c_2+c_2c_3+c_1c_3)}{\sum_{i=1}^{3}I_i(c_1c_2+c_2c_3+c_1c_3)}}. \tag{4.49}$$

The eigen frequency of this vibrational system taking into account all the elements mentioned in the dynamic model (Fig. 4.25) was verified experimentally: it was 305 ± 10 Hz. After supplying the stator windings with alternating current at a frequency of 1,000 Hz no changes in the eigen frequency were recorded. The connection of the power supply system with a high-frequency motor and with sensitive measuring transducers was carried out using a special power supply with the total friction torque not exceeding 10^{-5} nm [1].

In the electronic part of the apparatus the power supply to the electric motor is from a specially designed static electronic oscillator. This makes it possible to raise the rotation speed of the rotor gradually to 40,000 rpm, to regulate the voltage supplied and to eliminate the possible appearance in the rotor of low-frequency parasite vortex currents and their effect determined by the function of time $\varphi_r(t)$ on the vibrating system.

In order to measure the constant friction torque and its fluctuations with a frequency up to 100 Hz in a pair of high-speed ball bearings (HBB) under different working conditions it makes sense to use an apparatus working with semiconductor or resistance strain gauges bonded to the plate *1* (Fig. 4.24). The temperature effects and the drift in initial readings of the instrument are compensated by connecting the gauges in full bridge or half bridge circuits [78, 80, 106 and others]. The measurement of friction torque at high

temperatures (more than 100°C) has been considered using the capacitor-type transducer 7 (Fig. 4.24) and a capacitor-type transformer which reduce drift to zero during prolonged measurements [7, 8]. Fluctuations in friction torque are registered by the ELKAR-6 autorecorder of high sensitivity and high eigen frequency (100 Hz) or by oscilloscope.

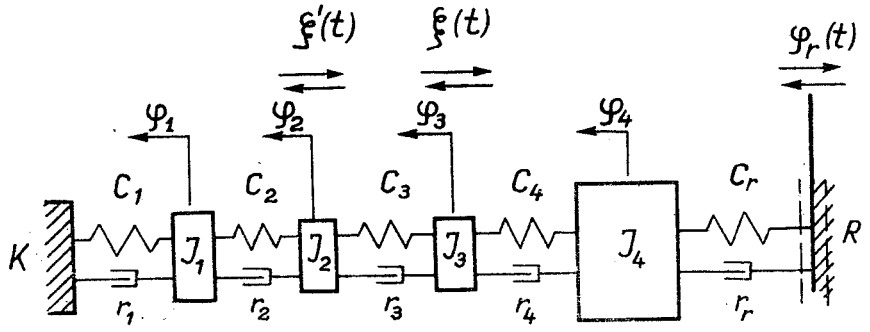

Fig. 4.25. Dynamic model of test stand: r_1, r_2, r_3, r_4—damping elements (dash pots) of corresponding segments of vibrating system; K—casing of test stand; R—rotor; I_1—moment of inertia of strap with respect to stator; I_2—carry-over moment of inertia of inner ring, cage and balls of sensitive bearing; I_3—moment of inertia of inner ring of bearing under test and fixing nuts; I_4—moment of inertia of stator; $\xi(t)$—random function of time, characterizing friction torque of pair of high-speed ball bearings and assembly errors of each component; $\xi'(t)$—random function of time characterizing change in friction torque of sensitive bearing; $\varphi_r(t)$—function of time of determination of effect of parasite vortex currents of rotor in absence of synchronization of stator vibration.

Intervals of time are marked on the oscilloscope screen and the recording of the number of revolutions of the rotor is carried out with the help of the capacitor transducer and capacitor transformer which register impulses when designed projections of the rotor pass by the plates of the transducer [111, 122].

The top of the test stand is placed in a hermetically sealed chamber having a free volume of 135 cm³ from which a vacuum pump evacuates air to 1×10^{-3} mm Hg. Resistance strain gauges, used as measuring transducers, are bonded from both sides to the steel plate and connected to a semibridge circuit. In order to avert shift of the null point of the measuring apparatus from temperature effects the bonded gauges are first subjected to thermal treatment [93, 94, 107]. The temperature in the chamber is maintained, registered and regulated using a setup incorporating the KSM-4 instrument. A platinum resistance thermometer is used as the temperature gauge. It is graduated in degrees and has a nominal resistance of $R_{nom}=46$ ohm (at 0°C).

As for all the other dynamic characteristics of a high-speed rotor the fric-

tion torque in bearings working in a vacuum also depends on the temperature of the stationary ring. This exceeds the temperature of the surrounding medium by tens of degrees and depends on working conditions and the range of the test. When carrying out basic tests with the rotor it is necessary to control the temperature of each bearing separately [11]. The improved EPP-09M3 instrument was used as the recording instrument. This instrument was adapted for recording the differential temperature of the rings of bearings relative to the surrounding medium with an accuracy of $\pm 0.2°C$ using a chromel-copal thermocouple of minimum dimensions [17, 62].

Accurate measurement of small differences in temperatures with the help of differential thermocouples can be ensured only when they are individually calibrated and when corresponding changes in the design of existing instruments are introduced [53, 109].

The final calibration of the instrument is carried out with the help of two thermostats. Thermocouples are mounted on the stator axis and the heads are tightly pressed to the most loaded upper part of the bearing inner ring. The length of the chrome and copal conductors of the thermocouples remains identical during assembly of the test head and also during calibration. The design of the apparatus, computation of the bridge and mounting of the thermocouples ensure the linearity of the scale [17, 75, 124].

A hydrodynamic film of lubricant introduces appreciable changes in the rotor dynamics of high-speed ball bearings. Its thickness and the hydrodynamic processes going on in it affect the damping characteristics of the rotor, the stiffness of the bearing and the whole rotor itself [10]. Besides this, study of the lubricating layer also establishes the causes of friction and wear and tear on ball bearings [29, 52, 92, 120].

Study of the stability of the film is associated with the stability of the dynamic characteristics of the rotor as a whole, especially in operating ranges of actual designs. Measurement of the thickness of the lubricating film and evaluation of its stability by direct methods without changing the assembly design are not possible in actual working conditions. Hence the determination of electric resistance of high-speed ball bearings is one of the basic methods of experimental verification of the nature of high-speed ball bearing lubricants [82, 119]. Analytical formulas and conclusions obtained on the basis of simplified hydrodynamic solutions as in the case of the hydrodynamic theory of lubricants do not take into account certain factors having a significant value in practice. Among these are the influence of individual properties of the lubricant used for lubricating the ball bearing of the support, the influence of the material and its properties on the friction, the influence of the design features of the bearing and the surrounding medium of the free volume of the chamber where the assembly is operating [47, 120]. For practical purposes it is necessary to study the ranges of stable operation of the lubricating layer in the actual design, to determine optimum operating ranges and to

control the condition of each ball bearing assembly of the rotor throughout its working life.

The following requirements must be met during the design of the above apparatus:

1. Independence of the chosen measurement technique from the effect of the temperature of the surrounding medium.
2. The selected method and design of the apparatus should not affect the lubricating, chemical and structural properties of the lubricating film.
3. Elimination of the effect of disturbances.
4. Linearity of measurement.

In spite of a large amount of work on the measurement of the film thickness a really suitable technique for determination of this thickness is yet to be developed, especially when the bearings work under specific conditions [52, 76].

As an example let us consider the apparatus for the control of the quality and condition of high-speed bearings (Fig. 4.26). The outer ring of the test bearing *1* is pressed to the top of the casing *2* through an isolating ceramic layer *3*, the high-speed shaft of the rotor *4* is mounted on the inner ring and welded at certain points. The shaft is separated along the center from the symmetric second end of the rotor by isolating ceramic bush *5*. At the end of the shaft of the rotor *4* an anode is screwed in and welded. The anode is the current receiver *6* made in the form of a ring with a taut nickel grid. Part of the bonded bulb of the vacuum photocell with photo-sensitive layers *8* serves at the photocathode *7*. The cathode is placed in the cartridge *9* which can be turned in the housing *10* near the axis of symmetry in the direction of the light flux indicated by arrows. In order to avoid unstable operation of the photocell in the event of the appearance of lubricant vapor in the chamber the outer end of the shaft *4* is sealed by vacuum packings *13*. The chamber consists of the cover with window for illumination *11* and base *12*. In order to protect the conducting parts of the rotor *4* and test bearing *1* from the effects of the variable electromagnetic field an insulator *14* is used and the casing of the machine *12* is earthed. In the chamber a vacuum (of the order of 10^{-5} to 10^{-7} mm Hg) is created. This is necessary for stable operation of the photocell. Voltage is supplied to the contacts *15* by insulated conductors *16* which are led out of the chamber through vacuum slides *17*.

At the time of operation of the apparatus a value of intensity of light flux falling on the photocathode *7* (Fig. 4.26) is chosen that corresponds to the photoelectric current $I\varphi_2$ (Fig. 4.27). This eliminates the possibility of puncture of the lubricating film being measured. This regulated stable light flux is focused on the photosensitive layer *8* (Fig. 4.26) of the photocathode *7*. Due to the potential gradient the electrons move in the direction of the rotating anode *6* (in Fig. 4.26 they are indicated by wavy arrows), completing the electric circuit consisting of series connection of cathode *7*, anode *6*, photocell and the

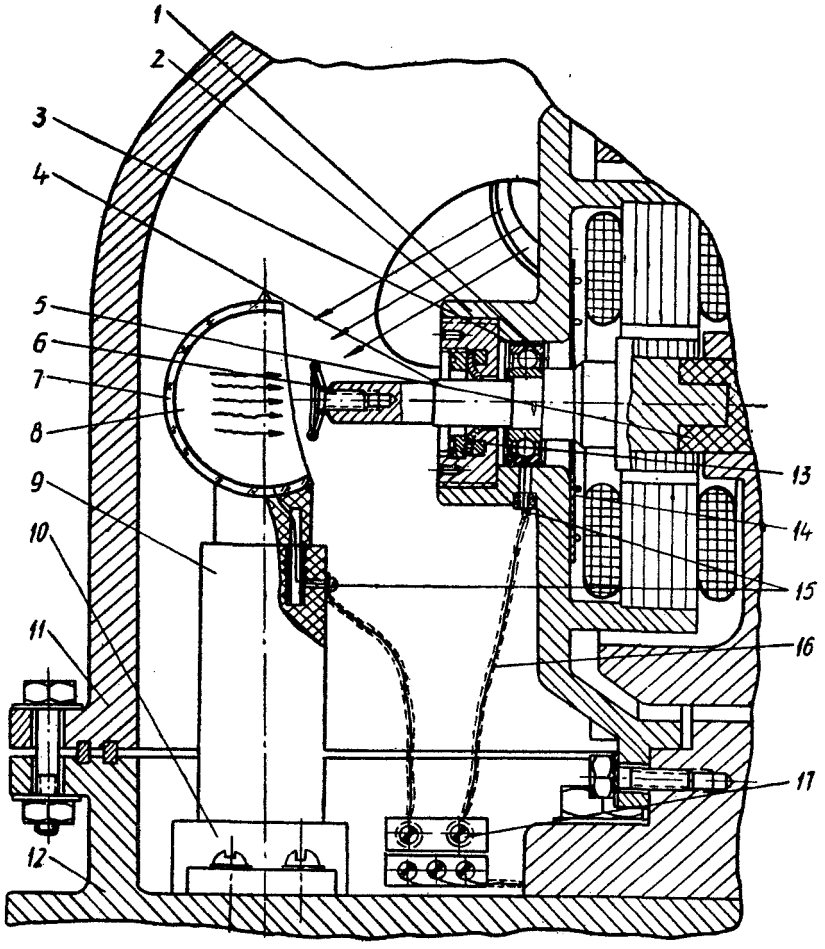

Fig. 4.26. Device for controlling bearings.

resistance of the bearing that is being measured. This scheme eliminates the effect of sources of errors in the geometric shape and vibrations of the shaft. It improves the sensitivity of the signal obtained without altering the operating conditions of the ball bearing.

In Fig. 4.27 the voltage-current characteristic of the photocell is shown where I_{φ_1}, I_{φ_2}, I_{φ_3} are the values of photoelectric current; straight lines R_{x_0}, R_{x_1} are the values of the resistance of the hydrodynamic lubricating film being measured; U_t is the voltage of the current source; U_a is the anodic voltage of the photocell; ΔU_1, ΔU_2, ΔU_3 are the voltages between the ends of the resistance; ΔU_{cr} is the voltage when the lubricating film is ruptured [18, 59, 65, 71].

For the purpose of studying the behavior of the lubricating film in high-speed ball bearings of a rotor which rotates in the chamber without a large free volume and at high working temperatures, another variation of the appa-

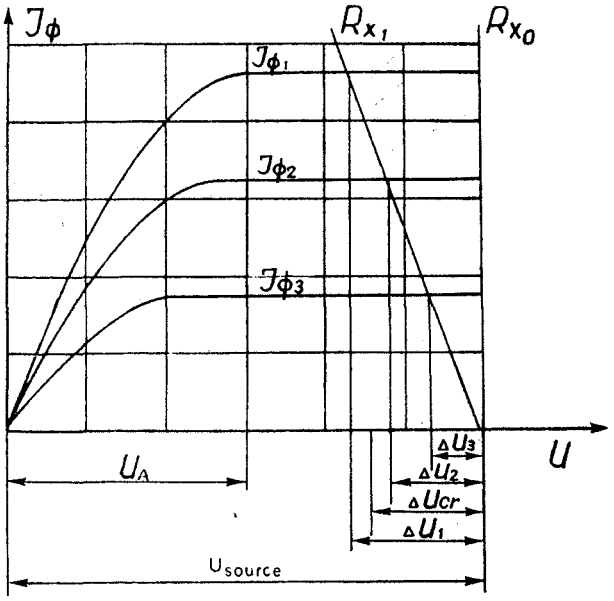

Fig. 4.27. Voltage-current characteristic of setup for control of bearing condition

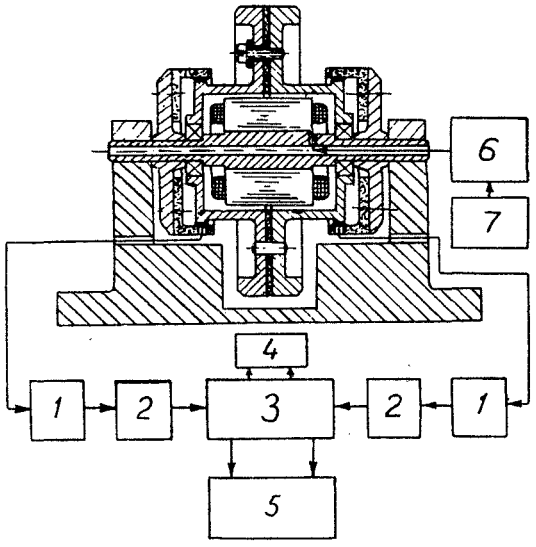

Fig. 4.28. Device for control of quality of high-speed ball bearing assemblies under working conditions by change in reactance.

ratus is used for control of the condition of high-speed ball bearings. It is based on measurement of the capacitance of the ball bearing, for which it is connected to a high-frequency generator by a capacitor-type variac [91]. The inclusion of the bearings in the measuring circuit by sliding variacs results in large errors while working at high temperatures in the vacuum chamber and does not yield the required reliability [2].

The basic diagram of the suggested apparatus for simultaneous control of the quality of the rotor's ball bearing supports is shown in Fig. 4.28. The design of the stand allows measurement and verification of other dynamic parameters of the rotor to be carried out without a detailed knowledge of the apparatus. Additional mounting errors are eliminated. Besides this, it is possible to carry out measurement of the capacitance of each bearing separately. For this purpose, ceramic plugs with a cone angle of 68′ 46″ ± 30″ and fiberglass packing are used, screwed between the covers of the rotor. This allows electrical insulation of the bearing from the other during measurement and ensures the necessary design rigidity.

The test stand includes a capacitor variac whose capacitance only negligibly affects the experimental results during the vibration of the rotor. The variac consists of two coaxial cylinders: an outer stator part made of a thin metal circular ring formed by a galvanized coating on a ceramic ring which is mounted on the axis of the stator with the help of a flange. The possibility of a shift of axes (value δ in Fig. 4.29) is thus avoided when the stand is assembled.

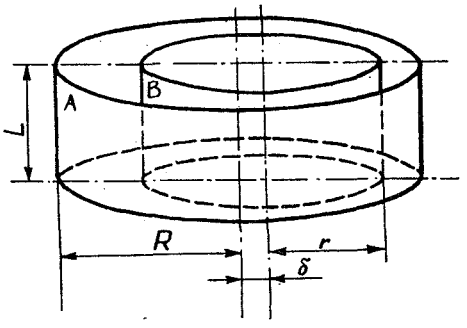

Fig. 4.29. Capacitor current pick-up.

The capacitance of such a condenser is determined by the relation (see Fig. 4.29) [44]:

$$C_m = \frac{2\pi\varepsilon L}{\tan^{-1}\text{h}\,\dfrac{r^2+R^2-\delta^2}{2\pi R}} \cong C_{m_0}\left(1-\frac{\delta^2}{4R\,(R-r)}\right), \qquad (4.50)$$

where

$$C_{m_0} = \frac{2\pi\varepsilon L}{\ln R/r},$$

Here L is the length of the rings;

R is the outer radius of the variac;

r is the inner radius of the variac;

δ is the shift in the axis of the moving ring relative to the stationary, caused by inaccuracy in manufacture and vibrations;

ε is the dielectric constant of the surrounding medium.

The allowable shift in the axes of cylinders is determined from the following condition:

$$\delta \leq \sqrt{R(R-r)\frac{\Delta C'}{C_{m_0}}}, \tag{4.51}$$

where $\Delta C'$ is the allowable deviation in the capacitance, determined by the accuracy of measurement.

With the help of small-diameter screened and insulated conductors the stationary rings of variacs are connected to the output heads *1* of the transformer, which has an initial capacitance adequate for operation of the apparatus in a linear domain (Fig. 4.28). The stand is connected to a two-channel capacitor convertor *3* through high-frequency generator *2* and indicator arrows record constant values of the capacitance of each bearing separately. From the capacitor converter the signal is transmitted either to the cathode oscillograph or through a filter to a highly sensitive multi-channel autorecording setup. This records the changing values of the capacitance of the ball bearings with the passage of time. The power supply for the rotor and regulation of its turning speed are from an EPCh-1 electronic frequency converter. The supply frequency of the stator winding is regulated by a noise generator. The assembled head with the experimental rotor and variacs is placed in a special chamber with a free volume of 145 cm^3. A temperature transducer is installed inside. The chamber allows the vacuum to be maintained at 10^{-3} mm Hg and temperature to be controlled with an accuracy of ± 1.5°C.

An equivalent electric circuit for the test head of the stand for measurement of the capacitance of the first ball bearing is shown in Fig. 4.30 where $C_{n_1}(t)$ is the variable capacitance of the experimental bearing. In the general case it is a random function of time: C'_{T_1} is the shunt parasite capacitance between the edges of the outer ring of the bearing and the stator of the head; $C_{n_2}(t)$ is the shunt capacitance between the covers of the experimental bearing through the isolating packing, plugs and screws through the second bearing on the casing of the stator (its value can also change with time); C_T is the capacitance of the variac; C_c is the shunt capacitance of all connecting wires

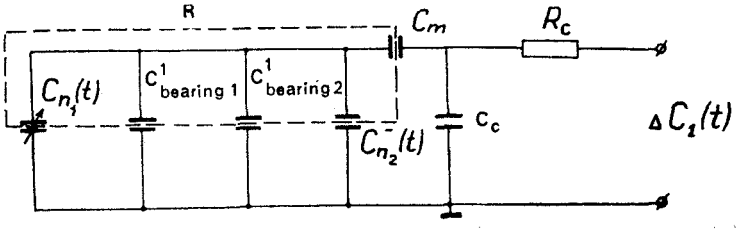

Fig. 4.30. Equivalent electric circuit for head of test stand for measurement of reactance of first bearing: *P*—rotor (broken lines indicate moving part).

and leads; R_c is the active resistance of connecting wires, contacts and metal supports.

In further computations the capacitance is not taken into account since the head is connected to the generator *2* (Fig. 4.28) of high frequency (5.0 MHz). In such conditions the active resistance is shunted [55]. On the basis of this circuit the capacitance of the *i*-th high-speed ball bearing is expressed in the following way:

$$C_{P_i}(t)=\Delta C_i(t)\{[C_{T_i}-\Delta C_i(t)]\,[C_{T_i}+C^i_{T_1}+C^i_{T_2}+C^-_{P_i}(t)] - C_{T_i}[C^i_{T_1}+C^i_{T_2}+C^-_{P_i}(t)]\}, \tag{4.52}$$

where $\Delta C_1(t)$ is the signal from the test head to the converter, varying in the limits of a few picofarads; $C_{P_i}(t)$ is the shunt capacitance from another bearing.

The reactance of the experimental ball bearings is determined by the formula:

$$X_{C_i}=\Delta C_i(t)\left\{2\pi f\left[\left(C_{T_i}-\Delta C_i(t)\right)(C_{T_i}+C^i_{T_1}+C^i_{T_2})-C_{T_i}(C^i_{T_1}+C^i_{T_2})\right]\right\}^{-1}, \tag{4.53}$$

where X_{C_i} is the reactance of the *i*-th ball bearing, $(i=1.2)$ Ohm;

f is the frequency of the current in the measurement circuit (5.0 MHz).

The values of shunt capacitance $C^1_{T_1}$, $C^1_{T_2}$, $C^2_{T_1}$ and $C^2_{T_2}$ corresponding to the first and second bearings were determined experimentally. The total shunt capacitance of these bearings was equal to 60 pF. The parasite capacitance $C^-_{P_i}(t)$, when compared to the above capacitances, did not exceed 5 per cent. The capacitances of the variacs are respectively

$$C_{T_1}=39.6 \text{ pF}, \; C_{T_2}=40.3 \text{ pF}.$$

The calibration of the measuring setup was carried out with the help of a special calibrating transducer, sensitivity 0.2 pF/mm, and the scale has a least count of 0.01 mm. During calibration the following condition was maintained:

$$C_{in_i}=C_{T_i}+C_c, \; (i=1.2), \tag{4.54}$$

where C_{in_i} is the initial capacitance of the calibrated transducer. This averted additional errors when calibrating the instruments.

References

1. Aganov, A.V. and others. 1969. Proizvodstvo i issledovanie (Production and Research). Moscow, Mashinostroenie.

2. Ageikin, D.I., I.N. Kostina and N.N. Kuznetsov. 1965. Datchiki kontrolya i regulinovaniya (Transducers for control and regulation). Moscow, Mashinostroenie.
3. Apirin, B.S. and B.B. Rodin. 1962. Pribor dlya kontrolya momenta teniya sharikopodshipnikov kacheniya (Instrument for the control of friction torque in ball bearings). *Podshipnikovaya promyshlennost*, No. 2.
4. Apirin, B.S. Sposob izmereniya momenta treniya podshipnikov kacheniya (Measurement techniques for friction torque in rolling contact bearing). Avt. svid. SSSR, N145042, Kl. 42K, 3801.
5. Arutyunov, V.O. 1949. Raschet i konstruirovanie elektrozimeritelnykh proborov (Design of electrical measuring instruments). Moscow, Gosenergoizdat.
6. Akhmetzhanov, A.A. 1962. Sinkhronno-sledyaschie sistemy povyshemoi tochnosti (High-precision synchronous-follower systems). Moscow, Oborongiz.
7. Atsyukovskii, V.A. 1960. Emkostnye differentsialnye datchiki peremeschcheniya (Capacitor-type differential displacement transducer). Moscow, Leningrad, Gosenergoizdat.
8. Atsynkovskii, V.A. 1966. Emkostnye preobrazovateli peremeshchleniya (Capacitor-type displacement converter). Moscow, Leningrad, Energiya.
9. Babaeva, N.F. and others. 1967. Raschet i proektirovanie elementov giroskopicheskikh ustroistv (Design of the components of gyroscopic instruments). Leningrad, Mashinostroenie.
10. Baranov, I.A. and I.I. Nevzorov. 1969. Vliyanie maslyanoi plenki na osevuyu zhestkost' bystrovrashchayuschegosya radial'no-upornogo sharikopodshipnika (Effect of oil film on axial stiffness of high-speed radial-thrust ball bearings). *Izv. vuzov. Priborostroenie*, No. 6.
11. Baranov, I.A. 1968. Izmenenie urovnya osevoi vibratsii, sozgavaemoi bystrovrashchayuschumsya sharikopodshipnikom v protsesse prirabotki (Change in the level of axial vibration of high-speed ball bearing during running-in). *Podshipnikovaya promyshlennost*, No. 2.
12. Baranovskii, S.N. 1964. Tenzodatchiki na osnove igolchatykh kristallov arsenida galliya (Strain gauges using needle crystals of gallium arsenide). In: *Poverkhnostnye i kontaktnye i kontaktnye yavleniya v poluprovodnikakh*, Izd. Tomskogo universitata.
13. Batalov, Kh.Kh. 1956. Avtomatizatsiya kontrolya momenta treniya pribornykh sharikopodshipnikov (Automatic control of friction torque in instrument ball bearings). *Izv. vuzov, Priborostroenie*, No. 8.
14. Belyaeva-Soloveva, E.A. 1967. Izmerenie dinamicheskogo momenta treniya v sharikopodshipnikakh s pomoschyu mayatnikovogo podvesa (Measurement of dynamic friction torque in ball bearings using a pendulum). *Izv. vuzov, Mashinostroenie*, No. 12.
15. Belyaeva-Soloveva, E.A. 1967. Fotoelektronnaya ustonovka dlya

otsillografirovaniya kolebanii v mekhanizmakh (Photoelectric device for obtaining the oscillogram of vibrations in machines). *Izmeritelnaya Tekhnika*, No. 3.

16. Bruevich, N.V., Z.M. Breitman and Yu.M. Reznikov. 1963. Tekhnicheskie izmereniya v podshipnikovoi promyshlennosti (Technological measurements in the bearing industry). Moscow, Mashgiz.
17. Butusov, I.V. 1963. Avtomaticheskie kontrolno-izmeritelnye i reguliruyuschie pribory (Automatically controlled and regulating instruments). Leningrad.
18. Vorontsev, L.N. 1965. Fotoelektricheskie sistemy kontrolya lineinykh velichin (Photoelectric systems of controlling linear quantities). Moscow, Mashinostroenie.
19. Vorontsev, L.N. and S.A. Maiorov. 1951. Pribornye sharikopodshipniki (Instrument ball bearings). Moscow, Oborongiz.
20. Gartel, L.A. Sposob opredeleniya momenta treniya v oporakh elektromekhanicheskikh priborov (Techniques for determining friction torque in bearings of electro-mechanical instruments). Avt. svid. SSSR, No. 153592, Kl. 42k 38 $_{02}$.
21. Gevodyan, T.A. and L.T. Kiselev. 1962. Pribory dlya izmereniya i registratsii kolebanii (Instruments for measuring and recording vibrations). Moscow, Mashgiz.
22. Germanov, G.S. and Yu.I. Sakharov. 1960. Izmerenie momenta treniya pribornykh podshipnikov metodom vybega (Measurement of friction torque in instrument bearings by the run-down method). *Podshipnikovaya Promyshlennost*, No. 1.
23. Goldman, V.S. and Yu.I. Sakharov. 1968. Induktivno-chastotnye preobrazovateli neelektricheskikh velichin (Inductance-frequency converters of non-electrical quantities). Moscow, Energiya.
24. Gordienko, P.L., I.M. Sivonenko and K.N. Yavlenskii. 1958. Laboratornaya ustanovka dlya izmereniya momentov sil treniya v oporakh priborov (Laboratory setup for measuring friction torque in instrument bearings). *Peredovoi nauchno-tekhnicheskii i proizvodstvennyi opit, Tema 32*, P-58–33/6.
25. Dovidenas, V.I. and V.N. Augutis. 1969. Izmerenie elektricheskogo soprotivleniya gidrodinamicheskoi maslyanoi plenki v podshipnikakh kacheniya (Measurement of the electrical resistance of a hydrodynamic oil film in rolling contact bearings).—*Nauchnye trudy vuzov Lit. SSR, Vibrotekhnika*, No. 3(5).
26. Dovidenas, V.I. 1968. Voprosy stabilizatsii skorosti v pretsizionnykh ustroistvakh magnitnoi zapisi (Velocity stabilization in precision units of tape recorders). Avtoreferat Kand. diss, Kaunas.
27. Dovidenas, V.I. 1970. Issledovanie dinamicheskikh momentov soprotivleniya sharikopodshipnikov (Study of dynamic friction torque in ball

bearings). *Nauchnye trudy vuzov Lit. SSR, Vibrotekhnika*, No. 3(8).
28. Dovidenas, V.I., K.M. Ragulskis and P.M.V. Kanapenas. Ustroistvo dlya kontrolya vrashchatelnykh kinematicheskikh par (A device for the control of a rotating kinematic pair). Avto. svid. SSSR, N252693, Kl. 42 K, 38_{02}.
29. Johns, F.S. and D.F. Wilcock. Protsess narusheniya smazki bystrokhodnykh sharikovykh podshipnikov (Destruction of lubrication in high-speed ball bearings). Perevod GPNTB N20792.
30. Dovbysh, V.D. Sposob izmereniya momenta treniya podshipnikov (Measurement techniques for friction torque in bearings). Avt. svid. SSSR, N219841, Kl. 42K, 38_{02}.
31. Dokuchalova, V.V., M.I. Lontser and A.S. Mikhailyuk. 1962. Izmerenie malykh momentov treniya (Measurement of small friction torque). *Izmeritelnaya Tekhnika*, No. 4.
32. Dolgov, V.A. and A.V. Kelin. 1968. Elektronnye datchiki dlya avtomaticheskikh sistem kontrolya (Electronic transducers for automatic control systems). Moscow, Sov. radio.
33. Dymshits, A.M. 1964. Indutsionnye datchiki ugla (Inductance transducers for angle). Moscow.
34. D'yakov, A.K. 1958. Podshipniki skolzheniya (Slide bearings). Moscow, Mashgiz.
35. Zheludev, I.S. 1969. Elektricheskie kristally (Electric crystals). Moscow, Nauka.
36. Zheludkov, V.N. 1963. Uprugie napravlyayushchie v priborakh (Elastic guides in instruments). *Izv. vuzov, Priborostroenie, LITMO*, Vol. 6, No. 2.
37. Izmeritelnye pribory dlya opredeleniya momenta treniya (Measuring instruments for determination of friction torque). Tekh. Perevod N 217/62, VNIPP. Moscow, 1962.
38. Ilisavskii, Yu.V. 1963. Poluprovodnikovye tenzometry (Semiconductor strain gauge technology). Izd. LDNTP.
39. Il'inskaya, L.S. 1962. Poluprovodnikovye tenzodatchiki (Semiconductor strain gauges). GOSINTI.
40. Il'inskaya, L.S. and A.N. Podmarkov. 1966. Poluprovodnikovye tenzodatchiki (Semiconductor strain gauges). Leningrad, Energiya.
41. Ilyukovich, A.M. 1966. Bokovoe davlenie na os' podvizhnoi chasti induktsionnogo schetchika (Lateral pressure on the axis of the moving part of an inductance counter). Leningrad, Energiya.
42. Iorish, Yu.I. 1963. Vibrometria (Vibration measurement). Moscow, Mashgiz.
43. Iorish, Yu.I. 1956. Izmerenie Vibratsii (Vibration measurement). Moscow, Mashgiz.
44. Iossel, Yu.Ya., E.S. Kachanov and M.G. Strunskii. 1969. Raschet elec-

tricheskoi emkosti (Computation of electrical capacitance). Moscow, Energiya.

45. Isaev, A.P. 1959. Issledovanie treniya v napravlyayushchikh osi balansa chasov (Study of friction in the guiders of the axis of a weights balance). *Izv. vuzov, Priborostroenie*, No. 3.
46. Kalvin, V.A. 1966. Eksperimentalnoe issledovanie momentov treniya skorostnykh podshipnikov kacheniya (Empirical study of friction torque in high-speed rolling contact bearings). *Trudy in-ta*, No. 1.
47. Same as [47], Chapter I.
48. Kio Kasakhiro. 1964. Podshipniki s malym shumom i treniem (Bearings with low noise and torque).—*Endzhiniya*, Vol. 6, No. 2 (Japanese).
49. Kaspler, V.A., E.F. Kolotii and I.G. Leschenko. 1966. Izmerenie dinanucheskogo momenta treniya sharikopodshipnikov Vremennym Metodom (Measurement of dynamic friction torque in ball bearings using the time method). *Izv. TPI im. S.M. Kirova*, Vol. 141.
50. Katsuo Kakuta. 1961. Issledovanie momenta treniya sharikopodshipnika, nakhodyashchegosya pod osevoi nagruzkoi (Study of friction torque in ball bearings under axial loading). *Nikhom kikari Gakkari rombunsyu*, Vol. 27, No. 178.
51. Kats, S.M. 1962. Balansirnye dinamometry dlya izmereniya vrashchayushchego momenta (Balancing dynamometers for the measurement of torque). Moscow, Leningrad, Gosenergoizdat.
52. Same as ref. [17], Chapter I.
53. Kozhukh, V.Ya. 1969. Avtomatichestkoe izmerenie raznosti temperatur (Automatic measurement of temperature difference). Moscow, Energiya.
54. Kolotenkov, V.I. and M.F. Kiselef. Pribor dlya opredeleniya momenta treniya v podshipnikakh kacheniya (Instrument for determination of friction torque in rolling contact bearings). Avt. svid. SSSR, No. 172527, Kl. 42K, 38_{02}.
55. Kolotii, E.F. 1966. Induktsionnyi metod izmereniya momenta troganiya pribornykh sharikopodshipnikov (Inductance method of measuring contact friction torque in instrument ball bearings). *Izv. TPI im. S.M. Kirova*, Vol. 141.
56. Kolotii, E.F. 1966. Primenenie induktsionnogo obrashchennogo preobrazovatelya dlya izmereniya dinamicheskogo momenta treniya priboznykh sharikopodshipnikov (Use of an inductance converter for measurement of dynamic friction torque in instrument ball bearings). *Izv. TPI im. S.M. Kirova*, Vol. 141.
57. Kolotii, E.F. and I.G. Leshchenko. 1966. K voprosu ob izmerenii momenta treniya pribornykh sharikopodshipnikov (Measurement of friction torque in instrument ball bearings). *Izv. TPI im. S.M. Kirova*, Vol. 141.

58. Kondakov, D.I. and B.Ya. Liberman. 1965. Mashiny dlya ispitanii vysokoskorostnykh podshipnikov kacheniya (Devices for testing high-speed rolling contact bearings). Moscow, VNIPP.
59. Kondorf, S.F. 1965. Fotoelektricheskie izmeritelnye ustroistva v mashinostroenii (Photoelectric measuring devices in machine design). Moscow, Mashinostroenie.
60. Korovin, N.I. and A.I. Eisurovich. Ustroistvo dlya kontrolya za sostoyaniem podshipnikov (Device for control of bearing conditions). Avt. svid. SSSR, No. 139128, Kl. 42K, 38_{02}.
61. Kosov, V.I. 1965. Tenzometricheskie podshipnikovye 'Vesy' (Strain gauge balance for bearings). GOSINTI, No. 18-65-643/46.
62. Kulakov, M.V. and B.I. Makarov. 1969. Izmerenie temperatury poverkhnosti tverdykh tel (Measurement of the surface temperature of solid bodies). Moscow, Energiya.
63. Kurendash, R.S. 1952. Issledovanie treniya v oporakh elektro-mekhanicheskikh priborov (Friction in the bearings of electromechanical instruments). Avtoreferat Kand. dis., L'vov.
64. Kutkov, A.A. 1958. Ustanovka dlya opredeleniya momentatroganiya podshipnikov kacheniya s avtomaticheskim fiksirovariem ego velichiny (Device for determination and automatic recording of contact friction torque in rolling contact bearings). *Izv. vuzov, Priborostroenie.* No. 2.
65. Lanis, V.A. and L.E. Lavina. 1963. Tekhnika vacuumnykhisnitanii (Vacuum technology). Moscow, Gosenergoizdat.
66. Leschenko, I.G., E.F. Kolotii and Yu.A. Bannov. 1966. Primenenie elektromagnitnogo preobrazovatalya dlya izmereniya momenta troganiya pribornykh sharikopodshipnikov (Use of an electromagnetic converter for measurement of contact torque in instrument ball bearings). *Izv. TPI im. S.M. Kirova*, Vol. 141.
67. Liberzon, K.Sh. Pribor dlya sortirovki pribornykh sharikopodshipnikov po momentu treniya (Instrument for sorting instrument ball bearings on the basis of friction torque). Avt. svid. SSSR, No. 145380, Kl. 42K, 38_{02}.
68. Liberzon, K.Sh. and G.I. Nedonoskov. Pribor dlya izmereniya momenta treniya vrascheniya v podshipnikakh kacheniya (Instrument to measure friction torque in rolling contact bearings). Avt. svid. SSSR, No. 164696, Kl. 42K, 38_{02}.
69. Liberman, B.Ya. 1965. Mashiny dlya ispitanii podshipnikov kacheniya (Devices for testing rolling contact bearings). Moscow, Mashinostroenie.
70. Liberman, B.Ya. and D.I. Kondakov. 1961. Tipazh mashin dlya ispitaniya podshipnikov kacheniya i rabochikh smazok (Devices for testing rolling contact bearings and lubricants). *Trudy VNIPPa*, No. 4 (28).
71. Litvak, V.I. 1966. Fotoelektricheskie datchiki v sistemakh kontrolya,

upravleniya i regulirovaniya (Photoelectric transducers in guidance and control systems). Moscow, Nauka.
72. Loginov, V.N. 1970. Elektricheskie izmereniya mekhanicheskikh velichin (Electrical measurement of mechanical quantities). Moscow, Energiya.
73. Martyushov, K.I. and Yu.V. Zaitsev. 1966. Rezistory (Resistors). Moscow, Energiya.
74. Matveevskii, R.M. 1957. Issledovanie treniya v pribornykh sharikopodshipnikakh (Study of friction in ball bearings of instruments). Moscow, Mashgiz.
75. Metody i sredstva izmereniya temperatury (Technique and procedures for measuring temperature). *Pribory i sistemy upravleniya*, No. 10, 1971.
76. Miller, Yu.G. and V.Ya. Ratkovskii. (?) Sposob opredeleniya nachala povrezhdeniya podshipnikov po poyavleniyu v smazke metallicheskikh chastits—produktov povrezhdeniya (Technique for early diagnosis of bearing failure upon appearance of metal debris in the lubricant). Avt. svid. SSSR, No. 148566, Kl. 42K, 38_{02}.
77. Mezon, Ch. 1952. Piezoelektricheskie kristally i ikh primenenie v elektroakustike (Piezoelectric crystals as used in electro-acoustics). Moscow, IL.
78. Nelits, I. 1970. Prakticheskoe primenenie tenzoresistorov (Practical use of resistance strain gauges). Moscow, Energiya.
79. Same as ref. [26], Chapter I.
80. Nybert, G.P. 1970. Izmeritelnye preobrazovateli neelektricheskikh velichin (Measuring converters of nonelectric quantities). Moscow, Energiya.
81. Pavlov, V.A. and others.(?) Ustroistvo dlya izmereniya momentor sil treniya v oporakh podvesa giroskopicheskikh priborov (Device for measurement of friction torque in the suspension supports of gyroscopic instruments). Avt. svid. SSSR, No. 150236, Kl. 42c, 25_{01}; 42K, 38_{02}.
82. Pokko, V.S. 1965. Pribor dlya izmereniya elektricheskogo soprotivleniya tonkikh maslyanykh plenok (Instrument for measurement of the electrical resistance of thin oil films). *Vestnik kharkovokogo politekhnicheskogo in-ta, Mashinostroenie*, vyp. I, No. 1 (49).
83. Polikarpov, P.N. and V.S. Vorobev.(?) Sposob izmereniya momenta treniya (Measurement of friction torque). Avt. svid. SSSR, No. 174408, Kl. 42K, 38_{02}.
84. Popov, I.N. 1967. Issledovanie treniya v napravlyayushchikh vrashchatelnogo dvizheniya priborov (Study of friction in the rotation guides of instruments). Avtoreferat kand. dis. Novocherkassk.
85. Popov, I.N. 1966. Ferrodinamicheskii datchik privedennogo momenta treniya i momenta inertsii miniatyurnykh sharikopodshipnikov (Ferrodynamic transducer of transformed friction torque and moment of

inertia in miniature ball bearings). *Izv. vuzov, Mashinostroenie.* No. 8.
86. Popov, I.N. 1968. Stend dlya issledovaniya treniya v napravlyayushchikh vrashchatelnogo dvizheniya priborov (Test-stand for study of friction in the rotation guides of instruments). Moscow, GOSINTI, 18-65-1071.
87. Porokhov, V.S. Sposob tarirovaniya mastin treniya (Calibration of friction-measuring devices). Avt. svid. SSSR, No. 179064, Kl. 42K, 38_{02}.
88. Portugalova, A.A. and N.A. Spitsyn. 1948. Podshipnikovye uzly vysokoskorostnykh privodov (Bearing assemblies of high-speed drives). Moscow, Mashgiz, vyp. 1.
89. 1963. Primenenie uprugikh sharnirov (Application of elastic joints). *Ekspress informatsiya. Isnytatelnye pribory i stendy, tochnayamekhanika i optika.* No. 29, Moscow.
90. Roiko, M.V., Trivailo. 1965. Metod izmereniya tolshchiny smazochnogo sloya v kontakte detalei mashin (How to measure the thickness of the lubricating layer in contact with machine components). *Fiziko-Khimicheskaya mekhanika materialov,* No. 5.
91. Ratnovskii, V.Ya., Yu.T. Miller and I.S. Voronin. Emkostnoi tokosemnik (Capacitor collector). Avt. svid. SSSR, No. 148600, Kl. 420, 12_{03}.
92. Rosenberg, Yu.A. 1970. Vliyanie smazochnykh masel na dolgovechnost' i nadezhnost detalei mashin (Effect of lubricating oils on the life and reliability of machine components). Moscow, *Mashinostroenie.*
93. Rudashevskii, G.V. 1957. Metodika rascheta i izgotovleniya termokompensinirovannykh tenzodatchikov (Methodology of the design and manufacture of temperature-compensated strain gauges). *Izmeritelnaya tekhnika,* No. 3.
94. Rudashevskii, G.V. 1956. Temperaturnaya kompensatsiya pritenzometripovanii (Temperature compensation in strain gauge measurement). *Izmeritelnaya tekhnika,* No. 1.
95. Sadovskii, A.S. 1957. Induktivnyi datchik povlyshennoi chuvstvitelnosti dlya registratsii lineinykh i uglovykh peremeshchenii (A highly sensitive inductance transducer for recording linear and angular displacements). *Avtomatika i telemekhanika,* Vol. 23, No. 9.
96. Sakharov, Yu.I. and V.A. Isaev. Pribor dlya izmereniya momenta treniya v podshipnikakh kacheniya (Device for measurement of friction torque in rolling contact bearings). Avt. svid. SSSR, No. 116016, Kl. 42K, 38og.
97. Same as ref. [86], Chapter III.
98. Solovev, A.I. 1955. Ustanovka dlya ispytaniya mikropodshipnikov natrenie (Setup for testing minibearings for friction). *Pribory i stendy,* Moscow, AN SSSR ITEI, Tema No. 2.
99. Solovev, A.I. and V.I. Kosov. Ustanovka dlya ispytaniya podshipnikov kacheniya (Setup for testing rolling contact bearings). Avt. svid. SSSR,

No. 207453, Kl. 42K, 38_{02}.
100. Same as ref. [35], Chapter I.
101. Same as ref. [37], Chapter I.
102. Sribner, L.A. 1966. Induktivnye putevye preobrazovateli transformatornogo tupa s differentsialnym vozdushnym zazorom (Inductance-tracked transformer-type converterws ith differential air clearance). *Mekhanizatsiya i avtomatizatsiya upravleniya*, Kiev, No. 1.
103. Sribner, L.A. 1966. Induktivnyi datchik lineinykh uglovykh peremeshchenii (Inductance transducer for linear angular displacements). Avt. svid. SSSR, No. 183628, Byulleten izobret, No. 13.
104. Sribner, L.A. 1966. Induktivnye i emkostnye preobrazovateli s differentisialnym rabochim vozdushnym zazorom (Inductance and capacitance converters with differential operating air clearance). *Stanki i instrument*, No. 5.
105. Stupel, F.A. 1965. Elektromekhanicheskie datchiki preobrazovateli neelektricheskikh velichin (Electro-mechanical transducers and converters of nonelectrical quantities). Moscow, Energiya.
106. Tisenko, N.G. 1960. K voprosu o kompensatsii temperaturnykh izmerenii soprotivleniya nakleennogo tenzodatchika (Compensation of temperature measurements of resistance with a bonded strain gauge). *Izmeritelnaya tekhnika*, No. 4.
107. Tisenko, N.G. and G.Kh. Borkunskii. 1968. Mikroporvoloka dlya termokompensirovannykh tensodatchikov (Micro-wires for temperature-compensated strain gauges). Moscow, Mashinostroenie.
108. Trukhachev, B.S. and N.P. Udalov. 1968. Poluprovodnikovye tenzopreobrazovateli (Semiconductor strain-converters). Moscow, Energiya.
109. Tumanov, V.A., V.N. Zharkov and V.V. Arkhiipov. 1970. Modernizatsiya promyshlennogo automaticheskogo potentiometra EMP-09 dlya otnositelnogo izmereniya temperatury (Improved version of the EPM-09 industrial automatic potentiometer for relative measurement of temperature). *Izmeritelnaya tekhnika*, No. 3.
110. Urazaev, E.F. Ustanovka dlya opredeleniya momenta treniya v podshipnikakh pri montazhnykh perekosakh (Setup for determination of friction torque in bearings skewed at the time of assembly). Avt. svid. SSSR, No. 130230, Kl. 42K, 38_{02}.
111. Utyamyshev, R.I. 1961. Tekhnika izmereniya skorostei vrascheniya (Measurement technique for speed of rotation). Moscow, Leningrad, Gosenergoizdat.
112. Fetisov, M.M. 1960. Novye automaticheskie kompensatsionnye pribory dlya izmereniya neelektricheskikh velichin (New automatic compensated instruments for the measurement of nonelectrical quantities). LDNTP, Ch.1, Leningrad.
113. Tsikerman, L.I. and R.Yu. Kotlyar. 1960. Induktinye preobrazovateli

dlya avtomatizatsii kontrolya peremeshchenio (Inductance converters for the automation of displacement control). Moscow, Mashinostroenie.

114. Chervyakov, V.V. Ustanovka dlya ispytaniya natenie i iznos podshipnikov kacheniya (Setup for testing rolling contact bearings for friction, wear and tear). Avt. svid. SSSR, No. 114971, Kl. 42K, 38_{02}.
115. Epstein, V.R. 1959. Pribory dlya kontrolya sharikopodshipnikov opor valov gladkikh barabanov (Instruments for the control of ball bearing supports with smooth drums). *Informatsionno-tekhnicheskii byulletin*, No. 3 (22).
116. Yurkauskas, A.Yu. 1969. Eksperimentalnoe issledovanie giroskopicheskikh podshipnikov po sostavlyayuschim momenta sil treniya (Empirical study of gyroscopic bearings using components of friction torque). *Nauchnye trudy vuzov Lit. SSR, Vibrotekhnika*, No. 5 (7).
117. Yurkauskas, A.Yu., K.M. Ragulskis and A.E. Vitkute. 1970. Izmerenie i analiz momentov soprotivleniya i vibratsii pribornykh sharikopodshipnikov (Measurement and analysis of friction torque and vibration of instrument ball bearings). *Nauchnye trudy vuzov Lit. SSR, Vibrotekhnika*, No. 2 (11).
118. Yakovlev, N.P. Ustanovka dlya opredeleniya momentov treniya v podshipnikakh kacheniya i skolzheniya (Setup for determination of friction torque in rolling contact and slide bearings). Avt. svid. SSSR, No. 112323, Kl. 42K, 38_{02}.
119. Adkins, R.W., C.S. Larson and J. Radzimovskye. 1968. Predicting the oil film thickness in hydrodynamically lubricated gears. *Pap. Amer. Soc. Mech. Eng.*, No. WA-5.
120. Anderson, W.J. 1970. Elastohydrodynamic lubrication theory as a design parameter for rolling element bearings.—*Pap. Amer. Soc. Mech. Eng.*, No. DE-19.
121. Giordano, Felix. 1961. Analyzer Discounts Machine Torque Accurate Bearing Record. *Product Engineering*, Vol. 32, No. 10.
122. Jones, B.E. 1970. Capacitance transducer—for high rotational speeds. *Control and Instrument*. Vol. 2, No. 3.
123. Kuhlenkamp, A. and J. Staraste. 1958. Melgerate zur Bestimmung Reibungsmomenten. *Feinwerktechnik*, Ig. 62, Heft 2.
124. Starr, C.D. and T.P. Wang. 1969. Thermocouples and extension wires. *Control and Instrument*, Vol. 42, No. 10.
125. Vieweg, R. and F. Gottwald. 1941. Nebverfahren zur Bestimmung Kleiner Reibungsmomente. *VDI-Zeitschrift*, Bd. 85, No. 18.

5

ERRORS IN THE MEASUREMENT OF FRICTION TORQUE AND THEIR REDUCTION

The process of measuring any physical quantity is an operation whose results show by how much the quantity being measured differs from the standard value. No single measurement can be carried out with absolute accuracy. When measurements are carried out with the help of measuring instruments errors are committed which are determined by the errors in the measuring instrument itself. The problem includes not only determination of the measured quantity but also an evaluation of the error involved in the measurement.

The measurement of friction torque is also accompanied by error. On its magnitude depends the accuracy of the information obtained by measurement on the processes taking place in the bearings.

Without lingering over a conditional division of errors into random and systematic, let us consider only the dominant and the most characteristic errors in the measurement of friction torque in precision bearings.

5.1 ADDITIVE ERROR IN THE MEASUREMENT OF FRICTION TORQUE AND ITS REDUCTION

In the majority of cases the measurement of friction torque can be considered linear. The linearity can be improved practically by introducing a negative inverse relation or by using compensatory measurement techniques. In these cases the output quantity from the measuring unit (MU) will depend linearly on the friction torque x:

$$y = A + Bx. \tag{5.1}$$

The instability of coefficients A and B gives rise to additive and multiplicational (change in B) components of error. It follows that the latter component can also be reduced by introducing a negative inverse relation.

The additive component determines the least measurable friction torque (the limiting sensitivity of the measuring instrument). It predominates in the measurement of friction torque for precision bearings. Hence the additive

component of error deserves special attention and requires careful study.

There is more than one reason for the appearance of additive error. It can be the effect of factors in the surrounding medium (temperature, pressure, humidity, radiation, etc.). The effect of temperature on MU has been most thoroughly studied, though in many cases it is difficult to account for.

The cause of additive error could also be the "aging" of the MU components, especially in the case of semiconductor devices.

The above factors responsible for the appearance of additive error develop slowly. For example, the "aging" of components may not arise throughout the working life of the device and in this case such errors can be excluded at the time of testing the MU.

More frequent sources of error are changes in supply voltages and flicker noise (in particular, the effect of the temperature of the surrounding medium).

The combination of all possible sources of error results in the additive error component σ_a. Reduction of this deserves special attention.

It is possible to reduce additive error by improving the design and manufacturing technology of transducers, amplifiers and other components.

There is also another method, though as yet not fully worked out: the cybernetic method associated with the search for an optimum design of MU, development of an accurate system using "crude" components. The most widespread techniques of stabilizing the real function of transformation and correction methods based on determination of the error signal and its elimination from the output signal of the MU belong to this type.

The correction of additive error when measuring friction torque is considered in work [3] in which it is shown that among the well-known methods of correction the most suitable is that of test signals.

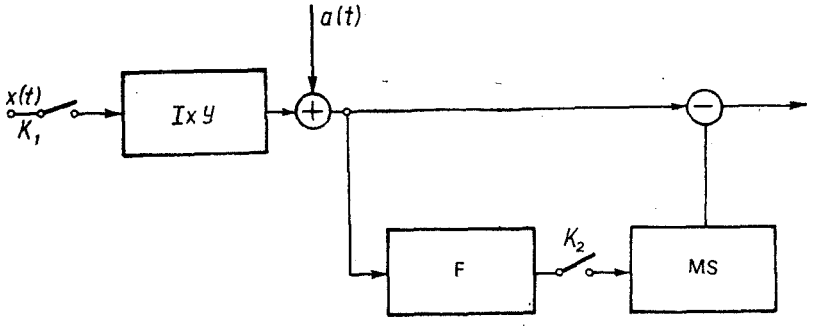

Fig. 5.1. Block-diagram of measuring unit with correction of additive error.

On the basis of general principles of correction using the method of test signals and the analysis carried out we may describe the block-diagram of MU with correction for additive error as shown in Fig. 5.1.

The working principle of this diagram is as follows:

When the switch key K_1 is closed the signal being measured arrives at the input of device $(I \times y)$, representing the converter, amplifier or other component. From the output of $(I \times y)$ the converted signal along with error enters the differential block and then the output of MU. The key K_1 periodically excludes the required signal when the switch K_2 is closed and the memory storage (MS) device registers the error signal. The filter takes into account the dynamic characteristics of the switch K_1. Besides this it can positively affect the correction process.

The switch K_1 will "switch off" the amplification from the converter in the measurement of torque. In the measurement of change in resistance the unbalanced bridge voltage is shut off from the input amplifier. It will switch off the small-power input signal and hence it must have small drift and low noise level. The requirements for the switch K_2 are less rigid because it commutes a high-level signal.

Like the input switch, the input system should have small drift and noise level.

The error $a\ (t)$ will be determined discretely. The problem consists in extrapolation of this error up to the next determination. These functions are carried out by MS, whose drift and noise level will also affect the residual error of MU with correction.

The simplest extrapolation formula can be expressed in terms of a polynomial of the fifth order. The extrapolator that carried out conversion of the input meshed function using such a formula will be called an extrapolator of the fifth order. The extrapolator of the zeroth order carries out step extrapolation and the extrapolator of the first order a linear extrapolation. Various methods of extrapolation are described in books on numerical analysis of experimental data. One of the simple types of extrapolation is based on expressing the function $a\ (t_n)$ in the form of a finite number of terms of a Taylor series. Since the data are given at a discrete number of points there is difficulty in the determination of the derivatives $a^v\ (t_n)$.

The power series formula for extrapolation can also be carried out using the interpolation formulas, for example, Newton's.

However, for the purpose of correction of errors of analog MU, only extrapolators of lower orders have practical interest, because of their complexity. We will restrict ourselves to study of the zeroth order and first order extrapolators.

5.2 DYNAMIC CONDITION OF CORRECTION OF ADDITIVE ERROR

It is found in practice that the shift in zero of friction torque measuring units is frequently a random process. Consequently, in the analysis of the dynamics of correction we have to use methods based on the theory of random processes. In what follows we will assume that the drift is a stationary

random process with a mathematical expectation $M=0$, energy spectrum $G_a(\omega)$, autocorrelation function $R_a(\tau)$ and dispersion D_a. Hence it is possible to judge the applicability of the results obtained below in each concrete case after initial tests for the drift of zero of MU. The region of application can be widened if the drift process contains explicitly expressed non-stationary components. In this case the residual error for them can be determined separately and then added to the residual error of the stationary component.

In the work of M.A. Zemel'man [17] residual error is considered for the correction of stationary random error by the method of auxiliary measurements. G.S. Safronov [36] has obtained the error of step extrapolation of a stationary random process.

On the basis of these works we will determine the dispersion and energy spectrum of residual error with step extrapolation of error. We will also study the hitherto unexplored problems of dispersion and energy spectrum of residual error in the case of linear extrapolation, determine the required (memory) storage of high-speed MU for effective correction and take up certain other problems connected with correction.

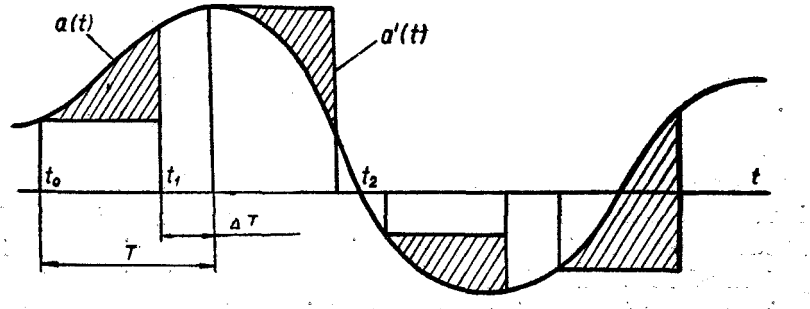

Fig. 5.2. Determination of residual error in case of stepped extrapolation.

Let us assume that the error is a stationary random process $a(t)$ (Fig. 5.2). The change in the value of $a(t)$ from t_0 to t_1 is made up of the residual error in the case of the application of step extrapolation. In the general case the residual error changes during the period of correction and if the measurement time for carrying out the correction is $\Delta T=0$, then

$$\varepsilon(T)=a(t)-a(t+T). \tag{5.2}$$

Since the differentiator does not carry out subtraction accurately,

$$\varepsilon(T)=a(t)-\varkappa a(t+T), \tag{5.3}$$

where $\varkappa$ is a coefficient determined by the differentiator ($\varkappa\approx 1$).

The autocorrelation function of $\varepsilon(T)$ has the form:

$$R_\varepsilon(\tau)=M[\varepsilon(t)\,\varepsilon(t+T)]=(1+\varkappa^2)\,R_a(\tau)-\varkappa[R_a(\tau-T)+R_a(\tau+T)]. \tag{5.4}$$

Hence the dispersion of the residual error is given by

$$D_\epsilon(T)=R_a(0)\,[1+\varkappa^2-2\varkappa\rho(T)], \tag{5.5}$$

where $\rho(T)$ is the normalized autocorrelation function.

The energy spectrum of the function $\varepsilon(T)$ can be expressed in the form

$$G_\epsilon(\omega)=\frac{1}{\pi}\int_{-\infty}^{\infty} R_\epsilon(\tau)\,e^{-j\omega\tau}\,d\tau=[(1+\varkappa^2)-2\varkappa\cos\omega T]\,G_a(\omega). \tag{5.6}$$

If

$$\varkappa=1,$$

then

$$G_\epsilon(\omega)=2\,G_a(\omega)\,(1-\cos\omega T) \tag{5.7}$$

and

$$D_\epsilon(T)=2\,D_a\,(1-\rho(T)]. \tag{5.8}$$

The nearer the normalized autocorrelation function $\rho(T)$ is to unity the smaller is the value of residual error. It changes in the limits of 1 to zero with changes in T from zero to infinity and consequently the dispersion of residual error changes from 0 to $2D_a$. Hence it follows that the correction can lead to an increase in dispersion.

As can be seen from formula (5.5), the dispersion of residual error depends on the value of $\varkappa$. The question arises as to the existence of the optimum value of $\varkappa_{\text{opt}}$ corresponding to the minimum of the expression

$$f(\varkappa)=1+\varkappa^2-2\varkappa\rho(T). \tag{5.9}$$

The minimum of the quantity $f(\varkappa)$ will be observed when $\varkappa_{\text{opt}}=\rho(T)$. Then

$$f(\varkappa_{\text{opt}})=1-\rho^2(T), \tag{5.10}$$

and

$$f(1)=2\,[1-\rho(T)]. \tag{5.11}$$

Comparing these expressions, we get

$$\frac{f(\varkappa_{\text{opt}})}{f(1)}=\frac{1+\rho(T)}{2}<1. \tag{5.12}$$

Given that, practically speaking, in the case of correction $\rho(T)\to 1$, then $\varkappa\to 1$. The increase in residual error due to noncorrespondence of the quantity $\varkappa$ to the optimum will not exceed 25%. This follows from the expression (5.12) for the condition of effective correction $\rho(T)>0.5$.

In the case of linear extrapolation the error (Fig. 5.3) can be predicted when its value is known not only at point t_0 but also at point t_0-T.

For determination of the dispersion of residual error during the period of correction we will write the residual error at the moment t_0+T':

$$\varepsilon(T')=[a(t_0)-a(t_0-T)]\frac{T'}{T}+[a(t_0)-a(t_0+T')]. \tag{5.13}$$

In the general case $t_0=t$.

Then

$$D_\varepsilon(T')=M[\varepsilon^2(t)]=2R_a(0)\left[1+\frac{T'}{T}+\frac{(T')^2}{T^2}-\left(1+\frac{T'}{T}\right)\rho(T')\right.$$
$$\left.-\frac{T'}{T}\left(1+\frac{T'}{T}\right)\rho(T)+\frac{T'}{T}\rho(T'+T)\right] \tag{5.14}$$

and before the next correction

$$D_\varepsilon(T)=2R_a(0)[3-4\rho(T)+\rho(2T)]. \tag{5.15}$$

As in the case of step extrapolation it is possible to find the energy spectrum of residual error:

$$G_\varepsilon(\omega)=2G_a(\omega)(3-4\cos\omega T+\cos 2\omega T). \tag{5.16}$$

After simple transformations we get

$$G_\varepsilon(\omega)=16\,G_a(\omega)\sin^4\frac{\omega T}{2}. \tag{5.17}$$

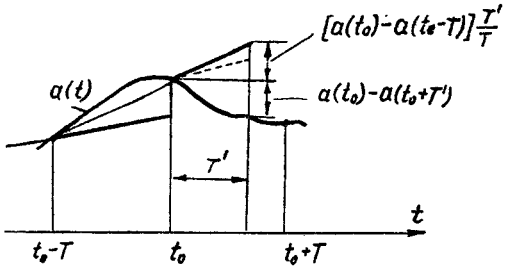

Fig. 5.3. Determination of residual error in case of linear extrapolation.

Usually, in linear extrapolation the function $a(t)$ in the interval of time t_0, t_0+T is expressed in the form of an extension of the straight line passing through points $a(t_0-T)$, $a(t_0)$. But extrapolation is possible even with a change in the curvature of this straight line in the interval of time t_0, t_0+T (broken line in Fig. 5.3). Let $\varkappa'$ be the coefficient which determines the change in curvature. Then

$$\varepsilon(t)=a(t)(1+\varkappa')-a(t+T)-\varkappa' a(t-T), \tag{5.18}$$
$$D_\varepsilon(T)=2R_a(0)[1+\varkappa'+(\varkappa')^2-(1+\varkappa')^2\rho(T)+\varkappa'\rho(2T)]. \tag{5.19}$$

The residual error depends on the value $\varkappa'$. Differentiating the expression (5.19) with respect to $\varkappa'$, we can find the minimum corresponding to

$$\varkappa_{\text{opt}}=\frac{2\rho(T)-1-\rho(2T)}{2[1-\rho(T)]}. \tag{5.20}$$

According to expressions (5.8) and (5.15), the correction has meaning in the case where the quantity $\rho(T)$ differs little from unity. Let us compare the residual error in the case of step and linear extrapolation for processes having characteristic spectra:

1) The spectrum

$$G_{a_1}(\omega)=\frac{2D_a\Omega}{\pi(\Omega^2+\omega^2)} \tag{5.21}$$

corresponds to "white noise" passing through the integrating RC circuit;

2) the spectrum

$$G_{a_2}(\omega)=\frac{D_a}{\Omega}\Pi\left(\frac{\omega}{\Omega}\right), \tag{5.22}$$

where

$$\Pi(t)=\begin{cases}1 \text{ when } 0<t<1\\ 0 \text{ when } t<0,\ t>1,\end{cases}$$

corresponds to "white noise" passing through an ideal filter;

3) the spectrum

$$G_{a_3}(\omega)=\frac{D_a}{\Delta\Omega}\Pi\left(\frac{|\omega-\Omega|}{\Delta\Omega}\right),\ \Delta\Omega\ll\Omega \tag{5.23}$$

corresponds to "white noise" passing through an ideal band filter;

4) the spectrum

$$G_{a_4}(\omega)=\begin{cases}g/\omega,\ \Omega_1<\omega<\Omega,\\ 0,\ 0<\omega<\Omega_1 \text{ and } \omega>\Omega,\end{cases} \tag{5.24}$$

where g is a coefficient proportional to the power, corresponds to flicker noise.

The following normalized autocorrelation functions are characterized by these processes:

$$\rho_1(\tau)=e^{-\Omega|\tau|}, \tag{5.25}$$

$$\rho_2(\tau)=\frac{\sin\Omega\tau}{\Omega\tau}, \tag{5.26}$$

$$\rho_3(\tau)=\frac{\sin\Delta\Omega\tau}{\Delta\Omega\tau}\cos\Omega\tau, \tag{5.27}$$

$$\rho_4(\tau)\approx 1-\frac{(\Omega\tau)^2}{4\ln\Omega/\Omega_1}+\frac{(\Omega\tau)^4}{96\ln\Omega/\Omega_1}. \tag{5.28}$$

The relation between the quantities $D_\epsilon(T)/D_a$ and ΩT is shown in Fig.

5.4 for these processes. The case of linear extrapolation is shown by broken lines. For flicker noise a value $\Omega/\Omega_1 = 10$ has been chosen.

As can be seen from the Figure, the linear extrapolation is worse than step extrapolation for a process with an unlimited upper frequency spectrum *1*. For a limited upper frequency linear extrapolation has an appreciable gain. For example, when $\Omega T < 0.1$ for the process *2*, the dispersion in the case of linear extrapolation is 1.6×10^2 times less than in the case of step extrapolation. Besides this, the dispersion of error in the presence of correction considerably decreases only when $\Omega T < 1$.

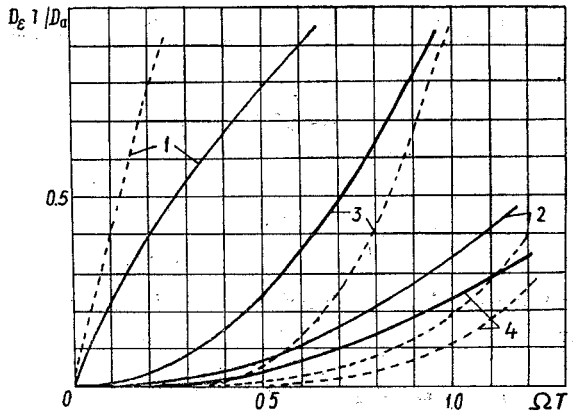

Fig. 5.4. Relation between ratio $\frac{D_\epsilon(T)}{D_a}$ and ΩT for processes having characteristic spectra from expressions (5.21) through (5.24).

5.2.1 Energy Spectrum of Residual Error

So far the dispersion of residual error has been considered before the sequential correction $D_\epsilon(T)$, answering the question as to the maximum probable error in measurement and the capacity of the MU to solve it. Energy spectra $G_\epsilon(\omega)$ obtained from formulas (5.7) and (5.17) are only auxiliary. With their help it is comparatively easy to compute the value of D_ϵ. A knowledge of the mean parameters of residual error is essential when measuring the parameters of random friction torque. The mean value of dispersion can be found from the expressions (5.8, 5.15):

$$D_\delta(T) = \frac{1}{T}\int_0^1 D_\epsilon(S)\, dS. \tag{5.29}$$

In order to find the component spectra approximately let us assume that the residual error consists of a sawtooth signal of unit amplitude $S(t)$ multiplied by the difference signal $\varepsilon(T)$:

$$\delta(t)=S(t)\,\varepsilon(T). \tag{5.30}$$

Expressing the quantity $S(t)$ in a series and multiplying each term by $\varepsilon(T)$, we get the spectrum of residual error.

Let us determine the exact expression for the energy spectrum of residual error which is the error in extrapolation of a stationary random process.

1. Stepped extrapolation

Let us assume that the function $a(t)$ is replaced by a step function

$$a'(t)=\sum_{n=-\infty}^{\infty} a(nT)\,1(t-nT)\,1[(n+1)T-t], \tag{5.31}$$

where $1(t)$ is a unit function.

The autocorrelation function of the difference process

$$q(t)=a(t)-a'(t) \tag{5.32}$$

is expressed [36] in the form

$$R_\delta(\tau)=R_a(\tau)+\sum_{k=-\infty}^{\infty} R_a(kT)\left(1-\frac{|kT-\tau|}{T}\right)1[\tau-(k-1)T]$$

$$\times[(k+1)T-\tau]-\frac{1}{T}\left[\int_{\tau}^{\tau+T} R_a(S)\,dS+\int_{-\tau}^{-\tau+T} R_a(S)\,dS\right], \tag{5.33}$$

and its energy spectrum in the form

$$G_\delta(\omega)=\left(\frac{\sin\frac{\omega T}{2}}{\frac{\omega T}{2}}\right)^2\sum_{n=-\infty}^{\infty} Ga\left(\omega+\frac{2\pi n}{T}\right)-G_a(\omega)\left(2\frac{\sin\omega T}{\omega T}-1\right). \tag{5.34}$$

From this expression, taking into account $\omega T<1$, for $n=0$, we get

$$G_{\delta_0}(\omega)=\frac{(\omega T)^2}{2}G_a(\omega), \tag{5.35}$$

and for $n=\pm1,\ \pm2,\ldots$

$$G_{\delta_n}(\omega)=\frac{(\omega' T)}{4(\pi n)^2}G_a(\omega'). \tag{5.36}$$

Here ω' is the deviation from the frequencies $\frac{2\pi n}{T}$.

2. Linear extrapolation

Let $a(t)$ be a stationary random process and $\bar{a}(t)$ its linear extrapolation (Fig. 5.5). Then the error in extrapolation is

$$g(t)=a(t)-\bar{a}(t). \tag{5.37}$$

The process $\bar{a}(t)$ can be expressed in the form

$$\bar{a}(t)=\sum_{n=-\infty}^{\infty}\left[\{a(nT)-a[(n-1)T]\}\lambda_1+a(nT)\right]\Pi\left(\frac{t-nT}{T}\right), \tag{5.38}$$

where

$$\lambda_1=\frac{1}{T}(t-nT).$$

To determine the correlation function of the error $q(t)$ we find

$$\bar{a}(t+\tau)=\sum_{n=-\infty}^{\infty}\left[\{a[(n+k)T]-a[(n+k+1)T]\}\lambda_2+a[(a+k)T]\right]\Pi \times\left[\frac{t+\tau+(n+k)T}{T}\right], \tag{5.39}$$

where

$$\lambda_2=\frac{1}{T}[t+\tau-(n+k)T].$$

Hence the correlation function of the error is expressed in the form

$$B(\tau_1 t)=M[q(t)q(t+\tau)]=M[a(t)a(t+\tau)-a(t)\bar{a}(t+\tau) -\bar{a}(t)a(t+\tau)+\bar{a}(t)\bar{a}(t+\tau). \tag{5.40}$$

Let us determine each term independently:

a) $$B_1(\tau_1 t)=M[a(t)a(t+\tau)]=R_a(\tau), \tag{5.41}$$

where $R_a(\tau)$ is the correlation function of the process $a(t)$;

b) $$B_2(\tau_1 t)=M[\bar{a}(t)a(t+\tau)], \tag{5.42}$$

assuming that $t=n+S$; then after substituting the value of $\bar{a}(t)$ we get

$$B_2(\tau_1 t)=\frac{S}{T}R_a(S+\tau)+R_a(S+\tau)-\frac{S}{T}R_a(S+\tau+T); \tag{5.43}$$

c) $$B_3(\tau_1 t)=M[a(t)\bar{a}(t+\tau)], \tag{5.44}$$

and similarly we get

$$B_3(\tau_1 t)=\frac{S}{T}R_a(S-\tau)+R_a(S-\tau)-\frac{S}{T}R_a(S-\tau+T); \tag{5.45}$$

d) $$B_4(\tau_1 t)=M[\bar{a}(t)a(t+\tau)]. \tag{5.46}$$

Substituting the values $\bar{a}(t)$ and $a(t+\tau)$ and considering that for the n-th interval of $\bar{a}(t)$ the value of $\bar{a}(t+\tau)$ changes from the interval $n+k$ to the interval $n+k+1$ (Fig. 5.5), we obtain

$$B_4'(\tau_1 t)=\lambda_1\lambda_2[2R_a(kT)-R_a(k-1)T-R_a(k+1)T]$$
$$+\lambda_1[R_a(kT)-R_a(k+1)T]+\lambda_2[R_a(kT)-R_a(k-1)T]+R_a(kT) \tag{5.47}$$

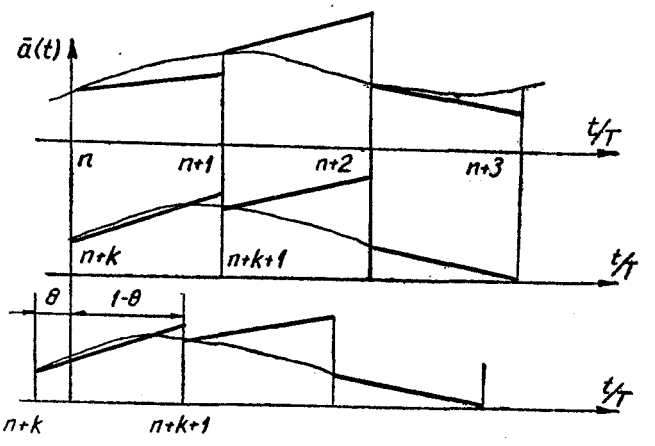

Fig. 5.5. Determination of energy spectrum of residual error in case of linear extrapolation.

when $nT\leqslant t\leqslant(n+1)T-\Theta$ and

$$B_4''(\tau_1 t)=\lambda_1\lambda_2[2R_a(k+1)T-R_a(kT)-R_a(k+2)T]$$
$$+\lambda_1[R_a(k+1)T-R_a(k+2)T]+\lambda_2[R_a(k+1)T-R_a(kT)]$$
$$R_a(k+1)T, \tag{5.48}$$

when $(n+1)T-\Theta\leqslant t\leqslant(n+1)T$.

The resulting correlation function is obtained, as expected, as a function of time. Averaging with respect to time, it is possible to make it stationary. After averaging and Fourier transformation we get the energy spectrum of residual error in the case of correction with the use of linear extrapolation of error:

$$G_8(\omega)=G_a(\omega)\left[1-2\frac{\sin^2\frac{\omega T}{2}}{\left(\frac{\omega T}{2}\right)^2}(\cos\omega T+\omega T\sin\omega T)\right]$$
$$+\frac{4(1-\cos\omega T)^2[1+(\omega T)^2]}{(\omega T)^4}\sum_{n=-\infty}^{\infty}G_a\left(\omega-\frac{2\pi n}{T}\right). \tag{5.49}$$

Then the spectrum of residual error around zero frequency will be

$$G_{8_0}(\omega)=G_a(\omega)\left[1+\frac{4(1-\cos\omega T)^2[1+(\omega T)^2]}{(\omega T)^4}\right.$$
$$\left.-4\frac{(1-\cos\omega T)(\cos\omega T+\omega T\sin\omega T)}{(\omega T)^2}\right]. \tag{5.50}$$

The spectral density in the range of frequencies which are multiples of the frequency of correction is found from formula (5.49):

$$G_{\delta_n}(\omega')=G_a(\omega')\frac{(\omega'T)^4}{(2\pi n)^2}, \tag{5.51}$$

where again ω' is the deviation from the frequency $\frac{2\pi n}{T}$.

Comparing formulas (5.35), (5.36) with formulas (5.50), (5.51) we see that when $\Omega T<1$ (where Ω is the upper frequency of the error spectrum) the spectral density of residual error in the case of linear extrapolation is less than in the case of stepped extrapolation.

The frequency of correction is an important parameter of MU. The higher the frequency the more accurate is the measurement. Without considering the speed of transmission of information the maximum frequency of correction will be determined at least by the high speed of MU. Let us find the relation between high-speed MU and frequency characteristics of the error and also the condition necessary for reduction of error in MU.

If it is required to reduce $D_\epsilon(T)$ n times, then for the stepped extrapolation according to (5.8) the following condition must be fulfilled.

$$1-\rho(T)\leqslant\frac{1}{2n},$$

and for linear extrapolation, according to (5.15), the condition

$$3-4\rho(T)+\rho(2T)\leqslant\frac{1}{2n}.$$

Let the MU have aperiodic transfer characteristics and F_B be the limiting frequency of its band pass. Then the duration of one measurement is $t_m=k'/F_B$,
where k' is a coefficient; $k'\approx 1$.

So the period of correction, in principle, cannot be less than $2t_m$ or $T>2k'/F_B$.

For processes 1, 2, 3 and 4 described by energy spectra (5.21) through (5.24) it is possible to compute the required ratio of frequencies F_B/F (here $F=\Omega/2\pi$) for an n-fold decrease in error dispersion. Computational results are given in Table 5.1. The quantities $\rho(\tau)$ are computed with approximate formulas.

$k'=1$ was assumed in the computations. Obviously, linear extrapolation is not always justified. Nevertheless, the minimum period of correction is taken to be the same as in the case of stepped extrapolation. This assumption is not correct for all linear extrapolation formulas but only when they are supplemented by one more storage scheme. Here only the ideal case has been considered.

TABLE 5.1

Process		1	2	3	4
$\rho(\tau)$		$1-\Omega\lvert\tau\rvert$	$1-\frac{(\Omega\tau)^2}{6}+\frac{(\Omega\tau)^4}{120}$	$1-\frac{(\Omega\tau)^2}{2}+\frac{(\Omega\tau)^4}{24}$	$1-\frac{(\Omega\tau)^2}{4ln\frac{\Omega}{\Omega_1}}+\frac{(\Omega\tau)^4}{96ln\frac{\Omega}{\Omega_1}}$
$\frac{F_B}{F}$	Stepwise Extrapolation	$8\pi n$	$4\pi\sqrt{n/3}$	$4\pi\sqrt{n}$	$4\pi\sqrt{\frac{n}{2ln\,\Omega/\Omega_1}}$
	Linear Extrapolation	$16\pi n$	$4\pi\sqrt[4]{n/5}$	$4\tau\sqrt[4]{n}$	$4\pi\sqrt[4]{\frac{n}{4ln\,\Omega/\Omega_1}}$

The above analysis of the dispersion and spectrum of residual error using correction with stepped or linear extrapolation shows that it is possible to prefer one or other method of extrapolation only after initially studying the nature of the error. From the point of view of simplicity of realization it is preferable, undoubtedly, to use the stepped extrapolation scheme.

5.3 SOME PROBLEMS OF CORRECTION PROCEDURE

From the examples on errors described by the energy spectra (5.21) through (5.23) it is possible to conclude that the frequency of correction should exceed by many times the upper limit of the frequency of error spectrum. When this condition is not fulfilled the correction may even increase the error dispersion.

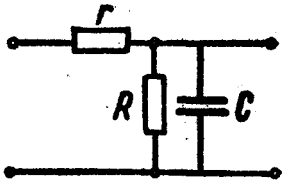

Fig. 5.6. R-C filter.

Often the low-frequency drift of MU is accompanied by high-frequency noise which adversely affects the conditions of correction. The negative influence of noise can be reduced by filtering it. As can be seen from the generalized diagram (5.1), filtration can be done either by a filter or by the memory unit. The use of a filter is unsuitable because of the long intervals between measurements. In the case of the simplest filter which is simultaneously a memory unit (Fig. 5.6) the time constant of the capacitor charge T_c should correspond to the condition

$$3T_c < \Delta T, \tag{5.52}$$

so that the capacitance is adjusted to the value of error by the correction time ΔT. On the other hand,

$$T_p = RC \gg T. \tag{5.53}$$

If the broad band width noise is described by the spectrum [21] and a stepped extrapolation is used, then the residual additive error of the noise in the case of filtration is expressed in the form

$$D_{\epsilon F} = D_{aB} + \frac{D_{aB}}{1 + \Omega_B T_c}, \tag{5.54}$$

where D_{aB} is the noise dispersion.

In the case of linear extrapolation

$$D_{\epsilon F} = D_{aB} + \frac{5D_{aB}}{1 + \Omega_B T_c}. \tag{5.55}$$

The value of the time constant of the filter is associated with the interval between measurements. An increase in this means a loss of information about the quantity being measured. On this basis we can conclude that filtration for the above cases will be effective if

$$\frac{\Omega_B}{\Omega_L} > 12 \frac{D_{aL}}{D_{aB}}, \tag{5.56}$$

where Ω_L and D_{aL} are the upper frequency and dispersion of low-frequency drift described by the spectrum (5.21).

5.3.1 Analysis of the Effect of Interrupting Measurement

When the correction is carried out by the method of standard signals the measurement is inevitably interrupted. Let the time during which MU does not give out information be ΔT. In certain cases the working principle of MU allows the effect of interruption to be easily avoided. For example, in oscillographs it is possible to synchronize the moments of correction by the reverse path of light. This corresponds to units of periodic action. In other cases, however, the interruption of measurement can affect the accuracy of the meas-

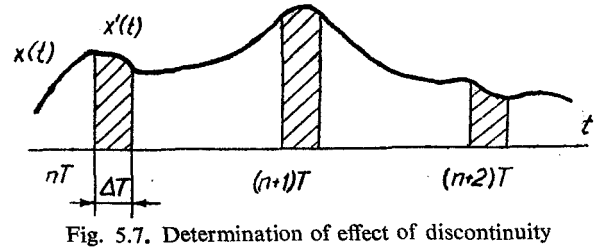

Fig. 5.7. Determination of effect of discontinuity in measurement process.

urement. To avoid this it is necessary to compute MU (if they are few in number) accordingly or determine and take into account the effect of interruption. Periodic impulse (Fig. 5.7, hatched portion) components in the form of

error $x'(t)$ are subtracted from the process being measured $x(t)$ for the interruption. The ratio of the mean value and power of the error signal to the mean value and power of the signal should be determined for the concrete signal that is measured. If, of example, the process being measured is given by impulses with duration ΔT, with a cycle period T, then if the beginning of the impulse and the interruption coincide no signal will appear at the output of MU. If the impulses do not coincide there will be no error signal. This shows that the general approach to the problem of interruption of measurement is very complex.

Studies described in the work [44] showed that friction torque in bearings is a random and practically stationary process. Hence we will also solve the problem of interruption of measurement for the particular case when the process being measured is random and stationary with a spectrum $G_x(\omega)$ and autocorrelation function $R_x(\tau)$.

The error process $x'(t)$ is determined in the form

$$x'(t)=\sum_{n=-\infty}^{\infty} x(t)\,1(t-nT)\,1(nT+\Delta T-t). \tag{5.57}$$

Hence

$$x'(t+\tau)=\sum_{n=-\infty}^{\infty} x(t+\tau)\,1[t+\tau-(n+k)\,T]\,1[(n+k+1)\,T + \Delta T-\tau-t]. \tag{5.58}$$

The autocorrelation function of the error process is

$$B_{x'}(t_1\,\tau)=M[x'(t)\,x'(t+\tau)]=R_x(\tau)\sum_{n=-\infty}^{\infty} 1(t-nT) \times 1(nT+\Delta T-t)\,1[t+\tau-(n+k)\,T]\,1[(n+k+1)\,T+\Delta T-t-\tau]. \tag{5.59}$$

Averaging (5.59) with respect to time, we get a time-independent expression for the autocorrelation function:

$$B_{x'}(\tau)=R_x(\tau)\sum_{n=-\infty}^{\infty} \Lambda\left(\frac{|kT-\tau|}{\Delta t}\right)\frac{\Delta T}{T}, \tag{5.60}$$

where

$$\Lambda(t)=\begin{cases} 1-t, & 0\leqslant t\leqslant 1;\\ t+1, & -1\leqslant t\leqslant 0;\\ 0, & |t|>1. \end{cases}$$

The spectral density of the error signal is expressed in the following way:

$$g_{x'}(\omega)=\frac{1}{\pi}\int_{-\infty}^{\infty} B_{x'}(\omega)\, e^{-j\omega\tau}\, d\tau. \tag{5.61}$$

It can be found for the concrete expression $R_x(\tau)$, limiting it to a finite number of terms in the series (5.60).

For certain cases of practical interest it is comparatively simple to obtain the expression for $g_{x'}(\omega)$ in closed form.

1. The correlation interval $\tau_{x_{cor}} \ll \Delta T$. This corresponds to the case where the interruption time is determined not by the band pass frequencies of MU but by other factors, i.e. it exceeds what the high-speed MU allows in continuous operation. It is natural to suppose that such a relation of values of $\tau_{x_{cor}}$ and ΔT exists with the measuring unit of friction torque with a mechanical deviation of the torque necessary for correction, using the technique of standard signals.

When $\tau_{x_{cor}} \ll \Delta T$ from expressions (5.60) we get

$$B_{x'1}(\tau)=R_x(\tau)\frac{\Delta T}{T} \tag{5.62}$$

and

$$g_{x'1}(\omega)=\frac{\Delta T}{T}G_x(\omega). \tag{5.63}$$

2. $\tau_{x_{cor}} \gg \Delta T$ but $\tau_{x_{cor}} < T$. The uncorrelated impulse of approximately rectangular form is subtracted from the signal being measured. Such an MU must have a greater capacity for high speed than the signal being measured.

From expression (5.60) we get

$$B_{x'2}(\tau)=\frac{\Delta T}{T}\Lambda\left(\frac{|\tau|}{\Delta T}\right)R_x(0). \tag{5.64}$$

After Fourier transformation we get

$$g_{x'2}(\omega)=\frac{2R_x(0)(\Delta T)^2}{T}\left(\frac{\sin\frac{\omega\Delta T}{2}}{\frac{\omega\Delta T}{2}}\right)^2. \tag{5.65}$$

3. $\tau_{x_{cor}} \gg \Delta T$ and $\tau_{x_{cor}} > T$. The low-frequency signal is measured and the correlated rectangular impulses are subtracted from it.

For this case we get from expression (5.60):

$$B_{x's}(\tau)=R_x(\tau)\sum_{k=-\infty}^{\infty}\Lambda\left(\frac{|kT-\tau|}{\Delta T}\right)\frac{\Delta T}{T}. \tag{5.66}$$

After Fourier transformation

$$g_{x'3}(\omega)=\left(\frac{\sin\frac{\omega\,\Delta T}{2}}{\frac{\omega\,\Delta T}{2}}\right)^2\frac{\Delta T}{T}\sum_{n=-\infty}^{\infty}G_x\left(\omega+\frac{2\pi n}{T}\right). \tag{5.67}$$

From equation (5.60), when $\tau=0$ we get the dispersion of error signal x':

$$B_{x'}(0)=R_x(0)\,\frac{\Delta T}{T}. \tag{5.68}$$

The mean value of the error signal is

$$M[x'(t)]=\frac{\Delta T}{T}M[x(t)]. \tag{5.69}$$

So reduction of the intervals between measurements leads to an increase in accuracy of measurement of the parameters of random friction torque.

5.3.2 Determination of the Parameters of Error

The solution of many problems on the correction of random additive error (choice of the type of extrapolation, determination of the frequency of correction, etc.) is associated with the determination of its parameters, more frequently, the normalized autocorrelation function.

There are many methods for the determination of parameters of a random process [7, 21, 28, 41]. The low-frequency error can be expressed, for example, by any recording device and the realization so obtained can be analyzed using a computer. For this it is necessary to prepare information for the computer input. In the Silvet computer multichannel automatic computation of curves (MASK) and others can be used. It is also possible to use the electronic analyzer of random processes (EARP) which is capable of analyzing the information recorded both on paper and on magnetic tape. These devices are characterized by complexity and demand considerable time for analysis of the results. Besides, they are always at the disposal of the researcher. The specific nature of demands to determine the parameters of random processes (it is necessary to determine the autocorrelation function at not too large intervals of time of correlation when the correlation coefficient hardly differs from unity), allows us to determine the correlation function in a comparatively simple way.

Let us assume that the error is a normal stationary random process whose normalized autocorrelation function at the point $\tau=0$ has derivatives up to n inclusive. To this case correspond processes described by energy spectra (5.22) and (5.23). As a rule, MU has a few inertial parts. Hence the process of error at the MU output can be described by energy spectra corresponding to "white noise" passing through a multi-capacitance filter:

$$G(\omega)=a\prod_{j=1}^{j_{max}}\frac{1}{1+\omega^2 Tj^2}\cdot \tag{5.70}$$

When $j_{max}>2$ the normalized autocorrelation function corresponding to the spectrum of expression (5.70) can be expressed in the form of a sum of exponents and is differentiable at the point $\tau=0$. For the majority of practically interesting cases $\rho'(0)=0$ (condition for a maximum). According to the work [2], for the stationary Gaussian random process with zero mean there exists a relation

$$\rho''(0)=-(\lambda_0 \Pi)^2, \tag{5.71}$$

where λ_0 is the frequency at the intersection of zero level of the process.

For processes described by energy spectra (5.22), (5.23) and (5.70) the normalized autocorrelation function can be expanded in a Maclaurin's series:

$$\rho(\tau)=\rho(0)+\rho'(0)+\frac{\rho''(0)}{2}+\ldots, \tag{5.72}$$

which is sign-variable. It is not difficult to show that when $\rho(\tau)\to 0$ it is possible to neglect terms of the series which are of an order greater than 3. Then

$$\rho(\tau)=1-\frac{(\pi\lambda_0\tau)^2}{2}\cdot \tag{5.73}$$

This expression can also be obtained when the spectrum of the process $G_a(\omega)$ is bounded, i.e. frequencies exceeding the quantity Ω can be neglected. Then

$$\rho(\tau)=\frac{R(\tau)}{R(0)}=\frac{\int_0^{\Omega} G_a(\omega)\cos\omega\tau\, d\omega}{\int_0^{\Omega} G_a(\omega)\,(d\omega)}=\frac{\int_0^{\Omega} G_a(\omega)\left[1-\frac{(\omega\tau)^2}{2}+\frac{(\omega\tau)^4}{24}-\ldots\right]}{\int_0^{\Omega} G_a(\omega)\,d\omega}\cdot \tag{5.74}$$

When $\omega T\ll 1$, bearing in mind that according to the work [2],

$$\frac{\int_0^{\Omega} G_a(\omega)\,\omega^2\,d\omega}{\int_0^{\Omega} G_a(\omega)\,d\omega}=(\Pi\lambda_0)^2 \tag{5.75}$$

we obtain an expression identical to expression (5.73).

For determination of the required duration for realization of the error the following expression [3] can be used:

$$\xi_{\lambda 0} < \frac{1}{\sqrt{N}}, \tag{5.76}$$

where $\xi_{\lambda 0}$ is the relative mean square error of the frequency of zeros of realization;

N is the number of zeros of realization.

From expressions (5.76) and (5.73) it follows that for the purposes of correction it is sufficient to have a duration of realization for which the number of zeros approaches 100.

5.3.3 Evaluation of the Effectiveness of Correction

1. *Evaluation of maximum dispersion*

Before the sequential correction the dispersion is expressed according to equations (5.8) and (5.15). The following expression serves the purpose of a criterion for the effectiveness of correction:

$$E_\epsilon = \frac{D_a}{D_\epsilon(T)} \cdot \tag{5.77}$$

The correction is effective if $E_\epsilon > 1$.

2. *Evaluation for average dispersion*

The mean dispersion over a period is determined by the expression

$$D_\delta(T) = \frac{1}{T} \int_0^T D_\epsilon(s)\, ds. \tag{5.78}$$

The criterion for the effectiveness of correction is expressed in the following way:

$$E_\delta(T) = \frac{D_a}{D_\delta(T)} \cdot \tag{5.79}$$

3. *Informative evaluation*

With a reduction in the period of correction the residual error decreases but the relative time for correction increases. Consequently the quick action of MU also suffers. Hence in a number of cases, for example in the case of a multichannel system, it is worthwhile considering the accuracy of measurement in connection with the high speed, i.e. speed of information transfer. The generalized parameter w [30] can serve as the quantitative measure of accuracy and high-speed action:

$$w=\xi^2 t_m, \tag{5.80}$$

where ξ is the relative error;

t_m is the time for one measurement.

Without correction we have

$$w_1=\xi_1^2 t_m, \tag{5.81}$$

and with correction

$$w_2=\xi_2^2 t_m\left(1-\frac{\Delta T}{T}\right)^{-1}, \tag{5.82}$$

where the quantity $\left(1-\frac{\Delta T}{T}\right)^{-1}$ takes into account the loss in high speed caused by the time ΔT required for correction. The effectiveness of correction can be expressed by the relation

$$E_{\text{inf}}=\frac{w_1}{w_2}=\frac{\xi_1^2}{\xi_2^2}\left(1-\frac{\Delta T}{T}\right)=\frac{D_a}{D_\epsilon(T)}\left(1-\frac{\Delta T}{T}\right). \tag{5.83}$$

The error can be practically reduced only to the noise level D_B. Then

$$E_{\text{inf}}=\frac{D_a}{D_B+D_\epsilon(T)}\left(1-\frac{\Delta T}{T}\right). \tag{5.84}$$

The effectiveness of correction depends on the correction period. From equation (5.84) it is possible to find the condition for maximum effectiveness:

$$\left(\frac{\Delta T}{T}-1\right)\frac{d[D_\epsilon(T)]}{dt}-D_\epsilon(t)-D_B=0. \tag{5.85}$$

For stepped extrapolation and the case where the residual error is expressed as $D_\epsilon(T)=2D_a(1-e^{-\Omega T})$ we get maximum effectiveness for the condition where

$$T=\Delta T\left(1+\sqrt{1+\frac{D_B}{D_a\Omega\Delta T}}\right). \tag{5.86}$$

5.4 FRICTION TORQUE MEASURING INSTRUMENT (FTMI) WITH CORRECTION FOR ADDITIVE ERROR

As mentioned earlier, among the well-known methods of friction torque measurement the best one is based on the conversion of force into electrical signal with the help of strain gauges. It is necessary to reduce the considerable additive error observed during prolonged measurement using this method. Correction is an effective means of doing this.

With the device described earlier (Chapter IV, Fig. 4.5) we will use stepped extrapolation with capacitance memory for the purpose of correction. Recording of the shift signal can be done either in a closed or in an open circuit.

Let us consider first of all the case where recording of the drift amplifier (UPT) with correction is carried out in a closed circuit (Fig. 5.8).

Here a_1, K_1 and a_2, K_2 are the drift and gain of the first and the second amplifier (a_1 takes into account the drift of the transducer IMSP also); r_c and r_0 are the resistance of the switch K_2 in closed and open positions; U_{ak} is the voltage of the shift of switch. To obtain a more general analysis the input

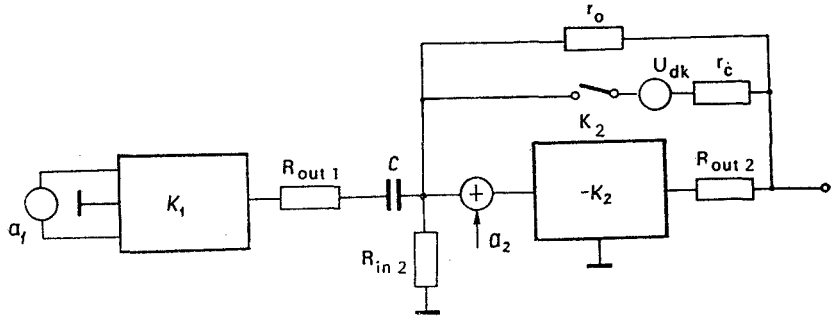

Fig. 5.8. Block diagram of instrument measuring friction torque in IMSP bearings with storage capacitor in closed loop circuit.

switch and transducer of the measuring device are not shown in the block diagram and only the drift a_1 due to them is considered. The switch K_2 will be in the off position for a period of time ΔT. During this time the torque being measured should be disconnected from the transducer. Having determined the equilibrium value of the voltage on the condenser:

$$U_c = a_1 K_1 + \frac{U_d + a_2 K_2}{1 + K_2}, \tag{5.87}$$

we find the drift voltage that is brought over to the input of the first amplifier after shifting the switch to the off position:

$$\varepsilon_1 = \frac{a_1 + U_{dk}}{K_1 (1 + K_2)} \cdot \tag{5.88}$$

The drift voltage at the output of the first amplifier is equal to $U_{ot\,1} = a_1 K_1$.

Assuming that $r_c \ll r_0$ and the capacitor charge is ahead of the amplifier with 100% feedback, the time constant of the circuit of the charge is determined in the following way:

$$T_{1c}^{*} = \left(R_{ot\,1} + \frac{r_c + R_{ot\,2}}{1 + K_2} \right) C. \tag{5.89}$$

Considering that $R_{ot\,1} \ll R_{in\,2}$, $R_{ot\,2} \ll r_0$, the time constant is expressed in the form

$$T_{10}^{*}=\left[\frac{R_{\text{in }2}\, r_0}{(1+K_2)\,(R_{\text{in }2}+r_0)}\right] C. \tag{5.90}$$

Let us consider the block-diagram of the measuring device with a storage capacitance in an open loop (Fig. 5.9). For this device, after the corresponding correction we get the residual drift voltage brought to the input of the first amplifier:

$$\varepsilon_2=\frac{a_2'+U_{\text{dk}}'}{K_1'}, \tag{5.91}$$

and at the output of the first amplifier, voltage:

$$U_{\text{ot }1}'=a_1' K_1'. \tag{5.92}$$

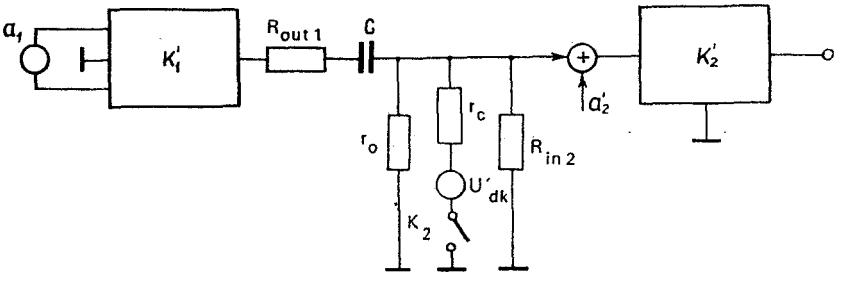

Fig. 5.9. Block-diagram of instrument measuring friction torque in IMSP bearings with storage capacitor in open loop circuit.

The time constant of the charging circuit of capacitance C, taking into account $R_c \ll R_{\text{in }2}$, will be

$$T_{2c}^{*}=(R_{\text{ot }1}+r_c)\, C, \tag{5.93}$$

and of the charging circuit when $R_{\text{ot }1} \ll r_0$,

$$T_{20}=\frac{r_0\, R_{\text{in }2}}{r_0+R_{\text{in }2}}\, C. \tag{5.94}$$

A comparison of these expressions with the expressions obtained for the first block-diagram (Fig. 5.8) shows that the value of the residual drift for identical gain $K=K_1 K_2=K_1' K_2'$ in the case of the first block-diagram (Fig. 5.24) is $(1+K_2')$ times less than in the second case. The drift voltage at the output of the first amplifier for identical transformed drift is $(1+K_2)$ times more in the case of the second block-diagram; the time constants of the charge when $r_c \ll R_{\text{ot }1}$ are practically the same; the time constant of the charge circuit of the first block-diagram is less when

$$r_0=R_{\text{in }2} \text{ by } \left(2+\frac{K_2}{2}\right) \text{ times.}$$

If the dynamic domain of the first amplifier allows, the residual drift of the second block-diagram will not exceed the residual drift of the first. From the point of view of registering the second block-diagram it is preferable since the storage capacitor has more charge resistance. Besides, in the case of the second block-diagram (open circuit) the danger of self-excitation is absent. Hence for further analysis of measuring devices we use the second block-diagram (Fig. 5.9).

The block-diagram IMSP (Fig. 5.10) designed on this basis consists of the device for rotation, strain gauge *SG*, signal amplifier of the strain gauge A_1, output amplifier A_2, control device *AA*, electromagnet *EM* and switch *S*.

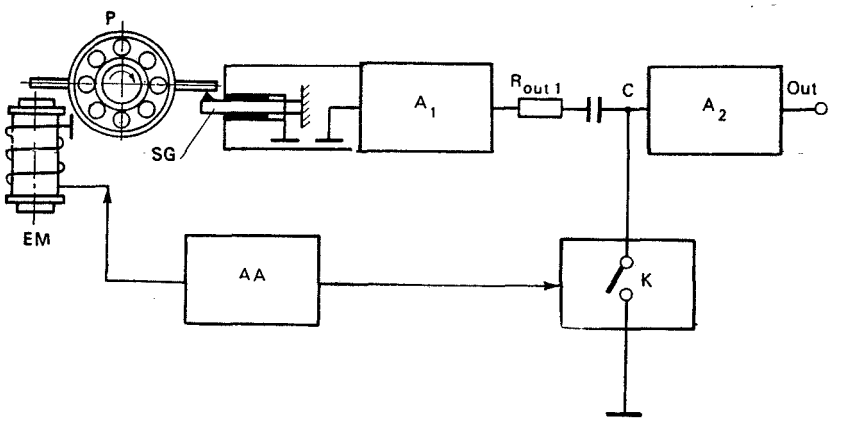

Fig. 5.10. Block-diagram of measuring unit of friction torque in IMSP bearings.

When the inner ring of the bearing *B* rotates the outer ring transmits friction torque through the beam.

Deflection of the beam of the strain gauge leads to unbalance in the bridge where there are two semiconductor resistance strain gauges fixed to the beam. The unbalance signal is amplified by the amplifier A_1 and then by A_2.

When the electromagnet responds the switch closes and the condenser *C* stores the voltage at the output of the amplifier A_1. This is made up of the total instrument drift of the amplifier and the gauge. The closing time of the switch *S* should be sufficient to stabilize the gauge after removing the torque from it. After switching on and releasing the electromagnet friction torque is again applied to the gauge. The time taken by the correction (important parameter) depends basically on transition processes of computation of friction torque to the gauge. It can be carried to a value not exceeding 0.1 sec.

Let us consider the cumulative error of IMSP (Fig. 5.10). Let the following be given: K_d is the gauge factor of the strain gauge (certain data on the gauge factor of strain gauges are given in Table 5.2); K_1 is gain in amplifier *1*; U_n is noise voltage applied to the input of the first amplifier; Ω_u is the upper

frequency of noise; i_{in} is input current of the second amplifier. Then from expression (5.27), taking into account the nonrandom current component of the drift of the second amplifier and possible coordination between the drifts of the two amplifiers, we get an expression for the cumulative error of IMSP when measuring the instantaneous value of friction torque:

$$\sigma_a = \left\{ \left[\left(\sqrt{D_{\epsilon n1}} + \frac{\sqrt{D_{\epsilon n2}}}{K_1} \right)^2 + U_n^2 + \frac{U_n^2}{1+\Omega_u T_c^*} \right]^{1/2} + \frac{i_{in} T}{K_1 C} \right\} \frac{1}{K_d}, \quad (5.95)$$

where $T_c^* = R_{ot\,1} C$;

$D_{\epsilon n1} = D_{\epsilon nd} + D_{\epsilon na}$ is the dispersion of the residual drift introduced by the gauge and the first amplifier determined by equation (5.8);

$D_{\epsilon n2}$ is the dispersion of the drift of the second amplifier.

TABLE 5.2

Type of Transducer	Dimension of plate mm	Natural resonance frequency Hz	Base of transducer mm	Supply voltage for bridge V	Sensitivity V/N
Semiconductor	40×10×0.2	120	10	4	0.5
Wire type	32×8×0.08	90	10	8	0.06
Foil type	32×8×0.08	90	10	8	0.05

The increase in the value of K_1 and reduction in the value of T lead to a reduction in the cumulative error. The limiting minimum value is given by the expression

$$T_{a\,min} = \frac{U_n}{K_d}. \quad (5.96)$$

If we assume that the amplifiers do not introduce noise and that all the noise is due to the strain gauge,

$$U_{ns} = 4 \times 10^{-3} \sqrt{R \Delta F}, \quad (5.97)$$

where U_{ns} is the noise voltage, μ V;

R is the bridge resistance of strain gauges, Ohm;

ΔF is the equivalent band width of amplifier noise, kHz.

Then for $R = 10^2$ Ohm, $\Delta F = 0.1$ kHz and $K_d = 1$ W/N we get minimum measurable load $\Delta P = 1.26 \times 10^{-8}$ N, which with a lever arm of $l = 2$ cm is the limiting sensitivity of IMSP given by $\Delta M = 2.52 \times 10^{-10}$ nm. In actual practice a larger value is obtained.

The realization of instrument drift of IMSP with a semiconductor strain gauge is shown in Fig. 5.11. Also shown is drift with correction in the case

where the correction interval T is equal to 5 and 1 sec. Each division of the time axis corresponds to 140 sec and on the torque axis corresponds to 20×10^{-3} nm. As shown by the curves, the instrument drift without correction

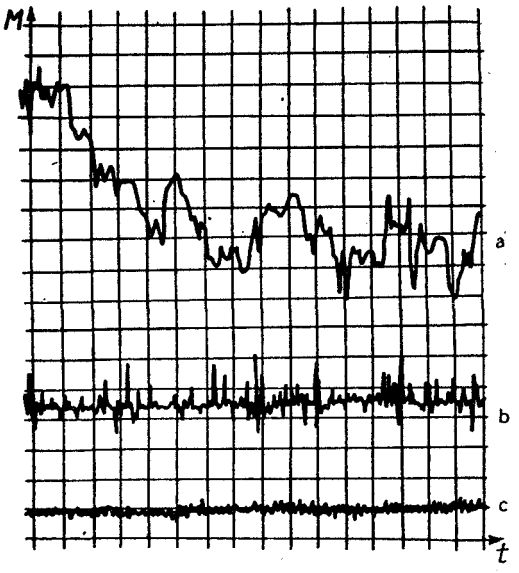

Fig. 5.11. Realizations of drift: *a*—without correction; *b*—correction period $T=5$ sec; *c*—correction period $T=1$ sec.

is 1.6×10^{-7} nm and with correction 5.3×10^{-8} nm and 1.25×10^{-8} nm. The effectiveness of correction E exceeds 10^2. This confirms the desirability of using correction of cumulative error for prolonged tests of precision bearings.

5.5 OTHER SOURCES OF ERROR IN THE MEASUREMENT OF FRICTION TORQUE

The dynamic error is determined as the difference between the true value of the measured quantity and the value shown by the instrument [16]:

$$\Delta x = x_t - x. \tag{5.98}$$

The basic reason for the appearance of dynamic error is the limited frequency range of measurement due to inertia of the moving part of the measuring system. In order to increase the frequency range it is necessary to raise the natural frequency of the system as high as possible:

$$\omega = \sqrt{\frac{K_s}{I}}, \tag{5.99}$$

where K_s is the stiffness of the system;

I is the moment of inertia of the moving part of the measuring system.

When computing the natural frequency in the instruments considered here the fundamental place in the moving system is occupied by the moving part of the test bearing. Hence it is necessary to compute the moment of inertia of the bearing accurately.

The kinetic energy of a rolling contact bearing is equal to the sum of the kinetic energy of its parts:

$$E=E_2+E_3+E_4, \tag{5.100}$$

where E is the kinetic energy of the moving parts of the bearing;

E_2 is the kinetic energy of the moving rings of the bearing;

E_3 is the kinetic energy of all rolling elements;

E_4 is the kinetic energy of the cage.

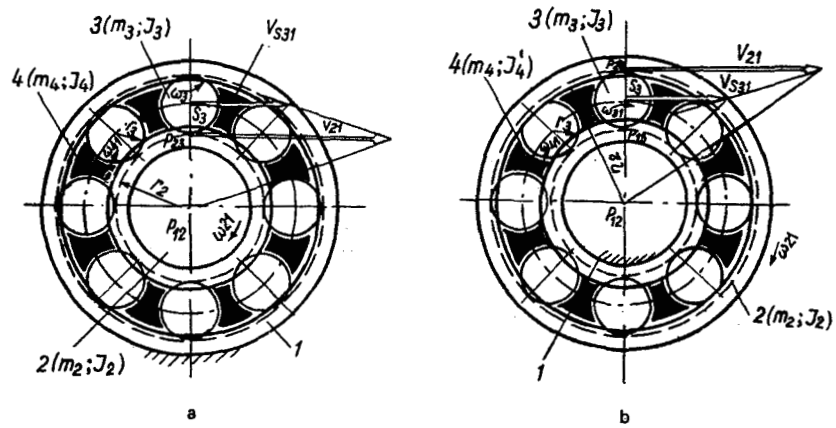

Fig. 5.12. Computation of moments of inertia of rolling contact bearings: *a*—moving inner ring of bearing; *b*—moving outer ring of bearing.

To compute the moments of inertia it is necessary to consider the bearings with moving outer and inner rings separately (in Fig. 5.12, *a* is for the moving inner ring of the bearing and *b* is for the moving outer ring).

The formulas developed below are suitable for the computation of moments of inertia of all types of rolling contact bearings except thrust bearings for which the concept of outer ring is not applicable.

Let us enumerate these formulas for a bearing with stationary outer ring:

$$E=I\frac{\omega_{21}}{2}, \tag{5.101}$$

$$E_2=I_2\frac{\omega_{21}^2}{2}, \tag{5.102}$$

$$E_3 = n\left(I_3 + \frac{\omega_{31}^2}{2} + m_3 \frac{v_{r\,31}^2}{2}\right), \tag{5.103}$$

$$E_4 = I_4 \frac{\omega_{41}^2}{2}, \tag{5.104}$$

where I is the transformed moment of inertia of the bearing;
I_2 is the moment of inertia of the moving ring of the bearing *2*;
I_3 is the moment of inertia of the rolling elements *3*;
I_4 is the moment of inertia of the cage *4*;
ω_{21} is the angular speed of the moving ring *2* relative to the stationary ring *1*;
ω_{31} is the angular speed of the rolling elements *3* relative to the stationary ring *1*;
ω_{41} is the angular speed of the cage *4* relative to the stationary ring *1*;
m_3 is the mass of rolling elements *3*;
$v_{r\,31}$ is the velocity of the center of gravity of rolling elements relative to the stationary ring *1*;
n is the number of rolling elements.

After respective transformations of the above expressions the moment of inertia of a bearing with a stationary outer ring will be given by

$$I = I_2 = n\left[I_3\left(\frac{\omega_{31}}{\omega_{21}}\right)^2 + m_3\left(\frac{v_{r-31}}{\omega_{21}}\right)^2\right] + I_4\left(\frac{\omega_{41}}{\omega_{21}}\right)^2. \tag{5.105}$$

Considering that

$$v_{r\,31} = r_3 \cdot \omega_{31}, \tag{5.106}$$

$$\omega_{41} = \frac{\omega_{21}}{2}\left(\frac{r}{(r_2 + r_3)}\right), \tag{5.107}$$

$$\frac{\omega_{31}}{\omega_{21}} = \frac{r_2}{2r_3}, \tag{5.108}$$

we get a formula suitable for computation

$$I = I_2 + \frac{n}{4}\left[I_3\left(\frac{r_2}{r_3}\right)^2 + m_3 r_2^2\right] + \frac{I_4}{4}\left(\frac{r_2}{r_2 + r_3}\right)^2. \tag{5.109}$$

In computation of the moment of inertia of a bearing with the stationary inner ring all the above formulas are used except (5.107), which has to be replaced by the formula

$$\omega_{41} = \frac{\omega_{21}}{2}\left(\frac{r}{r_2 - r_3}\right). \tag{5.110}$$

After corresponding transformations we get an expression for the moment of inertia of the bearing with stationary inner ring

$$I=I_2+\frac{n}{4}\left[I_3\left(\frac{r_2}{r_3}\right)^2+m_3 r_2^2\right]+\frac{I_4}{4}\left(\frac{r_2}{r_2-r_3}\right)^2. \tag{5.111}$$

The moments of inertia of the remaining moving components of the measuring system are computed using the well-known formulas.

In considering the natural frequency of the system it is necessary to keep in mind that it should be 2–3 times larger than the upper bound of the operating frequency of the process being studied, in this case, friction torque.

Knowing the transformed moments of inertia of the measuring system generalized with a large number of assumptions, we consider that the mass of a moving part of the instrument and the device

$$m=I/R, \tag{5.112}$$

where R is the distance from the center of rotation to the strain gauge which senses the torque being measured.

Error introduced by vibrations or wobbling of the device for rotation. Additional inertial forces F will act on the strain gauges with vibrations or wobbling and will cause an error:

$$F=ma, \tag{5.113}$$

where m is the transformed mass; a is the acceleration.

Then the error in the measurement of the variable component of friction torque of the bearing will be

$$\Delta F=\frac{F}{F_v}\cdot 100\%, \tag{5.114}$$

where F_v is the force acting on the system of gauges while measuring the variable component of the friction torque given by

$$F_v=\frac{M_v}{R}, \tag{5.115}$$

Here R is the distance of the bearing center to the gauge of the measuring system.

Error caused by nonuniform rotation. Another source of error in the measurement of friction torque components is the nonuniformity of rotation of the driving unit.

The principal sources of nonuniformity of rotation are the following:

a) nonuniform turning speed of electric motor transmitted to the bearing through the drive;

b) radial vibrations of pulleys (if any) which besides directly influencing the turning speed of the bearing also adversely affect the working of the system by exciting longitudinal vibrations in the belt, etc.;

c) unbalanced masses;

d) the rolling contact bearings of the drive, etc.

Tests for nonuniformity of rotation of synchronous motors of the DSG type showed that nonuniformity of rotation decreases with increased speed (Table 5.3).

TABLE 5.3

Electric Motor	Speed rpm	Nonuniformity in rotation, %
DSG-1	1,500	0.16
DSG-2	1,500	0.40
DSG-1	3,000	0.06
DSG-2	3,000	0.15

The tests also showed that in belt drives an increase in the tension of the belt increases the nonuniformity of the speed of rotation. This is explained by the fact that with the increased tension the stiffness of the belt increases, i.e. the natural frequency of the belt also changes. In the resonance region this leads to an increase in the amplitude of belt vibrations and thus to an increase in the coefficient of nonuniformity.

Hence determination of the coefficient of nonuniformity of rotation of the moving ring of the bearing is necessary in the study of errors in measurement. For this purpose it is possible to use different marking units (for example, a trigger marker of the 51E10 DISA type which gives a signal after a given angle of turn).

The coefficient of nonuniformity is determined thus: First the frequency of current pulse is determined. This depends on the turning speed of the marker disc:

$$f=\frac{n}{60}s, \tag{5.116}$$

where n is the turning speed of the moving ring, chosen according to the working range of the setup, rpm;

s is the number of impulses per revolution subject to the angle set for signal output.

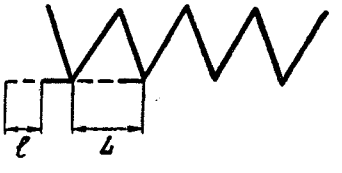

Fig. 5.13. Phase-shift and its inclination.

The recording element is a double beam oscilloscope. The standard signal from the generator is fed to one channel and the signal from the marker in the form of an impulse (better, in the form of a saw tooth) is fed to the other. The signals are compared. With the help of a chronometer the time for phase shift and the maximum deviation of the phase of the signal are recorded (Fig. 5.13).

For convenience of computation and increased accuracy both signals can be photographed.

The coefficient of nonuniformity in turning speed is determined by the formula

$$\delta = \frac{l}{Lf\Delta t}, \tag{5.117}$$

where l is the maximum phase shift;
L is the period of standard signal;
f is the pulse frequency;
Δt is the time for phase shift.

References

1. Anisimov, V.I. 1966. Nekotorye osobennosti rascheta dreifa nulya transistornykh UPT (Computational features of instrument drift of amplifiers). *Izv. vuzov, Priborostroenie*, No. 6.
2. Anisimov, V.I. and O.I. Tishchenko, 1967. Sposob periodicheskoi kompensatsii dreifa nulya transistornykh usilitelei (Periodic compensation of the instrument drift of transistor amplifiers). *Izv. vuzov, Priborostroenie*, No. 3.
3. Augutis, V.N. 1970. Issledovanie korrektsii additivnoi pogreshnosti pri izmerenii momenta sopravleniya elektricheskimi metodami (Study of correction of additive error in measurement of friction torque by electrical methods). Avtoreferat. Kand. diss., Kaunas.
4. Augutis V.N. and B.I. Gresyavichus, 1970. Korrektsiya additivnoi pogreshnosti pri izmerenii parametrov sluchainogo protsessa (Correction of additive error in measurement of random process parameters). *Nauchnye trudy vuzov, Lit. SSR, Vibrotekhnika*, No. 3 (12).
5. Augutis, V.N., B.I. Gresyavichus, and K.I. Rekvyavichus. 1968. Informatsionnaya otsenka korrektsii dreifa nulya izmeritelnykh ustrostv (Informed estimate of instrument drift correction of measuring devices). *Trudy nauchno-tekhnicheskoi konferentsii, ser. Radioelektronika*, Vol. 4, Kaunas.
6. Baglai, R.D. 1965. Usilenie slabykh signalov proizvolnoi formy (Amplification of weak signals of arbitrary form). Novosibirsk, Nauka.
7. Ball, G.A. 1965. Apparaturnyi korrelatsionnyi analiz sluchainykh protessessor (Instrument correlation analysis of random processes). Moscow, Energiya.
8. Bykovskii, Yu.Ya. 1966. Metody povysheniya tochnosti preobrazovatelei neelektricheskikh velichin (Ways of increasing the accuracy of converters

of nonelectric quantities). *Kiberneticheskie puti sovershenstvovaniya izmeritelnoi apparatury. Tezisy dokladov*, Leningrad.
9. Same as ref. [21], Chapter IV.
10. Gik, L.D. *et al.* 1967. Analiz poroga chuvstvitelnosti izmeritelnykh usilitelei (Analysis of the limits of sensitivity of measuring amplifiers). *Avtometriya*, No. 6.
11. Gik, L.D. and V.N. Nekuryashehev. 1969. Ispolzovanie e'lektromekhanicheskoi obratnoi svyazi v vibratorakh s magnitoelectricheskimi datchikami (Application of electromechanical reverse effect in vibrations with electromagnetic transducers). *Autometriya*. No. 6.
12. Gresyavichus, B.I. and V.N. Augutis. 1968. Opredelenie soothoshenii mezhdu pogreshnostyu, chastotoi ee korrektsii i bystrodeistvium izmeritelnogo ustroistva (Determination of the relations between frequency of error correction and the speed of response of the measuring device). *Trudy nauchno-tekhnicheskoi konferentsii, Ser. Radioelektronika*, Vol. 4, Kaunas.
13. Jilepsi, A.B. 1964. Signal, shum i razrushayushchaya sposobnost usilitelei (Signal, noise and distortion of amplifiers). Moscow, Atomizdat.
14. Same as ref. [25], Chapter IV.
15. Zemelman, M.A. 1969. O metodakh normirovaniya metrologicheskikh kharakteristik izmeritelnykh ustroistv (Ways of standardizing the metrological characteristics of measuring devices). *Izmeritelnaya Tekhnika*, No. 13.
16. Zemelman, M.A. 1966. K voprosu o pogreshnostyakh izmeritelnoi apparatury (Errors in measuring devices). *Izmeritelnaya Tekhnika*, No. 11.
17. Zemelman, M.A. 1968. Korrektsiya pogreshnostei izmeritelnykh ustroistv metodami vspomogatelnykh izmerenii (Correction of errors in measuring devices using auxiliary measurements). *Izmeritelnaya Tekhnika*, No. 1.
18. Zemelman, M.A. 1964. Tochnyi analogovyi preobrazovatel na grybykh elementakh (Precision analog converter on crude components). *Izmeritelnaya Tekhnika*, No. 9.
19. Zemelman, M.A., N.N. Vostrokhutov and A.P. Knyupfer. 1966. Transistornyi analogo-tsifrovoi preobrazovatel s avtomaticheskoi korrektsiei sistematicheskikh i silno korrelirovannykh sluchainykh pogreshnostei dlya tochnykh izmentelnykh sistem (Transistorized hybrid converter with automatic correction of systematic and closely correlated random errors for precision measuring systems). *Kiberneticheskie puti sovershenstovaniya izmeritelnoi apparatury. Tezisy dokladov.* Leningrad.
20. Kantere, V.M. and M.A. Karabegov. 1966. Avtomaticheskaya korrektsiya pokaganii promyshlennykh analizatorov (Automatic correction of the readings of industrial analyzers). *Avtometriya*, No. 1.
21. Klokov, Yu.L. and L.V. Zhuravlev. 1965. Metody otsenki uslovnogo vremeni zatukhaniya kovielatsionnykh funktsii nekotorogo klassa slucha-

inykh protsessov (Estimation of conditional damping time of correlation functions of one class of random processes). *Avtomatika i telemekhanika*, No. 10.

22. Kazubovskii, S.F. 1963. Avtomaticheskie korrelatsionnye izmeritelnoi skorosti (Automatic correlational velocity measuring instruments). Kiev. Izd. AN Ukr. SSR.
23. Konchakovskii, V.Yu. and R.R. Kharchenko. 1962. Izmeritelnyi usilitel postoyannogo toka s avtomaticheskoi korrektsiei dreifa nulya (Measurement DC amplifier with automatic correlation of instrument drift). *Priborostroenie*, No. 1.
24. Korshak, V.V. *et al.* 1970. Issledovanie momenta treniya samosmazyvayushchikhsya teplostoikikh pribornykh sharikopodshipnikakh (Study of the friction torque in self-lubricating thermally stable instrument ball bearings). *Pribory i sistemy upravleniya*, No. 3.
25. Kunov, V.M. 1969. Soglacovanie magnitoelektricheskogo datchika dlya dostizheniya minimalnogo koeffitsienta shuma (Matching of electromagnetic transducer to achieve minimum noise coefficient). *Avtometriya*, No. 1.
26. Levin, B.R. Teoreticheskie osnovy statisticheskoi radiotekhniki (Theoretical basis of statistical radio engineering). Moscow. Sov. Radio, kn. 1.
27. Malashenko, S.I. 1967. Raschet dreifa milya tranzistornykh usilitelei postoyannogo toka (Computation of instrument drift in transistor DC amplifiers). *Izv. vuzov, Radioelektronika*, No. 5.
28. Mirskii, G.Ya. 1967. Apparaturnoe opredelenie kharakteristik sluchainykh protsessov (Instrumental determination of the characteristics of random processes). Moscow, Energiya.
29. Nefedova, N.N., N.G. Sirnova and L.F. Shulmeister. 1969. Prebrazovatel napryazheniya v chastoty s kompensatsiei dreifa (Converter of voltage into frequency with drift compensation). *Avtometriya*, No. 4.
30. Novitskii, P.V. 1968. Osnovy informatsionnoi teorii izmeritelnykh ustroistv (Fundamentals of the information theory of measuring devices). Moscow, Energiya.
31. Pevzner, V.V. 1967. Amplifier (AC/DC) with small instrument drift on the base of a self-generating amplifier). *Pribbory i sistemy upravleniya*, No. 6.
32. Petukhov, V.I. and E.M. Porshin. 1967. Ob opredelenii staticheskoi pogreshnosti teleizmeritelnoi sistemy s avtomaticheskoi korrektsiei (Determination of statistical error in a telemetric system with automatic correction). *Trudy Ryazanskogo radiotekh. in-ta*, vyp. 6.
33. Avtomatizatsiya radioizmerenii (Automation of radio measurements). Ed. Balashova, Moscow, Sov. radio. 1966.
34. Polonnikov, D.E. 1962. Skhema avtomaticheskoi kompensatsii dreifa nulya v elektrometricheskikh usilitelyakh i ee analiz (Design of automatic

compensation of instrument drift in electrometric amplifier and its analysis). *Avtomatika i telemekhanika*, Vol. 23, No. 12.

35. Rykina, L.K. 1966. Ustroistvo avtomaticheskoi korrektsii nulya dlya tsifrovogo voltmetra sledyashchego uravnoveshivaniya (Device for automatic correction of the drift of a digital voltmeter after balancing). *Kiberneticheskie puti sovershenstvovaniya izmeritelnoi apparatury. Tezisy doklady*, Leningrad.
36. Safronov, G.S. 1962. Korrelyatsionnye funktsvi i spektralnye plotnoste dvykh sluchainykh funktsii, kvantovannykh po vremeni (Correlation functions and spectral densities of two random functions quantized by time). *Avtomatika i telemekhanika*, No. 6.
37. Stratonovich, R.L. 1961. Izbrannye voprosy teorii flynktuatsii v radiotekhnike (Selected problems in the theory of fluctuations in radio engineering). Moscow, Sov. radio.
38. Same as ref. [108], Chapter 4.
39. Kharkevich, A.A. 1965. Borba s pomekhami (Struggle with disturbances). Moscow, Nauka.
40. Khorna, O. 1962. Tenzometricheskie Mosty (Strain gauge bridges). Moscow, Leningrad, Gosenergoizdat.
41. Chegolin, P.M. 1969. Avtomatizatsiya spektralnogo i korrelyatsionnogo analiza (Automation of spectral and correlational analyses). Moscow, Energiya.
42. Chekhnadskii, I.A. 1969. Ispolzovanie yavleniya kompensatsii pogreshnostei dlya povysheniya tochnosti izmeritelnykh informatsionnykh sistem (Use of error compensation to increase the accuracy of measuring information systems). *Izmeritelnaya tekhnika*, No. 1.
43. Shenbrot, I.M. and M.Ya. Ginzburg. 1970. Raschet tochnosti sistem tsentralizovannogo kontrolya (Computation of the accuracy of systems of centralized control). Moscow, Energiya.
44. Jurkauskas, A.Yu. 1970. Issledoranie momentov soprotivleniya vrashcheniyu i sluchainykh kolebanii pretsizionnykh podshipnikov (Study of the friction torque and random vibrations in precision bearings). Avtoreferat kand. diss., Kaunas.
45. Jurovskii, A.Yu. 1967. Veroyatnostnyaya otsenka pogreshnosti dreifa nulya kompensatsionnykh priborov (Probabilistic estimation of the instrument drift error of compensated instruments). *Pribory i sistemy upravleniya*, No. 8.
46. Yakubovich, A.M. 1963. Operatsionnye usiliteli s kompensatsiei dreifa nulya po metody 'Printsa' (Operational amplifiers with compensated instrument drift by the Princes method). *Avtomatika i telemekhanika*, Vol. 24, No. 8.
47. Boden, H. 1969. Das Trägheitsmoment eines Walzlagers. *Mashinenmarkt*, Vol. 75, No. 28.

48. Brownr, F. 1968. Practical study of drift correction in P.R.S.N. cross-correlation. *Electronics Letters*, Vol. 4, No. 26.
49. Weltman, B.P. and H. Kwakernaak. 1961. Theorie und Technik der Polaritats—Korrelation für die dynamische Analyse Niederfrequenen. Signale und Systeme. *Regelungstechnik*, No. 9.

6

STATISTICAL ANALYSIS OF EXPERIMENTAL RESULTS OF PRECISION BEARING DYNAMICS

The process of the appearance of friction torque and vibrations in rolling contact bearings is extremely complex. The more complex phenomena are the ones that cause variable friction torque: in the working ranges they are supplemented by dynamic phenomena and by active forces caused by loading. In addition, functions of variable friction torque are complicated further by the random nature of the geometric defects in bearing components.

These problems can be solved by statistical methods based principally on the theory of stationary random functions.

Naturally, to obtain accurate results it is necessary to somehow limit the class of possible random processes that correspond to the disturbances. The possibility of replacing the actual noise and disturbances in the dynamic systems by white noise, which allows use of the theory of Marcovian processes for the analysis of dynamic systems, has been mentioned by A.A. Andronov, L.S. Pontryagin and A.A. Witt [31]. The method of Marcovian processes consists in using the Fokker-Planck-Kolmogorov equation for determination of the distribution law of the system's output signal.

Tests on the behavior of a linear system with random disturbances obtained by allowing white noise through a linear system (filter) with constant parameters, using the Fokker-Planck-Kolmogorov equation, are described in the work [39].

The work [22] describes the behavior of the linear system on which a nonstationary random process acts, determined as a result of passing nonstationary fractional noise through a linear filter.

Analysis of nonlinear systems is very difficult even in the case of known external effects. At present there is not a single mathematical technique suitable for the study of any nonlinear system in arbitrary working conditions.

Analytical study of random processes in nonlinear systems is even more difficult. In the analysis of nonlinear systems it is necessary to determine not only the mathematical expectation and correlation functions of random processes but also their distribution law. It is usually necessary to use approxi-

mate methods [9, 10, 15, 17, 18, 22, 28, 30, 32] based either on the linearization of the system or on the assumption that the processes have normal distribution or are Marcovian processes not of a high order. Certain methods (for example, the method of statistical linearization [12]) require simultaneous validity of both assumptions.

Study of dynamic systems by the method of correlation—spectral analysis [35, 36] is convenient because it is possible to use only the actual input and output signals observed in a normal operating system without any trial effects. But these methods are suitable only for study of linear systems, where they have the necessary accuracy. In the case of nonlinear systems only the mean characteristics are determined and use of these methods requires numerous repetitions of the experiment to obtain more accurate relations between the parameters of the system.

A complete study of ball bearing as a dynamic system subjected to random actions can be carried out only by statistical methods. It is necessary to know the principal statistical characteristics of action (reaction of the system to the effect): correlation function or spectral density associated with it, mathematical expectation (mean) and distribution law. These characteristics are determined by analyzing the curves plotted by the recorder (chosen curve, realization) of the random process during a finite interval of time that determines the computational error. The analysis is carried out using a digital computer which requires a description of the random process, i.e. substitution by a random sequence (grid function). This replacement affects the accuracy of determination of the characteristics. The limitations of the computer memory again lead to the problem of the effect on the accuracy of the evaluation of the length of realization and fixation interval of the process.

The evaluation of the accuracy of characteristics (*a posteriori*) is considered on the basis of preliminary (*a priori*) evaluation of the accuracy of the analysis of empirical results and choice (on the basis of this evaluation) of the duration of the experiment and fixation time of data.

Analytical study of the statistical and dynamic characteristics of any system as a rule leads to computations of stability, study of the type of transition processes and choice of parameters that will ensure the best completion of processes in the system. It is necessary to arrange the equations that describe the processes taking place in the system in the same way as the frequency characteristics or transfer functions. The latter can be determined by correlation and spectral methods which are convenient because they make use only of the information on the random changes in the input and output values under normal working (without test actions).

Using the simplified scheme of the bearing as a dynamic system with a few inputs and outputs it is possible to obtain logarithmic frequency characteristics and transfer functions corresponding to approximate logarithmic amplitude characteristics. The problem of determination of the degree of influence

of individual parameters (manufacturing defects, change in the film thickness, vibrations of rings relative to one another in the axial direction) on the total variable friction torque from the bearing as a whole is also solved within the framework of correlation theory.

6.1 REQUIREMENTS FOR THE EVALUATION OF STATISTICAL CHARACTERISTICS AND PREPARATION OF EXPERIMENTAL MATERIAL

Under working conditions every system, as a rule, experiences actions and responds to them by reactions of which random disturbances that change with time and are random functions of time form an integral part. According to the accepted terminology random functions of time are known as random processes. Unlike determined functions, random processes are determined by the combination of functions and laws characterizing the properties of this combination. Each function of the group is called a realization of the random process or chosen curve.

Many workers [5, 6, 14 and others] have shown that the principal cause of vibration of ball bearings is defects in the shape of the contact surfaces of the components in the form of so-called waviness (unevenness with a wavelength from 1/18 to 1/360 of the circumference) and sharp corners (wavelength of roughness varies from 1/3 to 1/18 of the circumference). A few authors [8] carry out visual analysis of error diagrams (waviness and sharp corners) of the bearing components obtained with the help of a Talyrond-51 or profilograph. G.K. Lipskii [24] and Yu.Yu. Kasnauskas [14] describe the surface profile normal to the axis of rotation in the polar coordinates

$$\rho = R + \Delta\rho\,(\varphi), \tag{6.1}$$

where ρ is the radius vector;

R is the radius of the normal circumference in the given plane;

$\Delta\rho\,(\varphi)$ is the deviation from the circular, measured in the radial direction, from the nominal circumference: a function of the polar angle φ.

Assuming that the quantity $\Delta\rho\,(\varphi)$ is a complicated periodic function with a period 2π, the authors carry out the expansion of the quantity $\Delta\rho\,(\varphi)$ in a Fourier series.

This representation of the quantity $\Delta\rho\,(\varphi)$ does not reveal the complete picture of the change in defects of the rolling surface. This is because the balls do not roll along just one raceway for every revolution of the ring (cage), because even for one revolution each ball may use different raceways. It can be assumed that defects in the shape of the raceway and rolling elements are described by complex, nonperiodic functions of the angle φ having a given amplitude distribution. The angle φ depends on the rotation speed of the bearing and may be expressed as a function of time. Hence the function $\Delta\rho\,(\varphi)$ may be called a random process. The action caused by the roughness

of contact elements on the variable friction torque should be determined by statistical characteristics $\Delta\rho(\varphi)$ or $\Delta\rho(t)$.

The dimensions, speed of rotation, magnitude of tension or clearance and thickness of the lubricating film, which is also a complicated function of time, affect both vibration and variable friction torque during the operation of the bearing. Hence variable friction torque, like the output of the dynamic system on which the random processes act, is also a random process though it can also have additive harmonic components.

For a correct analysis of random processes based on their realization it is necessary to establish whether they are stationary, random or normal.

Talking of stationary random process, it is necessary to verify whether their statistical characteristics change or not during a shift with time. Obviously, in practice such verification is impossible because the number of possible statistical characteristics is infinite and for a complete description of the random process it would be necessary to compute all these characteristics. However, it is possible to suggest a number of practical criteria for a stationary random process.

The first important assumption is that if the processes are not stationary statistical characteristics computed on the basis of one realization by averaging at short intervals of time will be different at different intervals, i.e. the changes in characteristics will be greater than what could have been expected assuming statistical selected variation. With this assumption verification as to whether the random process is stationary consists in the analysis of the behavior of individual realizations and not of the whole ensemble. In other words, proof that individual realizations are stationary in themselves argues that the random process to which these realizations belong is also stationary.

According to the second assumption, for a majority of applications it is sufficient to verify that the process is weakly stationary, i.e. confirm that the mean values and correlation function do not depend on time. This assumption can be accepted for two reasons. Firstly, in order to use such effective methods of analyzing stationary processes as correlation-spectral analysis it is only necessary that the condition of being weakly stationary be fulfilled. Secondly, random processes observed in actual physical phenomena are usually strictly stationary under the condition of being weakly stationary.

The third assumption states that the realization length be considered large when compared to the random oscillation contained in this realization. This assumption is necessary so that as a result of averaging at short intervals it is possible to obtain values that correctly reflect the mean characteristics of the process not subjected to the effect of random vibrations contained in the realization.

The assumption that leads to the statement that if the mean value of the square of the process (or dispersion) is stationary the correlation function is also stationary is not very well founded. However, it is usually assumed

because of the small probability of the correlation function of the nonstationary process depending on time for any shift τ except $\tau=0$. This assumption simplifies the use of the practical criteria of being stationary.

On the basis of these assumptions it is possible to carry out verification of a stationary random process using the examination of one realization $x(t)$ as described below:

1. The realization is divided into N equal intervals of such value that the divisions within each interval can be considered independent.

2. The mean values and mean square values are computed within each interval.

3. The sequence of mean values and mean square values is verified for the presence of a trend or deviation that exceeds the expected values of deviations due to the variation selected. For this purpose it is worth using non-parametric methods which do not require a knowledge of the sample distributions, i.e. to verify the hypothesis stating that the sequence of mean values and mean squares are sample values of a random quantity having a true mean value μ_x and mean square value ψ_x^2.

The presence of a nonstationary trend in the correlation function is determined in the following way:

1. By filtering the realization, the mixed narrow-frequency intervals whose total number equals c are determined.

2. Each narrow frequency interval of realization is divided into N equal parts.

3. The mean square values are computed within each such part in all frequency intervals and from these sample values c sequences are formed.

4. The verification of the sequence of mean square values is carried out in each particular interval in the presence of a trend (total c verification).

Nonconfirmation of the hypothesis as to the process being stationary arising from a particular check means a deviation of this hypothesis for the whole process.

It should be mentioned that if the probability of error of the first type at the time of verification in each frequency interval is equal to α' the probability of error of the first type for the verification as a whole is

$$\alpha=1-(1-\alpha')^c. \tag{6.2}$$

Consequently, if it is required that for the verification as a whole the probability of error of the first kind equal α, then verification for each of the c frequency intervals should be carried out at a level of significance of α' such that

$$\alpha'=1-(1-\alpha)^{\frac{1}{c}}. \tag{6.3}$$

The last method makes it possible to bring out the temporary trend in the

energy spectrum of the process, which is the same as determination of the trend of the correlation function.

In a random process that satisfies the criterion of being stationary the verification of randomness leads to determination of the composition in the process of harmonics due to the existence in the process of periodic or almost periodic components. Practical criteria of randomness are usually based on methods of analysis used on the assumption of randomness of processes.

In a spectrum of high resolution periodic components are brought out in the form of peaks even if the energy of these components is relatively small. Unlike a narrow-band random process, the measured peak width is always equal to the band-width of the passage of the filter used in the analysis and is independent of how narrow this filter is. This method of selection of periodicity is not applicable when the width of the narrowest possible band filter exceeds the range of frequencies of the possible narrow band process. In order to use the above method it is necessary that the realization length be large enough for the condition $BT \gg 1$ to be satisfied, where B is the passage band width and T is the duration of realization.

The presence of harmonics in the random process (in similar relations) can be observed even from the density distribution of the values of the process. Usually the distribution density of the random signal is very nearly (at least outwardly) the well-known bell-shaped Gaussian curve. The density distribution of harmonic process is cup-shaped. The sum of the signals has characteristic features of each of these.

The most effective method for singling out harmonic vibrations in a random process (in similar conditions) is construction of a correlationograph. In a purely random averaged process the correlation function always approaches zero with an increase in shift. On the other hand, the correlation function of harmonic process or sum of harmonics continues to oscillate independent of the magnitude of the shift.

The problem of obtaining maximum information is solved by so-called effective estimation. The evaluation of $\hat{\theta}\ (x_1,\ldots,\ x_n)$ of the unknown parameter carried out on the sample $x_1,\ x_2,\ldots,\ x_n$ is called effective estimation or optimum in the sense of minimum of mean square deviation if the dispersion of deviations of $\hat{\theta}$ with respect to $\hat{\Theta}$ is minimum in every class of different possible estimations.

It is also natural to introduce the requirement of tenability of the estimates. The estimation is called tenable if with an increase in the number to infinity, it leads by probability to the estimated parameter.

One must insist that the estimates should not be offset. This means that in the computational procedure of parameter systematic bias or errors should not be introduced, i.e. the mathematical expectation of the estimated parameter should coincide with the parameter being estimated.

Actually in the present case one has to encounter a whole series of difficulties. It appears that it is not always possible to carry out estimates that are simultaneously tenable and non-offset. In particular, the estimation of the spectral density is untenable, i.e. it cannot be corrected with increase within the number of observations. The estimation can be made tenable if it is possible to avoid the requirement of being offset, whereby the estimate becomes all the more effective, the larger the offset, i.e. the systematic error introduced during computations.

The second difficulty is that the effectiveness of estimates is very sensitive to violation of the initial assumption of normal distribution. It is reasonable to assume that most frequently we have to deal with offset distributions given as a sum of at least two functions of the distribution with a number of different parameters. Examples of such "impure" distributions are models of the type $0.9\,N(\mu, \delta^2)+0.1\,N(\mu+\lambda\delta, \delta^2)$, etc. Simulating the behavior of samples of this type on the computer shows that if we are dealing with a very bad sample the center of scattering can be better estimated from the median than from the arithmetic mean. The impurity affects the estimation of scattering by the variation span less than the estimation of dispersion. It is, of course, possible to "purify" the samples by rejecting crude (anomalous) observations with the help of one criterion or another. But this procedure also leads to a reduction in effectiveness since it is necessary to reduce the number of samples.

Finally, a third difficulty arises because estimation of parameters should frequently precede statistical analysis of the data, and during this we come across the problem of sensitivity of the criteria of analysis to the violation of basic assumptions. For example, Bartler's criterion, which is recommended for verification of the hypothesis on the homogeneity of sample dispersions is extremely sensitive to violation of the normal distribution. Here the most surprising fact is that for certain types of distributions the deviation becomes larger with an increase in the number of samples [42]. There is also a criterion which is very insensitive to the violation of normal distribution. The *F*-criterion (ratio of dispersion) is absolutely insensitive to violation of normality when comparing inter- with intragroup dispersion.

We must have a clear picture of the sensitivity of the criteria used to the basic assumptions. It is worth turning to the estimation of the degree of deviation from normality by computing asymmetry and excess. It is necessary to recall that estimation of these values based on the computation of third and fourth moments is associated with large errors which depend on the time of observation of the process and representation of the numerical sequence.

In order to determine the above and other statistical characteristics all the information on the results of experiments should be prepared before feeding into the computer. Preparation of the information consists in carrying out a

series of operations, the most important of which are: "discretization," which satisfies the requirements of quality of reproduction of the continuous process by quantized values of the quantity; coding of the values, which depends on the computer components and elements that are used for storing or processing the initial information; unification of all types and forms of initial information and transformation to a single scale (scaling); and concentration (building up and compression) without losing existing signs, which are important for further processing of information.

The modern recording unit (sweep oscilloscope, vibrograph, seismograph, etc.) makes it possible to record on one carrier a large number of graphs, each of which characterizes the dynamics of a certain part of a parameter of the system being studied. Such a recording is convenient for further analysis of the relations between the parameters whose characteristics of change were recorded. But this type of recording imposes certain requirements on the apparatus for computing the curves. These units reproduce all the graphs simultaneously or selectively in binary code, i.e. any of those in one cycle of observation of the carrier tape, provided the curves do not intersect, are not tangential and do not merge. The ordinates of each curve can be read with respect to its base level in the case of non-intersecting curves or with respect to the common base of all the curves. The output information of these devices is binary numbers proportional to the ordinates of the curves being read. Hence they can be collected from the computer using a digital punching machine or perforator. One can recommend use of the Siluet converter. It is most convenient to perforate the readout ordinates on five-channel tape in international code No. 2.

The curves to be fed into the Siluet converter should be drawn clearly, without gaps. If they are fed to photographic films and the reading interval does not exceed 0.25 mm, then the inclination of the curve relative to the basic level from which the ordinate is measured should not exceed 85°. If the curve is a markedly oscillating function the process should be recorded at a high speed of carrier tape. If the experimental conditions do not permit this it is necessary to increase the given realization (curve), after which the reading of ordinates is carried out with large intervals and the reading error is reduced.

When the recording of the process is done by autorecorder, which gives a picture of the function in curvilinear coordinates, and also in the absence of a reading unit, "discretization" has to be carried out by hand, using the appropriate network-pattern.

Hand computation is also possible for deviations from exact geometric shapes of raceways of bearing rings and of balls when circular diagrams are obtained and realization of deviations from the mean diameter is expressed in polar coordinates.

The numbers obtained by "discretization" should be scaled. Before scal-

ing, the sequence must be centered. This means that from each number $x_i \in x$, where x is the sequence, the mean value is subtracted:

$$m = \frac{1}{N} \sum_{i=1}^{N} x_i, \tag{6.4}$$

where N is the number of terms in the series.

Thus we get a new series whose terms are

$$x_i^0 = x_i - m, \; i = 1, 2, \ldots, N, \tag{6.5}$$

i.e. we get a series of readings corresponding to the basic level (basic level is the mean value of the process).

The series (6.5) is scaled, i.e. it is multiplied by a number 'a' which is inversely proportional to a number k:

$$a = \frac{1}{k}, \tag{6.6}$$

where k is the coefficient of elongation (compression) of the ordinates of the process when it is recorded on the carrier tape from which the ordinates are read out. In determining this coefficient, the condition that "ordinate" usually means the distance between the basic level and deviation expressed in millimeters is also taken into account. These are expressed in units corresponding to the particular nature of the process (torque, voltage, etc.).

If the maximum y_{max} and minimum y_{min} of the value of the process expressed in units corresponding to the nature of the process are known, then the value of the coefficient k can be determined from the expression

$$k = \frac{x_{max} - x_{min}}{y_{max} - y_{min}}, \tag{6.7}$$

where x_{max}, x_{min} are respectively the maximum and minimum values of the process in the readout units with "discretization" (basic level not necessarily zero).

Recomputation using formulas (6.4), (6.5) and by formula

$$x'_{im} = \frac{1}{k} x_i^0 \tag{6.8}$$

is carried out after feeding data into the computer until the statistical characteristics are determined.

The process of obtaining spectral-correlational characteristics of bearings can be broken down as follows:

a) measurement and recording of process;

b) computation of realizations for input to computer;

c) compilation of programs to be fed into the computer and determination of the desired statistical characteristics;

d) determination of statistical characteristics of bearings in the form of digital or graphic data (correlation functions, spectral densities, curves of distribution, transfer functions).

The question of determination of the observation time and fixation interval "discretization" of the random process is fundamental for the preparation of experimental data to determine statistical characteristics using a computer. The solution is made difficult by the lack of *a priori* information on the nature of the correlation function of the process, on the basis of which the observation time and fixation interval are determined, taking into account the requirement for accuracy of the estimations of probable characteristics of the process.

Usually when running tests, the following formula is used for determination of observation time T_0 of the random process:

$$T_0=\eta\,\tau_d, \tag{6.9}$$

where η is a coefficient that characterizes the volume of samples, in practice taken equal to 8–10;

τ_d is the conditional time for damping of the correlation function $K(\tau)$, determined from the condition of validity for $\tau\geqslant\tau_d$ of the inequality

$$\frac{|K(\tau)|}{K(0)}=|\rho(\tau)|\leqslant 0.05. \tag{6.10}$$

For determination of τ_d different relations are used, in particular [34],

$$\tau_d=\int_{-\infty}^{\infty}|\rho(\tau)|\,d\tau,$$

$$\tau_d=\int_{-\infty}^{\infty}\rho^2(\tau)\,d\tau \tag{6.11}$$

and others (if there is an assumption as to the type of correlation function).

The approximate method of estimating the conditional damping time of correlation function [11] is well known. It is based on the use of the relation of the mean number of zeros (cross-section of zero mean level) in unit time of a normal stationary differentiable random process with the second derivative of a normalized correlation function $\rho(\tau)$ when $\tau=0$:

$$n_0=\frac{1}{\pi}\sqrt{-\rho''(0)}. \tag{6.12}$$

For processes with rational-fraction spectral densities which can be approximated by the expression $a\prod_{j}^{j_{max}}1/(T^2\omega^2+1)$, the quantity τ_d changes in

the interval from

$$\tau_{d\,min}=0.78/n_0$$

to

$$\tau_{d\,max}=3.12/n_0. \tag{6.13}$$

The mean number of zeros is satisfactorily stabilized in the interval of time containing 50–70% zeros of the process.

There is another method for finding τ_d. Let the range of frequencies be known: ω_l lower and ω_u upper frequency. Taking the process for "white noise" in this range of frequencies, we have

$$\rho(\tau)\leqslant\frac{2}{(\omega_u-\omega_l)\tau}\,.$$

Hence

$$\tau_d\leqslant\frac{40}{\omega_u-\omega_l}\,. \tag{6.14}$$

In choosing the "discretization" step of continuous processes it is necessary to estimate the error in replacing the continuous process by discrete ones. In considering a concrete problem the error of "discretization" should be determined as the value of deviations of results of the solution using discrete and continuous processes. It is not always possible to determine in advance what "discretization" may lead to. Usually by error of "discretization" of processes we mean an error with which the continuous process could be restored using its discrete values, i.e. it corresponds to the error in the problem of interpolation of the continuous process at a discrete number of points.

The restoration of continuous process $x(t)$ based on the corresponding process x_i can usually be represented as the allowable series of "instantaneous" impulses (δ-functions) with the envelope x_i and period Δt through a linear interpolating filter with certain transfer characteristics $k_0(t)$. The signal

$$x_*(t)=\sum_{i=-\infty}^{\infty}x_i\,k_0(t-i\Delta t). \tag{6.15}$$

is formed.

The correlation function, energy spectrum and error dispersion

$$\Delta x(t)=x(t)-x_*(t) \tag{6.16}$$

on the assumption that $x(t)$ is a stationary centered random process, are expressed respectively in the following way:

$$K_\Delta(\tau)=K(\tau)+\frac{1}{\Delta t}\sum_{m=-\infty}^{\infty}K[m]\,g_0(\tau-m\Delta t)$$

$$-\frac{1}{\Delta t}K(\tau)*k_0(\tau)-\frac{1}{\Delta t}K(\tau)*k_0(-\tau), \tag{6.17}$$

where $g_0(\tau)=k_0(\tau)*k_0(-\tau)$ is the convolution operation;

$$f_1(t)*f_2(t)=\int_{-\infty}^{\infty} f_1(\Theta)\,f_2(t-\Theta)\,d\Theta=\int_{-\infty}^{\infty} f_1(t-\Theta)\,f_2(\Theta)\,d\Theta;$$

$$S_\Delta(\omega)=\int_{-\infty}^{\infty} K_\Delta(\tau)\,e^{-j\omega\tau}\,d\tau=S(\omega)\left[1-\frac{2}{\Delta t}\operatorname{Re}K_0(j\omega)\right]+\frac{1}{\Delta t}\Phi(\omega)\,|K_0(j\omega)|^2, \tag{6.18}$$

where $K_0(j\omega)=\int_{-\infty}^{\infty} k_0(t)\,e^{-j\omega t}\,dt$ is the spectrum of interpolation function $k_0(t)$;

$$\sigma_\Delta^2=K_\Delta(0)=\delta^2+\frac{1}{\Delta t}\sum_{m=-\infty}^{\infty}K[m]\,g_0[m]-\frac{2}{\Delta t}\int_{-\infty}^{\infty}K(\Theta)\,k(\Theta)\,d\Theta.$$

There are different ways of determining the "discretization" step Δt in order to obtain estimates of statistical characteristics.

If the random stationary process has a correlation function $K(\tau)$ whose first derivative $K'(\tau)$ in the region of zero is not equal to zero and the remaining drivatives are bounded, then the fixation step Δt is obtained on the basis of the solution of equation [11]:

$$\frac{4}{9}K\left(\frac{\Delta t}{2}\right)-\frac{5}{18}K(\Delta t)=\frac{1}{2}K(0) \tag{6.19}$$

in terms of Δt. This interval is optimum for a mean arithmetic estimate of the mathematical expectation, i.e. reduction of this interval does not lead to an improvement in the accuracy of estimation. For an estimate of the dispersion and correlation function this interval does not yield enough measurements.

When one has no idea whatever as to the form of the correlation functions of the random process it is possible to use the V.A. Kotelnikov [20] theorem on amplitude-impulse transformation for preliminary choice of the constant fixation interval Δt. According to this theorem exact reproduction of the signal is possible in the case of transmission of successive discrete values at intervals not exceeding half the period of the higher harmonic of the spectrum.

On the other hand, the distance $\Delta\tau$ between successive values of the correlation function being estimated is chosen from the condition of allowable error of approximation δ_a.

In linear approximation of the curve by parts the relative error δ_a is associated with the interval Δt by the well-known formula that allows the com-

putation of $\Delta\tau$ [25] in terms of the concrete form of the correlation function:

$$\Delta\tau=\sqrt{\frac{8\delta_a}{|K''(\tau)/K(\tau)|_{max}}}, \tag{6.20}$$

where $K''(\tau)$ is the second derivative of the correlation function (the maximum is taken in the interval $0\leqslant\tau\leqslant\tau_d$).

The sample interval Δt is usually kept equal to the interval $\Delta\tau$:

$$\Delta t=\Delta\tau \tag{6.21}$$

In the work [25], for typical correlation functions computation of the quantity $\Delta t=\Delta\tau$ as a function of δ_a is carried out using formula (6.20). An expression is obtained that determines the number of readings k within a period of upper frequencies ω_u:

$$k=\frac{2\pi}{\Delta t\omega_u}.$$

For a very wide class of correlation functions the expression for k has practically identical form:

$$k=\frac{2\pi}{\sqrt{8\delta_a}}, \tag{6.22}$$

so that the quantity Δt is determined only by the allowable error and upper frequency:

$$\Delta t=\Delta\tau=\sqrt{\frac{\delta_a}{\omega_u}}. \tag{6.23}$$

In particular, $k=16$ when $\delta_a=2\%$ and $k=10$ for $\delta_a=5\%$. In practice the choice $\Delta t=\Delta\tau$ from the conditions (6.20), (6.23) results in good linear interpolation of the random process and corresponds to the recommended 10–20 readings during an upper frequency period.

This method for selecting the fixation interval Δt is equivalent to continuous integration based on the accuracy of the data obtained. However, it leads to unjustifiably large samples because there are considerable correlational relations between sample values of the random process and there is an appreciable redundance in the information obtained on the characteristics of the random process. In addition the choice of the value $\Delta t=2\pi/(10\text{–}20)\omega_u$ imposes very rigid requirements on the computer.

The invariance with time of the statistical characteristics of stationary processes allows us to carry out sampling with arbitrary frequency, with a lower bound decided in practice solely by the required interval of realizations T_0. The choice of the value $\Delta t\geqslant\tau_d$ practically corresponds to the uncorrelated sample.

The size of sample N in this case is practically equal to the minimum. It

can work out random processes whose upper frequency is $\tau_d/\Delta t=m$ times higher than in the case of sampling with interval $\Delta t=\Delta\tau$. For processes with an exponential correlation function the choice $\Delta\tau=\tau_d$ where τ_d is determined by the relation (6.10) requires a threefold increase in the duration of realization. For other forms of $K(\tau)$ this increase can be even greater (five to ten times).

Such increase in the analysis time is not desirable especially for low-frequency processes but is quite suitable when analyzing the function of change in errors of the roughness of raceways of rings and rolling elements since this is a stationary ergodic random process. In the analysis of the function of variable friction torque as a random process we come across analysis of the realization of fixed duration determined by the recording of realization, or the case where the duration time of observation T_0 is limited by the condition of being stationary. In such cases the impossibility of a multiple increase in T_0 leads to an increase in error by 1.5 to 3 times when compared to the frequency of sampling [3].

So before determining statistical characteristics it is necessary to replace infinite realization by realization of finite duration T_0 on the basis of purely practical considerations as to the form of the correlation function and the fact that excessively long realizations may be nonstationary.

Choice of the fixation interval $\Delta t=\Delta\tau$ determined by the condition (6.20) is not rational because of the large amount of computational work. The method of uncorrelated sampling is free from this disadvantage but to maintain accuracy it requires a considerable increase in the length of realization. The best choice from this point of view is

$$\Delta t=\frac{\tau_d}{5-8}. \tag{6.24}$$

For realizations of equal duration the accuracy of the estimates obtained is practically the same as in the first method (frequent sampling). At the same time the amount of computations required exceeds the amount of computations for uncorrelated sampling by only 1.5 to three times. The upper bound of the frequency range is exceeded by four to eight times when compared to the first method.

The number of readings

$$N=E\left[\frac{T_0}{\Delta t}\right]+1, \tag{6.25}$$

where $E[T_0/\Delta t]$, indicates the maximum integer number less than $\frac{T_0}{\Delta t}$.

In practice the realizations of the processes are expressed in the form of oscillograms on photographic films or paper tape. The length of such a realization (in meters) necessary for understanding the spectral structure of

the process in the range of frequencies from ω_l to ω_u is obtained from the inequality

$$L \geqslant \frac{4\pi^2 v}{\omega_u \omega_l}, \tag{6.26}$$

where v is the speed of the tape (film, photopaper) during the recording of the realization of the process, μ/sec.

The fixation interval in units of length is

$$\Delta L \leqslant \frac{L}{N-1}. \tag{6.27}$$

When analyzing the spectral structure of the process in a wide range of frequencies the number N may be too large when compared to the limited memory capacity of the computer. In order to distinguish low frequencies it is not necessary to sacrifice higher ones or, in other words, it is necessary to carry out the analysis in steps. Here the analyzed realization is replaced by random series-samples to a maximum number N determined by the memory of the computer, and with different intervals (by length) of fixation. Considering that to distinguish any frequency it is necessary to arrange realizations containing eight to ten corresponding periods, each having eight to ten reading points, it is possible to determine roughly the range of frequencies in which the estimates will correspond to the required specifications for given values of N and Δt. This range consists of frequencies from 2π (8–10)/$N\,\Delta t$ to 2π/(8–10) Δt radians.

When determining the statistical characteristics of the functions of bearing component profiles (geometric defects) it is necessary to solve the problem of finding the center of the circle diagram which represents surface roughness. In order to get the diagrams it is most convenient to use instruments of the Talyrond-51 type for verification of circular shape. In Fig. 6.1 examples are shown of the verification of the raceways of ball bearing rings. In this case deviations from the theoretical circle due to manufacturing defects in the raceways of both inner and outer rings of the bearings were recorded. The raceways were determined by the method of charging. Location of the center of theoretical circle can be only approximately determined using the procedure in the instructions for use of instruments to record oscillograms. In the work [14] an algorithm is suggested for accurately locating the center, but it follows from the Fourier series for $\Delta\rho\,(\varphi)$ given there that even using the algorithm the center is displaced. An algorithm for centering the circle diagram free from this defect is given here.

Let us introduce the following notations: ρ_i ($i = 1, 2, \cdots, N$, where N is the number of readings) and the radii relative to the approximately located center O (Fig. 6.2); r_i are radii relative to the actual center O_1; x, y are the coordinates of the actual center; φ_i is the angle between the x-axis and radius

ρ_i; ψ_i is the angle between the x-axis and the radius passing through the actual center; c is the distance between the approximately located and actual centers. For each value of i ($i=1, 2, \cdots, N$)

$$r_i^2=\rho_i^2+c-2\rho_i\cos(\varphi_i-\varphi_c). \tag{6.28}$$

Considering

$$\cos\varphi_c=\frac{x}{c},\ \sin\varphi_c=\frac{y}{c},\ c=\sqrt{x^2+y^2}, \tag{6.29}$$

we get

$$r_i^2=\rho_i^2+c^2-2\rho_i x\cos\varphi_i-2\rho_i y\sin\varphi_i. \tag{6.30}$$

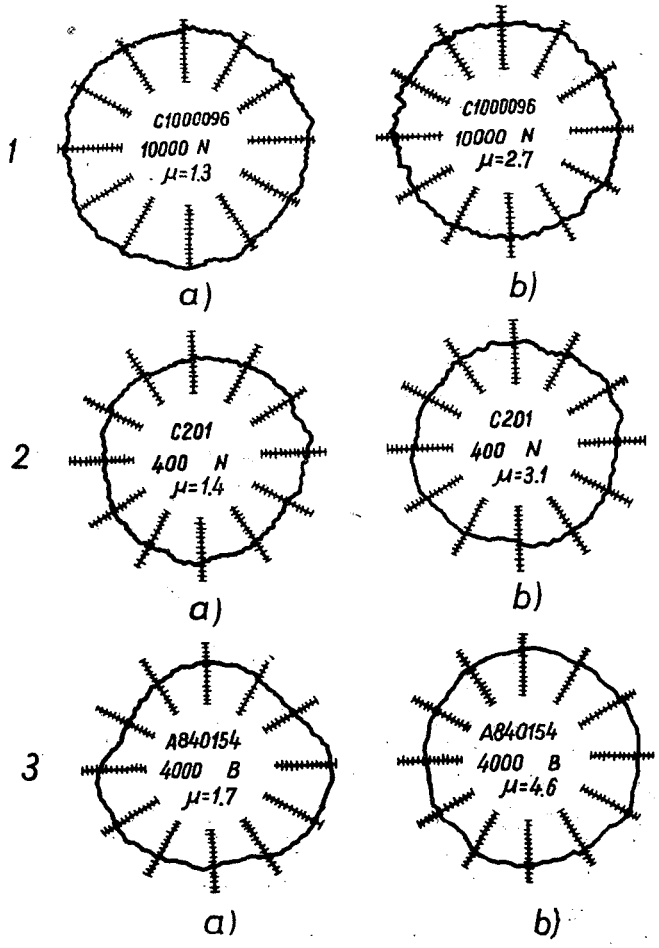

Fig. 6.1. Examples of circle diagrams describing surface roughness of raceways: *a*—outer ring, *b*—inner ring; *1*—bearing of C1000096 type; × 10000 times; *2*—bearing of C201 type; × 4000 times (sic); *3*—bearing of A840154 type; × 4000 times.

The coordinates of the real center are determined from the condition for minimum dispersion of deviations from the mean radius

$$\bar{r}=\frac{1}{N}\sum_{i=1}^{N} r_i, \qquad (6.31)$$

corresponding to the actual center. This is adequate to obtain the values of x and y from the minimizing criteria

$$Q(x, y)=\frac{1}{N}(r_i-r)^2. \qquad (6.32)$$

Conditions for the minimum lead to a system of two transcendental equations:

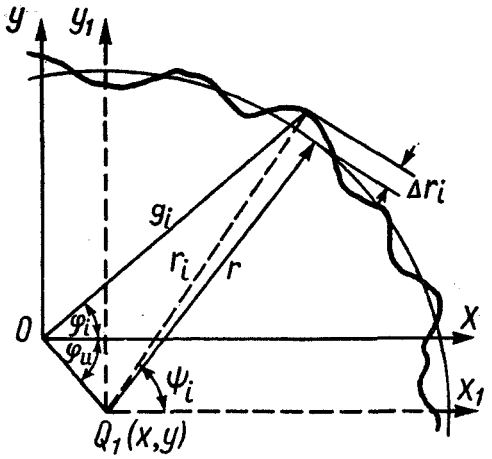

Fig. 6.2. Determination of center of circle diagram.

$$x=\frac{1}{N}\sum_{i=1}^{N}\rho_i\cos\varphi_i-\frac{1}{N}\,\mathrm{r}\sum_{i=1}^{N}\frac{x-\rho_i\cos\varphi_i}{r_i}=f_1(x, y),$$

$$y=\frac{1}{N}\sum_{i=1}^{N}\rho_i\sin\varphi_i-\frac{1}{N}\,\mathrm{r}\sum_{i=1}^{N}\frac{y-\rho_i\sin\varphi_i}{r_i}=f_2(x, y). \qquad (6.33)$$

By direct calculation it has been established that the right-hand sides of equations (6.33) satisfy Lifshits' conditions and the system has a unique solution which can be found with the iterative method. It is possible to start the iteration with zero initial values $x=0$, $y=0$ or with

$$x_0=\frac{1}{N}\sum_{i=1}^{N}\rho_i\cos\varphi_i,$$

$$y_0=\frac{1}{N}\sum_{i=1}^{N}\rho_i\sin\varphi_i, \qquad (6.34)$$

which corresponds to the first iteration x_1, y_1 with zero initial values. The values of x_1, y_1 in the first iteration are found from the formulas:

$$x_i=f_1(x_{i-1}, y_{i-1}),$$
$$y_i=f_2(x_{i-1}, y_{i-1}). \qquad (6.35)$$

The condition for terminating the iterative procedure for computing x and y is determined by the inequality:

$$|Q_i - Q_{i-1}| < \varepsilon, \tag{6.36}$$

where Q_i and Q_{i-1} are values of the criterion Q, computed for the values x_i, y_i; and x_{i-1}, y_{i-1} obtained for the i-th and $(i-1)$-th iterations respectively; ε is a small positive number which is arbitrarily chosen or corresponding to conditions

$$\begin{aligned} |x_i - x_{i-1}| &< \delta_1, \\ |y_i - y_{i-1}| &< \delta_2, \end{aligned} \tag{6.37}$$

where δ_1 and δ_2 are small positive numbers that indicate the allowable absolute error in the estimates of x and y respectively; they can be computed as a percentage for each iteration i with respect to the given relative error δ in the estimation of x and y:

$$\begin{aligned} \delta_{1i} &= \frac{\delta x_i}{100}, \\ \delta_{2i} &= \frac{\delta y_i}{100}. \end{aligned} \tag{6.38}$$

Actual computations showed that the iterative procedure converges within 12–24 iterations. This means that it is possible to avoid analysis of results after each iteration and instead give a constant number of iterations equal to 25–30.

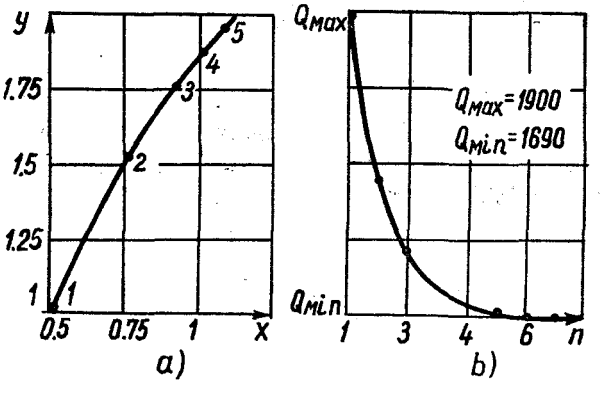

Fig. 6.3. Shift in location of center in iteration procedure (*a*) relation between shift in number of iterations of dispersion and mean radius; (*b*) Q_{max}=1,900, Q_{min}=1,690.

In Fig. 6.3 results of the solution of equations (6.33) by the iterative procedure are shown. Here the center of the circular diagram of geometric defects in the inner ring of ball bearing C1000096 was found. The number *1* refers to the initial point (x_0, y_0) of the iteration.

An example of change in the criterion Q is shown in Fig. 6.3 b. The num-

ber of iterations is given along the abscissa and the ordinates give Q computed using formula (6.32), starting from Q_0 up to the last iteration.

Usually the quantity ρ_i is read at equal polar angles $\Delta\varphi$

$$\Delta\varphi=\varphi_i-\varphi_{i-1}=\frac{2\pi k}{N}$$

or

$$\varphi_i=\frac{2\pi k}{N}i, \qquad i=1, 2, \ldots, N, \tag{6.39}$$

where k is the number of readings.

After transfer of the center to the point O_1 radii r_i correspond to angles

$$\psi_i=\tan^{-1}\frac{y-\rho_i\sin\varphi_i}{x-\rho_i\cos\varphi_i}$$
$$+\pi\left[1-\frac{1}{2}\operatorname{sign}(y-\rho_i\sin\varphi_i)\{1+\operatorname{sign}(x-\rho_i\cos\varphi_i)\}\right],$$
$$\operatorname{sign}x=\begin{cases}1, & x\geqslant 0,\\ -1, & x<0,\end{cases} \tag{6.40}$$

i.e. the angle between neighboring radii is not a constant. Fourier analyses were carried out for the deviations from mean radii corresponding to the centers of circular diagrams determined by using the procedure [14] and the iterative procedure. In all cases the amplitude of the first harmonic for the first period exceeded by several times the amplitude of the first harmonic of deviations from the mean radius corresponding to the center determined by the method suggested. This indicates determination of the center without displacement. This phenomenon is illustrated by the Fourier spectra (Fig. 6.4). The dots indicate amplitudes of the spectrum of deviations from the mean radius determined by the iterative procedure. The abscissa gives the number of harmonics.

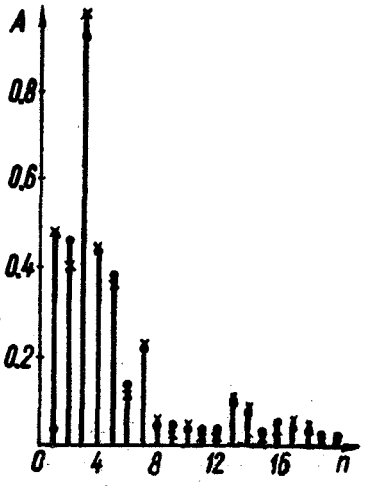

Fig. 6.4. Amplitudes of Fourier spectrum of function of geometric errors: "*"—after first iteration; "·"—after determination of center of profilograph.

When computing the estimates of a correlation function for the series r_i $(i=1, 2, \ldots, N)$ it is necessary to use linear interpolation to obtain new values of equally spaced radii along polar angles:

$$r_i^*=\frac{r_j-r_{j-1}}{\psi_j-\psi_{j-1}}\left(\frac{2\pi k}{N}i-\psi_{j-1}\right)+r_{j-1}, \qquad i=1, 2, \ldots, N. \tag{6.41}$$

Here ψ_j is the minimum of angles ψ_i larger than $\frac{2\pi k}{N}i$:

$$\psi_j = \min_L \left\{ \psi_L : \psi_L > \frac{2\pi k}{N} i \right\}, \qquad i = 1, 2, \ldots, N. \tag{6.42}$$

6.2 ESTIMATION OF STATISTICAL CHARACTERISTICS

The distribution density, mathematical expectation, dispersion and correlation function of the process being studied are the principal statistical characteristics to be estimated.

The correlation function characterizes the degree of dependence between the quantities $x(t_1)$ and $x(t_2)$ of the random process, separated by an interval of time $t_2 - t_1$.

The correlation function of the friction torque and vibrations of bearings is damped with an increase in time τ and does not depend on the initial reading, which shows the randomness of the friction torque and vibrations of bearing rings as a stationary ergodic process.

In the physical sense the correlation function characterizes the inertia of a system subjected to the action of random disturbances.

In the estimation of the dynamic characteristics of rolling contact bearings the correlation function is principally used as an intermediate stage for estimating the spectral density.

The exposure of hidden periodicity, i.e. analysis of the spectral structure of real processes based on the results of measurements, is very important when studying the vibration phenomenon. Analysis of a vibrogram makes it possible to show the periodic components and discover the principal sources of friction torque and vibrations in bearings.

The spectral density shows a mean dispersion density, i.e. dispersion per unit length of the given interval of frequencies.

From spectral density of friction torques and vibrations of bearing rings it is possible to come to conclusions as to the expected levels and frequencies of the processes, both for individual instrument rolling contact bearings and for assemblies of which they are part.

The stationary process $x(t)$ having the property of ergodicity is characterized by the following relations, using the ergodicity theorem under certain conditions which are practically always satisfied with a probability equal to unity:

$$m = \lim_{T \to \infty} \int_0^T x(t)\, dt;$$

$$K(\tau) = \lim_{T \to \infty} \int_0^T x^0(t)\, x^0(t+\tau)\, dt; \tag{6.43}$$

$$x^0(t) = x(t) - m.$$

In computing estimates of m and $K(\tau)$ using the known experimental recording of random functions $x(t)$ formulas (6.43) have been used. Estimates computed on the basis of one realization $x(t)$ by averaging with respect to argument t in the interval $[0, T]$ are expressed by m_T and K_T:

$$m_T=\frac{1}{T}\int_0^T x(t)\,dt,$$

$$K_T(\tau)=\frac{1}{T}\int_0^T x(t)\,x(t+\tau)\,dt. \tag{6.44}$$

Depending on the choice of T based on the available observation time T_o of realization of the random process, it is possible to use a number of ways to compute $K_T(\tau)$ [16]. But the following formula is most frequently used:

$$K_T(\tau)=\frac{1}{T_o-\tau}\int_0^{T_o-\tau} x^0(t)\,x^0(t+\varepsilon)\,dt. \tag{6.45}$$

The mean square deviation of the function $K_T(\tau)$ from functions $K(\tau)$:

$$\sigma^2(\tau)=M\Big(K_T(\tau)-K(\tau)\Big)^2 \tag{6.46}$$

is expressed through an integral of functions containing the quantities m and $K(\tau)$. In practical computations, when the values of m and $K(\tau)$ are usually unknown, they are replaced by estimates m_T and $K_T(\tau)$. It is possible to evaluate roughly the accuracy of the estimates obtained by using the approximate value $\sigma^2(\tau)$.

In numerical integration equations (6.44) and (6.45) are replaced by the equations

$$m=\frac{1}{N}\sum_{\nu=1}^{N} x(\nu\Delta t),$$

$$x(\nu\Delta t)=x(t)\,|_{t=\nu\Delta t},\ x^0(\nu\Delta t)=x(t)\,|_{t=\nu\Delta t}-m;$$

$$K_N(i\Delta t)=\frac{1}{N-i}\sum_{\nu=1}^{N-i} x^0(\nu\Delta t)\,x^0(\nu\Delta t+i\Delta t),\quad i=1,2,\ldots,M, \tag{6.47}$$

$$M=E\left[\frac{\tau_3}{\Delta t}\right]+1.$$

In practice, usually

$$M\approx\frac{N}{8-10}. \tag{6.48}$$

The normalized correlation function has the following form:

$$\rho_N(i\Delta t)=\frac{K_N(i\Delta t)}{\sigma_N^2}, \tag{6.49}$$

where σ_N^2 is the estimate of the dispersion of random process:

$$\sigma_N^2=K(0). \tag{6.50}$$

The dispersion of the estimate (6.47) of mathematical expectation

$$\sigma_m^2=\frac{\sigma_N^2}{N^2}\left[N^2+2\sum_{i=1}^{N-1}(N-i)\,\rho(i\Delta t)\right], \tag{6.51}$$

and the estimate of correlation function

$$\sigma_{K_N}^2=\frac{\sigma_N^2}{(N-k)^2}\sum_{l=-(N-k)}^{N-k}(N-k-|l|)\{\rho^2(l\Delta t) + \rho[(l+k)\,\Delta t]\,\rho[(l-k)\,\Delta t]\}. \tag{6.52}$$

When computing the estimates σ_m^2 and $\sigma_{K_N}^2$ it is necessary to use the estimate obtained from realization instead of the values $\rho(k\Delta t)$.

To study vibrations of bearings using the method of statistical tests it is necessary to approximate correlation functions. Compilation of the algorithm for modeling the random process is most convenient with analytical expression of the correlation function.

In this sense the suitable approximating expression for the values of $K(\tau)$ can be found by a linear combination of functions $\varphi_n(\tau)$ in particular, by a possible approximation of one of them by suitable functions, for example, by the function $\varphi(\tau)=ce^{-\alpha|\tau|}\cos\beta\tau$ or by other methods described in the work [34].

Let us consider the requirements for the approximating functions.

1. Correlation functions $K(\tau)$ must if possible be expressible through functions $\psi_n(\tau)$, whose operational Laplace images are rational-fractional functions of the variable ω.

2. Approximating functions should represent a complete family of orthogonal functions, which ensures simplicity of control of approximation in the mean quadratic sense.

3. The computations of the coefficients of the $K(\tau)$ series should be simple operations as far as possible.

4. The approximating functions should satisfy the limiting relation

$$\lim_{\tau\to\infty}\varphi_n(\tau)=0.$$

5. The approximating functions should reflect the oscillating nature of the change in the correlation function.

The most convenient and most general family of approximating functions is

$$c_\nu e^{-\alpha_\nu |\tau|} \cos \beta_\nu \tau.$$

The problem of approximating correlation functions practically leads to the determination of parameters c_ν, α_ν, β_ν which enter the series expansion

$$K(\tau)=\sum_{\nu=1}^{n} c_\nu e^{-\alpha_\nu |\tau|} \cos \beta_\nu \tau. \tag{6.53}$$

These parameters should be computed starting from the condition for the minimum of the function:

$$F=\sum_{i=1}^{M}\left[K(\tau_i)-\sum_{\nu=1}^{n} c_\nu e^{-\alpha_\nu |\tau|} \cos \beta_\nu \tau_i\right]^2. \tag{6.54}$$

The conditions for minimum are described by a system of three transcendental equations:

$$\begin{aligned}
\frac{\partial F}{\partial c_\nu} &= -2\sum_{i=1}^{M} f_i \cos \beta_\nu \tau_i e^{-\alpha_\nu \tau_i}=0,\\
\frac{\partial F}{\partial \alpha_\nu} &= 2\sum_{i=1}^{M} f_i c_\nu \tau_i \cos \beta_\nu \tau_i e^{-\alpha_\nu \tau_i}=0,\\
\frac{\partial F}{\partial \beta_\nu} &= 2\sum_{i=1}^{M} f_i c_\nu \tau_i \sin \beta_\nu \tau_i e^{-\alpha_\nu \tau_i}=0,
\end{aligned} \tag{6.55}$$

where

$$f_i=K(\tau_i)-\sum_{\nu=1}^{M} c_\nu e^{-\alpha_\nu \tau_i}\cos \beta_\nu \tau_i,\ \tau_i>0,\ i=1, 2, \ldots, M.$$

The system of equations (6.55) can be solved by the iterative method, the method of gradient or the method of steepest descent. Let us choose the method of steepest descent.

Let us determine the new variables x_ν, $\nu=1, 2, \ldots 3n$:

$$\begin{aligned}
x_\nu &= c_\nu,\ \nu=1, 2, \ldots, n,\\
x\nu &= \alpha\nu_{-n},\ \nu=n+1, n+2, \ldots, 2n,\\
x\nu &= \beta\nu_{-2n},\ \nu=2n+1, 2n+2, \ldots, 3n.
\end{aligned} \tag{6.56}$$

In this case the $(j+1)$ th approximation of x_ν $(j+1)$ of parameters x_ν is computed using formulas

$$x_\nu(j+1)=x_\nu(j)-h\frac{\partial F}{\partial x_\nu},\quad \nu=1, 2, \ldots, 3n, \tag{6.57}$$

and the optimum interval h is determined by the relation

$$h=\frac{\sum_{\nu=1}^{3n}\left(\frac{\partial F}{\partial x_\nu}\right)^2}{\sum_{\nu=1}^{3n}\sum_{\mu=1}^{3n}\frac{\partial^2 F}{\partial x_\nu\,\partial x_\mu}\cdot\frac{\partial F}{\partial x_\nu}\cdot\frac{\partial F}{\partial x_\mu}}, \tag{6.58}$$

in which the derivatives are computed for the values $x_\nu(j)$, $\nu=1, 2, \ldots, 3n$, obtained at the previous approximation of j.

The second-order derivatives have the following form:

$$\frac{\partial^2 F}{\partial x_\nu\,\partial x_\mu}=2\sum_{i=1}^{M}\exp\{-(\alpha_\nu+\alpha_\mu)\tau_i\}\cos\beta_\nu\tau_i\cos\beta_\mu\tau_i,$$

$$\nu,\ \mu=1, 2, \ldots, n;$$

$$\frac{\partial^2 F}{\partial x_\nu\,\partial x_\mu}=-2\sum_{i=1}^{M}c_\mu\tau_i\exp\{-(\alpha_\nu+\alpha_\mu)\tau_i\}\cos\beta_\nu\tau_i\cos\beta_\mu\tau_i$$

$$+\delta_{\nu,\,\mu-n}\,2\sum_{c=1}^{M}f_i\tau_i\exp\{-\alpha_\mu\tau_i\}\cos\beta_\mu\tau_i,$$

$$\nu=1, 2, \ldots, n,\ \mu=n+1, n+2, \ldots, 2n;$$

$$\delta_{i,j}=\begin{cases}1, & i=j,\\ 0, & i\neq j,\end{cases}$$

$$\frac{\partial^2 F}{\partial x_\nu\,\partial x_\mu}=-2\sum_{i=1}^{M}c_\mu\tau_i\exp\{-(\alpha_\nu+\alpha_\mu)\tau_i\}\cos\beta_\nu\tau_i\sin\beta_\mu\tau_i$$

$$+\delta_{\nu,\,\mu-2n}\,2\sum_{i=1}^{M}f_i\tau_i\exp\{-\alpha_\mu\tau_i\}\sin\beta_\mu\tau_i, \tag{6.59}$$

$$\nu=1, 2, \ldots, n,\ \mu=2n+1, 2n+2, \ldots, 3n;$$

$$\frac{\partial^2 F}{\partial x_\nu\,\partial x_\mu}=2\sum_{i=1}^{M}c_\nu c_\mu\tau_i^2\exp\{-(\alpha_\nu+\alpha_\mu)\tau_i\}\cos\beta_\nu\tau_i\cos\beta_\mu\tau$$

$$+\delta_{\nu,\,\mu}\,2\sum_{i=1}^{M}f_i\tau_i^2\,c_\mu\exp\{-\alpha_\mu\tau_i\}\cos\beta_\mu\tau_i,$$

$$\nu, \mu = n+1,\ n+2,\ldots,\ 2n;$$

$$\frac{\partial^2 F}{\partial x_\nu\, \partial x_\mu} = 2 \sum_{i=1}^{M} c_\mu\, c_\nu\, \tau_i^2 \exp\{-(\alpha_\nu+\alpha_\mu)\,\tau_i\} \cos\beta_\nu\,\tau_i \sin\beta_\mu\,\tau_i$$

$$+\delta_{\nu,\,\mu-n}\, 2 \sum_{i=1}^{M} f_i\, \tau_i^2 \exp\{-\alpha_\mu\,\tau_i\} \sin\beta_\mu\,\tau_i \cdot c_\mu\,,$$

$$\nu = n+1,\ n+2,\ldots,\ 2n,\ \ \mu = 2n+1,\ 2n+2,\ldots,\ 3n,$$

$$\frac{\partial^2 F}{\partial x_\nu\, \partial x_\mu} = 2 \sum_{i=1}^{M} c_\nu\, c_\mu\, \tau_i^2 \exp\{-(\alpha_\nu+\alpha_\mu)\,\tau_i\} \sin\beta_\nu\,\tau_i \sin\beta_\mu\,\tau_i$$

$$+\delta_{\nu\mu-n} - 2 \sum_{i=1}^{M} f_i\, c_\mu\, \tau_i^2 \exp\{-\alpha_\mu\,\tau_i\} \cos\beta_\mu\,\tau_i\,,$$

$$\mu,\ \nu = 2n+1,\ 2n+2,\ldots,\ 3n;$$

$$\frac{\partial^2 F}{\partial x_\nu\, \partial x_\mu} = \frac{\partial^2 F}{\partial x_\mu\, \partial x_\nu}\,,\quad \nu, \mu = 1,\ 2,\ldots,\ 3n.$$

The iteration is started from values determined from the spectral density corresponding to the approximating correlation function. Choose the values of $x_{\nu+2n}\,(0) = \omega_\nu$, $\nu = 1,\ 2,\ldots,\ n$, for which the spectral density has maximum values, $x_\nu = S\,(\omega_\nu)$, $\nu = 1,\ 2,\ldots,\ n$, i.e. values of spectral density for the frequencies ω_ν. Damping coefficients $\alpha_\nu = x_{\nu+n}$ are chosen near the value

$$\alpha = \frac{1}{\tau} \ln \frac{K\,(0)}{K\,(\tau)}, \tag{6.60}$$

where $K\,(0)$ and $K\,(\tau)$ are the values of correlation function for the zero value of time $\tau = 0$ and for the value $\tau > 0$ respectively, when the correlation function has a global maximum.

The solution is terminated when the inequality

$$\left| h\, \frac{\partial F}{\partial x_\nu} \right| < \varepsilon \tag{6.61}$$

is satisfied for all values of x_ν ($\nu = 1,\ 2,\ldots,\ 3n$), where ε is the given small positive number or the number determined for each iteration based on the given allowable relative error δ in percent, for the variable x_ν:

$$\varepsilon_\nu\,(j) = \frac{\delta_\nu\, x_\nu}{100}\,. \tag{6.62}$$

Curves of correlation function and functions of spectral density (in Fig. 6.5 a and b respectively they are indicated by solid lines) and also approximat-

ing curves (shown by broken lines) are shown below. Obviously, the approximation offers the required accuracy.

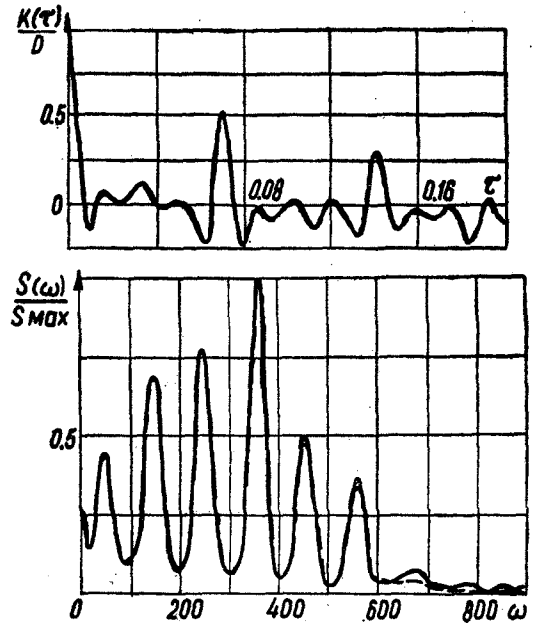

Fig. 6.5. Empirical (solid lines) and approximate (broken lines) curves of correlation function $K(\tau)$ and spectral density $S(\omega)$.

The spectral density (energy spectrum) of a stationary and ergodic random process is determined as a cosine Fourier transformation of the correlation function:

$$S(\omega)=\frac{1}{\pi}\int_0^{\infty} K(\tau)\cos\omega\tau\, d\tau. \tag{6.63}$$

For a finite length of realization the upper limit of integration in the expression (6.63) is replaced by a finite limit ($M\Delta t$). This leads to untenability and a shift in the estimate of spectral density and necessitates the use of various methods to improve the effectiveness of estimates with the help of weighted functions, i.e. "smoothing" of estimates. It is well-known [41] that for certain conditions of "regularity" in stationary process the estimate

$$S_N(\omega)=\int_{-\pi}^{\pi} \lambda_N(\mu,\omega)\, I_N(\omega)\, d\mu \tag{6.64}$$

of the spectral density $S(\omega)$, where

$$I_N(\omega)=\frac{1}{2\pi N}\left[\sum_{k=1}^{N} x^0(k\Delta t)\, e^{ik\omega}\right]^2$$

$$=\frac{1}{2\pi}\sum_{k=-(N+1)}^{N+1}\left(1-\frac{|k|}{N}\right) K_N(k\Delta t)\, e^{ik\omega}. \tag{6.65}$$

The periodgraph of the series $\left\{x(k\Delta t)\right\}$, $k=1, 2,\ldots, N$, and the series of even functions $\left\{\lambda_N(\mu, \omega)\right\}$ with increase in the number N "converges" to the δ-function has a dispersion

$$\sigma^2_{S_N}=\begin{cases}\dfrac{2\pi S^2(\omega)}{N}\displaystyle\int_{-\pi}^{\pi}\lambda_N^2(\mu,\omega)\,d\mu, & \omega\neq 0,\\[2ex] \dfrac{4\pi S^2(0)}{N}\displaystyle\int_{-\pi}^{\pi}\lambda_N^2(\mu,\omega)\,d\mu, & \omega=0\end{cases} \tag{6.66}$$

if the spectral density $S(\omega)$ of the process $x(t)$ is different from zero.

The rate at which the functions $\lambda_N(\mu)$ concentrate near the origin is inversely proportional to the rate of reduction of the dispersion $S_N(\omega)$ and directly proportional to the rate at which the displacement of $S_N(\omega)$ decreases. For a fixed number N the mean value of the estimate will be a smoother function than the true $S(\omega)$ so that certain characteristic features will be lost. In spite of the limitation this combination of two effects has obvious merits and is worth using.

In practice there are many well-known types of weighted functions (truncated, Bartlett, Daniel and others) but the clear, all-around superiority of any concrete weighted function has not been established. In the present book Xemming's weighted function [37] has been used. On the basis of the estimation of the spectral density

$$S_N(\omega)=\frac{1}{2\pi}\sum_{k=-M}^{M}\left(1-\frac{|k|}{N}\right) K_N(k\Delta t)\left\{0.54+0.46\cos\frac{\pi k}{M}\right\}e^{ik\omega}, \tag{6.67}$$

considering that $K_N(k\Delta t)$ is even, we obtain

$$S_N(\omega)=\frac{1}{\pi}\left[\frac{1}{2}K(0)\right.$$

$$\left.+\sum_{k=1}^{M}\left(1-\frac{k}{M}\right) K_N(k\Delta t)\left\{0.54+0.46\cos\frac{\pi k}{M}\right\}\cos k\omega\right]. \tag{6.68}$$

This corresponds to use of the simplest formulas of numerical integration for computation of the integral

$$\bar{S}(\omega)=\int_0^{M\Delta t} K_N^*(\tau)\cos\omega t\,d\tau, \tag{6.69}$$

where

$$K_N^*(k\Delta t)=K(k\Delta t)\left(1-\frac{k}{N}\right)\left\{0.54+0.46\cos\frac{\pi k}{M}\right\}. \tag{6.70}$$

The function within the integral sign in equation (6.69) contains a term $\cos(\omega t)$ in connection with which the curve at large values of ω oscillates rapidly. Hence the quantity $S(\omega)$ cannot be obtained with sufficient accuracy when using the simplest formulas of numerical integration. When computing such integrals by numerical methods the integration intervals should be divided into a large number of parts. In the present case this number is given when computing the quantities $K_N(k\Delta t)$. It is possible to use the method suggested by M.V. Nikolaeva [27] for an approximate computation of oscillating integrals: With the help of interpolating polynomials to approximate not the complete function under the integral but only the multiple $K_N^*(\tau)$, which does not depend on ω. According to the work [19], when approximating the correlation function in the elementary interval $[(i-1)\,\Delta t,\ i\Delta t]$ by an arc of the second-order parabola we get

$$S_N(\omega)=\frac{1}{\pi}\left\{L_1 K_N^*(0)+L_2\sum_{k=1}^{\frac{M-1}{2}} K_N^*[(2k-1)\,\Delta t]\cos\omega\,(2k-1)\,\Delta t\right.$$

$$\left.+2L_1\sum_{k=1}^{\frac{M-1}{2}} K_N^*(2k\Delta t)\cos\omega 2k\,\Delta t+L_3 K_N^*(M\Delta t)\right\}, \tag{6.71}$$

where

$$L_1=\frac{1}{\omega^2\Delta t}\left[1+\cos^2\omega\Delta t-\frac{1}{\omega\Delta t}\sin 2\omega\Delta t\right],$$

$$L_2=\frac{4}{\omega^2\Delta t}\left[\frac{1}{\omega\Delta t}\sin\omega\Delta t-\cos\omega\Delta t\right],$$

$$L_3=\frac{1}{\omega}\left[\sin M\,\omega\Delta t+\frac{1}{\omega\Delta t}\cos M\,\omega\Delta t\right]$$

$$+\frac{1}{\omega^2\Delta t}\cos[(M-1)\,\omega\Delta t]\left\{\cos\omega\Delta t-\frac{2}{\omega\Delta t}\sin\omega\Delta t\right\},$$

and $K_N^*(k\Delta t)$ is determined from the relation (4.70). The use of formula (4.71) leads to a minimum of error in numerical integration for large values of ω, for which $\frac{1}{\omega}\leqslant(5-8)\,\Delta t$.

As shown in the work [40], with a reliability of about 95% the following inequalities are true:

$$e^{-d}-1\leqslant\frac{S_N(\omega)-S(\omega)}{S(\omega)}\leqslant e^{d}-1,$$

$$d\leqslant 2\left\{\frac{M}{N}\int_{-1}^{1}(0.54+0.46\cos\pi u)^2\,du\right\}^{1/2}. \tag{6.72}$$

Where $\frac{M}{N}=0.05$ we have $d=0.4$; $e^{-d}-1=0.33$; $e^{d}-1\approx 0.49$ and for $\frac{M}{N}=0.1$ $-d\approx 0.5$; $e^{-d}-1=0.39$, $e^{d}-1\approx 0.65$.

When the value of $\frac{M}{N}$ is increased the difference between the estimation of spectral density and the actual spectral density increases, which reduces the accuracy. For $\frac{M}{N}\leqslant 0.1$ the error is tolerable.

When computing the quantity $S_N(\omega)$ with the computer the values of ω are chosen with an interval $\Delta\omega$ on the basis of the observation time T_0 and fixation interval Δt. These determine the value ω_u (upper) and ω_l (lower) of circular frequency as the interval within which the estimation has the desired accuracy:

$$\Delta\omega=\frac{\omega_u-\omega_l}{n},$$

$$\omega_u=\frac{2\pi}{(6-10)\,\Delta t},\quad \omega_l=\frac{(6-10)\,2\pi}{T_0}, \tag{6.73}$$

where n is the number of points at which the spectral density is estimated.

The distribution function $F(x)$ is estimated using the formula

$$F_T(x)=\frac{T_x}{T_0}, \tag{6.74}$$

where T is the index that indicates that the characteristic of random process $x(t)$ is determined on the basis of the realization of finite duration T_0;

T_x is the value of random time during which the random process $x(t)\leqslant x$. Here the error depends on the time T_0 of observation of the process, the number of points x_k at which $F_T(x)$ are computed and on their position [1, 13]. The dispersion of this estimation is given by

$$\sigma_F^2=\frac{2}{T_0}\int_0^{T_0}\left(1-\frac{\tau}{T_0}\right)K(\tau)\,d\tau-F^2(x). \tag{6.75}$$

As can be seen, the dispersion is of the order of $\frac{1}{T}$ and depends on two-

dimensional distribution (of correlation function $K(\tau)$) and on the true distribution $F(x)$. It is possible to get rid of the last two only by approximation, i.e. by replacing the actual values of $K(\tau)$ and $F(x)$ by their estimates (6.47) and (6.74) respectively.

An integral series of distribution is compiled using the computer (discrete case). Here the observations of the random function quantities (sampling) are combined in groups and a computation is made as to how many times the values are met in each group. The length of the group is

$$\lambda=\frac{x_{max}-x_{min}}{k}, \tag{6.76}$$

where x_{max} and x_{min} are respectively the maximum and minimum terms of the series $\{x\ (i\Delta t)\}$ $(i=1, 2,..., N)$. The number k is usually taken equal to 12 where a deviation by two-three units in either direction from this number is permissible. This agrees with the determination of k using the formula

$$k=E\,[\log_2 N]+1. \tag{6.77}$$

The middle of the groups $x_j=x_{min}+(j-0.5)\,\lambda$ $(j=1, 2,..., k)$ corresponds to the number of the group $j=\frac{1}{\lambda}\left[x_j-(x_{min}-0.5\,\lambda)\right]$ and the number of "hits" in the group Δj $(j=1, 2,..., k)$ is equal to

$$m_j=\sum_{j=1}^{N}\mu_i, \tag{6.78}$$

where

$$\mu_i=\begin{cases}1, & x_i\in\Delta_j,\\ 0, & x_i\overline{\in}\,\Delta_j.\end{cases}$$

The frequency of hitting the group Δj

$$f_j=\frac{m_j}{N},\ j=1, 2,..., k. \tag{6.79}$$

The empirical distribution function, i.e. the estimate of the distribution function, takes the form:

$$F_l=\sum_{j=1}^{l}f_j,\ l=0, 1,..., \mathrm{k}. \tag{6.80}$$

If it is necessary to determine to which class the law of distribution of the process belongs it is more convenient to use the estimation of the distribution density.

The empirical distribution series (histogram) is the statistical analogy of

the unidimensional function of distribution density and the values $x_j (j = 1,..., k)$ taken to indicate groups and frequencies f_j correspond to them.

When representing the distribution series (histogram) the values of the group x_j, $j=1, 2,..., k$ are given on the horizontal axis and the frequencies f_j on the vertical. Here the scales are chosen so that the whole graph is situated inside the rectangle whose height h to length a ratio is approximately 5/8 (rule of "golden section" [26]).

In the statistical calculus there are a number of factors characterizing the degree of divergence (or agreement) between empirical series and true (hypothetical) distribution. The factors are random quantities and conclusions are based on their distribution with the use of any level of significance.

Using K. Pearson's [26] criterion for agreement (χ^2 test) for the measure of divergence or "fit" of the distribution series and hypothetical distribution, we take the quantity

$$\chi^2 = \sum_{j=1}^{k} \frac{N}{p_j} (m_j - Np_j)^2, \tag{6.81}$$

where m_j are the observed frequencies [see (6.78)];

N is the size of the sample;

p_j is the probability of the random number x (t) falling in the group computed for the hypothetical distribution.

The probability $P(\chi^2)$ is found from tables. We take α % level of significance as the boundary between random and actual values. The meaning of this is that, for example, for $P=0.05$ (5% level of significance) and on the assumption that the test hypothesis is true for the type of distribution, an appreciable difference can be expected approximately five times in 100 tests (the test conditions are not changed). If for the chosen α % level of significance

$$P(\chi^2) < \frac{\alpha}{100}, \tag{6.82}$$

then the criterion indicates insufficient agreement between the hypothesis and observation.

The normal distribution with function of probabilistic density

$$f(x) = \frac{1}{\sigma\sqrt{2\pi}} \exp\left\{-\frac{(x-m)^2}{2\sigma^2}\right\} \tag{6.83}$$

is often chosen instead of the hypothetical law of distribution. Here the mathematical expectation m and disperison σ^2 are estimated using the distribution series:

$$\overline{m} = \sum_{j=1}^{k} x_j f_j,$$

$$\bar{\sigma}^2 = \sum_{j=1}^{k} (x_j - \overline{m})^2 f_j, \tag{6.84}$$

where x_j is the point of the j-th group;

f_j is the frequency corresponding to the j-th group.

The reliable intervals of accurate values of m and σ^2 are the following:

$$\overline{m} - t_q \frac{\bar{\sigma}^2}{\sqrt{N}} < m < \overline{m} + t_q \frac{\bar{\sigma}^2}{\sqrt{N}},$$

$$\bar{\sigma}^2 - t_q \sqrt{\frac{\overline{m_4 - m_2^2}}{N}} < \sigma^2 < \bar{\sigma}^2 + t_q \sqrt{\frac{\overline{m_4 - m_2^2}}{N}}, \tag{6.85}$$

where

$$m_k = \frac{1}{N} \sum_{i=1}^{N} \Big(x(i\Delta t) - m \Big)^k,$$

and the quantity t_q for the chosen value of q (%) is determined by the formula

$$\frac{1}{2}\left(1 - \frac{q}{100}\right) = \frac{1}{2\pi} \int_0^{t_q} \exp\left\{-\frac{v^2}{2}\right\} dv. \tag{6.86}$$

Approximating by the Edgeworth series [38] the distribution series deviating from the normal distribution and confining ourselves to the first four terms forming a Shark A series, we get the distribution function:

$$F(x) = 0.5 + 0.5\Phi(x) - \frac{A_s}{6} f_2(x) + \frac{E_k}{24} f_3(x), \tag{6.87}$$

where $f_2(x)$ and $f_3(x)$ are the second-order and third-order derivatives of the normal probabilistic density $f(x)$ respectively;

Φ is the normal distribution;

$$A_s = \frac{m_3}{\sigma^3} \text{ is the estimate of asymmetry;} \tag{6.88}$$

$$E_k = \frac{m_4}{\sigma^4} - 3 \text{ is the estimate of the excess.} \tag{6.89}$$

The dispersion of estimates A_s and E_k is determined by the relations

$$\sigma_{A_s} = \sqrt{\frac{6(n-1)}{(n+1)(n+3)}}, \quad \sigma_{E_k} = \left\{\frac{24n(n-2)(n-3)}{(n+1)(n+3)(n+5)}\right\}^{\frac{1}{2}}. \tag{6.90}$$

To verify the hypotheses the quantities $\Phi(x), f_1(x), f_2(x)$ are taken from the tables (see, for example, [26]).

6.2.1 Special Correlation Characteristics of Rolling-Contact Bearing Parameters and the Dependence of Friction Torque on Different Operating Conditions

A large number of experimental results were analyzed using the methodology described.

The bearing and bearing assemblies under study should be initially operated and checked before carrying out experimental research in order to eliminate additional sources of errors that might distort the actual characteristics of the bearings and to reject very unsuitable bearings.

One preliminary treatment is complete elimination of sticky deposits, products of oxidation and dirt from the surface of the rolling elements in the bearings, using Benzene B-70. During preliminary cleaning the rings are slowly rotated in opposite directions, subjecting them simultaneously to a compressed air blast.

The final cleaning immediately follows the first, using Benzene B-70 again, until all the deposits which separated from the surface of the bearing components during the first cleaning are removed.

The ease of rotation should be the criterion of satisfactory functioning of bearings and assemblies.

Jamming, i.e. relatively free rotation except at certain points where force is needed to rotate the ring indicates abnormal condition of the raceways of the rings and rolling elements. This can be caused by the presence of any local deposits of the products of lubricant decomposition, sticking of particles or creation of mechanical defects in the form of bumps or displacement of material on the working surfaces of rings and rolling elements. Another cleaning is necessary.

If after cleaning with dehydrated kerosene and Benzene B-70 the bearing or assembly still jams it is rejected.

Preliminary rejection is also done when checking bearings and assemblies for noise. Loud noise in a bearing can occur as a result of: increased inner clearances in the bearings, large nonuniformity in the sizes of rolling elements and dirt on the working surfaces of rings and rolling elements. Since the noise check is of a subjective nature any final judgment on noise should be passed when the bearing or assembly is well lubricated.

Characteristics of bearings like friction torques, vibrations of bearing rings with respect to one another and their interrelation and the interrelation of these parameters with the geometric parameters of the bearings are of great interest.

Dynamic characteristics can be observed using different instruments. The characteristics described here were observed principally with the help of strain gauges with inductance transducers.

Before starting the checks it is necessary to rotate the washed bearing in

both directions (not less than 10 revolutions) until there is complete lubrication of all interacting parts.

Bearings of different classes, precision and typical sizes were used for the study of stationary friction torque. As an example, the basic results are given below for tests on bearings of types C1000096 and A840154. These can be taken as a basis when determining the causes of the principal errors. In each series one bearing was taken with comparatively large variable friction torque and another with small variable friction torque. The division of bearings into

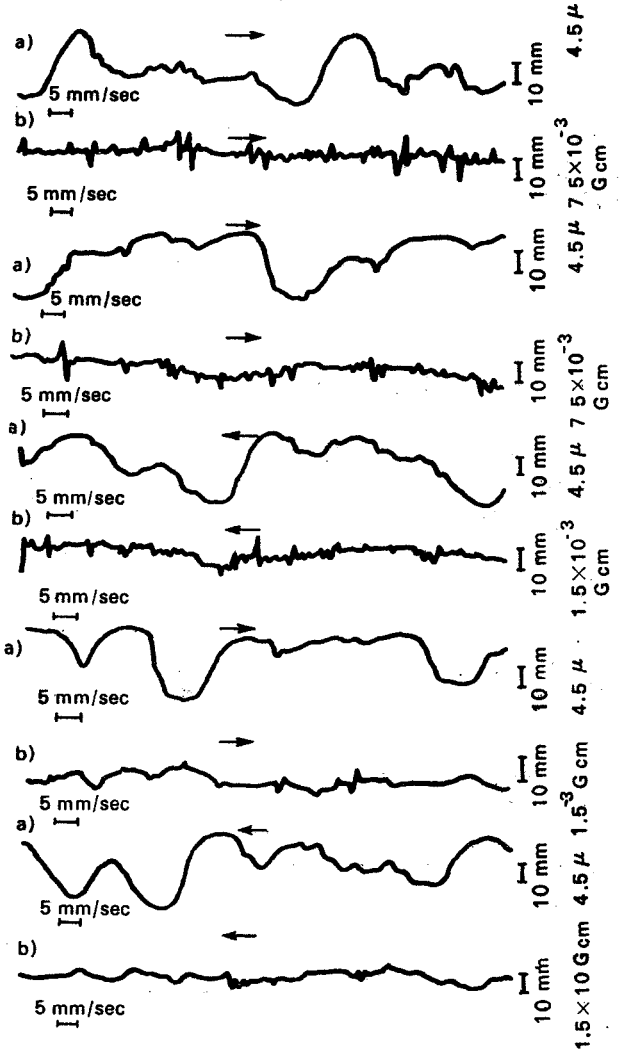

Fig. 6.6. Curves of vibrations in axial direction (*a*) and variable component of friction torque; (*b*) in washed bearing of A840154 type.

"bad" and "good" was done by comparing the amplitudes characterizing the value of friction torque and by the change in the amplitude with time.

Ten series of measurements with a length of realization of not less than 20 revolutions (Fig. 6.6) were carried out. The constant component of friction torque was brought out for one revolution, two revolutions, etc.

From these values the relative variation of mean values of friction torque depending on the number of revolutions was obtained, using the expression

$$\delta = \frac{\overline{M}_{max} - \overline{M}_{av}}{M_{av}} \cdot 100, \tag{6.91}$$

where M_{max}, M_{av} are respectively the maximum and average values of friction torque, %. The curve relating the constant components of friction torque and the number of revolutions is drawn (Fig. 6.7) using the values obtained for the variation in torques.

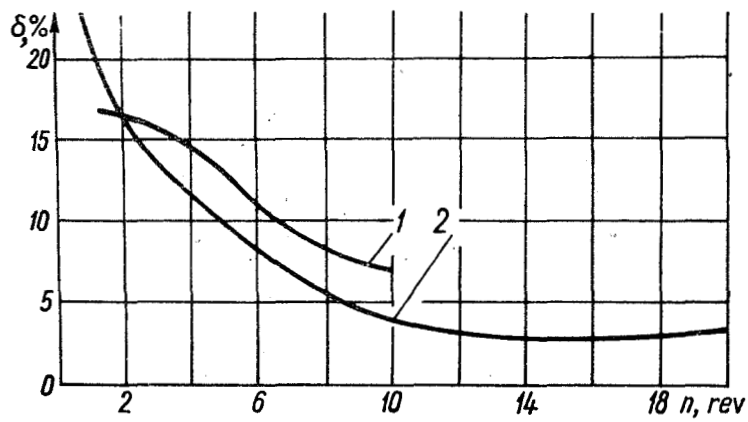

Fig. 6.7. Relation between shift in constant component of friction torque and number of revolutions in case of (*1*) "good" and (*2*) "bad" bearings.

It is necessary to know the distribution of bearings based on the constant friction torque component M_{cc} for statistical control of the quality of bearings.

In order to determine the nature of distribution a tested set of bearings is taken, on the basis of which it is possible to characterize the whole group. Two sets of precision bearings of the types 2C45 and A840154 with 50 pieces in each were taken as standard.

The bearings were treated to obtain statistical characteristics and to plot the histogram of the direct and reverse movement of the constant (Fig. 6.8) and variable (Fig. 6.9) components of friction torque.

The curves of correlation functions in Fig. 6.10 show the dependence of the process on the working conditions. In the majority of cases the correlation functions have an oscillating nature which can be caused by the presence

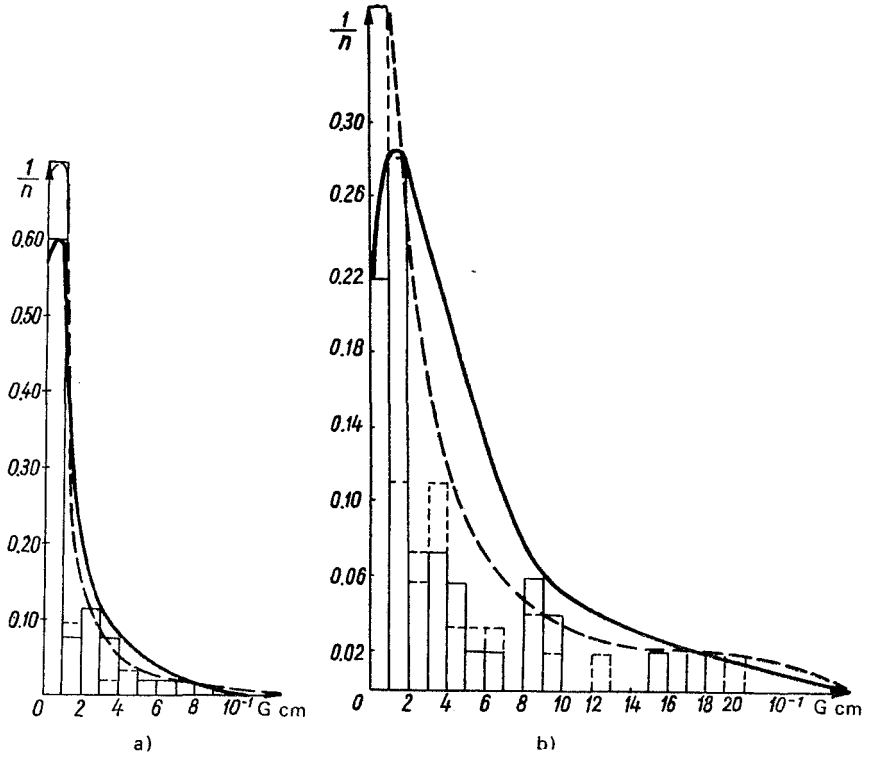

Fig. 6.8. Histograms and functions of distribution of constant component of friction torque in bearings of (*a*) A840154 and (*b*) 2C45 type with rotation in clockwise direction (broken) and anticlockwise direction (solid lines).

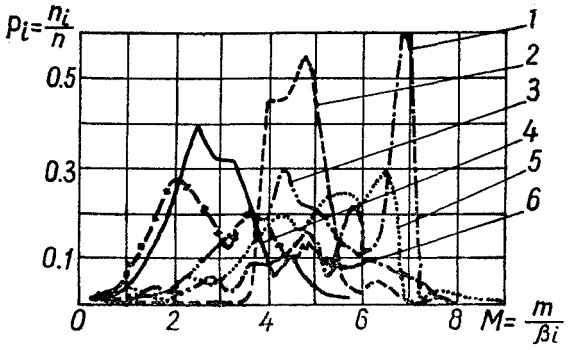

Fig. 6.9. Distribution of VFT under following conditions: *1*—bearing lubricated, magnetized (3.5μV); *2*—bearing dry, not magnetized; *3*—bearing dry, magnetized (5μV); *4*—bearing lubricated, not magnetized (3.5μV); *5*—bearing lubricated, magnetized (4μV).

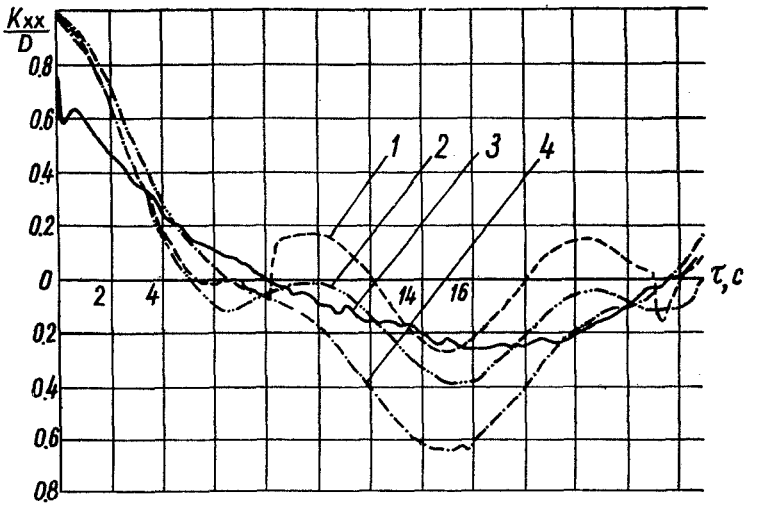

Fig. 6.10. Correlation functions of (*1*, *2*)—VFT; (*3*, *4*)—vibration of rings of bearing of A840154 type with radial load R=0, axial—A=0.1 kg, n=2 rpm; (*1*, *3*—bearing dry; *2*, *4*—bearing lubricated with three drops of lubricant).

of clearly indicated vibrations of a certain frequency and with an additive noise. The presence of noise indicates a rapid damping of the correlation function in the region of small values when compared to damping in the region of other values of τ. Here the oscillating nature of correlation functions is such that the following conclusion can be drawn: in processes with high frequencies the noise level is higher than in processes with an abundance of low frequencies.

Test results show that the friction torque and spatial vibrations of rolling contact bearings in general are stationary random functions of an ergodic nature. Depending on the shape of the bearing, the characteristics of bearings contain periodic components. The curves of spectral densities confirm this (Fig. 6.11).

Analysis of the frequency composition of the process obtained in tests on a set of small-sized A840154 bearings justifies certain conclusions on the behavior of variable friction torque in bearings with an inner diameter φ_{in}= 0.6–3 mm and a speed of 2 rpm.

1) The fundamental harmonic of frequencies is a multiple of the number of revolutions of the outer ring of the bearing (when the inner ring is stationary);

2) The second harmonic of frequencies is a multiple of the number of revolutions of the cage, and the frequency level very much depends on the lubrication, installation of the bearing and defects in the geometric shape;

3) The number of revolutions of the cage depends on the axial loading

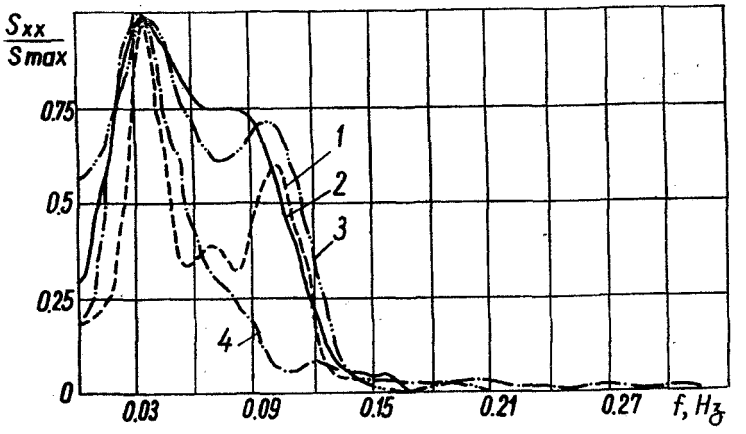

Fig. 6.11. Typical spectral densities of friction torque in (*1*, *2*)—unlubricated; (*3*, *4*)—lubricated bearing, rotating (*1*, *3*)—clockwise and (*2*, *4*)—anticlockwise.

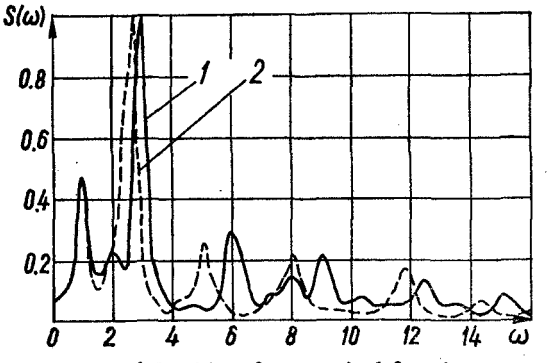

Fig. 6.12. Spectral densities of geometric defects in raceways of (*1*) inner and (*2*) outer rings of bearing of C 1000096 type.

and the number of revolutions of the moving ring of the bearing (especially at low speeds);

4) The level of other harmonics is negligible.

A comparison of the spectral densities of individual representations of the working of bearings is of interest.

Spectral densities are given (Fig. 6.12) for the geometric defects in the raceways of balls along the inner (solid) and outer (broken lines) rings of a 1000096 bearing. The number 1 indicates a frequency corresponding to the complete circumference of the ring. As can be seen from the curves, in this case on both inner and outer rings a frequency corresponding to a roughness with a period of one-third of the circumference abounds.

It is interesting that this affects the spectral densities of vibrations of variable friction torques of the same bearing, i.e. in the spectral densities a fre-

quency triple that of the frequency of rotor rotation is clearly indicated. In cases where analysis of geometric errors indicates the presence of ovality, in the corresponding densities of the variable friction torques a frequency double that of the frequency of rotor rotation predominates. This is explained by the effect of ovality and sharp corners on the factors of rotation (variable friction torque, vibration between rings).

The above is illustrated in Fig. 6.13, where the fundamental maximum corresponds to the rotor revolutions, the second and third to the number of balls (in this bearing there were eight) and rotor revolutions and the last to the number of balls and revolutions of the cage, i.e. they are combined frequencies. It may be mentioned that the number of rotations of the cage in the case where the inner ring was stationary was computed by the formula [29]:

$$n_c = -0.5\, n\,(1 + \frac{D_b}{d_b}\cos\alpha), \tag{6.92}$$

where n_c is the turning speed of the cage;
n is the rotational speed of the inner ring;
D_b is the diameter of the rolling element, mm;
α is the contact angle;
d_b is the mean diameter of the bearing.

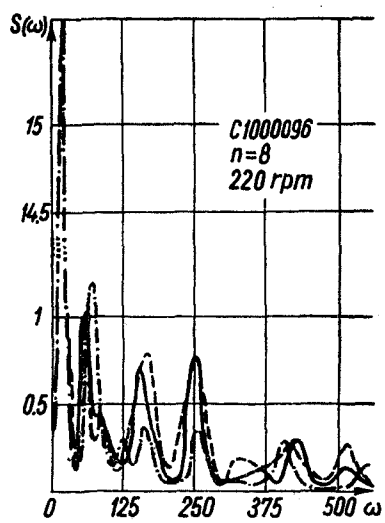

Fig. 6.13. Spectral densities of VFT in bearing C1000096 type with eight balls, speed 220 rpm.

A similar analysis can be carried out for spectra of the same bearings for rotation with a frequency of 1,000 rpm and with other loads. The same picture is observed in cases of the spectra of C201 and C26 bearings.

Spectral densities of variable friction torque of a bearing of the A840154 type are shown in Fig. 6.14 for rotation with a frequency of 2 rpm and different operating conditions. From a comparison of the maximum values of spectral densities shown in this Figure it may be seen that the dispersion of friction torque of a dry bearing is more than that of a lubricated one. This is explained by the influence of geometric defects in the manufacture of raceways on friction torque when there is no lubricating film.

Spectral densities of vibrations of rings of two A840154 bearings with respect to one another in the axial direction are shown in Fig. 6.15 (the inner ring rotated in the clockwise direction at 2 rpm). Comparison of their maximum values indicates the effect of lubrication on the reduction of vibrations.

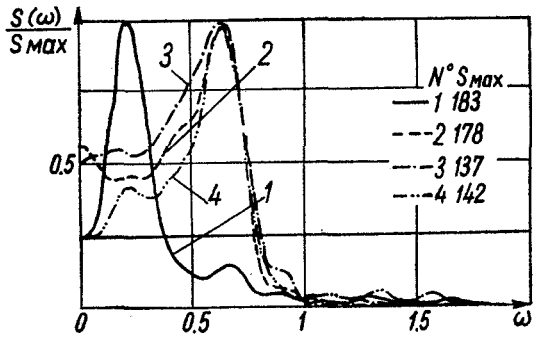

Fig. 6.14. Spectral densities of VFT in (*1*, *2*) lubricated and (*3*, *4*) dry bearings of A840154 type rotating at 2 rpm in (*2*, *4*)—clockwise and (*1*, *3*)—anticlockwise directions.

It may be mentioned that the presence of frequencies double and triple the frequency of rotation $\omega \approx 0.21$ rad/sec (curves 2 and 3) is explained by the action of geometric defects. Profilographs of the raceways of this bearing had roughness of wavelengths of one-half and one-third of the circumference.

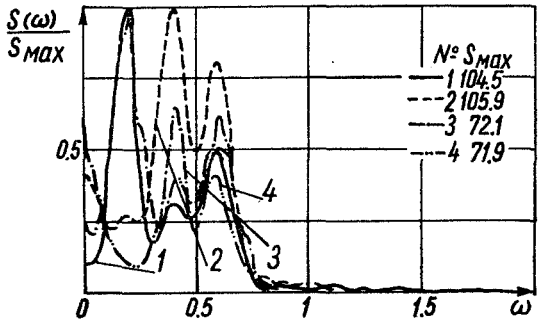

Fig. 6.15. Spectral densities of vibration of rings in bearings of A840154 type rotating at 2 rpm: (*1*, *2*)—dry bearing; (*3*, *4*)—lubricated bearing.

An example of spectral density of amplitudes of change in the lubricating film of a C201 bearing when the frequency of rotation was 300 rpm is shown in Fig. 6.16. In this and other cases the fundamental frequency in the spectrum corresponds to the frequency of rotation. High frequencies were not observed.

For a convenient representation in one scale and for comparison with normal distribution of the function of densities the distributions were normalized, i.e. the amplitudes of the processes were transformed into new ones:

$$x^* = \frac{x-m}{\sigma}, \tag{6.93}$$

having zero mean value and unit dispersion.

Examples of functions of distribution density of the amplitudes of variable friction torque in bearings are shown in Fig. 6.17 a and b. The working conditions are given in the Table.

TABLE 6.1

Fig.	No.	n	R	A	A_s	E_k
	1	400	1	0.4	−0.335	0.56
a	2	220	1	0	−0.175	−0.5
	3	220	4	0	−0.107	−0.4
	1	220	1	0	0.12	−0.2
b	2	220	4	0	−0.09	−0.04
	3	1000	1	1	0.05	0.01

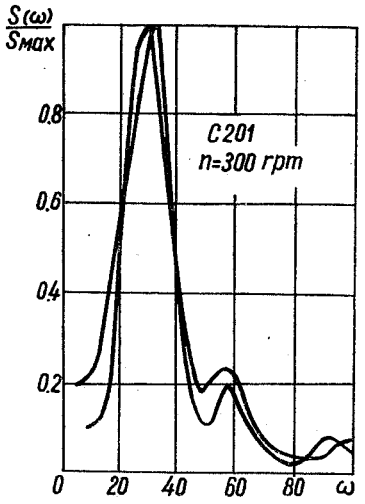

Fig. 6.16. Spectral densities of variation in oil film in bearings of C201 type rotating at 300 rpm.

where n is the speed of rotation (rpm); R and A are the radial and axial loads respectively, kg; A_s is the coefficient of asymmetry; E_k is the coefficient of excess. It has been established that the latter in general decreases with an increase in radial load. The coefficient of asymmetry, on the contrary, increases with an increase in load, as can be seen from the graphs. With an increase in the number of revolutions the deviations from the normal law appreciably increase in the majority of cases. Only in certain cases do they satisfy the conditions of normality according to the criterion χ^2 at 5% significance level. The approximation of these laws of distribution

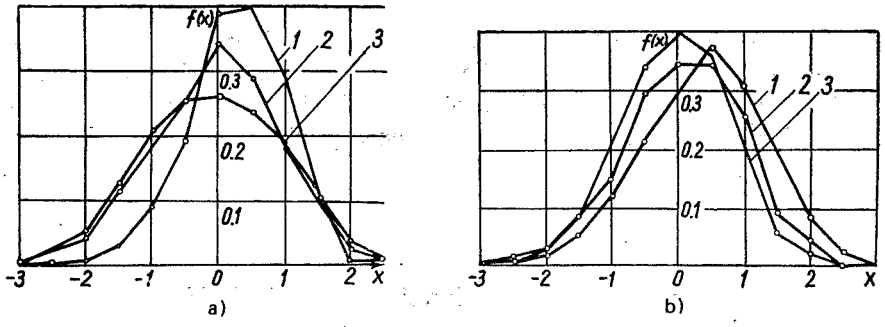

Fig. 6.17. Distribution density of friction torque in bearings of (*a*) C1000096 and (*b*) C201 type: n—rpm; A—axial load; R—radial load (kg); A_s—coefficient of asymmetry; E_k—coefficient of excess.

by the first terms of the Edgeworth series is a good approximation in the sense of the above criterion.

For functions of the distribution density of amplitudes of variable friction torque in an A840154 bearing at a frequency of rotation of the inner ring of 2 rpm the hypothesis on normal distribution was confirmed in all cases (criterion of agreement χ^2, significance level 5%).

Functions of distribution of amplitudes of change in the lubricating film also show approximately normal distribution.

The analysis carried out for a large number of estimations of functions of distribution density of real processes observed at the time of operation of bearings leads us to conclude that for their probable reproduction on simulating units, in the majority of cases it is possible to replace them by processes with normal distribution.

The estimates of probabilistic densities of geometric defects in bearings of the same class are shown in Fig. 6.18. For comparison, the curve of normal distribution N (0.1) (solid line) is also shown. K. Pearson's criterion (χ^2 test) with 1% significance level indicates the correctness of the hypothesis on the normality of distribution.

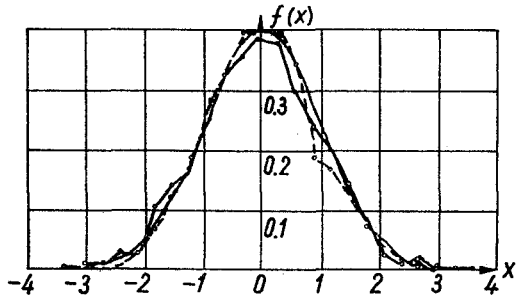

Fig. 6.18. Distribution densities of geometric defects in manufacture of raceways of bearings of C1000096 type solid line—normal distribution (nil).

It may be mentioned that in the analysis of realizations recorded at different intervals of time in succession (i.e. after every 5 and 10 min from the beginning of operation) no appreciable difference in the spectra and densities of distribution was observed. This to some degree justifies the hypothetical assumption that the processes are stationary.

6.3 DETERMINATION OF RELATIONS BETWEEN BEARING PARAMETERS

As we mentioned, one source of vibration and variable friction torque in ball bearings is defects in manufacture and assembly. Incomplete balancing of moving elements, nonuniform loading and working of the motor in the operating conditions and their interaction and other factors contribute to such

defects. The factors affecting variable friction torque and vibration will be considered within the framework of the correlation theory of random functions. Here a schematic representation of a bearing as a mechanical system with a given approximation is shown in the form of a linear object with n inputs and m outputs (Fig. 6.19). In the analysis of such a system the well-known formulation of the problem of identification can be used when the optimum estimate of the system operator in the class of linear operators is found on the basis of the reactions of inputs and outputs (for example, on the basis of the criterion of the minimum of mean square deviation).

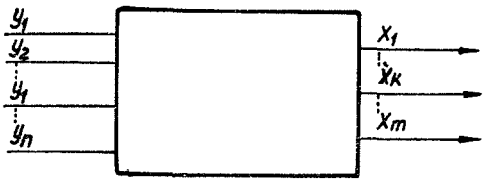

Fig. 6.19. Bearing in form of 2 $(n+m)$ poles.

The correlation method of determining the dynamic characteristics of a unidimensional system leads to the solution of the integral equation:

$$K_{yx}(\tau)=\int_{-\infty}^{\infty} K_{xx}(\lambda-\tau)\,\omega(\tau)\,d\lambda,\ \omega(\tau)=0,\ \tau<0 \tag{6.94}$$

with respect to the impulse characteristic $\omega(\tau)$. This is sought for the given correlation function $K_{xx}(\tau)$ of the signal x observed at the input and the cross-correlated function $K_{yx}(\tau)$ between signals at the input x and output y. In the discrete case

$$K_{yx}(k\Delta t)=\frac{1}{N-k}\sum_{i=1}^{N-k} y^0(i\Delta t)\,x^0[(i+k)\,\Delta t],$$

$$k=0,\ \pm 1,\ \ldots,\ \pm M,\ M\approx\frac{N}{10},$$

$$y^0(i\Delta t)=y(t)\,|_{t=i\Delta t}-m_y,$$

$$m_y=\frac{1}{N}\sum_{i=1}^{N} y(i\Delta t). \tag{6.95}$$

If the input process observed at the instant $t=t_0$ remains stationary it is more convenient to use not the instantaneous but the spectral method of analysis. Then, from the equation

$$S_{yx}(j\omega)=W(j\omega)\,S_{xx}(\omega), \tag{6.96}$$

where $S_{xx}(\omega)$ is the spectral density of the input signal;

$S_{yx}(j\omega)$ is the cross-correlation density between output and input signals,

we find the required amplitude-phase characteristic (transfer function) $W(j\omega)$ of the system. It may be mentioned that the real part of the function Re $S_{yx}(j\omega)$ is determined from equation (6.68), replacing the quantities $K_N(k\Delta t)$ by $K_{yx}(k\Delta t)+K_{yx}(-k\Delta t)$, and the imaginary part from the formula

$$\operatorname{Im} S_{yx}(j\omega)=\frac{1}{\pi}\left[\frac{1}{2}K_{yx}(0)+\sum_{k=1}^{M}\left(1-\frac{k}{N}\right)[K_{yx}(k\Delta t) - K_{yx}(-k\Delta t)]\left\{0.54+0.46\cos\frac{\pi k}{M}\right\}\sin\omega k\right]. \tag{6.97}$$

When computing the estimation for large values of ω formula (6.71) is used both for the real part and for the imaginary part and in the latter case cos ωt is replaced by sin ωt.

Logarithmic amplitude $A(\omega)$ and phase $\varphi(\omega)$ frequency characteristics are determined from the expressions

$$A(\omega)=20\log|W(j\omega)|=20\log\frac{|S_{yx}(j\omega)|}{S_{xx}(\omega)},$$

$$\varphi(\omega)=\tan^{-1}\frac{\operatorname{Im} S_{yx}(j\omega)}{\operatorname{Re} S_{yx}(j\omega)}+\pi\left[1-\frac{1}{2}\operatorname{sign}\operatorname{Im} S_{yx}(j\omega)\left\{1+\operatorname{sign}\operatorname{Re} S_{yx}(j\omega)\right\}\right]. \tag{6.98}$$

Here

$$|S_{yx}(j\omega)|=\sqrt{[\operatorname{Re} S_{yx}(j\omega)]^2+[\operatorname{Im} S_{yx}(j\omega)]^2},$$

and Im $S_{yx}(j\omega)$ and Re $S_{yx}(j\omega)$ are respectively the imaginary and real parts of the cross-correlation density $S_{yx}(j\omega)$. It is convenient to use logarithmic characteristics because they are easily approximated by segments of straight lines—asymptotes which greatly simplify construction. The inclination of these asymptotes is expressed in decibels per decade, i.e. for an interval of frequencies separated from each other by the order of 10.

Determining the logarithmic frequency characteristics using numerical methods gives us only a graphical representation of $A(\omega)$ and $\varphi(\omega)$. Here the approximation of the function $A(\omega)$ by asymptotes should be carried out by graphical-analytical means, giving the possible deviations from the theoretical of random peaks of empirical amplitude-phase characteristics. Usually a deviation up to 6 db is permitted.

From the graph for $A(\omega)$ we chose the segments where the forms of characteristics are nearly straight with inclinations of 20 k db/dec ($k=0,\pm1,\ldots$). In the same way the conjugate frequencies (ends of the chosen segments) ω_i ($i=1, 2, \ldots, M$) are determined with the condition that the number of segments should equal M.

The coefficient k of inclination of the straight line in the segment (ω_{i-1}, ω_i) is indicated by k_i, where ω_0 is the frequency at the origin.

Using one decade as the unit in the frequency axis and a decibel in the vertical axis we get angular coefficients of straight lines:

$$m_i=\frac{k_i}{20}, \qquad i=1, 2, \ldots, M. \tag{6.99}$$

Segments n_i $(i=1, \ldots, M)$ intersected by asymptotes with the vertical axis are determined by the method of least squares [23], i.e. from the condition of the minimum of the sum of squares of deviations

$$\varepsilon_j=A(\omega_j)-A^*(\omega_j). \tag{6.100}$$

Here $A^*(\omega_j)$ is found from the asymptotic equation that approximates the function $A(\omega_j)$. In Cartesian coordinates (with units of one decade along the frequency axis and one decibel along the ordinate) these equations take the form

$$A_i^*(\omega)=\frac{k_i}{20}[\log \omega_j-\log \omega_0]+n_i, \quad i=1, 2, \ldots, M, \tag{6.101}$$

if, during the shift from the logarithmic scale to the linear, the origin of coordinates does not move to the point $\omega=1$.

Using the method of least squares we find

$$n_i=\frac{1}{N_i}\sum\left[A_i(\omega_j)-\frac{k_i}{20}(\log \omega_i-\log \omega_0)\right], \tag{6.102}$$

where the summation is for all points of ω_j from the interval (ω_{i-1}, ω_i) in which the quantities $A(\omega)$ were computed by formula (6.98) in the numerical determination of $A(\omega)$ (N_i is the number of additives in the summation).

The straight lines described by the relations (6.101) and (6.102) and the corresponding neighboring intervals do not as a rule intersect at the points of conjugate frequencies chosen when separating these intervals. It is worth taking the points of intersection of straight lines as corrected conjugate frequencies ω_i $(i=1, 2, \ldots, M)$ and estimating new values n_i $(i=1, 2, \ldots, M)$ according to formula (6.102). The operation is repeated until we obtain conjugate frequencies ω_i that differ from the ones obtained in the previous stage by not more than the value $\Delta\omega/2$, where $\Delta\omega$ is a "discretization" interval in the numerical determination of $A(\omega)$.

After this the time constants are computed

$$T_i=\frac{1}{\omega_i}, \qquad i=1, 2, \ldots, M \tag{6.103}$$

and the analytical expression for $W(j\omega)$ is written. If $k_i-k_{i-1}=l>0$ (positive integer), which corresponds to the change in inclination of the straight line by $+20\,l$ db/dec, then we multiply the expression for $W(j\omega)$ by $(1+j\omega T_i)^e$ corresponding to the series connection l of the differentiating links with the time constant T_i.

If $k_i - k_{i-1} = m < 0$ ($-$ve integer), then the expression for $W(j\omega)$ is multiplied by $1/(1+j\omega T_i)^m$, corresponding to the series connection m of inertial links, or (if $|m|>1$) by two multiples:

$$1/(1+j\omega T_i)^{m-2p} \text{ and } 1\Big/\left[(j\omega)^2+2\xi_i\frac{1}{T_i}j\omega+\frac{1}{T_i^2}\right]^p,$$

from which the latter corresponds to the series connection p of the oscillating links. The presence of the oscillating link is established by comparing the correction curves (for example, [21]) of asymptotic characteristics with the deviation of $A(\omega)$ determined by numerical methods from the approximating zigzag line for $A^*(\omega)$. Using the same correction curves the damping coefficient ξ_i and "order" p are determined. If $k_0 \neq 0$, then we multiply by $\frac{1}{(j\omega)^{k_0}}$ corresponding to the series connection k_0 of integrating links. The gain k is computed from the condition of equality of ordinate (when $\omega=1$) 20 log$k$. Finally we get

$$W(j\omega)=\frac{k\prod_{s=1}^{t}(1+j\omega T_s)^{l_s}}{(j\omega)^{k_0}\prod_{i=1}^{n}(1+j\omega T_i)^{m_i-2p_i}\prod_{q=1}^{r}\left[(j\omega)^2+2\xi_q\frac{1}{T_q}j\omega+\frac{1}{T_q^2}\right]^{p_q}}. \quad (6.104)$$

Since the argument $\varphi(\omega)$ is equal to the algebraic sum of arguments of the products the phase characteristic of the system with a transfer function $W(j\omega)$ (6.104) takes the form

$$\varphi(\omega)=k_0\frac{\pi}{2}-\sum_{i=1}^{n}(m_i-2p_i)\tan^{-1}\omega T_i+\sum_{s=1}^{t}l_s\tan^{-1}(1+j\omega T_s)$$
$$-\sum_{q=1}^{r}p_q\tan^{-1}\frac{2\xi_q\frac{1}{T_q}\omega}{\frac{1}{T_q^2}-\omega^2}. \quad (6.105)$$

During the experiment measurements were made on type 26, 201 and 1000096 sets of bearings (25 each) of precision class C and sets (50 each) of A840154 bearings. When determining the analytical expressions of transfer functions corresponding to the logarithmic characteristics the latter were averaged with respect to the number of estimates.

Logarithmic amplitude frequency characteristics of the dependence of friction torque on the vibration of rings with respect to one another in the axial direction for a lubricated bearing of class A of type 840154 with rightly fixed inner ring and rotation of the outer ring at 2 rpm, estimated with the above methodology using the Razdan-3 computer, are shown in Fig. 6.20 (curve

1). The zigzag line *2* in the Figure corresponds to the approximating function constructed by graphic-analytical means. The transfer function

$$W(j\omega)=\frac{0.297\,(1+1.45\,j\omega)^2}{(1+2.37\,j\omega)^2}. \tag{6.106}$$

corresponds to it.

Analogous curves are shown in Fig. 6.21 for the same bearing, cleaned. In this case

$$W(j\omega)=\frac{0.492\,(1+1.51\,j\omega)^2}{(1+0.38\,j\omega)\,(1+0.446\,j\omega)}. \tag{6.107}$$

Comparing the expressions (6.106) and (6.107) we notice that the dependence of variable friction torque on the vibration of rings in the axial direction is more complex in the case of a cleaned bearing. The parameters are commensurate in the two cases for low frequencies, as we mentioned during the analysis of spectral densities.

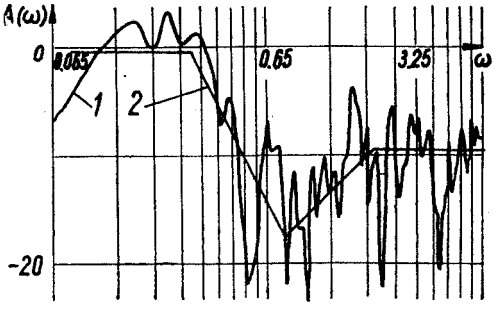

Fig. 6.20. Logarithmic amplitude characteristic (*1*) and its approximate asymptotic characteristic (*2*) of dependence of friction torque on vibration of rings of lubricated bearing A840154 (speed =2 rpm).

It is possible to come to similar conclusions even in the case of the dependence of variable friction torque on the vibration of rings in the axial direction when the inner ring rotates in an anticlockwise direction.

The transfer function

$$W(j\omega)=\frac{0.3548\,(1+0.0108\,j\omega)\,(1+0.0047\,j\omega)^2}{(1+0.0369\,j\omega)\,(1+0.0123\,j\omega)\,(1+0.0024\,j\omega)} \tag{6.108}$$

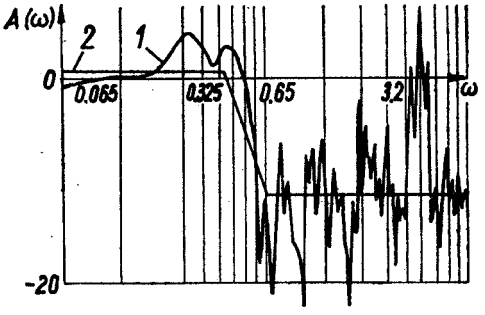

Fig. 6.21. Same as Fig. 6.20 for a dry bearing.

corresponds to the approximating logarithmic amplitude characteristic of the dependence of variable friction torque on the thickness of the lubricating film (Fig. 6.22, curve *3*).

In this case appreciable dependence is noticeable only in the range of low frequencies (of the order of the frequency of rotation). This can be explained

by the effect of the lubricant on the reduction of high frequencies.

The dependence of variable friction torque and vibrations between rings in the axial direction on manufacturing defects in the grooves of rings is determined by the transfer function of the corresponding system.

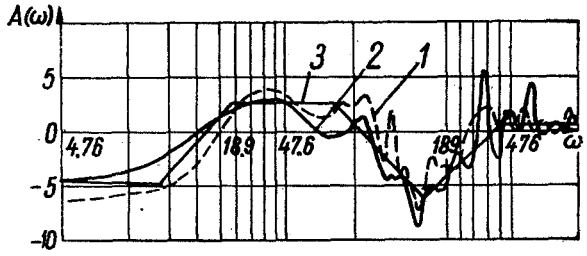

Fig. 6.22. (*1*, *2*)—Logarithmic amplitude characteristics of dependence of VFT on change in oil film thickness in bearing of C1000096 type rotating at 220 rpm; curve (*3*)—approximate logarithmic characteristic.

On further analysis, defects in the manufacture of the ring (ball) correspond to the magnitude of deviations from the mean radius of the circle diagram, determined by formula (6.31).

The turning speed of the cage is represented by ω_c, the speed of rotation of the rotor by ω_r, and

$$R(k)=R(k\Delta\varphi),\quad \Delta\varphi=\frac{2\pi}{N},\quad k=1, 2, \ldots, E\left[\frac{T\omega_c}{\Delta_\varphi}\right]+1 \qquad (6.109)$$

are the values of the function of defects in manufacture of the outer ring, measured at points $k\Delta\varphi$ (read in the anticlockwise direction). T is the observation time of the random function of the variable friction torque, vibrations and change in lubricating film. Correspondingly (for the inner ring)

$$r(l)=r(l\Delta\psi),\quad \Delta\psi=\frac{2\pi}{M},\quad l=1, 2, \ldots, E\left[\frac{T(\omega_p-\omega_c)}{\Delta\psi}\right]+1. \qquad (6.110)$$

This corresponds to a certain quantization by time of the functions of manufacturing defects. The quantization interval depends on the speed of rotation of the bearing and in general does not coincide with the interval for quantization of the signal of variable friction torque. Comparison of these intervals is carried out by the following procedure:

OA (Fig. 6.23) is taken as the reference radius and *OB* as the moving radius, rotating with the rotor. Manufacturing defects at the contact points of balls with rings at any instant t are

$$x_j(t)=R(\varphi_{jt})-r(\psi_{jt}),\qquad j=1, 2, \ldots, n, \qquad (6.111)$$

where n is the number of balls:

$$\varphi_{jt}=\varphi(t)+\frac{2\pi}{n}(j-1), \quad \psi_{jt}=\psi(t)+\frac{2\pi}{n}(j-1), \; j=1, 2, \ldots, n \qquad (6.112)$$

are the angles between radii at the contact points of balls and reference radius and moving radius respectively.

The value of the input signal at an instant t is determined as a sum of errors:

$$x(t)=\sum_{j=1}^{n} x_j. \qquad (6.113)$$

In order to determine the values of total error (4.106) at any instant of time $i\Delta t$ linear interpolation is used.

After a time $i\Delta t$ we get

$$\varphi(t)=\omega_c\, i\Delta t,$$
$$\varphi(t)=(\omega_r-\omega_c)\, i\Delta t \qquad (6.114)$$

if the inner ring rotates in the clockwise direction and the outer ring is fixed. Using these values the values of φ_{ji} and ψ_{ji} are determined at the same instant of time $i\Delta t$. When the quantities φ_{ji} and ψ_{ji} do not agree with any of $k\Delta\varphi$, $k=1, 2, \ldots, E\left[\frac{\omega_c T}{\Delta\varphi}\right]$ and $l\Delta\psi$, $l=1, 2, \ldots, E\left[\frac{T(\omega_r-\omega_c)}{\Delta\psi}\right]+1$ respectively, the quantities $r(\psi_{ji})$ and $R(\varphi_{ji})$ for the moment of time $i\Delta t$ are computed using linear interpolation:

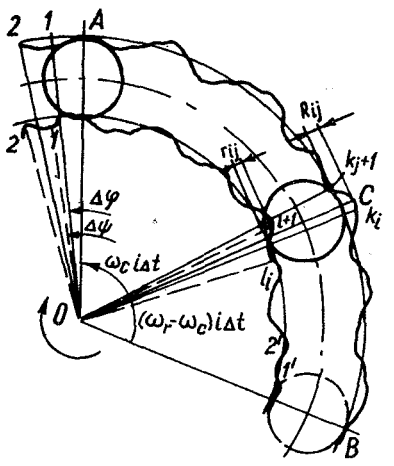

Fig. 6.23. Effect of geometric defects in manufacture of raceways.

$$R(\varphi_{ji})=R(E[k_{ji}])+\left[R(E[k_{ji}]+1)-R(E[k_{ji}])\right]\cdot E\{k_{ji}\},$$
$$r(\psi_{ji})=r(E[l_{ji}])+\left[r(E[l_{ji}]+1)-r(E[l_{ji}])\right]\cdot E\{l_{ji}\}. \qquad (6.115)$$

Here $E[\cdot]$ is the integer part of the number and
$E\{\cdot\}$ is the fractional part;

$$k_{ji}=N(p_j-1)+\left\{2\pi p_j-\omega_c\, i\Delta t-\frac{2\pi}{n}(j-1)\right\}\frac{1}{\Delta\varphi}=E[k_{ji}]+E\{k_{ji}\};$$
$$p_j=\min_{p_j=1, 2, \ldots}\left\{p_j: 2\pi j-\omega_c\, i\Delta t-\frac{2\pi}{n}(j-1)>0\right\};$$
$$l_{ji}=\left[(\omega_r-\omega_c)\, i\Delta t+\frac{2\pi}{n}(j-1)\right]\frac{1}{\Delta\psi}=E[l_{ji}]+E\{l_{ji}\}. \qquad (6.116)$$

In the case of rotation of the inner ring in the anticlockwise direction (6.114) we determine the angles measured in the direction opposite to the

turning of the circle diagram, replacing it by a series of values of deviations from the mean radius. Hence the quantities k_{ji} and l_{ji} (6.115) determined from equation (6.116) are replaced by quantities k^*_{ji} and l^*_{ji} respectively:

$$k^*_{ji}=\left[\omega_c\, i\Delta t+\frac{2\pi}{n}(j-1)\right]\frac{1}{\Delta\varphi}=E[k^*_{ji}]+E\{k^*_{ji}\},$$

$$l^*_{ji}=M(q_j-1)+\left\{2\pi q_j-(\omega_r-\omega_c)\, i\Delta t-\frac{2\pi}{n}(j-1)\right\}\frac{1}{\Delta\psi}=E[l^*_{ji}]+E\{l^*_{ji}\},$$

$$q_j=\min_{q_j=1,2,\ldots}\left\{g_j: 2\pi q_j-(\omega_r-\omega_c)\, i\Delta t-\frac{2\pi}{n}(j-1)>0\right\}. \qquad (6.117)$$

Similarly we get formulas for $x(i\Delta t)=x(t)\mid_{t-i\Delta t}$ when the inner ring is rigidly fixed and the outer ring rotates at a constant angular speed ω_{ot}.

It is necessary to have the following values:

$$R(k)=R(k\Delta\varphi),\quad \Delta\varphi=\frac{2\pi}{N},\quad k=1,2,\ldots,E\left[\frac{T(\omega_{ot}-\omega_c)}{\Delta\varphi}\right]+1,$$

$$r(l)=r(l\Delta\psi),\ \Delta\psi=\frac{2\pi}{M},\quad l=1,2,\ldots,E\left[\frac{T\omega_c}{\Delta\psi}\right]+1. \qquad (6.118)$$

At the instant of time $i\Delta t$ we have

$$\varphi(t)=(\omega_{ot}-\omega_c)\, i\Delta t,$$
$$\psi(t)=\omega_c\, i\Delta t, \qquad (6.119)$$

and instead of equations (6.116)—

$$k_{ji}=\left[(\omega_{ot}-\omega_c)\, i\Delta t+\frac{2\pi}{n}(j-1)\right]\frac{1}{\Delta\varphi}=E[k_{ji}]+E\{k_{ji}\},$$

$$l_{ji}=M(q_j-1)+\left[2\pi q_j-\omega_c\, i\Delta t-\frac{2\pi}{n}(j-1)\right]\frac{1}{\Delta\psi}=E[l_{ji}]+E\{l_{ji}\},$$

$$q_j=\min_{q_j=1,2,\ldots}\left\{q_j: 2\pi q_j-\omega_c\, i\Delta t-\frac{2\pi}{n}(j-1)>0\right\} \qquad (6.120)$$

with rotation of the outer ring in the clockwise direction. If the rotation of the outer ring is anticlockwise, instead of the expression (6.120) we get

$$k^*_{ji}=N(p_j-1)+\left[2\pi p_j-\left\{(\omega_{ot}-\omega_c)\, i\Delta t+\frac{2\pi}{n}(j-1)\right\}\right]\frac{1}{\Delta\varphi}=E[k^*_{ji}]+E\{k^*_{ji}\},$$

$$p_j=\min_{p_j=1,2,\ldots}\left\{p: 2\pi p_j-\left[(\omega_{ot}-\omega_c)\, i\Delta t+\frac{2\pi}{n}(j-1)\right]>0\right\},$$

$$l^*_{ji}=\left[\omega_c\, i\Delta t+\frac{2\pi}{n}(j-1)\right]\frac{1}{\Delta\psi}=E[l^*_{ji}]+E\{l^*_{ji}\}. \qquad (6.121)$$

Formulas (6.112) and (6.116) through (6.121) are valid for the case of balls

rolling along one and the same raceway. If it is possible to measure deviations:

$$R_j(k)=R_j(k\Delta\varphi),\quad k=1, 2, \ldots, E\left[\frac{\omega_c T}{\Delta\varphi}\right]+1,$$

$$r_j(l)=r_j(l\Delta\psi),\quad l=1, 2, \ldots, E\left[\frac{T(\omega_r-\omega_c)}{\Delta\psi}\right]+1 \qquad (6.122)$$

when the inner ring rotates and

$$k=1, 2, \ldots, E\left[\frac{(\omega_{ot}-\omega_c)T}{\Delta\varphi}\right]+1,$$

$$l=1, 2, \ldots, E\left[\frac{\omega_c T}{\Delta\psi}\right] \qquad (6.123)$$

when the outer ring rotates for each ball $j=1, 2, \ldots, n$, then instead of the expressions (6.115) we get

$$R(\varphi_{ji})=R_j(E[k_i])+\left[R_j(E[k_i]+1)-R_j(E[k_i])\right]\cdot E\{k_i\},$$

$$r(\psi_{ji})=r_j(E[l_i])+\left[r_j(E[l_i]+1)-r_j(E[l_i])\right]\cdot E\{l_i\}. \qquad (6.124)$$

When the inner ring rotates in the clockwise direction we determine

$$k_i=N(p-1)+(2\pi p-\omega_c\, i\Delta t)\frac{1}{\Delta\varphi}=E[k_i]+E\{k_i\},$$

$$p=\min_{p=1, 2, \ldots}\{p: 2\pi p-\omega_c\, i\Delta t>0\},$$

$$l_j=\frac{\omega_r-\omega_c}{\Delta\psi}\, i\Delta t=E[l_i]+E\{l_i\}. \qquad (6.125)$$

When the inner ring rotates in the anticlockwise direction

$$k_i=\omega_c\, i\Delta t\,\frac{1}{\Delta\varphi}=E[k_i]+E\{k_i\},$$

$$l_i=\left[\frac{2\pi q}{\Delta\psi}-\frac{\omega_r-\omega_c}{\Delta\psi}\right] i\Delta t+M(q-1)=E[l_i]+E\{l_i\},$$

$$q=\min_{q=1, 2, \ldots}\{q: 2\pi q-(\omega_r-\omega_c)\, i\Delta t>0\}. \qquad (6.126)$$

When the outer ring rotates in the clockwise direction

$$k_i=N(p-1)-\frac{(\omega_{ot}-\omega_c)}{\Delta\varphi}\, i\Delta t+\frac{2\pi p}{\Delta\varphi}=E[k_i]+E\{k_i\},$$

$$p=\min_{p=1, 2, 3, \ldots}\{p: 2\pi p-(\omega_{ot}-\omega_c)\, i\Delta t>0\},$$

$$l_i=\frac{\omega_c}{\Delta\psi}\, i\Delta t=E[l_i]+E\{l_i\}. \qquad (6.127)$$

When the outer ring rotates anticlockwise

$$k_i=\frac{\omega_{ot}-\omega_c}{\Delta\varphi}\, i\Delta t=E[k_i]+E\{k_i\},$$

$$l_i=M(q-1)+[2\pi q-\omega_c\, i\Delta t]\,\frac{1}{\Delta\psi}=E[l_i]+E\{l_i\},$$

$$q=\min_{q=1,2,\ldots}\{q: 2\pi q-\omega_c\, i\Delta t>0\}. \tag{6.128}$$

Assuming that all the balls in the ball bearings are ideal products and roll along one and the same raceway it is possible to describe the manufacturing defects of one raceway of the inner ring and one of the outer ring with the help of circle diagrams. Here

$$R(k)=R(k\Delta\varphi),\quad \Delta\varphi=\frac{2\pi}{N},\quad k=1, 2, \ldots, N,$$

$$r(l)=r(l\Delta\psi),\quad \Delta\psi=\frac{2\pi}{M},\quad l=1, 2, \ldots, M \tag{6.129}$$

and in the cases (6.116), (6.117), (6.120) and (6.121) the quantities $E[k_{ji}]$, $E[l_{ji}]$, $E[k^*_{ji}]$, $E[l^*_{ji}]$ are replaced by the respective quantities

$$E[k_{ji}]-E\left[\frac{k_{ji}}{N}\right]\cdot N,\quad E[l_{ji}]-E\left[\frac{l_{ji}}{M}\right]M,$$

$$E[k^*_{ji}]-E\left[\frac{k^*_{ji}}{N}\right]\cdot N,\quad E[l^*_{ji}]-E\left[\frac{l^*_{ji}}{M}\right]M. \tag{6.130}$$

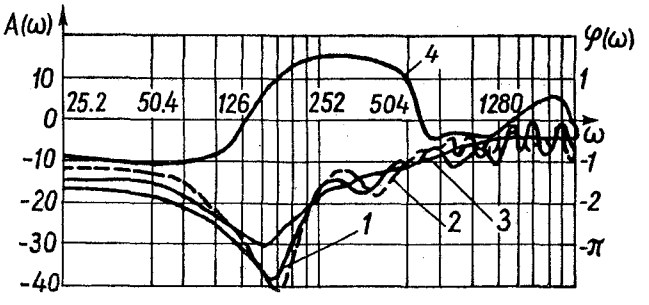

Fig. 6.24. Logarithmic amplitude characteristics (empirical curves: *1*, *2* and approximate curve: *3*) and phase (curve *4*) characteristic of dependence of VFT on manufacturing defects in raceways; bearing C1000096 with eight balls, radial load 1 kg, speed 200 rpm.

Curves of empirical (curves *1*, *2*) and approximating (curve *3*) functions of the logarithmic, amplitude and phase (curve *4*) frequency characteristics of manufacturing defects in raceways of rings are shown in Fig. 6.24 for the

1000096 ball bearing with eight balls with a radial load of 1 kg and a speed of 200 rpm. The approximating transfer function in this case is:

$$W(j\omega)=\frac{0.1778\,(1+0.041\,j\omega)^7}{(1+0.125\,j\omega)\,(1+0.078\,j\omega)^2\,(1+0.023\,j\omega)^3\,(1+0.005\,j\omega)}. \quad (6.131)$$

It corresponds to curve *3* drawn using graphic-analytical means.

An example of the logarithmic amplitude characteristic of the dependence of variable friction torque on geometric errors in a lubricated A840154 bearing is shown in Fig. 6.25 (curve *1*). The transfer function given for the approximating curve *2* has the form

$$W(j\omega)=\frac{1.82\,(1+6.35\,j\omega)}{j\omega}. \quad (6.132)$$

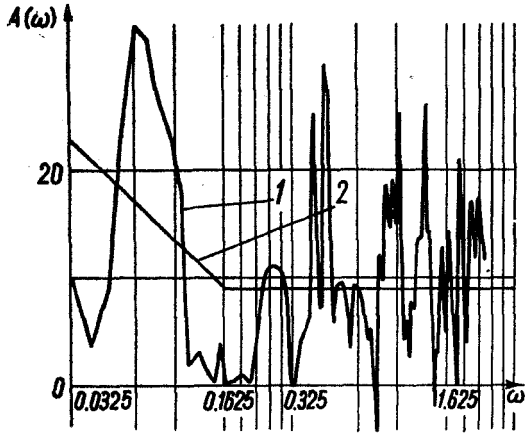

Fig. 6.25. (*1*) Empirical and (*2*) approximate logarithmic amplitude characteristics of dependence of VFT on geometric defects in lubricated bearing of A840154 type.

The same characteristics for the cleaned bearing are shown in Fig. 6.26. In this case

$$W(j\omega)=\frac{4.677\,(1+3.13\,j\omega)^2\,(1+1.11\,j\omega)}{(1+12.4\,j\omega)^2\,(1+0.12\,j\omega)}. \quad (6.133)$$

Transfer functions between geometric defects in the manufacture of raceways and vibrations were estimated separately for inner and outer rings. It was established that geometric defects in the rotating ring considerably affect the vibrations. In order to illustrate this statement curves are shown in Fig. 6.27 representing the logarithmic amplitude characteristic (curve *1*) and approximating asymptotic logarithmic characteristic (curve *2*) drawn using graphic-analytical means for a lubricated A840154 bearing when the outer ring rotates at 2 rpm. The corresponding asymptotic transfer function is given by

$$W(j\omega)=6.918. \quad (6.134)$$

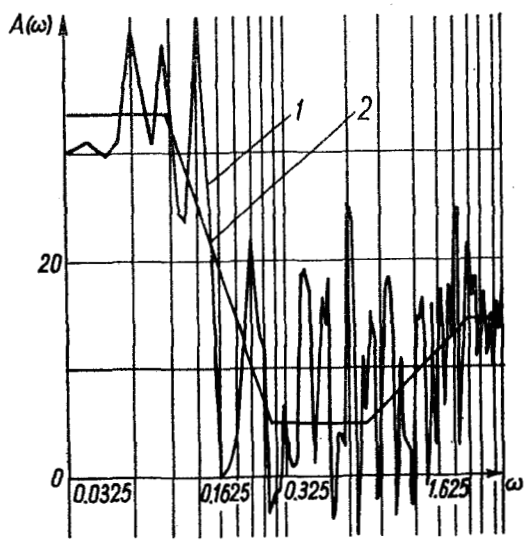

Fig. 6.26. (*1*) Empirical and (*2*) approximate logarithmic amplitude characteristics of dependence of VFT on geometric defects in raceways in dry bearing of A840154 type.

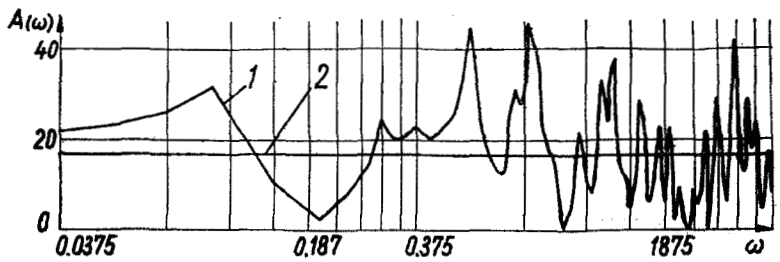

Fig. 6.27. Logarithmic amplitude characteristics of dependence of vibration of rings in axial direction on geometric defects in manufacture of raceways in lubricated bearing: *1*—empirical; *2*—approximate characteristics.

Similar characteristics for the cleaned bearing are shown in Fig. 6.28. The corresponding expression for the transfer function is

$$W(j\omega)=\frac{6.839\,(1+0.362\,j\omega)^3}{(1+0.88\,j\omega)^3}. \tag{6.135}$$

A comparison of the curves and the corresponding expressions for transfer functions indicates that lubrication acts as a damper of vibrations.

In accurate modern instruments local magnetic fields are almost always set up by different electronic circuits. Hence the effect of an external magnetic field on the dynamic characteristics of the bearing is of interest.

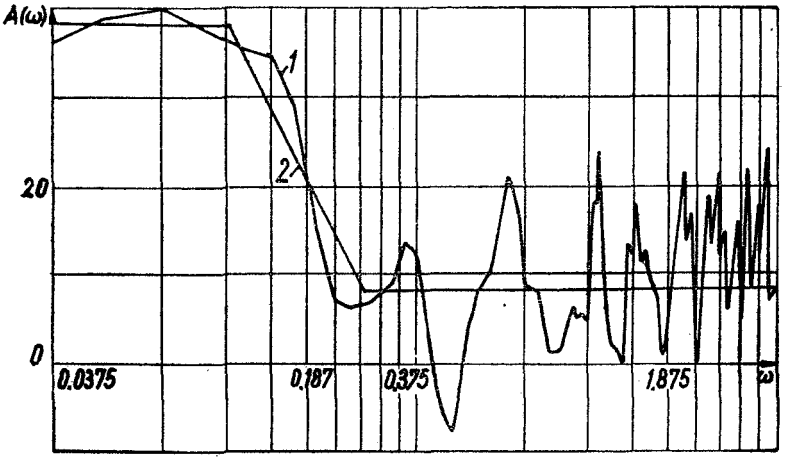

Fig. 6.28. Same as Fig. 6.27 in dry bearing.

During the tests the degree of magnetization was evaluated in Maxwells along the magnetic flux created by the magnetized bearing. Magnetization was carried out with the help of a solenoid by orienting the magnetic moments on the faces of the bearing.

The spectral densities of vibrations of rings in the axial direction and of variable friction torques and the transfer functions between them were estimated for different values of magnetization. As an example we use Fig. 6.29

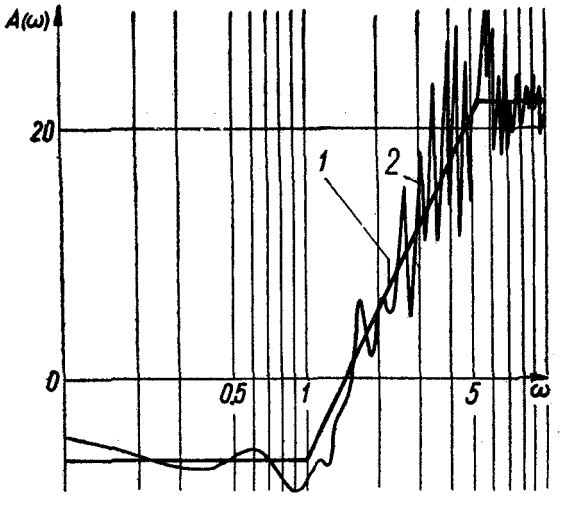

Fig. 6.29. (*1*) Asymptotic and (*2*) empirical logarithmic amplitude characteristics of dependence of vibrations of rings on VFT without magnetization of surrounding medium.

showing the characteristics, drawn on the basis of the above methods, which determine the relation between vibration of rings and friction torque of a lubricated non-magnetized bearing. The transfer function

$$W(j\omega)=\frac{0.093\,(1+j\omega)^2}{(1+0.194\,j\omega)^2}. \tag{6.136}$$

corresponds to curve *1*.

The same characteristics for a bearing magnetized to three Maxwells are shown in Fig. 6.30 for comparison. In this case

$$W(j\omega)=\frac{0.092\,(1+2\,j\omega)}{1+0.21\,j\omega}\,. \tag{6.137}$$

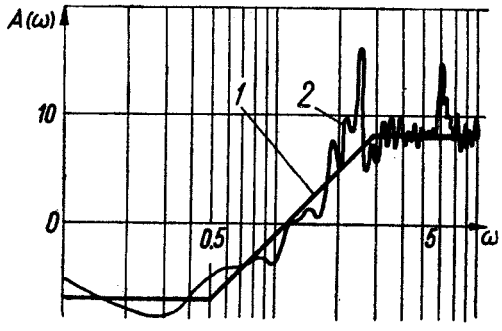

Fig. 6.30. (*1*) Asymptotic and (*2*) empirical logarithmic amplitude characteristics of dependence of vibrations of rings on VFT with magnetization equal to 3 Maxwells.

Analysis of estimates of spectral densities and transfer functions leads to the conclusion that small magnetization (up to five Maxwells) lowers the level of friction torque and high frequencies. For large magnetization a sharp increase in the mean level of friction torque has been observed.

Let us determine the degree of influence of individual parameters on the total variable friction torque of the ball bearing.

The method of localization of sources for the appearance of variable friction torque is the simplest method. Following this method it is possible to estimate their effectiveness based on the value of the coefficient of cross-correlation between the variable friction torque and the source. It is necessary to fulfill the condition of statistical independence and normal distribution of the stationary processes that cause the appearance of variable friction torque. This leads to significant limitations in the formulation of the problem. In particular, in such a formulation it is not possible to determine the degree of influence of parameters having different relations with the variable friction torque. As a result it is not possible to obtain a clear maximum of the correlation coefficient. In the work [2] the procedure for the solution of this problem is given for the case of narrow-band processes. We will follow a more general procedure [7].

Let us estimate the influence of three basic parameters on variable friction torque: geometric defects in the manufacture of rings, vibration of rings with respect to one another in the axial direction and variation in the thickness of

the lubricating film. The mechanical system with the number of parameters $n=3$ is expressed in the form of 2 (3+1) poles (Fig. 6.31).

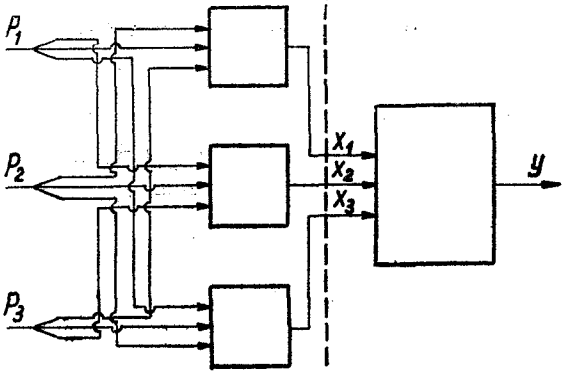

Fig. 6.31. Determination of influence of individual parameters of bearing on VFT.

The external uncorrelated actions are indicated by p_i, the response of the system at the k-th input ($k=1, 2, 3$) by $x_k(t)$ and at the output by $p_0(t)$. The spectral densities S_{kk} of signals $x_k(t)$ and cross spectral densities S_{mk} (m, $k=1, 2, 3$) and S_{ok} ($k=1, 2, 3$) obtained by experimental methods are used as the initial data.

The solution of the problem formulated is given by solution of the system

$$S_{kk}=\sum_{i=1}^{3} W_{ki}\, W_{ki}^{*}\, S_i,$$

$$S_{mk}=\sum_{i=1}^{3} W_{mi}\, W_{ki}^{*}\, S_i,$$

$$S_{ok}=\sum_{i=1}^{3} W_{0i}\, W_{ki}^{*}\, S_i, \qquad (6.138)$$

where W_{ki}^{*} is the transfer function that is the conjugate of the function W_{ki}. The unknowns are the spectral densities S_i and transfer function W_{0i}.

The spectral density of the output of variable friction torque can be written in the form [33]:

$$S_{00}(\omega)=\sum_{i=1}^{3} |W_{0i}|^2\, S_i(\omega). \qquad (6.139)$$

The right-hand side of equation (6.139) contains the expressions that determine the contribution of each parameter (source) in the band of frequencies $d\omega$ to energy at the system output.

In equations (6.139) the following notations are introduced:

$$S_{kk}=a_k,\quad S_{mk}=a_{mk}+jb_{mk},\quad S_{ok}=\alpha_k+j\beta_k,\quad S_k=x_k,$$
$$W_{kk}=A_k+jB_k,\quad W_{mk}=y_{mk}+jz_{mk},\quad W_{ok}=u_k+jv_k, \tag{6.140}$$

using which we get:

$$\left.\begin{aligned}
&-a_1+(A_1^2+B_1^2)\,x_1+(y_{12}^2+z_{12}^2)\,x_2+(y_{13}^2+z_{13}^2)\,x_3=0,\\
&-a_2+(y_{12}^2+z_{12}^2)\,x_1+(A_2^2+B_2^2)\,x_2+(y_{23}^2+z_{23}^2)\,x_3=0,\\
&-a_3+(y_{13}^2+z_{13}^2)x_1+(y_{23}^2+z_{23}^2)x_2+(A_3^2+B_3^2)\,x_3=0,\\
&-a_{12}+A_1\,y_{12}\,x_1-B_1\,z_{12}\,x_1+A_2\,y_{12}\,x_2\\
&+B_2\,z_{12}\,x_2+y_{13}\,z_{23}\,x_3-z_{13}\,y_{23}\,x_3=0,\\
&-b_{12}+A_1\,z_{12}\,x_1+B_1\,y_{12}\,x_1+A_2\,z_{12}\,x_2\\
&-B_2\,y_{12}\,x_2+y_{23}\,z_{13}\,x_3-z_{23}\,y_{13}\,x_3=0,\\
&-a_{13}+A_1\,y_{13}\,x_1-B_1\,z_{13}\,x_1+y_{12}\,y_{23}\,x_2-z_{12}\,z_{23}\,x_2\\
&+A_3\,y_{13}\,x_3+B_3\,z_{13}\,x_3=0,\\
&-b_{13}+B_1\,y_{13}\,x_1+A_1\,z_{13}\,x_1+y_{12}\,z_{23}\,x_2+y_{23}\,z_{12}\,x_2\\
&+A_3\,z_{13}\,x_3-B_3\,y_{13}\,x_3=0,\\
&-a_{23}+y_{12}\,y_{13}\,x_1+z_{12}\,z_{13}\,x_1+A_2\,y_{23}\,x_2-B_2\,z_{23}\,x_2\\
&+A_3\,y_{23}\,x_3+B_3\,z_{23}\,x_3+0,\\
&-b_{23}+y_{12}\,z_{13}\,x_1-z_{12}\,y_{13}\,x_1+A_2\,z_{23}\,x_2+B_2\,y_{23}\,x_2\\
&+A_3\,z_{23}\,x_3-B_3\,y_{23}\,x_3=0.
\end{aligned}\right\} \tag{6.141}$$

$$\left.\begin{aligned}
&\alpha_1+A_1\,u_1\,x_1+B_1\,v_1\,x_1+u_2\,y_{12}\,x_2+v_2\,z_{12}\,x_2\\
&+u_3\,y_{13}\,x_3+v_2\,z_{13}\,x_3=0,\\
&\beta_1+A_1\,v_1\,x_1-B_1\,u_1\,x_1-u_2\,z_{12}\,x_2+v_2\,y_{12}\,x_2\\
&-u_3\,z_{13}\,x_3+v_3\,y_{13}\,x_3=0,\\
&\alpha_2+u_1\,y_{12}\,x_1-v_1\,z_{12}\,x_1+A_2\,u_2\,x_2+B_2\,v_2\,x_2\\
&+u_3\,y_{23}\,x_3+v_3\,z_{23}\,x_3=0,\\
&\beta_2+v_1\,y_{12}\,x_1+u_1\,z_{12}\,x_1-B_2\,u_2\,x_2+A_2\,v_2\,x_2\\
&-u_3\,z_{23}\,x_3+v_3\,y_{23}\,x_3=0,\\
&\alpha_3+u_1\,y_{13}\,x_1-v_1\,z_{13}\,x_1+u_2\,y_{23}\,x_2-v_2\,z_{23}\,x_2\\
&+A_3\,u_3\,x_3+B_3\,v_3\,x_3=0,\\
&\beta_3+u_1\,z_{13}\,x_1+v_1\,y_{13}\,x_1+u_2\,z_{23}\,x_2+v_2\,y_{23}\,x_2\\
&-B_3\,u_3\,x_3+A_3\,v_3\,x_3=0.
\end{aligned}\right\} \tag{6.142}$$

Equations (6.138) are thus brought down to two subsystems of algebraic equations (6.141) and (6.142) where the first is nonlinear with respect to x_i, y_{ij}, z_{ij} $(i, j=1, 2, 3)$ and the second is linear with respect to u_k, v_k $(k=1, 2, 3)$ after substituting the solutions of the subsystem (6.141) therein.

The general scheme for solving the complete problem using the computer is as follows. The initial data (up to 4,000 points of realization of each process) are fed in. In the case of variation in the lubricating film the counting is carried out at equal intervals Δt. For geometric defects in the manufacture of

components counting is carried out for each degree of the circle diagram. Using the methodology described in the preceding paragraph computations are carried out for the effects caused by errors and estimates are found for all correlation and cross-correlation functions according to formulas (6.47) and (6.95) respectively. The corresponding "weighted" functions are determined using formula (6.70). Spectral and cross-spectral densities are computed for values of ω for which it is desirable to have an estimate of the effectiveness of the causes of variable friction torque.

The subsystem (6.141) is solved by the iterative procedure. The unknown quantities x_1, x_2, x_3, y_{12}, z_{12}, y_{13}, z_{13}, y_{23}, z_{23} are expressed in terms of the remainder from the first, second, etc. equations respectively. The solution is started from zero initial values of the quantities y_{12}, z_{12}, y_{13}, z_{13}, y_{23}, z_{23} and unit initial values of the quantities x_1, x_2, x_3.

The condition for concluding the iteration is determined with an accuracy based on relative error $\delta \leqslant 0.5\%$ for all unknowns.

The subsystem (6.142) is solved by the Gauss method using the principal diagonal at each stage.

Fig. 6.32 shows graphs of the spectral density of variable friction torque (curve *4*) and the additions which determine the part contributed to the energy of processes by changes in the thickness of the lubricating film, vibrations of rings with respect to one another in the axial direction and geometrical defects in the manufacture of raceways (curves *1*, *2*, *3* respectively) for a C201 bearing with zero axial load and for a radial load of 1 kg (inner ring rotating at 220 rpm). It can be seen from a comparison of curves that the maximum influence is due to geometrical defects in manufacture. This effect is especially marked in the region of high frequencies exceeding the frequency of rotation of the bearing by two to three times.

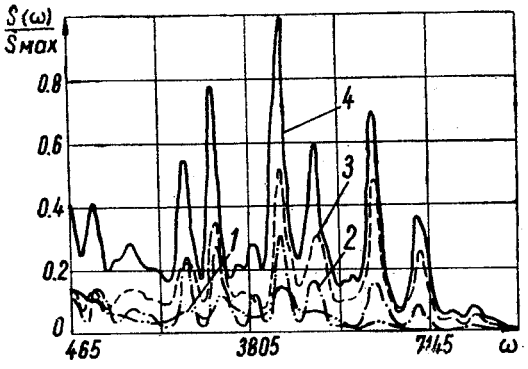

Fig. 6.32. (*4*) Spectral density of VFT and its components due to (*1*) thickness of oil film, (*2*) vibrations of rings (*3*) and geometric defects in manufacture of raceways of rings in bearing of C201 type rotating at 220 rpm.

An analogous picture was observed for C1000096 and C26 bearings at different speeds of rotation and loads.

The smallest effect on the spectrum of variable friction torque is due to changes in the thickness of the lubricating film.

References

1. Baburin, V.M. et al. 1962. O vychislenii funktsii raspredeleniya sluchainykh protsessov po eksperimentalnym dannym (Computation of the distribution function of random processes based on empirical data). *Avtomatika i telemekhanika*, Vol. 23, No. 5.
2. Balitskii, F.Ya., M.D. Genkin and A.G. Sokolova. 1966. Korrelyatsionnyi metod lokalizatsii statisticheski zavicimykh istochnikov shuna (Correlational method of localizing statistically dependent sources of noise). In *Borba s shumani i vibratsiyami*, Moscow.
3. Venchkovskii, L.B. 1962. Postroenie otsenok matematicheskogo ozhidaniya i dispersii po nekorrelirovannoi vyborke sluchainogo protsessa (Plotting of estimates of mathematical expectation and dispersion according to uncorrelated samples of random process). *Avtomatika i telemekhanika*, Vol. 29, No. 5.
4. Vergiles, A.M. 1969. Issledovanie fluktuatsii momentov sil treniya sharikopodshipnikov v atmospfere i vacuume pri povyshennykh temperaturakh (Study of fluctuation in the friction torque of ball bearings in the atmosphere and in a vacuum at high temperatures). Avtoreferat kand. diss., Moscow.
5. Veselova, G.P. and Yu.I. Gribanov. 1968. Oboptimalnom shage vyborki pri rychislenii korrelyatsionnykh funktsis stuchainyka protsessov na tsifrovykh vychislitelnykh ustroistvakh (Best sampling interval when computing correlation functions of random processes using the computer). *Avtomatika i telemakhanika*, No. 12.
6. Vilenkin, S.Ya. 1967. Statisticheskie metody issledovaniya statsionarnykh protsessov i sistem avtomaticheskogo regulirovaniya (Statistical approach to stationary processes and automatic control systems). Moscow, Sov. radio.
7. Genkin, M.D., V.I. Sergeev and A.G. Sokolova. 1969. Nekotorye voprosy statisticheskoi dinamiki mekhanicheskikh kolebatelnykh sistem (Some problems in the statistical dynamics of mechanical vibration systems). Mashinovedenie, No. 2.
8. Same as ref. [31], Chapter III.
9. Evlanov, L.G. 1968. Metody analiza dinamicheskikh sistem, Soderzhashchikh strutainye parametry (Analysis of dynamic systems incorporating

random parameters). I. *Avtomatika i Telemekhanika*, No. 8 and 11. *Avtomatika i Telemekhanika*, No. 12.

10. Evalanov, L.G. 1967. Priblizhennyi metod issledovaniya tochnosti lineinykh sistem, soderzhashchikh sluchainye parametry (Approximate method of ascertaining the accuracy of linear systems incorporating random parameters). In *Optimalnye sistemy. Statisticheskie metody*. Moscow, Nauka.
11. Zotov, Yu.A. 1965. Mnogokanalnyi elektricheskii korrelyator (Multichannel electric correlator). *Voprosy radio-elektroniki*, ser. 12, vyp. 21.
12. Kazakov, I.E. and B.G. Dostupov. 1962. Statisticheskaya dinamika nelineinykh avtomaticheskikh sistem (Statistical dynamics of nonlinear automatic systems). Moscow, Fizmatgiz.
13. Kazakov, I.E. 1965. Opredelenic zakonov raspredeleniya peremennykh nelineinoi stokhasticheskoi sistemy (Determination of the distribution laws of the variables in stochastic systems). *Avtomatika i telemekhanika*, No. 11.
14. Kasnauskas, Yu.Yu. 1969. Issledovanie dvizheniya vertikalnykh zhestikikh rotorov, vrashchayushchikhsya v vysokochastotnykh predvaritelno natyanutykh sharikopodshipnikakh (The motion of vertical rigid rotors turning in high-speed preloaded ball bearings). Avtoreferat kand. diss., Kaunas.
15. Same as ref. [44], Chapter III.
16. Same as ref. [48], Chapter III.
17. Kotov, E.O. 1965. K analizu lineinoi sistemy s peremenrym parametrani I Sluchainyi Ogranichennogo izmeneniya parametrov (Analysis of a linear system with variable parameters. I. The case of limited variation in parameters). *Avtomatika i Telemekhanika*, No. 26, No. 12.
18. Same as ref. [53], Chapter III.
19. Lazaryan, V.A., V.F. Ushkalov and E.M. Tenenbaum. 1967. K voprosy ob opredelenii s pomoshchyu E Ts VM chastot i amplitud garmonicheskikh sostavlyayushchikh kolebatelnykh protsessov, zanisannykh pri ispytanii zheleznodorozhnykh ekipazhei (Computer-aided determination of frequencies and amplitudes of harmonic components of vibrating processes recorded when testing trainmen). Moscow, *Transport*, vyp. 72.
20. Same as ref. [26], Chapter V.
21. Lerner, A.Ya. 1958. Vvedenie v teoriyu avtomaticheskogo regulirovaniya (Introduction to the theory of automatic control). Moscow, Mashgiz.
22. Lin, V.K. 1963. Primenenie modeli nestataonannogo drobovogo shuma dlya issledovaniya povedeniya sistemy pri deistvii nekotorykh tipov nestatsionarynykh vozmyshchenii (The nonstationary fractional noise model applied to the behavior of a system subject to nonstationary disturbances). *Prikladnaya Mekhanika*, Vol. 30, ser. E, No. 4.

23. Linnik, Yu.V. 1962. Metod naimenishikh kvadratov i osnovy teorii obrabotki nablyudenii (The method of least squares and fundamentals of the theory of data processing). Moscow, Fizmatgiz.
24. Linskii, G.K. and B.T. Sheftel. Issledovanie radialnykh vibratsii sharikopodshipnika ot pogreshnostei formy poverkhnostei kacheniya metodom spektralnogo analiza (Spectral analysis of radial vibrations of ball bearings due to defects in rolling surfaces). *Podshipnikovaya Promyshlennost*, No. 4.
25. Same as ref. [28], Chapter V.
26. Mitropolskii, A.K. 1961. Tekhnika statisticheskikh vychislenii (Statistical computation techniques). Moscow, Fizmatgiz.
27. Nikolaeva, M.V. 1949. O priblizhennom vychislenii otsilliruyushchikh integralov (Approximate computation of oscillating integrals). *Trudy matematicheskogo in-ta in. Steklova*, Vol. 28, Moscow-Leningrad, Izd. AN SSSR.
28. Nikolaenko, N.R. 1967. Veroyatnostnye metody dinamicheskogo rascheta mashinostroitelnykh konstruktsii (Probability methods of dynamic computation of machine designs). Moscow, Mashinostroenie.
29. Palmgren, A. 1949. Sharikovye i rolikovye podshipniki (Ball and roller bearings). Moscow, Mashgiz.
30. Pervozvanskii, A.A. 1962. Sluchainye protsessy v nelineinykh avtomaticheskikh sistemakh (Random processes in nonlinear automatic systems). Moscow, Fizmatgiz.
31. Same as ref. [75], Chapter III.
32. Same as ref. [77], Chapter III.
33. Pugachev, V.S. 1960. Teoriya sluchainykh funktsii i ee primenenie k zadacham avtomaticheskogo upravleniya (Theory of random control and its application to problems of automatic control). Izd. 2-e. pererab. i dop. Moscow, Fizmatgiz.
34. Same as ref. [81], Chapter III.
35. Sveshnikov, A.A. 1961. Prikladnye metody teorii sluchainykh funktsii (Applied theory of random functions). Sudpromgiz.
36. Solodovnikov, V.B. 1960. Statisticheskaya dinamika lineinykh sistem avtomaticheskogo uprovleniya (Statistical dynamics of linear systems of automatic control). Moscow, Fizmatgiz.
37. Same as ref. [101], Chapter III.
38. Chuberkis, V.P. 1968. Proverka gipotezy o normalnosti odnomernogo zakona raspredeleniya statsionarnogo sluchainogo protsessa (Confirming the hypothesis as to the normal unidimensional distribution of a stationary random process). *Avtomatika i telemekhanika*, No. 11.
39. Chan, S.Y. and K. Chuang. 1966. A study of linear time-varying systems subject to stochastic disturbances. *Avtomatika*, Vol. 4, No. 1.
40. Parzen, E. 1957. On consistent estimates of the spectrum of a stationary

time series. *Ann. Math. Statistics*, Vol. 28, No. 2.
41. Rosenblatt, M. 1959. Statistical analysis of stochastic processes with stationary residuals. Probability and statistics. Stockholm, Almqvist and Wilkseli, New York. John Willey and Sons.
42. The Design and Analysis of Industrial Experiments (ed. by O.L. Dacies), Int. ed. Oliver and Boyd, 1960.

7

EXPERIMENTAL STUDY OF THE DYNAMIC CHARACTERISTICS OF PRECISION BEARINGS AND ASSEMBLIES

The continuous progress in technology poses fundamentally new demands on the working of the rolling contact bearings used in flight vehicles, ships, instruments, etc.

In many units the support is provided basically by precision rolling contact bearings and sliding bearings which have a minimum loss to friction torque and a low level of disturbance due to vibrations.

One could list a whole series of devices of precision instrumentation in which friction torque causes appreciable deterioration of the dynamic characteristics. They include gyroscopic instruments, information input and output systems, computers, audio and video recording apparatus and counters.

For example, in tape recorders oscillations in the speed of tape movement evaluated by the coefficient of detonation are caused by defects in the geometric sizes, accuracy of rotation and variation in friction torque in the ball bearings used as rolling contact support of all the rotating components (tone channel, guides, etc.). In the gyroscopic instruments used in modern flight vehicles the gyroscope rotor should have very large kinetic moment and low level of vibration in the working condition and the gimbal suspension should have high sensitivity and rotational accuracy. To ensure the required accuracy, reliability and longevity the support for rotation and bearings of these devices should be of high quality. They are complex vibrating systems that excite vibrations in the shafts and rotors mounted on them with parameters which depend on the actual working conditions. Theoretical study of the dynamics of bearing supports is often complicated by the impossibility of taking into account all the factors affecting the level of vibration that are met with in practice. Hence experimental study of the dynamic and vibrational characteristics of bearing supports under near-real working conditions is the only way to obtain accurate data on the behavior of the system.

7.1 STUDY OF FRICTION TORQUE IN BEARINGS AND BEARING ASSEMBLIES

Friction torque in rolling contact bearings is a complex, physical process

caused by contact deformations of rubbing elements, macro- and micro surface roughness of raceways, properties of the lubricant, resistance to the flow of lubricant or the surrounding medium, loads, the number of revolutions and the physical properties of the materials of contact elements.

Since it is difficult to compute friction torque it is necessary to use the results of tests showing the effect of various operational parameters on the components of friction torque. This is very important for selection of the optimum working conditions of bearings and assemblies.

7.1.1 Dependence of Friction Torque on Loading

Axial load has an appreciable effect on the friction torque components. As can be seen from the curves (Fig. 7.1), radial load affects friction torque to a lesser degree.

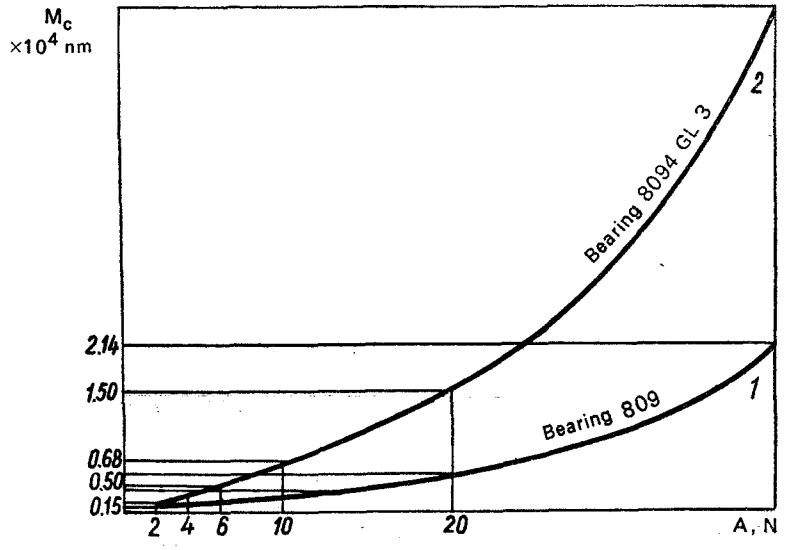

Fig. 7.1. Variation in constant component of friction torque with load and varying surface smoothness of raceways of mass-produced ball bearings: *1*—ball bearing with normal surface smoothness; *2*—ball bearing with rough raceway surface.

The curves shown here were obtained on the basis of a large number of measurements of the constant friction torque component of a ball bearing of bulk class 809 loaded in the axial direction. Experiments were carried out with bearings without lubrication. From an analysis of the curves it follows that for a load up to 20 N the friction torque is nearly proportional to the load [35]:

$$M_n = AQ, \tag{7.1}$$

where A is the coefficient of proportionality;

Q is the load.

Up to a certain value, if the load is gradually increased friction torque increases negligibly. However, with a load around 5 N its value goes up appreciably [35]. With an increase in load up to 20 N and more and also with any deterioration in the cleanliness of raceway surfaces the friction torque considerably increases.

Similar results were obtained by the Japanese worker K. Kakuta for bearings of the 6310 series without a cage. The bearings were lubricated with MIL-L-7870A lubricant, and the number of balls was three (Fig. 7.2). All the notations used are according to the standards of Japanese industry. The nature of the curve is similar to that in the previous example [21].

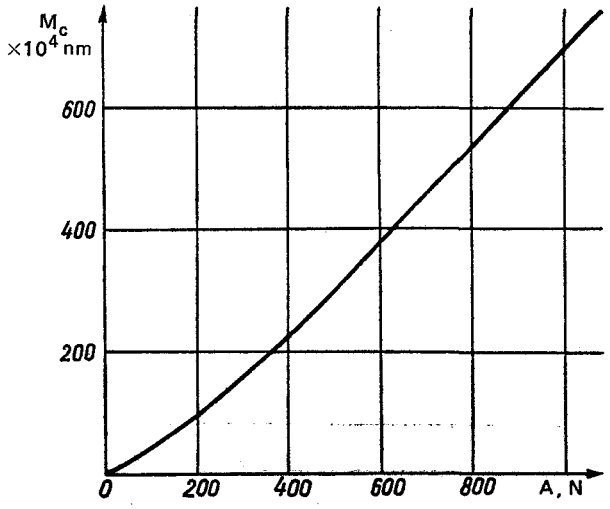

Fig. 7.2. Effect of axial load on constant component of friction torque in bearing of 6310 type.

It is seen from Fig. 7.3 that the relative change of moment of resistance at higher loads is less than that at smaller loads. Thus, in the first case at $A = 15.0$ N the moment of resistance increases 3.7 times but at a load of 60 N, only 2.5 times [43].

The change of variable component of the moment of resistance has been shown very clearly in Fig. 7.4 which indicates that the variable component increases very sharply.

In conclusion it may be said that axial load, on which the value of the contact angle and the forces acting on the balls and raceways depend, appreciably affects the working of radial-thrust ball bearings.

With an increase in axial loading the friction torque increases irrespective of lubrication and speeds of rotation. In the majority of cases a very nearly

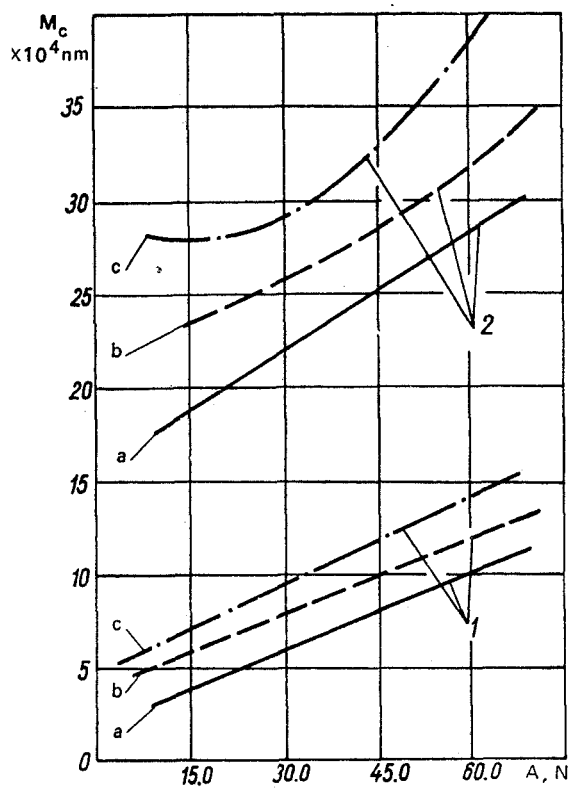

Fig. 7.3. Relation between constant component of friction torque and axial load: *1*—speed of moving ring, n=10,000 rpm; *2*—speed of moving ring, n=40,000 rpm; *a*—VNIINP-260 lubricant; *b*—VNIINP-228 lubricant; *c*—MVP oil.

linear dependence of friction torque on loading is obtained. Only at high speeds does the friction torque change more intensively with the use of viscous lubricants. This is because, firstly, all manufacturing defects in bearings and defects in the mounting in the assembly are more apparent at higher speeds and, secondly, with an increase in speed viscous lubricants cause a greater increase in friction torque.

With an increase in loading the relative change in friction torque is greater at low speeds. The use of VNIINP-280 lubricant increases the value of friction torque by 1.97 and 1.35 times [43]. For identical speeds, the friction torque changes with an increase in loading by a practically constant value independent of the lubricant used. An increase in loading always leads to an increase in friction torque because all types of losses take place:

a) elastic hysteresis;

b) differential sliding;

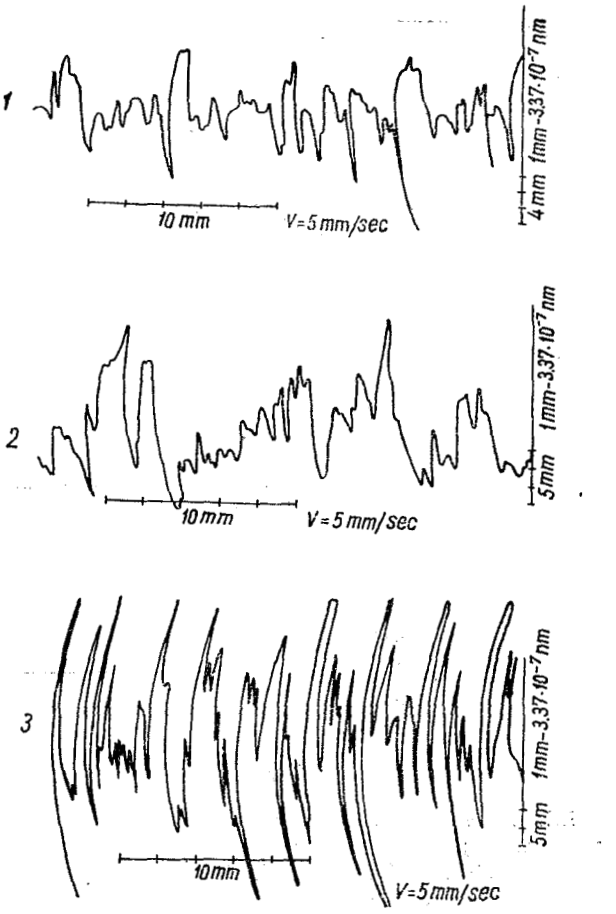

Fig. 7.4. Variation in VFT with axial load of bearing of C45 type:
1—zero load; *2*—load 30.00 N; *3*—load 5.00 N.

c) differential sliding of balls relative to one of the rings;

d) increase in lubricant viscosity in the contact zone of balls with raceways caused by the increase in normal pressure in the contact zone.

The effect of combined loading on friction torque is shown in Fig. 7.5. Analysis of the graphs of the relationships confirms the above remarks on the major influence of axial loading [43].

In combined loading the balls are loaded with unequal forces and have different contact angles with the raceways. As a result losses to friction are increased due to increased sliding of the rolling elements along the raceways and the inertial effect on the cage. The ratio of loads also affects the friction torque to a considerable degree: the larger the ratio of the axial load to the radial, the less the latter affects the working of the bearing.

At certain speeds friction torque is less in the case of combined loading than for axial loading alone.

All the rules for purely axial loading will be true even for the case of combined loading of an assembly which is not large, when the radial loading R is equal to 8 ± 2 N.

Since the effect of loads is associated with the action of other factors the analysis of the dependence of friction torque has a complex nature. Study of the dominating influence of individual factors makes it possible to select optimum working conditions.

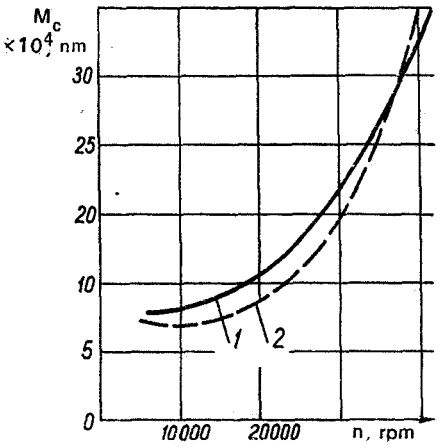

Fig. 7.5. Effect of combined loading on friction torque (VNIINP-260 lubricant): *1*—axial load 15 N; radial load 4 N; *2*—axial load 15 N; no radial load.

7.1.2 Study of Friction Torque in Bearing Assemblies

Owing to certain structural factors (preloading, mounting errors, etc.) the operation of ball bearings in special assemblies is different by comparison with bearings in isolation.

When discussing the friction torque in bearing assemblies it was assumed that the process is stationary and ergodic. The duration of realizations was chosen according to the method of computation shown.

In order to determine optimum loading, for minimum impact on the characteristic of assemblies, the ranges of parameters of rotation corresponded to ranges existing in actual mechanisms. In the present case concrete assemblies of tape mechanisms (LPM), initially cleaned according to the above procedure, were used.

In the study of friction torque components of LPM assemblies an important role is taken by the constant friction torque component which characterizes the total energy losses to friction in each specific assembly and correspondingly in the whole machine. This is very important in computing the required power and other design computations of low-power machines.

For measurement of the constant friction torque component basically two characteristic assemblies (assembly No. 1 with 1000094 bearings and assembly No. 2 with 1000096 bearings) were used. The assemblies were tested at different working conditions, i.e. at speeds of rotation from 50 to 550 rpm with a radial load varying from 0 to 5 N and axial load from 1 N to 5 N. The mass of the assembly itself was taken into account. The assemblies were tested with and without lubricant.

It is obvious that in the case of lubricated bearings the constant friction torque component of small-sized bearings increases somewhat more than in the case of unlubricated ones. With larger assemblies this difference is less sharp, the variable friction torque component decreases, rotation is more uniform and the process is stabilized.

With an increase in rotational speed (Fig. 7.6), however, the constant friction torque component increases all the time and the applied radial load does not appreciably affect the change in torque.

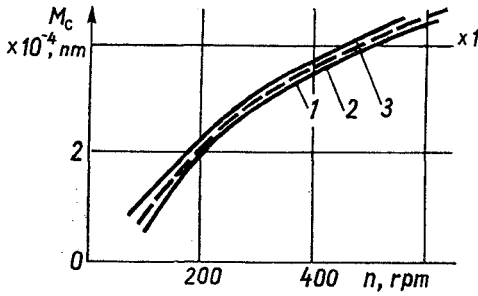

Fig. 7.6. Relation between constant component of friction torque and speed of lubricated assembly No. 2 for various radial loads: *1*—1 N; *2*—3.0 N; *3*—5.00 N.

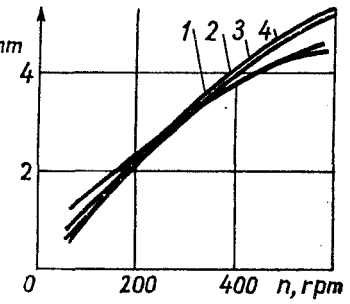

Fig. 7.7. Relation between constant component and speed of assembly No. 1 lubricated with MS-20 oil for various radial loads: *1*—1.0 N; *2*—2.0 N; *3*—3.0 N; *4*—5.0 N.

It can be seen from an analysis of Fig. 7.7 that the increase in friction torque has the same character as in a change in radial loading.

A clear picture of the dependence of the constant component on axial and radial loads can be obtained from Figs. 7.8 and 7.9. For this design of LPM assemblies both axial and radial loads up to 5 N hardly affect friction torque, but an increase in the rotational speed sharply increases the constant friction torque component.

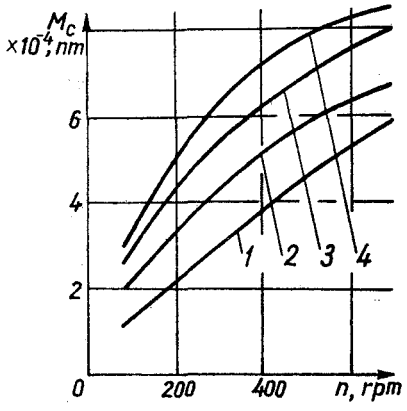

Fig. 7.8. Relation between constant component of friction torque and speed of assembly No. 1 lubricated with MS-20 oil for various axial loads: *1*—1.0 N; *2*—2.0 N; *3*—3.0 N; *4*—5.0 N.

The study of the behavior of LPM assemblies with unlubricated bearings appears to be more interesting. Bearings with axial and radial loads and those without loads (Figs. 7.8–7.12) tend to show an increase in the constant friction torque component with an increase in the rotational speed of the assembly. However, after reaching a certain speed the friction torque

decreases with a further increase in speed. This is because at a certain speed, in this case 200–300 rpm, the unlubricated bearing lacks stability of the process. The process is stabilized with an increase in speed. The sensitivity to

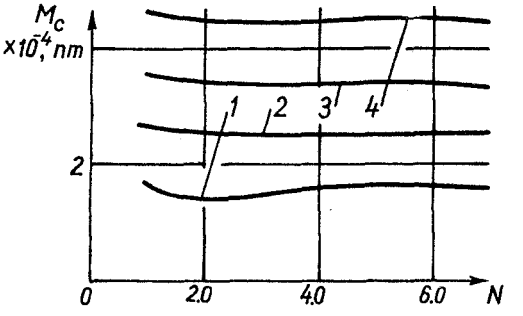

Fig. 7.9. Relation between constant component of friction torque and radial load of assembly No. 2 lubricated with MS-20 oil at various speeds: *1*—100 rpm; *2*—200 rpm; *3*—300 rpm; *4*—500 rpm.

small geometric defects is lowered, leading to a reduction in the constant friction torque component. In lubricated bearings this process is subject to the lubricating film.

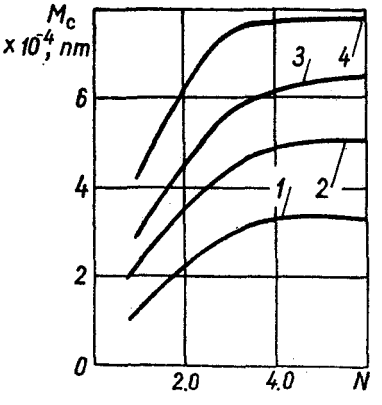

Fig. 7.10. Relation between constant component of friction torque and axial load of assembly No. 2 lubricated with MS-20 oil at various speeds: *1*—100 rpm; *2*—200 rpm; *3*—300 rpm; *4*—500 rpm.

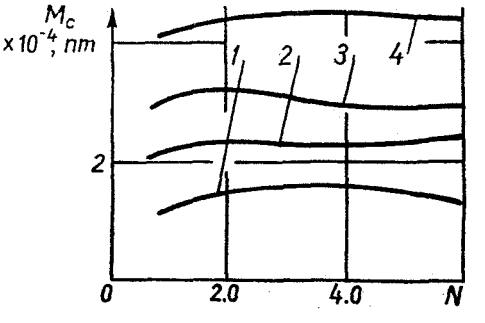

Fig. 7.11. Relation between constant component of friction torque and axial load of assembly No. 1 lubricated with MS-20 oil at various speeds: *1*—100 rpm; *2*—200 rpm; *3*—300 rpm; *4*—500 rpm.

Analysis of the constant friction torque component gives a general picture of the energy losses. Study of the variable component along with a study of its basic frequency characteristics, i.e. spectral density, indicates the limited possibilities of the effect of disturbances on the quality of magnetic recording.

It is worth mentioning the complexity of the phenomena that determine the friction torque in bearing assemblies when a large number of components rotate. Variable friction torque components depend to a large degree on dynamic (in particular, vibrational) processes observed in bearings.

We can come to certain conclusions based on our studies. It should be mentioned here that the effect of different factors on the variable component should be considered individually.

The effect of axial loading on the variable component of friction torque is not directly proportional. The variable component of individual, bearings increases sharply with an increase in the axial load but the variable component under the action of axial load of unloaded LPM assemblies increases proportionally though not so sharply as in the case of individual bearings.

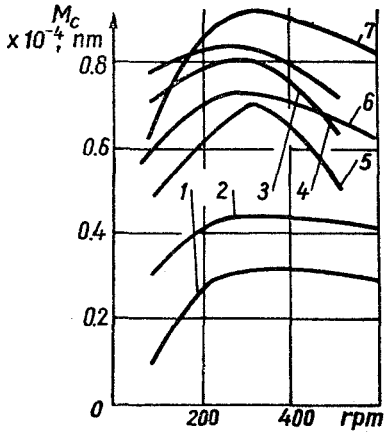

Fig. 7.12. Relation between constant component of friction torque and speed of dry (unlubricated) assembly No. 2 for various radial and axial loads: *1*—axial 1.00 N; *2*—radial 1.0 N; *3*—radial 3.0 N; *4*—radial 5.0 N; *5*—axial 2.0 N; *6*—axial 3.0 N; *7*—axial 5.0 N.

The periodicity of the variable component is almost always a multiple of the number of revolutions of the moving rings, which is evident from the very lowest turning speeds.

The amplitude of the variable component increases with the turning speed but basically on account of high-frequency components. If the low-frequency component with a periodicity equal to the number of revolutions increases it does so negligibly.

The variable component of unlubricated bearing assemblies is considerably higher than that of lubricated ones whereas the constant component of unlubricated bearing LPM assemblies is several times less than the variable component of lubricated bearings.

This is because assemblies with unlubricated bearings work by jerks, with irregular movement of the rolling elements along the raceways because of geometric defects.

7.1.3 Dependence of Friction Torque (M_B) in Bearings on Other Factors

The dependence of M_B on the turning speed for different durations of work is shown in Fig. 7.13. The tests were carried out at working temperatures of 20–200°C. Friction torque was measured after every 10 hours of

work over the bearings' entire service life. It was established that friction torque in bearings is reduced from 25×10^{-4} (after 10 hours of work) to 14×10^{-4} mm (after 100–150 hours) and then increases (around 300 hours). Two pairs of ball bearings worked around 400 hours and one pair for 515 hours. An increase in friction torque by 2.5 to 3 times with respect to the value of friction torque measured after 10 hours of operation corresponded to these service lives. The increase in friction torque as a rule was accompanied by an increase in the noise level and vibration in bearings, indicating the approach of pull-out torque as a result of the failure of cages. Thus it is possible to judge the service life of self-lubricating ball bearings at high temperatures on the basis of the change in kinematic torque.

The change in friction torque with constant speed of rotation and identical loading conditions as a function of radial loading is shown in Fig. 7.14. It may be mentioned here that the radial load affects the friction torque very little and in the present case the basic losses were due to the type of lubricant. At the time of the test the bearing bath was filled to the lower contour of the shaft with lubricants of different viscosities.

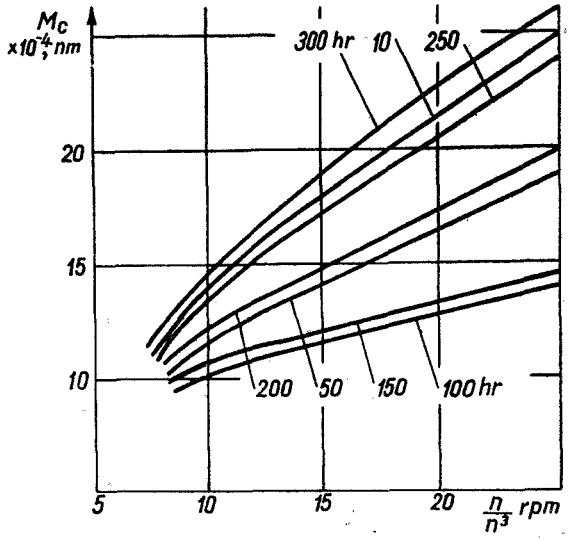

Fig. 7.13. Relation between friction torque and speed in bearings for different spells of operation. Ball bearings of A36025 Yu.T type, rings covered by molybdenum-sulphide lubricant (MoS_2), cage of AMAN material (reinforced).

Fig. 7.15 shows a family of curves characterizing the heating of a bearing at different rotational speeds and Fig. 7.16 the same thing at different loads. From an analysis of these curves we can conclude that the intensity of increase in the temperature of the bearing is linearly dependent on the rotational speed and parabolically dependent on the loading.

Heating of the bearing is an obstacle to the reduction of losses in the region of optimum loading. However, it is also worth considering that losses

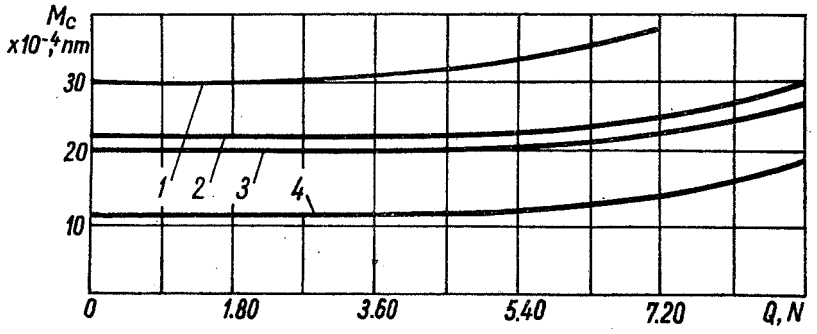

Fig. 7.14. Variation of friction torque in ball bearing of 200 type with radial load and bearing bath filled with oils:
1—castor; *2*—machine L; *3*—spindle oil; *4*—bearing cleaned with benzine.

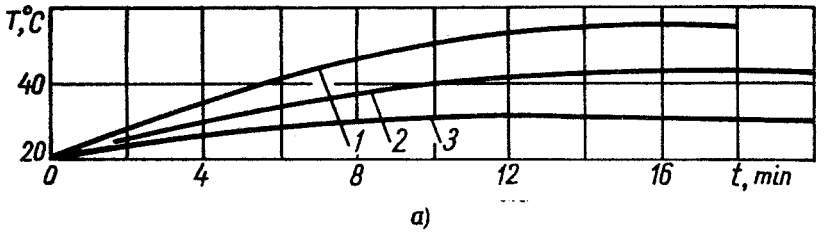

a)

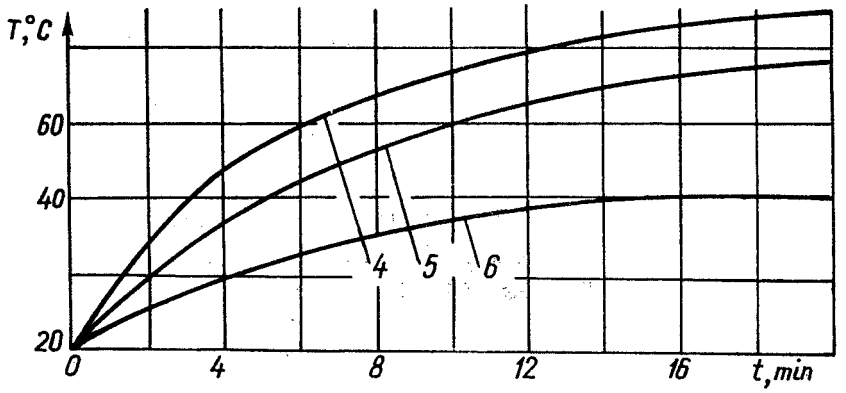

b)

Fig. 7.15. Variation with time in temperature of bearing 5 mm φ:
a—depending on speed; *b*—depending on radial load (at constant speed of 4,400 rpm); *1*—speed 4,800 rpm; *2*—33,000 rpm; *3*—16,080 rpm; *4*—without load; 5—load 5.40 N; *6*—load 3.0 N.

sharply increase with any increase in loading above the design value (Fig. 7.16). The increase in losses is due to the contact surfaces squeezing out lubricant under the increased radial load when the rise in temperature thins the lubricant.

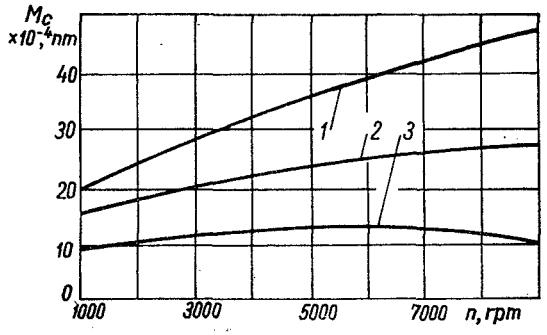

Fig. 7.16. Relation between friction torque and power transmitted in bearing of diameter 5 mm:
1—radial load 7.20 N; *2*—load 3.60 N; *3*—no load.

7.2 EFFECT OF LUBRICANT ON FRICTION TORQUE IN BEARINGS

A reduction in the variable friction torque component in bearings is basically achieved by raising the accuracy of manufacture of the contact elements of the bearing. However, there are limits to the increase in accuracy. Hence a proper choice of lubricant is of fundamental importance in this difficult and complex problem.

There are many studies on the influence of the type of lubricant on the operational qualities of bearings. Many works [6, 12, 23, 32, 35, 50, 51 and others] are devoted to the experimental determination of friction torque either in bearings or between rolling surfaces with the participation of lubricant. The works [7, 27, 34, 37 and others] give the results of studies on the physical phenomena taking place in the lubricating film.

In spite of a large number of works in this field it must be mentioned that there are no data on the influence of the type of lubricant on the variable friction torque component.

In order to study this factor a device was selected based on balancing the friction torque by the measuring torque. Semiconductor strain gauges were used as converters. Axial and radial loads were created with the help of elastic components (the device is described in detail in Chapter IV).

In order to measure the electrical resistance of a hydrodynamic lubricating film a measuring instrument working on AC [62] was used. This instrument can record both the constant and the variable components of friction torque. The power output makes possible recording by electromagnetic oscillograph.

Determination of the effect of lubricant on the variable component helps in the selection of the best working conditions of precision ball bearings used in the rolling contact supports of an LPM.

For this purpose ball bearings of type C26, C201 and C80202 were tested for a period of 10 hours of operation. Deslushing, cleaning and lubrication were carried out in the way followed in plants manufacturing magnetic recording apparatus. Preliminary tests showed that with a liquid lubricant friction torque in a bearing reached equilibrium value after 10 min and with grease, after one hour of operation of the bearing. The initial reduction in the friction torque of the bearing is associated mainly with the expulsion of excess lubricant.

These liquid lubricants were used in the tests: Velosit L, OKB 122–5, industrial oil of types 12, 20, 45, and 50, aviation oil MS-20 and transmission oil TAp-15. Grease of the following types was used: TsIATIM 221S, TsIATIM 201, TsIATIM 221, OKB 122–7 and Starfak-2.

In the study of the components of friction torque in bearings an important role is taken by the constant component which characterizes the total energy losses to friction in the bearing and consequently in the whole machine. This is important when computing the power required and for other design computations of low-power machines.

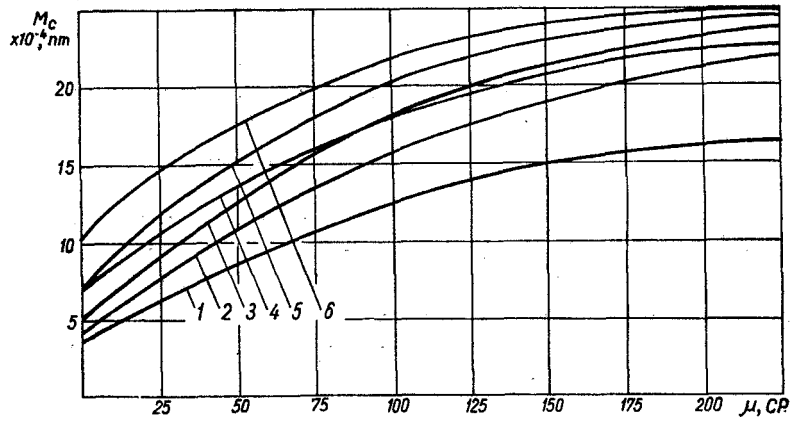

Fig. 7.17. Relation between friction torque in bearing of C26 type and viscosity of oil at speed of 50 rad/sec and radial load: *1*—no load; *2*—10 N; *3*—20 N; *4*—30 N; *5*—40 N; *6*—50 N.

Test results show that with an increase in the viscosity of the lubricant constant friction torque increases sharply (Fig. 7.17). This supplies a basis for the assumption that in instrument ball bearings considerable hydrodynamic resistance results if there is a large amount of lubricant. To reduce this resistance in ball bearings it is advisable to use lubricants of very low viscosity. However, the design features of ball bearings do not always allow reduc-

tion in the viscosity of the lubricants used. Lubricants of low viscosity may ooze out through the seal of the bearing assembly. It is interesting to note that unlubricated bearings have the lowest friction torque. However, this is at the cost of abrasion resistance, anti-corrosion, etc.

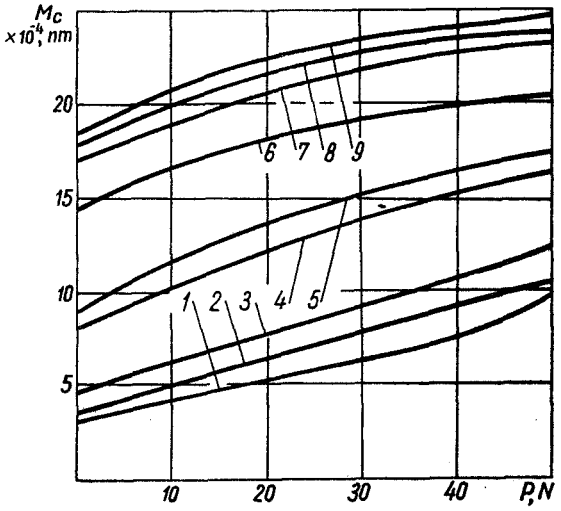

Fig. 7.18. Relation between friction torque in bearing of C26 type and radial load at speed of 25 rad/sec:
1—unlubricated and lubricated with oils; *2*—OKB 125–5; *3*—Ind. 12; *4*—Ind. 45; *5*—Ind. 50; *6*—TAp-15; *7*—MS-20; *8*—OKB 122–7; *9*—TsIATIM 221.

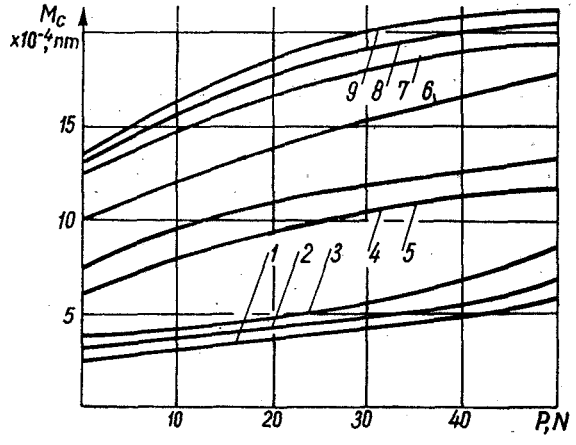

Fig. 7.19. Relation between friction torque in bearing of C26 type and radial load at speed of 50 rad/sec:
1—unlubricated and lubricated with oils: *2*—OKB-5; *3*—Ind. 12; *4*—Ind-45; *5*—Ind-50; *6*—TAp-15; *7*—MS-20; *8*—OKB 122–7; *9*—TsIATIM 221.

On the basis of an analysis of Figs. 7.18, 7.19 and 7.20 it is possible to say that with an increase in radial load friction torque gradually increases for all types of lubricants. This is due to the pressure increase in the lubricating

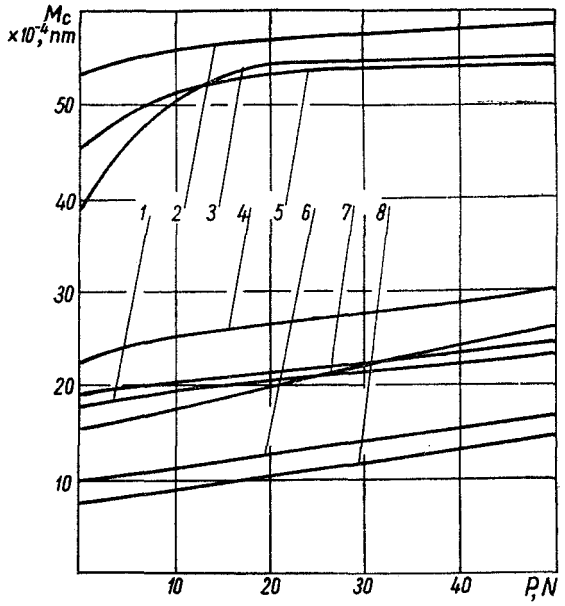

Fig. 7.20. Relation between friction torque in bearing of C201 type and radial load at speed of 50 rad/sec and lubrication by oils: *1*—OKB 122–7; *2*—MS-20; *3*—TAp-15; *4*—Ind-50; *5*—TsIATIM 221; *6*—Velosit L; *7*—Ind-12; *8*—(unlubricated); *9*—OKB 122–5.

layer with the increase in load. Besides, the deformation of contact surfaces increases the area of the separating film. Losses to friction increase when the film layers are displaced with respect to each other. It is worth mentioning that for all lubricants friction torque in the C26 bearing increased more slowly than in the C201 bearing.

Along with the measurement of friction torques in the bearing the complex electrical resistance GMP was measured. Certain works assume a directly proportional dependence of the electrical resistance of the lubricating film on its thickness. According to this the change in the value of electrical resistance qualitatively characterizes the variations in the thickness of the lubricating film. Owing to the difficulty of reliable calibration we will confine ourselves to study of the behavior of electrical resistance GMP.

The results obtained from the study of electrical resistance refute the claims of certain workers that with an increase in loading the thickness of the layer does not change. From analysis of Figs. 7.21, 7.22, 7.23 and 7.24 it is

clear that in almost all cases the electrical resistance sharply falls with an increase in loading except in the case of resistance marked by curves *2*, *3* (Fig. 7.23) and *2*, *3*, *5* (Fig. 7.24).

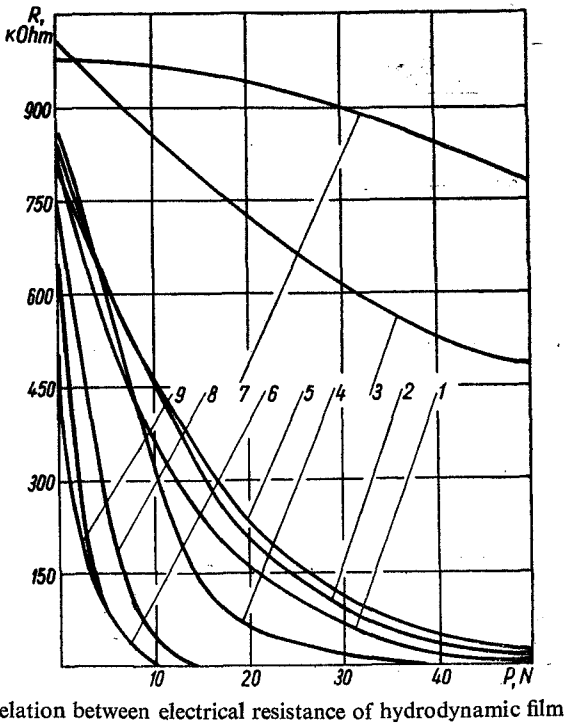

Fig. 7.21. Relation between electrical resistance of hydrodynamic film in bearing of C26 type and radial load at speed of 50 rad/sec and lubrication with oils: *1*—Ind. 12; *2*—Starfak-2; *3*—Ind. 40; *4*—TsIATIM 221; *5*—MS-20; *6*—OKB 122–7; *7*—TAp-15; *8*—Velosit L; *9*—Ind. 12.

Of special interest is the fact that in the range of loads considered the electrical resistance of certain types of lubricants falls to zero. This indicates that a metal contact develops between contact surfaces and this is a very bad working condition. Lubricants of the types OKB 122–7, OKB 122–5, Velosit-L and industrial type 12 used for lubricating the C201 bearing belong to this category. In the C26 bearing the most stable film developed with 50 industrial oil and TAp-15 transmission oil. With an increase in speed the thickness of the film of all lubricants increases. With an increase in the size of the bearings in the same loading conditions a more stable film is observed with bearings of larger sizes (C26 and C201).

It is worth mentioning that a definite relationship between electrical resistance and the viscosity of the lubricant was not established. It is clear that electrical conductivity is almost independent of the viscosity of the lubricant. The

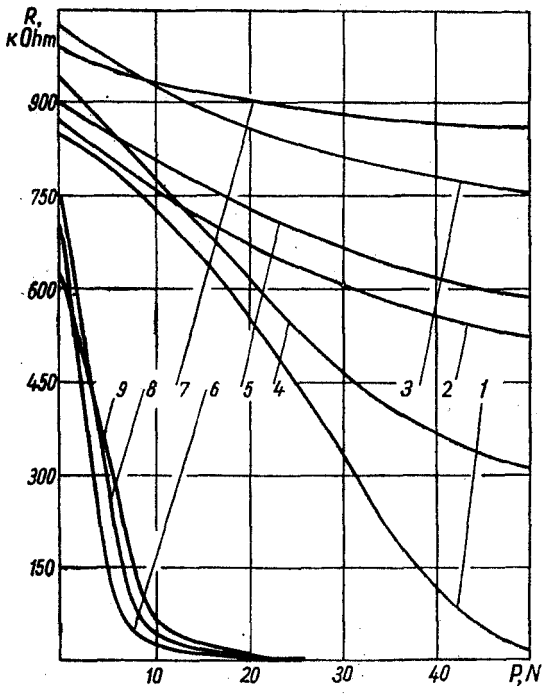

Fig. 7.22. Relation between electrical resistance of hydrodynamic film in C26 bearing and radial load at speed of 50 rad/sec and lubrication with oils: *1*—Ind. 12; *2*—Starfak-2; *3*—Ind. 50; *4*—TsIATIM 221; *5*—MS-20; *6*—OKB 122-7; *7*—TAp-15; *8*—Velosit-L; *9*—Ind. 12.

chemical composition of the lubricant and its internal structure have the maximum effect on the value of electrical resistance. Besides, the values of electrical resistance GMP depend on the content of mechanical impurities and water entering the lubricant during its preparation and use.

The electrical resistance of all types of lubricants increases sharply (Fig. 7.25) with an increase in the speed of rotation. It is worth emphasizing that the lubricating film is developed not immediately but on achieving a certain speed of rotation whose value depends on the type of lubricant, loading and size of the bearing.

Study of the variable component of friction torque yielded limited characteristics on the effect of possible disturbances on uniform motion. The effect of the type of lubricant is the most neglected among all the causes of the variable component of friction torque in bearing.

The results of tests showed a close relation between the state of the lubricating layer and the variable component of friction torque. Fig. 7.26 gives characteristic oscillograms of the variable component of friction torque and

the variable component of electrical resistance (VCER) of the C26 bearing. It can be seen from Fig. 7.21 that for a load of 25N using lubricant OKB 1–7, metal contact occurs. This state of the film affects the variable component of friction torque amplitudes of oscillations in VCER. It is considerably greater

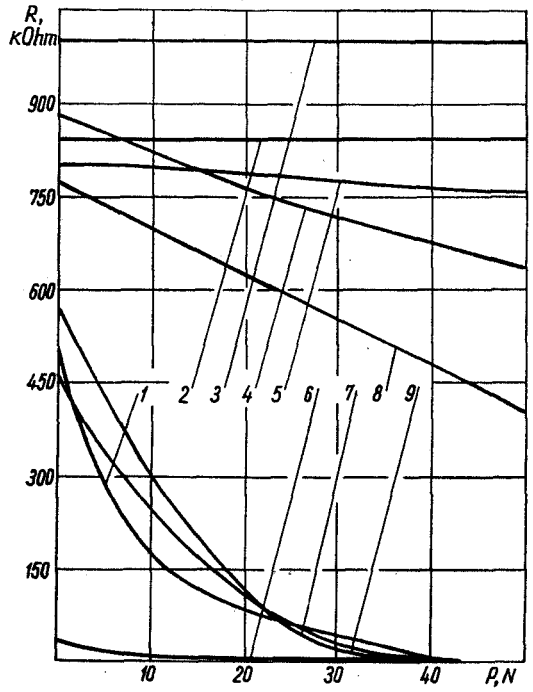

Fig. 7.23. Same as Fig. 7.22 for bearing of C201 type, speed 25 rad/sec and lubrication with oils:
1—OKB 122–7; *2*—MS-20; *3*—TAp-15; *4*—Ind. 50; *5*—TsIATIM 221; *6*—Velosit-L; *7*—Ind. 12; *8*—(unlubricated); *9*—OKB 122–5.

(Fig. 7.26 c) than the variable component of friction torque amplitudes (Fig. 7.26 b) where the metal component is absent. This change of state in GMP also distorts the character of VCER: the smooth curve (Fig. 7.26 a) becomes a series of jumps (Fig. 7.26 c).

With an increase in the viscosity of the lubricant the peak values of the variable component of friction torque appreciably increase (Fig. 7.27). It is also worth mentioning that with the increase in the viscosity high frequencies are cut off. The value of these frequencies corresponds to the frequency of geometric defects in the raceways, whose wavelength is commensurate with the length and width of the lubricating film.

We must note that with the use of certain greases the amplitude of vibrations of the variable component of friction torque (VFT) can be less than with

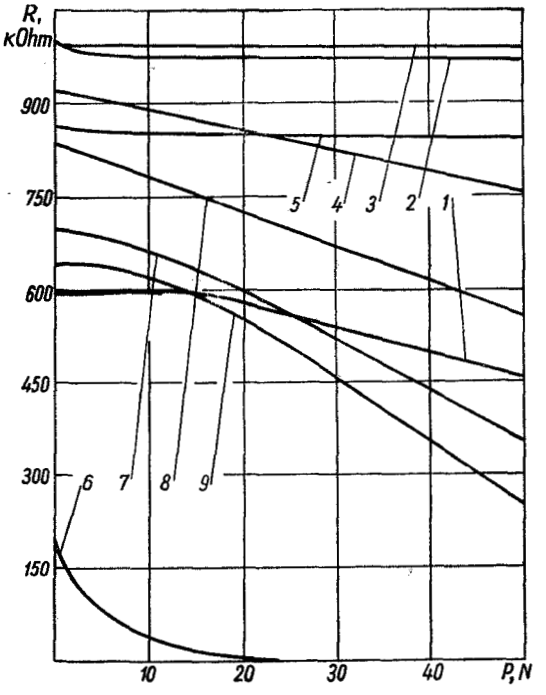

Fig. 7.24. Same as Fig. 7.23 at speed of 50 rad/sec.

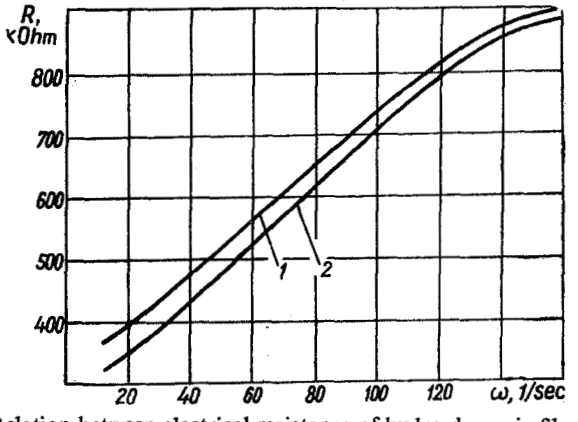

Fig. 7.25. Relation between electrical resistance of hydro-dynamic film in bearing of C18 type and speed for radial load of 30 N: *1*—OKB 122–7; *2*—MS-20.

the use of certain liquid lubricants (Fig. 7.27) (lubricants OKB 122–7, Starfak-2). This is because the physical and chemical properties of the lubricants are not only dependent on their viscosity. In certain working conditions of rubbing components of ball bearings, the thickness of the film and the value of

friction torque may be appreciably affected by the capacity of the lubricating layer to separate the rubbing surfaces of the bearing and to avert metal contacts between them, ensuring a coefficient of friction that is not too large (the so-called lubricating capacity of oil).

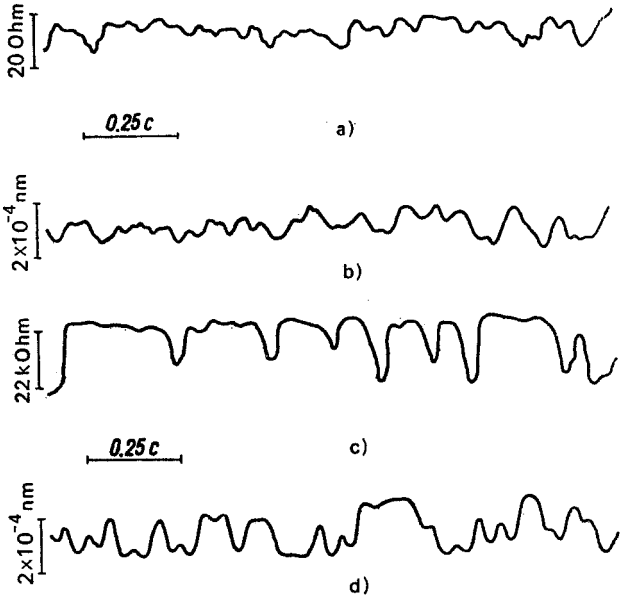

Fig. 7.26. Oscillogram of variable components of (*a*, *c*): electrical resistance and (*b*, *d*) friction torque in bearing of C26 type; lubricant OKB 122–7; radial load 10 N (curves *a*, *b*) and 25 N (*c*, *d*).

This property of lubricants does not depend on their viscosity and appears basically in conditions of boundary friction when the rubbing surfaces are separated by a thin molecular layer of the lubricant. Many workers have established that the molecules of lubricants can orient themselves on metal surfaces by forming structural layers having the capacity to bear high normal pressures and ensure a low coefficient of friction during relative movement of the surfaces. The lubricating capacity of oils depends on the degree of orientation of the molecules of the specific lubricant on the given metal, on the strength of bonding between molecules of the lubricant and of the metal and between molecules of the oriented lubricating layer. The breaking of these bonds leads to destruction of the oriented layer and to the occurrence of metal contact between rubbing surfaces, i.e. to loss of the capacity of the oil to lubricate.

However, quantitative criteria characterizing the lubricating capacity of lubricants are not available. Hence it is not possible to obtain a definite relationship between VFT and the type of lubricant on the basis of its physical properties alone. We can only say that among the greases tested OKB 122–7

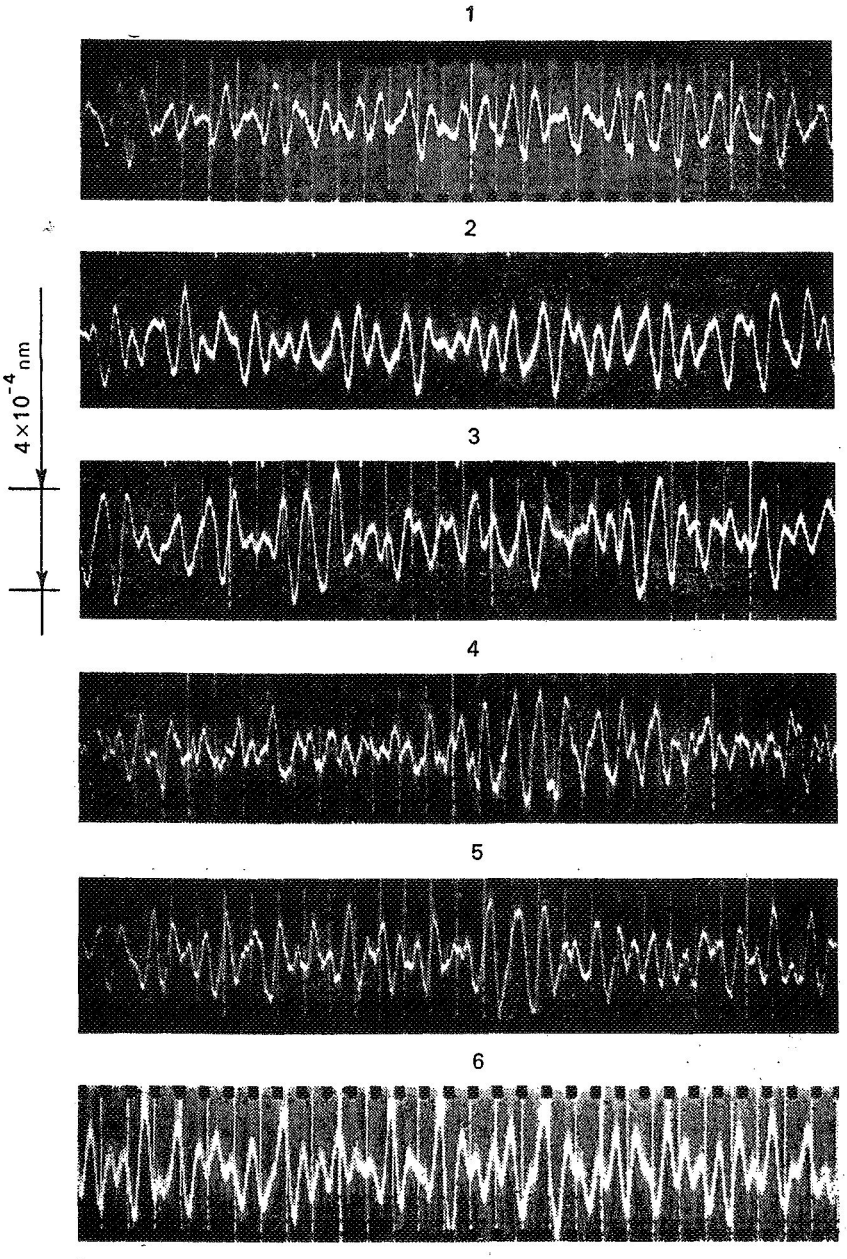

Fig. 7.27. VFT of C80202 bearing using different lubricants. Speed: 120 rad/sec. Radial load 30 N. Types of lubricants: *1*—Ind. 20; *2*—Ind. 50; *3*—TAp-15; *4*—OKB 122–7; *5*—Starfak-2; *6*—TsIATIM 221. Time scale: 0.01 sec for each interval.

and Starfak-2 created VFT whose amplitudes were less than those with certain liquid lubricants. Lubricants of the types TsIATIM 201, TsIATIM 221 and TsIATIM 221S develop maximum VFT.

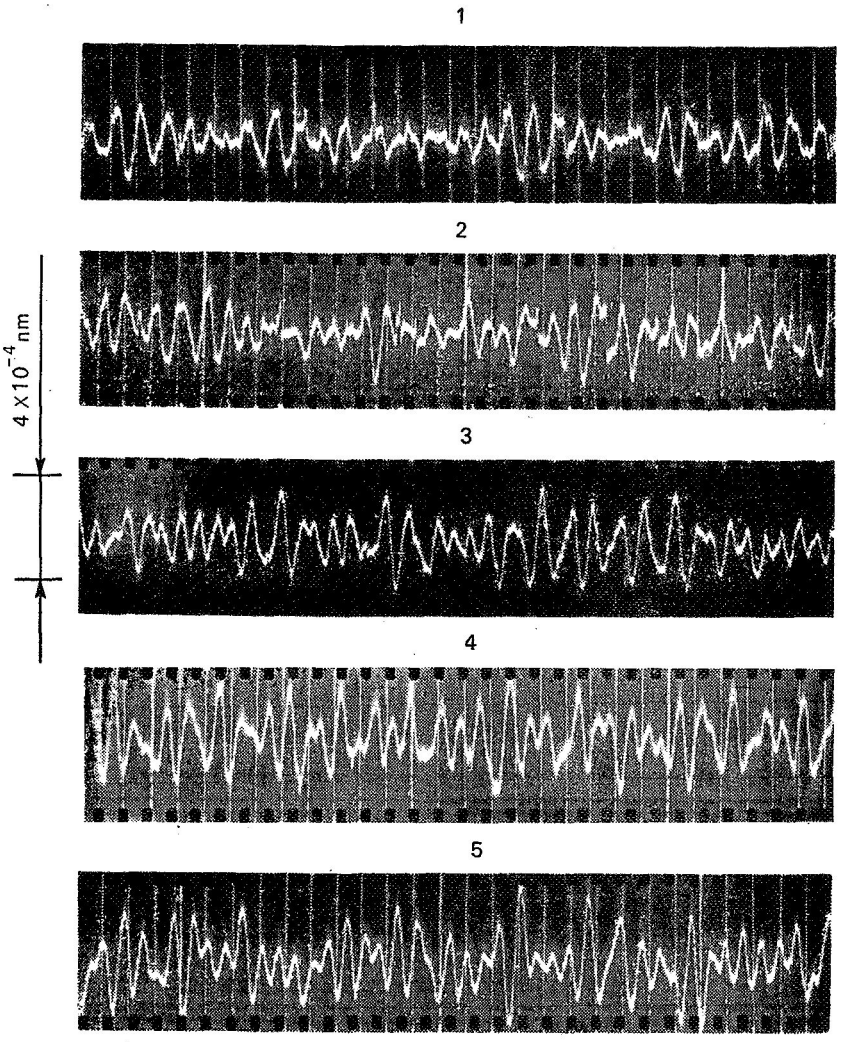

Fig. 7.28. VFT of C80202 bearing for various radial loads. Speed: 120 rad/sec; lubricant: TsIATIM 221; *1*—no load; *2*—10 N; *3*—20 N; *4*—30 N; *5*—40 N. Time interval 0.01 sec.

The increase in radial load relative to VFT is similar to the increase in the viscosity of the lubricant. With an increase in loading the peak values of the amplitudes of VFT are considerably increased (Fig. 7.28). This is because with the increase in load the pressure and viscosity of the film also increase and

friction losses between neighboring layers of lubricant likewise. Besides this, the contact area increases and with it the losses due to differential sliding and the role of geometric defects.

Parallel recording of the VFT of all types of lubricant and oscillation of the electrical resistance GMP was carried out. The analogous nature of the two curves confirms that the principal cause of the appearance of VFT in the hydrodynamic working condition of the bearing is the change in the total thickness of the film due to geometric defects in the rings and rolling elements. Electrical resistance is not a complete analogy of VFT. When the lubricant clogs or when there is metal contact large differences (Fig. 7.26 c, d) arise between VFT and the electrical resistance.

However, the complex nature of curves for the hydrodynamic working condition of the bearing indicates the possibility of describing VFT in terms of changes in the electrical resistance GMP. This method can be especially effective, for example, when determining the VFT due to vibrations, impacts, high and low temperatures and other cases, because the direct determination of VFT is difficult.

7.3 STUDY OF THE DYNAMIC PARAMETERS OF HIGH-SPEED ROTORS IN BALL BEARING SUPPORTS

Modern rotor systems mounted on high-speed precision ball bearings mostly use precision radial-thrust ball bearings with preload. In many mechanisms like high-frequency electrical shafts, inertial navigation instruments,

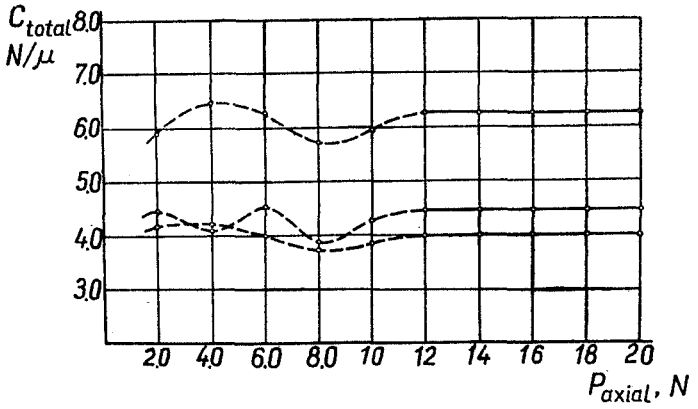

Fig. 7.29. Stiffness characteristics of three designs of rotors.

aviation engines and other instruments with the high-speed parameter of $D_{av} \times n_p = 2-3 \times 10^6$ mm rpm a suitable substitute is yet to be found for rolling contact bearings [1]. In the field of the dynamics of high-speed precision ball

bearings and assemblies there are many unsolved problems. The axial vibrations of a high-speed rotor, flexible in the axial direction and rotating in two precision ball bearings, have not been sufficiently studied. Accurate data on the level of vibrations of one bearing and a rotor of this design are not available at all. The nature of lubricant, the stability of the lubricating layer and their effect on the dynamic characteristics of the rotor are unknown.

The complexity of vibrational phenomena in rolling contact bearings and their dependence on a large number of factors (speed of rotation, loading, surface smoothness of raceways, state of lubricant, temperature, design, rotor stiffness, etc.) make an exact analytical description of all the physical phenomena occurring in high-speed ball bearings difficult. We have to tackle this problem and verification of theoretical computations by experimental methods.

This section gives the results of experimental studies on the principal dynamic parameters and axial vibrations of individual components of a high-speed rotor flexible in the axial direction and working in a vacuum at temperatures ranging from 40 to 120°C.

One of the dynamic characteristics of this rotor is its axial stiffness in the assembled form, which depends on axial loading. Theoretical computations of displacement of the rotor center under the action of external axial loading were carried out by M.P. Kovalev [24]. They are described by a linear function of axial load. The stiffness of the cover, geometric and design data on the ball bearings and their axial tension are the parameters affecting the displacement of the rotor center.

In order to determine the stiffness characteristics of rotors mounted in bearings of the 406075 type use is made of an inductance transducer of high sensitivity and a matching amplifier unit. The stiffness characteristics obtained are given in Fig. 7.29. The broken lines indicate a certain scatter in experimental results which straightens out when the external axial loading exceeds 12 N, indicating the true value of stiffness. The scatter of points at small external

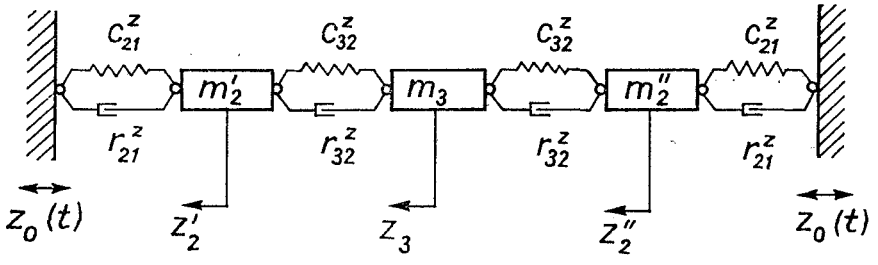

Fig. 7.30. Dynamic model of setup for determining amplitude-frequency characteristic of rotors: c_{21}^z, r_{21}^z—stiffness and damping elements of bearings; c_{32}^z, r_{32}^z—stiffness and damping element of rotor cover; m^3—rotor mass; m_1', m_2''—mass of outer rings and components of fixture of first and second bearings respectively.

axial loading is due to certain errors in measurements and nonuniform deformation of the bearing components caused by defects in their geometric shapes.

Besides stiffness characteristics the experimental amplitude-frequency characteristics of rotors of the above design have also been drawn. For this purpose the assembled cover was mounted on a vibration test stand with vertical axis of rotation of the rotor. The dynamic model of the setup is shown in Fig. 7.30. Forced vibrations of the rotor were calibrated in the following way: The rotor was deformed in the axial direction by the external load and its displacement was measured by the inductive transducer and amplifier with a sensitivity of 0.2 μm. The deflection of the light ray was simultaneously noted on the oscilloscope. The source of vibrational excitation was the vibration test stand. During the experiments the amplitude of vibrations of the test stand was kept constant: $2A_0=0.211$ μm. Resonance amplitudes were read on the oscilloscope screen. The accelerations were measured with the help of a set of devices which included piezoelectric transducers of high sensitivity. Later the rotor was run up to 15,000 rpm and the tests were repeated in the dynamic condition. The errors in the values of resonance amplitudes read from the screen are greater in this case because vibrations of the rotor caused by the ball bearings are introduced. Since the magnitude of resonance amplitudes exceeds these vibrations of the rotor by 10–16 times the determination of resonance amplitudes does not pose difficulties. The amplitude-frequency characteristics obtained in the range 500–1,700 Hz are shown in Fig. 7.31, where

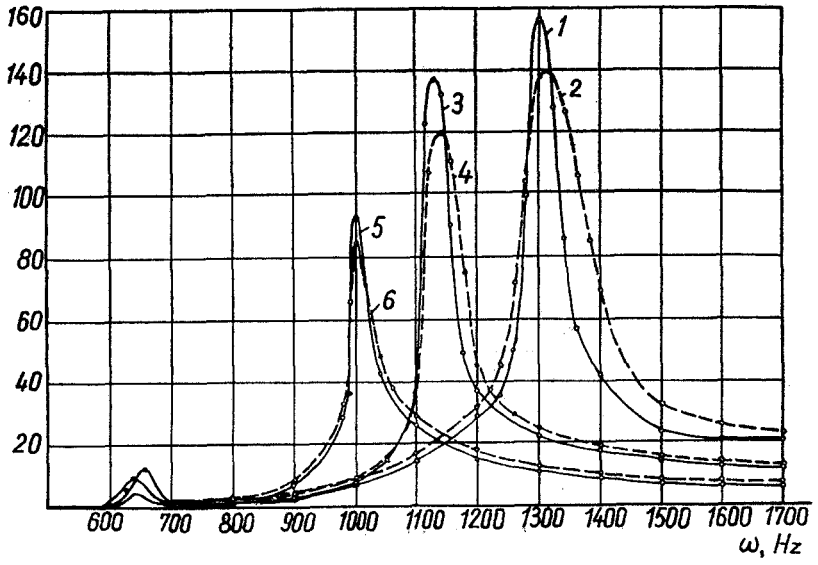

Fig. 7.31. Amplitude-frequency characteristic of rotors of first, second and third designs respectively: *1, 3, 5*—instatic; *2, 4, 6*—at rotor speed of 15,000 rpm.

the ordinate represents the ratio of resonance to excitation amplitudes, ξ_a. The characteristics obtained describe only the first fundamental eigen frequencies of the rotor. The second and third eigen frequencies caused by masses m_2' and m_2'' (Fig. 7.30) are observed in the range of frequencies 2,600–3,000 Hz. However, the quantity ξ_a is several times smaller in these cases and for our purposes is of no interest. It is important to mention, however, that when rotors of this design are run at a speed of 15,000 rpm the amplitude-frequency characteristics are somewhat changed: the quantity ξ_a in all cases is reduced and the natural frequency has a tendency to shift upward by 20–25 Hz. For a rotor of a third design this difference was smaller, a mere 5–8 Hz.

The relation between axial stiffness of rotors and the corresponding eigen frequencies is shown in Fig. 7.32. The empirical relation obtained is nonlinear and tallies well with published theoretical results [18, 52]. A reduction in the ratio of amplitudes ξ_a (see Fig. 7.31) during the rotation of the rotor is explained by the increase in the damping coefficient of the ball bearings. This is due to the appearance of a lubricating layer between the rolling elements and the raceways and also to the absorption of vibrational energy during the impacts of rolling elements on the surface of the raceways.

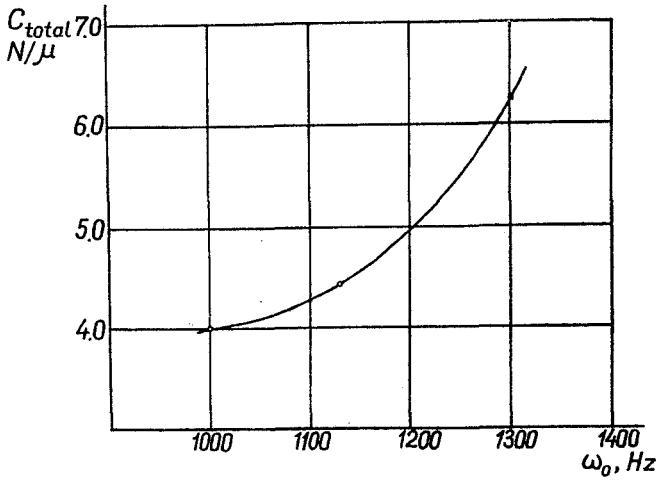

Fig. 7.32. Relation between axial stiffness of rotor and corresponding fundamental frequencies.

Damping forces caused by bearings, especially high-speed ones, have not been adequately studied and the data characterizing their magnitude are contradictory [49, 58, 66]. Yet the damping coefficient is one of the most important factors determining the state of the system [39, 40, 42] and one of the most important parameters for determination of the conditions for instability of rotor vibrations. The value of the damping coefficient can be judged on the basis of the following parameters: high-Q, width of resonance peak, logarith-

mic decrement vibrations, etc. [41, 52, 63 and others]. The design of the mechanical part of the test stand makes it possible to determine the nondimensional damping coefficient using the amplitude-frequency characteristics obtained earlier (Fig. 7.31), taking into account the changes in the ratio of amplitudes of fundamental resonance.

It is assumed that for this system (Fig. 7.30) the following condition is satisfied

$$m_3 \gg m_2' + m_2''.$$

Then it can be regarded as a single-mass system having a single degree of freedom. In the dynamic condition where the rotor runs at 15,000 rpm damping parameters r_{32}^z do not change relative to the static condition. Hence a change in damping will be entirely due to the change in the hydrodynamic condition in the bearings. In the case of a single-mass system (Fig. 7.30) capacitor transducers record the vibrations of the rotor relative to the casing. The equation of motion has the following form:

$$m_3 \ddot{z}_3 + h(\dot{z}_3 - \dot{z}_0) + k(z_3 - z_0) = 0. \tag{7.2}$$

The movement of the casing on the vibration test stand is determined by the function

$$z_0(t) = A_0 \sin \omega t, \tag{7.3}$$

and the relative vibrations recorded by capacitor transducers $z(t)$ have the following expression:

$$z(t) = z_3(t) - z_0(t). \tag{7.4}$$

In such a case equation (7.2) is transformed into the form

$$m_3 \ddot{z} + h\dot{z} + kz = m_3 \omega^2 A_0 \sin \omega t, \tag{7.5}$$

whose solution is

$$z = \frac{A_0 r^2 \sin(\omega t - \varphi)}{\sqrt{(1-r^2) + (2\zeta_n r)^2}}. \tag{7.6}$$

In the case of resonance, when $r = 1$, the nondimensional damping coefficient is determined from the relation [61]

$$\zeta_n = \frac{1}{2\xi_{a_{max}}}, \tag{7.7}$$

The change in the nondimensional damping coefficient during rotation of the rotor is given by

$$\Delta\zeta_n = \frac{\xi_{a_{max}} - \xi'_{a_{max}}}{2\xi_{a_{max}}\xi'_{a_{max}}}, \tag{7.8}$$

where $\xi_{a_{max}}$ and $\xi'_{a_{max}}$ are the maximum ratios of amplitudes for static resonance and for rotation of the rotor at $n_r = 15{,}000$ rpm, respectively.

The empirical results show that in the dynamic domain, when the rotor rotates at 15,000 rpm the nondimensional damping coefficient is increased in all cases. The principal cause of this is the appearance of a hydrodynamic lubricating film in the bearings when the rotor rotates. Consequently the change in the damping coefficient of the bearings should entail a change in the vibrational process of the rotor components in different working conditions of the bearing. These assumptions have been verified by experiment.

For measurement of axial vibrations of individual components of a high-speed rotor of the third design—outer rings of ball bearings and the basic mass of rotor z_2' and z_3 (Fig. 7.30)—special capacitor-type transducers were used with adequate stiffness and temperature stability. The axial stiffness of the rotor was equal to $4N/\mu M$ and natural frequency of vibration 1,000 H_z. The design of the transducers reduces to a minimum errors in measurement due to the incorrect geometric shape of the rotor components resulting from manufacturing defects. The working surface of the transducers is a thin palladium-coated layer of copper spread over the ceramic ring. The design of the transducer also provides for simultaneous measurement of the capacitance-impedance of each bearing without rearranging the test stand.

The capacitance of the transducer changes as a function of the vibration level. This variable capacitance in combination with the constant reactance forms an electric circuit whose resonance frequency determines the working frequency of the high-frequency oscillator. The physical quantities to be measured (in this case the rotor vibrations) are converted into vibrations with the signal frequencies given out by the oscillator. The frequency-modu-

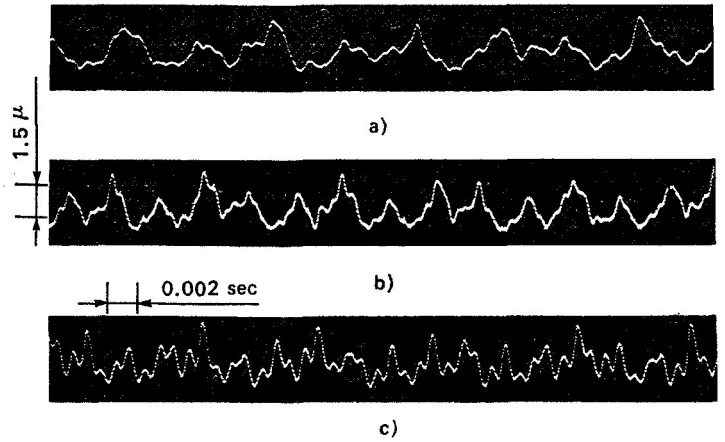

Fig. 7.33. Oscillograms of vibrations of outer ring of first bearing: $T_e = 60°C$; *a*—10,000 rpm; *b*—15,000 rpm; *c*—20,000 rpm.

lated signal is fed into the block of the capacitance converter in which a DC voltage is formed that changes in accordance with the modulation. The signal shows up on the indicator or is amplified and recorded by a loop-oscilloscope.

Calibration of the setup should be done with the help of instruments working with inductance transducers whose sensitivity is 0.02 μM. Preliminary tests show that the type of connection of the instruments affects the readings. Hence calibration of the instruments is carried out immediately after testing. Experiments were carried out at different speeds of the rotor, chamber temperatures of 40, 60, 80, 100 and 120°C and a vacuum in the chamber of 10^{-3} mm of Hg. The free space in the chamber was 145 cm^3. The temperature of the stationary rings of the bearings was measured with respect to the surrounding medium and was recorded by the improved EPP-09M3 instrument.

Figs. 7.33 and 7.34 show oscillograms of axial vibrations of the rotating ring of the first ball bearing at different temperatures and rotor speeds. Fig. 7.35 shows oscillograms of axial vibrations of the rotating rotor at different speeds with the temperature of the surrounding medium 100°C.

Defects in the geometric shape of the bearing component and of the rotor on the surface of which vibrations were measured and the setup of the transducer itself adversely affect the measurement of axial vibrations using capacitor contactless transducers. The edge effects of the capacitor-transducer and harmful effect of rough components are minimized by a proper selection of transducer design [38, 59]. Only the oscillations due to edge effects have any influence on the oscillograph reading. A periodic component equal to 100 Hz observed in all working conditions of the rotor was not taken into

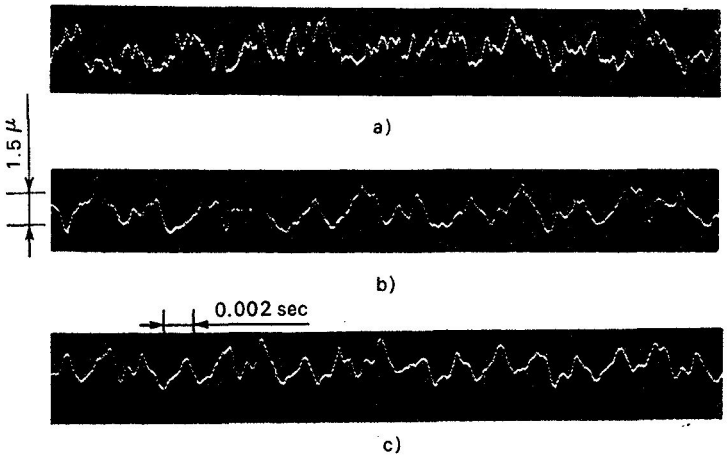

Fig. 7.34. Same as Fig. 7.33; $T_c = 100$°C.

account in the oscillograms and in the analyses of rotor vibrations. The cause of this effect was the additional amplifier unit. Since these harmonics are not considered in the analysis of oscillograms and the study of vibrations caused by ball bearings the signals obtained can be assumed to correspond to the axial vibrations of the components of the bearing and the rotor.

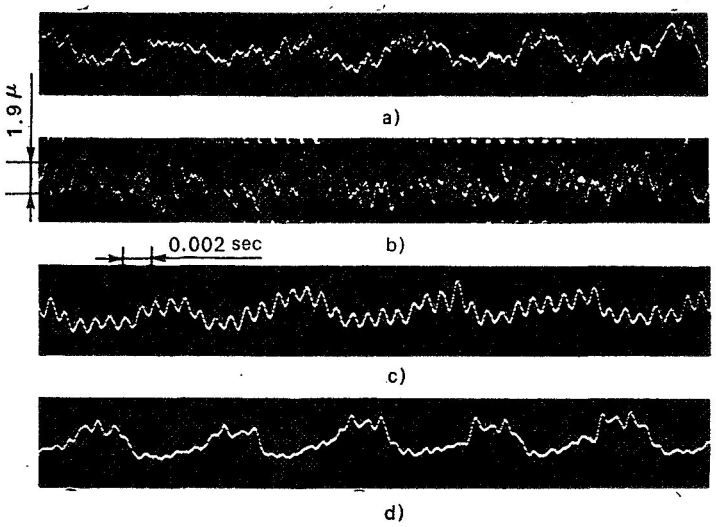

Fig. 7.35. Oscillograms of axial vibrations of rotor: T_c=100°C; *a*—10,000 rpm; *b*—15,000 rpm; *c*—20,000 rpm; *d*—30,000 rpm.

From an analysis of the oscillograms obtained it is not difficult to see that the amplitudes of vibrations of the first and second bearings are different. The amplitude of axial vibrations of the outer rings of the bearings in the steady state (for example at rotor speeds of 10,000 and 30,000 rpm) is 5–10% more than the amplitude of rotor vibration.

The configuration of the raceways plays an important part in the vibrational processes of bearings. After conducting the experiments the bearings are cleaned and with the help of a caliper the deviations from the circular of the raceways of the inner and outer rings and balls of both the bearings are recorded. Comparing the recordings of vibrations of the outer rings of the bearings and the deviation of the raceways from the correct geometric shape, it is possible to conclude that their maximum values are of the same order and the imperfect geometric shape of the raceways is one of the principal causes of axial vibrations of the outer ring of the ball bearing.

It can be seen from the oscillogram of rotor vibrations that at rotor speeds of approximately 20,000 rpm vibrations with a frequency of 1,000 Hz are excited corresponding to the natural frequency of the rotor (the phenomenon of parametric resonance). These vibrations dominate in the working

range of the rotor corresponding to a temperature of 120°C of the surrounding medium. The amplitude of vibrations in this case is appreciably larger than when the rotor is in a chamber at a temperature of 40°C, when analogous excitation of vibrations was observed at higher speeds (20,400–20,600 rpm). These phenomena are explained by the effect of the magnitude and nature of damping in the bearings with the rise in ambient temperatures to 120°C on the magnitude of one of the critical speeds of the rotor in the 20,000–20,600 rpm range. A more detailed analysis of the effect of ambient temperature on the vibrations of bearings and rotor can be made by spectrum analysis.

The normalized spectral densities of vibrations of the moving ring of the first bearing are shown as an example in Fig. 7.36. In Fig. 7.37 analogous spectral functions of rotor vibrations are shown.

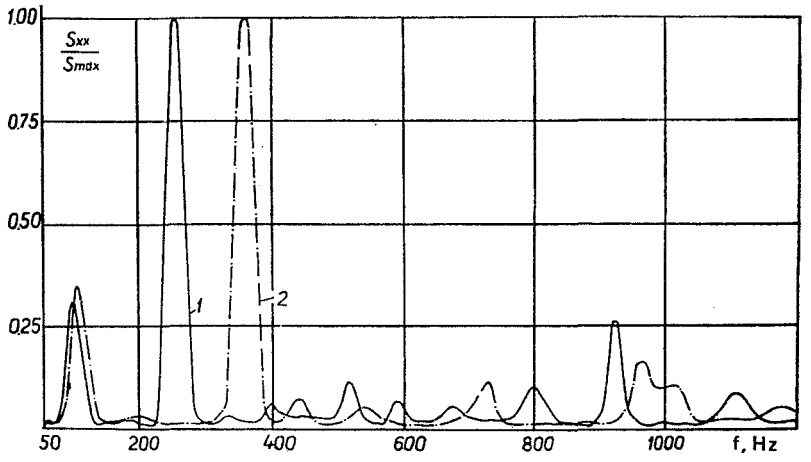

Fig. 7.36. Energy spectral densities of vibrations of moving ring of first bearing: *1*—T_c=120°C; n_r=15,000 rpm; *2*—T_c=100°C; n_r=20,000 rpm.

The vibrations of the bearing and of the rotor as a whole assume different natures with a rise in the ambient temperature to 100°C and higher. When the chamber temperature is 100–120°C and the rotor speed is 10,000 rpm or a little more, completely different, higher frequencies appear in the spectra, indicating a change in the working conditions of the bearings. If the allowable working temperature range (not more than 150°C) of the VNIINP-260 lubricant used in the bearing and the controllable heating of the bearing working in a vacuum are considered for the duration of the tests it is possible to conclude that the cause of the appearance of higher frequency components could be the change in the hydrodynamic condition of high-speed ball bearings at low speeds and the allowable temperature extremes of the lubricant. The introduction of these components may be the result of the more intense effect

on the vibrations of defects in the geometric shape and the surface roughness of bearing rings and the instability of the lubricating layer. According to existing analytical data [11, 22] a stable layer of lubricant in a high-speed bearing does not cause appreciable vibrations in the bearing components but is responsible for a certain amount of damping of high frequencies. It follows that a more comprehensive study is necessary using special techniques to stabilize the lubricating layer at different working conditions of the rotor.

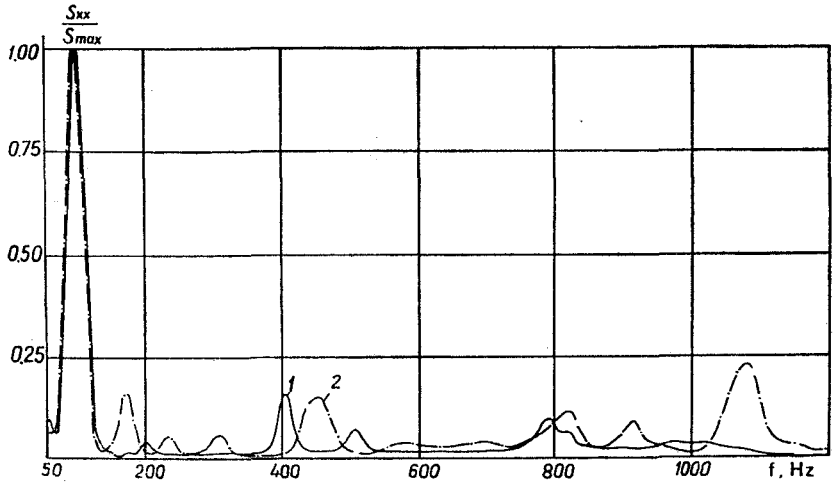

Fig. 7.37. Energy spectral densities of rotor: *1*—T_c=60°C; n_r=10,000 rpm; *2*—T_c=100°C; n_r=10,000 rpm.

7.4 EXPERIMENTAL STUDY OF HEATING, FRICTION TORQUE AND LUBRICATING CONDITIONS OF HIGH-SPEED BALL BEARINGS

High-speed ball bearings differ from others in that apart from external loads, the centrifugal forces acting on the balls and also the lubricating film appearing between the rolling elements and the raceways of the rings affect the displacement of the moving rings.

The main parameters characterizing the dynamics of a high-speed rotor in ball bearings are the friction torque in the ball bearings; electrical resistance of the hydrodynamic lubricating film characterizing its stability, thickness, the hydrodynamic condition between the rolling elements and the raceways and simultaneously determining the quality of the whole support; and the heating of the stationary bearing ring. For example, in gyroscopic instruments, under the action of axial vibrations of the rotor the friction torque changes in suspension supports [1]. A change in the hydrodynamic state of the lubricant in one of the bearings entails changes in vibrational phenomena and displacement of the rotor's center of gravity. The VFT in high-speed

ball bearings increases the wear and tear of raceways, causing instrument drift and reducing the reliability of the system.

The heating of the stationary ring of the bearing relative to the surrounding medium is not a decisive dynamic characteristic of the rotor system being studied. But it has an important role in determination of certain causes of change in the constant quantities of friction torque and the electrical resistance of high-speed ball bearings working in a vacuum at high temperatures and different conditions. The dynamic characteristics of the rotor and wear and tear of bearings are also subject to extreme heating of bearings [60].

Here we will study the rotor whose design and parameters have been described in preceding chapters.

While carrying out tests with the help of the EPP-09M3 instrument it was observed both during acceleration of the rotor and after the required speed was reached that the temperature of the bearing increased. After a period of 50–80 min its operation stabilized. When the motor operated in an atmosphere of air the stabilization period and the magnitude of heating were 50–60 percent less. The heating of a bearing working in a vacuum chamber is subject to two factors: heating of the rotor under the action of the supply current and frictional forces in the bearing itself. Heat transfer from individual parts of the rotor to the casing of the stand was effected by conduction and radiation [13 and others]. As a result of these tests it was established that the heating of the bearing ring depended on the means of reaching the working conditions of the rotor and also on how many times the rotor was accelerated to the desired speed: after a long period at rest or immediately after a continu-

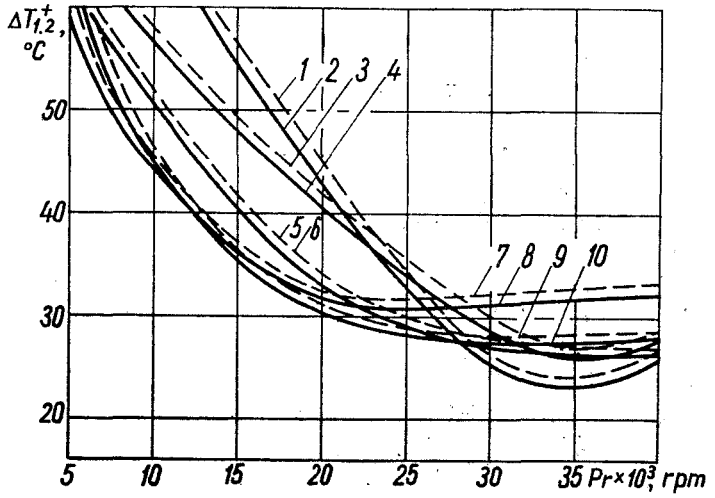

Fig. 7.38. Relation between heating of ball bearings and rotor speed with gradual increase in speed: *1, 3, 5, 7, 9*—of first bearing, respectively at T_c=40, 60, 80, 100, 120°C; *2, 4, 6, 8, 10*—of second bearing at same temperatures.

ous series of experiments. During the second and third runs of the motor the temperature of the bearing came down on the average by 10–15%. Hence all the measurements are carried out in a given sequence: before the test the motor is run at the rotor speed of 20,000 rpm for a period of 1.5 hours and then after a short stoppage the temperature of the bearings is measured simultaneously along with other parameters, namely friction torque and electrical resistance. First the rotor speeds are gradually increased (I range) (the values of differential temperatures in this case are indicated by ΔT_i^+, where i is the number of the bearing) and then gradually decreased by braking the rotor with the help of an electronic frequency converter (II range) $-\Delta T_i^-$. The readings of the values of temperatures and other parameters were carried out after stabilizing the heating of the bearings. The main results of the measurements are shown in Figs. 7.38 and 7.39. Approximate recordings of the change in differential temperature for different means of establishing the working speed of the rotor are given in Figs. 7.40 and 7.41.

The relations obtained show that during braking the differential temperature of the bearing is 2–5% higher than during acceleration in almost all cases. The extra heating is explained by overheating of the rotor and forced

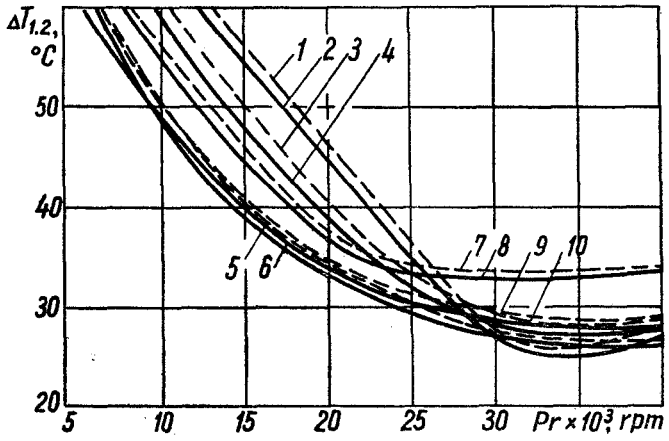

Fig. 7.39. Relation between heating of ball bearings and rotor speed during deceleration of motor: *1, 3, 5, 7, 9*—of first bearing for T_0=40, 50, 80, 100, 120°C; *2, 4, 6, 8, 10*—of second bearing for T_0=40, 50, 80, 100, 120°C.

mixing of the lubricant in the bearing. Besides this, the temperature of the first bearing relative to the surrounding medium is in all cases more than the second (except during acceleration of the motor, when they are occasionally equal). One more regularity is obvious. For this design of test stand the temperature of the bearings falls to a certain value with an increase in rotor speed and then in the interval 25,000–40,000 rpm has a tendency to increase. Besides

this, the results of the experiments are also somewhat affected by the power source of the EPCh-1 whose voltage output (especially at low rotor speeds) has not the ideal sinusoidal form but a stepped form [5, 10]. As a result of repeated running of tests with the help of an improved converter giving voltage of correct sinusoidal form on all phases analogous phenomena were recorded with one difference: the inclination of the family of curves (for rotor speeds up to 20,000 rpm) was not so steep.

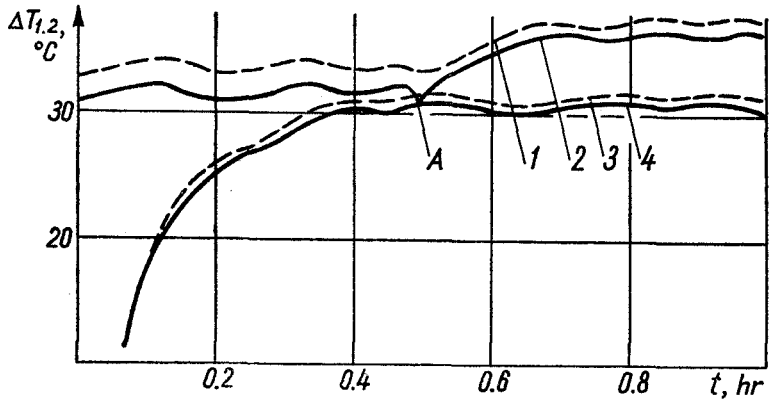

Fig. 7.40. Variation in differential temperature: $T_c = 100°C$; *3*, *1*—of first bearing in first (acceleration up to 20,000 rpm) and second conditions; *4*, *2*—of second bearing in first and second conditions; *A*—instant when motor running at 40,000 and 20,000 rpm, respectively, is switched off.

Comparing the recordings of the change in the heating of the bearing rings and the surrounding medium (readings on EPP-09M3 and KSM-4 instruments), we can conclude that vibrations of the temperature of the bearings in the steady state conditions are basically due to vibrations of the temperature of the surrounding medium and have an indentical frequency. Before measuring the friction torque, the components of the precision ball bearings of the 406075 type and the cage are carefully cleaned with Benzine and dried in the air. The film of oxide and moisture that forms evaporates during the initial run of the motor in a vacuum and does not significantly affect the results. Then, observing the technical conditions of the assembly of the bearings they are lubricated with VNIINP-260 grease. This has certain advantages compared to other forms of lubricants of the same type (large range of operating temperatures, better chemical composition, corrosion resistance and others).

Graduation of the apparatus for measurement of the constant and variable friction torques of bearings is carried out by applying an external torque of known value to the axis of the stator. In order to avoid additional errors the graduation is carried out according to a scheme analogous to the scheme of measurements without resetting the cover of the test stand. In order to

improve the accuracy of reading the constant components of friction torque of bearings a second, arrow-type indicator with a finer limit of measurement is introduced after balancing the measuring instrument.

The friction torque of high-speed ball bearings is a function that depends on many design, technological and operational parameters: speed of rotation of the moving rings; loads acting on the bearing; the viscosity, quantity and state of the lubricant; temperature and chemical composition of the surrounding medium, the state of contact surfaces; and the design and technology of manufacture of the bearing and of the rotor as a whole [8, 16, 19, 21, 54, etc.]. As a result of measurements it was established that even secondary factors affect friction torque (especially the constant component): time taken to make the bearing, test procedure and conditions, direction of rotation of the rotor

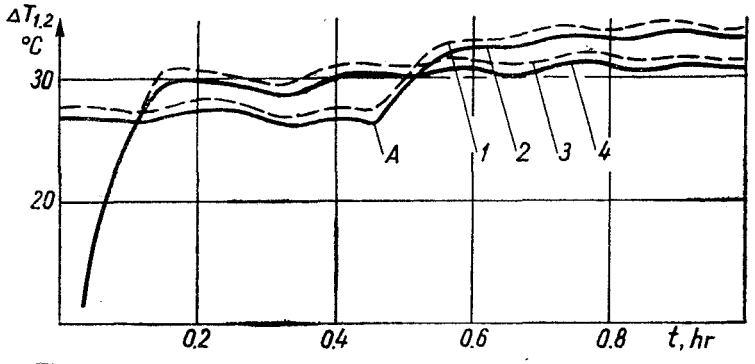

Fig. 7.41. Curves of variation in differential temperature: $T_c = 120°C$. Other conditions same as Fig. 7.40.

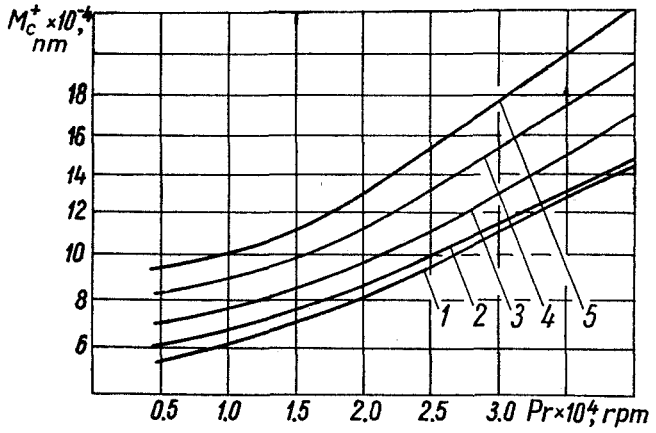

Fig. 7.42. Relation between change in constant value of friction torque of pair of ball bearings and rotor speed with increasing rotor speed: *1*—$T_c = 120°C$; *2*—$T_c = 100°C$; *3*—$T_c = 80°C$; *4*—$T_c = 60°C$; *5*—$T_c = 40°C$.

and method of establishing the desired speed conditions (with gradual increase or by reduction in speed).

Before the start of tests, after evacuating air from the chamber to 10^{-3} mm of Hg and establishing the required temperature of the surrounding medium, the rotor is run up to 20,000 rpm and heated for a period of 1.5 hours. The temperature of both the bearings relative to the surrounding medium is regulated by an improved automatic potentiometer EPP-09M3. After stabilizing the temperature of the bearings measurements of the constant and variable components of the friction torque of bearings are carried out at a given temperature and in all ranges of speeds. This is followed by an increase (m_p^+) and immediately afterward by a forced gradual decrease in speed—braking the rotor with the help of an electronic converter of frequency (m_p^-).

Empirical data from the study of the constant friction torque component are given in the form of graphs (Figs. 7.42 and 7.43). Fig. 7.43 shows dependence of the friction torque of bearings on the temperature of the surrounding medium.

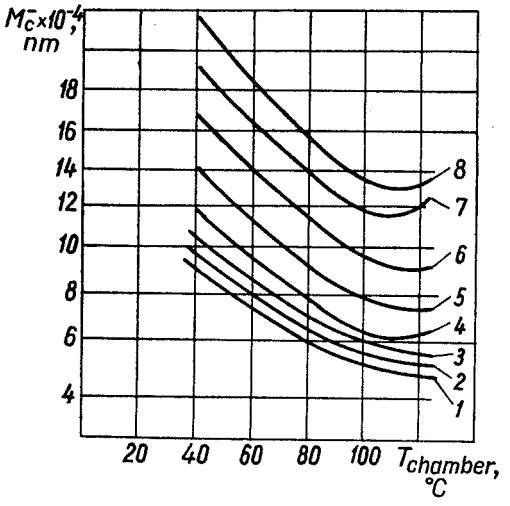

Fig. 7.43. Relation between change in constant component of friction torque of pair of ball bearings and temperature in chamber with gradual increases in rotor speed: *1*—n_r=5,000 rpm; *2*—n_r=10,000 rpm; *3*—n_r=15,000 rpm; *4*—n_r=20,000 rpm; *5*—n_r=25,000 rpm; *6*—n_r=30,000 rpm; *7*—n_r=35,000 rpm; *8*—n_r=40,000 rpm.

Analyzing the relations obtained, we may conclude that with an increase in the rotor speed the friction torque in the chamber decreases. The latter relation, apparently, is associated with a decrease in the viscosity of the lubricant and thereby with a reduction in the loss of power needed to overcome the resistance to motion. However, when the rotor operates in the range of temperatures 100–120°C at higher speeds a certain violation of this depend-

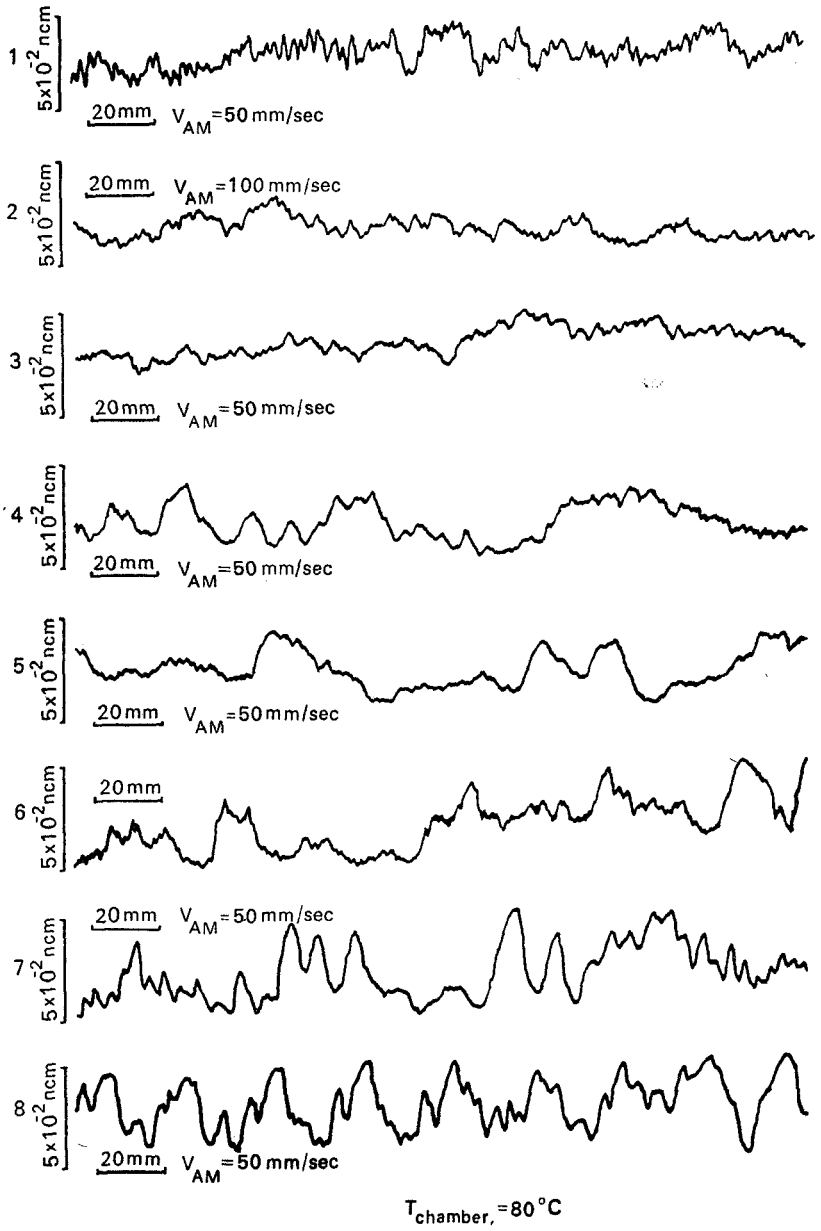

Fig. 7.44. Recording of variable values of friction torque in ball bearings:
T_c=60°C; *1*—n_r=5,000 rpm; *2*—n_r=10,000 rpm; *3*—n_r=15,000 rpm;
4—n_r=20,000 rpm; *5*—n_r=25,000 rpm; *6*—n_r=30,000 rpm;
7—n_r=35,000 rpm; *8*—n_r=40,000 rpm.

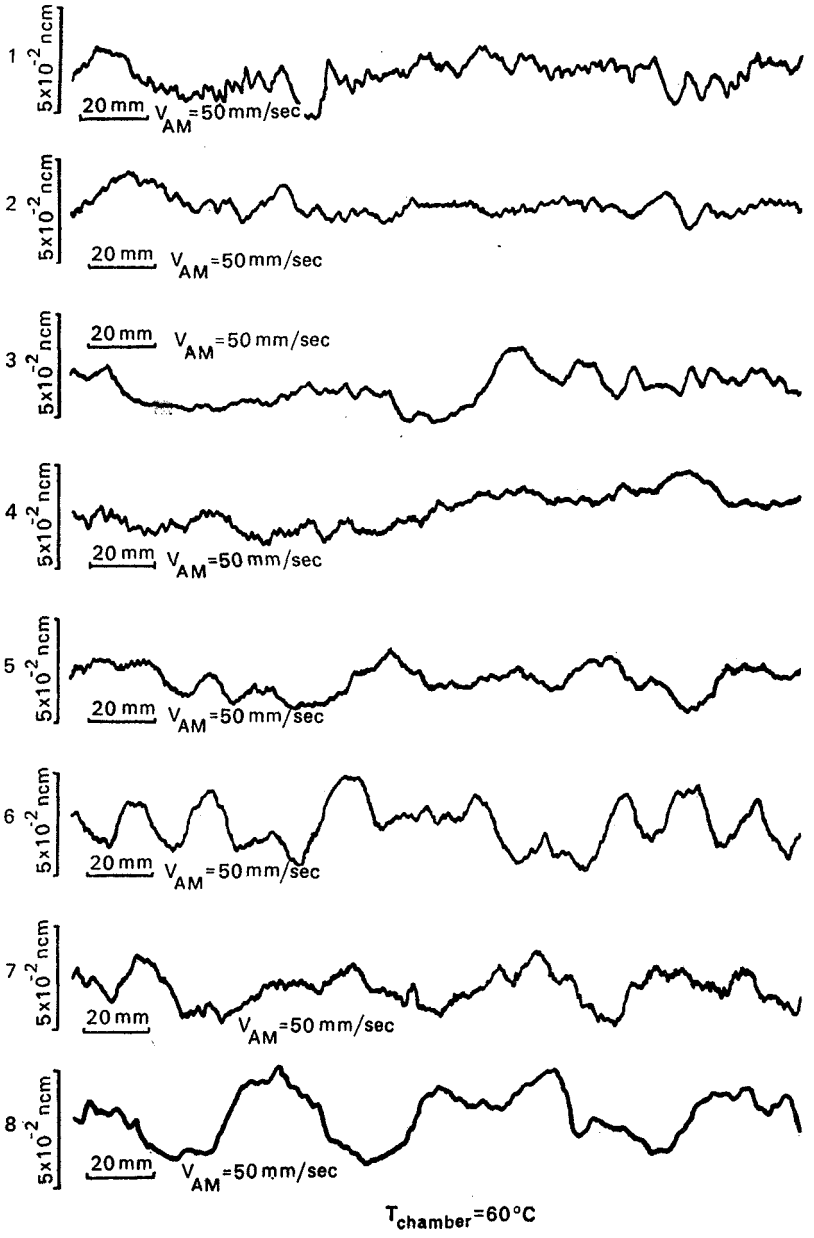

Fig. 7.45. Recording of variable values of friction torque of ball bearings: T_c=80°C. *1* to *8*—same as Fig. 7.44.

ence is noticed. This is explained by the nonuniform change in the geometric dimensions of individual parts of ball bearings as a result of the action of higher temperatures (the phenomenon of the squeezing of rolling elements). The point of minimum friction torque at rotor speeds from approximately 5,000 to 15,000 rpm is shifted in the direction of higher temperatures.

It was also established that with a gradual increase in rotor speed (Figs. 7.42 and 7.43) the high-speed friction of bearings was greater by 5–7% than during the smooth reduction in the speed of rotation (braking of the rotor) that followed. This is explained by the corresponding change in shear stresses in the lubricating layer when there is mechanical action in the processes of mixing of the lubricating layer and also by a certain increase in the temperature and heating of ball bearings during lengthy tests.

The variable components of friction torque (Figs. 7.44 and 7.45) obtained represent only the low-frequency fluctuations with a frequency up to 30–40 Hz having the maximum value in practice. Friction in high-speed ball bearings is not a regular but a purely random process.

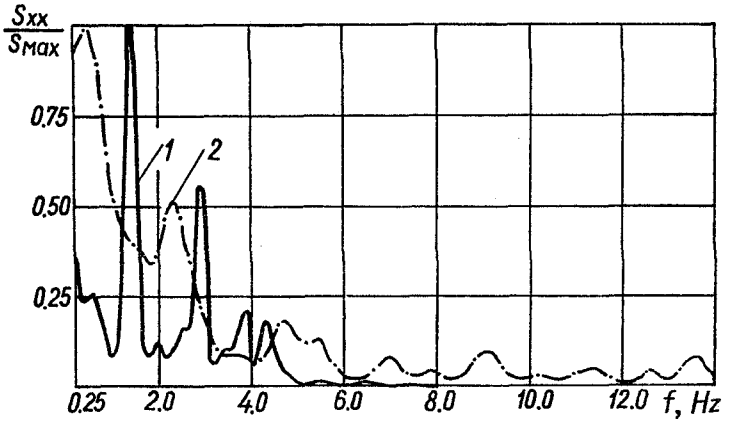

Fig. 7.46. Energy spectral densities of friction torque at $T_c=40°C$: *1*—$n_r=40{,}000$ rpm; *2*—$n_r=5{,}000$ rpm.

Figs. 7.46 and 7.47 show normalized spectral densities of the oscillations of friction torque in bearings.

The analysis carried out for the functions obtained allows us to determine certain regularities in the oscillations of friction torque in bearings. When the rotor speed is increased the energy spectrum in the majority of cases has a tendency to shift in the direction of lower frequencies. When the speed is 25,000–40,000 rpm more sharply expressed narrow bands of dominating frequencies are observed in the energy spectrum. The ambient temperature does not appreciably affect the energy spectrum of friction torque. The appearance of separate, more sharply expressed dominating frequencies when the speed of the moving rings of bearings is increased cannot be the result only of imper-

fections in the surfaces of raceways and the assembly of bearings. Apparently it is a result of hydrodynamic action of the lubricating layers of both bearings on high-speed friction.

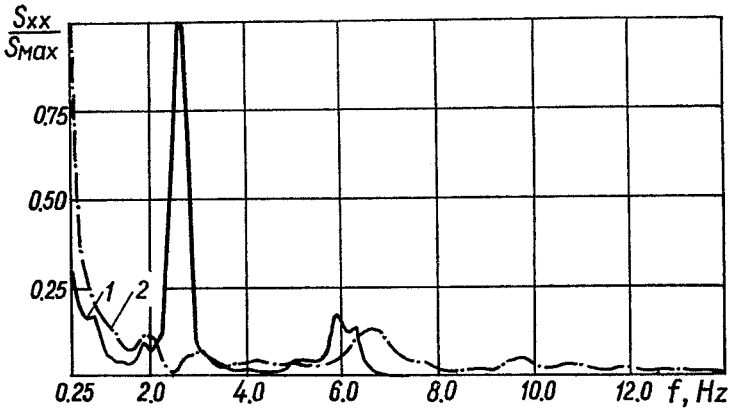

Fig. 7.47. Same as Fig. 7.46 with $T_c = 60°C$.

Simultaneously it is necessary to determine the variable magnitude of the total thickness of the hydrodynamic lubricating film of high-speed ball bearings.

In order to verify the stability and thickness of the lubricating layer measurements were carried out to find the constant and variable components of capacitor impedance of two ball bearings in which a high-speed rotor rotates. The design and basic dynamic parameters of the rotor were considered earlier.

The change in reactance of bearings working in a vacuum chamber weakens the role of oxidized films, especially those intensively formed by interaction with air at high temperatures. In that case we can exclude the value of reactance created by the oxidized film from the value of the reactance being measured and more correctly assess the interrelation of capacitive reactance of the lubricating layer and the rotor dynamics. The interaction of the test stand with the air before the tests marginally affects the results of observations because the oxidized layer and also the boundary layers are quickly removed and are not restored in the vacuum [45].

The results of the study of constant values of reactance of each ball bearing are illustrated by graphs: in Figs. 7.48 and 7.49 by the dependence of the reactance of the first and second bearings respectively on the rotor speed for different working conditions; in Fig. 7.50 by the dependence of the reactance of the first bearing on the temperature in the chamber with increased rotor speed; in Fig. 7.51 by a similar dependence for the second bearing. Each point on the graphs is the average value of three results successively obtained in identical conditions.

Analyzing the graphs in Figs. 7.48 and 7.49, it is possible to conclude that in all cases the reactance of a high-speed ball bearing of this design increases with an increase in the speed of the moving ring, though the increase is less marked when the rotor speed exceeds 10,000 rpm. During the test certain ranges were observed in which the readings of instruments of the converter were very unstable and the indicating arrow either returned to the initial position or went off the scale. Simultaneously the oscilloscope and the autorecorder also went off the scale. Such phenomena were observed for both bearings at rotor speeds up to 16,000–17,000 rpm and temperatures in the chamber of 10 and 120°C. When the change in rotor speed was smooth similar situations were observed even at lower temperatures of the surrounding medium, though to a much smaller degree. During the change in speed the readings of the instruments stabilized. This is associated, perhaps, with the mechanical vibrations of the rotor. In Figs. 7.48 and 7.49 the regions of instability are shown by points.

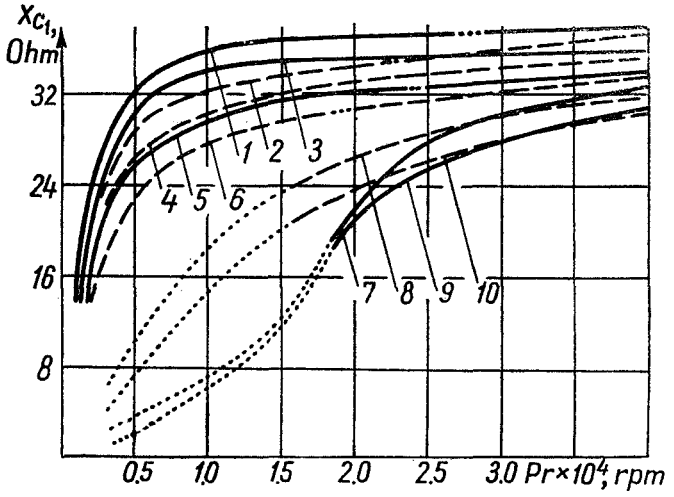

Fig. 7.48. Relation between change reactance of first ball bearing and rotor speed with increasing (solid line) and decreasing (broken lines) speeds: *1, 2*—T_c=40°C; *3, 4*—T_c=60°C; *5, 6*—T_c=80°C; *7, 8*—T_c=100°C; *9, 10*—T_c=120°C.

At higher temperatures in the chamber and at low speeds of rotation (in the given conditions) the boundary lubricant comprising a very thin layer of oil dominates the friction in bearings and this thin layer is most frequently made up of a few molecules; but in other conditions, the fluid lubrication is reliable. The presence of boundary lubricant in bearings affects the working capacity of the whole support. The condition of the lubricant also depends on the surface roughness of rubbing components of the bearing. The service life

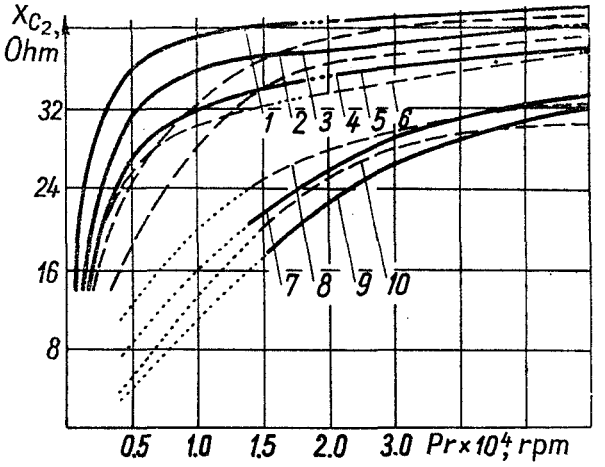

Fig. 7.49. Same as Fig. 7.48 for second ball bearing.

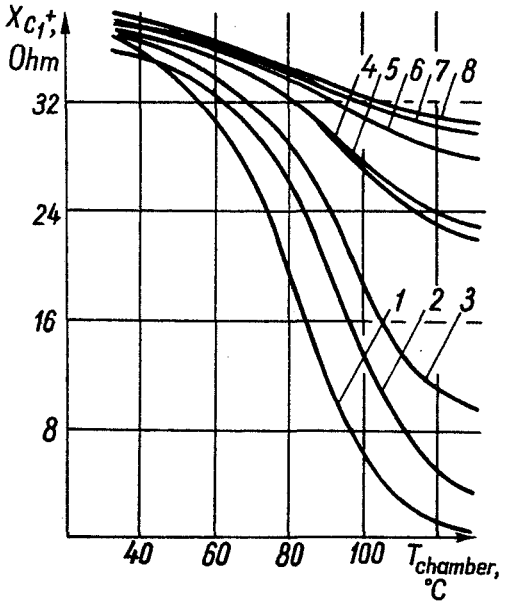

Fig. 7.50. Relation between change in reactance of first bearing and temperature in chamber with increasing speeds: 1—n_r=5,000 rpm; 2—n_r=10,000 rpm; 3—n_r=15,000 rpm; 4—n_r=20,000 rpm; 5—n_r=25,000 rpm; 6—n_r=30,000 rpm; 7—n_r=35,000 rpm; 8—n_r=40,000 rpm.

of rolling contact bearing is determined by a few authors as the ratio of minimum thickness of the lubricant to the resulting surface roughness [64]. Hence the above experiments are the simplest and most reliable means of controlling the quality of a bearing working in difficult conditions.

According to the conventional hydrodynamic theory of lubrication of high-speed, lightly loaded ball bearings [20] the thickness of the lubricating layer at the contact points between the balls and the raceways of the rings increases sharply with an increase in rotor speed and in the viscosity of the oil. Fig. 7.52 shows the design value of the total thickness of the lubricating layer of type VNIINP-260 oil for ball bearings of this design. According to

the works of other authors [64] the increase in the minimal layer of lubricant due to high speed of the rotor is smoother. A certain disagreement as to the nature of the dependences of reactance to motion and total thickness of lubricating layer h_t on an increase in the speed of rotation is apparently due to complex phenomena not covered by the hydrodynamic theory of lubrication of rolling contact bearings. Analogous phenomena for the lubrication of machine parts have been recorded by other authors [45, 46]. In high-speed ball bearings the increase in sliding speeds and reduction in rolling speeds are especially noticeable. Skidding of balls, especially at small axial loads, is increased at contact points [4, 57, 71, 72, 74 and others]. The thickness of the lubricant film decreases at the contact points of machine parts during acute sliding but pure rolling helps to form a lubricating layer [45, 70] The leveling off of the increase in reactance of a bearing with an increase in the speed of rotation in the tests is explained by the increase in sliding, decrease in the sensitivity of the viscosity of the lubricant to pressure and structural changes in the lubricant in the contact zones.

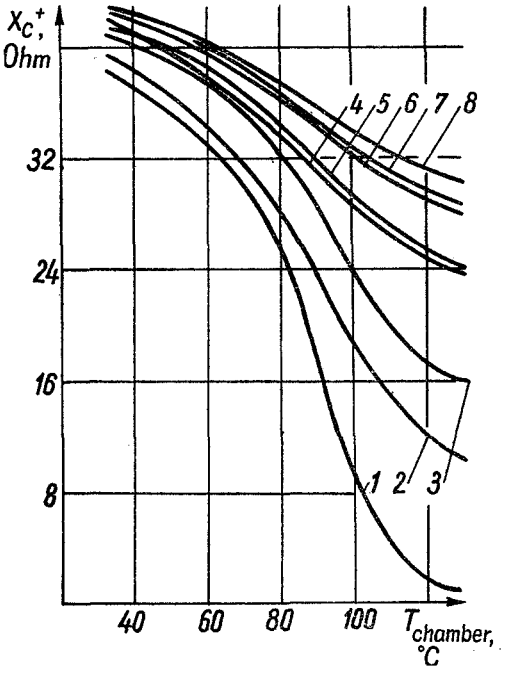

Fig. 7.51. Same as Fig. 7.50 for second bearing.

The data obtained (see Figs. 7.50 and 7.51) very clearly demonstrate that with an increase in temperature in the chamber the reactance of bearings falls, the more rapidly the higher the temperature. As it goes up the polar bonding energy of the molecules with the adsorbing surface of the bearing rings appears to be reduced as also the thickness and mechanical properties of the boundary layers. At lower temperatures the lubricating oil assumes a viscous state; at high temperatures chemical phenomena are intensified, the viscosity of the particular type of lubricant is reduced to a few percent of its normal value and the lubricating layers are separated. Taking into account the heating of the bearing, the maximum temperature of the external medium for steady operation of the rotor in a vacuum chamber at a speed of up to 15,000 rpm may be put at 80–90°C. When the rotor operates for a long spell in a chamber at a temperature of 120–130°C the raceways may be spoiled even at

higher speeds of rotation.

The results of tests shown in Figs. 7.48 through 7.51 were obtained after 60 min of operation of the rotor at each given condition. The change from one speed to another was gradual without stopping the rotor. The motor was warmed before the tests.

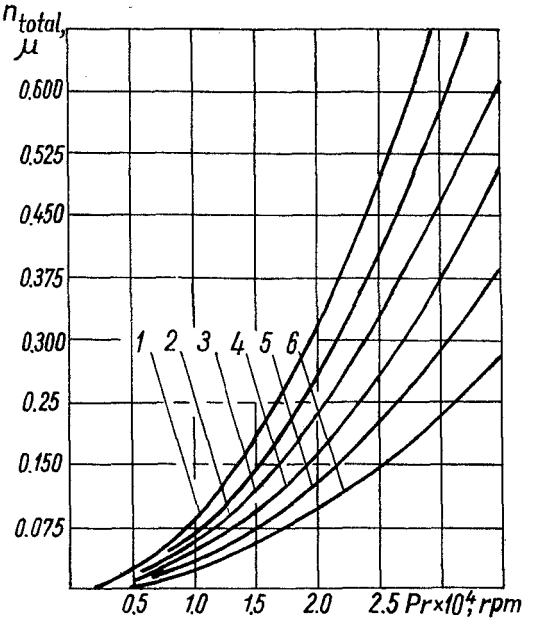

Fig. 7.52. Relation between total thickness of lubricating layer in bearings computed from hydrodynamic theory of lubricating rolling contact bearings and speed: *1*—μ=5.5 Poise; *2*—5.0 P; *3*—4.5 P; *4*—4 P; *5*—3.5 P; *6*—3.0 P.

The value of reactance to rotation of the bearing also depends on how the given speed condition was achieved: by a gradual increase in speed (X_{si}^{+}) or by a gradual reduction (X_{si}^{-}). Speed was reduced by forced braking of the motor with the help of an electronic frequency converter, by switching the noise generator to a low supply frequency. In this situation the constant value of reactance was reduced by a certain value at all temperatures and rotor speeds.

Such phenomena associated with the change in the value of reactance on switching from one regime to another should be considered as the result of temperature and structural changes in the lubricating layers. According to hydrodynamic theory a particular state of the lubricating layer should be reached immediately on establishing stable speed and should not depend on the sequence of speeds: acceleration or braking. It follows that the equilibrium of a structurally organized layer of oil is not static and is associated with the

phenomena of separation and reattachment of oil particles. The new condition of friction requires a new equilibrium state.

In the study of the dynamic characteristics of the rotor it is also necessary to know the regularity of the change in the variable component of the reactance bearings of lower frequencies (up to 100 Hz), since higher harmonics do not appreciably affect the dynamic behavior of the rotor. Approximate curves of the variable components of reactance in ball bearings studied at different working conditions are shown in Figs. 7.53 and 7.54. A comprehensive analysis of the curves obtained shows that at low rotor speeds the amplitude of vibrations of the reactance is less than at higher speeds and increases especially from 30;000 to 35,000 rpm. When the ambient temperature is 120°C and the rotor speed is 15,000 rpm the amplitude of the variable component sharply increases (the pointer goes off the scale). This indicates the existence of an

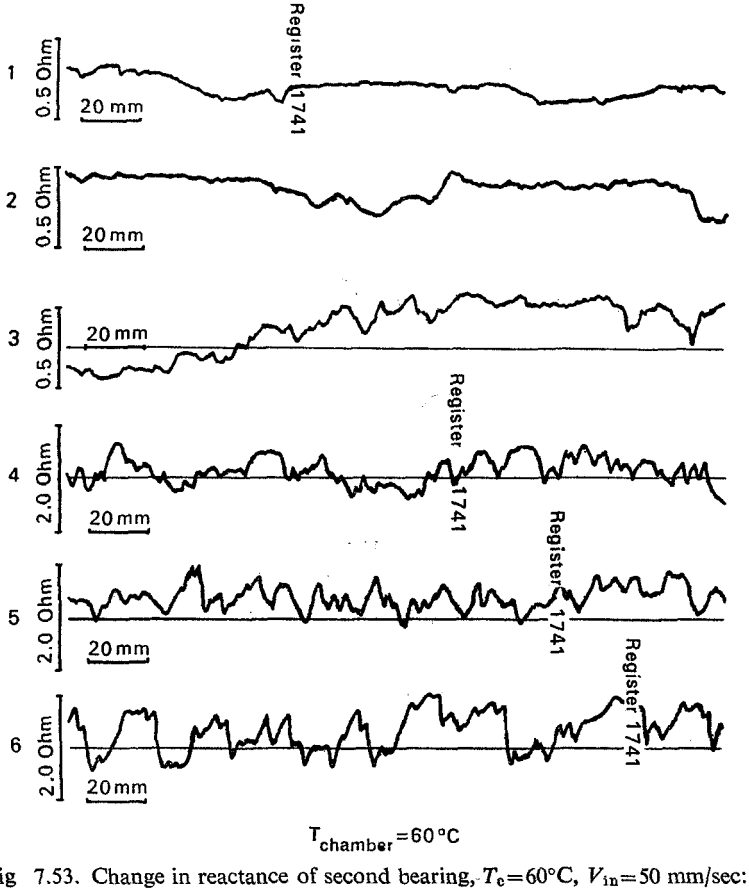

Fig 7.53. Change in reactance of second bearing, $T_c=60°C$, $V_{in}=50$ mm/sec: *1*—$n_r=15{,}000$ rpm; *2*—$n_r=20{,}000$ rpm; *3*—$n_r=25{,}000$ rpm; *4*—$n_r=30{,}000$ rpm; *5*—$n_r=35{,}000$ rpm; *6*—$n_r=40{,}000$ rpm.

unstable hydrodynamic region and the separation of the lubricating film. Curves of the variation in reactance of the first and second bearings are analogous under given conditions.

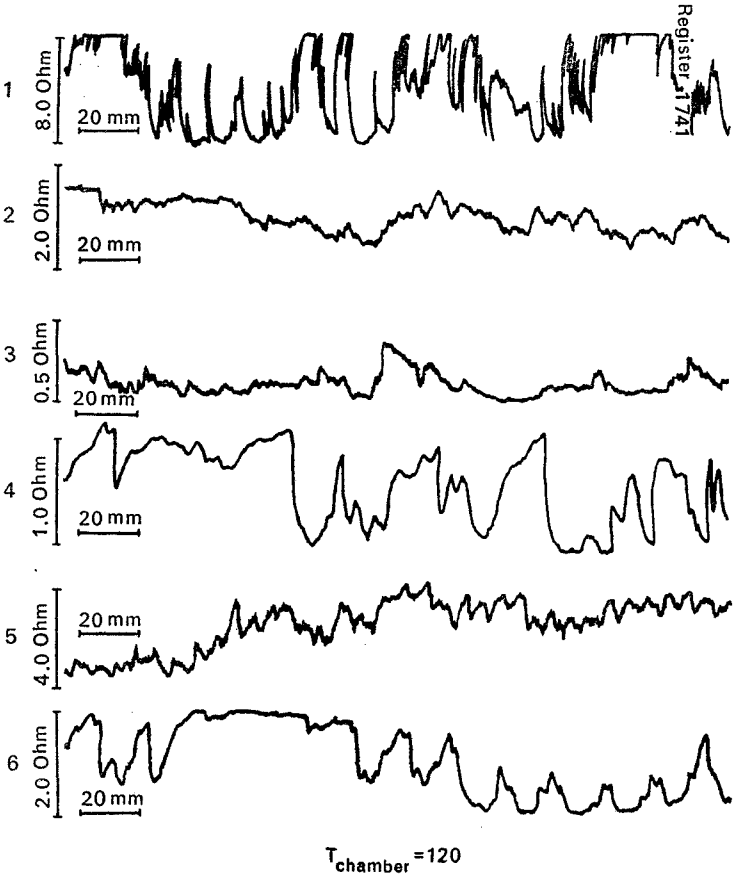

Fig. 7.54. Same as Fig. 7.53 for second ball bearing $T_c = 120°C$.

The presence of regions of unstable lubricating film in the above working conditions tallies with the results of the tests described in the preceding section. The importance of the oil film for the dynamics of high-speed rotor working at high temperatures is confirmed.

For a more complete explanation of the relation between VFT and the vibrations of electrical resistance in ball bearings and also for the determination of the change in this relation at different operating conditions it is convenient to use transfer functions. The most typical logarithmic amplitude frequency characteristics obtained with the help of a computer and approximated by graphic-analytical methods are shown in Figs. 7.55 and 7.56. These

characteristics reflect the relation between reactance of a pair of ball bearings of the rotor under test and VFT in different working conditions. The reactance characterizing the mean thickness of the hydrodynamic oil film reduces the level of higher frequencies of friction torque. For relatively high frequencies (in this case more than 2–2.5 Hz) the lubricant acts as a damper. The transfer functions of a system having reactance at the input and VFT at the output confirm the conclusions drawn in the preceding chapters.

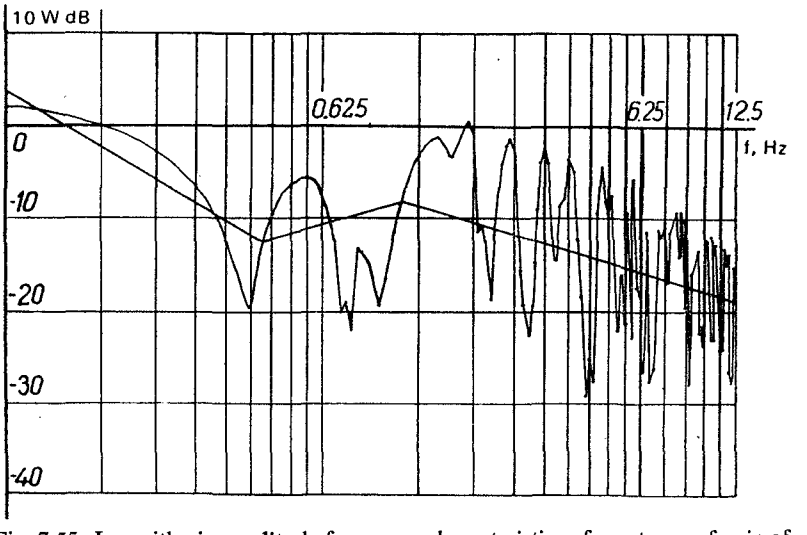

Fig. 7.55. Logarithmic amplitude-frequency characteristics of reactance of pair of high-speed ball bearings with friction torque: $T_0=60°C$; $n_r=30{,}000$ rpm.

7.5 INVESTIGATION OF FRICTION TORQUE IN PRECISION SLIDE BEARINGS

The perfection of modern precision instruments and the need to reduce errors therein pose a great challenge for the development of key moving parts, in particular, rotors and rotary slide bearings, which should have very high precision, sensitivity, reliability and long life when working under specific operating conditions.

Wide applications in precision instruments are found for rotating systems which include precision slide bearings with curvilinear working surfaces capable of working in conditions of vibrations with combined loading, in different media, and also in conditions of radiation and vacuum. The accuracy of operation of such dynamic systems (counters of electrical energy, Wattmeters, gyroscopic instruments and magnetic tape recorders, aviation instruments and instruments for standard time, accelerometers, stepping motors, etc.) is basically determined by the variation in the components of dynamic friction torque in precision bearings due to design and technological errors. The principal causes are:

—absence of symmetry in rotating elements;
—incorrect choice of design parameters of the rubbing working surfaces;
—wrong choice of location of the rotor and bearing;
—absence of provision to eliminate imbalance in rotating parts;
—manufacturing defects in individual components;
—poor quality of the assembly, lubrication and mounting.

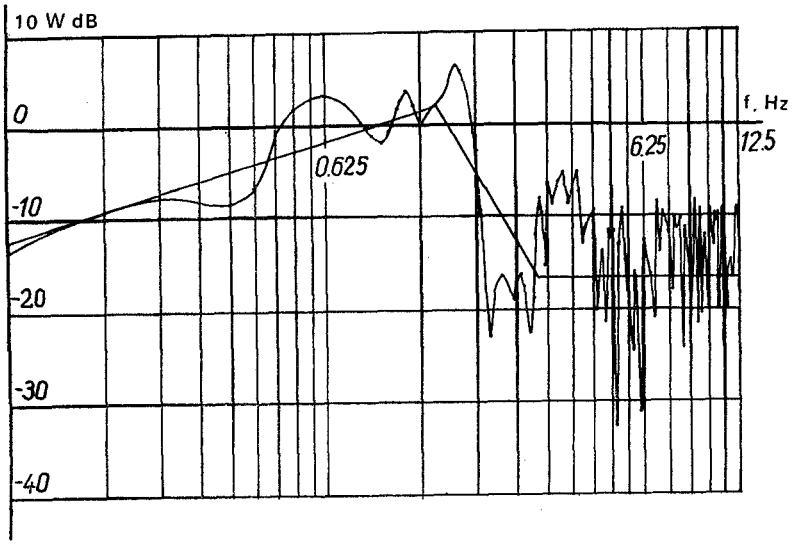

Fig. 7.56. Same as Fig. 7.55 for n_r=35,000 rpm.

We should mention that imbalance in a rotating part of a precision rotor system makes itself felt during actual operation. As a result of research it has been established that a change in ambient temperature and heating affect the magnitude of imbalance, as a result of which the VFT may appreciably increase. Such operating conditions can lead to rapid wear of bearings. Hence assemblies and components of moving parts must be made as far as possible from materials with the same coefficient of linear expansion.

The constancy of friction torques is practically of the highest importance in precision systems. In the majority of highly sensitive precision systems almost all the energy of drives is spent on overcoming friction losses. Hence the problems of stabilizing and reducing the components of dynamic friction torques in precision slide bearings are very real. The variability of friction torque of moving parts in precision bearings of such instruments is in most cases the principal cause of error which affects the accuracy of the motion of the dynamic system and is responsible for failure to function properly. The magnitude and stability of the constant component M_c of friction torque depend on many external factors of static and dynamic character and on the geometric and design parameters of the system. In many works [3, 17, 25, 26, 73]

friction torque is considered as friction torque in the supporting bearing and is expressed by design formulas:

$$M_c = 0.534 f \sqrt{G^4 \frac{\frac{1-\mu_R^4}{E_R} + \frac{1-\mu_b^2}{E_b}}{\frac{1}{R_H} - \frac{1}{R_s}}} \tag{7.9}$$

where μ_R, E_R, μ_b, E_b are respectively Poisson's ratio for the materials of the rotor head with radius R_H and of the support with a radius of working surface R_s.

Formula (7.9) does not give the complete characteristics of M_c in the dynamic regime of the rotor system. As shown by tests carried out with a vertical rotor system, the value of M_c in the lower supporting precision bearing with a spherical working surface changes as a function of rotor speed.

Fig. 7.57 shows the results obtained experimentally for the dependence of M_c on the angular speed ω of the vertical rotor of a dynamic system in the case of elastic suspension on elastic components of the lower load-carrying precision bearing.

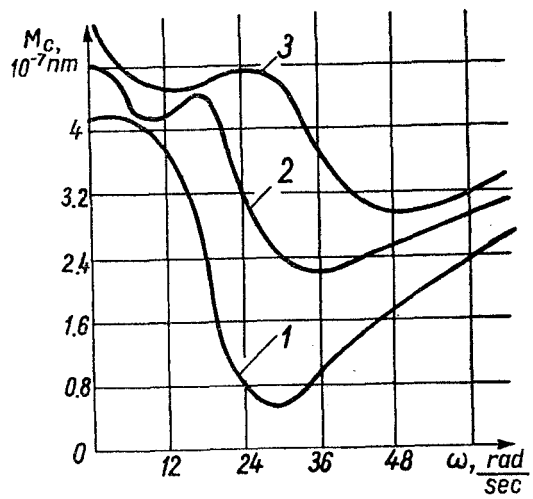

Fig. 7.57. Relation between characteristics of M_c in elastically suspended support and rotor speed for rubbing pair (ball ShKh 15; bearing PAS) with axial loads: *1*—$G=2.8\times10^{-1}$ N; *2*—$G=3.3\times10^{-1}$ N; *3*—$G=3.8\times15^{-1}$ N.

The value of M_c obtained by using formula (7.9) is considerably less than the value obtained experimentally. This is due to the under-estimation of the following factors observed in the analytical system:

—the axis of rotation of the rotor and the geometric axis of the bearing net did not coincide;

—only the axial force of load G of the rotating part was considered for the normal pressure force;
—the force acting on the rotor axis is also of a lateral-radial nature;
—the friction coefficient in the zone of the working area of contact is not a constant;
—constant values of speed with respect to the complicated sliding and unit pressure in the zone of contact area.

Depending on the type of contact in the zone of the contact area of rubbing components, the coefficient of friction changes non-linearly depending on the load. With an increase in the normal load it is reduced for elastic contact and increased for plastic contact. The value of M_c depends on the type of contact.

The value of the quantity M_c has a very complex relationship to the angular speed of the rotor axis ω (Fig. 7.57). It is a nonlinear function which changes in character at different axial loads of the rotating part. For curve *1* a mathematical expression for M_c has been obtained as a function of the difference in angular speeds $\dot{\varphi}(t)=\omega+\dot{\varphi}_1(t)$ and $\dot{\varphi}_2(t)$:

$$M_c(\dot{\varphi}, \dot{\varphi}_2)=\begin{cases} p_1(x) & [0, 30] \\ p_2(x) & [30, 64], \end{cases} \tag{7.10}$$

where

$$p_1(x)=[12+1.46(\dot{\varphi}-\dot{\varphi}_2)-0.75(\dot{\varphi}-\dot{\varphi}_2)^2-0.05(\dot{\varphi}-\dot{\varphi}_2)^3 +0.07(\dot{\varphi}-\dot{\varphi}_2)^4]\,0.342\cdot 10^{-7}, \tag{7.11}$$

$$p_2(x)=[-7+1.42(\dot{\varphi}-\dot{\varphi}_2)-0.03(\dot{\varphi}-\dot{\varphi}_2)^2]\,0.342\cdot 10^{-7}, \tag{7.12}$$

ω and $\dot{\varphi}_1=\dot{\varphi}_1(t)$ are respectively the constant and variable angular speeds of the rotor around its own axis;

$\dot{\varphi}_2=\dot{\varphi}_2(t)$ is the variable angular speed of rotation of the elastically supported lower bearing.

The quantities $\dot{\varphi}_1$ and $\dot{\varphi}_2$ are very small when compared to ω. To obtain the empirical expressions (7.11) and (7.12) it is possible to neglect them and take $\dot{\varphi}_1-\dot{\varphi}_2\approx\omega$. Systems with a vertical rotor work in complex working conditions since the rotating part is affected by lateral radial loads, imbalance, design-technological factors, etc.

Let us analyze the change in constant components of friction torque for the case where the rotor head of radius R_H completes a complex sliding motion along the curvilinear working surface of the support bearing with angular speeds $\dot{\varphi}, \dot{\psi}, \dot{\Theta}$ (Fig. 7.58).

During this motion of the rotor corresponding additional friction torque that differs in magnitude and rate of change is introduced. In the lower precision slide bearing the movement of the rotor is affected by the friction torques M_φ, M_ψ and M_Θ. The value of the friction torque due to the rotation of the rotor around its own axis with an angular speed ω does not correspond to the value of M_c obtained with the working condition of the rotor for $\Theta=0$ from formula (7.9). Since the axis of rotation of the rotor about its own axis does not coincide with the contact point of sliding A, when the displaced rotor moves in a rigidly fixed bearing additional friction torques are introduced whose general design value can be expressed in the following way:

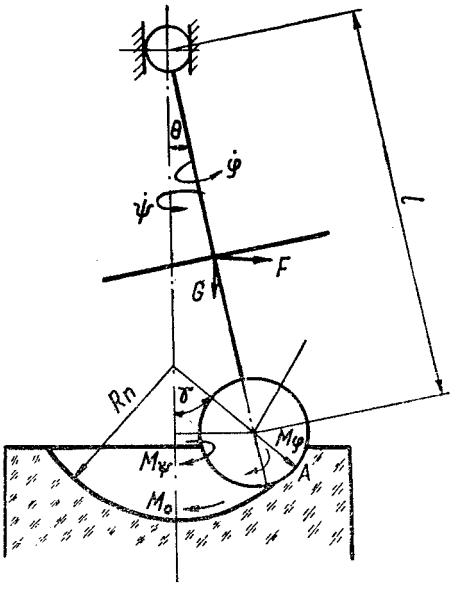

Fig. 7.58. Kinematic diagram of rotor movement along spherical surface of support.

$$M_{c.a}=M_\varphi+M_\psi+M_\Theta. \quad (7.13)$$

Friction torque due to the rotation of the rotor around its own axis through an angle $\varphi=\varphi\ (t)$ is expressed in the form:

$$M_\varphi=G f\cos\gamma\, R_H \sin\alpha, \quad (7.14)$$

where

$$\alpha=\gamma-\Theta;$$

$$\sin\alpha=\frac{1}{R_\Delta}\sin\Theta\,(l\cos\Theta-\sqrt{R_\Delta^2-l^2\sin^2\Theta});\quad R_\Delta=R_s-R_H.$$

The friction torque due to the rotation of the axis of rotation of the rotor about the vertical

$$\psi=\frac{K}{n}\omega t+\psi_1\,(t)\ (K=0, 1, 2, \ldots; n=1, 2, \ldots, \infty)$$

is given by

$$M_\psi=Gf\sin\gamma\,\frac{R_n}{R_\Delta}\,l\sin\Theta. \quad (7.15)$$

When the axis of rotation of the rotor turns through an angle relative to the vertical $\Theta=\Theta\ (t)$ the friction torque takes the form

$$M_\Theta = Gf \sin \gamma \, R_{\text{H}}. \tag{7.16}$$

When $R_\Delta > l \sin \Theta$ the value of friction torque M_ψ cannot be more than M_Θ.

Results of tests show that the friction torque in precision slide bearings changes when the direction of rotor rotation is changed in magnitude and character. The value of the constant component of the friction torque caused by the change in the direction of rotation of the rotor can vary a number of times for one and the same value of the angle of turn.

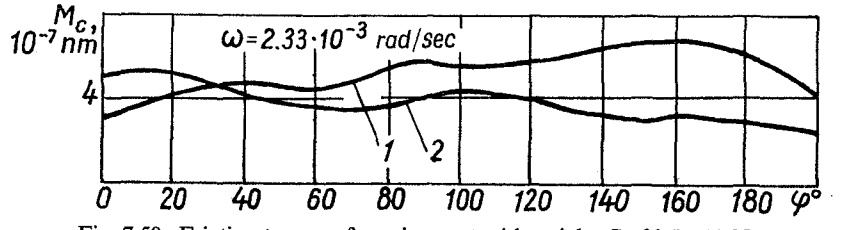

Fig. 7.59. Friction torque of moving part with weight $G = 30.5 \times 10$ N in supports of electronic counter with turning angle φ:
1—anticlockwise rotation of rotor; *2*—clockwise rotation.

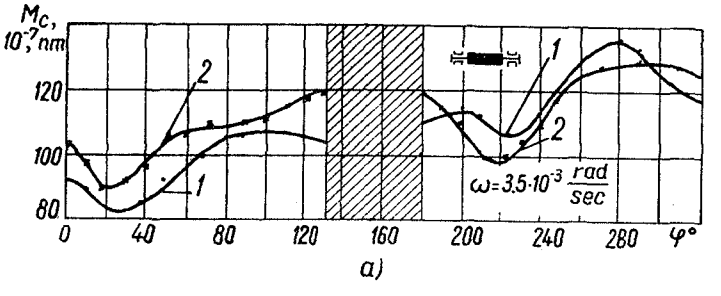

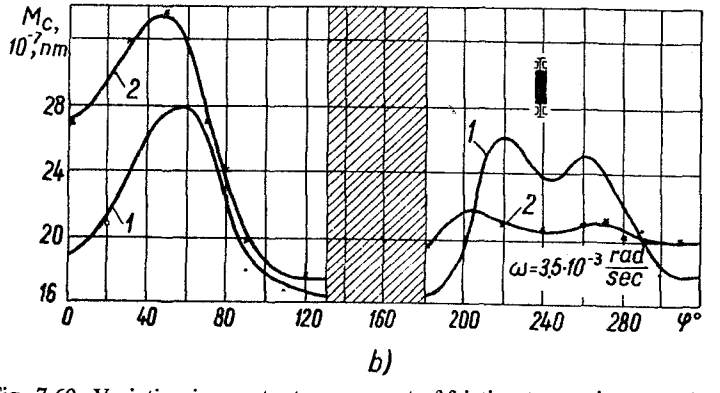

Fig. 7.60. Variation in constant component of friction torque in supports of suspended gyroscope when axis of rotor is:
a—vertical; *b*—horizontal; and rotation is: *1*—anticlockwise; *2*—clockwise.

Fig. 7.59 shows the empirical partial dependence of M_c on the angle of turn of the rotor of the rotating part of an electronic counter of the SO-I445 type for the most representative speed range in the region of small loads and in the range of 'autorotating-sensitivity.'

An appreciable change in the constant component of friction torque was observed during tests on rotors in precision slide bearings of suspension-type gyroscopes (Fig. 7.60). The hard metal alloy VK 10 (rotor) and leucosaphire (bushing, step bearing) were the materials used for the rubbing surfaces. The rotor weighed 4.5×10^{-2} N. The change in the value of M_c for the same angles of turn of the rotor is perhaps explained by the different roughness, nonuniform running-in of working surfaces of the rubbing components, geometric defects in the shape and large clearance of the rotor in the bearings that leads to a twisting of the axis and appearance of unbalancing loads. Typically, the change in the value of M_c when the axis of the rotor is vertical (Fig. 7.60 a) is more than when it is horizontal. This can be explained by smaller contact area, the greater effect of the combination of geometric deviations in the contact zone, the reduced stability of a rotor rotating in the vertical position and other factors.

In order to improve the accuracy and sensitivity of high-precision dynamic systems with slowly rotating rotors (for example, electrical counters, suspension gyroscopes, etc.), it is very important to reduce friction losses sharply. Hence dynamic systems should be made with optimum geometric and design parameters and minimum manufacturing defects. The fulfillment of these requirements is hampered by the limitations of manufacturing technology and the building of individual assemblies and components (for example, bushings, step bearings). Hence for a maximum reduction of friction torques in precision bearings it is necessary to look for other means to improve the qualitative characteristics of high-precision instruments.

One of the most effective methods of reducing friction torque in bearings is the method of moving the elements of rubbing components in conditions excited by axial vibrations.

It is worth mentioning that with vibrations, if the torque needed to set the rotor in motion can be reduced appreciably the energy needed to excite axial vibrations in the rotor and bearings goes up.

Reduction in the expenditure of energy during axial vibrations indicates a reduction in friction torques as a result of physical changes in the rubbing components.

Let us consider the case of reduction in M_c in bearings of an electronic counter.

Let us assume that with axial vibrations and $\Theta = 0$ the rotating axis shown in Fig. 7.58 is acted on by an axial load G and a load which varies harmonically, $B_m = B_0 \sin \omega t$, acting in the axial direction of the rotor. To turn the rotating part from rest, the minimum torque $M_{r_{min}}$ must exceed the

maximum value of friction torque of the rotor in the upper and lower bearings by an equal margin:

$$M_{r_{min}} = M_{B_1} + M_{B_2}, \tag{7.17}$$

where $M_{B_1} = \frac{4}{\pi} f_1 F_c R_c$ is the friction torque in the upper bearing support [68, 73];

$M_{B_2} = \frac{3}{16} \pi f_2 G\rho$ is the friction torque in the lower spherical support [26, 56];

ρ is the radius of the contact surface of the rotor and support [56].

In the dynamic domain friction torque equals the minimum and exceeds the maximum resistance in the supports if the effective action of disturbing load B_M is directed upward.

Thus the following condition is satisfied:

$$M_{r_{min}} + M_d = \frac{4}{\pi} f_1 F_c R_c + \frac{3}{16} \pi f_2 G\rho, \tag{7.18}$$

where M_d is the friction torque in the supports when the disturbing load $B_M = B_0 \sin \omega t$ acts.

From the expression (7.18) we get

$$M'_{r_{min}} = f_1 \left(\frac{4}{\pi} F_c R_c + \frac{3}{16} \pi \frac{f_2}{f_1} G\rho \right) - M_d = f_1 Q - M_d. \tag{7.19}$$

In evaluating the friction torque with no disturbing variable load B_M we find the effective coefficient of friction:

$$f' = f_1 \left(1 - \frac{M_d}{f_1 Q} \right). \tag{7.20}$$

It is necessary to mention that the coefficient f' is not the physical friction coefficient. However, its dependence on the quantity $M_d / f_1 Q$ does not indicate the variation in the true coefficient of friction in the presence of vibrations.

In certain works it is argued that the reason for the reduction in the effective coefficient of friction between a vibrating rough surface and the element touching it may be the resonant elastic vibrations of this element [2, 36, 48]. Resonant vibrations of a dynamic system [9, 53] can also be used to reduce the disturbance amplitude of self-vibrations.

In both cases we are considering resonant vibrations. Experiments were carried out with actual dynamic systems to determine the effectiveness of reduction in M_c in the range of disturbing vibrational oscillation of the displacements of frequencies from 10 Hz to 20 kHz. The direction of vibrations excited by the vibroelement was lined up with the axis of rotation of the rotor

and with the geometric axes of the upper and lower supports. For this purpose the supports were rigidly fixed to the vibrating surface of the shaker whose amplitude and frequency of vibrations were regulated by the excitation block.

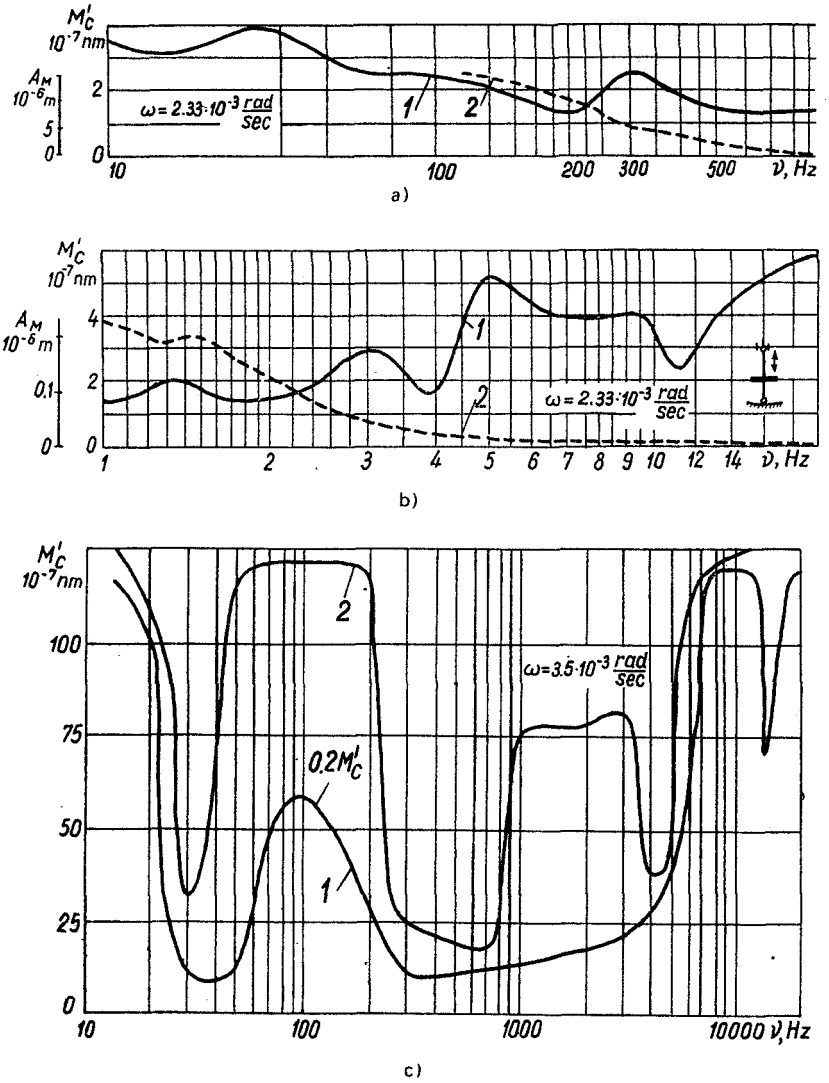

Fig. 7.61. Relation between constant component of friction torque and frequency of axial vibrations in supports of: *a*, *b*—electronic counter; *c*—suspended gyroscope.

Fig. 7.61 shows the results of reducing M_c, depending on the frequency of axial vibrations. Tests were run on the same equipment used for the results shown in Figs. 7.59 and 7.60 a.

To reduce M_c in the supports of an electronic counter its maximum value was chosen and the tests were run turning the rotor only within the limits of the angle of turn from 165° to 170° (see Fig. 7.57, curve 1). As a result of tests it was established that M_r in electronic counters of the SO-I445 type is reduced several times in the presence of effective axial vibrations of a certain frequency (Fig. 7.61 a and b, curve 1). The characteristic of M_r is a nonlinear function. With effective amplitude of disturbance in the frequency range 10 Hz–20 kHz its value changes by approximately 3.5 times.

The reduction in M_r with axial vibrations is found to be closely associated with the value of M_r when there are no vibrations. The maximum reduction in M_r is observed when M_c is small, i.e. the less the value of friction torque in precision slide bearings, the more it can be reduced by the action of axial vibrations.

The accuracy and stability of a precision rotor system is largely affected by the VFT M_v, whose magnitude, nature of change in amplitude and disturbance frequency basically depend on the nonlinearity of the characteristic of constant component of friction torque M_c, absent for the particular speed range, on geometric errors in the contact zone of the rubbing components, on

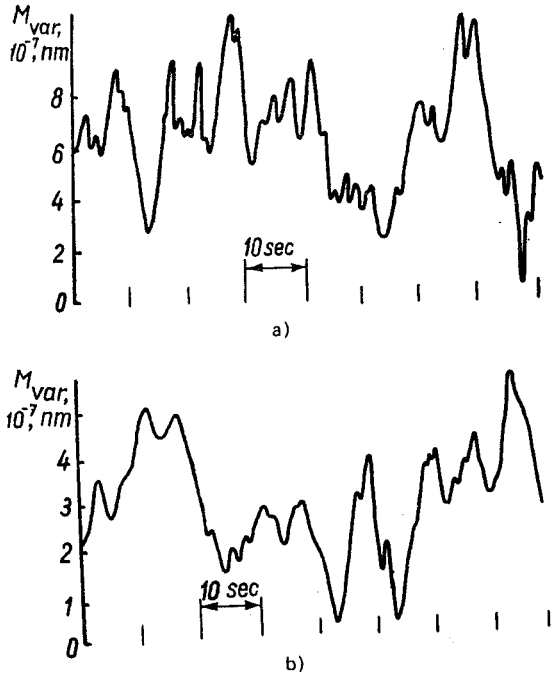

Fig. 7.62. Variable component of friction torque in supports of float-type gyroscope at rotor speed of $\omega=3.5\times10^{-3}$ rad/sec in: *a*—vertical and *b*—horizontal positions.

inertial disturbance, on properties of the particular dynamic system and on other factors. In the majority of cases the excited M_v in precision slide bearings is of torsional vibrations of a random nature. Fig. 7.62 a shows the empirical oscillograms M_v of a rotor with journals made of VK10 material with a diameter of 4×10^{-2} m, rotating in two leucosaphire slide supports without lubrication representing bushing and step bearing.

We find another picture with an elastically suspended precision slide support. Often such supports, working without lubrication, have free vibration processes whose excitation takes place in particular ranges of rotor speeds. They are due to a sharp fall in the nonlinear characteristics of the constant components of dynamic friction torque M_c. The presence of free vibrations in such bearings is confirmed by the change in the magnitude of the amplitude M_r (Fig. 7.63).

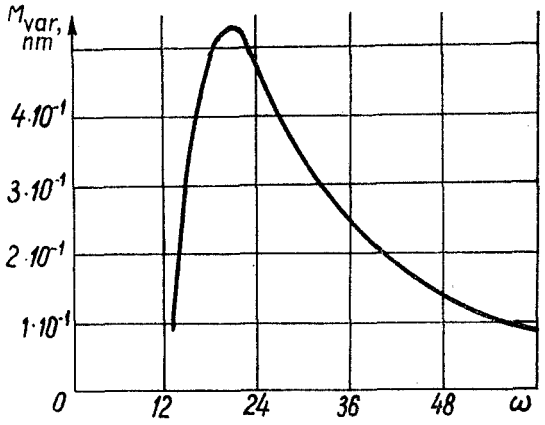

Fig. 7.63. Change in maximum values of M_v of elastically suspended agate support of PAS type.

When the rotor speed is between 0 and 12.2 rad/sec the value of the amplitude (Fig. 7.63) is very small when compared to the smallest amplitude of free vibrations. The rate of increase in amplitude of free vibrations is determined by the stiffness of the vibrating system, the frictional properties of the contact of the rubbing components, the relative sliding speed and the degree of fall in the characteristic $M_c - \omega$.

When the rotor speed is gradually increased the form and nature of change in amplitude of vibrations M_v attains a more random character. This is explained by the change in the characteristic $M_c - \omega$, the effect of inertial disturbance, the change in the value of the contact area of curvilinear working surfaces of the rotor and the bearing, twist and deflection from the vertical position of the rotor's axis of rotation and the more effective influence of geometric deviations in the contact zone. The frequency of vibrations of M_c also depends on the rotor speed, since in the case of the curvilinear working

surface of an elastically suspended bearing, forces of inertial disturbance due to poor balancing of the rotating part act on the suspension and change the stiffness of the elastic components of the bearing suspension. The presence of geometric errors in the contact zone also affects the frequency of M_v.

If the contact elements of the rubbing components are made of different types of material generation of electric charges of opposite signs may occur during rotation of the rotor. The triboelectricity so produced in the contact zone adversely affects the antifriction qualities of the rubbing pair, introducing additional frictional forces of constant or variable nature which considerably affect the magnitude and character of changes in characteristics M_v and M_c in precision slide bearings.

At low rotor speeds the elastically suspended bearing has disturbing vibrations whose form is nearly sinusoidal. In this case the effect of inertial forces is reduced, the nature of dissipative forces acting between the rotor and the bearing changes, the axis of rotation of the rotor is more accurately centered relative to the geometric axes of the upper and lower bearings and the dynamic system operates in the steady-state condition of vibrations.

An increase in the axial load of a rotor in precision slide bearings affects the magnitude and form of characteristic M_c (Fig. 7.57, curves *2* and *3*). Here self-vibrations of very low frequency appear in the dynamic system more rapidly than at low rotor speeds on the first falling branch of M_c. It has been established that in the zone of low rotor speeds, when the characteristic $M_c-\omega$ has an increasing or constant character, M_v does not appear in the elastically suspended bearing or has a very small amplitude when compared to the amplitude of free vibrations. In other speed ranges a large number of factors have a more effective influence and their action increases the number of spectral frequency components of M_v.

For a deeper analysis of the disturbances of M_v in an elastically suspended precision slide bearing at different rotor speeds a test was run for a dynamic precision system made up of a vertically placed rotor whose axial load could be changed. The upper part of the rotor lies in a rigidly fixed precision slide bearing (bushing) and the lower end is made in the form of a spherical head. The rotor rests on an elastically suspended bearing (step bearing) with a concave spherical working surface in which the M_v is registered in the form of an oscillogram. The ratio of the radii of curvature of working rubbing surfaces of the bearing and the steel head of the rotor $(R_n/R_H)=2.4$. As a result of the analysis of empirical values of M_v using a digital computer it was found that the general level of spectral frequencies of the components of M_v has a very nearly normal distribution. The fundamental frequency component of M_v coincides with the number of rotations of the rotor in the case of imbalance of the rotating part (rotor with inertial mass in the form of a disc rigidly fixed to it) and has a directly proportional dependence. Analysis of spectral frequencies showed that the accuracy of motion of the rotor axis in

an elastically suspended bearing is determined to a large degree by the maximum values of M_v. An increase in the rotor speed with unchanged axial loads increases the level of high frequencies of M_v.

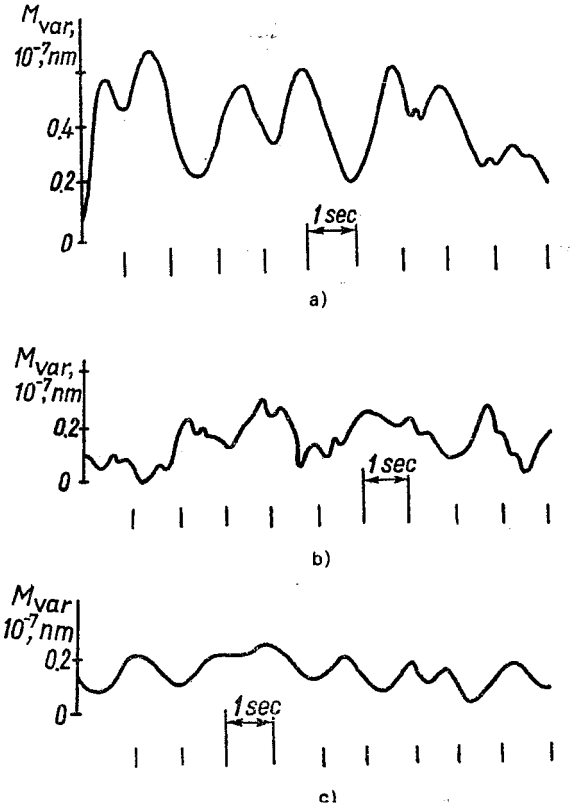

Fig. 7.64. VFT in supports of electronic counter of SO-I445 type when rotor is: *a*—rotating "forward"; *b*—in reverse; *c*—rotating "forward" with axial vibrations: $\omega = 2.33 \times 10^{-3}$ rad/sec.

The VFT of the rotating part of an electronic counter of the SO-I445 type in bearings without lubrication is shown in Fig. 7.64. From the oscillograms it may be seen that the amplitude and frequency of M_v differ as between forward and reverse drive of the rotor. This is apparently to be explained by the different form and appreciable effect of geometric deviations in the contact zone of the rubbing pair. For axial vibrations (Fig. 7.64 c) the change in M_v is of a steadier nature. The magnitude of amplitude is less than without vibrations. From what has been said it follows that in the case of axial vibrations of the rotor it is possible to reduce effectively the magnitude of the constant component and amplitude of the variable component of friction torque. This can be explained by the change in the frictional properties of the elastic con-

tact since the actual contact area and unit load in the region of the contact surfaces are changed during mechanical vibrations.

7.6 DIAGNOSIS OF ERRORS AND MOUNTING-CUM-OPERATIONAL DEFECTS IN BEARINGS ACCORDING TO CHARACTERISTICS OF FRICTION TORQUES

Errors in rolling contact bearings and bearing assemblies can be diagnosed using different characteristics and indications. One of the most reliable methods of diagnosis is the method of determining the state of bearings and their assemblies from the characteristics of friction torques.

Spectral-correlational analysis is carried out according to the methodology described in Chapter VI. However, in production conditions, for a faster and frequently direct analysis to bring out possible defects in bearings and assemblies it is important to be able to determine these errors from the nature of the curve obtained by the recording unit or observed in the cathode ray oscilloscope.

The dependence of changes in friction torque on different working conditions will be dealt with below. In the present section let us consider the effect of individual errors in geometric shape, the cleanliness of the treatment of surfaces, deposition of dirt and other factors on the components of friction torque and the nature of the curve for friction torque, since these errors cause changes in the components of friction torque.

It is possible to evaluate the characteristics on the basis of a number of selected parameters or their combination.

Some of them are:

1) average torque in the steady-state condition-constant component of the torque;
2) peak torque in the steady-state working condition;
3) average maximum torque in the steady-state working condition;
4) frequency of the torque characteristics.

The constant component of the torque in the steady-state working condition is the average number of all values of the torque during the complete cycle of tests. Lines are drawn on the realization (Fig. 7.65) to describe the mean value of the curve drawn in each direction from the zero position, i.e. in the clockwise rotation of the assembly. The zero line is drawn in the case where the pointer of the instrument (vibration torque measuring instrument) indicates zero. The load is not transferred to the transducers that measure the torque. In some cases, first the mean lines of torques are drawn in the clockwise and anticlockwise direction and the zero line is found by division into equal parts of the distance between mean lines.

Multiplying the value of M_c by the scale, we get the value of the constant component. The constant component can also be determined from the deflec-

tion of the pointer of the instrument. The peak torque M_{peak} in the steady-state working condition is the maximum instantaneous value of friction torque observed during the complete cycle of tests. Having determined, as shown above, the zero line of the characteristic, the peak value of the friction torque is found by multiplying the value M_{peak} by the scale in nm.

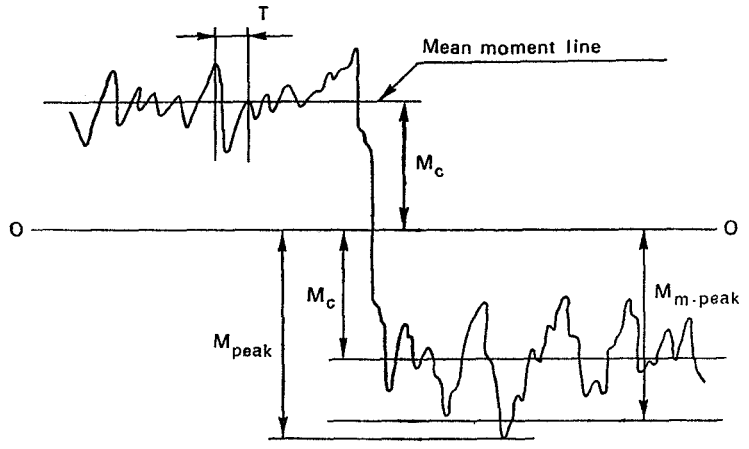

Fig. 7.65. Realization of friction torque.

The mean peak torque in the steady-state working condition is the mean value of instantaneous peak values of the torque observed throughout the experiment. Computation of the magnitude of each instantaneous peak in the recorded curve, taking their mean value, is the accurate way of determining this characteristic. A more rapid, and effective, method is to draw a line passing through all the instantaneous peaks and approximately compute the mean peak line for each revolution with the help of a transparent ruler. The mean peak torque is equal to half the sum of two peak values multiplied by the scale in nm.

The frequency of characteristics of torque is basically determined by spectral-correlational analysis though it is possible to determine it approximately by visual means from the recorded curve and also on the screen of a cathode ray oscilloscope. The frequency f is determined by the period T:

$$f=\frac{1}{T}=\frac{\omega}{2\pi}, \tag{7.21}$$

where ω is the circular frequency, rad/sec.

Since the lowest frequency f_{min} is well-defined it can be determined from the curve. The highest frequency f_{max} can also be easily determined from the curve.

7.6.1 Effect of the Shape of Bearings

The characteristic of the curve of friction torque recorded or observed on the screen of a cathode ray oscilloscope is also a function of the shape of the bearing. Ovality of the raceways, concentricity of inner and outer diameters of the ball bearing ring with respect to the inner and outer diameter of the raceways, eccentricity of raceways relative to the lateral surface and its distortion, etc. affect the ultimate characteristic of the friction torque. Typical curves characterizing the effect of individual deviations on the friction torque components are shown in Fig. 7.66.

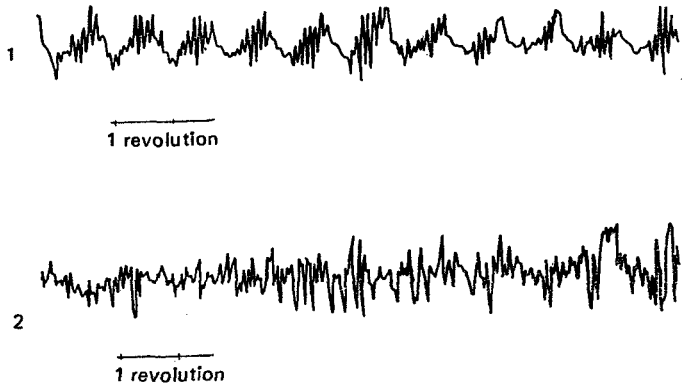

Fig. 7.66. Characteristics of friction torques with defects in raceways:
1—bearing 2 of 26 type with scratches on raceway of outer ring;
2—bearing 1 of 26 type with furrows in raceway.

Inspection of the friction torque curve allows us to determine the degree of geometric perfection of the bearing.

7.6.2 Effect of the Cage

Jamming of the cage and stress therein have a considerable effect on variable friction torque.

Frequent jamming of the cage can be confused with geometric defects in rolling elements. But since this is a random defect, in the majority of cases it can be recognized, whereas geometric deviation from the correct shape is expressed by a nearly sinusoidal curve.

Typical characteristics of friction torque when the cage is deformed and when it is jammed are shown in Fig. 7.67.

One of the principal causes of stresses in the cage, leading to destruction, is twisting of the inner ring of the bearing relative to the outer. These stresses can be reduced to a minimum by ensuring the necessary radial clearance bet-

ween balls and the raceways of rings. As shown by experiments [69], for each value of twist the maximum amplitude of stresses does not depend on the speed of rotation of the ball bearing in the range 0–3,000 rpm. Fig. 7.68 shows curves which describe the nature of stresses in the cage and the rise in the amplitude of oscillations with an increase in angular twist. The characteristics of

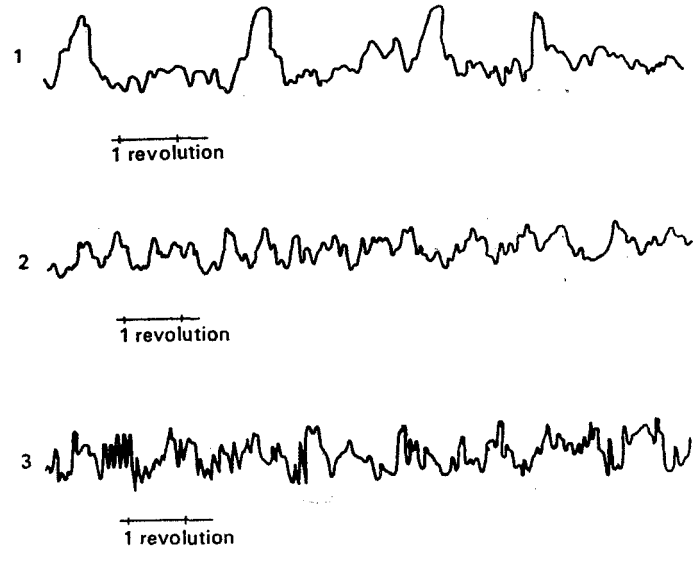

Fig. 7.67. Friction torque with defects: *1*—bearing 2 of 26 type with concave cage; *2*—bearing 3 of 26 type with deformed cage; *3*—bearing 1 of 201 type with slight jamming of cage.

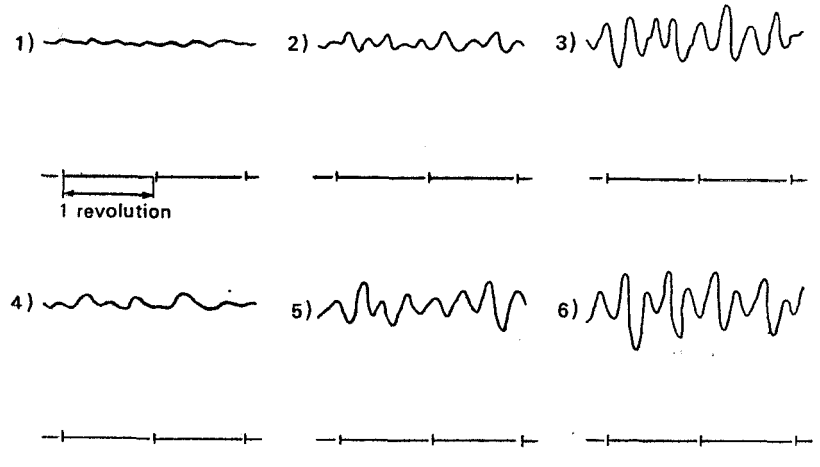

Fig. 7.68. Stresses in cage depending on skew angle of bearing rings: *1*—0.26°; *2*—0.39°; *3*—0.46°; *4*—0.51°; *5*—0.56°; *6*—0.61°.

friction torque are analogous to the nature and amplitudes of stresses in the cage.

7.6.3 Effect of Surface Smoothness

The curve of friction torque offers excellent qualitative analysis of the surface smoothness of raceways, balls and cages and also other random defects.

Random defects (pits, scratches, Brinnel indents) are expressed in the recorded curve of friction torque in the form of disorderly located random scatters.

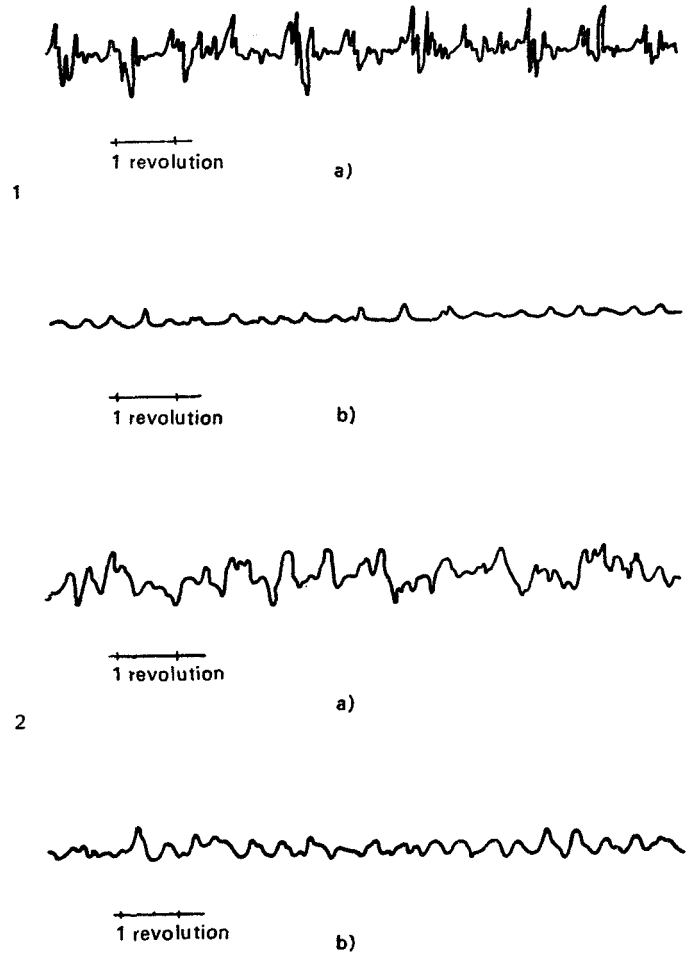

Fig. 7.69. Friction torque in bearings: *a*—contaminated (by sand particles); *b*—clean; *1*, *2*—number of bearings.

7.6.4 Effect of Dirt

Fig. 7.69 shows typical curves of friction torque corresponding to washed bearings and bearings with different degrees of contamination.

Peaks in the curve of friction torque caused by dirt usually differ from scatter due to random defects (smoothness of surface treatment) by the fact that dirt causes narrow scattering in the torque curve. However, this is not always so because the scatter caused by a large particle of dust can add up to

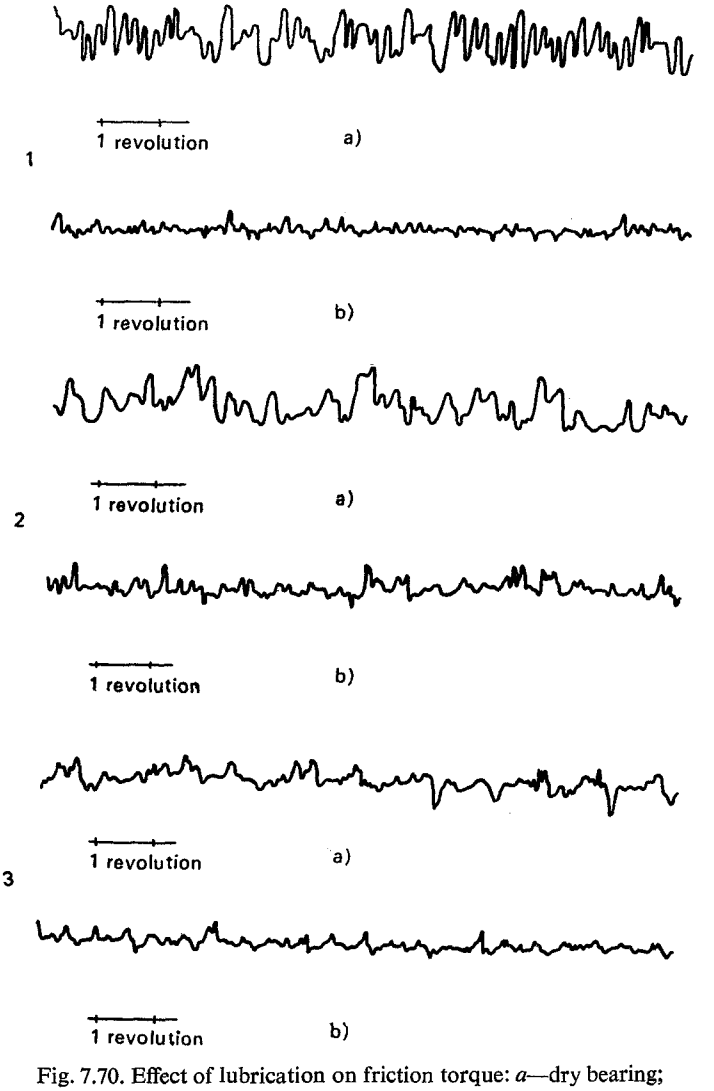

Fig. 7.70. Effect of lubrication on friction torque: *a*—dry bearing; *b*—lubricated; *1, 2, 3*—no. of bearings.

the instantaneous value of friction torque. In order to determine accurately the nature of the scatter (contamination by particle) it is necessary to clean the bearing carefully and then repeat the test.

7.6.5 Effect of Lubrication

The effect of lubrication on the characteristic of friction torque in bearings was considered earlier. The curves drawn in Fig. 7.70 once again show the effect of lubrication on the characteristic of friction torque under different conditions.

Standard lubricants usually cause an increase in the constant component of friction torque in bearings and a reduction in the variable component.

7.6.6 Effect of Ring Deformation

When there is wobbling, ovality or deformation of bearing rings the characteristics of friction torque have an especially typical form. In these cases a clearly expressed periodicity whose frequency is sharply defined among other frequencies is obtained (Fig. 7.71). The circle diagram obtained with a circle meter is shown in Fig. 7.71, which describes deviation of the raceways of bearing rings from the correct shape (the outer ring was deliberately deformed).

The characteristics of the friction torque of one bearing in different conditions are shown in Fig. 7.72 for comparative analysis.

In 1966 the firm SKF developed an impact-impulse technique for determination of deformations in bearings using electrical measurement of high-frequency vibrations, which are always present in a defective bearing [67].

In considering all the characteristics listed it is necessary to take into account the condition that in each case not one but many factors are at work, although one predominates.

Visual analysis always gives only preliminary data on the state of the bearing and requires high expertise of the controller. For an objective diagnosis other methods of examining a bearing are necessary.

The purpose of interpreting the variable friction torque during the analysis of realizations is to obtain estimates of the state of the bearing. In the case of a complex interpretation it is necessary to carry out a selection from the possible qualitative states of the bearing (qualitative interpretation) and evaluate the unknown parameters on which these states depend. Here the presence of even very small random component (compared to other, known components) excludes the "null" criterion since the difference between the values of assumed moduli of the empirical data and the measured values is a random function, different from zero. All attempts to formulate any criterion come up against the law of probabilistic distribution of the difference obtained.

The interpretation can be expressed in two stages. These consist in describing a certain function of "response" $\lambda(\rho)$ in the space of bearing states and determining the values of the parameters $\vec{\rho}=\hat{\rho}$ for which the value of $\lambda(\hat{\rho})$ has a minimum (maximum). In the case of least squares

$$\lambda(\rho)=\sum_k \sum_i [U_{ki}-f_{ki}(\rho)]^2, \tag{7.22}$$

where $f_{ki}(\rho)$ are theoretical functions characterizing the possible states; U_{ki} are the empirical data.

In the present case the complete set of observations is divided into separate groups which are identified by index k ($k=0, \pm 1, \pm K$). Hence any pair of observations taken from different groups can be considered statistically

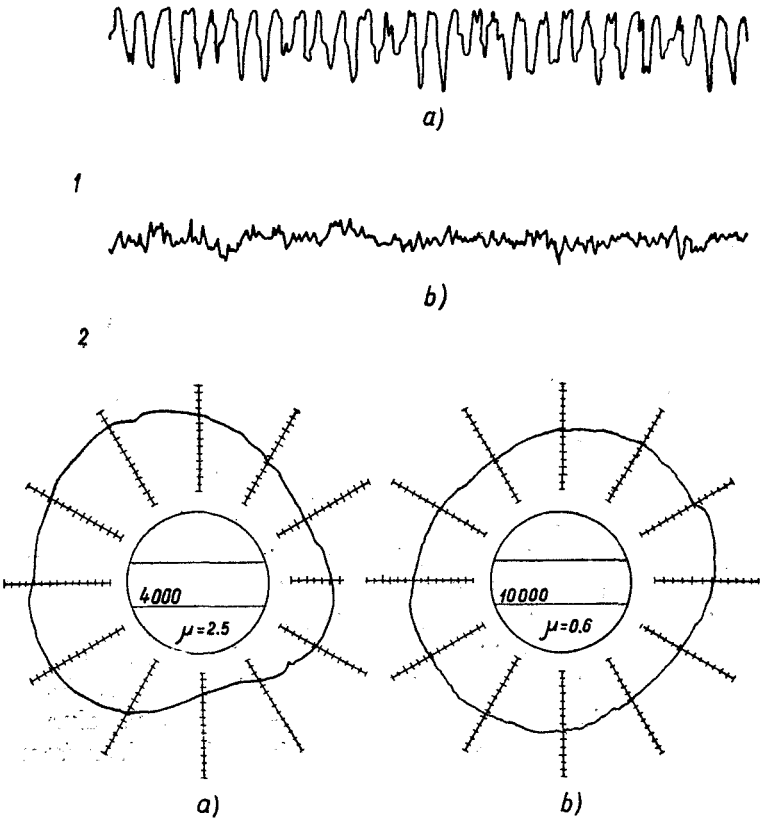

Fig. 7.71. *1*—Friction torque with deformation of rings: *a*—outer ring deformed; *b*—undeformed, same bearing; *2*—shape of raceways of bearing; *a*—inner ring; *b*—outer ring.

independent. At the same time, observations included in any k-th group are correlationally associated among themselves. The index i indicates the number of observations within the k-th group, for example, the group of realizations of variable friction torque in bearings with scratches on the outer groove for a bearing with deformed cage (ring) contaminated by sand, etc.

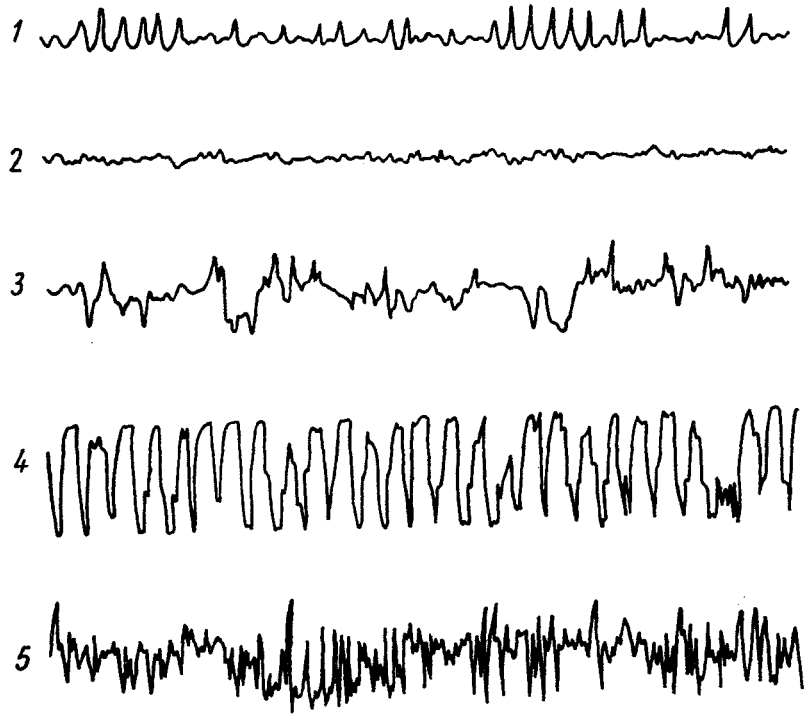

Fig. 7.72. VFT of bearing of 26 type: *1*—dry bearing; *2*—lubricated with IS-45 oil; *3*—contaminated by dust; *4*—outer ring deformed; *5*—cage deformed.

The problem consists in determining the optimum choice of the probable state based on the given realization of observations. To ensure the possibility of obtaining a very effective result it is desirable to choose for the "response" function conditional probability $P_u(n)$ for the possible states $n=1, 2, \ldots, N$, which can be determined after obtaining the empirical values of U_{ki}.

The probabilistic density $p(\mathbf{U})$ of the appearance of the given vectors U_k ($k=0, \pm 1, \ldots, \pm K$) as a result of the experiment is obtained from Bayes formulas:

$$P_u(n)=\frac{1}{p(\mathbf{U})}P(n)\,p_n(\mathbf{U}). \tag{7.23}$$

Here P_n is the *a priori* density of each of the possible states; $p_n(\mathbf{U})$ is the value

of the conditional probabilistic distribution density of empirical data for one of the possible states of the bearing. These densities are determined according to the particular model of empirical data using the well-known theorems of the probability theory. Let us consider them as functions of bearing state for this sample of empirical values, i.e. functions of probability. In a purely qualitative interpretation the probability function is a discrete set of numbers (probability coefficients) characterizing individual states of the bearings.

Using this theory we determine N quantities λ_ν ($\nu=1, 2, \ldots, N$) of the logarithm of the ratios of *a posteriori* probabilities:

$$\lambda_\nu=\ln\frac{P_u(\nu)}{P_u(0)}=\ln\frac{P(\nu)\,L_\nu}{P(0)\,L_0}, \quad L_n=P_n(U) \tag{7.24}$$

and choose a state for which the quantity λ_ν is maximum and positive. If all values of λ_ν are negative we choose the state for which $n=0$.

Observe that the determination of the state of the bearing is carried out not only on the basis of information obtained while analyzing the data of realization of variable friction torque but also taking into account *a priori* knowledge of these states, obtained by the analysis of the data of earlier tests. In this case for determination of the quantity λ_ν a known quantity which takes into account the *a priori* probabilistic distribution:

$$L_n\frac{P_0(\nu)}{P_0(0)}\,. \tag{7.25}$$

is added to the expression (7.24). All results concerning the rules for acceptance of the solutions and estimates of the effectiveness of the qualitative interpretation continue to operate.

The method of maximum probability leads to asymptotically empirical, effective and normal estimates [44]. Their effectiveness is determined by the covariant matrix

$$B=|\,b_{ss'}\,|\,{}_{ss'=1}^{N},\; b_{ss'}=\sum_i\sum_k U_{ski}\,U_{s'ki}, \tag{7.26}$$

where s is the number of the state.

The diagonal elements of the matrix indicate the dispersion of corresponding estimates and nondiagonal elements-correlation coefficients of relations between estimates which have to be considered when estimating a few different states of the bearing from the same empirical data. The need to take into account the relation between estimates (and states) entails a requirement for simultaneous variation of parameters in the search for the maximum of the probability function. In selecting the parameters of the scheme of observations we must remember that it appreciably depends on the expected qualitative states of the bearing, the nature of the random component and the

number and expected values of the vector of parameters, since the observations selected should ensure acquisition of the desired information to the states of the bearing.

The following groups of bearings were chosen: with scratches on the outer rolling groove (1); with deformed cage, lubricated (2); lubricated with IS-45 oil (3); lubricated and dirty (4); dry (5); with deformed ring, lubricated (6); dry, with deformed cage (7); with wobbling (8); contaminated with sand (9); with deformed outer ring (10).

The parameters on the basis of which qualitative interpretation of the state was carried out were mean numbers of scatters beyond a given level A_i ($i=1, 2, 3, \ldots, N$) in 20 revolutions. Results of this study of bearings of the 201C type are given in Table 7.1.

TABLE 7.1

Group of bearings	Parameters												
	A_1	A_2	A_3	A_4	A_5	A_6	A_7	A_8	A_9	A_{10}	A_{11}	A_{12}	A_{13}
1	59	33.5	15.5	5	2								
2	55	54	56.5	50	42	29	20.5	9.5	4	2	0	0	0
3	70	50	29.5	19	16.5	10	8	4	2	0	0	0	0
4	36	39.5	33.5	25	18.5	14	10	8.5	6.5	4	3	2	2
5	61	45	45.5	30.5	24	13	7	5.5	1.5	1	0	0	0
6	35	35	35	35	34	33	23	15	10	4	1.5	0	0
7	23	19.5	1	0	0	0	0	0	0	0	0	0	0
8	51	51	51	51	51	51	51	51	51	51	51	38	11.5
9	145	145	138.5	71	65.5	88	64.5	34.5	7	2.5	0	0	0
10	27	29.5	24	23.5	19.5	7.5	5.5	3.5	2	2	1	0	0

It may be mentioned that when the state of the bearing has been decided it is possible to use the criteria of comparing mean values and dispersions of the number of scatter as in the case of dispersion analysis.

References

1. Same as ref. [1], Chapter IV.
2. Blekhman, I.I. and S.A. Molasyan. 1970. O Koeffitsientakh treniya pri vzaimodeistvii uprugogo tela s vibruyushchei ploskostyu (Friction coefficients due to the interaction of an elastic body with a vibrating plane). *Mekhanika tverdogo tela*, No. 4.
3. Bodner, V.A. 1969. Aviatsionnye pribory (Aircraft instruments). Moscow, Mashinostroenie.

4. Bowden, F.P. and D. Taybor. 1960. Trenie i smazka (Friction and lubrication). Moscow, Mashgiz.
5. Bulgakov, A.A. 1966. Chastotnoe upravlenie asinkhronnymi dvigatelyami (Frequency control of asynchronous motors). Moscow, Nauka.
6. Same as ref. [4], Chapter I.
7. Gvozdev, M.M. 1952. Uprugo-plasticheskie svoistva i povedenie konsistentnykh smazok v podshipnikakh kacheniya (Elasto-plastic properties and the behavior of grease in rolling contact bearings). Avtoreferat kand. diss., Kaunas.
8. Same as ref. [24], Chapter IV.
9. Grigoreva, S.O., D.M. Tolstoi and A.V. Chichinadze. 1972. Ob ustranenii friktsionnykh avtokolebanii (Elimination of friction self-vibrations). *Doklady AN SSSR*, Vol. 202, No. 1.
10. Gruzov, V.L. and Yu.A. Sabininin. 1970. Asinkhronnye malomoshchnye privody a staticheskimi preobrazovatelyami (Asynchronous low-powered drives with static converters). Leningrad, Energiya.
11. Gustafson, O.G. Vliyanie konsistentnoi smazki na vibratsiyu podshipnikov kacheniya (Effect of grease on the vibrations of rolling contact bearings). Per. GPNTB, No. 69/9832-B.
12. Deinega, Yu.F. and Ya.A. Verbitskii. 1967. Reologicheskie svoistva plastichnykh smazok i soprativlenie vrashcheniyu podshipnikov kacheniya na nizkikh skorostyakh (Rheological properties of plastic lubricants and frictional torque of rolling contact bearings at low speeds). *Doklady AN SSSR*, Vol. 172, No. 3.
13. Delektorskii, B.A. *et al.* 1968. Proektirovanie giroskopicheskikh elektrodvigatelei (Design of gyroscopic motors). Moscow, Mashinostroenie.
14. Same as ref. [26], Chapter IV.
15. Dovidenas, V.I. 1967. Eksperimentalnoe issledovanie dinamicheskikh peremennykh momentov soprotivleniya sharikopodshipnikov, primenyaemykh v magnitnoi zapisi (Empirical study of dynamic variable friction torque in ball bearings used in tape recorder). In *Tekhnika*, Vilnyus.
16. Zhilnikov, E.P. and M.I. Kurushin. 1969. Eksperimentalnoe i teoreticheskoe issledovanie rezhima treniya v radial'no-upornom podshipnike (Theoretical and empirical study of friction in radial-thrust bearings). *Trudy Kuibyshevskogo aviatsionnogo in-ta*, vyp. 40.
17. Ilyukovich, A.M. 1963. Elektricheskie schetchiki (Electrical counters). Moscow-Leningrad, Gosenergoizdat.
18. Same as ref. [42], Chapter IV.
19. Kalvan, V.A. 1966. Eksperimental nye issledovaniya momentov treniya skorostnykh podshipnikov kacheniya (Empirical study of friction torque in high-speed rolling contact bearings). *Trudy VNIPPa*, No. 1 (45).
20. Same as ref. [10], Chapter I.
21. Same as ref. [50], Chapter IV.

22. Same as ref. [45], Chapter III.
23. Klimov, K.I. 1967. Otsenka stabilnosti masei i plastichnykh smazok v zone treniya kacheniya (Estimation of the stability of oils and plastic greases in the zone of rolling friction). In *Metody issledovaniya neftei i nefteproduktov, prisadok, katalizatorov i adsorbentov.* Moscow.
24. Kovalev, M.P. 1968. K raschetu smeshchenii tsentra rotora giroskopa pri chisto osevoi nagruzke (Computation of the displacement of the rotor center of a gyroscope due to purely axial load). *Izv. vuzov, Priborostroenie*, No. 6.
25. Kovalev, M.P. 1970. Opory i podvesy giroscopicheskikh ustroistv (Supports and suspensions of gyroscopic devices). Moscow, Mashinostroenie.
26. Same as ref. [12], Chapter I.
27. Kolesnichenko, L.F. 1966. Metodika i prisposoblenie dlya izucheniya vliyaniya smazochnykh sred na sostoyanie tonkoi kristallicheskoi struktury poverkhnostnogo sloya metallov pri trenii (Methodology and devices for study of the effect of lubricant on the thin surface crystal structure of metals under friction). *Fiziko-khimicheskaya mekhanika polimerov*, No. 2.
28. Same as ref. [20], Chapter I.
29. Same as ref. [22], Chapter I.
30. Kraskovskii, E.Ya. 1964. O soprotivlenii, voznikayushchem pri trenii kacheniya (Resistance due to rolling friction). *Sbornik trudov Leningradskogo in-ta inzhenerov zheleznodorozhnogo transporta*, vyp. 217.
31. Kutkov, A.A. 1959. Izmerenie tolshchiny smazochnykh sloev (Measurement of the thickness of lubricating layers). *Izmeritelnaya Tekhnika*, No. 10.
32. Kutkov, A.A. 1959. O staticheskom momenta treniya podshipnikov kacheniya (Static friction torque of rolling contact bearings). *Izv. vuzov, Mashinostroenie*, No. 2.
33. Kutkov, A.A. and V.I. Vishnyakov. 1968. Novye issledovaniya v oblasti treniya i iznosa mashin (New studies in friction wear and tear in machines). Rostovskoe knizhnoe izd.
34. Loncaster, D.K. 1967. Smazochnoe deistvie plenok tverdykh smazok (Lubricating action of films of solid lubricants). In: *Novoe o smazochnykh materials. Izbrannye doklady na mezhdunarodnoi konferentsii po smazochnym materialan.* Translated from English, Moscow, Khimiya.
35. Same as ref. [74], Chapter IV.
36. Mikhelman, A.I. and A.N. Mashchinov. 1969. Vliyanie ultrazvykovykh kolebanii na trenie tverdykh tel (Effect of ultrasonic vibrations on the friction of solid bodies). *Vestnik mashinostroeniya*, No. 1.
37. Nazarenko, M.V. and M.A. Runets. 1968. Vliyanie svoistv smazochnykh masel na protsessy treniya i iznos (Effect of lubricating oil qualities on friction, wear and tear). *Promyshlennost' Byelorussii*, No. 10.
38. Same as ref. [80], Chapter IV.

39. Same as ref. [27], Chapter II.
40. Panovka, Ya.G. and I.I. Gubanova. 1964. Ustoichivost' i kolebaniya uprugikh sistem (Stability and vibrations of elastic systems). Moscow, Nauka.
41. Pisarenko, G.S. 1962. Rasseyanie energii pri mekhanicheskikh Kolebaniyakh (Energy dispersion during mechanical vibrations). Kiev. Izd. AN Ukr USSR.
42. Poznyak, E.L. 1971. Nelineinye kolebainiya neuravnoveshennykh vertikalnykh rotorov na podshipnikakh kacheniya (Nonlinear vibrations of unbalanced vertical rotors on rolling contact bearings). *Mashinovedenie*. No. 1.
43. Prichiny shuma i vibratsii v podshipnikakh kacheniya (Sources of noise and vibration in rolling contact bearings). Rotoprintnaya VNIPPa, Moscow, 1967.
44. Pugachev, V.S. 1960. Teoriya sluchainykh funktsii (Theory of random functions). Moscow, Fizmatgiz.
45. Raiko, M.V. 1970. Smazka zubchatykh peredach (Lubrication of toothed-gear transmissions). Kiev., Tekhnika.
46. Raiko, M.V. and V.P. Kadomskii. 1970. O svoistvykh nezhidkikh plenok, obrazuemykh maslami na poverkhnostyakh kontakta detalei mashin (Properties of nonliquid films formed by oils on the contact surfaces of machine components). *Prikladnaya Mekhanika*, vyp. 3.
47. Same as ref. [90], Chapter IV.
48. Reguliririvanie rezhima vibratsionnykh isnytanii po sile i uskoreniyu (Control of vibration tests by force and acceleration). *Ekspress-informatsiya. Ser. Detali mashin*, No. 4, 1971.
49. Reshetov, D.N. and E.I. Levina. 1956. Dempfirovanie kolebanii v soedineniyakh detalei mashin (Damping vibration in couplings of machine components). *Vestnik Mashinostroeniya*, No. 12.
50. Sinitsyn, V.V. and L.S. Vasileva. 1968. Vliyanie vyazkostnykh smazochnykh materialov na soprativleniye vrashcheniyu podshipnikov kacheniya (Effect of viscous lubricants on friction torque in rolling contact bearings). In: *Voprosy treniya i problemy smazki. Moscow, Nauka.*
51. Sinitsyn, V.V. and L.S. Vasileva. 1966. Issledovanie peremeshcheniya plastichnykh smazok v podshipnikakh (Study of the displacement of plastic lubricants in bearings). *Zavodskaya laboratoriya*. No. 5.
52. Sluchainye kolebaniya (Random vibrations) ed. S. Krendel, Moscow, Mir, 1967.
53. Snizhenie kineticheskogo treniya putem prilozheniya razlichno napravlenny, garmonicheskikh Kolebanii (Reduction of kinetic friction using multidirectional harmonic vibrations). *Ekspress-informatsiya, Ser. Detali mashin*, No. 24, 1971.
54. Solov'ev, A.I. 1958. Issledovanie poter na trenie v podshipnikakh kache-

niya pri razlichnykh rezhimakh (Study of friction losses in rolling contact bearings under different conditions). *Vestnik mashinostroeniya*, No. 3.
55. Solov'ev, A.I. 1959. O trenii u podshipnikakh kacheniya priborov (Friction in rolling contact bearings of instruments). *Priborostroenie*, No. 9.
56. Solov'ev, A.I. 1966. Raschet mekhanizmov izmeritelnykh vychislitel'nykh i avtomaticheskikh ustroistv (Design of the mechanisms of measuring, computing and automatic devices). Moscow-Leningrad, Energiya.
57. Solov'ev, A.I., V.I. Kosov and I.N. Popov. 1969. Skolzhenie v podshipnikakh kacheniya (Sliding in rolling contact bearings). *Vestnik Maschinostroeniya*, No. 6.
58. Faingauz, V.M. 1968. Izmerenie koeffitsientov dempfirovaniya podshipnikov kacheniya (Measurement of damping coefficients of rolling contact bearings). *Izv. vuzov, Mashinostroenie*, No. 12.
59. Foreit, I. 1966. Emkostnye datchiki neelektricheskikh velichin (Capacitance transducers of nonelectric quantities). Moscow-Leningrad, Energiya.
60. Haerning Walter. Ustanovka podshipnikov kacheniya v metallore zhushchikh stankakh pri pomoshchi diagnoza uzla Doklady (Setup of rolling contact bearings in metal-cutting lathes for different assemblies). Lectures. FAG kugelfischer Georg Schafer co Schweinfurt.
61. Same as ref. [102], Chapter III.
62. Jurkauskas, A.Yu and A.Yu. Palionis. 1970. Issledovanie elektricheskogo soprotivleniya gidrodinamicheskoi plenki sharikopodshipnikov (Electrical resistance of the hydrodynamic film in ball bearings). *Nauchnye trudy vuzov. Lit. SSR, vibrotekhnika*. No. 4 (13).
63. Yatsura, E.S. and P.I. Yashcheritsyn. 1969. Issledovanie dempfiruyushcheii sposobnosti uprugoi sistemy rotor-podshipnik pri impulsnom nagruzhenii (Study of the damping characteristic of a rotor-bearing elastic system under impact loading). In: *Kachestvo i nadezhnost' metallo-obrabatyvayushchego oborudovaniya*, Moscow.
64. Anderson, W.J. 1970. Elastohydrodynamic lubrication theory as a design parameter for rolling element bearings. *Pap. Amer. Soc. Mech. Eng.*, No. DE-19.
65. Barnard, T.P. and R.S. Guyett. 1960. Determination and correlation of fundamental instrument bearing parameters. *J. of the Amer. Soc. of Lubrication Eng.*, No. 2.
66. Bassler, O. 1963. Der Einfluss von Walzlagern auf die Biegeschwingungen von Wellen. *Konstruction*, Bd. 15, H. 5.
67. Boto, P.A. 1971. Detection of bearing damage by shock-pulse measurements. *Eng. Dig.*, Gr. Brit., 32, No. 9.
68. Buczynski, L. and S. Mikulski. 1968. Aktualnye problemy konstruirovaniya podshipnikov skolzheniya (Practical problems of sliding-bearing design). *Przeglad mechanizmy*, No. 17.

69. Crawford, T.S. 1970. The experimental determination of ball bearing cage stress.—*Wear*, 16, No. 1.
70. Dowson, D. 1965. Thin Film Lubrication. Proc. Int. Symp. on Lubrication and Wear, Muster and Sternlicht, Ed. Me Cuthan Pub. Corn.
71. Harris, T.A. 1970. An analytical method of predicting skidding in thrust-loaded, angular-contact ball bearings. *Pap. Amer. Soc. Mech. Eng.*, No. S-7.
72. Lutz Otto, Brune Gerhard. 1970. Berechnung des Kafigschlupfes axia-libe-laster Schragkugellager. *Motortechnische, Zeitschrift'*, 31, Nr. 7.
73. Onnen, O. 1969. Kalsruhe, Verbesserung der Mess genauigkeit in der Dehnungs-mebstreifen-Technik. *Feinwerktechnik*, Nr. 2.
74. Paplawski, J.V. and J.A. Mauriello. 1969. Skidding in lightly loaded high-speed thrust ball bearings. *Pap. Amer. Soc. Mech. Eng.*' No. 20.

8

WAYS OF REDUCING FRICTION TORQUE AND VIBRATIONS IN BEARINGS

The correct choice of the optimum design of bearings and the magnitude of friction losses therein have a major role in the accuracy of motion and sensitivity to rotation of the rotating parts of rotary systems.

There is a wide variety of types and designs of precision bearings used in important high-precision rotary systems working in specific temperature conditions and media in static, transitional and dynamic domains [1, 2, 5, 6]. As a rule, relatively large friction losses are inherent in these types of precision bearings. These do not measure up to the growing requirements of technology and greatly restrict the range of application.

Improvement of existing types of bearing and assemblies of new types are called for along with use of the favorable influence of external vibrations. It is worth remembering that there are very strict requirements for constancy of magnitude of friction torque in new types of bearings and assemblies.

The present chapter describes techniques for reducing the harmful effect of friction and vibration of bearings on the basis of the conclusions of theoretical and experimental research in the field of the dynamic parameters of friction.

8.1 EFFECT OF VIBRATIONS ON FRICTION TORQUE IN BALL BEARINGS

In working conditions instruments are subjected to the effect of vibrations that affect the life and accuracy of the instruments, in particular, the friction torque of ball bearings. Both dissipative and restoring friction torque affect the accuracy of instruments. In certain cases the major role is taken by restoring torque (in taperecorders) and in others by restoring and dissipative torques simultaneously (in gyroscopic instruments). Hence the effect of vibrations on both kinds of torque is of special interest.

Many Soviet and foreign scientists are involved in study of the effect of vibration on friction torque. The following have contributed notably to the

solution of this problem: I.M. Sivokonenko, A.V. Fuseev, Yu.V. Skopynin, K.N. Yavlenskii, I.I. Blekhman, G.Yu. Janelidze, D.S. Pal'nor, V.A. Matveev, S.V. Karpov, A.P. Isaev, Z.M. Akcel'rod, Yasyo Iokoyama, Sakiiti Okobe, Ken'iti Isikiwa and others. The majority of authors conduct research on different aspects of the problem of vibrational effects on dissipative friction torque. Restoring friction torque has been left practically untouched.

In order to measure friction torque in ball bearing assemblies with vibrations an original setup was developed to measure restoring and dissipative friction torque. Measurement is carried out by the null method using semiconductor strain gauges. This method most completely corresponds to the actual operating conditions of the assembly being tested. The block-diagram of the setup is shown in Fig. 8.1 and the working principle of the mechanical part is shown in Fig. 8.2.

The drive is transmitted to the assembly casing off a PMU-IMI through two-step belt transmission, spindle with platform, lever and universal shaft. The speed of rotation of the assembly is between 2 and 200 rpm. The torsional vibrations are created by a DC minielectric motor mounted on the rotating platform. A circular cam is fixed to the shaft, whose eccentricity can be varied from 0 to 5 mm corresponding to amplitudes of vibrations from 0 to 0.056 rad.

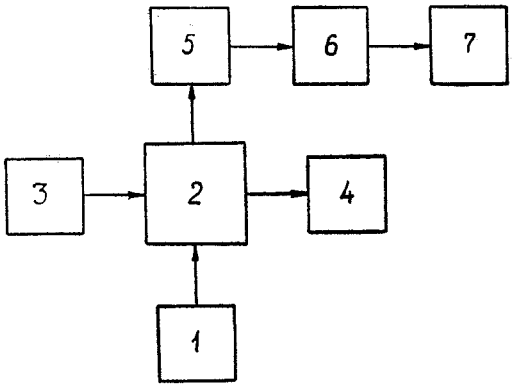

Fig. 8.1. Block-diagram of setup:
1—drive for assembly; *2*—assembly; *3*—source of torsional vibrations; *4*—control of torsional vibrations; *5*—transducers; *6*—strain amplifier; *7*—recorder.

The torsional vibrations can be expressed by the formula:

$$\psi = \tan^{-1}\frac{b\sin\omega t}{L+b\cos\omega t} + \tan^{-1}\frac{R}{\sqrt{L^2+b^2-R^2+2Lb\cos\omega t}}, \qquad (8.1)$$

where ψ is the angle of turn of the vibrating lever relative to the rotating platform;

ω is the angular speed of the minielectric motor;

t is the time;

b is the eccentricity of the circular cam;
R is the radius of the cam;
L is the distance between the axes of the minimotor and the lever.

It can be seen from formula (8.1) that the torsional vibrations are not purely sinusoidal. Expressing equation (8.1) in a Fourier series for maximum eccentricity, we get the following values of amplitudes of harmonic components of the motion:

$\psi_1 = 0.056$ rad;
$\psi_2 = 0.0016$ rad;
$\psi_3 = 0.0002$ rad, when $b = 5$ mm; $R = 14$ mm;
$L = 90$ mm.

The coefficient of nonlinear distortion

$$k = \sqrt{\frac{\psi_2^2 + \psi_3^2}{\psi_1^2}}\, 100\% = 2.9\%.$$

The frequency of torsional vibrations can be changed by changing the supply voltage of the minimotor. The frequency of vibrations is measured with a stroboscope.

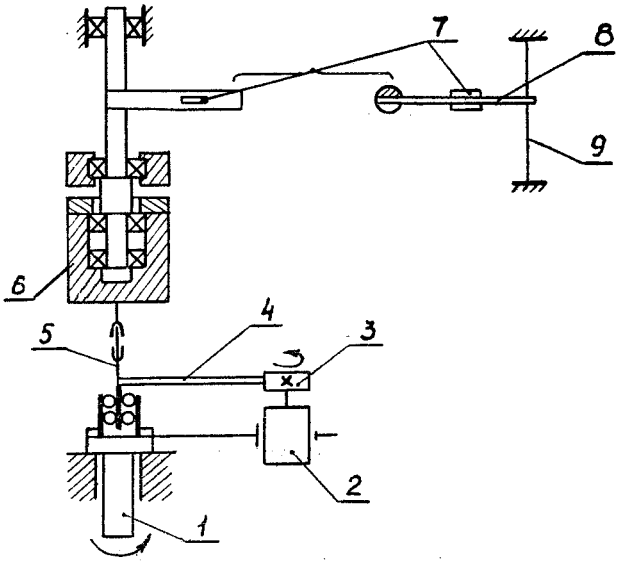

Fig. 8.2. Working principle of mechanical parts:
1—spindle with platform; *2*—minielectric motor; *3*—circular cam; *4*—lever; *5*—universal shaft; *6*—assembly under test; *7*—strain gauges; *8*—beam; *9*—taut string.

Tests were run with ball bearing assemblies on vertical axes. C1000900 and C1000094 bearings were tested. The weight of the assembly with the C1000900 bearings was 1.9 N and with the C1000094 bearings, 1.1 N. The

tests were run with dry friction without axial load. The dissipative friction torque of the assembly with C1000900 bearings was measured. The signal of dissipative torque traveled from the strain gauges to a strain amplifier with a high frequency filter at the output. It was read on the screen of an electronic oscilloscope. The frequency range of the strain amplifier was 0 to 300 Hz, nominal sensitivity 0.3 mV for a unit volt output signal. The time constant of the filter was set at 10 revolutions of the assembly. Readings on the screen of the oscilloscope were taken for steady signals.

The following notations are introduced: friction torque with vibrations will be indicated by the index 'V', dissipative by the index 'D' and restoring torque by the index 'R'.

With an increase in frequencies of vibrations at constant rotational speed ω_i of the assembly the ratio M_{DV}/M_D is reduced (Fig. 8.3 a). The ratio M_{DV}/M_D varies depending on the amplitude of vibrations f_0 (Fig. 8.3 b). With an increase in the rotational speed of the assembly, other conditions being the same, the effect of torsional vibrations is reduced (Fig. 8.3 c). In conclusion it may be mentioned that the change in the ratio M_{DV}/M_D depends on the product of amplitude and angular frequency of vibrations $f_0\omega$, i.e. on the maximum speed of vibrations for a given rotational speed of the assembly (Fig. 8.3 d).

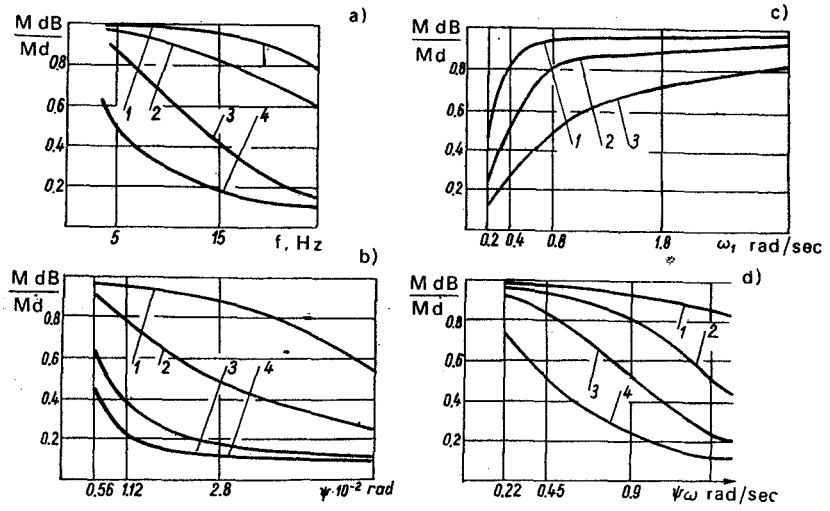

Fig. 8.3. Effect of torsional vibrations on dissipative friction torque: *a*—M_{DV}/M_D vs f (torsional vibration frequency) for amplitude $\psi=1.12\times10^{-2}$ rad; *1*—$\omega_1=3$ rad/sec; *2*—$\omega_1=0.8$ rad/sec; *3*—$\omega_1=0.4$ rad/sec; *4*—$\omega_1=0.2$ rad/sec; *b*—M_{DV}/M_D vs amplitude ψ of torsional vibrations when frequency $f=15$ Hz; *1*—$\omega_1=3$ rad/sec; *2*—$\omega_1=0.8$ rad/sec; *3*—$\omega_1=0.4$ rad/sec; *4*—$\omega_1=0.2$ rad/sec; *c*—effect of torsional vibrations depending on speed of assembly when $\psi=1.12\times10^{-2}$ rad: *1*—$f=5$ Hz; *2*—$f=10$ Hz; *3*—$f=20$ Hz; *d*—M_{DV}/M_D vs speed of vibrations $\psi\omega$: *1*—$\omega_1=3$ rad/sec; *2*—$\omega_1=0.8$ rad/sec; *3*—$\omega_1=0.4$ rad/sec; *4*—$\omega_1=0.2$ rad/sec.

On the basis of empirical data and graphs (Fig. 8.3) it is possible to draw the following conclusions:

1. For dry friction of the given ball bearing assembly under the given load with a vertical axis of rotation and ball bearings without axial tension dissipative friction torque depends on angular speed of vibrations $f_0\omega$. The dissipative friction torque is reduced with an increase in angular speed of vibrations.

2. The ratio M_{DV}/M_D depends on the rotational speed of the assembly. At high speeds of rotation the effect of vibrations is reduced.

Tests were also run to determine the restoring torque M_R of an assembly with C1000094 bearings. The signal from the strain gauges traveled to the strain amplifier. It was then recorded by a highly sensitive autorecorder of the Elkar type whose range of recordable frequencies is 0–100 Hz. Each experiment covered 10 revolutions of the assembly. It can be seen from the realizations obtained (Fig. 8.4) that the diagram of M_R is "modulated" by the

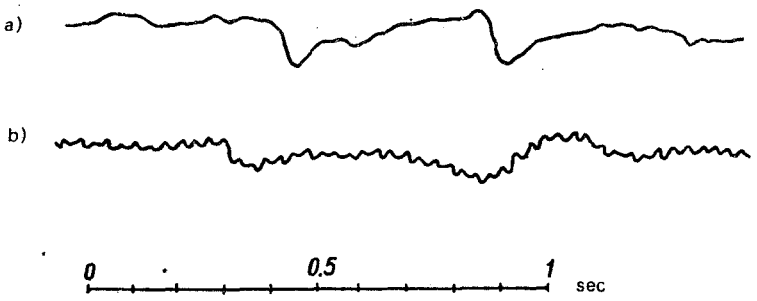

Fig. 8.4. Effect of torsional vibrations on restoring torque M_R: *a*—realization of M_R for $\omega_1=0.4$ rad/sec; *b*—realization of M_{RV} for $\omega_1=0.4$ rad/sec; $\psi=1.12\times10^{-2}$ rad; $f=30$ Hz.

frequency of torsional vibrations, i.e. one can clearly distinguish the variable component with a frequency equal to the frequency of torsional vibrations. With an increase in the frequency of torsional vibrations the amplitude of "modulation" is reduced and with an increase in the amplitude of vibrations it increases.

To obtain spectral density a spectrum analyzer is introduced instead of the Elkar autorecorder.

Graphs of spectral densities are shown in Fig. 8.5. The abscissa represents frequencies of the components M_R (in Hz) and the ordinate their amplitudes in (db). Amplitude A_0 is arbitrarily chosen. Analyzing the realizations obtained (Fig. 8.4) and graphs of spectral densities (8.5), we can draw the following conclusions:

1. Under the action of torsional vibrations in ball bearing assemblies a component of conservative torque appears with a frequency equal to the fre-

quency of the torsional vibrations. The amplitude of this component has a maximum value for large amplitudes and low frequencies of torsional vibrations.

2. With an increase in the frequency of torsional vibrations the excited amplitude of the component M_{RV} is reduced.

3. Torsional vibrations help widen the range of frequencies of M_R and reduce peak values of amplitudes of low frequencies. The frequency range is widened from low frequencies in the direction of high frequencies and around an excited frequency equal to the frequency of torsional vibrations.

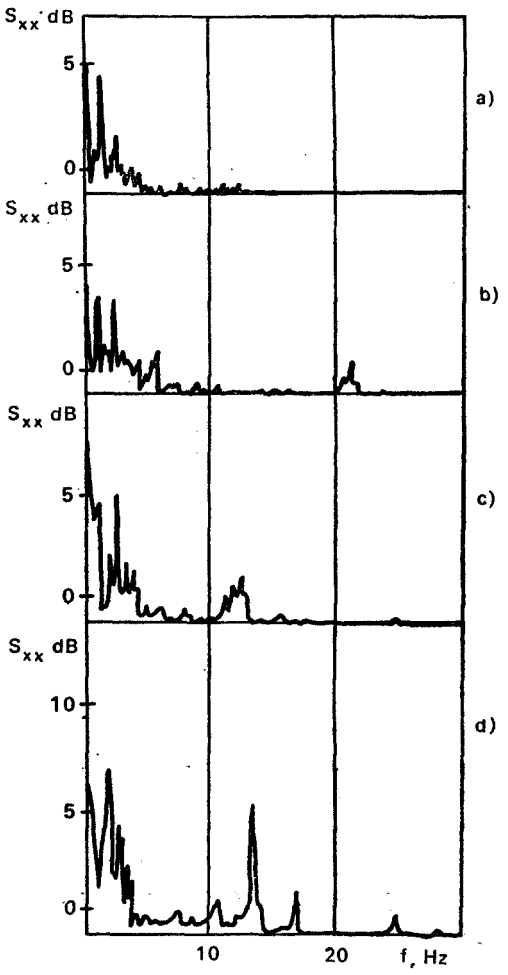

Fig. 8.5. Spectral densities of restoring torque M_R: *a*—$\omega_1=0.4$ rad/sec; $f=0$; *b*—$\omega_1=0.4$ rad/sec; $f=22$ Hz; $\psi=0.56\times10^{-2}$ rad; *c*—$\omega_1=0.2$ rad/sec; $f=13$ Hz; $\psi=0.56\times10^{-2}$ rad; *d*—$\omega_1=0.2$ rad/sec; $f=13$ Hz; $\psi=1.12\times10^{-2}$ rad.

8.2 NEW DESIGNS OF ROLLING-CONTACT BEARINGS AND ASSEMBLIES WITH REDUCED FRICTION TORQUE

In Chapter I it was shown that VFT in bearings with preloading appears as a result of different value of loads acting between individual rolling elements and rings. The magnitude of the amplitude of VFT depends on the magnitude of the difference in these loads. To reduce VFT it is necessary to reduce the difference in loads to a minimum. This is achieved by reducing the loads acting on the bearings, especially the axial loads, by reducing macro-geometric defects and by using low-viscosity lubricant. Fig. 8.6 is a drawing of a tape recorder assembly with a vertical-axis drum loaded in the axial direction. There is no axial load on the bearings of the drum when

$$P=ps,$$

where P is the weight of the rotor;
p is the air pressure;
s is the area of the end surface of the fluid static bearing.

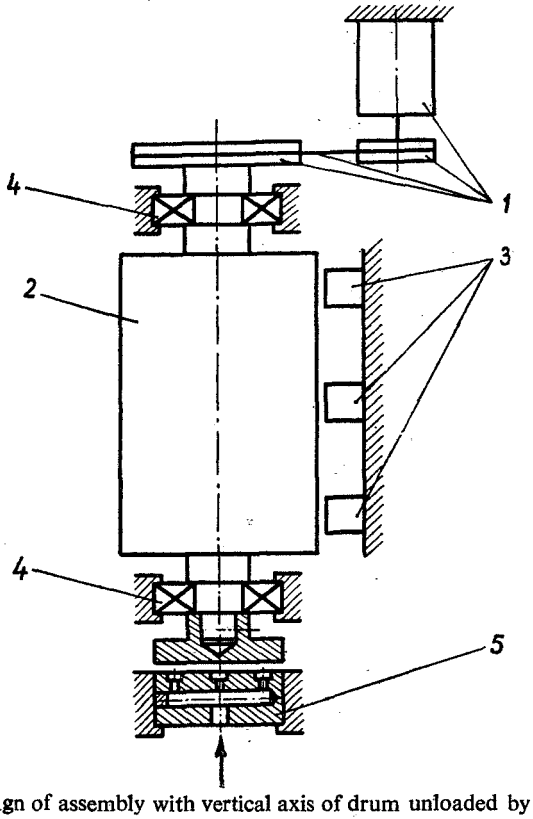

Fig. 8.6. Design of assembly with vertical axis of drum unloaded by air pressure: *1*—drive; *2*—magnetic drum; *3*—magnetic head; *4*—rolling contact bearings; *5*—fluid static bearing.

Fig. 8.7 shows the design of a suggested tape recorder with radial loading of the drive shaft. This load is achieved by adjusting the pulley-flywheel of the drive shaft to a constant horseshoe magnet whose ends are directed toward the cylindrical surface of the flywheel and placed symmetrically with respect to the circular groove of the flywheel.

The bearings *3* of the shaft *2* are loaded with a force R_N during operation of the drive *1*. With the adjustment of constant magnet *4* whose axis coincides with the line of action of force R_N, an attractive force R_a is created in the opposite direction. By selecting the constant magnet *4* with a corresponding inductance and regulating the clearance between the magnet and the pulley-flywheel of drive *1* we achieve an equilibrium of forces R_N and R_a. Thanks to this the bearings *3* are loaded in the radial direction.

Besides this, the magnet also helps to damp torsional vibrations of the drive shaft, which strongly affect detonation.

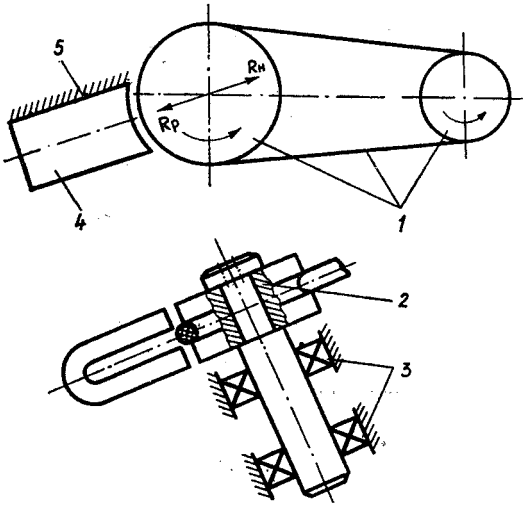

Fig. 8.7. Assembly of tape-winding mechanism with radial unloading of drive shaft:
1—drive; *2*—drive shaft; *3*—bearings; *4*—permanent magnet; *5*—casing.

The difference in loads acting on each rolling element due to geometric defects in the bearing assembly with preloading can be considerably reduced by using a tensile element with a stiffness a few orders of magnitude less than the contact stiffness in the bearing.

The working of the assembly, shown in Fig. 8.8, consists of the following: preloading is achieved by the cover *4* whose resting end has an elastic spring. Besides this, the bearing *2* and casing *5* are divided by the elastic ring *3*. The

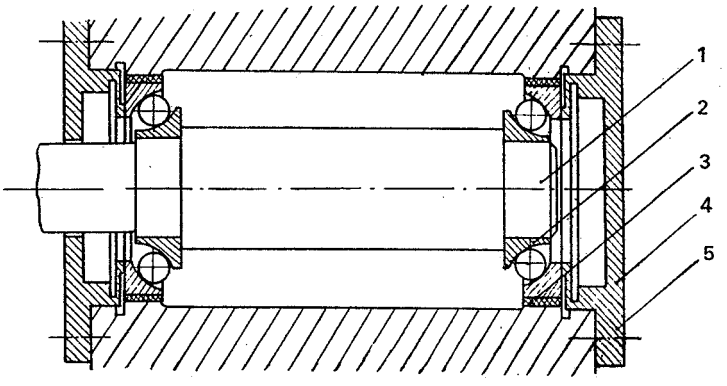

Fig. 8.8. Device for preloading in assembly:
1—shaft; *2*—bearing; *3*—elastic ring; *4*—top cover; *5*—casing.

resulting axial displacement due to geometric defects in the rolling elements and raceways of rings of the bearing *2* cause the deformation of rings *3* and spring of the cover *4*. The resulting difference in loads at the contact of rolling elements (thanks to slight stiffness in the axis *1*, direction of ring *3* and cover *4*) is negligible when compared to the difference in loads which would have resulted from a stiff tensile cover.

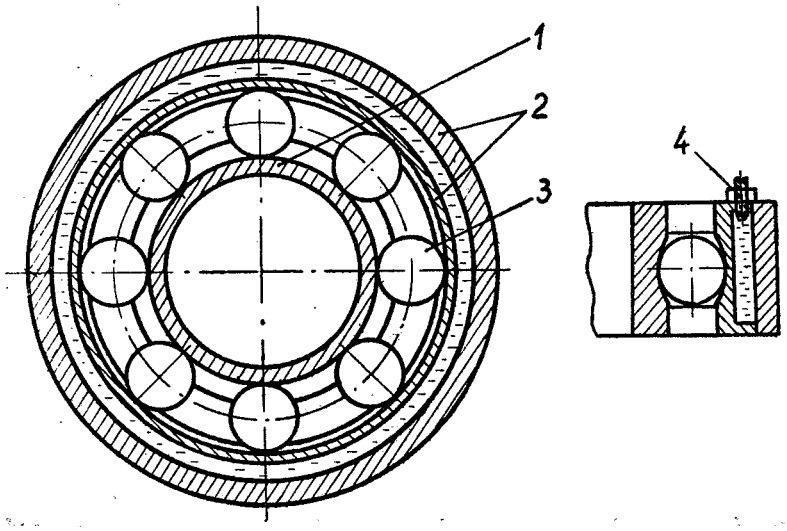

Fig. 8.9. Bearing with rings filled by incompressible liquid *1* and *2*—rings; *3*—rolling elements and cage; *4*—regulating unit.

Thus the variable component of a load with preloading at contact points of a bearing with raceways of rings and rolling elements having geometric defects reduces to a minimum, thanks to which the VFT of the rotor of the assembly is also reduced.

Macrogeometric defects in raceways are reduced by increased manufacturing accuracy. But this improvement has its limits. Fig. 8.9 is the drawing of a bearing in which the influence of macrogeometric defects in the rolling elements and raceways is brought to a minimum without increasing manufacturing accuracy.

The above bearing differs from the usual ones in that one or both of its rings have a cavity filled with incompressible liquid. The dimensions of the rings are chosen such that the contact stiffness at points of contact in the bearing is one order of magnitude greater than the flexural stiffness of the raceways.

Due to macrogeometric defects when the inner ring *1* rotates, rolling elements *3* enter either a narrow or a broad stretch of raceway. The load at the contact points either increases or decreases. Since the liquid is incompressible and pressure acts uniformly in all directions, the less loaded elements get an

additional load on account of the release of load from higher-loaded elements. Thus all the rolling elements are identically loaded during working.

Besides this, an important property of such a bearing is the simultaneous reduction in noise and vibration. It may also be mentioned that it is possible to regulate the radial clearance using the screw *4*.

A new design of bearing (Fig. 8.10) has been suggested. This uses separating elements instead of a cage, in which the variable and especially the constant components of friction torque are reduced. The reduction in components is achieved because each one of the separating elements is made in the form of a flexible continuous tape round a pair of rollers and placed between rolling elements.

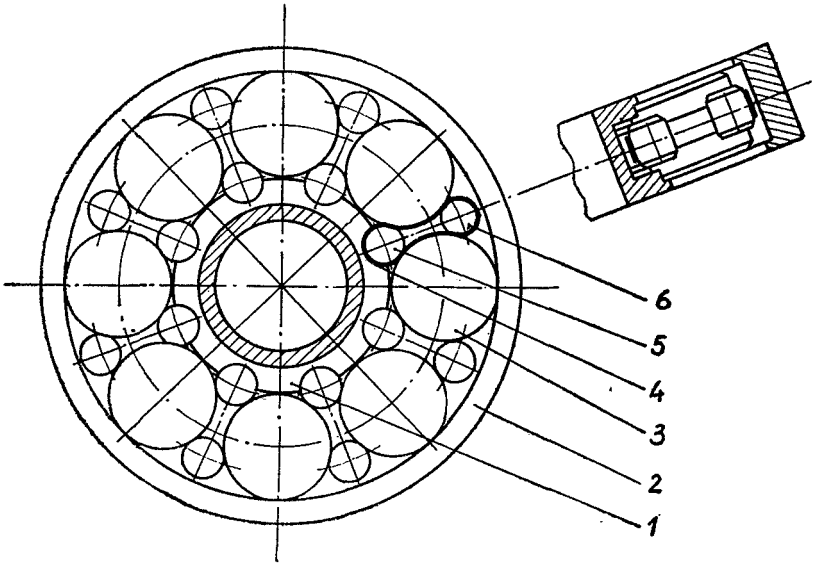

Fig. 8.10. Bearing with separating elements:
1 and *2*—rings of bearing; *3*—rolling elements; *4*—flexible endless tape; *5* and *6*—rollers.

The bearing operates in the following way: when the inner ring *1* rotates, rolling elements *3* rotating around their own axis transmit the motion to the separating element through tape *4* around rollers *5* and *6*. These in turn rotate on their axes and the axis of the separate rolling elements *3*. Rollers *5* and *6* are placed between rolling elements *3* such that the tape remains stretched. During the operation of the bearing, the rolling friction of rolling elements *3* about the separating element is considerably less than the sliding friction (in the usual cage) and thereby both constant and variable components of friction torque in the bearing are reduced.

As shown in Chapter 1, the constant and variable components are reduced

with a decrease in the viscosity of the lubricant. However, it is difficult to use low-viscosity lubricant in the usual bearings.

In order to improve the conditions of lubrication of a bearing with low-viscosity lubricants, moving separating elements are placed in the partitions of the cage, separating the rolling elements, and at the ends of the cage circular pockets with lubricants are located. They are connected by holes with the points of the separating elements farthest from the centers of the bearing and with the centers of the rolling elements. Let us study the working principle of such a bearing (Fig. 8.11).

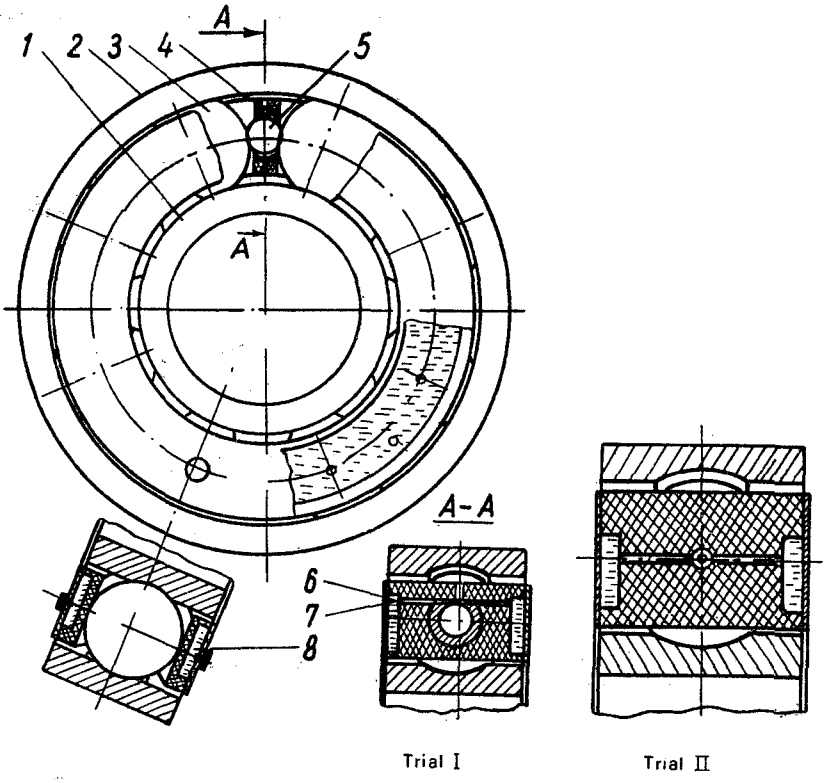

Fig. 8.11. Bearing with self-lubricating cage: *1* and *2*—rings; *3*—rolling elements; *4*—cage; *5*—separating element; *6*—pocket; *7*, *8*—holes.

Rolling elements *3* and separating element *5* start rotating on their own axis and in combination with the cage *4* all the elements rotate about the bearing axis when the inner ring *1* rotates. This results in a centrifugal force and consequently pressure, due to which the lubricant passes through the hole *7* with the help of the rotating separating element *5* and through the hole *8* and thereby lubricates the rolling elements *3*.

Consequently the contact points are continuously lubricated in this design

of bearing. With the help of a self-lubricating cage lubrication "starvation" and concentration of too much lubricant are avoided. This bearing can also work under vacuum conditions.

8.3 NEW DESIGNS OF SLIDE BEARINGS WITH REDUCED FRICTION TORQUE

For an effective reduction of friction losses and to increase the sensitivity of the rotation of rotors in bearings a few techniques have been developed: introduction of lubricant between rubbing components, forced motion of the bearing relative to the rotor and operation of the bearings in vibration conditions [5, 7]. Use of the first two reduces the friction loss negligibly.

Precision bearings finding wide application in instruments work under forced vibration conditions. The vibration of such bearings is achieved with the help of vibrators connected to the elements of the rubbing components. The vibrators of the bearings could be of the following types: mechanical (cam mechanisms), electromagnetic, membrane (electrodynamic), and piezoelectric. The first three types of vibrators have not found wide practical application because they work only at low frequencies of excited vibrations, they are large in size and allow the development of vibrations principally of the reciprocating type. Piezoelectric vibrators find very wide applications. They work with frequencies from 10 Hz to 10 MHz with uniform control of amplitude and frequencies in the given range. Depending on the design of piezoelectric vibrators it is possible to excite longitudinal, torsional and radial vibrations in bearings.

In order to excite mechanical vibrations piezoelectric elements with reverse effect are used as vibrators. They are divided into the following groups depending on their purpose:

—high-sensitivity piezoelements used in receivers or transmitters;
—piezoelectric elements used in receivers or transmitters under the action of strong electric fields;
—piezoelectric elements having high stability;
—piezoelectric elements with high amplitude-frequency characteristics in a certain range of temperatures and time;
—high-temperature piezoelectric elements working at temperatures above +250°C.

Piezoelectric elements with large values of piezoelectric and dielectric parameters and also high dynamic and temperature characteristics can find the widest practical application for purposes of effective excitation of vibrations in bearing components. Piezoelectric materials made of barium titanate, zirconate-titanate-lead, columbite-barium-lead, semicrystallic ferroelectric materials of the VK type [8] and quartz elements made of natural or artificial

quartz crystals working in resonance harmonics [9] are examples of such piezoelectric elements.

There are different designs of piezoelectric elements. The optimum designs of piezoelements take the form of plates, rods, discs, rings and cylinders. The form of polarized piezoelectric element is chosen depending on the required form of the excited vibrations. The frequency of mechanical resonance depends on the size of piezoelectric element and the way it is installed. The amplitude of excited vibrations depends on the type of piezoelectric element. If a voltage of 10 kV is applied to a piezoelectric element along the axis of polarization its length is increased by not more than a few microns. It is necessary to pay special attention to the correctness of installation and geometric form of piezoelectric elements in the exciter. Twists, curvature, cleavage and cavities of piezoelectric elements can appreciably distort the amplitude-frequency characteristics of the vibrations exciter and affect the stability of operation.

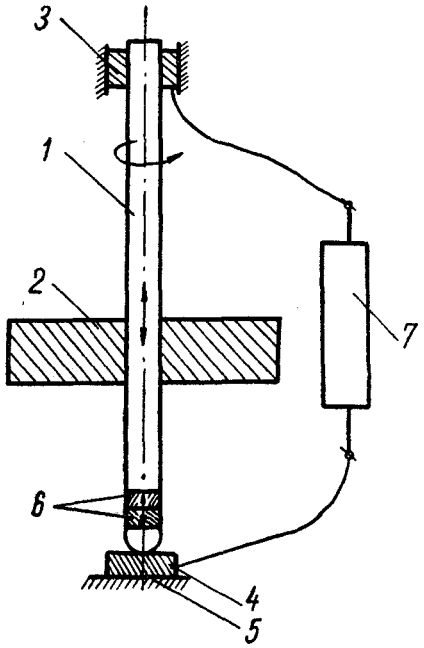

Fig. 8.12. Support with piezoelectric vibration exciter:
1—rotor; *2*—inertial mass; *3*—current conducting bearing; *4*—support; *5*—plate; *6*—piezoelectric element; *7*—frequency exciter block.

Certain typical precision slide bearings of instruments containing vibration exciters with uniform control of frequency and amplitude of excited vibrations are described below. These vibrations bring about an effective reduction of friction torque to a few percent of the usual value.

Use of a small-sized piezoelectric vibration exciter to excite axial vibrations in the rotor is illustrated in Fig. 8.12. When the rotor *1* rotates with the inertia mass *2* in the bearings *3* and in the support *4* constant and variable friction torques are developed. A block of piezoelectric elements of the reverse effect *6* is installed between the component parts of the rotor. This block is electrically connected through the current-conducting bearing *3* and support *4* with the block of frequency exciter *7* and insulated by the dielectric plate *5*.

By lining up the electrical axes of piezoelectric elements of reverse effect with the axis of rotation of the component parts of the rotor it is possible to obtain the maximum excitation amplitude of axial vibrations at the same supply voltage. Axial vibrations of the rotor are principally due to elongation

of the piezoelectric discs along their thickness. Depending on the amplitude of their vibrations, the upper part of the rotor along with the inertial mass undergoes oscillatory motion. Depending on the value of supply voltage applied to the block of piezoelectric elements, the upper part of the rotor along with the inertia mass can slide in the bearing *3* with a given amplitude of vibrations. In the support *4*, meanwhile, only the value of unit pressure varies because it is impossible for the lower part of the rotor to jump from the working surface of the support. Owing to the action of axial vibrations of the rotor, both in the bearing *3* and in the support *4* friction torques are reduced. This helps to increase the sensitivity to turning of the rotating part, especially during transition.

In the majority of high-precision instruments use is made of supports with spherical inner working surfaces between which the ball rests. Such a support (Fig. 8.13) shows the ball divided into two magnetized hemispheres between which reverse-effect piezoelectric elements are installed. These are electrically connected to the exciter.

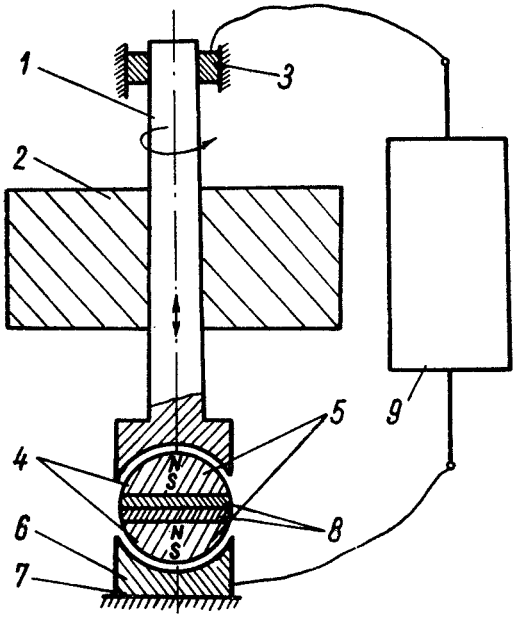

Fig. 8.13. Support with reverse-effect piezoelectric elements: *1*—rotor; *2*—disc; *3*—bearing; *4*—hemispheres; *5*—corrosion resistance shells; *6*—support; *7*—dielectric plate; *8*—piezo- electric elements; *9*—frequency block.

The support works in the following way:

The rotor *1* with the disc *2* rotates in the bearing *3*. The axial loads of the rotating part are taken by the support *6* through the hemispheres *4* covered

with a corrosion-resistant shell *5*. The support is electrically insulated from the casing of the instrument by the plate *7*. Under the action of friction torque in contact areas, hemispheres with shells and piezoelectric elements *8* rotate like a rigid body. The vibrations in the axial direction of the rotating rotor are caused by the mechanical deformations of elongation and compression of the piezoelements. Their frequency is controlled with the help of frequency block *9* by changing the polarity of the electric signal voltage. This changes the voltage vector of the external electric field of the connected plates and the piezoelectric elements. The hemispheres are magnetized in such a way that their opposite magnetic poles coincide with the axis of rotation of the ball. This allows the electrical axes of the piezoelectric elements to be lined up with the axis of rotation of the rotor and the geometric axis of the support. Thus the magnetized hemispheres ensure more stable movement of the ball in the support. A reduction in friction torque takes place at contact areas (Fig. 8.13) on account of the reduction in effective friction coefficients in the rubbing pair.

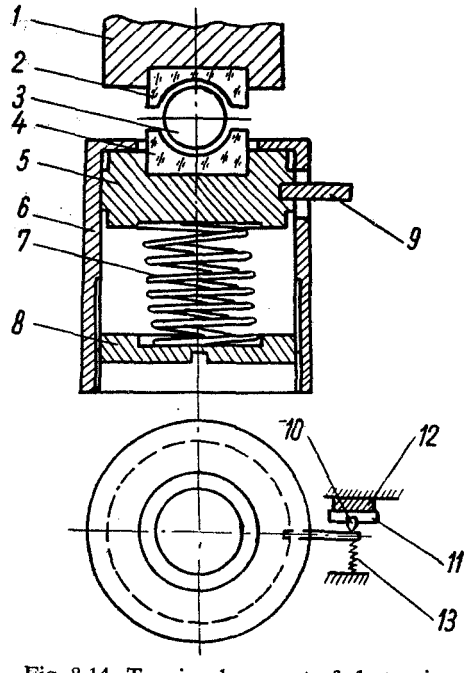

Fig. 8.14. Two-jewel support of electronic counter with piezoelectric element: *1*—rotor; *2*—industrial jewel; *3*—ball; *4*—support; *5*—holder; *6*—bushing; *7*—elastic element; *8*—nut; *9*—lever; *10*—needle; *11*—plate; *12*—piezoelectric element; *13*—elastic element.

The design of a two-jewel instrument bearing is shown in Fig. 8.14 consisting of the vibration exciter which converts the longitudinal vibrations excited by the piezoelectric element into torsional vibrations of the support. The working principle of this assembly is as follows:

The rotating rotor *1* with industrial jewel *2* set in the lower end makes the ball *3* move in the support *4*. The axial load of the rotor is taken through the holder *5* by the elastic element *7* set on the nut *8*, which is moved in the axial direction in the bushing *6*. A stiff needle *10* connected by the plate *11* to the effectively deforming plane of the reverse-effect piezoelectric element *12* rests on the free end of the lever *9* fixed to the holder.

The vibrations excited by this element cause torsional vibrations of the support *4* along with its holder about the geometric axis. The elastic

element *13* whose stiffness can be changed regulates the value of the exciting resonance amplitude of the free end of arm *9*.

Fig. 8.15 shows another design of instrument precision slide bearing which reduces the friction torque at the point of contact with the help of two vibration exciters.

The essence of this design is that in order to reduce friction losses of the rotor *1* in the bearing, reverse-effect piezoelectric elements *3*, *7* are installed in the upper and lower ends *4*, *6*. The ball *5* is freely suspended in their spherical sockets. Piezoelectric elements *3*, *7* are placed such that their electrical axes are parallel to one another and relative to the axis of rotation of the rotor. They are inclined at an angle exceeding the friction angle of the ball in the upper and lower ends respectively. This location of piezoelectric elements is determined by the minimum energy needed to bring about vibrational motion of the spherical ends.

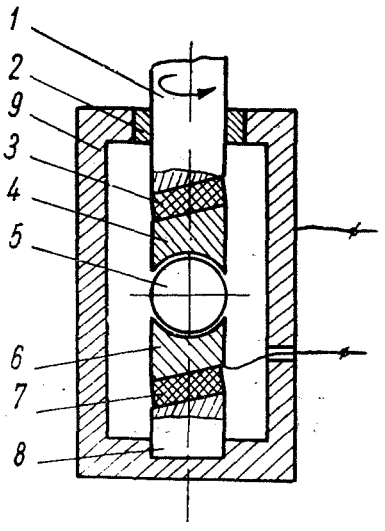

Fig. 8.15. Support with two piezoelectric vibration exciters: *1*—rotor; *2*—bearing; *3* and *7*—piezoelectric elements; *4* and *6*—ends; *5*—ball; *8*—support; *9*—casing.

The designs of the precision slide bearings described above can be successfully used in different precision instruments and rotor systems. The application of small-sized vibration exciters using reverse-effect piezoelectric elements will allow the development of new, improved designs and types of bearings. Such types of bearing can find wide application in precision instruments: gyroscopic instruments, tape recorders, Wattmeters, accelerometers, minielectric motors, and other rotary systems where high sensitivity to the turning of the rotating part and minimum friction losses are necessary.

References

1. Same as ref. [9], Chapter IV.
2. Vostroknutov, N.G. and A.M. Ilyukovich. 1961. Ispytanie elektricheskikh schetchikov (Tests of electric counters). Leningrad, Gosenergoizdat.
3. Kanapenas, P.M.V. and K.M. Ragulskis. 1970. Ustrostvo dlya opredelniya momenta samokhoda elektroschetchikov (Device for determination

of the torque of powered electric counters). Avtorskoe svidetelstvo po zayavke No. 133376/24–27.
4. Kanapenas, P.M.V., L.Yu. Michenis and K.M. Ragulskis. Ustroistvo dlya kalibrovki datchikov (Setup for the calibration of transducers). Avtorskoe svidetelstvo po zayavke No. 1615977/18–10.
5. Kovalev, M.P., I.M. Sivokonenko and K.N. Yavlenskii. 1968. Opory priborov (Instrument bearings). Moscow, Mashinostroenie.
6. Kopeikin, A.M. 1968. Napravlyayushchie i opory podvizhnykh elementov priborov (Guides and supports of moving components of instruments), Yaroslavl, Verkhnevolzhskoe kn. izd.
7. Sivokonenko, I.M. and K.N Yavlenskii. 1963. Vliyanie vibratsii na velichinu sil treniya v oporakh (Effect of vibrations on the magnitude of frictional resistance in supports). *Trudy LIAPa*, Vol. 40.
8. Same as ref. [33], Chapter I.
9. Yakimov, K.S. 1969. Vibratsionnoe peremeshchenie dvukhmassnoi kolabatelnoi sistemy (Vibrational displacement of a two-mass vibration system). *Izv. AN SSSR, MTT*, No. 5.

TT 75-52090
NASA TT F-679